Cretaceous-Cenozoic Evolution of the Crocodylia, and the Role of Environmental Change in Driving Diversity

Russell, Hannah

Award date:
2019

Awarding institution:
University of Bath

Cretaceous-Cenozoic Evolution of the Crocodylia, and the Role of Environmental Change in Driving Diversity

Hannah Polly Russell

A thesis submitted for the degree of Doctor of Philosophy

University of Bath

Department of Biology and Biochemistry

May 2018

Declaration of any previous submission of the work

The material presented here for examination for the award of a higher degree by research has not been incorporated into a submission for another degree.

Candidate's signature

……

Declaration of Authorship

I am the author of this thesis, and the work described therein was carried out by myself personally, with the exception of co-authored manuscripts presented in chapters 2-4 where the contribution of the work was carried out by other researchers is detailed at the start of each manuscript.

Candidate's signature

……

For Dad, the other Dr. Russell

Contents

List of Figures:

Chapter 3: Diverse assemblage of marine Crocodylia following the K-Pg mass extinction

Chapter 4: An Alligatoroid from the Early Paleogene of North Africa and the Post-Extinction Dispersal of Alligators

List of Tables:

Abstract:

The Cretaceous-Paleogene (K-Pg) mass extinction, 66 Ma, was one of five major extinctions in Earth history. Crocodylomorpha, originating in the Late Triassic, were affected with only three lineages surviving into the Cenozoic. However, the severity of the mass extinction on crown crocodilians remains unexplored. The primary aim of this thesis is to examine the impact of the K-Pg event on crown crocodilians, and how environmental changes across the boundary influenced their diversity, disparity, and biogeographical spread. A case study is made of the phosphate deposits of Morocco which span the K-Pg boundary and multiple new crown crocodilians are described from the Paleocene-Ypresian beds. The first four new species described are diagnosed as members of Gavialoidea and Tomistominae, highly specialised slender-snouted crocodilians which range from the Cretaceous to the present day. The phylogenetic position of these groups within the crown group is debated. Therefore, both morphological and combined datasets were examined in a time-calibrated framework to examine how the conflict influences our understanding of macroevolutionary patterns across the K-Pg extinction. The morphology and size of the new material prompted additional investigations into disparity, using linear and geometric morphometrics. Results show a distinct peak in disparity in the aftermath of the K-Pg. The second set of specimens described are diagnosed as a new species of Alligatoroidea. This species represents the first diagnostic material of Alligatoroidea in Africa. Using a time-calibrated phylogenetic framework, the results from this study suggest a pattern of rapid biogeographic dispersal for alligatoroids following the K-Pg. The results presented in this thesis find that the K-Pg was a strong driver for macroevolutionary patterns amongst the crown crocodilians. A thorough understanding of patterns of survival and extinction of crocodilians will ultimately help us to more fully understand the modern biota and how global environmental changes threaten this group.

Chapter 1: Introduction

Originating nearly 250 million years ago, the Crocodylomorpha are a distinctive group of reptiles classed within Archosauria, which also contains the dinosaurs and birds (Nesbitt, 2011; Bronzati, Montefeltro and Langer, 2012). The Crocodylomorpha have persisted through a series of mass extinction events and substantial transitions in global climate throughout their evolutionary history. Though incredibly diverse throughout their fossil record, comprising hundreds of species, the extant fauna constitutes just 23 species, of primarily large, semi-aquatic predators restricted to tropical and subtropical environments (Grigg and Kirshner, 2015). To more fully understand the modern biota and how global environmental changes threaten crocodylians in the future, we must develop and improve our knowledge of the evolutionary history of this iconic group. In this thesis, the evolutionary dynamics of the crown group are of particular interest, with a focus on the effects of the most recent major mass extinction in Earth history, the Cretaceous-Paleogene extinction (K-Pg).

Historically, it has been a widely accepted belief that the crocodile group are "living fossils". The term, originally introduced by Darwin (1859), describes the phenomenon whereby extant taxa remain largely unchanged from their distant fossil counterparts, suggesting very reduced rates of evolution or stasis (Darwin, 1859). The general similarity observed between the morphology and size of the extant crocodile fauna and fossils in the Jurassic and Cretaceous have driven this belief (Guggisberg, 1972; Meyer, 1984; Schwarz, 2002; Brochu, 2003; McGregor, 2005). This became exaggerated by the work of early taxonomists who classed fossil material based on overall similarity- phenetics (Richard, 1888; Zittel *et al.*, 1890). Since the 1980's, a combination of new fossil discoveries (de Gasparini, 1971; Buffetaut, 1981; Wu, Sues and Sun, 1995; Buckley *et al.*, 2000), improved phylogenetic reconstructions (Salisbury and Willis, 1996; Brochu, 1997c) and molecular analysis (Densmore and Dessauer, 1984; Oaks, 2011) have challenged this long held belief, revealing a more dynamic crocodylian history .

The Mesozoic record of Crocodylomorpha is now understood to show high levels of diversity (number of species), exhibiting disparate body plans. These included terrestrial herbivores (Notosuchia), marine carnivores and piscivores (Thalattosuchia and Neosuchia) and gracile insectivores (Sphenosuchia) (Langston, 1973; Clark, 1994; Wu, Sues and Sun, 1995; Russell and Wu, 1997; Storrs and Efimov, 2000; Clark *et al.*, 2004; Sereno and Larsson, 2009; Young *et al.*, 2010; Bronzati, Montefeltro and Langer, 2012; Stubbs *et al.*, 2013; Toljagić and Butler, 2013). Crown crocodylians (Crocodylia), however, demonstrate much lower levels of overall disparity- the variation is morphological form (Brochu, 2001; Wilberg, 2017). Rather than being reconcilable with the “living fossil” concept, present phylogenetic hypotheses have indicated that this low overall disparity in the crown is the result of convergence between multiple crocodylian groups over time (Brochu, 2001, 2012; Bronzati, Montefeltro and Langer, 2012; Jouve *et al.*, 2014). Convergent evolution is the process by which unrelated taxa evolve similar morphological traits independently, classic examples include the development of wings in bats and birds. Amongst crocodilians, convergence is typically observed in skull shape, which is considered to be strongly linked to ecology (Brochu, 2001; McHenry *et al.*, 2006; Walmsley *et al.*, 2013).. For example, the fish-eating (piscivorous) crocodylians typically develop a long-slender snout and in the crown group alone this morphology has evolved in at least three

independent lineages (Langston, 1973; Busbey, 1994; Brochu, 2001; Sadleir and Makovicky, 2008). Therefore, though the overall range in disparity in the crown group is low, this is masking a more complex evolutionary history, with multiple clades independently evolving similar skull morphologies. This tallies with molecular reconstructions of extant relationships, which indicate that the evolutionary rate implied by the phylogeny is not slow enough to be reconciled with a "living fossil" theory (Oaks, 2011).

1.1 Early History of the Crocodylomorpha:

The Crocodylomorpha belong to a larger group of archosaurs called the pseudosuchians, which also appear in the fossil record in the Early Triassic, approximately 250Ma (Mannion *et al.*, 2015). The Crocodylomorpha are the only members to have survived the Triassic/Jurassic extinction (Figure 1.1). In the Late Triassic, most of the pseudosuchian diversity and disparity is attributed to non-crocodylomorph groups including the phytosaurs, aetosaurs, and rauisuchians (Stubbs *et al.*, 2013). Crocodylomorpha were not very diverse in the Triassic occupying only the small terrestrial predator niche (Russell and Wu, 1997; Stubbs *et al.*, 2013). The earliest members of the Crocodylomorpha, the sphenosuchians, were small, gracile animals with long slender limbs directly beneath the body and limited body armour (Nesbitt, 2011; Bronzati, Montefeltro and Langer, 2015).

The first wave of crocodylomorph diversification occurred during the Jurassic, with a radiation of a number of clades into the marine environment (Stubbs *et al.*, 2013; Bronzati, Montefeltro and Langer, 2015; Mannion *et al.*, 2015). This radiation included the diversification of Thalattosuchia (Figure 1.1), which comprised the slender snouted teleosaurs and the metriorhynchids (Bronzati, Montefeltro and Langer, 2015). The Metriorhynchidae represent some of the most extremely adapted members of the Crocodylomorpha, looking superficially similar to the Mosasauroidea: through the evolution of paddle-like hydrofoil limbs, streamlined skull, elongate body and tailfins (Langston, 1973; Pierce, Angielczyk and Rayfield, 2009; Young *et al.*, 2010). Contemporaneously, terrestrial crocodylomorphs (Protosuchia and Sphenosuchia), semi-aquatic goniopholidids and small bodied atoposaurs continued to diversify in the Jurassic (Stubbs *et al.*, 2013; Bronzati, Montefeltro and Langer, 2015). At the Jurassic-Cretaceous boundary another extinction caused the loss of 55-75% of generic diversity of Crocodylomorpha (Tennant, Mannion and Upchurch, 2016). A period of sea-level lowstand during this time caused the loss of shallow marine habitats and has been suggested as the cause for this extinction (Benson and Butler, 2011; Tennant, Mannion and Upchurch, 2016).

In the Cretaceous, a second wave of diversification was dominated by terrestrial crocodyliforms, including the Notosuchia, Gobiosuchidae and Peirosauridae (Figure 1.1) (Stubbs *et al.*, 2013; Bronzati, Montefeltro and Langer, 2015; Mannion *et al.*, 2015; Pol and Leardi, 2015). The Notosuchia represent one of the most diverse crocodyliform groups, including semi-aquatic, terrestrial and fossorial forms, one of which convergently resembles an armadillo (Wu, Sues and Sun, 1995; Buckley *et al.*, 2000; Marinho and Carvalho, 2009; O'Connor *et al.*, 2010; Pol and Powell, 2011; Pol and Leardi, 2015; Wilberg, 2017). Although notosuchians were typically small in size, they showed a range of dietary adaptations from carnivores to herbivores, and a range of specialised dentitions similar to the morphological range observed in extant mammals (Clark, Jacobs and Downs, 1989; Wu, Sues and Sun, 1995; Buckley *et al.*, 2000; Sereno and Larsson, 2009; O'Connor *et al.*, 2010).

Throughout the Cretaceous, multiple independent radiations into the marine environment are observed, including pholidosaurs, dyrosaurs and crown crocodylians; and the continued diversification of semi-aquatic neosuchians. The Neosuchia include bizarre forms such as Stomatosuchids in Africa, which exhibited large broad duck-billed rostra (Sereno and Larsson, 2009) as well as gigantic forms *Sarcosuchus* and the alligatoroid *Deinosuchus* which ranged from 8-12m in length (Erickson and Brochu, 1999; Sereno *et al.*, 2001). Generally, much of the crocodylomorph diversity declined into the Late Cretaceous, tracking global cooling trends, to which crocodylians have been demonstrated to be highly sensitive (Lang and Andrews, 1994; Markwick, 1994, 1998b; Mannion *et al.*, 2015). However, there was a peak in disparity in the Late Cretaceous and this can largely be attributed to the Notosuchia (Wilberg, 2017).

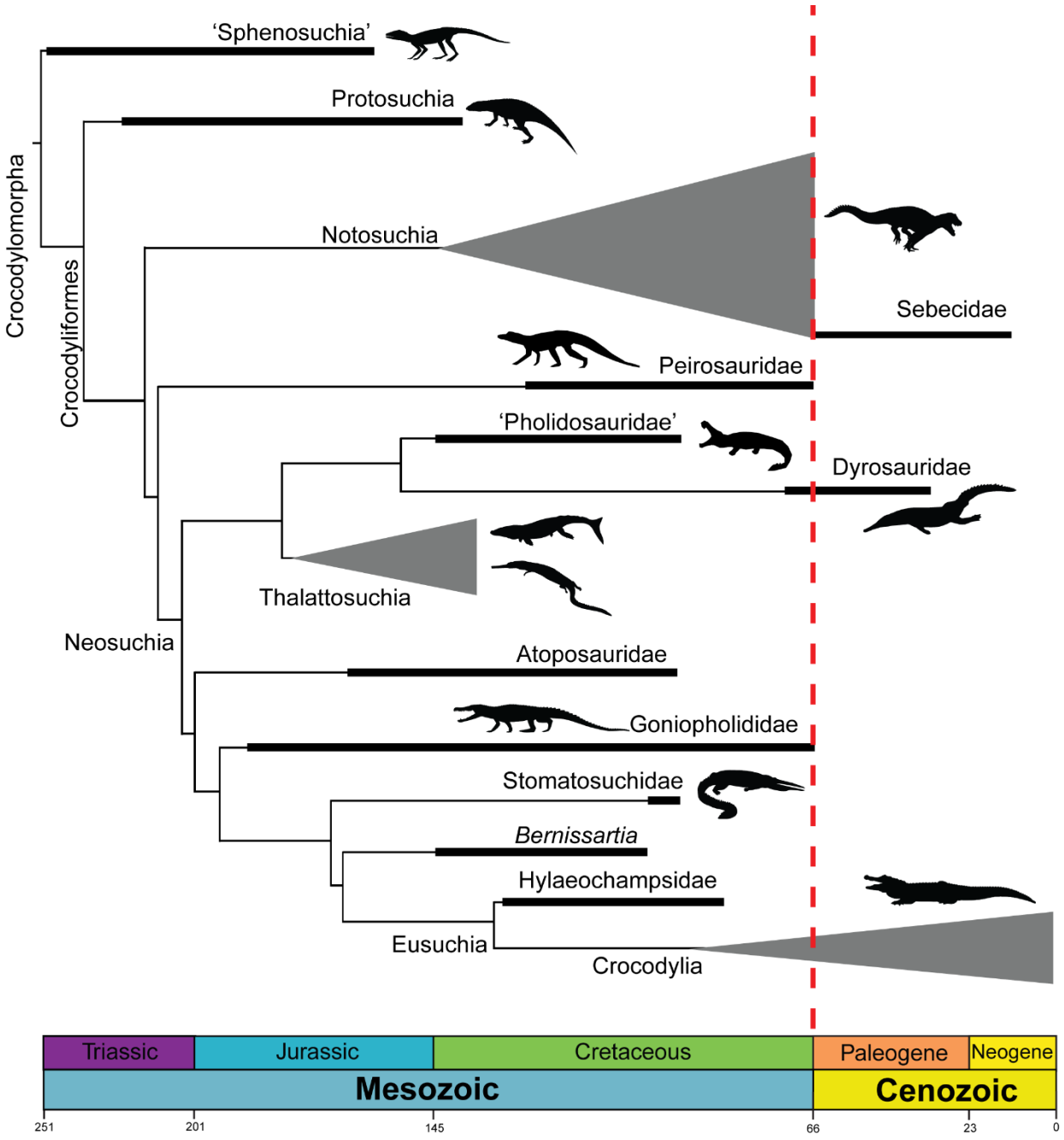

Figure 1.1: Simplified phylogeny of the Crocodylomorpha showing key groups over geologic time. Fossil ranges and phylogeny sourced from (Kellner, Pinheiro and Campos, 2014; Bronzati, Montefeltro and Langer, 2015). Silhouettes are modified from work by Stubbs et al. (2013) and by Smokeybjb, Nobu Tamura, T. Michael Keesey, Todd Marshall, Zimices, Scott Hartman, Stanton F. Fink (hosted on http://phylopic.org), available via CC BY-NC-SA 3.0 or CC BY-SA 3.0 licenses.

1.2 The Cenozoic record:

The diversity and disparity of the Mesozoic record of Crocodylomorpha contrasts starkly to that of the Cenozoic (66-0Ma), which is greatly reduced (Wilberg, 2017). The Cenozoic record includes fossil material from only three crocodylian lineages, the marine dyrosaurs, semi-aquatic and terrestrial sebecids (Notosuchia) and the crown Crocodylia, which includes marine, semi-aquatic and terrestrial forms (Jouve, Bardet and Jalil, 2008; Pol and Powell, 2011; Kellner, Pinheiro and Campos, 2014; Bronzati, Montefeltro and Langer, 2015). Dyrosauridae were particularly abundant in the Paleocene of Africa and South America but disappeared in the early Eocene (Jouve, 2007; Hastings, Bloch and Jaramillo, 2014; Puértolas-Pascual *et al.*, 2016). Sebecidae were restricted to South America and (Kellner, Pinheiro and Campos, 2014). persisted until the Miocene

In the Paleocene, there was an initial peak in diversity in marine (dyrosaurs and gavialoids) and terrestrial environments, linked to both climate and post- extinction opportunism (Mannion *et al.*, 2015; Puértolas-Pascual *et al.*, 2016). Throughout the Cenozoic, there is a general transition in global climate from "hothouse" to "icehouse" conditions (Zachos *et al.*, 2001). Crocodyliform diversity in the terrestrial environment has been correlated with reconstructions of global climate, favouring warmer conditions (Sill, 1968; Markwick, 1994, 1998a, 1998b; Zachos *et al.*, 2001; Mannion *et al.*, 2015). In particular, the climatic optima in the Eocene and Miocene saw strong increase in both diversity and disparity (Markwick, 1994; Böhme, 2003; Mannion *et al.*, 2015; Wilberg, 2017). A severe drop in diversity was observed with cooling at the Eocene-Oligocene boundary (34Ma) and with the onset of permanent ice caps on both poles into the Plio-Pleistocene (Zachos *et al.*, 2001; Mannion *et al.*, 2015; Wilberg, 2017). Marine crocodyliform diversity peaked in the Paleocene and then remained low from the Eocene to the present day, this early peak was predominantly due to the dyrosaurs and crown group gavialoids (Mannion *et al.*, 2015). Marine biodiversity has been linked to both temperature and sea level, with reduction in sea level over the Cenozoic contributing to the loss of marine biodiversity (Martin, Amiot, *et al.*, 2014; Mannion *et al.*, 2015). Crocodylians also became geographically restricted to the sub-tropics with cooler climate, whereas during the Eocene “hot house”, crocodylian occurrences in the Arctic and Antarctic are documented (Estes and Howard Hutchison, 1980; Willis and Stilwell, 2000).

Disparity patterns appear to track these trends in diversity and remain low compared to the Late Cretaceous peak (Wilberg, 2017). The correlation between the peaks in diversity and disparity during the Cenozoic suggest that there may be a link between disparity and climate, but this remains to be more rigorously tested. High disparity in the Miocene was largely the result of endemism (Hutchison, 1982; Scheyer *et al.*, 2013; Salas-Gismondi *et al.*, 2015). These endemic populations included a range of crocodylian species from duck-billed caimans, shovel-jawed caimans with crushing dentition, longirostrine gavialoids and ziphodont sebecids (Salas-Gismondi *et al.*, 2007). Though there are no studies on body size evolution amongst the crocodylians, exploration of the literature indicates what appears to be a distinct trend towards giant sizes in the Miocene, reaching sizes similar to giant forms in the Cretaceous (Sill, 1970; Willis, Murray and Megirian, 1990; Kraus, 1998; Brochu, 1999; Katsura, 2004; Aguilera, Riff and Bocquentin-Villanueva, 2006; Kobayashi *et al.*, 2006; Riff, Conquista and Aguilera, 2008; Aureliano *et al.*, 2015; Salas-Gismondi *et al.*, 2015).

1.3 Disparity:

There are various ways in which disparity can be measured in macroevolutionary studies (Zelditch *et al.*, 2004; Wagner, 2010; Ciampaglio, Kemp and Mcshea, 2016). We can use disparity in conjunction with other metrics such as diversity to gain a greater understanding of underlying evolutionary processes and external drivers. A measure of disparity usually looks for average dissimilarity or variance between a set of species. Commonly used methods to quantify disparity include using discrete character matrices (Hughes, Gerber and Wills, 2013; Lloyd, 2016) or shape-based analyses such as linear or geometric morphometrics or extended eigenshape analyses (Macleod, 1999; Zelditch *et al.*, 2004). Once shape has been quantified, disparity can be calculated from the resultant morphospace data (Wills, Briggs and Fortey, 1994).

The two more commonly used morphometric approaches are based on linear measurements or geometric morphometrics. Geometric morphometrics employs a landmark based approach to quantify shape, this is a much more detailed approach than linear measurements and filters out aspects such as size and orientation (Zelditch *et al.*, 2004). Landmarks are discrete points that must be homologous across all specimens; typical landmarks used are type 1 landmarks- points of intersection of bone, and type 2- points of maximal/minimal curvature or maximal extension of an anatomical feature (Zelditch *et al.*, 2004). Unlike linear measurements, geometric morphometrics approaches require that there are no missing data, therefore if a landmark cannot be positioned on a fossil (due to incomplete preservation) this fossil must be excluded. The choice of landmarks is therefore critical- more landmarks will more accurately capture overall shape variation but at the expense of a smaller sample size. Semilandmarks can also be used to quantify a curve or outline between species, for example the outline of the crocodylian rostrum. Semilandmarks are particularly useful when the sample contains distantly related taxa and homologous (fixed) landmarks become difficult to assign; this was the approach used in (Wilberg, 2017) to examine disparity in the Crocodylomorpha.

Disparity studies on Crocodylia focus on skull morphology, as this is the primary way in which crocodilians interact with their environment, and the skull has been demonstrated to evolve much more plasticly than the postcrania (Brochu, 2001; Pierce, Angielczyk and Rayfield, 2008; Piras *et al.*, 2010; Stubbs *et al.*, 2013). The Crocodylia are frequently split into different skull shape categories (Busbey, 1994; Brochu, 2001; Sadleir and Makovicky, 2008). Early attempts to characterise skull morphology were over-simplistic, binning taxa into two broad shape categories: the longirostres- long slender snouts, and the brevirostres- everything else (Troxell, 1925). More recent works have examined functional aspects of snout morphology, based on linear metrics, cross sectional area, biomechanical models and geometric morphometrics in extant taxa (Langston, 1973; Busbey, 1994; Russell and Wu, 1997; Brochu, 2001; McHenry *et al.*, 2006; Sadleir and Makovicky, 2008; Erickson *et al.*, 2012). The most commonly utilised skull shape categories based on variations in the rostrum were discussed by Brochu (2001) and comprise the generalist, longirostrine, blunt-snouted, ziphodont and duck-bill (Figure 1.2).

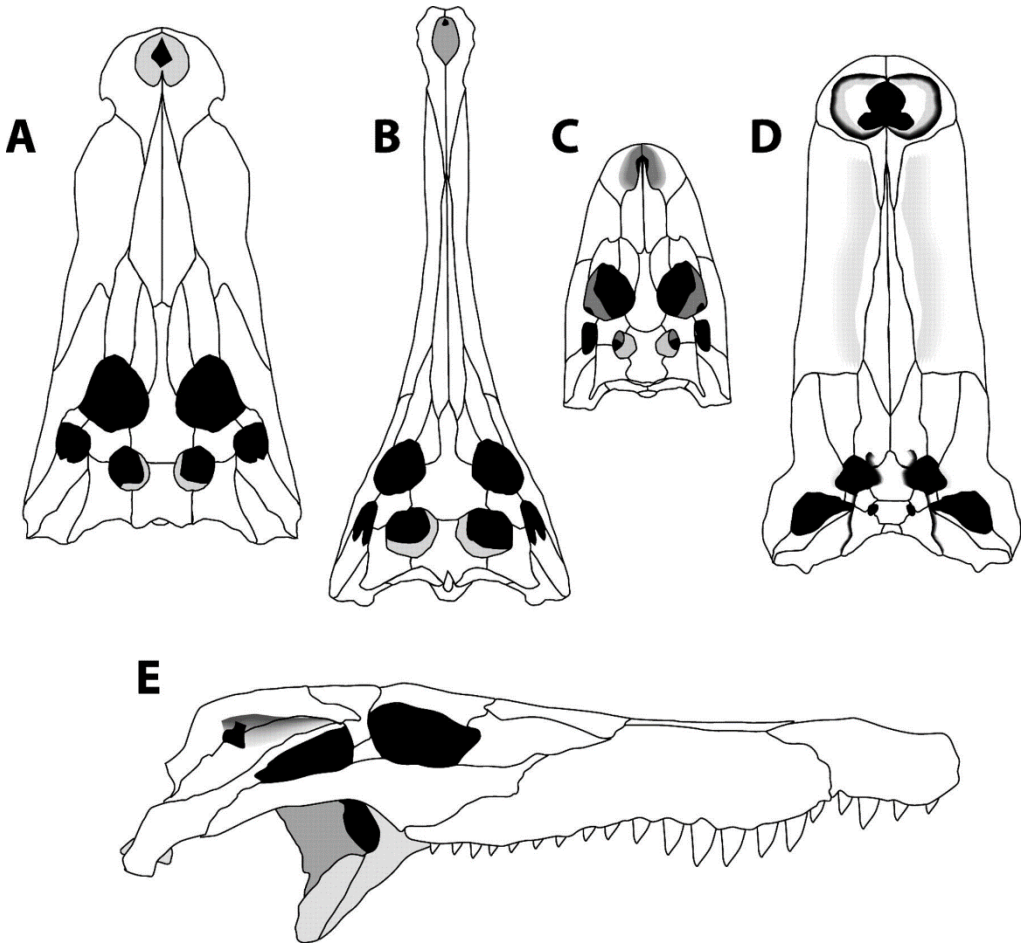

Figure 1.2: Examples of the snout shape categories used in Brochu (2001). **A** generalist, *Leidyosuchus canadensis,* **B** longirostrine, *Thoracosaurus macrorhynchus,* **C** blunt-snouted, *Alligator mcgrewi,* **D** duck-bill, *Mourasuchus,* **E** ziphodont, *Pristichampsus.* Taken from Brochu (2001), Figure 1.

The generalist skull morphology is characterised by a dorsoventrally flattened rostrum which is broad and tapers anteriorly. Typically, species in this category, including numerous species of extant crocodiles and the American alligator, have heterodont dentition and are dietary generalists (Grigg and Kirshner, 2015). The longirostrine skull morphology has a long and slender rostrum and is more tubular in cross-section; dentition is typically more uniform with long slender teeth. The blunt-snout represents the last skull type attributable to the extant crocodylian species, and is reduced in anteroposterior length, it is observed in extant dwarf species (Brochu, 2001; Grigg and Kirshner, 2015). Ziphodont forms have a dorsoventrally deep and laterally compressed skull. The duck-billed rostrum, is unusual with a very broad, flattened elongate rostrum with numerous small teeth (Brochu, 1999; Sereno and Larsson, 2009).

Convergence of these skull types within the crocodylomorphs is common, for example longirostry is observed in teleosaurs, dyrosaurs, pholidosaurs and in the crown this feature is observed in numerous clades (Russell and Wu, 1997; Brochu, 2001; Sereno *et al.*, 2001; Wu, Russell and Cumbaa, 2001; Schwarz, 2002; Schwarz and Salisbury, 2005; Stubbs *et al.*, 2013; Turner, 2015). This has caused a lot of taxonomic confusion between groups and their position in the Crocodylomorpha (Bronzati, Montefeltro and Langer, 2012). Mechanical studies on the crocodylian skull and direct observation of the extant fauna suggest that these high levels of convergence are driven by ecology (Russell and Wu, 1997; McHenry *et al.*, 2006; Stubbs *et al.*, 2013). The dietary mode of a species is constrained by the skull morphology: a long slender snout and slender teeth will experience increased stress and high loading pressures, but minimal drag forces in water, specialised to small agile prey, whereas generalised snouts are broad, heavily ornamented with robust teeth which can withstand high loading pressures, suited to larger prey and crushing mode (Langston, 1973; Busbey, 1994; Russell and Wu, 1997; McHenry *et al.*, 2006; Pierce, Angielczyk and Rayfield, 2008).

The majority of studies investigating disparity of the crocodylian skull in the crown group focus on extant species with the aim of understanding ontogeny, ecology or phylogenetic signals (Pierce, Angielczyk and Rayfield, 2008; Sadleir and Makovicky, 2008; Piras *et al.*, 2009, 2014; Watanabe and Slice, 2014). Macroevolutionary studies (studies of trends in evolution within groups over long periods of time) on crocodilian disparity are less common and tend to focus on the more inclusive Crocodylomorpha during the Mesozoic (Pierce, Angielczyk and Rayfield, 2009; Young *et al.*, 2010; Stubbs *et al.*, 2013; Toljagić and Butler, 2013; Stubbs and Benton, 2016; Wilberg, 2017). Few studies examine disparity over the Cenozoic and the K-Pg (Brochu, 2001; Salas-Gismondi *et al.*, 2015; Wilberg, 2017). The first and only comprehensive analysis of disparity through the Cretaceous-Cenozoic to date is focussed on the Crocodylomorpha, with less emphasis on the crown group (Wilberg, 2017). Using a geometric morphometrics approach, the landmarking scheme used was primarily restricted to the skull outline, in order to quantify shape effectively across the total group (Wilberg, 2017). In this thesis, as a result of new material described in chapter 2, disparity within the crown crocodylians over this interval is investigated. The work presented here differs from this previous analysis by focussing on a smaller group of crocodylians, by doing this, a more detailed landmarking scheme could be utilised as the species are more closely related. In doing so, the results here pick up finer scale variations in disparity that are not detected in the more generalised study above, suggesting higher disparity than expected after the K-Pg.

1.4 Crown group crocodylians:

Crocodylia first appeared in the fossil record in the Campanian of North America including the gavialoid, *Eothoracosaurus mississippiensis* (Carpenter, 1983; Brochu, 2004a), and the numerous alligatoroid species, *Leidyosuchus canadensis* (Brochu, 1997a), *Deinosuchus* spp. (Rivera-Sylva *et al.*, 2011) and *Brachychampsa* spp. (Williamson, 1996; Sullivan and Lucas, 2003). Diversity remained low during the Late Cretaceous but species were geographically widespread (Koken, 1888; Mook, 1941; Efimov, 1982; Storrs and Efimov, 2000; Jouve, Bardet and Jalil, 2008; Brochu *et al.*, 2012). Following the K-Pg mass extinction Crocodylia became diverse, and by the Eocene, all major clades had diversified, including extinct clades such as the borealosuchids and the planocraniids (Brochu, 2001, 2012; Brochu *et al.*, 2012; Wilberg, 2017). The borealosuchids are a North American clade which share broad similarities to basal alligatorines (Brochu, 2003). The planocraniids are unusual in having dorsoventrally deep snouts, contrary to the flattened profile typical of most crocodylians. In addition, some

planocraniid species developed labiolingually compressed and serrated teeth- ziphodont morphology (Brochu, 2012). The extant species are divided into three groups, the Crocodyloidea, Alligatoroidea and Gavialoidea, the position of these families varies depending on the phylogenetic interpretation (Figure 1.3).

Crocodyloidea:

The Crocodyloidea includes *Crocodylus niloticus* and all crocodylians closer to it than to *Alligator mississippiensis* or *Gavialis gangeticus* (Brochu, 2003). Crocodylinae is a subfamily within the Crocodyloidea (Figure 1.3), and is defined as *Crocodylus niloticus* and all crocodylians closer to it than *Tomistoma schlegelii* (Brochu, 2003). Found in a range of freshwater and marine habitats, the Crocodylinae are the only group with a global distribution throughout their fossil record and in the present (Brochu, 2001, 2003; Grigg and Kirshner, 2015). The subfamily contains 13-15 extant species, uncertainty has arisen due to cryptic species of *Crocodylus niloticus* and *Osteolaemus tetraspis* identified by molecular studies (Eaton *et al.*, 2009; Hekkala *et al.*, 2011; Oaks, 2011). The majority of the Crocodylinae are dietary generalists, however they are the most disparate group amongst the Crocodylia, including blunt snouted (*Osteolaemus*, *Mekosuchus* (Salisbury and Willis, 1996), *Trilophosuchus* (Salisbury and Willis, 1996)), longirostrine (*Mecistops*, *Crocodylus johnstoni*, *Crocodylus intermedius*, *Euthecodon* (Ginsburg and Buffetaut, 1978)) and a ziphodont form, *Quinkana* spp. (Salisbury and Willis, 1996; Brochu, 2001; Pierce, Angielczyk and Rayfield, 2008). Earliest fossils known for the Crocodylinae, *Arenysuchus* (Puértolas, Canudo and Cruzado-Caballero, 2011) and *Prodiplocynodon* (Mook, 1941) are from the latest Cretaceous of Europe and North America respectively.

Alligatoroidea:

The Alligatoroidea are a group of freshwater crocodylians, recognised by eight extant species which include two alligators and six caimans. The basalmost member of the group, *Leidyosuchus canadensis* (Brochu, 1997a), is from the Campanian of Canada. The Alligatoroidea is split into two groups, the Globidonta and the Diplocynodontidae (Brochu, 1999). The Diplocynodontidae are an extinct basal clade, known exclusively from the Paleocene-Miocene of Europe (Brochu, 1999; Piras and Buscalioni, 2006; Martin and Gross, 2011; Martin, Smith, *et al.*, 2014; Díaz Aráez *et al.*, 2015). Within the Globidonta are the two subfamilies, the Caimaninae and the Alligatorinae (Figure 1.3). Basal globidontans are typically blunt snouted, compared to the more derived members such as *Alligator* spp. and *Caiman* spp. which show a generalist morphology (Brochu, 2001). In addition to the blunt snout morphology, earlier members of the Alligatorinae such as *Allognathosuchus* (Brochu, 2004b), *Eoalligator* (Wang, Sullivan and Liu, 2016), *Krabisuchus* (Martin and Lauprasert, 2010) and the Caimaninae, *Kuttanacaiman* and *Gnatusuchus* (Salas-Gismondi *et al.*, 2015) have globular posterior teeth which are considered to be an adaptation for a crushing hard-shelled prey. The alligatoroids retain the overbite, plesiomorphic for the crown group and typically have broader rostra (Brochu, 1999, 2003).

Alligatorinae occur predominantly in North America but there are also occurrences in Europe (Kälin, 1939; Wassersug and Hecht, 1967) and Asia (Martin and Lauprasert, 2010; Iijima, Takahashi and Kobayashi, 2016; Wang, Sullivan and Liu, 2016); including the extant Chinese alligator, *Alligator sinensis*. The earliest members of this clade were from the Paleocene of North America (*Navajosuchus mooki* (Mook, 1942) and *Wannaganosuchus brachymanus* (Erickson, 1982)). Caimans are found predominantly in South America, though some earlier members in the Paleocene indicate early dispersals back into North America

(Brochu, 1999, 2010). The caimanines are more disparate than the rest of the Alligatoroidea due to the nettosuchids, a peculiar group of “duck-billed” caimans which look similar to the distantly related stomatosuchids (Langston Jr., 1966; Brochu, 1999; Aureliano *et al.*, 2015). Though their fossil record extends back to the Paleocene, the early fossil record for caimanines is sparse, the most abundant fossil material is not known until the Miocene-Pliocene (Salas-Gismondi *et al.*, 2015).

Gavialoidea:

The Gavialoidea are highly derived members of the Crocodylia, made distinctive by their longirostrine morphology. The sole extant species, *Gavialis gangeticus*, is found in freshwater habitats in India with a highly restricted geographical range (IUCN, 2015). However, fossil evidence suggests a much more widespread distribution of this group in the past, with evidence for marine tolerance in the clade- which can be reconciled with anatomical features in the extant species, such as the keratinised tongue and lingual salt glands (Taplin, Grigg and Beard, 1985; Hua and Jouve, 2004; Vélez-Juarbe, Brochu and Santos, 2007; Jouve, Bardet and Jalil, 2008; Grigg and Kirshner, 2015). The fossil record of this group extends to the Late Cretaceous of North America with the stratigraphically earliest member, *Eothoracosaurus mississippiensis* (Brochu, 2004a). The early members of this group are known as the "thoracosaurs" and are found in a range of coastal/marine deposits from North America and Europe up until the earliest Eocene (Koken, 1888; Carpenter, 1983; Zarski, Jakubowski and Gawor-Biedowa, 1998; Delfino, Piras and Smith, 2005; Brochu, 2006b). The status of the "thoracosaurs" has been the focus of much debate, and until recently these members were classed within Tomistominae (see Brochu, 2004 and references therein). Poor classification of the "thoracosaur" group has led to a lot of confusion in the literature, and it is unclear whether newly described African species from the Cretaceous and Paleocene, *Ocepesuchus eoafricanus* and *Argochampsa krebsi,* are inclusive to this group (Hua and Jouve, 2004; Vélez-Juarbe, Brochu and Santos, 2007; Jouve, Bardet and Jalil, 2008). The Eocene record of gharials is largely unknown and has been referred to as the "Gharial Gap" (Brochu, 2004a). In contrast to other longirostrine species in the Crocodylia, gavialoids show homodont dentition and high variability in tooth count. The verticalisation of the braincase, typical of crocodylians, is also not apparent in the gavialoids (Brochu, 2004a; Gold, Brochu and Norell, 2014).

Tomistominae:

The Tomistominae (Kälin, 1955; Brochu, 2003) are a subfamily of longirostrine crocodylians, recognised by the sole extant species *Tomistoma schlegelii* from Indonesia. Dependent on the phylogenetic interpretation (Figure 1.3), the Tomistominae are grouped within either the Crocodyloidea (morphology) or the Gavialoidea (molecular) (Brochu, 2003). Similar to gharials, the extant *Tomistoma,* is found in freshwater habitats, but the fossil record of the group indicates saltwater tolerance and was geographically widespread (Grigg and Kirshner, 2015). Basalmost members of the group are known from the Ypresian of Morocco, *Maroccosuchus zennaroi* (Jonet and Wouters, 1977) and Eocene of the UK, *Kentisuchus spenceri* (Brochu, 2007). The tomistomines are closely related to the Crocodylinae and basal members of the clade retain similarities with the Crocodyloidea (Brochu, 2012). These plesiomorphic states include a more generalist skull morphology, retention of the nasal-premaxilla contact and enlarged 5th maxillary tooth (Brochu, 1997b, 2003). More derived members of the Tomistominae show an evolutionary trend towards longirostry and demonstrate typical gavial apomorphies such as linear shape of the maxilla, long splenial

symphysis, anteriorly flaring squamosal groove and wedge-like process of the palatine (Jouve *et al.*, 2014).

Numerous taxa currently classed as gavialoids such as *Eogavialis* (Andrews, 1906; Müller, 1927; Storrs, 2003) and *Thoracosaurus* (Koken, 1888; Brochu, 2004a) have previously been assigned to Tomistominae, similarly *Gavialosuchus* (Erickson and Sawyer, 1996) in current phylogenetic analyses places amongst the Tomistominae over the previously gavialoid affinities. Structural requirements of this derived skull design has resulted in high levels of convergence between the gavials and tomistomines and has caused much taxonomic confusion (Toula and Kail, 1885; Iordansky, 1973; Langston, 1973; Carpenter, 1983; Busbey, 1994; Brochu, 2004a, 2006a, 2007). There is additional conflict between the morphological (Norell, 1989; Tarsitano, Frey and Riess, 1989; Brochu, 1997b) and molecular phylogenies on the position of the Gavialoidea (Poe, 1996; Gatesy *et al.*, 2003; Harshman *et al.*, 2003; Janke *et al.*, 2005; Man *et al.*, 2011; Oaks, 2011).

1.5 Controversial Relationships -the gharial problem:

There are many examples in the fossil record where there is a conflict between morphological and molecular data for phylogenetic reconstruction (Donoghue and Sanderson, 1992; Benton, 1999; Rieppel and Reisz, 1999; Jenner, 2004; Debiasse and Hellberg, 2015). The gavialoids and tomistomines represent an example of this classic conflict. In many cases, this conflict can arise where species that have convergently evolved are drawn together in phylogenetic analysis of morphological data. However, in the case of the gavialoids, the reverse is true, and morphology favours convergence and the molecular signal does not. Morphological data recovers a basal position for the Gavialoidea (Tarsitano, Frey and Riess, 1989; Vélez-Juarbe, Brochu and Santos, 2007; Jouve, Bardet and Jalil, 2008; Riff, Conquista and Aguilera, 2008; Moraes-Santos, Villanueva and Toledo, 2011; Brochu and Storrs, 2012), with the Tomistominae nested within the Crocodyloidea (Piras *et al.*, 2010). The similar morphology of the gavialoids and tomistomines in this scenario indicate convergence. However, the molecular hypothesis favours a sister-group relationship between the *Gavialis* and *Tomistoma* (Densmore and Dessauer, 1984; Norell, 1989; Aggarwal *et al.*, 1994; Poe, 1996; Gatesy *et al.*, 2003; Harshman *et al.*, 2003; Janke *et al.*, 2005; McAliley *et al.*, 2006; Roos, Aggarwal and Janke, 2007; Piras *et al.*, 2010; Feng *et al.*, 2010; Oaks, 2011; Man *et al.*, 2011; Meganathan *et al.*, 2011; Green *et al.*, 2014) (Fig 1.2).

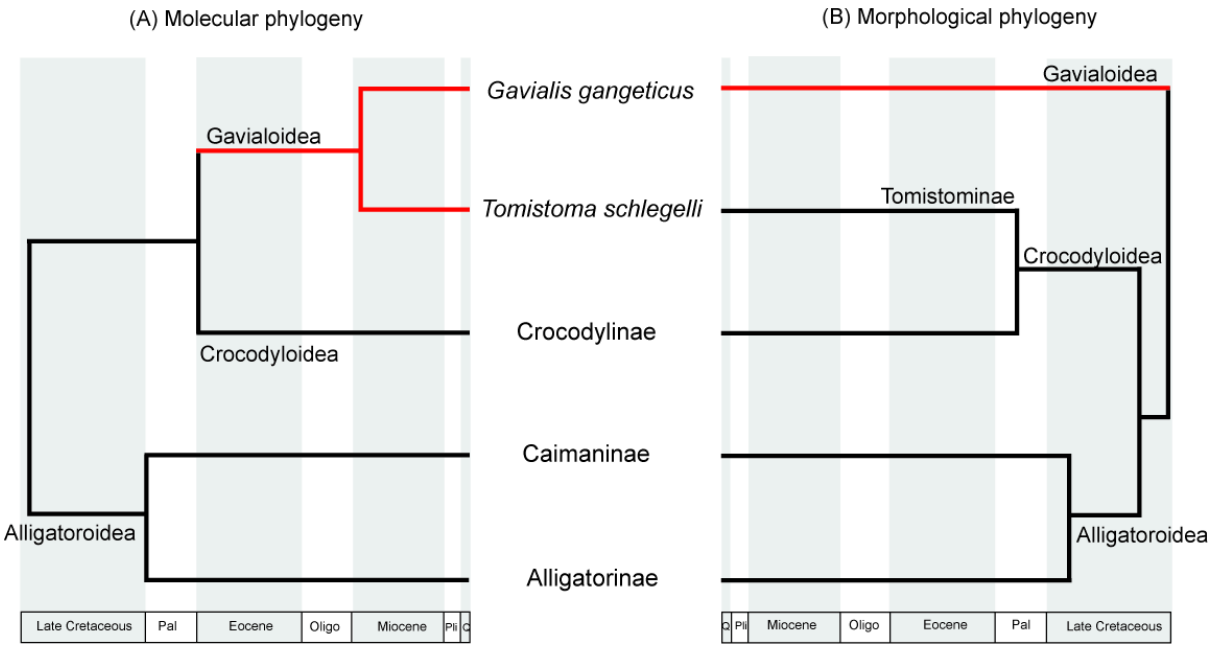

Figure 1.3: The two competing phylogenetic hypotheses for the position of the Gavialoidea. **(A)** Result from the molecular data, time calibration based on (Oaks, 2011). **(B)** result from the morphological data (including fossils), time calibration based on (Puértolas, Canudo and Cruzado-Caballero, 2011).

Morphology:

Analyses of the morphological character matrices consistently place Gavialoidea basally within Crocodylia (Vélez-Juarbe, Brochu and Santos, 2007; Brochu, 2012; Bronzati, Montefeltro and Langer, 2012; Jouve *et al.*, 2014). Only one early study, Buffetaut (1985) suggested that there may be some morphological characters congruent with the molecular hypothesis, however the work was heavily criticised due to the inclusion of predominantly plesiomorphic and ontogenetic characters (Buffetaut, 1985b; Norell, 1989). Though other character matrices exist (Norell, 1989; Salisbury and Willis, 1996), the Brochu matrix (Brochu, 1997c, 1999) has formed the basis of nearly all phylogenetic analyses over the last 20 years. With subsequent modifications and addition of new taxa over time, this matrix represents the most extensive and well-studied character matrix available to study crown crocodylian relationships.

Numerous characters within the morphological matrix commonly correlate with different skull shape categories. For example, a long splenial symphysis, linear maxilla and wedge-like palatine process and reduction in the length of the nasal, are all associated with a long slender rostrum, and therefore observed convergently in different longirostrine groups (McHenry *et al.*, 2006; Brochu and Storrs, 2012). Numerous workers have hunted for a secondary signal in the morphological dataset to see if there are a set of characters uniting *Gavialis-Tomistoma*, congruent with the molecular signal. Some characters have been identified (including the above mentioned) but are highly homoplastic (Brochu, 1997c; Trueman, 1998; Gatesy *et al.*, 2003; Harshman *et al.*, 2003), therefore it has been proposed

that there is no strong secondary signal within the Brochu dataset (Sadleir and Makovicky, 2008).

Molecular:

The molecular hypothesis is similarly robust. Early analyses uniting *Gavialis-Tomistoma* employed methods using immunological reactions, DNA fingerprinting and preliminary studies of mitochondrial DNA sequences (Densmore and Dessauer, 1984; Aggarwal *et al.*, 1994; Poe, 1996). These early studies were criticised for poor data selection and not using outgroups to root the molecular tree, and instead employing distance-based algorithms. Rooting the molecular trees remains problematic as the closest living outgroup to crocodylians is the birds (Aves) which diverged from the group over 250 Myrs ago (Harshman *et al.*, 2003). Functional convergence and long branch attraction are additional criticisms applied to these studies, which may have produced an incorrect relationship (Harshman *et al.*, 2003; McAliley *et al.*, 2006; Willis *et al.*, 2007). However, advances in molecular systematics reveal a consistent and robust sister group relationship between the *Gavialis-Tomistoma*. These studies have analysed both mitochondrial (Harshman *et al.*, 2003; Janke *et al.*, 2005; McAliley *et al.*, 2006; Roos, Aggarwal and Janke, 2007; Willis *et al.*, 2007; Feng *et al.*, 2010; Man *et al.*, 2011; Meganathan *et al.*, 2011; Oaks, 2011)and nuclear data (Harshman *et al.*, 2003; Gatesy, Baker and Hayashi, 2004; McAliley *et al.*, 2006; Willis *et al.*, 2007; Oaks, 2011), including the whole genome of three crocodylian species (*Crocodylus, Alligator* and *Gavialis*) (Green *et al.*, 2014).

Possible solutions:

Attempts to clarify the conflict between these two phylogenetic hypotheses have used a combined approach and constrained searches (Poe, 1996; Brochu, 1997b; Gatesy *et al.*, 2003; Gatesy, Baker and Hayashi, 2004; Gold, Brochu and Norell, 2014). The combined analyses have utilised both molecular and morphological character matrices in the same search. As molecular data is only available for extant species, molecular characters for the fossil taxa are coded as missing. Constrained searches, on the other hand, use the morphological character matrix only, and the molecular topology is constrained as a backbone during the tree search. Fossil taxa, which are not constrained to a particular relationship are allowed to "float" in the search (Wilkinson, Thorley and Upchurch, 2000). This allows the fossil taxa to position in the most parsimonious solution, given the enforced topology. To date, all combined analyses have only employed parsimony-based methods. These methods have reproduced the molecular signal with the morphological data, with Gavialinae forming a sister group with Tomistominae.

A number of papers have utilised a geometric morphometrics approach to examine overall disparity and ontogenetic trajectories of the extant fauna (Pierce, Angielczyk and Rayfield, 2008; Piras *et al.*, 2010; Gold, Brochu and Norell, 2014; Watanabe and Slice, 2014). The overarching result of these studies show that *Gavialis* and *Tomistoma,* though similar in morphology, occupy distinct areas of morphospace (Pierce, Angielczyk and Rayfield, 2008; Piras *et al.*, 2010). Ontogenetic trajectories of *Tomistoma schlegelii* in particular are distinct from all other crocodylian taxa (Piras *et al.*, 2010). These studies lend support to the morphological hypothesis, as you would expect stronger overlap of the species if the molecular signal were true. Another study focussed on geometric morphometrics of the braincase and the eustachian system, as the braincase evolution is considered more conserved compared to the plasticity of the rostrum (Gold, Brochu and Norell, 2014). Whole braincase morphology provided support for the molecular signal, whereas the eustachian system supports the

morphological hypothesis. All these studies have been applied to the extant fauna only, which is limiting as there are only two extant species (*G. gangeticus* and *T. schlegelii)*. Incorporation of fossil material is needed to better sample ancestral shape variation.

Molecular clocks and stratigraphic incongruence:

Molecular clock estimates for crocodylian phylogenies are based on both mitochondrial and nuclear data (Janke *et al.*, 2005; Roos, Aggarwal and Janke, 2007; Oaks, 2011). Here we find a marked inconsistency between the predicted divergence times and the stratigraphic position of fossil taxa. The oldest date predicted for the *Gavialis-Tomistoma* split is ≈42Mya in the Eocene (Janke *et al.*, 2005), though dates as recent as the Miocene have been predicted (Roos, Aggarwal and Janke, 2007; Oaks, 2011). However, numerous gavialoid species have been found between the Late Cretaceous-Eocene, including the "thoracosaurs" (Koken, 1888; Troedsson, 1924; Carpenter, 1983; Zarski, Jakubowski and Gawor-Biedowa, 1998; Brochu, 2004a, 2006b; Delfino, Piras and Smith, 2005) and the Moroccan species *Ocepesuchus* (Jouve, Bardet and Jalil, 2008) and *Argochampsa* (Hua and Jouve, 2004). Similarly numerous tomistomine fossils are known from the Eocene including basal members (Brochu, 2007; Piras *et al.*, 2007; Jouve *et al.*, 2014) and more derived species such as, *Tomistoma cairense* (Müller, 1927) and *Paratomistoma courti* (Brochu and Gingerich, 2000).

A noted feature of the gharial fossil record is this distinct lack of fossil material in the middle Eocene, known as the "Gharial Gap". The timing of this gap in the fossil record correlates with some molecular divergence dates for the *Gavialis-Tomistoma* split (Brochu, 1997b, 2004a, 2006a; Harshman *et al.*, 2003; Gatesy, Baker and Hayashi, 2004). One hypothesis to explain the incongruence between the fossil record and molecular divergence dates is that the molecular divergences are accurate and that all fossils known prior to the "Gharial Gap" have been erroneously assigned to the Gavialoidea. Numerous authors have suggested that a reassessment of taxonomic affinities of the "thoracosaurs" would resolve the conflict between the stratigraphic record and the molecular clock data (Brochu, 2006a; Vélez-Juarbe, Brochu and Santos, 2007; Riff, Conquista and Aguilera, 2008). This has been suggested as "thoracosaurs" demonstrate primitive characters not present in gavialoids as a whole, such as a verticalisation of the braincase and confluent 3rd-4th dentary alveoli (Brochu, 2004a, 2006a, 2006b; Vélez-Juarbe, Brochu and Santos, 2007). Alternatively, the discovery of any new fossil material during or prior to the gharial gap may help to shed light on evolutionary relationships amongst early gavialoids and clarification of the incongruence between the molecular clocks and the fossil record.

Molecular clock studies have not addressed the presence of fossil material before the divergence times. Similarly, no combined analyses have been considered in a time calibrated framework. As the earliest Tomistomines are known in the Eocene and earliest gavialoids in the Cretaceous, if the molecular signal is the true signal, this would project ghost lineages for the tomistomines back into the Late Cretaceous and has strong implications for crocodylian survival across the K-Pg mass extinction. This has not yet been examined in detail in the literature and is something addressed in this thesis.

1.6 The Cretaceous-Paleogene transition:

The Cretaceous-Paleogene (K-Pg) boundary at 66 Ma is marked by a thin clay layer, that can be identified worldwide in a range of environmental settings (Nichols *et al.*, 1992; Nichols and Johnson, 2008; Ferrow *et al.*, 2011; Vajda and Bercovici, 2014). The boundary clay shows unusual enrichment in Iridium and other platinum groups elements, in addition to shocked quartz grains (Bohor, Modreski and Foord, 1987; Claeys, Kiessling and Alvarez, 2002), glass spherules, Ni-rich spinels (Alvarez *et al.*, 1980; Claeys, Kiessling and Alvarez, 2002; Schulte *et al.*, 2010; Ferrow *et al.*, 2011; Vajda and Bercovici, 2014). Iridium is depleted in the earth's crust and therefore the iridium spike at the K-Pg boundary is indicative of an extra-terrestrial origin (Alvarez *et al.*, 1980; Smit and Hertogen, 1980). Supernova, comet showers and multiple impact scenarios have all been proposed as the source of this enrichment at the K-Pg boundary (Alvarez *et al.*, 1980; Buffetaut, 1990; Pope *et al.*, 1997; Keller *et al.*, 2004). However, over the last 30 years, increasing evidence indicates that these deposits are the result of a single asteroid impact of roughly 10km diameter, which caused the Chicxulub crater, located in the Yucatan peninsula in Mexico (Alvarez, 1997; Kring, 2007; Schulte *et al.*, 2010). The shocked quartz and glass spherules associated with these deposits correspond to a high energy impact event with an extra-terrestrial object (Alvarez *et al.*, 1980; Schulte *et al.*, 2010). The distribution of the ejecta deposits, decreasing in thickness and abundance of glass spherules and shocked quartz distal to the impact site, corroborate the location of the impact (Claeys, Kiessling and Alvarez, 2002; Schulte *et al.*, 2010).

The K-Pg boundary coincides with a severe and global mass extinction, which is currently thought to have wiped out somewhere between 75% of species (Sepkoski, 1996) and 40% of genera (Bambach, 2006). This mass extinction comprises one of the "big five" mass extinctions in Earth history, of which this is the most recent. This extinction event is most popularly known for wiping out the non-avian dinosaurs, however other major groups such as the ammonites, marine reptiles (mosasaurs and plesiosaurs) also became extinct (Robertson *et al.*, 2013b; Landman *et al.*, 2014; Polcyn *et al.*, 2014; Brusatte *et al.*, 2015). The extinction was globally widespread and affected all trophic levels, including foraminifera, primary producers, invertebrates and all major vertebrate groups (Archibald and Bryant, 1990; Sheehan and Fastovsky, 1992; Cavin, 2002; Labandeira, Johnson and Lang, 2002; Wilf *et al.*, 2006; Bambach, 2006; Kring, 2007; Longrich, Tokaryk and Field, 2011; Longrich, Bhullar and Gauthier, 2012; Wilson, 2013; Robertson *et al.*, 2013b; Adolfssen and Ward, 2014; Vajda and Bercovici, 2014). The extinction was highly selective, affecting the marine and terrestrial environments much more than freshwater ecosystems (Robertson *et al.*, 2013b). The selectivity of the extinction has caused controversy in the literature in relation to the mechanism, and explanation of why some groups such as Crocodyliformes survived, whereas other groups such as the non-avian dinosaurs did not.

Controversies:

Though the impact hypothesis has become the most widely accepted hypothesis for the cause of the K-Pg mass extinction, controversies remain in the literature. The alternative hypothesis, that still receives support, suggests that Deccan volcanism caused a more protracted extinction in the Late Cretaceous (Keller, 2014). The Deccan traps in India resulted from a Large Igneous Province that underwent its main phase of volcanism over the Cretaceous-Paleogene boundary, 66.25-65.5Ma (Font *et al.*, 2016). The flood basalts would have released vast quantities of sulphur and carbon dioxide, resulting in greenhouse warming,

acid rain, terrestrial aridification and ocean acidification, this has been proposed as the kill mechanism (Keller *et al.*, 2004, 2010; Keller, 2014; Schoene *et al.*, 2015; Punekar *et al.*, 2016).

In support of this alternate hypothesis, numerous arguments against the impact hypothesis have arisen. In particular, it has been argued that the Chicxulub impact crater predates the K-Pg (iridium layer) by up to 300 Kyrs (Keller *et al.*, 2004). This is based on the sequence stratigraphy of the deposits near to the impact site. Between the impact breccia and the K-Pg boundary clay, a 50m sequence of dolomitic beds containing Late Cretaceous foraminifera has been reported (Keller *et al.*, 2004). It was argued that these beds formed by natural sedimentation rates, which would take hundreds of thousands of years to form. A multiple impacts scenario is proposed instead to explain the iridium enrichment at the K-Pg (Keller *et al.*, 2003, 2004). However, there is no stratigraphic/ejecta sequences or isotopic support for a multiple impact scenario (Alvarez, Asaro and Montanari, 1990; Mukhopadhyay, Farley and Montanari, 2001; Kring, 2007) and recent radiometric dating puts the Chicxulub impact coincident with the K-Pg boundary (Renne *et al.*, 2013). The sequence stratigraphy near the impact site has been attributed to erosion and reworking after the impact, and backwash from tsunamis and sediment slumping (Kring, 2007; Schulte *et al.*, 2010).

Recent studies are in general support of a combined hypothesis whereby, the Deccan volcanism produced stress on the Earth system for up to 200 Kyrs prior to the K-Pg boundary, increasing ocean acidity (Dameron *et al.*, 2017) and causing greenhouse warming (Schoene *et al.*, 2015; Petersen, Dutton and Lohmann, 2016; Punekar *et al.*, 2016). The Chicxulub impact caused the main extinction, but it is likely that the effects of the impact were amplified as the global ecosystem was already vulnerable to extinction.

Mechanism:

The effect of the impact is thought to have been particularly catastrophic due to the target rocks at Chicxulub. The oil-rich, carbonate-anhydrite target rock would have released vast quantities of carbon dioxide, sulphur and soot into the atmosphere and stratosphere (Schulte *et al.*, 2010; Ohno *et al.*, 2014; Kaiho *et al.*, 2016). The interaction of the sulphur with the atmosphere would have resulted in acid rain and ocean acidification (Ohno *et al.*, 2014).

In the short term, direct effects of the impact would have caused megatsunamis, earthquakes and slumping, air blasts/shockwaves, and intense heat and fires, especially with closer proximity to the impact fireball (Albertão and Martins, 1996; Kring, 1997, 2007; Norris *et al.*, 2000; Bourgeois, 2009). In addition to this, re-entering ejecta would have heated the atmosphere, causing an infrared pulse on a global scale (Goldin and Melosh, 2009; Robertson *et al.*, 2013a). It has been suggested that this pulse could have caused global firestorms and wildfires (Kruge *et al.*, 1994; Robertson *et al.*, 2004). However, recent modelling techniques combined with stratigraphic evidence indicate that due to shielding from settling debris (glass spherules), the pulse was likely to be less severe, but still enough to ignite localised fires and death to any animals exposed to the pulse (Robertson *et al.*, 2004, 2013a; Belcher, 2009; Goldin and Melosh, 2009; Morgan, Artemieva and Goldin, 2013). Robertson et al. (2004) suggested that this could explain extinction selectivity in the terrestrial environment, favouring smaller animals able to burrow or shelter from the effects of this pulse.

In the longer term, a shut-down of primary productivity causing food chain collapse is considered the causal mechanism for the mass extinction (Alvarez *et al.*, 1980). This likely occurred via the injection of dust, sulphur aerosols and/or soot into the stratosphere, which would deflect sunlight, causing darkness and drastic cooling (impact winter) (Ohno *et al.*, 2014;

Vellekoop *et al.*, 2014; Kaiho *et al.*, 2016). Residence times in the stratosphere are much greater than the atmosphere, and therefore anything reaching the stratosphere will achieve global distributions. These conditions could have prevailed from months to decades after the impact (Pope *et al.*, 1997; Pierazzo, Kring and Melosh, 1998; Vellekoop *et al.*, 2014; Kaiho *et al.*, 2016; Brugger, Feulner and Petri, 2017).

The marine ecosystem relies completely on primary productivity. Darkness combined with the effects of ocean acidification on calcareous organisms help explain why the marine environment was so severely affected. Benthic foraminifera, which are typically detritus feeders were less strongly affected than planktonic forms reliant on primary productivity (Ohno *et al.*, 2014). Freshwater ecosystems rely less on primary productivity and more on incoming detritus and are buffered against the effects of acidification, up to 90% of freshwater species are reported to have survived the extinction event (Sheehan and Fastovsky, 1992; Maruoka and Koeberl, 2003; Robertson *et al.*, 2013b; Ohno *et al.*, 2014; Kaiho *et al.*, 2016). In the terrestrial environment, ferns and mosses show a quicker recovery than angiosperms and gymnosperms following the K-Pg (Kring, 2007; Nichols and Johnson, 2008; Vajda and Bercovici, 2014). The 'fern spike' and abundance of fungal spores immediately after the K-Pg boundary is considered to reflect the low light, acidic conditions prevailing at the time (Kring, 2007; Schulte *et al.*, 2010; Ohno *et al.*, 2014; Vajda and Bercovici, 2014).

Survival:

Following the K-Pg extinction, there was a shift from the reptile dominated fauna of the Mesozoic to the mammal and avian fauna that dominate ecosystems in the Cenozoic. We can observe a rapid recovery and diversification of a number of groups including foraminifera (Coxall, D'Hondt and Zachos, 2006), teleosts (Friedman, 2010), mammals (Alroy, 1999; Grossnickle and Newham, 2016; Longrich, Scriberas and Wills, 2016), birds (Feduccia, 1995) and amphibians (Feng *et al.*, 2017). Groups reliant on primary productivity in the food chain were decimated and evidence suggests that marine pelagic recovery took up to 3-4 million years after the extinction (D'Hondt *et al.*, 1996; Coxall, D'Hondt and Zachos, 2006; Wilf *et al.*, 2006). Examination of the fossil record before and after the mass extinction have identified that a greater chance of survival is linked to diet, geographic range, body size, energy consumption and environment.

In terms of diet, omnivores, insectivores, detritus and carrion eaters were more successful than more specialised species such as carnivores (Wilson, 2013). Geographically widespread taxa (Jablonski, 2005; Lockwood, 2005; Longrich, Bhullar and Gauthier, 2012; Wilson, 2013; Landman *et al.*, 2014) had a greater chance of survival and in fact, for mammals especially, the recovery was fuelled by immigrants, radiating into new regions no longer hindered by competition or predation (Longrich, Sciberras and Wills, no date; Wilson, 2013; Longrich *et al.*, 2015; Feng *et al.*, 2017). Small body size is considered to have been a selective advantage over larger species (Alvarez *et al.*, 1980; Robertson *et al.*, 2004, 2013b; Wilson, 2013); this has been particularly noted in the terrestrial environment where animals less than 25kg are thought to have greater chance of survivorship over the extinction event (Alvarez *et al.*, 1980; Buffetaut, 1990; Wilson, 2013). This hypothesis is called the "Lilliput effect" and has been documented in terrestrial ecosystems through insects (Wiest *et al.*, 2018), trace fossils (Wiest *et al.*, 2015; Łaska, Rodríguez-Tovar and Uchman, 2017), birds (Berv and Field, 2017), lizards (Longrich, Bhullar and Gauthier, 2012) and mammals (Wilson, 2013) and in marine ecosystems through marine planktonic foraminifera (Elewa and Dakrory, 2008), veneroid bivalves (Lockwood, 2005), coccolithophores (Gardin and Monechi, 1998), lamniform sharks

(Belben *et al.*, 2017) and decapod crustaceans (Martínez-Díaz *et al.*, 2016). Any taxa that have large energy requirements had a far greater chance of extinction because of food chain collapse. Endotherms would be particularly susceptible, but even fast swimming ectotherms such as pliosaurs and mosasaurs would have been more susceptible to extinction (Bernard *et al.*, 2010; Robertson *et al.*, 2013b). Similarly active/fast swimming fish and sharks have been shown to show similar extinction risk due to starvation (Cavin, 2002; Friedman, 2009; Belben *et al.*, 2017).

Crocodylomorpha:

The effect of the K-Pg mass extinction on crocodyliformes is considered minimal, though this has been attributed to high origination rates in the Paleocene as opposed to low extinction rates in the Cretaceous (Bryant, 1989; Archibald and Bryant, 1990; Markwick, 1998b; Silber, Geisler and Bolortsetseg, 2011; Kellner, Pinheiro and Campos, 2014; Martin, Amiot, *et al.*, 2014; Bronzati, Montefeltro and Langer, 2015; Mannion *et al.*, 2015; Puértolas-Pascual *et al.*, 2016). Regions such as the USA, are more extensively studied over the K-Pg as the sedimentary record is continuous across the boundary and very well dated, to within a few million years of the boundary (Longrich, Bhullar and Gauthier, 2012; Puértolas-Pascual *et al.*, 2016). However, there has been a recent study of European deposits which provides comprehensive analysis and re-examination of fragmentary fossil remains, improving our understanding of the effects of the extinction in a more global perspective (Puértolas-Pascual *et al.*, 2016). Diversity curves show that terrestrial/semi-aquatic crocodylians suffered a greater extinction than marine forms.

Of the three surviving lineages, body size selectivity only seems to apply to the terrestrial/semi-aquatic fauna, the Sebecidae and Alligatoroidea (Erickson, 1982; Brochu, 1997a; Erickson and Brochu, 1999; Pol and Powell, 2011; Kellner, Pinheiro and Campos, 2014). Marine taxa including the dyrosaurids and gavialoids retain larger body sizes before and after the boundary, though this has not been explicitly tested (Troedsson, 1924; Brochu, 2004a; Jouve *et al.*, 2005; Hastings, Bloch and Jaramillo, 2014; Callahan *et al.*, 2015). Few species of Crocodylia or Dyrosauridae are known before the extinction boundary, but are highly diverse in the Paleocene (Archibald and Bryant, 1990; Puértolas, Canudo and Cruzado-Caballero, 2011; Hastings, Bloch and Jaramillo, 2014; Puértolas-Pascual *et al.*, 2016). Amongst the sebecids, small body size and dietary non-specialists represent the survival fauna (Pol and Powell, 2011; Kellner, Pinheiro and Campos, 2014). This is reflected in disparity patterns, where the loss of highly specialised notosuchians explained the decrease in disparity over the boundary (Wilberg, 2017).

Marine crocodylians that survive over the K-Pg represent specialised forms (longirostrine) adapted for piscivory. Given the devastating effect of the extinction on the marine food chain, the survival of these marine crocodyliforms is surprising. It has been suggested that these crocodyliforms found refugium in freshwater ecosystems, which would have contained a more abundant food supply during the extinction interval (Hill *et al.*, 2008; Jouve, Bardet and Jalil, 2008; Robertson *et al.*, 2013b). As ectotherms, crocodylians are not required to feed as regularly and larger forms especially have a better chance at avoiding starvation in the aftermath. Also, in periods of cold temperatures or drought, extant crocodylians have been known to go dormant, this may help explain how crocodylians survived in the unstable environment following the K-Pg (Robertson *et al.*, 2013b; Grigg and Kirshner, 2015).

1.7 Geology of Morocco and the phosphates:

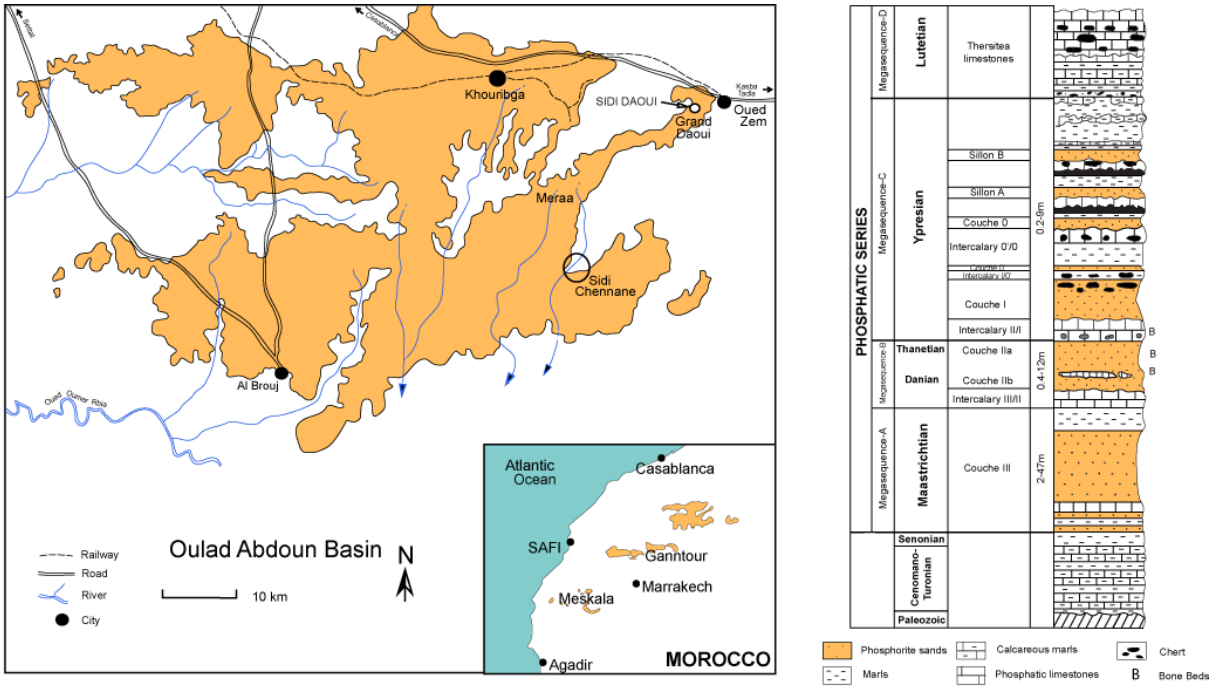

Figure 1.4: Geographic location of the Oulad Abdoun basin in Morocco, with stratigraphic column. Modified from Yans et al. (2014) and Kocsis et al. (2014).

By the Late Cretaceous Africa had become completely isolated from other continental landmasses following the fragmentation of Pangea in the Jurassic and the opening of the Atlantic Ocean (Gheerbrant and Rage, 2006; Michard *et al.*, 2008). During this time, the two major oceans the Atlantic and the Tethys seaway converged around Morocco. In the Late Cretaceous (Cenomanian-Turonian) a period of eustatic sea-level highstand, linked to climatic warming, lead to the flooding of the Atlantic margin of the continental platform into Africa (Lucas and Prevot-Lucas, 1996; Michard *et al.*, 2008; Kocsis *et al.*, 2014). These large inland seas retreated towards the end of the Cretaceous, though portions of inland Africa, including parts of Morocco remained submerged in a set of shallow marine gulfs till the Eocene (Michard *et al.*, 2008; Noubhani, 2010). Evidence of these shallow marine conditions are preserved today in a series of large phosphatic basins, located in the structural zone of the western Meseta (Haddi, Benbouziane and Mouflih, 2014), north of the Atlas Mountains. The phosphatic basins in this region of Morocco include the Ganntour, Meksala and the Oulad Abdoun basin, and collectively represent one of the largest phosphate deposits in the world (Michard *et al.*, 2008). The phosphate series was deposited between the Late Cretaceous and Eocene, the sediments are continuous throughout this interval with no major hiatus in the succession and host a diverse fossil fauna. The continuity of the sequence makes these basins an ideal area to study the effects of the K-Pg mass extinction.

The sedimentary succession between the Late Cretaceous and Eocene is known as the phosphatic series. In the Oulad Abdoun basin the phosphatic series overlies Upper Jurassic-Cretaceous substratum, which comprise red beds, shallow marine marly limestone and evaporites (Cenomanian-Turonian) and Senonian gypsum, limestone and yellow marls (Michard *et al.*, 2008; Yans *et al.*, 2014). The phosphatic series is overlain by a Lutetian dolomitic cap and then Neogene continental deposits (Yans *et al.*, 2014) (Figure 1.4). Presence of dolomite and traces of halite within the deposits indicate that the seaway became restricted from the open ocean between the Maastrichtian and the Lutetian (Michard *et al.*, 2008). In the Oulad Abdoun basin, the phosphatic series is more condensed and phosphate rich in the north-eastern part of the basin becoming thicker in the south-westerly direction (Bardet, Suberbiola, Iarochène, Amalik, *et al.*, 2005; Michard *et al.*, 2008). The condensed series was likely deposited in a more energetic, coastal environment, and the thicker sequence, more typical of the series in the Ganntour basin, deposited in a deeper, open-ocean environment (Lucas and Prevot-Lucas, 1996; Bardet, Suberbiola, Iarochène, Amalik, *et al.*, 2005).

The stratigraphy of the phosphate series is traditionally based on selachian biozonation correlated to European faunas. The phosphates contain an abundant selachian fauna, originally described and utilised by Arambourg (1952). Since then, the fauna has been revised and updated by Noubhani (2010) and Noubhani and Cappetta (1997), and remains the most commonly used tool for stratigraphic dating of the series. However, this dating scheme is not flawless, reworking of the sediments, particularly at the base of units is frequent (Kocsis *et al.*, 2014). Numerous other studies have been carried out to assess biostratigraphic value of invertebrates (Salvan, 1954), pollen (Ollivier-Pierre, 1982), foraminifera (Salvan, 1954), however poor preservation and in cases, poor biostratigraphic value limit their usefulness in the phosphates. Recent investigations have focussed on stable isotopes, such as carbon and oxygen, to correlate the stratigraphy with the global isotopic record. These were found to broadly support the selachian biostratigraphy, but also found that the Selandian is incorporated with Couche IIa in the lower, *Eritherium* bone bed (Noubhani and Cappetta, 1997; Kocsis *et al.*, 2014).

The phosphate series is split into a series of beds, locally known as couches, and these are separated by intercalary beds which are often composed of calcareous phosphate and yellow clay horizons (Kocsis *et al.*, 2014). Couche III, Maastrichtian, is composed of sandy phosphorites, calcareous bonebeds, phosphatic marls, interbedded with limestones at the top of the succession (Michard *et al.*, 2008; Haddi, Benbouziane and Mouflih, 2014; Kocsis *et al.*, 2014). Couche II forms the Paleocene beds, characterised by uncemented sandy phosphorites overlain by phosphatic limestone. Couche II is split into two levels where the Danian and Thanetian are easily identified (Couche IIb and Couche IIa respectively); the Danian section lacks marl and clay levels (Haddi, Benbouziane and Mouflih, 2014). The Selandian is not distinguishable in the series using selachian biostratigraphy (Arambourg, 1952; Yans *et al.*, 2014). Couche IIa (Thanetian) contains two bone beds, iconic for preserving a range of afrotherian mammal taxa (Gheerbrant *et al.*, 2003; Solé *et al.*, 2009; Yans *et al.*, 2014). Intercalaire I/II between the Couch II and Couche I is earliest Ypresian and composed of phosphatic limestone with nodular flints and coprolites. This horizon includes the *Otodus obliquus* bone bed and represents the third bone bed well known for containing mammal material (Gheerbrant *et al.*, 2003). The Ypresian is distinguished by several units, of with Couche I and 0 are highly fossiliferous. The horizons alternate between marly and phosphatic limestone and course yellow and grey sandy phosphorites with coprolites (Haddi, Benbouziane and Mouflih, 2014). Chert horizons are common up section interbedded with phosphorite levels and thinner phosphatic horizons higher up in the Ypresian section are referred to as sillon A and B. Four megasequences of marine transgressive-regressive cycles can be observed up section in the Oulad Abdoun basin. These megasequences separate the Maastrichtian, Paleocene, Ypresian ad Lutetian (Kocsis *et al.*, 2014).

The phosphate series has yielded an abundant and diverse fossil fauna, including actinopterygians (Cavin *et al.*, 2000; Cappetta *et al.*, 2014), selachians (Arambourg, 1952; Noubhani, 2010; Cappetta *et al.*, 2014) and marine reptiles (Bardet *et al.*, 2004, 2010; Bardet, Suberbiola, Iarochène, Bouya, *et al.*, 2005; Jouve *et al.*, 2006; Jouve, 2007; Jouve, Bardet and Jalil, 2008; Vincent *et al.*, 2013) as well as rarer occurrences of birds (Bourdon, Amaghzaz and Bouya, 2010), placental mammals (Gheerbrant *et al.*, 2003; Gheerbrant, 2009; Solé *et al.*, 2009) and non-avian dinosaurs (Suberbiola *et al.*, 2004; Jalil *et al.*, 2009; Longrich *et al.*, 2017). The continuity of the phosphatic series allows for direct comparison of the fauna before and after the K-Pg mass extinction. Couche III is abundant in selachians, actinopterygians and mosasaur material. Also present, but much rarer in the Maastrichtian deposits are species of plesiosaur, chelonii, crocodyliformes, dinosaur and pterosaur (Jouve, Bardet and Jalil, 2008; Bardet *et al.*, 2010; Vincent *et al.*, 2013). In the Paleocene deposits, key taxa including the mosasaurs, large selachians and actinopterygians are no longer present. Instead, there is an abundant turtle and crocodyliform fauna, including numerous species of dyrosaur (Jouve, 2005, 2007, Jouve, Bouya and Amaghzaz, 2005, 2008; Bardet *et al.*, 2010) and crown crocodylians (Jonet and Wouters, 1977; Hua and Jouve, 2004; Jouve *et al.*, 2006, 2014). Rarer fossil occurrences of snake, birds and mammals have also been recovered. New species are continuously being described from the deposits. Therefore, these deposits provide an excellent case study for continued research, not only into the impact of the mass extinction but also the dynamics of the recovery interval.

1.8 Aims of the study:

The effect of the K-Pg extinction on crocodyliformes remains understudied. The extinction event marks a dramatic shift in crocodylian evolutionary dynamics, from the highly diverse and disparate fauna in the Mesozoic, to the largely semi-aquatic forms with low disparity which comprise the Cenozoic fauna. The aim of this thesis is to describe an abundant new crocodylian fauna from the Paleo-Eocene phosphates of Morocco. In doing so, they are placed into an evolutionary context to gain a greater understanding about crocodylian evolution over the K-Pg boundary and the subsequent recovery. The thesis is presented in the alternative format, as specified by the University of Bath. In this format each chapter contains research presented in the style of an academic paper, with an associated commentary text to incorporate the paper into the thesis with additional research and supplemental material for the paper.

Chapter two is focussed on the description of a four new species of gavialoid and tomistomine from the Paleocene-Ypresian of the Oulad Abdoun basin. Three of the new species described form a new clade, suggesting that an endemic fauna in Morocco diversified rapidly following the K-Pg. The fossils described in this chapter provided an opportunity to re-examine the phylogenetic conflict on the position of the Gavialoidea.

Chapter three, incorporates the new fossils described in chapter 2 into a macroevolutionary study of disparity and body size over the K-Pg and throughout the Cenozoic. The new fossil species are stratigraphically early in the evolutionary history of these groups and before the “gharial gap”. Due to the timing of these fossils, in a novel approach, the phylogenetic conflict between the gavialoids and tomistomines is explored in a stratigraphic framework, calculating stratigraphic congruence between the morphological and molecular signals.

Chapter four is focussed on the description of a new species of alligatoroid based on two nearly complete skulls, also from the Oulad Abdoun basin. This material represents the first conclusive proof of Alligatoroidea dispersing into Africa and represents a new species of

Diplocynodontidae. Using biogeography, the work presented in this chapter challenges previous ideas about alligatoroid dispersal in the Cenozoic and suggests that the K-Pg played a significant role in driving alligatoroid diversity and biogeography.

Chapter 2: New crocodylian fossils from the Paleocene-Eocene of Morocco, North Africa

2.1 Pre-paper commentary:

The purpose of this chapter is the description of new fossil material from the Paleocene-Ypresian phosphate deposits of the Oulad Abdoun basin from Morocco. The fossils belong in the crown group, Crocodylia, recovered as relatives of the extant *Gavialis gangeticus* and *Tomistoma schlegelii*. These taxa are significant as they occur in the recovery interval in the aftermath of the K-Pg mass extinction. The gavialoids and tomistomines are poorly understood from this time period, and this represents an early stage in their evolutionary history (Brochu, 2004a, 2006b, Jouve *et al.*, 2006, 2014; Jouve, Bardet and Jalil, 2008). As a result, any new species from this time are critical to improve our understanding of the evolution of these longirostrine taxa. There is significant phylogenetic uncertainty between these groups as the molecular and morphological signals recover conflicting tree topologies. We examine both phylogenetic hypotheses in this paper to compare the relationships. The new species described in this chapter also exhibit a range of skull morphologies from a broad flattened rostrum to hyperelongate tubular rostrum. The morphology of the rostrum is considered to impact the niche occupation of a species and therefore their palaeobiology is discussed.

This declaration concerns the article entitled:									
New crocodylian fossils from the Paleocene-Eocene of Morocco, North Africa									
Publication status (tick one)									
draft manuscript		**Submitted**		**In review**	X	**Accepted**		**Published**	
Publication details (reference)	Resubmission to PloS ONE								
Candidate's contribution to the paper (detailed, and also given as a percentage).	Fossils recognised as novel and obtained by N. Longrich. Preparation carried out by P. Russell and M. Topham (in acknowledgments). Both P. Russell and N. Longrich discussed ideas on how to approach the phylogenetic analyses and possible feeding strategies. All phylogenetic analysis, new scorings were done by P. Russell. Collections visited by P. Russell to collect comparative material on ontogeny. The manuscript was written by P. Russell with edits provided by N. Longrich, A. Roberts, C. Klein and E. Randle (in acknowledgements). All photographs and figures were made by P. Russell. Supplemental material compiled by P. Russell and N. Longrich, with additional discussions with C. Underwood (acknowledgements). 85% Polly Russell and 15% Nicholas Longrich.								
Statement from Candidate	This paper reports on original research I conducted during the period of my Higher Degree by Research candidature.								
Signed						**Date**			

New crocodylian fossils from the Paleocene-Eocene of Morocco, North Africa

Polly Russell[a, b] and Nicholas R. Longrich[a, b,]

[a] Department of Biology and Biochemistry and [b] Milner Centre for Evolution, University of Bath, Claverton Down, Bath, BA2 7AY, United Kingdom

Abstract:

The phosphate deposits of Morocco have historically yielded a rich fossil reptile fauna. The geological setting of these deposits suggests a highly productive shallow warm sea environment relatively closed off to the open ocean. To date, a large number of longirostrine crocodyliformes have been described from these deposits, including species within the crown group, Crocodylia. Amongst the crown group, only two species of gavialoid, *Ocepesuchus eoafricanus* and *Argochampsa krebsi* and one species of tomistomine, *Maroccosuchus zennaroi* have previously been described from the phosphates. Here we describe four new species of crocodylian from the Paleocene-early Eocene deposits of the Oulad Abdoun basin, Morocco. The new species described here include three new species of gavialoid, *Parvosuchus daouiensis* gen. et sp. nov.*, Argochampsa microrhynchus* sp. nov. and *Phasmatosuchus decipulae* gen. et sp. nov., which show a range of brevirostrine and longirostrine morphologies. An additional brevirostrine *Maroccosuchus* species is described, *Maroccosuchus brachygnathus* sp. nov. The variety of skull morphologies suggest a range of trophic adaptations amongst these new species. The robust skull and crushing dentition displayed by *Maroccosuchus* indicate a possibly durophagous diet. In contrast, the slender and elongate skull of the new gavialoid species suggest adaptations towards piscivory. *Phasmatosuchus decipulae* differs from the other gavialoids, exhibiting horizontally projected recurved teeth and a hyperelongate rostrum, suggesting that this species uses a different feeding strategy. Possibilities include the trapping of prey using a comb-like mesh of teeth or mimicking of the modern-day sawfish, agitating benthos with the elongate rostrum. The phylogenetic affinities of the Gavialoidea with respect to the Tomistominae are debated depending on whether morphological or molecular data are used. Adding the new species described here, we re-examined this phylogenetic conflict using the both the morphological character matrix and a combined morphological and molecular matrix. The result of the morphological analysis is consistent with prior analyses, finding Gavialoidea basal within Crocodylia, and *Maroccosuchus* classed as a basal member of the Tomistominae. The new gavialoid species form a new clade with *A. krebsi*, the Argochampsinae, which is endemic to Morocco. The combined (morphological and molecular) analysis produces a result consistent with the molecular phylogeny, gavialoids and tomistomines forming a sister group. The results obtained here are largely consistent with previous combined analyses and the conflict between these two datasets remains unresolved.

Introduction:

The phosphatic deposits of the Oulad Abdoun basin of Morocco have been extensively studied (Bardet et al. 2010; Arambourg 1952; Arambourg 1935; Salvan 1954), yielding a rich vertebrate fossil fauna including bony fish, selachians, reptiles, birds, and mammals. The phosphates span the Late Cretaceous through to the Early Eocene and were deposited in a warm, shallow marine setting, as part of the Tethyan province (Yans et al. 2014; Lucas & Prevot-Lucas 1996; Kocsis et al. 2014). The abundance of fossils has helped document faunal turnover across the K-Pg boundary, from the mosasaurid-dominated fauna of the Cretaceous to a fauna dominated by crocodylomorphs, chelonians, and palaeophiid snakes in the Paleocene (Bardet et al. 2010; Jouve, Bardet, et al. 2008; Bardet et al. 2004; Bardet, Suberbiola, Iarochène, Bouya, et al. 2005; Bardet, Suberbiola, Iarochène, Amalik, et al. 2005).

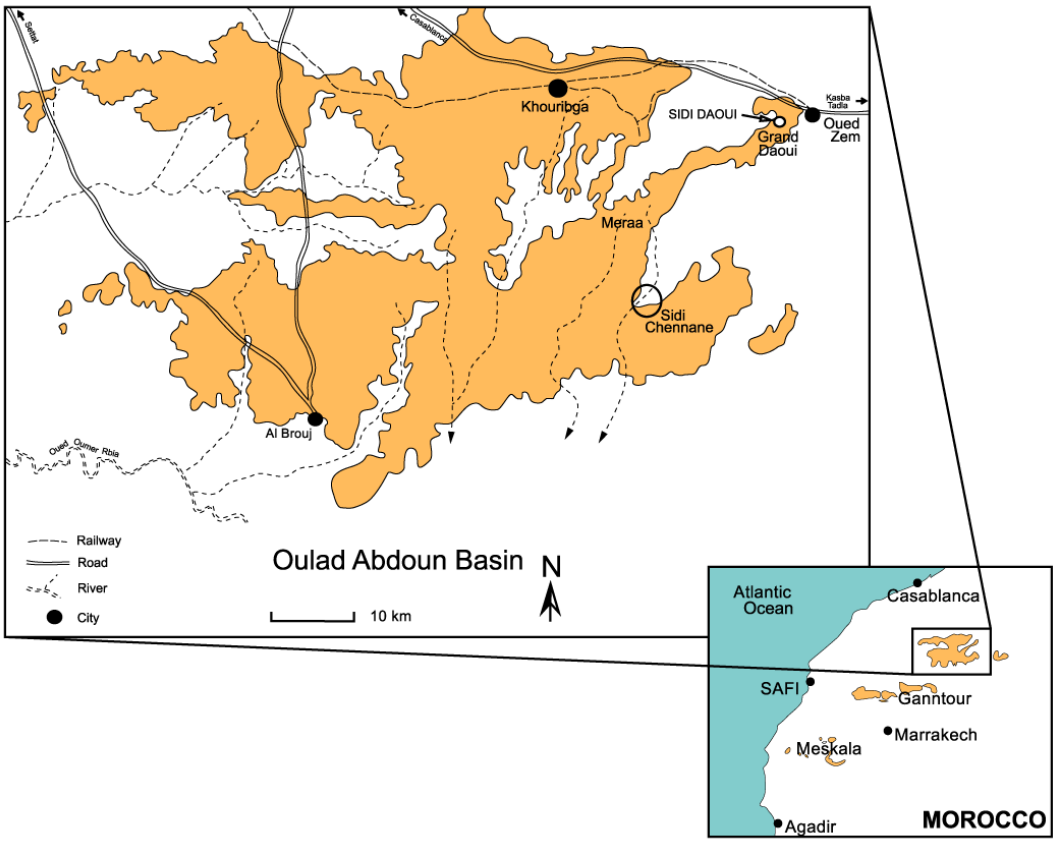

Figure 2.1 Geographical position of the phosphate basins in Morocco. The position of the Oulad Abdoun basin in Morocco is indicated on the smaller map (modified from (Yans et al. 2014))

The Paleogene has produced a particularly diverse assemblage of crocodylomorphs, comprising several species which classify within Dyrosauridae, Gavialoidea, and Tomistominae (Bardet et al. 2010; Jouve et al. 2014; Jouve, Bardet, et al. 2008; Hua & Jouve 2004; Jouve, Bouya, et al. 2008; Jouve, Ne, et al. 2005; Arambourg 1952; Jouve et al. 2006b; Jouve et al. 2006a). The Dyrosauridae, an extinct group of marine Crocodyliformes, represent the most abundant Crocodyliformes in the phosphates (Bardet et al. 2010). All species have a longirostrine morphology which ranges between the short-snouted form seen in *Chenanisuchus lateroculi,* and the extremely long-snouted form of *Atlantosuchus caupatezi* (Jouve, Bouya, et al. 2008; Jouve, Bouya, et al. 2005). Gavialoids described from the phosphates of Morocco have only been found in Oulad Abdoun basin, one of several phosphatic basins that outcrop in this region (Figure 2.1). The gavialoids are less common in the phosphates, represented by two species, *Argochampsa krebsi* (Paleocene) (Hua & Jouve 2004) and *Ocepesuchus eoafricanus* (Maastrichtian) (Jouve et al. 2006b; Jouve, Bardet, et al. 2008). *Maroccosuchus zennaroi* (Ypresian) represents the only known tomistomine from the deposits (Jouve et al. 2014).

The crown group, Crocodylia, comprises three extant groups, Alligatoroidea, Crocodyloidea and Gavialoidea. All Gavialoidea exhibit a highly specialised longirostrine morphology. Their fossil record extends to the Late Cretaceous (Brochu 2004), and the sole extant species, *Gavialis gangeticus,* is restricted to freshwater habitats in India. Anatomical features and fossil record indicate that this transition to freshwater was relatively recent (Taplin et al. 1985; Grigg & Kirshner 2015). The primitive gavialoids, the 'thoracosaurs', are generally found in North America and Europe in coastal/deltaic settings (Brochu 2004; Carpenter 1983; Koken 1888).

The Tomistominae are nested within the Crocodyloidea (all taxa more closely related to *Crocodylus niloticus* than *Gavialis gangeticus* and *Alligator mississippiensis* (Brochu 2003)). The earliest members of the Tomistominae, including *Maroccosuchus zennaroi* (Jonet & Wouters 1977; Jouve et al. 2014) (Morocco) and *Kentisuchus spenceri* (Brochu 2007) (UK), first appear in the Eocene. These early members retain the plesiomorphic crocodylid skull morphology, with broad flattened rostrum with lateral maxillary waves, whereas more derived members exhibit the longirostrine morphology. Similar to the Gavialoidea, the extant species *Tomistoma schlegelii*, is found in freshwater ecosystems, although fossil evidence suggests that marine affinities were widespread in extinct members of the group.

The phylogenetic relationship between Gavialoidea and Tomistominae remains controversial. Using the morphological data, the Gavialoidea are recovered basal within Crocodylia and the Tomistominae, nested in Crocodyloidea (as above). Molecular data, on the other hand, consistently recovers a sister taxon relationship between the extant species, *Gavialis gangeticus* and *Tomistoma schlegelii*, shifting *Gavialis* from the basal position (hypothesised by the morphological data) to a derived position within Crocodylia (Brochu 1997a; Oaks 2011; Gatesy et al. 2004; Harshman et al. 2003; Janke et al. 2005). Combined analyses including fossil taxa also recover a topology consistent with the molecular data (Gatesy et al. 2003; Gold et al. 2014). According to this hypothesis the Gavialoidea (all taxa more closely related to *Gavialis gangeticus* than *Crocodylus niloticus* and *Alligator mississippiensis*) would include Tomistominae, and the Tomistominae would no longer be part of the Crocodyloidea. The Tomistominae are defined as all taxa more closely related to *Tomistoma schlegelii* than to *Gavialis gangeticus* or *Crocodylus niloticus*, dependent on the phylogenetic context. Previous combined analyses indicate that basal tomistomines (in the

morphological context), such as *Maroccosuchus, Kentisuchus,* and *Dollosuchoides*, cannot be classed as tomistomines in the molecular/combined context and are instead classed as basal members of the Gavialoidea (Gatesy et al. 2003; Gold et al. 2014).

Here, we describe multiple new fossils from the Paleocene and Eocene of the Oulad Abdoun basin (see supplementary for provenance information). The variation in skull morphology seen amongst the new taxa suggests that they were adapted to a range of diets, from generalists to highly specialised piscivory and perhaps other ecologies. Four new species are diagnosed as members of the Gavialoidea and Tomistominae using the morphological character matrix. In light of this new fossil data, we also used a combined (morphology-with-molecular) dataset to compare the phylogenetic relationships between the two analyses.

Although both phylogenetic hypotheses are examined here, for the sake of clarity, throughout this work we will refer to the phylogenetic definitions based on the morphological hypothesis (unless otherwise stated). This was chosen to avoid confusion with associated literature on fossil species within the Gavialoidea and Tomistominae, as the morphological data is the primary way to make phylogenetic inferences about fossil material.

Materials and Methods:

Nomenclatural acts: (pending)

Institutional abbreviations:

OCP: Office Chérifien des Phosphates, Direction des Exploitations, Khouribga, Morocco; **MHNLM**: Muséum d'Histoire Naturelle, Le Mans, France; **MHNM**: Museum of Natural History Cadi Ayyad University, Marrakech, Morocco.

Phylogenetic analysis

Phylogenetic analysis was conducted using a modified version of the matrix from Jouve et al. (2014), which was in turn based on previous cladistic studies (Brochu 1997b; Brochu 1997a; Brochu 1999). Modifications made by Jouve et al. (2014) included the addition of 11 gavialoid taxa and reduction in the number of Alligatoroidea and Crocodyloidea species, which allowed for a targeted analysis of the Gavialoidea and Tomistominae.

We added 6 novel characters and 13 new taxa to the matrix (see supplementary information). The new matrix consists of 244 characters and 77 ingroup taxa, with *Bernissartia fagesii* as an outgroup. New taxa include 9 extant species and 4 new fossil taxa described here, *Argochampsa microrhynchus* sp. nov.*, Parvosuchus daouiensis* gen. et sp. nov.*, Phasmatosuchus decipulae* gen. et sp. nov. and *Maroccosuchus brachygnathus* sp. nov.*.* Character 165, 169 and 171 were modified (see supplementary information), and character codings were updated for the following taxa; *Eothoracosaurus mississippiensis, Thoracosaurus neocesariensis, Ikanogavialis gameroi, Euthecodon arambourgi*, *Euthecodon brumpti, Argochampsa krebsi* and *Maroccosuchus zennaroi.*

Due to the conflict in the position of the Gavialoidea within the Crocodylia, we ran two phylogenetic analyses; the first using the morphological character matrix only, and the second using a combined analysis of morphology-with-molecular data.

In the morphology-only analysis, the phylogenetic matrix was analysed in TNT v 1.1 (Goloboff et al. 2003) using a traditional search of 1000 replicates of Wagner trees, holding 100 trees per replicate (TBR branch swapping). Characters were equally weighted and unordered. In the second analysis, we performed a combined analysis of the morphological and molecular data using parsimony (Figure 2.4, File S2). The molecular alignment was sourced from Gold et al. (2014) the molecular matrix contains 11,564 base pairs for 16 extant taxa. The matrix was input into TNT v 1.1 in an interleaved format and the same heuristic tree search as above.

Results:

Systematic Palaeontology:

Eusuchia Huxley 1875
Crocodylia Gmelin 1789
Gavialoidea Hay 1930
Argochampsinae tax. nov.
Argochampsa Hua and Jouve 2004

Type species: *Argochampsa krebsi* Hua and Jouve 2004
Diagnosis: Premaxilla transversely broad with two foramina anterior to the nares; first 3 alveoli form a linear transverse row; diastema between the 4th and 5th premaxillary alveoli; paroccipital processes form two postero-laterally directed long narrow points; exoccipitals form long nearly horizontal plate broadly visible in dorsal view. The genus also has fused nasals, which are observed in Argochampsinae.

Argochampsa microrhynchus sp. nov. (Figure 2.2-2.7)

Etymology: *micro* (μικρό), Greek, "small", and *rhynchus* (ρύγχος), Greek, "snout".
Holotype: MHNH.KHG.169, nearly complete skull
Horizon and locality: Couche II, Paleocene from the Sidi Daoui locality in the Oulad Abdoun basin, Morocco
Diagnosis: Distinguished from *Argochampsa krebsi* by a quadrate with an expanded medial hemicondyle, <20 maxillary alveoli (at least 12), proportionally shorter and broader rostrum, strongly scalloped maxillary edge with lateral protrusion of the alveoli well developed anteriorly. Foramen incisivum larger than *A. krebsi* and does not extend anteriorly beyond the anterior border of the external nares.

Description:

Preservation and general form:

The cranium of *Argochampsa microrhynchus* (MHNH.KHG.169) is incomplete, missing the lower temporal bar (jugal and quadratojugal), shows significant dorsoventral compression

and the rostrum is bowed dorsally (Figure 2.4). This deformation has displaced the occipital condyle posterolaterally and the entire occipital condyle surface is visible in dorsal view (Figure 2.2,2.5). As a result, the foramen magnum is not preserved and the exoccipital and basioccipital are damaged. As the lower temporal bar has not been preserved, the lateral margins of the orbits are incomplete. The postorbital bar and infratemporal fenestrae are not preserved. The dorsal surface has been reconstructed with plaster where damaged (Figure 2.2,2.6). The damage is pronounced in the preorbital region and sutural contacts between the frontal, prefrontals, lacrimals and jugals cannot be discerned. The posterior border of the left squamosal and left quadrate are also missing. The right quadrate is preserved but matrix obscures the nature of the contact with the exoccipital.

In ventral view the rostrum is highly fractured and on the left premaxilla the second and third alveoli are damaged. Posteriorly, near the anterior orbital margin the maxillae are incomplete, therefore total maxillary tooth count is uncertain. The ectopterygoids, pterygoids and suborbital fenestrae are not preserved. However, the contact surface for the attachment of the pterygoid to the basisphenoid is visible. The braincase and associated cranial bones are missing.

The cranium measures 31.1cm from the back of the skull table to the tip of the rostrum, exhibiting a general longirostrine morphology (Table 2.1) (Brochu 2001). The rostrum is linear anteroposteriorly, lacking maxillary waves. At the level of the ninth maxillary alveolus the rostrum flares posteriorly up to the anterior border of the orbits. The rostrum is proportionally shorter and broader than *Argochampsa krebsi* (Hua & Jouve 2004), with a reduced tooth count. The linear morphology of the maxilla, in combination with maxillary homodonty, is diagnostic to Gavialoidea within crown Crocodylia (Brochu 1997a).

Cranial openings:

The external naris is large, comprising nearly half of the premaxillary width (Table 2.1), subcircular and bordered entirely by the premaxilla. It opens dorsally with no ridge or notch visible around the narial rim. Like *Argochampsa krebsi*, the premaxilla bears two reception pits (diameter: 6mm) on the dorsal surface, which are positioned anterior to the external nares but posterior to the first three premaxillary alveoli (Figure 2.2,2.7). These reception pits are observed in extant taxa such as *Crocodylus porosus*, where the first dentary teeth protrude through the cranial bone to the dorsal surface of the skull (Jouve et al. 2006b; Iordansky 1973; de Lapparent de Broin 2002). The incisive foramen (Figure 2.3) is roughly circular and smaller than the external nares (Table 2.1). It is bordered entirely by the premaxilla and does not extend beyond the margins of the external naris. The orbits are roughly elliptical in shape, based on the anteroposterior length of the orbits, and are dorsally positioned. The telescoped orbits observed in *Gavialis gangeticus* are not observed in *A. microrhynchus*. The supratemporal fenestrae are roughly circular, however the right supratemporal fenestra is smaller due to preservation. The fenestrae are large, occupying most of the skull table, consistent with gavialoid affinities. On the occipital face, the foramen vagi are clearly preserved within the exoccipitals, lateral to the occipital condyle. The medial eustachian foramen is visible in ventral view between the basioccipital and basisphenoid contact, the lateral eustachian foramina are not preserved and therefore their position with respect to each other in uncertain.

	A. microrhynchus MHNM.KHG.169	*P. daouiensis* MHNM.KHG.168	*P. decipulae* MHNM.KHG.166	*P. decipulae* MHNM.KHG.167	*M. brachygnathus* MHNM.KHG.170	*M. zennaroi* MHNM.KHG.171	*M. zennaroi* MHNM.KHG.172	*M. zennaroi* MHNM.KHG.173
Total length (posterior border of supraoccipital to tip of rostrum)	30.3	33.3*	59.8*	33.3*	50	49.9	47.1	42.8
Rostral length (from anterior border of the orbits to tip of rostrum)	22.1	24.9*	50.9*	24.1*	34.7	35.8	34.4	31
Length from supraoccipital to anterior border of the orbits	8.2	8.4*	8.9	9.2	15.3	14.1	12.7	11.8
Rostrum width at anterior border of orbit	7.9	6.8*	8.3*	6.6	18.9	15.3	15.7	12.4
Width at first lateral wave of rostrum	-	-	-	-	14.8	10.6	10.9	8.1
Rostrum width at mid-snout constriction	3.3	2.7	3.6	3	11.3	9.3	9.2	7.1
Width at narial constriction	2.8	1.8	-	-	6.5*	5	5.3	4
Nasal length	12.9	14.6	13.4	-	26.1	29.2	27.3	25.3
Frontal length in front of orbits	1.7	2.8*	2.4	-	3.6	3.6	4.1	3.9
Width between lateral quadrate condyles	12.8*	9.9	13.4*	12.4	32.5*	24.6	23.8*	18
Width skull table	8.8*	7.1	11.8*	7.5	19.5	14.4	13.1	11.5
Orbit length	3.6*	-	-	-	5.1	5.7	5.1	5.5
Orbital width (maximum)	-	-	-	3.4	5.1	3.4	3.9	3.3
Supratemporal fenestra length	2.8*	-	-	3.4*	4.8	3.6	4	3.6
Supratemporal fenestra width	3	-	-	3.6*	5	3.8	4	2.7
External naris length	2.7	1.25	-	-	5.6	4.3	4.2	3.5
External nares width	2.3	1.1	-	-	4.1	3.7	3.7	2.3
Premaxilla maximum width	5.5	2.6	-	-	9.1	8.6	8.6	5.9
Interorbital width	2.5	-	1.7	2	5.5	3.8	3.6	3.2
Interfenestral bar width	0.6	-	0.8*	0.6	1.4	1.2	0.7	1
Incisive foramen length	1.7	-	-	-	-	-	-	1.1
Incisive foramen width	1.5	-	-	-	-	-	-	1.1
Occipital condyle height	1.4	1.3	1.3	1.7	-	-	-	-
Occipital condyle width	2.3	1.7	2.4	2.1	-	-	-	-
Foramen magnum height	-	1.4	-	1.1	-	-	-	-
Foramen magnum width	-	0.4	-	1.5	-	-	-	-
Suborbital fenestra length	-	-	-	-	-	-	-	9.2
Suborbital fenestra width	-	-	-	-	-	-	-	3.1
Choana length	-	-	1	2*	-	-	-	1.4*
Choana width	-	-	2.2	2.1*	-	-	-	1.6*
Maxillary tooth count	12-18?	>22	>50	>30	-	-	-	14

Table 2.1: Comparative measurements of the new taxa (in cm). Asterisks highlight estimated measurements due to poor or incomplete preservation.

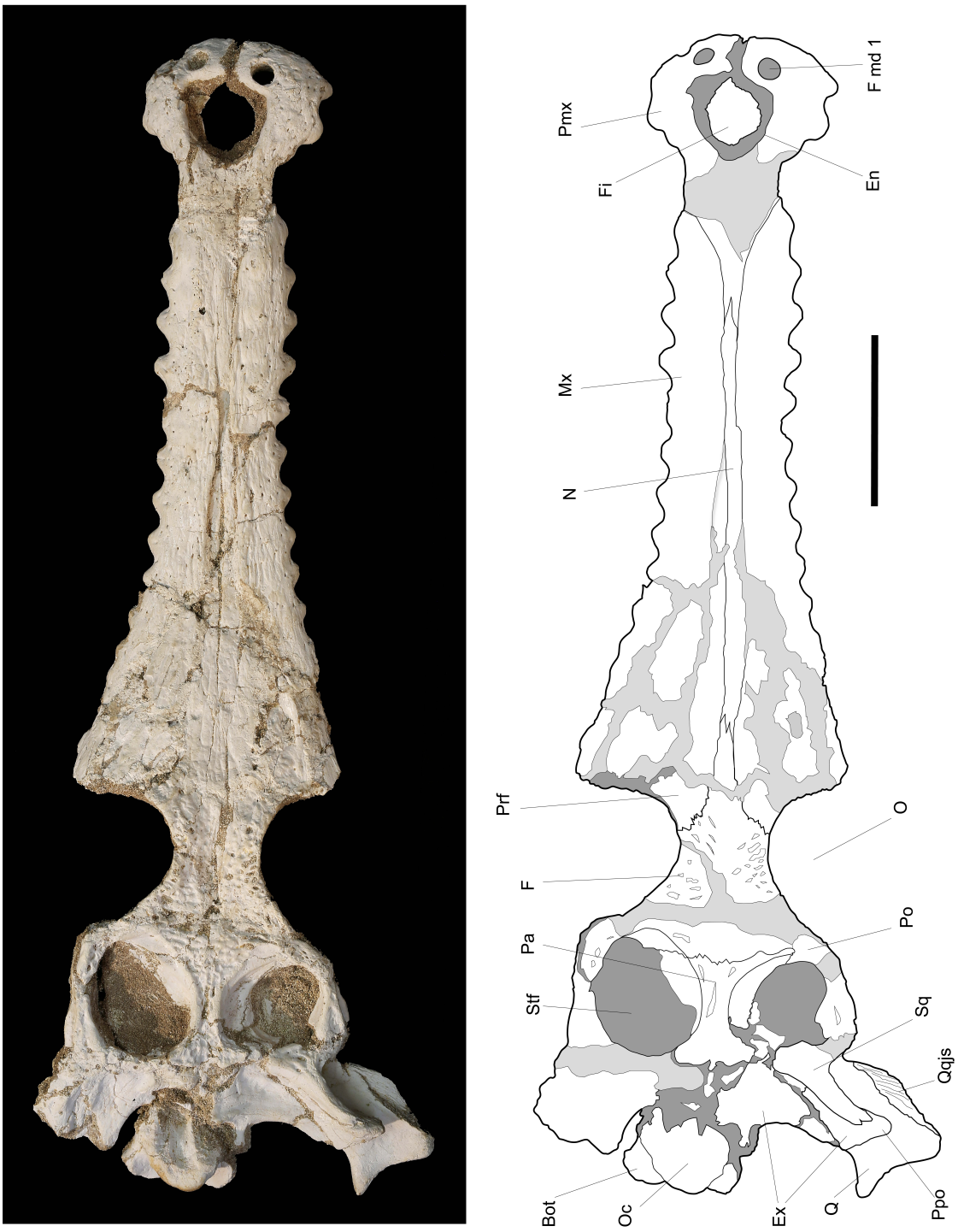

Figure 2.2 *Argochampsa microrhynchus* sp. nov., holotype MHNM.KHG.169 from Paleocene of Morocco. Skull in dorsal view. Scale bar = 5cm. Light shading indicates areas of plaster reconstruction. Areas of dark shading are areas obscured by matrix. **Abbreviations: Bot,** basioccipital tuberosities, **En,** external nares, **Ex,** exoccipital, **Fi,** foramen incisivum, **F md 1,** foramen for first mandibular tooth, **F,** frontal, **Mx,** maxilla, **N,** nasal, **O,** orbit, **Oc,** occipital condyle, **Pa,** parietal, **Ppo,** paroccipital process, **Pmx,** premaxilla, **Po,** postorbital, **Prf,** prefrontal, **Q,** quadrate, **Qqjs,** quadratojugal suture, **Sq,** squamosal, **Stf,** supratemporal fenestra

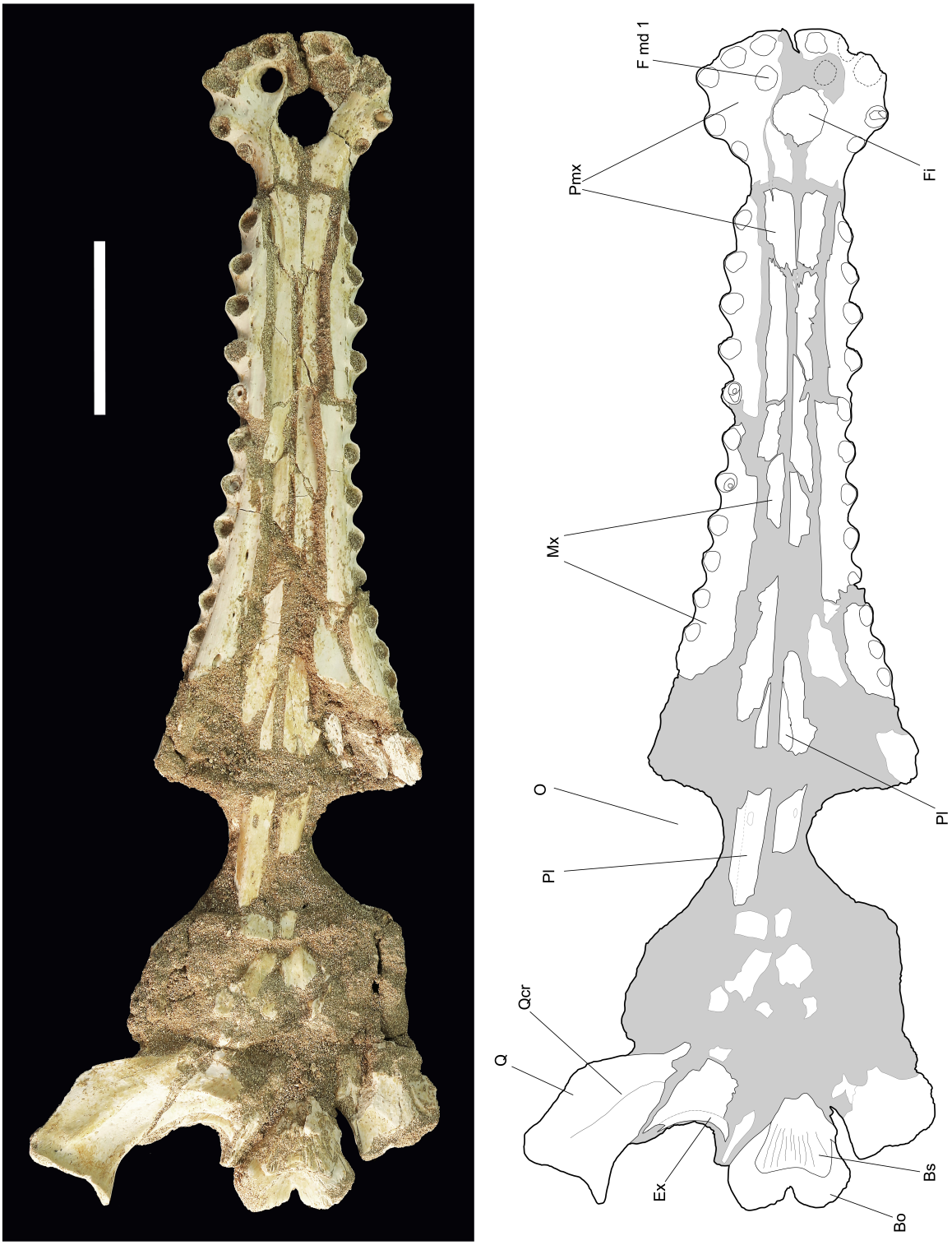

Figure 2.3 *Argochampsa microrhynchus* sp. nov., holotype MHNM.KHG.169 from Paleocene of Morocco. Skull in ventral view. Scale bar = 5cm. Areas of shading are areas are matrix. **Abbreviations: Bo,** basioccipital, **Bs,** basisphenoid, **Ex,** exoccipital, **F md 1,** foramen for first mandibular tooth, **Fi,** foramen incisivum, **Mx,** maxilla, **O,** orbit, **Pl,** palatine, **Pmx,** premaxilla, **Q,** quadrate, **Qcr,** quadrate crest

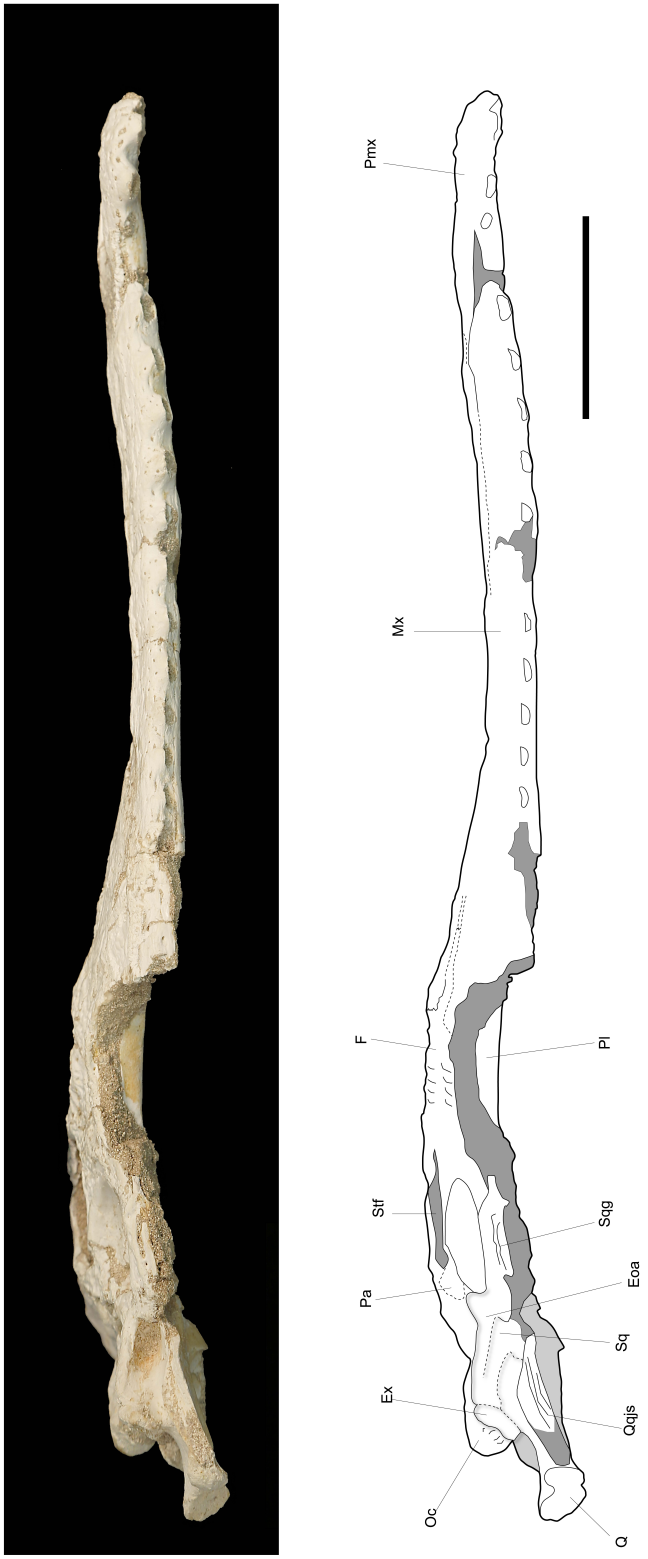

Figure 2.4 *Argochampsa microrhynchus* sp. nov., holotype MHNM.KHG.169 from Paleocene of Morocco. Skull in right lateral view. Scale bar = 5cm. Areas of shading are matrix. **Abbreviations: Eoa,** external otic aperture, **Ex,** exoccipital, **F,** frontal, **Mx,** maxilla, **Oc,** occipital condyle, **Pa,** parietal, **Pmx,** premaxilla, **Pl,** palatine, **Ppo,** paroccipital process, **Q,** quadrate, **Qqjs,** quadratojugal suture, **Sq,** squamosal, **Sqg,** squamosal groove for external ear muscle attachment, **Stf,** supratemporal fenestra

Cranial bones:

The premaxilla is mediolaterally broad at the level of the third-fourth premaxillary alveoli, 67% wider than the mediolateral width of the rostrum. Each premaxilla bears five alveoli, plesiomorphic to Crocodylia. The first three alveoli are equal in diameter (6mm) oriented in a posterolateral row. The fourth and fifth alveoli are smaller, 5mm and 4.5mm respectively, and separated from the first three alveoli by a 6mm anteroposteriorly long diastema. The fifth alveolus is posteromedial to the fourth alveolus. Posterior to the fifth alveoli the premaxilla narrows and a 13mm diastema separates the final premaxillary alveolus and the first maxillary alveolus. The morphology and arrangement of the premaxillary dentition is a synapomorphy for *Argochampsa* (Hua & Jouve 2004) and convergent with distantly related Crocodyliformes, Pholidosauridae (Sereno et al. 2001; Fortier et al. 2011; de Lapparent de Broin 2002). Compared to *A. krebsi* the premaxillae in *A. microrhynchus* are mediolaterally broader. Dorsally the posterior process extends to the level of the third maxillary alveolus. Ventrally, the posterior premaxillary process extends to the level of the second maxillary alveolus, forming a broad contact with the maxilla. This short process is homologous to that seen in *Eosuchus lerichei* and *Eosuchus minor* (Delfino et al. 2005; Dollo 1907; Brochu 2006b), but in all other gavialoids, including *A. krebsi,* the process is more elongate posteriorly.

In dorsal view, the maxillae have a scalloped edge due to the lateral projection of the maxillary alveoli (Figure 2.2). Anteriorly the lateral projection of the alveoli is more exaggerated, and the alveoli are oriented anteroventrally. The scalloped edge of the maxilla is more pronounced in *Argochampsa microrhynchus* than in *A. krebsi* and is more similar to that seen in the South American gharial *Ikanogavialis gameroi* (Sill 1970) and the African long-snouted crocodylid, *Euthecodon* (Ginsburg & Buffetaut 1978; Storrs 2003). There are 12 alveoli preserved on the right maxilla and 11 on the left side, comparison with the arrangement of alveoli in *A. krebsi* indicates that there could be up to 18 maxillary teeth in total. The maxillary alveoli are circular and uniform in size (5mm diameter) with equal interalveolar spacing. Posterior to the tenth alveolus the alveoli decrease in diameter and show mediolateral compression. No complete teeth are preserved in the specimen, but fragments are preserved within three alveoli. These are rounded in cross section, ~1.5mm in diameter and homodont. In ventral view, the anterior palatine process is narrow, this morphology is a feature shared by Gavialoidea and Tomistominae. The palatine terminates in an acute point at the level of the twelfth maxillary alveolus. Posteriorly the lateral margins of the palatines form the medial border of the suborbital fenestrae and are parallel sided. The posterior contact with the pterygoid is not preserved.

The nasals are narrow and fused. Anteriorly, the nasals contact the premaxillae in line with the third maxillary alveolus. The nasals do not penetrate far anteriorly into the premaxilla, a condition shared with the primitive gharials and *Argochampsa krebsi.* The contact with the frontal is broad, with an interdigitating suture at the level of the twelfth maxillary alveolus.

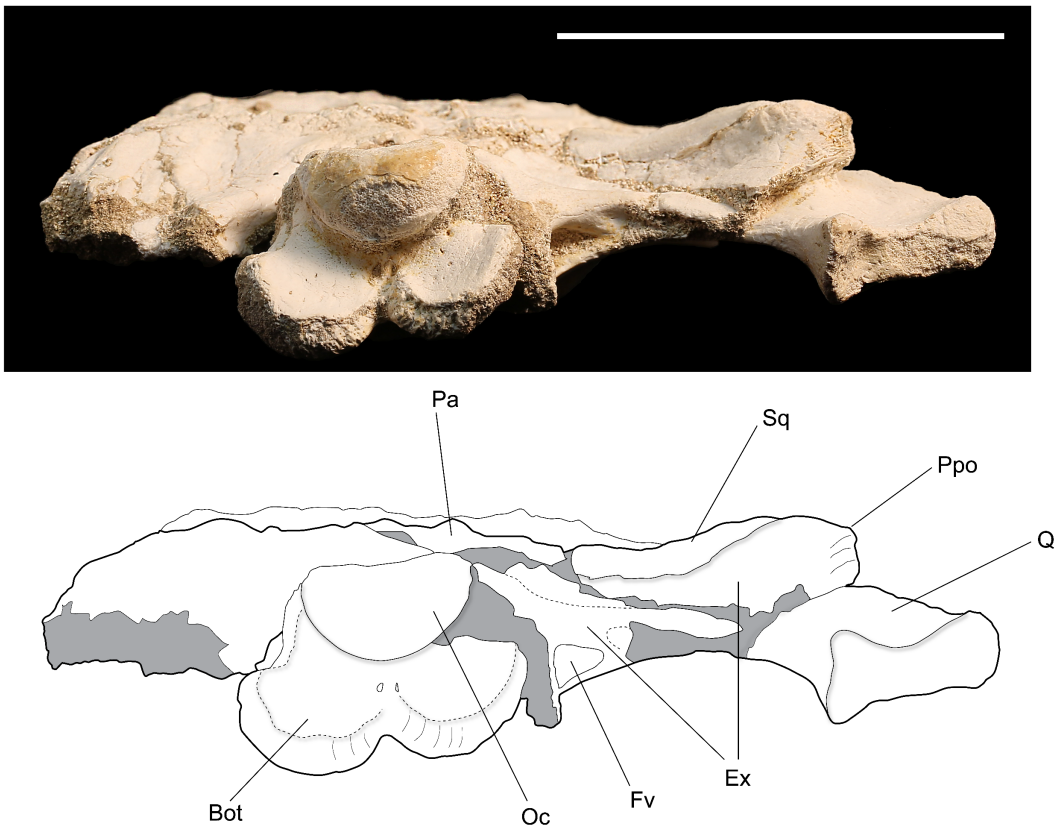

Figure 2.5 *Argochampsa microrhynchus* sp. nov., holotype MHNM.KHG.169 from Paleocene of Morocco. Skull in occipital view. Scale bar = 5cm. Areas of shading are matrix. **Abbreviations: Bot**, basioccipital tuberosity, **Ex,** exoccipital, **Fv,** vagus foramen, **Oc,** occipital condyle, **Pa,** parietal, **Ppo,** paroccipital process, **Q,** quadrate, **Sq,** squamosal

The frontal is concave between the orbits and shows modest ornamentation in the form of small and rounded shallow pits. The frontal forms the posteromedial border of the orbits and the anterior border of the supratemporal fenestrae but does not participate in the interfenestral bar. The frontoparietal suture is linear and modestly penetrates the walls of the supratemporal fenestra; these characters are also observed in *Argochampsa krebsi*, *Aktiogavialis puertoricensis* (Vélez-Juarbe et al. 2007)*, Gryposuchus colombianus* (Langston & Gasparini 1997; Riff et al. 2008) and *Gavialis gangeticus* (Iordansky 1973; Martin et al. 2012).

The postorbital contributes to the anterolateral border of the supratemporal fenestrae. The postorbital-squamosal suture on the lateral border of the skull table passes ventrally under the postorbital. The parietal forms the interfenestral bar and posteromedial border of the supratemporal fenestrae. The sutures with the squamosal and supraoccipital on the posterior region of the skull table are poorly defined. The squamosal forms the posterior and posterolateral border of the supratemporal fenestrae. Laterally, the quadratosquamosal suture extends along the caudal margin of the external otic aperture. The morphology of the squamosal groove for external ear muscle attachment is unclear. The posterior squamosal prong is elongate and extends posterolaterally to contact the exoccipital on the paroccipital process.

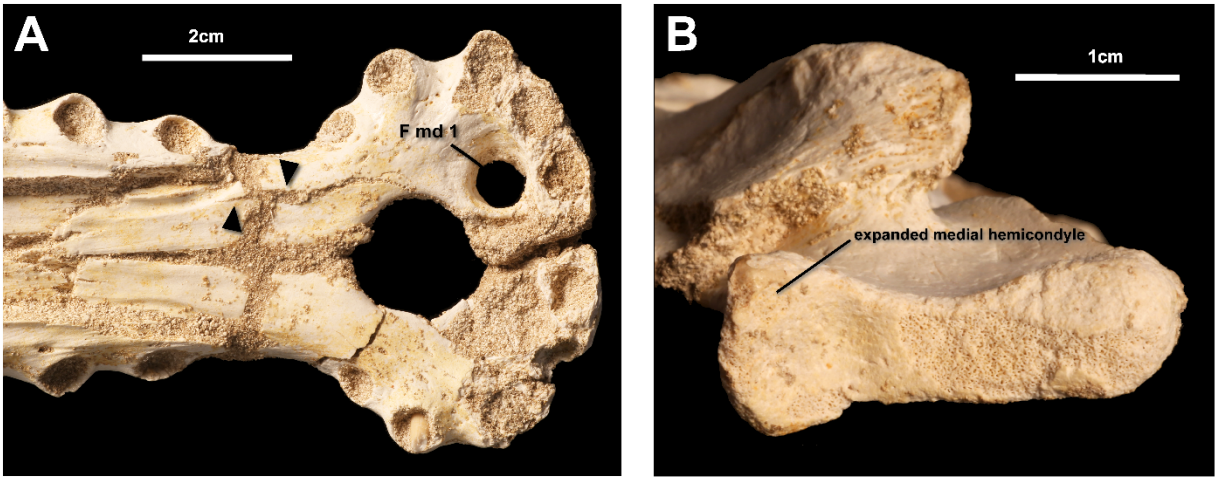

Figure 2.6 *Argochampsa microrhynchus* sp. nov., holotype MHNM.KHG.169. **A** Ventral view of the premaxilla. Black triangles show fracture in premaxilla is continuous across a break in the fossil, where plaster reconstruction is evident on the dorsal surface. **B** Occipital view of the quadrate, indicating the dorsal expansion of the medial hemicondyle.

The quadratojugal forms a contact with the quadrate anterior to the lateral articulation surface of the quadrate, as shown by the sutural contact surface on the right quadrate (Figure 2.2). The articular surface of the quadrate exhibits a sigmoidal shape, with the medial hemicondyle larger than the lateral hemicondyle. The medial hemicondyle is directed posteromedially and dorsoventrally expanded (Figure 2.5, 2.6). This condition is observed the most primitive gharials *Eosuchus* spp. (Delfino et al. 2005; Brochu 2006b), and in a number of tomistomines (Jouve et al. 2014; Shan et al. 2009; Kobayashi et al. 2006). On the ventral surface, the quadrate crest B (Iordansky 1973) runs parallel to the posteromedial margin of the quadrate. The foramen aereum appears absent on the surface of the quadrate. In general, the foramen aereum is present, amongst Crocodylia, the absence of this feature may be an apomorphy of *Argochampsa*, as the foramen aereum is also not present on *A. krebsi* (Jouve et al. 2006b).

The occipital face is inclined and visible in dorsal view, a synapomorphy of Gavialoidea. The contact between the exoccipital and squamosal can be seen on the occipital surface, it is smooth, and curves upwards at the termination of the squamosal to form the paroccipital process. The basioccipital has two large, pendulous tubera similar in morphology to *Gavialis* and medially separated by a distinct groove (Hecht & Malone 1972). The basisphenoid is broadly exposed on the ventral surface of the basioccipital tubera, roughly triangular and measuring 23mm at its widest point.

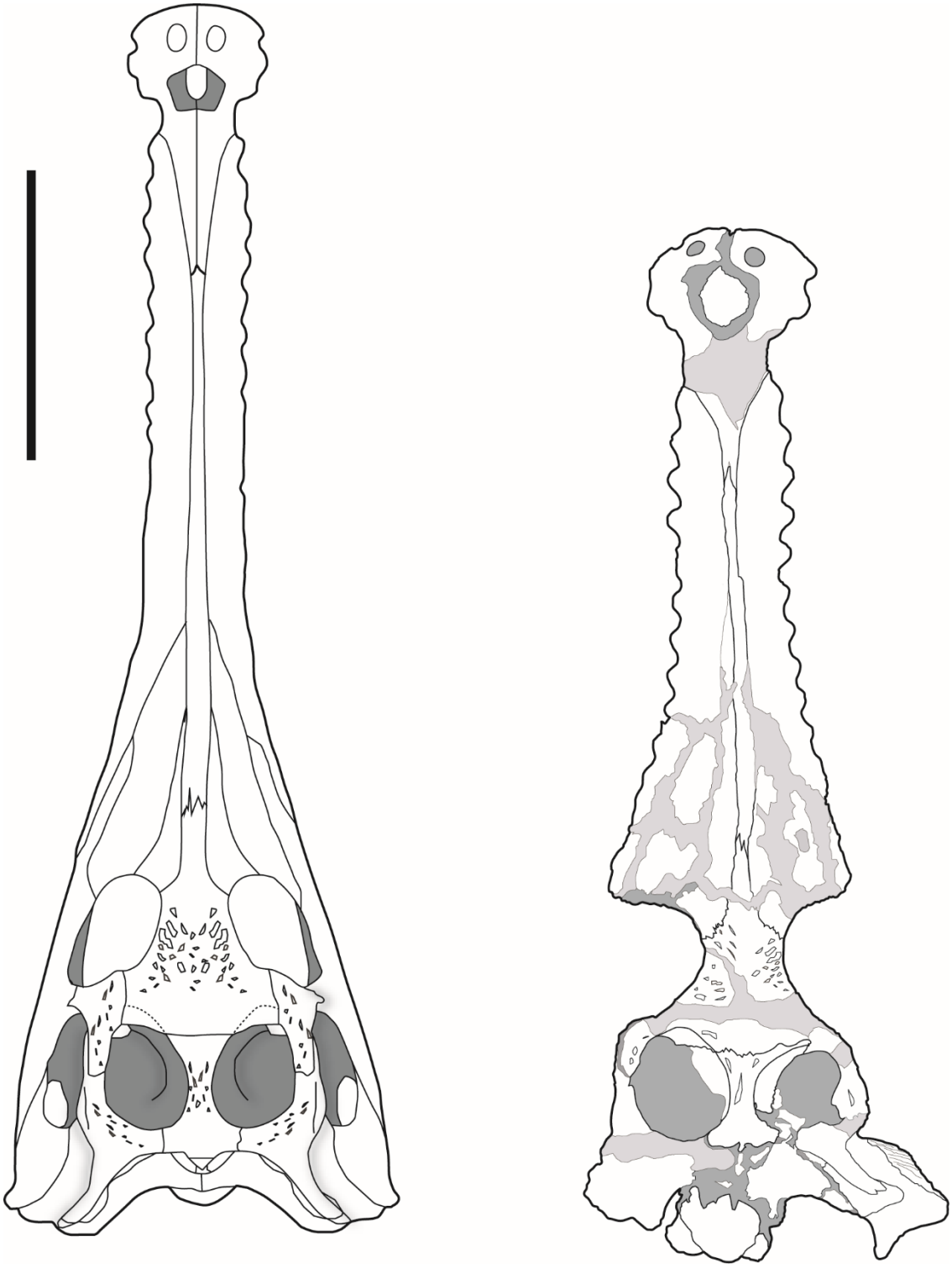

Figure 2.7 Comparative figure of *Argochampsa* species to scale. **A** reconstruction of *A. krebsi* in dorsal view (modified from (Jouve et al. 2006b)). **B** *A. microrhynchus* in dorsal view. Scale bar is equal to 10cm.

Parvosuchus n. gen

Type species: *Parvosuchus daouiensis* gen. et sp. nov.
Etymology: *parvos*, Latin, "small"; *suchu*s, Greek, "crocodile".
Diagnosis: as diagnosis for species

Parvosuchus daouiensis sp.nov (Figure 2.8-2.13)

Etymology: The species name comes from the type locality of the specimen at Sidi Daoui.
Holotype: MHNM.KHG.168 Nearly complete skull, missing the skull table and the orbital region. The skull is damaged and fractured along the rostrum, the posterior region of the skull shows half of the braincase in cross section.
Type Horizon and Locality: Couche II, Danian, Sidi Daoui locality in the Oulad Abdoun basin, Morocco
Diagnosis: Gavialoid of small size that can be distinguished from all other gavialoids by the following autapomorphies: a shallow, antero-posteriorly elongate fossa on the dorsal surface of the premaxilla posterior to the nares, anteroposteriorly elongate diastema between the premaxillary and maxillary alveoli, cranioquadrate passage not hidden by exoccipitals in occipital view, 22 maxillary teeth, rostrum approx. 73% of medial skull length. Fused nasals are synapomorphic to the Argochampsinae.

Description:

Preservation and general form:

The cranium is small (33.3cm) compared to most species within the Gavialoidea, which typically range between 55-117cm. Gavialoids of similar size are restricted to *Eosuchus* and other Moroccan species (*Argochampsa* and *Ocepesuchus).* The cranium demonstrates a longirostrine morphology, the rostrum is straight lacking maxillary waves, and flares laterally posterior to the 13th maxillary alveolus.

The skull is highly fractured and damaged, particularly in the postorbital region. The rostrum and postorbital region of the skull are separated in the matrix, however the configuration of bones and distance between the two regions suggest these are close to the life position (Figure 2.8). The damage to the skull was likely incurred during excavation/discovery of the skull rather than taphonomic processes. The rostrum is broken at the level of the anterior border of the orbits, inferred from the surrounding anatomy.

The rostral region of the skull is only visible in dorsal view. The right premaxilla is heavily damaged, and much of the original dorsal surface is missing and broken. The posterior dorsal processes are not preserved, but suture surfaces on the maxillary surface (Figure 2.8, 2.13) can be used to infer the position of the premaxilla. Posteriorly, the anterior process of the jugals are also inferred from suture surfaces on the right maxilla (Figure 2.8). The palate is not visible and therefore the position of the suborbital fenestra and foramen incisivum are not known.

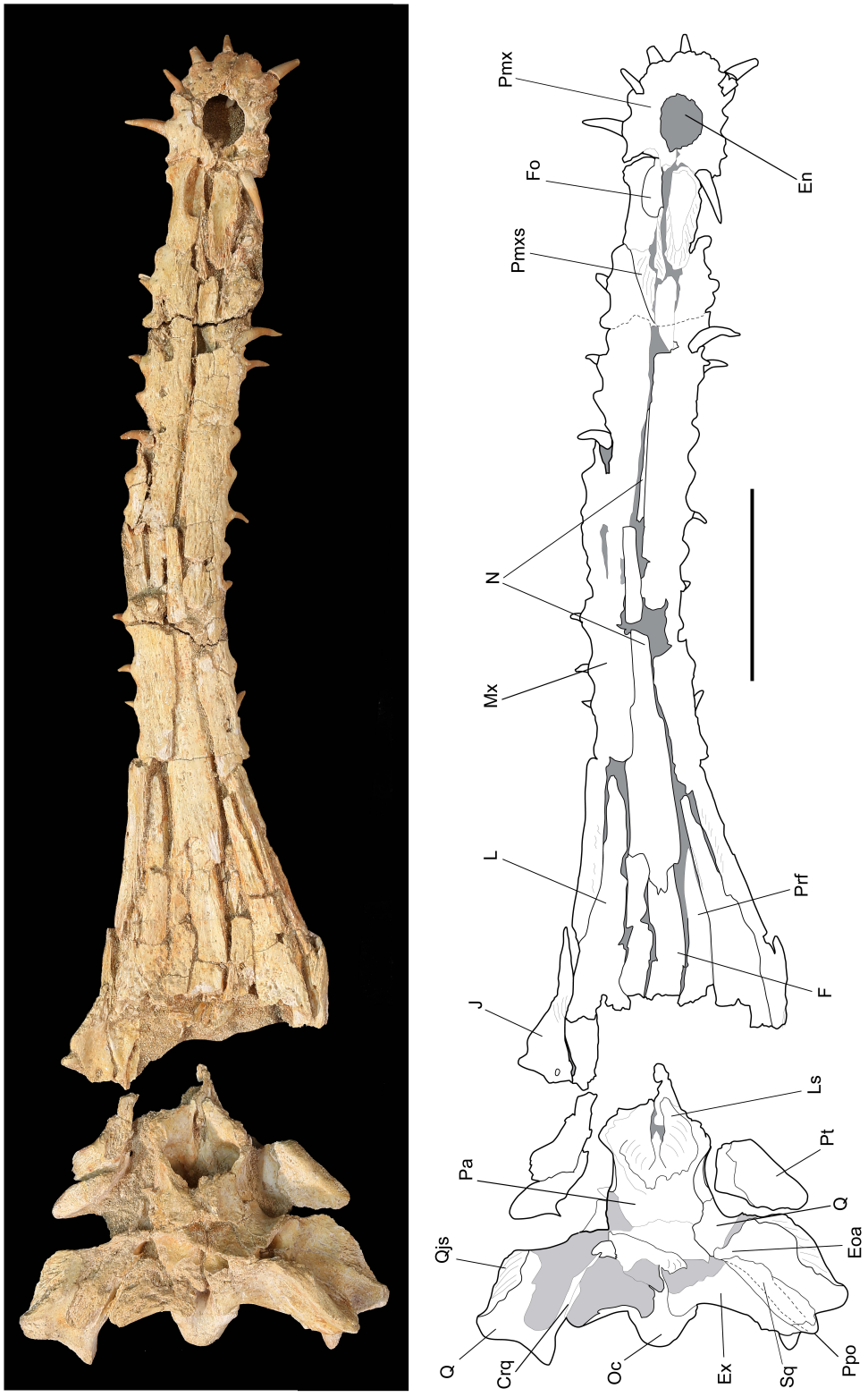

Figure 2.8 *Parvosuchus daouiensis*, holotype MHNM.KHG.168 from Paleocene, Couche II, of Morocco. Skull in dorsal view. Light shading indicates areas where the surface is broken. Areas of dark shading are matrix. Scale bar= 5cm **Abbreviations: Crq**, cranioquadrate passage, **Eoa,** external otic aperture, **En,** external nares, **Ex,** exoccipital, **F,** frontal, **Fo,** fossa, **J,** jugal, **L,** lacrimal, **Ls,** laterosphenoid, **Mx,** maxilla, **N,** nasal, **Oc,** occipital condyle, **Pa,** parietal, **Ppo,** paroccipital process, **Pmx,** premaxilla, **Pmxs,** premaxilla suture surface, **Prf,** prefrontal, **Pt,** Pterygoid, **Q,** quadrate, **Qjs,** quadratojugal suture, **Sq,** squamosal

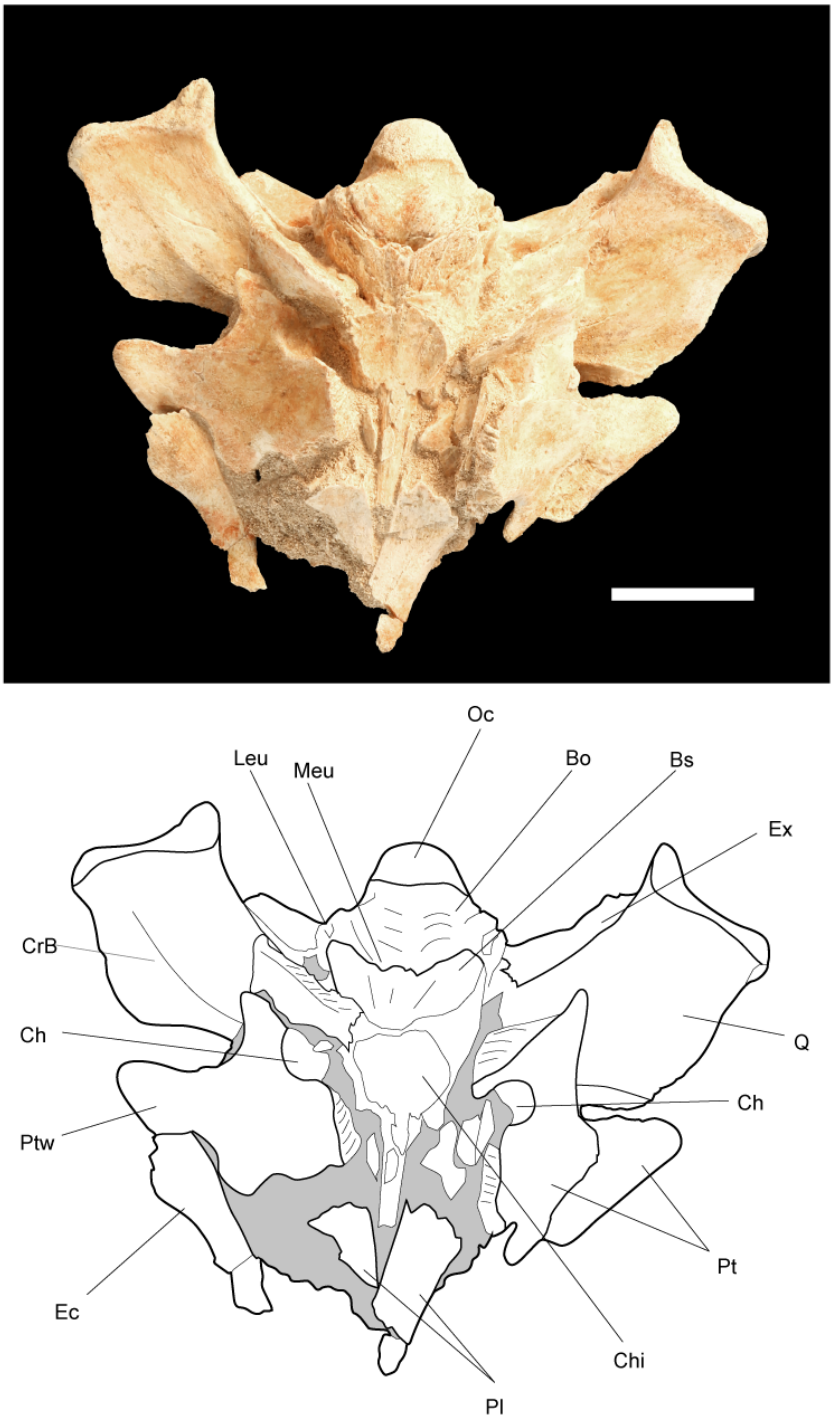

Figure 2.9 *Parvosuchus daouiensis,* holotype MHNM.KHG.168. Prepared, posterior portion of the skull in palatal view. Scale bar = 2cm. **Abbreviations: Bo,** basioccipital, **Bs,** basisphenoid, **Ch,** choana, **Chi,** internal choana, CrB**,** quadrate crest, Ec**,** ectopterygoid, **Ex,** exoccipital, **Leu,** lateral eustachian foramen, **Meu,** medial eustachian foramen, **Oc,** occipital condyle, **Pl,** palatine, **Pt,** pterygoid, **Ptw,** pterygoid wing, **Q,** quadrate,

The skull table (frontal, postorbital, parietal and squamosal) and lower temporal bars (jugals and quadratojugals) are missing therefore the morphology and position of the orbits, supratemporal fenestra and infratemporal fenestra are unknown. Because of the damage to this region of the skull however, the braincase/cerebral fossa is visible. The walls of the supratemporal fenestra are partially preserved. Lateral to the braincase, the pterygoid wings are visible in the matrix in dorsal view due to dorsoventral deformation. In the posterior region of the skull much of the left side is missing, however fractured surfaces allow for reconstruction of the position of some bone elements. The left exoccipital is incomplete, preserving only the ventral region in occipital view. The caudal projections of the pterygoids are visible in occipital view lateral to the basioccipital. The curved shape is a result of deformation (Figure 2.10).

The postorbital region of the skull has been fully prepared and the ventral surface is visible (Figure 2.9). In ventral view the postorbital region of the skull shows evidence of compression however the nature of the contacts between the bones can be reconstructed and the position of the choana and posterior border of the suborbital fenestra can be inferred. The left ectopterygoid is partially preserved, showing the posteriormost fragment.

Cranial openings:

The external naris is circular and relatively large, occupying nearly half the total mediolateral width of the premaxilla (Figure 2.13). The naris opens dorsally and is flush with the dorsal surface of the premaxilla, it is bordered entirely by the premaxilla. The external otic aperture is well preserved on the right lateral view, it is bordered by the squamosal and the quadrate (Figure 2.11). The foramen magnum has a compressed ovoid shape, bordered by the exoccipital and the basioccipitals (Figure 2.10). The foramen vagi is positioned lateral to the occipital condyle. The lateral eustachian foramina are level with the base of the occipital condyle and position dorsal to the medial eustachian foramen, plesiomorphic to Crocodylia (Figure 2.9, 2.10). The medial eustachian foramen is visible in ventral view between the medial groove in the basioccipital and the basisphenoid. The choana positions anterior to the medial eustachian foramen (Figure 2.9). The choana is formed completely by the pterygoids and when reconstructed, the choana is circular in shape, and not septate. There is no evident depression anterior and lateral to the choana. The pterygoids form the posterior angle and the palatines the medial border of the suborbital fenestrae.

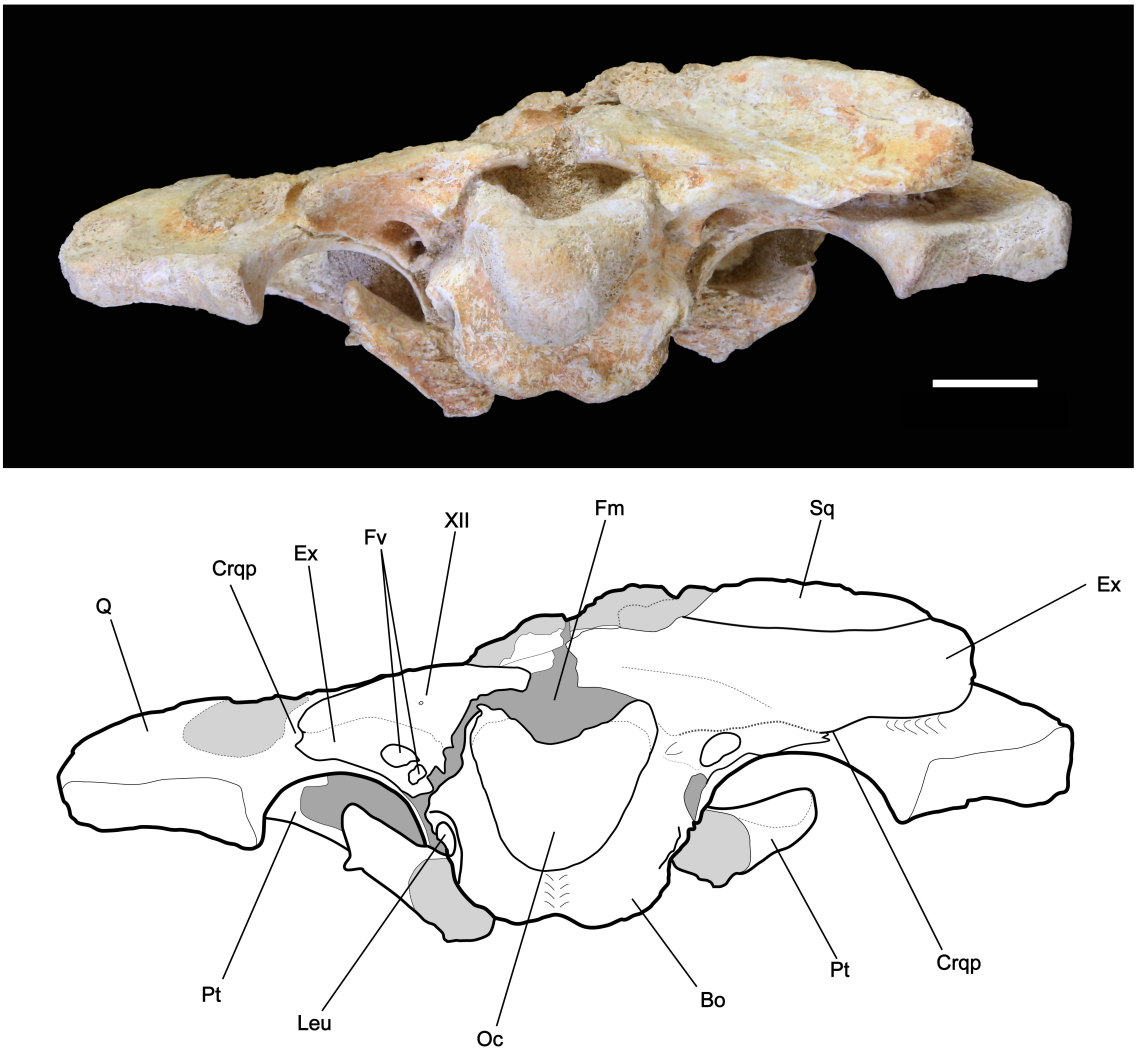

Figure 2.10 *Parvosuchus daouiensis,* holotype MHNM.KHG.168. Skull in occipital view. Scale bar = 10mm. Areas of dark shading are obscured by matrix, areas of light shading mark breakage surfaces on the bone. **Abbreviations: Bo**, basioccipital, **Crqp,** cranioquadrate passage, **Ex,** exoccipital, **Fm,** foramen magnum, **Fv,** foramen vagi, **Leu**, lateral eustachian foramen, **Oc,** occipital condyle, **Pt,** pterygoid, **Q,** quadrate, **Sq,** squamosal, **XII,** foramen for cranial nerve XII

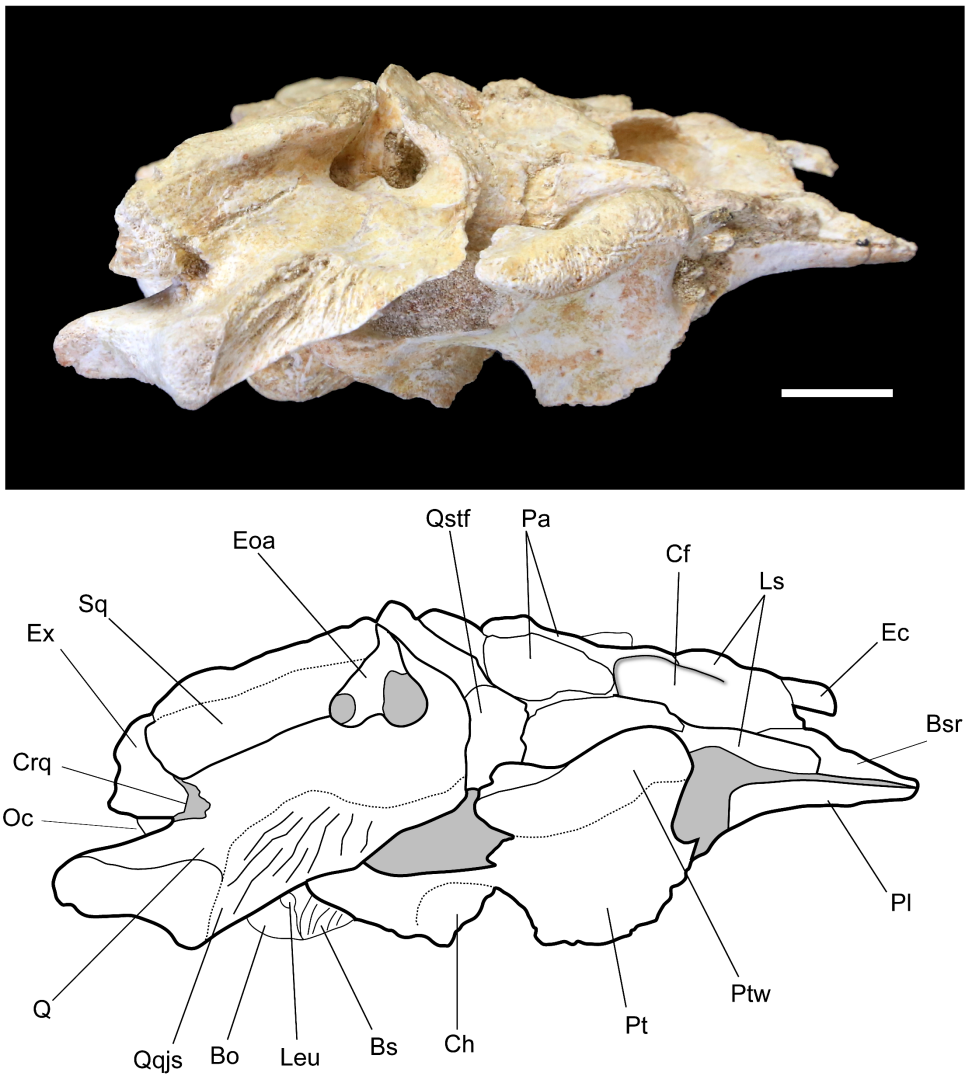

Figure 2.11 *Parvosuchus daouiensis,* holotype MHNM.KHG.168. Prepared, posterior portion of the skull in right lateral view. Scale bar = 10mm. Areas of dark shading indicate the presence of matrix. **Abbreviations: Bo,** basioccipital, **Bs,** basisphenoid, **Bsr**, basisphenoid rostrum, **Cf**, cerebral fossa, **Ch,** choana, **Crq,** cranioquadrate opening, **Ec,** ectopterygoid, **Eoa,** external otic aperture, **Ex,** exoccipital, **Ls**, laterosphenoid, **Pa**, parietal, **Pl,** palatine, **Pt,** pterygoid, **Ptw,** pterygoid wing, **Q,** quadrate, **Qqjs**, suture surface for the attachment of the quadratojugal, **Qstf**, quadrate on the supratemporal fenestra wall, **Sq,** squamosal

Cranial bones:

The premaxillae contrast to *Argochampsa* spp., as they are narrower and not wider than the mediolateral width of the rostrum. The premaxilla has five alveoli and on the left premaxilla four complete teeth are preserved in situ. Three alveoli are visible on the right premaxilla in the first, second and fifth position, with teeth preserved in the second and fifth position. The teeth are homodont and equally spaced. The first and second premaxillary teeth are positioned anteriorly and the final alveolus is positioned posterior to the external naris. An elongate diastema (16mm anteroposterior length) is present between the last premaxillary alveolus and the first maxillary alveolus. A diastema is also observed in the genus *Argochampsa* (Hua & Jouve 2004; Jouve et al. 2006b); however, it is not as elongate as in *Parvosuchus.* The posterior dorsal process of the premaxilla can be inferred to extend to the level of the second maxillary alveolus. The short posterior process (terminating anterior to the third maxillary alveolus) is shared with *A. microrhynchus*. This feature is uncommon amongst the Gavialoidea and Tomistominae, but is frequently observed in Crocodyloidea and Alligatoroidea (Brochu et al. 2012; Brochu 1999).

Figure 2.12 *Parvosuchus daouiensis,* holotype MHNM.KHG.168. Right lateral view of the rostrum, the matrix has been shaded out. Scale bar= 5cm.

Posterior to the external nares there is a shallow fossa (3.5mm depth) which is anteroposteriorly longer than wide. The lateral and posterior walls are visible on the left side (length: 14mm, width to midline: 5mm) but there is too much damage to the right. The anterior border is equivalent to the level of the last premaxillary alveolus and it extends posteriorly along the length of the diastema (Figure 2.13). There appears to be a defined wall between the nares and the fossa which would suggest these two regions are separate, however due to damage this cannot be concluded with certainty. Although different in morphology to the narial fossa observed in *Rhamphosuchus* and *Gavialis*, it may serve a similar function only visible in soft tissue; in the extant species this soft tissue ghara has a sexual selection function (Martin & Bellairs 2009; Young et al. 2010). Alternatively it might be homologous to the narial fossa seen in the large caimans such as *Purussaurus* (Aguilera et al. 2006) and *Mourasuchus* (Langston Jr. 1966). However, the function of this is unclear.

The maxillae show minor ornamentation in the form of sinuous shallow grooves, typical for gavialoids. Nineteen alveoli can be confirmed on the left maxilla and twenty on the right. Comparing both sides of the maxilla, a tooth count of at least 22 can be inferred, although this count may be higher as the posterior process is missing. There are 9 teeth preserved on the left and 10 on the right (Figure 2.12), these show homodont dentition and the alveoli are equally spaced along the length of the rostrum. The alveoli project

anterolaterally, giving the maxilla a scalloped appearance along the lateral margins, though not as extreme as in *Argochampsa microrhynchus* and *Ikanogavialis gameroi* (Sill 1970). All teeth along the maxilla are positioned in a similar direction and angle, suggesting that that the teeth have not been strongly displaced during preservation. The teeth are slender and gently recurved posteriorly, there are no clear carinae or striations on the tooth surface.

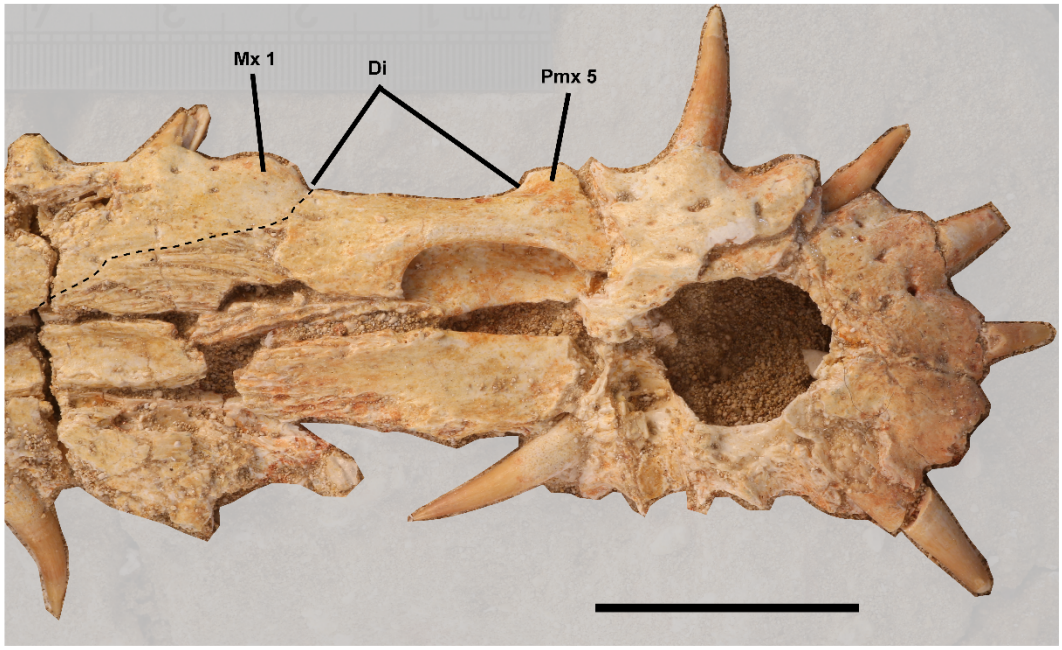

Figure 2.13 *Parvosuchus daouiensis,* holotype MHNM.KHG.168. Close up view of the premaxillary region of the rostrum showing the shape of the fossa, posterior to the external naris. The broken surfaces on the right premaxilla mirror the position of bone on the left suggesting that pit on the right premaxilla would be symmetrical. The matrix has been shaded out. Scale bar= 2cm. The dashed line shows the outline of the suture surface on the maxilla for the attachment of the premaxilla. **Abbreviations: Di,** diastema, **Mx 1,** first maxillary tooth, **Pmx 5,** 5th premaxillary tooth

The nasals are fused medially and visibly extend to the level of the third maxillary alveolus, but the anterior extent of the contact between the nasals and premaxilla is not clear. The nasals are laterally expanded posteriorly, which differs from the uniform width observed in *Argochampsa* (Figure 2.7, 2.8). The broad, serrate contact between the frontal and nasal is shared with *Argochampsa* and *Eosuchus lerichei*, differing from the condition in most gavialoids and tomistomines in which the contact terminates in an acute point. Only the anteriormost process of the frontal is preserved extending well anterior of the orbits, but posterior to the prefrontal and lacrimal.

The prefrontal anterior process extends beyond the level of the frontal-nasal contact, which is observed in more primitive members of Gavialoidea such as *Thoracosaurus, Eosuchus* and the African gharials (Jouve, Bardet, et al. 2008; Brochu 2006a; Delfino et al. 2005;

Carpenter 1983; Koken 1888; Storrs 2003; Andrews 1906). The anterior extension of the prefrontal is modest in *Parvosuchus daouiensis* unlike the extreme degree of extension seen in *Ocepesuchus eoafricanus* (Jouve, Bardet, et al. 2008). The lacrimals extend anteriorly to the level of the 14-15th maxillary alveoli, far anterior to the prefrontals, a plesiomorphic trait of Eusuchia.

The anterior process of the jugal terminates level with the 22nd maxillary alveolus, posterior to the anterior extent of the frontal; a character shared with gavialoid taxa including *Gavialis*, *Piscogavialis jugaliperforatus, Ikanogavialis gameroi* and *Eothoracosaurus mississippiensis* (Brochu 2004; Sill 1970; Kraus 1998). Posterior to the contact, the jugal strongly flares laterally. The medial jugal foramen is small.

The posterior portion of the cranium is poorly preserved, with only fragments of the parietal and the squamosal available for comparative comments. The parietal is partially preserved on the dorsal surface of the cerebral fossa (Figure 2.8, 2.9, 2.11) and contacts the laterosphenoid ventrally, on the lateral walls of the braincase. Posteriorly, the parietal contacts the quadrate on the posterior wall of the supratemporal fenestra. However, the nature of the parietal-squamosal contact is uncertain. Laterally the squamosal contacts the quadrate with a linear suture that extends to the caudal margin of the external otic aperture. Anterior to the aperture the squamosal is not preserved, therefore the shape of the squamosal groove cannot be determined. The squamosal prong is elongate and projects posterolaterally, contacting the exoccipital at the paroccipital process. The elongate squamosal prong is observed in the Argochampsinae and Gryposuchinae (Vélez-Juarbe et al. 2007).

Suture surfaces on the quadrates show that the quadratojugals contact the quadrate anterior to the lateral articulation surface. The quadrates are well preserved and project only a short distance posterior of the paroccipital process (4mm). The medial hemicondyle is small and ventrally reflected, observed in *Borealosuchus* and Gavialoidea to exclusion of the rest of the Crocodylia. The cranioquadrate canal is visible on the occipital surface and is formed between the quadrate and the exoccipital paroccipital process. The foramen aereum is not visible on the dorsal surface of the quadrate.

The exoccipitals form a large portion of the occipital surface, which is inclined and visible in dorsal view. The exoccipital contact with the squamosal is smooth and visible on the occipital face (Figure 2.10). The ventral border of the exoccipital is slightly convex and does not hide the posterior opening of the cranioquadrate passage in occipital view, this is expressed in Eusuchia to the exclusion of Gavialoidea and is apomorphic to *Parvosuchus daouiensis.* The exoccipital contacts the quadrate medial to the cranioquadrate canal and projects ventromedially, lateral to the basioccipital tubera. The ventral extent of the exoccipitals is uncertain.

The basioccipital forms the lateral and ventral margins of the foramen magnum and the occipital condyle (Figure 2.10). Ventral to the occipital condyle the basioccipital is dorsoventrally short and gently curved with a medial groove. The short basioccipital is common for more derived members of the Gavialoidea, relative to the long, flattened morphology typical of the Crocodylia. The medial groove is not as deep in *Parvosuchus daouiensis*, compared to *Argochampsa* and *Gavialis* (Hua & Jouve 2004; Hecht & Malone 1972). The basisphenoid is visible in ventral view and is present as a very thin lamina anterior to the basioccipital (Figure 2.9). The basisphenoid forms the anterior margin of the medial eustachian foramen. The preserved portion is roughly triangular and shows the suture surface for contact with the pterygoids. The laterosphenoids are preserved on the lateral walls and the ventral wall of the cerebral fossa. The anterior portion of the braincase is missing and the capitate process of the laterosphenoid is not preserved.

The posterior wings of the pterygoids position posterior to the posterior border of the choanal opening (Figure 2.8, 2.9, 2.11). The posterior processes of the pterygoids are tall and prominent**.** Only the posteriormost portion of the palatine is visible. Reconstruction of the contacts would suggest a linear contact between the palatines and pterygoids, far from the posterior angle of the suborbital fenestra**.** The ectopterygoid contacts the pterygoid laterally, close to the posteriormost extension of the pterygoid wing.

Phasmatosuchus n. gen

Type species: *Phasmatosuchus decipulae* gen. et sp. nov.
Etymology: The genus is derived from *phasma*, Greek, "apparition", and *suchus* Greek *soûkhos (*σοῦχος) "crocodile".
Diagnosis: as diagnosis for species

Phasmatosuchus decipulae sp. nov. (Figure 2.14-2.20)

Etymology: The species name is derived from *decipula*, Latin, trap. This is based on the arrangement of teeth in the species.
Holotype: MHNM.KHG.166 partial skull with associated vertebrae and skull fragments
Paratype: MHNM.KHG.167 incomplete skull
Horizon and locality: Couche II, Thanetian, Sidi Daoui locality in the Oulad Abdoun basin, Morocco
Diagnosis: Quadrates are short, terminating posteriorly at the same level as the paroccipital process; quadrate participates in the infratemporal fenestra; fronto-parietal suture concavo-convex. Autapomorphies include: >43maxillary teeth, maxillary alveoli oriented laterally on the rostrum, snout length >83% total skull length. The nasals terminate far posterior to the premaxilla and external nares (nasals and premaxilla not in contact); maxillae meet medially, anterior to the nasals.

Description:

Preservation and general form:

This species is described based on two incomplete specimens, both lacking the tip of the rostrum (Figure 2.14, 2.18). The species is longirostrine, with a hyper-elongate rostrum, accounting for a minimum of 83% of the total skull length. In the associated matrix of the holotype, an additional fragment of maxilla was found and is assumed to belong to this specimen. This increases the rostral proportion of the dorsal skull length to 85%. The maxilla is mediolaterally narrow (Table 2.1) with straight maxillary margins and homodont dentition. The maxillary alveoli position laterally on the rostrum projecting laterally and anteriorly. The quadrates do not extend posteriorly beyond the level of the paroccipital process.

There is minimal ornamentation on both specimens. For the rostrum, this is typical for gavialoids, which show minimal/no ornament on the rostrum. Ornamentation on the lacrimal, prefrontal, frontal is greatly reduced in the form of small shallow pits. Ornamentation is typically denser with deep pitting in gavialoids in this region of the skull.

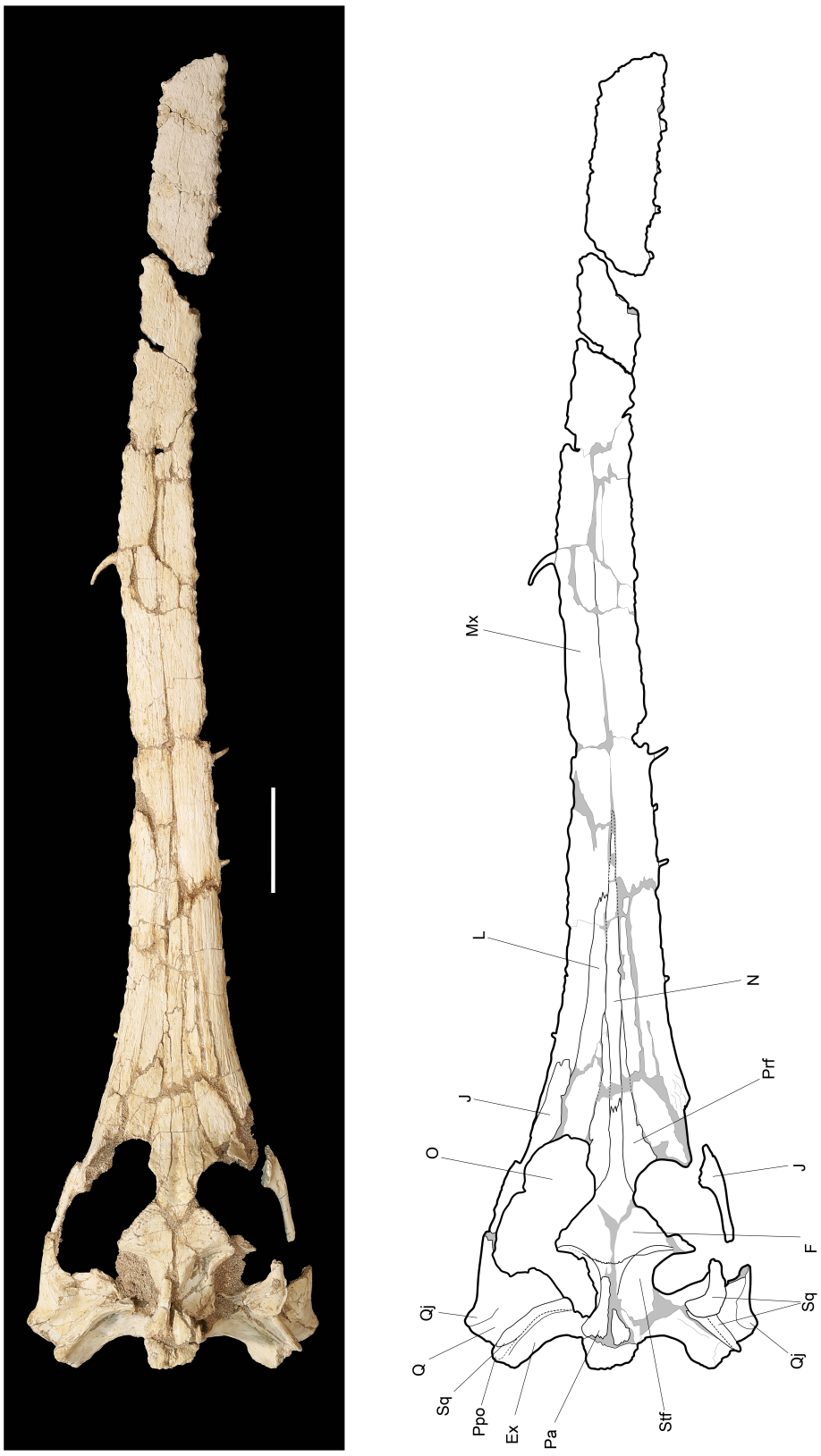

Figure 2.14 *Phasmatosuchus decipulae,* holotype MHNM.KHG.166, Paleocene, Couche II, Oulad Abdoun basin, Morocco. Skull in dorsal view. Scale bar = 5cm. **Abbreviations: Ex,** exoccipital, **F,** frontal, **J,** jugal, **L,** lacrimal, **Mx,** maxilla, **N,** nasal, **O,** orbit, **Pa,** parietal, **Ppo,** paroccipital process, **Prf,** prefrontal, **Q,** quadrate, **Qj,** quadratojugal, **Stf,** supratemporal fenestra, **Sq,** squamosal

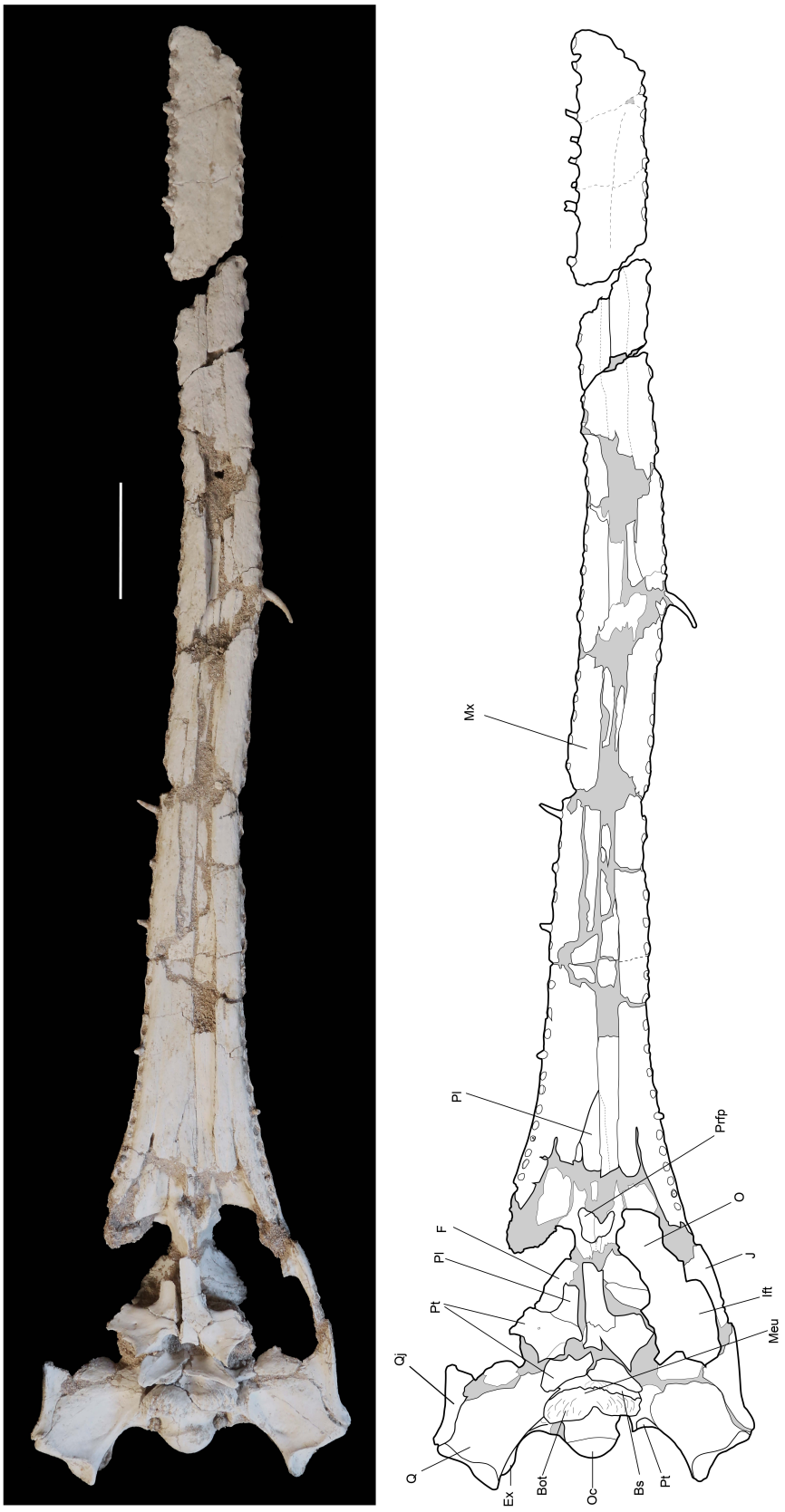

Figure 2.15 *Phasmatosuchus decipulae,* holotype MHNM.KHG.166. Skull in ventral view. Scale bar = 5cm. **Abbreviations: Bot,** basioccipital tubera, **Bs,** basisphenoid, **Ex,** exoccipital, **F,** frontal, **Itf,** infratemporal fenestra, **J,** jugal, **Mx,** maxilla, **Meu,** medial eustachian foramen, **O,** orbit, **Oc,** occipital condyle, **Pl,** palatine, **Prfp,** prefrontal pillar, **Pt,** pterygoid, **Q,** quadrate, **Qj,** quadratojugal

The holotype is relatively complete, and several bone fragments were preserved in associated matrix, which are assumed to belong to this specimen. The anterior tip of the rostrum is missing and therefore the total length/tooth count is equivocal, the holotype rostrum is more complete than the paratype. The premaxilla is not preserved and there is no evidence of the posterior processes of the premaxilla on the rostrum. When compared to the length of the posterior premaxillary process in other gavialoids, this suggests that there would be a minimum of at least three additional teeth on the maxilla (see character matrix-Appendix 1). The holotype is dorsoventrally compressed, and the posterior and lateral section of skull table is missing- the postorbitals are not preserved and the squamosals incomplete (Figure 2.14, 2.17). As a result, only the anteromedial borders of the supratemporal fenestrae are preserved. In palatal view the skull is heavily fractured; the infratemporal fenestra, suborbital fenestra, pterygoid wings and palatine are incompletely preserved and the ectopterygoids are missing (Figure 2.15). Associated material includes the posterior extension of both ectopterygoids with the contact with the pterygoids. The anterior and posterior regions of the palatine are preserved, but the middle region corresponding to the position of the medial borders suborbital fenestrae is missing. As a result, the prefrontal pillar is exposed, though the ventral surface is broken. On the occipital face the occipital condyle and basioccipital have been displaced dorsally and the top of the skull table displaced dorsally and laterally (Figure 2.16).

The paratype shows minimal dorsoventral compression but the rostrum is less complete than the holotype (Figure 2.17, 2.18). The postorbital region of the skull is more complete has been partially reconstructed (Figure 2.17-2.20). The posterior region of the left side of the frontal, the postorbitals and jugals are the areas reconstructed (highlighted in Figure 2.18, 2.20) and will not be included in the anatomical interpretation of this fossil. In ventral view the matrix is embedded and the skull highly fractured, as a result, the anterior morphology of the palatine cannot be discerned and the ectopterygoids are missing. The pterygoid wings are missing, and the pterygoids are broken and dorsally displaced around the lateral borders of the choana. The occipital face of the paratype is more complete than the holotype (Figure 2.19).

Cranial openings:

The external nares and foramen incisivum are not preserved in either specimen. The orbits are more complete in the paratype (Fig. 2.17-2.20), and the orbital margins are upturned vertically by the prefrontals, lacrimals and jugals. This gives the “telescoped” orbit observed in *Gavialis* and *Gryposuchus* (Langston Jr. & Gasparini 1997; Salas-Gismondi et al. 2016). The borders of the supratemporal, infratemporal and suborbital fenestrae are incompletely preserved. The supratemporal fenestrae (paratype) are large, occupying most of the skull table (Figure 2.18).

The choana is oval with no septum and inset, it is bordered entirely by the pterygoid. The choana is positioned posteriorly, close to the medial eustachian foramina and basisphenoid (Figure 2.15, 2.18). The foramen magnum is bordered by the basioccipital and the exoccipital, and the supraoccipital does not participate in the border. The foramen aereum is not visible on either specimen. The medial eustachian foramen is located between the basioccipital tubera and basisphenoid and the vagus foramina (holotype) are preserved on each exoccipital, lateral to the occipital condyle (Figure 2.16).

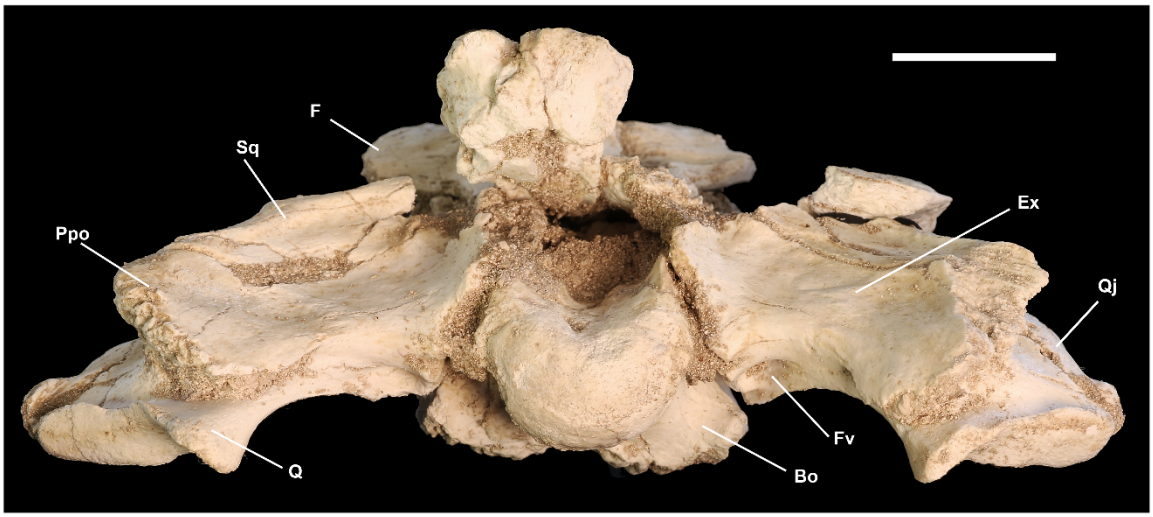

Figure 2.16 *Phasmatosuchus decipulae,* holotype MHNM.KHG.166. Skull in occipital view. Scale bar = 2cm. Dorsoventral compression has displaced the occipital condyle relative to the skull table. **Abbreviations: Bo,** basioccipital, **Ex,** exoccipital, **F,** frontal, **Fv,** foramen vagi, **Ppo,** paroccipital process, **Q,** quadrate, **Sq,** squamosal

Cranial bones:

The maxilla has a scalloped lateral margin due to laterally directed maxillary alveoli, though less pronounced than *Argochampsa* spp. and *Parvosuchus daouiensis*. The maxillae meet medially, anterior to the termination of the nasals. Anteriorly, the maxillae are fused (Figure 2.14, 2.18). The alveoli are circular in cross section (4mm diameter), on the left maxilla 43 alveoli are preserved and on the right 50, including the associated maxillary piece. There are five partial teeth preserved on the left maxilla and one complete tooth (this is not preserved in life position). There are remains of seven teeth on the right maxilla and an additional seven incomplete teeth preserved on the right maxilla of the associated piece. The teeth are similar in morphology to the other Moroccan gavialoids. They are small, slender and recurved, showing minimal striations or carinae on the surface. The posteriormost alveoli are oriented ventrally, anteriorly the alveoli rotate to a lateral position along the rostrum (Figure 2.15, 2.17, 2.20). The spacing between the alveoli and the curvature of the teeth suggest that the teeth might interlock in a comb-like arrangement, projecting laterally from the rostrum and curving ventrally to create a mesh.

The nasals are fused and have a limited anteroposterior length. They do not form a contact with the premaxilla or the external nares, a character shared with *Gavialis*. The nasals form a broad sutural contact with the frontal and do not extend posteriorly between the frontals and prefrontals, this unites the Argochampsinae to the exclusion of all other gavialoids.

Figure 2.17 *Phasmatosuchus decipulae,* **A** paratype MHNM.KHG.167 **B** MHNM.KHG.166. Skulls in right lateral view. Scale bar = 5cm. Grey shading on the paratype indicates areas of reconstruction on the skull.

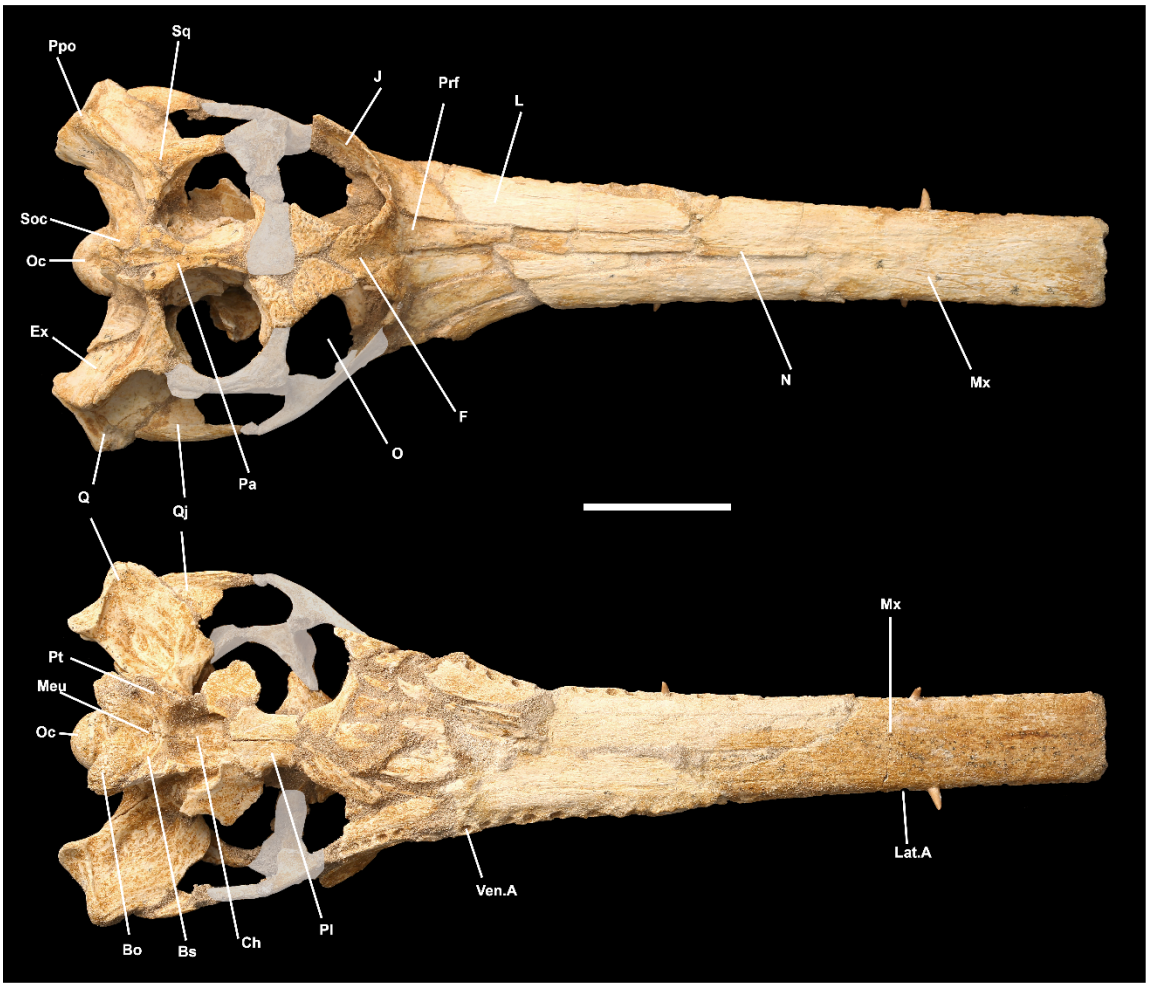

Figure 2.18 *Phasmatosuchus decipulae,* paratype MHNM.KHG.167. Skull in dorsal and ventral view. Scale bar = 5cm. Grey area indicates where the skull has been reconstructed (not included in the anatomical interpretation). **Abbreviations: Bo,** basioccipital, **Bs,** basisphenoid, **Ch,** choana, **Ex,** exoccipital, **F,** frontal, **J,** jugal **L,** lacrimal, **Lat.A,** laterally projecting alveolus, **Meu,** medial eustachian foramen, **Mx,** maxilla, **N,** nasal, **O,** orbit, **Oc,** occipital condyle, **Pa,** parietal, **Pl,** palatine, **Ppo,** paroccipital process, **Prf,** prefrontal, **Pt,** pterygoid, **Q,** quadrate, **Qj,** quadratojugal, **Soc,** supraoccipital, **Sq,** squamosal, **Ven.A,** ventrally projecting alveolus

The prefrontals terminate anterior to the frontals but posterior to the lacrimals (Figure 2.14). The dorsal portion of the prefrontal pillar is preserved in the holotype, in line with the anterior border of the orbits (Figure 2.15). The prefrontal pillar is solid, lacking a large pneumatic sinus. The dorsal half is anteroposteriorly expanded. The paratype preserves the contact with the palatine on the ventral portion of the pillar, the medial process is expanded dorsoventrally. The lacrimals form part of the anterior margin of the orbits. The anterior extent of the lacrimals is not clear. The lacrimal duct is visible on the left orbit of the paratype.

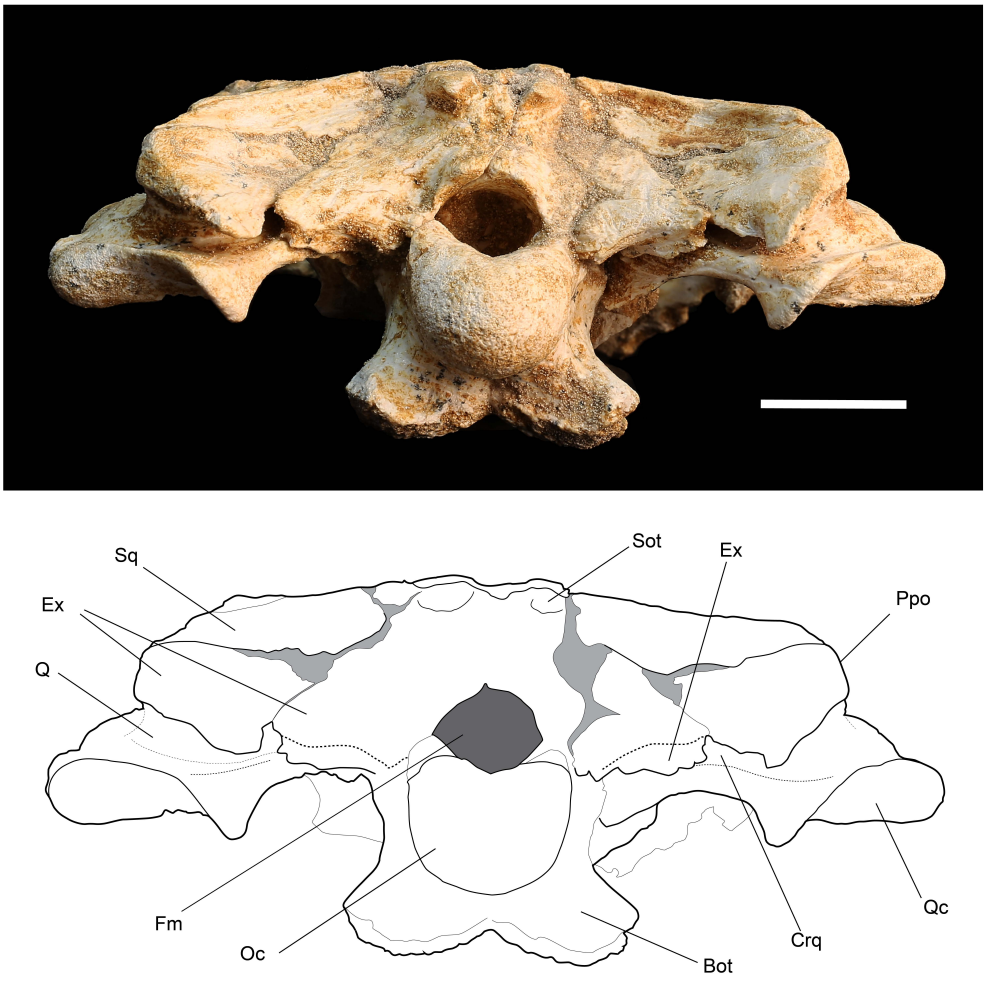

Figure 2.19 *Phasmatosuchus decipulae,* paratype MHNM.KHG.167. Skull in occipital view. Scale bar = 2cm. **Abbreviations: Bot,** basioccipital tubera, **Crq,** cranioquadrate passage, **Ex,** exoccipital, **Fm,** foramen magnum, **Oc,** occipital condyle, **Ppo,** paroccipital process, **Q,** quadrate, **Qc,** quadrate condyle, **Sot,** supraoccipital tuberosity, **Sq,** squamosal

The frontal anterior process does not extend far beyond the anterior border of the orbits. The interorbital bar is narrow. The frontoparietal suture is concavo-convex and makes a modest entry into the supratemporal fenestra (Figure 2.14). The anterior process of the jugal extends anterior to the anterior process of the frontal, plesiomorphic to Crocodylia. The jugals form the anterolateral border of the orbits, which are raised vertically (Figure 2.17).

The parietal forms the medial and posteromedial border of the supratemporal fenestra. It contacts the frontal at the anteriormost portion of the interfenestral bar. It is unclear if the supraoccipital is exposed on the dorsal surface, but a contact is visible with the parietal on the occipital face on the paratype (Figure 2.19). The supraoccipital has large lateral posterior tuberosities which are visible in dorsal view, a character shared amongst gavialoids and tomistomines to the exclusion of Crocodylia.

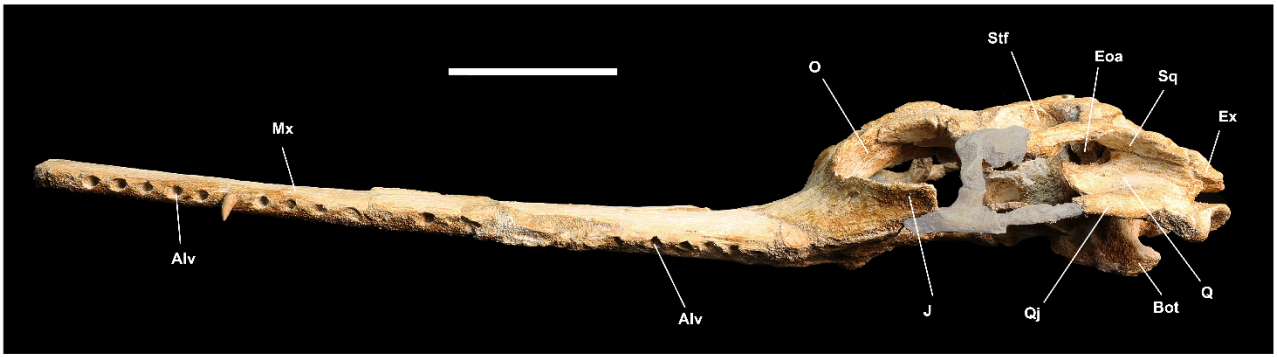

Figure 2.20 *Phasmatosuchus decipulae,* paratype MHNM.KHG.167. Skull in left lateral view. Scale bar = 5cm. Grey area indicates where the skull has been reconstructed (not included in the anatomical interpretation). **Abbreviations: Alv,** alveoli, **Bot,** basioccipital tubera, **Crq,** cranioquadrate passage, **Eoa,** external otic aperture, **Ex,** exoccipital, **J,** jugal, **Mx,** maxilla, **O,** orbit, **Q,** quadrate, **Qj,** quadratojugal, **Sq,** squamosal, **Stf,** supratemporal fenestra

The squamosals make up the posterolateral margin of the supratemporal fenestra. The squamosal prongs project posterolaterally, terminating at the tip of the paroccipital process (Figure 2.14, 2.18). The squamosal prongs are very long, a character shared with *Argochampsa* and *Parvosuchus*, and the South American gavialoids (Sill 1970; Kraus 1998; Brochu & Rincon 2004). In lateral view, the contact with the quadrate extends along the caudal margin of the external otic aperture (Figure 2.17, 2.20).

Unlike *Parvosuchus daouiensis*, the quadrates of *Phasmatosuchus decipulae* are not posteriorly extended. In dorsal view, they extend to almost the same level as the paroccipital processes. The medial hemicondyle of the quadrate is ventrally projected (Figure 2.16, 2.19). The cranioquadrate passage is visible in the paratype due to damage to the bone, but this is hidden by the exoccipital in the holotype. It is not clear if the quadrate participates in the infratemporal fenestra. The contact with the quadratojugal extends to the lateral corner of the lateral hemicondyle.

The exoccipital is visible in dorsal view as the occipital face is inclined, a typical gavialoid feature. The basioccipital forms the ventral margin of the foramen magnum and the occipital condyle (Figure 2.16, 2.19). The condyle is distinctly larger than the foramen magnum (Table 2.1). The basioccipital tuberosities are large and pendulous with a deep medial groove separating the two tuberosities. They are more strongly developed than in *Parvosuchus daouiensis* and the overall morphology is similar to *Argochampsa* and derived gavialoids, *Gryposuchus* and *Gavialis.* The basisphenoid is thin and not broadly exposed ventral to the basioccipital.

In ventral view, the palatine anterior process projects significantly beyond the anterior margin of the suborbital fenestra and terminates in an acute point. The palatine forms the medial border of the suborbital fenestra, the lateral edges of the palatines are parallel sided. The contact with the pterygoid is positioned far from the posterior angle of the suborbital fenestra (Figure 2.15, 2.18).

Eusuchia Huxley 1875
Crocodylia Gmelin 1789
Crocodyloidea Fitzinger 1826 *sensu* Brochu 2003
Tomistominae Kälin 1955 *sensu* Brochu 2003
Maroccosuchus Jonet and Wouters 1977

Type species: *Maroccosuchus zennaroi* Jonet and Wouters 1977
Genus Diagnosis. Robust and largely wider than high snout; pterygoid surface pushed inward anterolateral to the choanal aperture; maxillary foramen for palatine ramus of cranial nerve V very large; mandibular symphysis nearly twice wider than high; 11th dentary tooth is the largest, larger than the 4th, plesiomorphic to Crocodylidae. The mandibular symphysis reaching the level of the 9th tooth unites gavialoids and tomistomines, and the splenial participating in the symphysis over a length corresponding to three teeth is shared amongst basal Tomistominae.

Holotype: IRSNB R408, skull, mandible and postcranial material from Couche 1, Ypresian, Sidi Daoui, Oulad Abdoun Basin, Morocco
Referred specimens: MHNM.KHG.171 skull, MHNM.KHG.172 skull and vertebrae, MHNM.KHG.173 skull (juvenile) (Figure 2.21, 2.22, 2.23)
Horizon and Locality: MHNM.KHG.171 and 172, Couche 0, Sidi Chennane locality in the Oulad Abdoun Basin, Morocco. MHNM.KHG.173 from Couche I (Ypresian), Sidi Daoui locality.
Revised species diagnosis: *Maroccosuchus* characterised by a moderately elongate rostrum, 70-74% of median skull length; narrow interorbital bar; supraoccipital not exposed on the dorsal surface of the skull table.

Description:

Preservation and general form:

Three new skulls are here referred to *Maroccosuchus zennaroi*. All specimens are relatively small in size compared to the published material (Jouve et al. 2014) and are inferred to represent ontogenetically younger specimens (Table 2.1 and discussion). MNHM.KHG.171 and MHNM.KHG.172 (Figure 2.21) are only visible in dorsal view. The skull of MNHM.KHG.171 is complete, though there is some damage to the posteriormost extension of the quadrates. MHNM.KHG.172 represents a nearly complete skull and in the associated matrix, four vertebrae in articulation are preserved. The left side of the skull is more complete, though due to damage on the postorbital bar the contact between the jugal and postorbital is not discernible. On the right side of the cranium, part of the rostrum is missing anterior to the orbits and the anterior margin of the orbits is damaged. The right lower temporal bar is partially preserved but displaced laterally in the matrix. The postorbital bar and infratemporal fenestra are not preserved. The right quadrate is poorly preserved posteriorly, the articulation surface with the lower jaw is missing and therefore the posterior extent of the quadrate-quadratojugal contact cannot be confirmed.

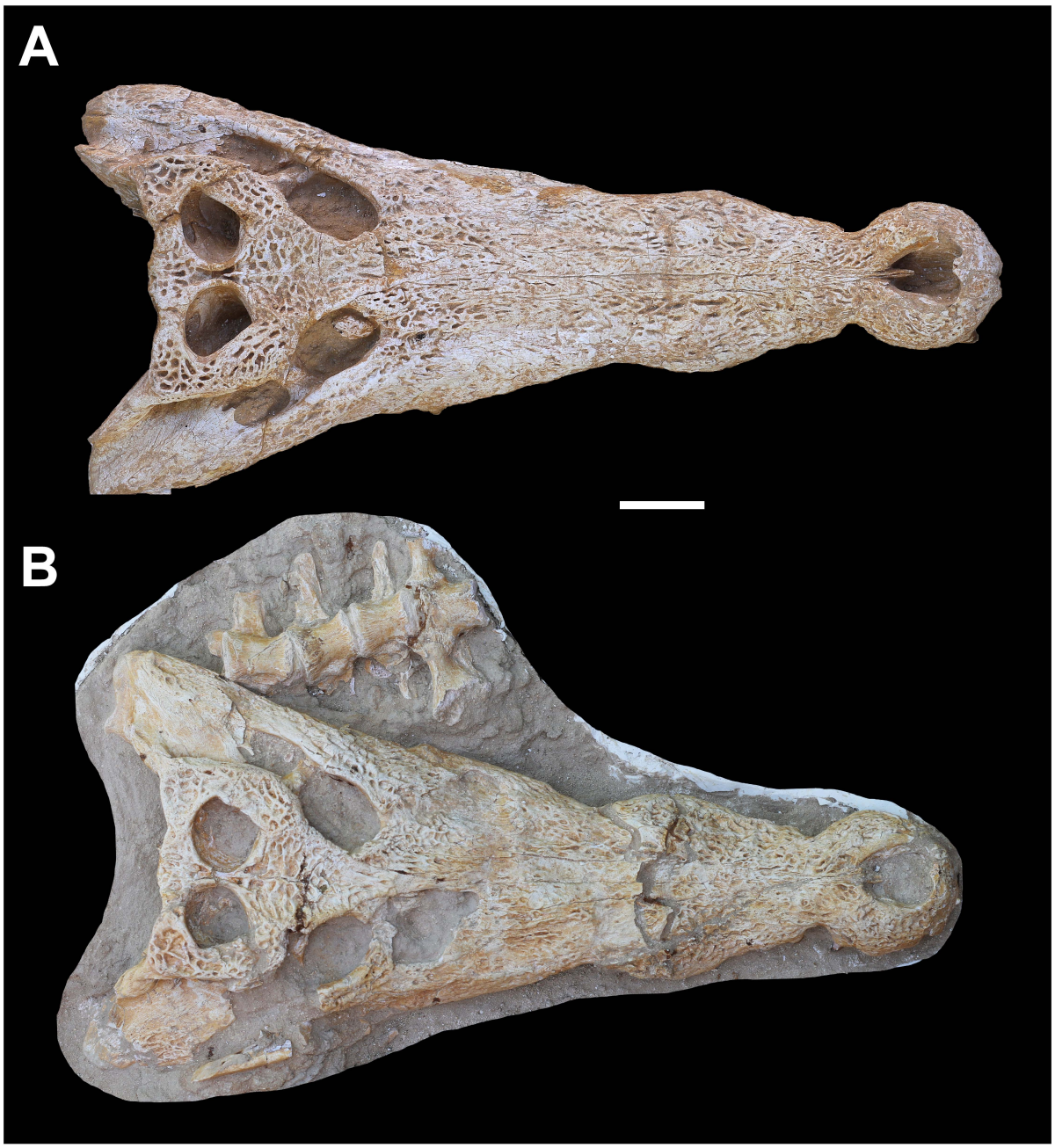

Figure 2.21 *Maroccosuchus zennaroi* referred material, skulls in dorsal view. **A** MHNM.KHG.171, **B** MHNM.KHG.172. Scale bar = 5cm.

The smallest of the three skulls, MHNM.KHG.173 (Figure 2.22, 2.23), is complete showing minimal dorsoventral compression. In dorsal view, there is some damage to the postorbital bars and quadrates, obscuring anatomical sutures. The quadrates are incomplete posteriorly and the articulation surface with the lower jaw is missing. In ventral view, the palate is complete, though the left premaxilla is partially broken anteriorly. The first and third premaxillary alveoli are incompletely preserved. Posteriorly the pterygoids are incomplete, only the medial region surrounding the choana is preserved. The external surface of the pterygoid surrounding the choana is heavily fractured and due to damage posterior to the choana, the basioccipital and basisphenoid morphology is equivocal.

The overall morphology of the skull material shows the plesiomorphic condition for the Crocodyloidea, exhibiting broad flattened rostra, with lateral maxillary waves and heterodont dentition. The sinusoidal margins of the rostra vary between the three specimens; MHNM.KHG.171 and MHNM.KHG.173 are more slender in overall morphology compared to MHNM.KHG.172, and the lateral waves are less pronounced. This difference in skull morphology is within the level of variation expected in an ontogenetic growth series, where younger members are typically more slender and less robust (Kälin 1933; Hall & Portier 1994; Webb & Messel 1978).

The ornamentation on all three specimens is consistent with ornamentation typically observed in crocodylians, to the exclusion of the Gavialoidea. Modest ornamentation is observed on the rostrum in the form of shallow pits and grooves. Posteriorly, around the orbital margins, lower temporal bars and skull table the ornamentation becomes more densely packed with deeper pitting. There is no ornament on the quadrates.

Cranial openings:

The external naris is large, occupying just less than half the width of the premaxilla. It is bordered laterally and anteriorly by the premaxilla and the anterior border has a short posterior process of the premaxilla. Posteriorly, the nasals contact and project anteriorly into the naris but do not bisect it. The naris is roughly teardrop shaped and larger than the foramen incisivum which does not extend beyond the narial borders. The foramen incisivum is small, roughly triangular and bordered entirely by the premaxilla. The posterior margin is posterior to the third premaxillary alveolus and the first dentary occlusion pit. The orbits are large, larger than the supratemporal fenestrae, and elliptical in shape. The infratemporal fenestra is smaller than the supratemporal fenestra and is bordered by the jugal, post-orbital and quadratojugal; the quadrate and the squamosals make a minor contribution to the dorsal margin. The supratemporal fenestrae vary in shape between all three specimens, MHNM.KHG.171-172 are roughly D-shaped, whereas MHNM.KHG.173 is longer than wide, the long axis 45° from the medial plane. The D-shape results from the linear margin from the postorbital. This level of variation is within the range expected for an ontogenetic series when compared to extant species (pers. obs.). The walls of the supratemporal fenestra are highly fractured and so the nature of contacts on the internal walls cannot be determined.

In ventral view, the suborbital fenestrae are large and anteroposteriorly elongate. The anterior border of the fenestrae is level with the 11th maxillary alveolus and anteriorly projects far beyond the anterior margin of the orbits. The posterior margin of the orbit is posterior/same level as the posterior margin of the suborbital fenestra. The choana is circular with no septum and projects at a posteroventral angle. In occipital view, the foramen magnum is dorsoventrally compressed; dorsally and laterally it is bordered by the exoccipital, ventrally by the basioccipital.

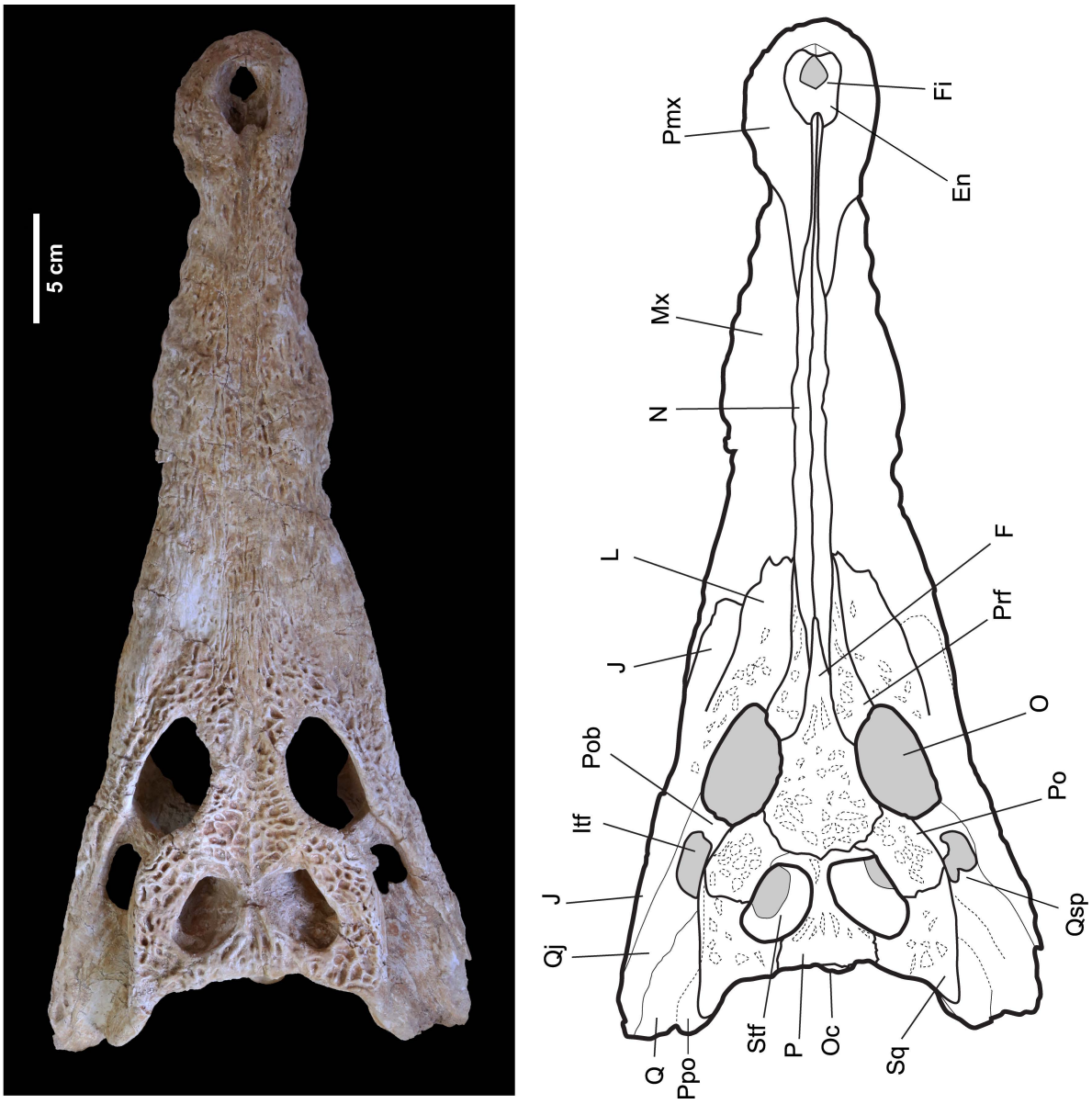

Figure 2.22 *Maroccosuchus zennaroi (juvenile)*, MHNM.KHG.173. Skull in dorsal view. Scale bar= 5cm. **Abbreviations: En,** external nares, **Fi,** foramen incisivum**, F,** frontal, **Itf,** infratemporal fenestra, **J,** jugal, **L,** lacrimal, **Mx,** maxilla, **N,** nasals, **O,** orbit, **Oc,** occipital condyle, **P,** parietal, **Po,** postorbital, **Pob**, postorbital bar, **Ppo,** paroccipital process, **Pmx,** premaxilla, **Prf,** prefrontal, **Q,** quadrate, **Qj,** quadratojugal, **Qsp,** spina quadratojugalis, **Sq,** squamosal, **Stf,** supratemporal fenestra

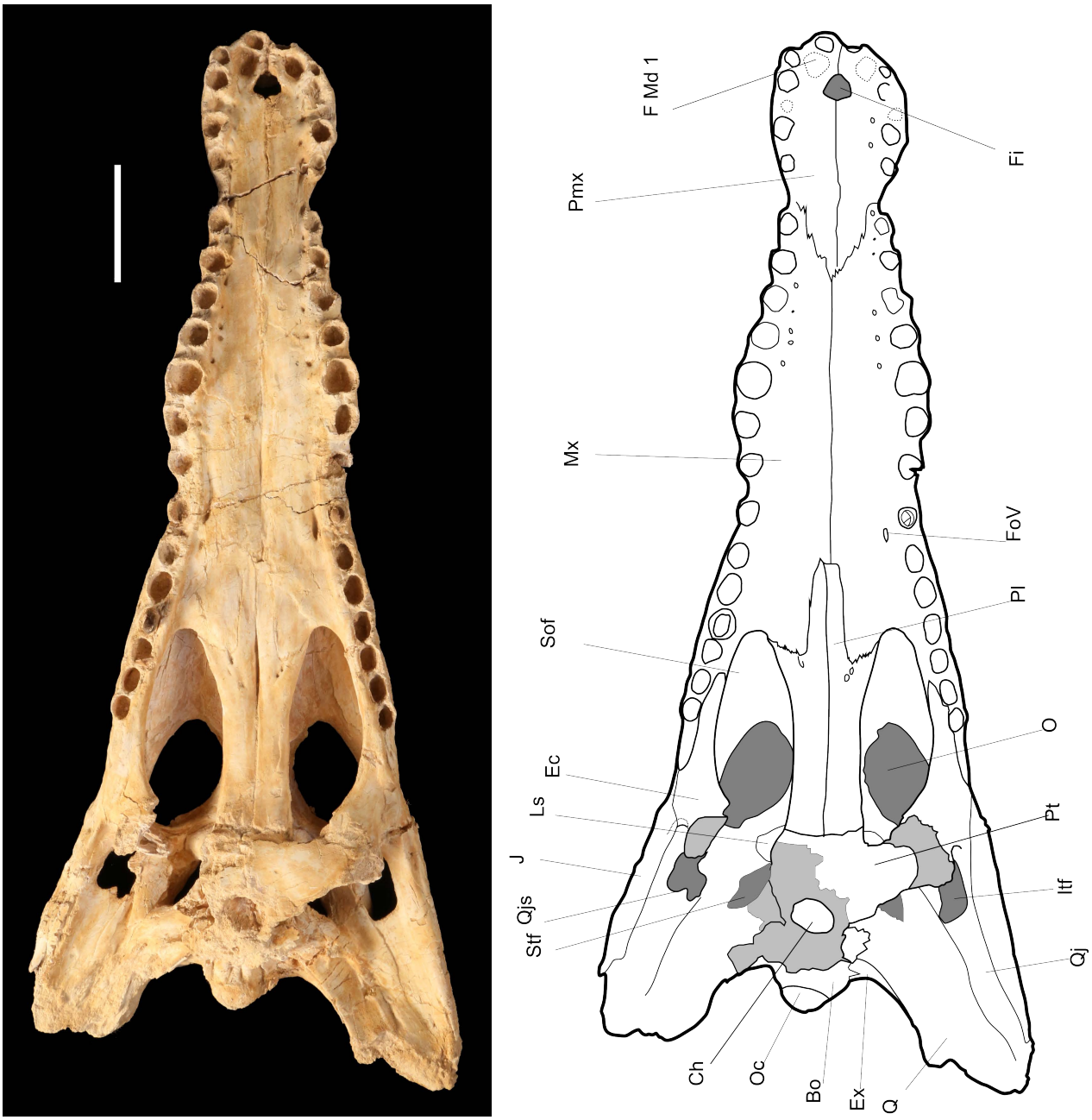

Figure 2.23 *Maroccosuchus zennaroi (juvenile)*, MHNM.KHG.173. Skull in ventral view. Light shading indicates areas where the surface is broken. Areas of dark shading are matrix. Scale bar= 5cm. **Abbreviations: Bo,** basioccipital, **Ch**, choana, **Ec,** ectopterygoid, **Ex,** exoccipital, **Fi,** foramen incisivum, **F Md1,** notch to receive of the first dentary tooth, **FoV,** foramen for palatine ramus of cranial nerve, **Itf,** infratemporal fenestra, **J,** jugal, **Ls,** laterosphenoid, **Mx,** maxilla, **O,** orbit, **Oc,** occipital condyle, **Pl,** palatine, **Pmx,** premaxilla, **Pt,** Pterygoid, **Q,** quadrate, **Qj,** quadratojugal, **Qjs,** spina quadratojugalis, **Sof,** suborbital fenestra, **Stf,** supratemporal fenestra

Cranial bones:

The premaxilla contains five alveoli with heterodont dentition. The fourth alveolus is the largest and all are roughly circular in shape. The interalveolar spacing is varied; there is wider spacing between the first and second alveoli and the third and fourth. This wider spacing corresponds to the position of occlusion pits in the ventral surface of the premaxilla, for the dentary teeth. The occlusion pit for the first dentary tooth is wide and deep, positioned posteriorly between the first and second alveoli. The second occlusal pit is small and shallow. The second premaxillary alveolus is smaller than the third and are very close together. The premaxillae are separated by the nasals posterior to the external nares. Dorsally, the posterior process of the premaxilla extends between the level of the third and fourth maxillary alveoli. In ventral view, the contact with the maxilla is anteroposteriorly short, extending to the second maxillary alveolus and forms a broad V.

In palatal view, MHNM.KHG.173 has 14 alveoli and two teeth are preserved in the eleventh position on the right and eighth on the left (Figure 2.23). As in the published description of *Maroccosuchus zennaroi* (Jouve et al. 2014) the teeth are robust, blunt and bullet shaped. The first lateral maxillary wave contains the first seven maxillary alveoli, constricting between the seventh and eighth alveoli. The maxillary alveoli are heterodont and the fifth alveolus is the largest. The maxilla flares laterally in a second wave posterior to the eighth alveolus. Posterior to the tenth alveolus the alveoli decrease in size becoming more laterally compressed. The maxillary foramen for the palatine ramus of cranial nerve V is large (Figure 2.23). The maxilla contributes to the anterolateral corner of the suborbital fenestra, contacting the exoccipital on the lateral border of the fenestra parallel to the 13th maxillary alveolus. The lateral maxillary posterior process is short and projects posteriorly for over one alveolar length behind the final alveolus. The palatine-maxillary suture intersects the suborbital fenestra posterior to the anteromedial corner of the fenestra and the maxilla sends a short process posteriorly into the palatine, not exceeding the level of the anterior quarter of the fenestrae.

In the published description for *Maroccosuchus zennaroi*, the prefrontals terminate posterior to the lacrimals. This is consistent with the two skulls MHNM.KHG.171 and MHNM.KHG.172. In MHNM.KHG.173, the prefrontals and lacrimals extend anteriorly to the same level. In ventral view, the position of the prefrontal pillar is preserved (MHNM.KHG.173) though the nature of the medial process cannot be determined as it is obscured by matrix. The dorsal half of the pillar is anteroposteriorly expanded. The anterior border of the lacrimal is broad and lateral to the nasal-lacrimal contact the maxilla sends a short posterior process within the lacrimal.

The frontal forms the posteromedial border of the orbits and does not participate in the supratemporal fenestra. The frontal process extends anteriorly between the nasals to form an acute point. In the published description of *Maroccosuchus zennaroi,* the frontal process ends level with the prefrontals; in all three new specimens the frontal ends posterior to the prefrontals (character 171) but this does not affect the coding of the character in the phylogenetic matrix. The position of the frontal with respect to the anterior extent of the jugal is variable in the referred material and published *M. zennaroi* skulls. In the referred material described here, the jugal extends anterior of the frontal, as observed in MHNT.PAL.2006.80.11 (Jouve et al. 2014), though in other published material the jugal and frontal terminate level with one another. This does not affect the phylogenetic inference as the coding remains the

same (character 174). The frontal is concave between the orbits. The frontoparietal suture is concavo-convex and is positioned entirely on the skull table and does not penetrate the supratemporal fenestra.

Behind the posterior process of the maxilla the jugals raise dorsally to contact the ectopterygoids, forming the anterolateral half of the border of the infratemporal fenestra. A gutter separates the lateral edge of the jugal and the postorbital bar. The jugal extends posteriorly just anterior to the lateral articulation surface of the quadrate.

The squamosals form the posterolateral margin of the supratemporal fenestra, contributing equally to the posterior border with the parietal. The squamosals form two short posteriorly directed prongs posterolateral to the supratemporal fenestra. In lateral view, the contact with the postorbital-squamosal contact passes ventrally beneath the postorbital. The dorsal and ventral rims of the squamosal groove for external ear musculature are parallel.

The quadratojugal participates in the posterior border of the infratemporal fenestra. The quadratojugal does not exclude the quadrate from the superior angle of the fenestra and sends a very short anterior process along the lateral margin of the fenestra. The spina quadratojugalis is small and low. The quadratojugal extends posteriorly to the corner of the lateral hemicondyle but does not contribute to the articulation surface. The quadrate forms the ventral margin of the external otic aperture, but the extension of the quadratosquamosal contact is unclear. The foramen aereum is not discernible on any of the skulls. The quadrates extend slightly posterior of the paroccipital process in the caudal region of the skull.

The supraoccipital is not exposed on the dorsal skull table. The lateral supraoccipital tuberosities on the occipital surface are small and not visible in dorsal view. The exoccipitals contact the squamosals at the base of the paroccipital process and form the ventral half of the occipital face. The ventral process of the exoccipital extends lateral to the basioccipital.

The palatine forms the medial margin of the suborbital fenestra and sends a broad process anteriorly into the maxilla to the level of the ninth alveolus. Palatine foramina are clearly visible just posterior to the maxilla-palatine contact (Figure 2.23). The nature of the contact with the pterygoid is unclear, but the contact appears to be linear at the posterior border of the suborbital fenestra.

The ectopterygoid comprises the posterior three quarters of the lateral margin of the suborbital fenestra. The contact with the maxilla runs medial to the toothrow, in the form of a thin wedge and abuts the last two maxillary teeth. The pterygoids form the posterior angle of the fenestra and contact the ectopterygoid on the posterolateral edge.

The anterior margin of the capitate process of the laterosphenoid projects posterolaterally from the medial plane. The bones are fully ossified and meet medially dorsal to the basisphenoid rostrum. The basisphenoid and prootic are not visible. The laterosphenoids contribute to at least the anterior border foramen ovale in MHNM.KHG.173.

Vertebrae:

Three cervical vertebrae and one sacral vertebra are preserved in articulation (MHNM.KHG.172). The vertebrae are proceolous, plesiomorphic to Crocodylia. As they are only visible in ventral view, little can be said about their anatomy.

Maroccosuchus brachygnathus sp. nov. (Figure 2.24)

Holotype. MHNM.KHG.170, skull and mandible
Horizon and Locality. Lower Ypresian Intercalary Bed (*Otodus obliquus* bed). The matrix is a heavily indurated sandstone with greenish mudstone inclusions that are characteristic of the intercalary bed that separates Couche I and Couche IIA (Kocsis et al. 2014).
Diagnosis. *Maroccosuchus* characterised by a short, broad rostrum, 69% of the median skull length. The species demonstrates the following characters which are inconsistent with the currently *Maroccosuchus zennaroi*: frontals strongly expanded and trapezoidal in dorsal view; wide interorbital bar, skull table width is double the length and rectangular in shape; small supraoccipital exposure on dorsal surface of the skull.

Description:

Preservation and general form:

The cranium is nearly complete, with some damage posteriorly along the lower temporal bars and the quadrates. Due to the hardness of the matrix, the specimen is only partially prepared (Figure 2.24). On the right side of the cranium, the postorbital bar, infratemporal fenestra and quadrate surface are incomplete. There is minimal dorsoventral compression in the specimen and the anatomy (including postorbital bars) is well preserved. The occipital face is partially exposed to the level of the dorsal surface of the occipital condyle, but the whole occipital surface is very damaged.

The lower jaw is preserved in articulation and therefore only partially visible, showing the anterior symphyseal region, left lateral side and the retroarticular processes. The anteriormost tip of the dentary is missing and the lower jaw is highly damaged and therefore minimal sutural information is preserved. However, what is visible is anatomically consistent with *Maroccosuchus* (Jouve et al. 2014). The glenoid fossa is visible on the left side of the jaw, but no sutural information about the articular can be discerned.

The cranium is large and robust with pronounced lateral maxillary waves (Table 2.1). The rostrum comprises 69% of the skull length, proportionally shorter than all other published *Maroccosuchus zennaroi* specimens, which range between 70-74% skull length (Jouve et al. 2014). The skull table is also broad compared to other *Maroccosuchus zennaroi* specimens. The width of the skull table is twice the length of the skull table (measured from the posterior margin of the orbits) (Table 2.1).

In medial skull length, this specimen is similar in size to MHNM.KHG.171 (49cm), MHNM.KHG.172 (47cm) and MHNT.PAL.2006.80.11 (53cm). However, in postorbital length, it is similar to MHNT.PAL.2006.80.11, OCP DEK-GE 13, MHNLM 2003.1.5082 and OCP DEK-GE 385, which are consistently larger in overall size. As crocodylian skulls increase in size with age, these larger specimens are assumed to be much older individuals. The blunt and reduced snout in MHNM.KHG170 is unexpected when compared these specimens with similar postorbital proportions and difficult to explain in terms of ontogeny. Due to the similarity between this new specimen and *Maroccosuchus zennaroi*, here we provide a condensed description of the new species, mostly highlighting anatomical differences between the two.

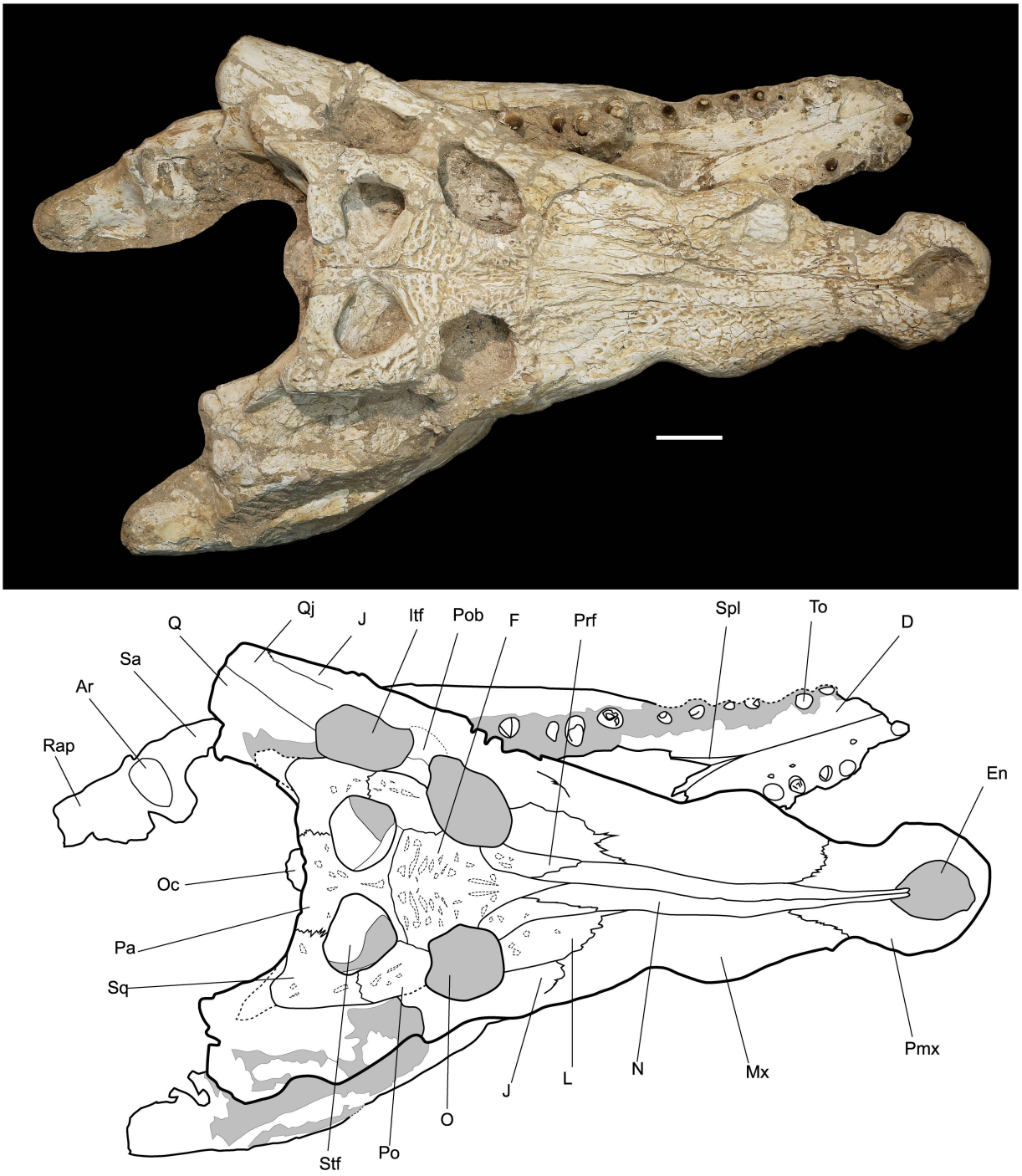

Figure 2.24 *Maroccosuchus brachygnathus* sp.nov.., holotype MHNM.KHG.170 from Ypresian of Morocco. Skull in dorsal view. Areas of dark shading are obscured by matrix. Scale bar= 5cm. **Abbreviations: Ar,** articular, **D,** dentary, **En,** external nares, **F,** frontal, **Itf,** infratemporal fenestra, **J,** jugal, **L,** lacrimal, **Mx,** maxilla, **N,** nasals, **O,** orbit, **Oc,** occipital condyle, **Pa,** parietal, **Po,** postorbital, **Pob**, postorbital bar, **Pmx,** premaxilla, **Prf,** prefrontal, **Q,** quadrate, **Qj,** quadratojugal, **Rap,** retroarticular process, **Sa,** surangular, **Spl,** splenial, **Sq,** squamosal, **Stf,** supratemporal fenestra, **To**, tooth

Cranial openings:

The external naris is circular and large, occupying 45% of the premaxillary width. The nasals extend a short distance anteriorly into the nares as in *Maroccosuchus zennaroi* and do not bisect the nares. The orbits are larger than the supratemporal fenestra and circular, in contrast to *M. zennaroi* where they are elliptical. The frontal is very broad between the orbits, displacing the orbits laterally. The supratemporal fenestrae are angular giving a subtriangular shape. The infratemporal fenestrae are smaller than the orbits.

Cranial bones:

The dorsal premaxillary process is short and does not extend beyond the third maxillary tooth, typical for tomistomine and gavialoid species. The lateral waves of the maxilla are more pronounced than in Maroccosuchus zennaroi. As in *M. zennaroi*, the prefrontal is longer than the frontal, but does not extend as far anteriorly as the lacrimal. The lacrimal has a short posterior process of the maxilla at its anterior margin. The jugal extends to the same level as the frontal, this character is variable amongst *M. zennaroi* material (see above).

The anterior process of the frontal is relatively short and does not extend far beyond the anterior margin of the orbits. The interorbital bar is wider than any of the *Maroccosuchus zennaroi* material. The frontal-postorbital suture runs parallel to the medial plane making the frontal broader posteriorly relative to *M. zennaroi* (Figure 2.22-2.24). The frontoparietal suture is concavo-convex and the postorbital-parietal-frontal contact is on the dorsal surface of the skull.

The parietal forms the medial half of the supratemporal fenestra margin and the interfenestral bar. The position of the squamosal and postorbitals are consistent with the description of *Maroccosuchus zennaroi,* though the postorbital has a straight anterior margin which forms the anterior border of the skull table and posterior margin of the orbits. This gives the skull table a rectangular shape and the orbits are more circular as a result. In *M. zennaroi,* the postorbital is more curved, elongating the orbits to an elliptical shape.

Posteriorly the jugal forms the ventral half of the postorbital bar and a gutter separates the lateral edge of the jugal from the postorbital bar. The jugal extends far posterior to the infratemporal fenestra but does not reach the level of the jaw joint. The quadratojugal contributes to the posterior border of the fenestra but due to preservation the nature of the contact with the quadrate is not clear. Posteriorly, the quadratojugal extends to the quadrate condyle, but the shape of the articular surface on the lower jaw indicates that it does not participate in the jaw joint. The quadrates extend well posterior of the occipital condyle and paroccipital process. The width across the back of the quadrates is wider than published *Maroccosuchus zennaroi* material. The supraoccipital exposure on the dorsal surface of the skull is small, in contrast to *M. zennaroi*, where it is absent on the dorsal skull table. The occipital face is vertical and therefore not visible in dorsal view, plesiomorphic for Crocodylia to the exclusion of Gavialoidea.

On the lower jaw, ten teeth are preserved on the left dentary and five on the right. The dentary is ~6.2cm wide and is proportionally wider than the published *Maroccosuchus zennaroi* specimens**.** The splenial participates in the mandibular symphysis, for a length of 3cm. On the right side of the lower jaw the external mandibular fenestra is partially preserved. The surangular-dentary contact intersects the mandibular fenestra anterior to the posterodorsal corner. The retroarticular process is short and projects posterodorsally.

Phylogenetic Relationships:

Morphology-only

The overall relationships of the morphology-only analysis (Figure 2.25) were consistent with previous research using morphological matrices, with regards to the position of the Gavialoidea (Jouve et al. 2014; Vélez-Juarbe et al. 2007; Brochu 2012). The Gavialoidea (all taxa more closely related to *Gavialis gangeticus* than *Alligator mississippiensis* and *Crocodylus niloticus* (Brochu 2003)) are recovered in a position basal to the Crocodyloidea and the Alligatoroidea, and the Tomistominae (all taxa more closely related to *Tomistoma schlegelii* than to *Crocodylus niloticus* (Brochu 2003)) are nested in the Crocodyloidea. Our analysis recovered 1023 most parsimonious trees with 1018 steps (CI=0.32, RI= 0.725).

In the morphology only tree, *Maroccosuchus zennaroi* and *Maroccosuchus brachygnathus* sp. nov. are recovered in a polytomy at the base of the Tomistominae, consistent with the position of *M. zennaroi* in previous research (Jouve et al. 2014). Character support for the clade Tomistominae is consistent with the results in Jouve et al (2014) (see supplement for details on character support).

In the strict consensus there is poor resolution amongst the Gavialoidea, particularly amongst the basal taxa, often referred to as the thoracosaurines (Brochu 2003; Brochu 2004; Carpenter 1983). The new taxa described here form a clade that is more closely related to *Gavialis gangeticus* and the Gryposuchinae (*Gryposuchus jessei* and all crocodylians closer to it than to *G. gangeticus* or *Tomistoma schlegelii)* than to the thoracosaurs. The new clade includes *Argochampsa krebsi, Argochampsa microrhynchus*, *Parvosuchus daouiensis* and *Phasmatosuchus decipulae.* Here, we define this group as the Argochampsinae, which includes *Argochampsa krebsi* and all crocodylians closer to it than *Gavialis gangeticus, Crocodylus niloticus, Alligator mississippiensis* and *Tomistoma schlegelii*. Within the Argochampsinae, the two species of *Argochampsa* are sister taxa, and *Parvosuchus* and *Phasmatosuchus* form a polytomy within the Argochampsinae.

Gavialoid characters observed amongst the Argochampsinae include: an inclined occipital face visible in dorsal view (ch. 167), homodont dentition with evenly spaced maxillary teeth (ch. 203, 235), a squamosal groove for external ear valve musculature groove which flares anteriorly (ch. 84), a palatine which forms a thin wedge anteriorly (ch. 118), nasal does not contact the external nares (ch. 95) and toothrow underlined (ch. 165). Character support for individual taxa is discussed in the supplemental material.

Combined (morphology-with-molecular) analysis:

Our second phylogenetic analysis was performed using the combined matrix of morphological and molecular data, which retained 32 most parsimonious trees of 17,985 steps (CI= 0.562, RI= 0.628). The overall relationships in the strict consensus topology are consistent with previous phylogenetic analyses on molecular and combined datasets (Gold et al. 2014; Gatesy et al. 2003; Harshman et al. 2003; Roos et al. 2007; Oaks 2011; Janke et al. 2005; McAliley et al. 2006). Gavialoidea is recovered as the sister group to Crocodyloidea, with Alligatoroidea diverging prior to this. All taxa assigned to Tomistominae in the morphology-only analysis become incorporated in Gavialoidea in this combined analysis (Figure 2.26). In addition, Alligatoroidea position basal in the consensus, and the *Borealosuchus* clade has moved closer to the Crocodyloidea.

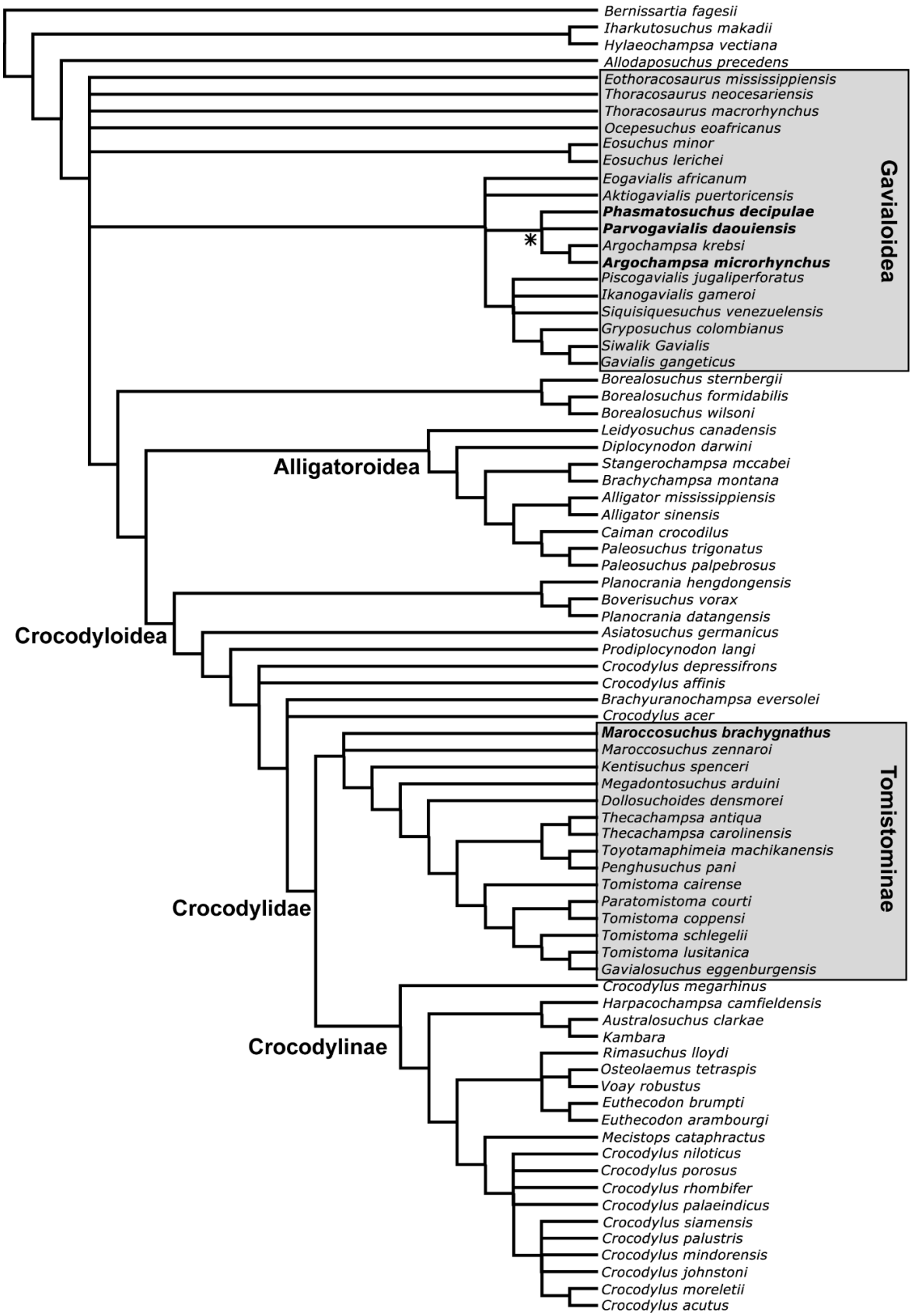

Figure 2.25 Phylogenetic relationships recovered by the parsimony analysis of 244 characters. Strict consensus topology of the 1012 most parsimonious trees. (Length, 1022 steps, CI=0.32, RI= 0.725). Asterisk marks the new clade, the Argochampsinae.

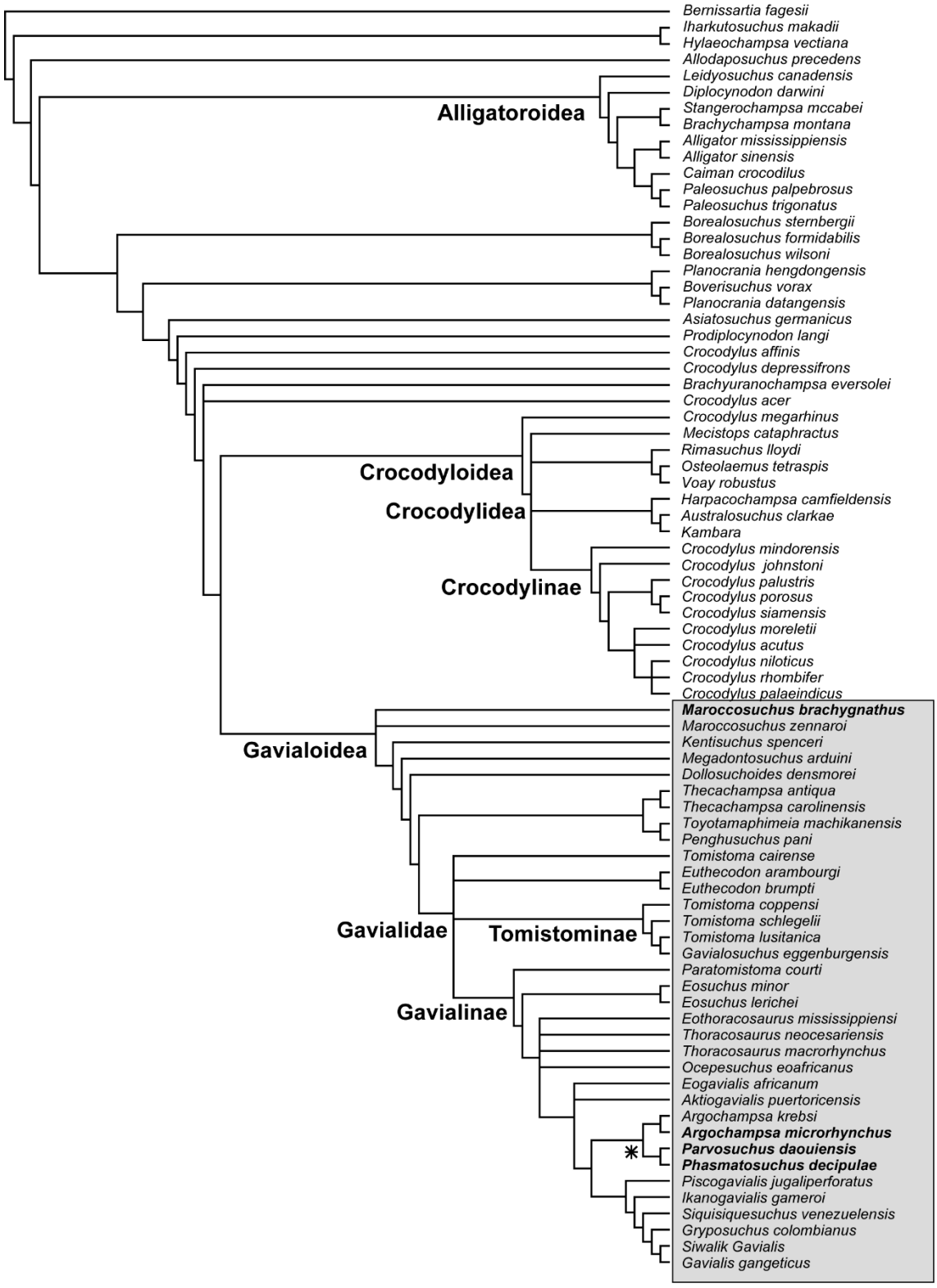

Figure 2.26 Phylogenetic relationships recovered by the parsimony analysis of 244 characters.50% majority rule consensus topology of the 1012 most parsimonious trees. (Length, 1022 steps, CI=0.32, RI= 0.725). Asterisk marks the position of the Argochampsinae.

As outlined in Brochu (2003), the terminology in this phylogenetic context has to be emended. Tomistominae becomes all taxa more closely related to *Tomistoma schlegelii* than to *Gavialis gangeticus*. As a result, in our strict consensus, numerous species referred to the Tomistominae in the morphological context are not classed as Tomistominae in the combined analysis. These species are recovered on the stem of Gavialidae in the combined topology, including *Maroccosuchus,* which is classed as the deepest branching member of the Gavialoidea in this context (see Figures 2.25, 2.26 for clarification of terms). In the combined data tree, *Euthecodon* spp. (Ginsburg & Buffetaut 1978; Storrs 2003) is also included in the Gavialidae, whereas, in the morphological dataset it is positioned within the Crocodylidae.

The Gavialinae (all taxa more closely related to *Gavialis gangeticus* than to *Tomistoma schlegelii* (Brochu 2003)) includes all species referred to Gavialoidea in the morphological context, with the addition of *Paratomistoma courti*, which forms the deepest branch. The resolution amongst the Gavialinae is improved relative to the morphological analysis. Argochampsinae is still recovered as a clade and forms a sister group to the more derived gryposuchines and *Gavialis.* The only other known Moroccan gavialoid, *Ocepesuchus* (Jouve, Bardet, et al. 2008), is in both phylogenies recovered in a polytomy with *Thoracosaurus* and *Eothoracosaurus* towards the root of the Gavialinae.

Discussion:

Phylogenetic conflict:

The ongoing conflict between the morphological and molecular signals remains the source of much debate in the literature. Here, with the discovery of multiple new species of gavialoid and tomistomine, we reinvestigated this conflict to see if these new species change our understanding of this conflict. In comparison to previous research, this dataset contains a much larger number of gavialoid and tomistomine species and can therefore provide a more targeted analysis of these groups.

The results of the morphological analysis, as stated above, remains largely consistent with previous morphological analyses (Jouve et al. 2014). The addition of new species has had the effect of reducing the resolution amongst the gavialoids, however the relationships amongst the Tomistominae remain largely unchanged. This reduced resolution is likely due to high levels of homoplasy in the dataset, indicated by the low consistency index (CI). The formation of the new clade, Argochampsinae, however indicates an endemic fauna in Morocco.

In the combined analysis, our results differ markedly from prior attempts to combine dataset by increasing the number of taxa significantly. However, the results remain similar to previous combined analyses, with Tomistominae and Gavialinae forming sister group, and taxa such as *Kentisuchus, Dollosuchoides, Megadontosuchus* and *Maroccosuchus* falling onto the stem of the Gavialidae. Compared to previous analyses presented by Gold (2014) and Gatesy (2004), which had poor resolution in the gavialoids and tomistomines respectively, the resolution in our analysis is much greater. The addition of the problematic genus *Euthecodon* to the Gavialoidea in our analysis is interesting as these species have been the source of much taxonomic confusion- previously assigned to Gavialoidea, Tomistominae and Crocodyloidea (Ginsburg & Buffetaut 1978; Storrs 2003; Brochu et al. 2012).

Overall, we found that the new species did impact our understanding of the individual relationships amongst the gavialoids and tomistomines but has done little to resolve the ongoing

conflict between these two phylogenetic datasets. Each result obtained here (as with previous research) remained robust. Future research directed towards different tree-searching methods or examining this conflict with the use of stratigraphy may help shed new light on this conflict.

Ontogenetic considerations:

Of the four new species described here, *Parvosuchus* and *Phasmatosuchus* are clearly distinct from any known fossil gavialoid taxa described to date. *Argochampsa microrhynchus* and the *Maroccosuchus* specimens, however, closely resemble previously described species *A. krebsi* (Hua & Jouve 2004) and *M. zennaroi* (Jouve et al. 2014; Jonet & Wouters 1977) respectively. Given this, it is important to determine whether the observed differences in the new material might have arisen through ontogeny or intraspecific variation. To assess this, we examined growth series and intraspecific variation in extant crocodylian skull material across a range of species, from both the literature and museum collections.

Crocodylians exhibit allometric growth, and therefore differences observed in the rostral proportions in the described material could conceivably result from ontogeny (Iordansky 1973; Kälin 1933; Monteiro & Soares 1997; Watanabe & Slice 2014; Piras et al. 2010). For example, early in ontogeny, it is typical to find proportionally larger orbits and a proportionally shorter and narrower rostrum (Iordansky 1973). Lateral maxillary waves (where present) are generally less exaggerated in ontogenetically younger specimens. In extant species, skulls become proportionally wider and more robust throughout ontogeny (Kälin 1933; Hall & Portier 1994; Platt et al. 2011; Iordansky 1973; Grigg & Kirshner 2015; Piras et al. 2010; Iijima 2017).

Argochampsa microrhynchus:

Due to its small size, *Argochampsa microrhynchus* might be considered as a juvenile of *Argochampsa krebsi*. The main differences between the two taxa are the proportionally shorter and broader rostrum in *A. microrhynchus,* as well as the reduced tooth count, large foramen incisivum and expanded medial hemicondyle. The proportionally wider rostrum of *A. microrhynchus* is inconsistent with an ontogenetically younger specimen (Figure 2.7). Additionally, *Gavialis gangeticus* exhibits narrowing of the interfenestral bar as the supratemporal fenestra increases in size throughout ontogeny, and during this process the frontoparietal suture becomes incorporated into the supratemporal fenestra wall (Brochu 2004; Kälin 1933). In the type of *A. microrhynchus*, the narrow interfenestral bar and incorporation of the frontoparietal suture within the fenestra, as well as the similarity in postorbital proportions to *A. krebsi* (Figure 2.7), suggest that the animal was a mature individual.

In addition to the shorter rostrum, *Argochampsa microrhynchus* has fewer maxillary teeth than *A. krebsi*. At least twelve maxillary alveoli are preserved in *A. microrhynchus*, but due to incomplete preservation an additional 6-7 alveoli is possible, for a total of 18-19 teeth. This differs markedly from the tooth count of *A. krebsi*, which has spaces for 26 maxillary teeth, similar to the primitive gavialoids *Eosuchus lerichei* (Dollo 1907; Delfino et al. 2005) and *Eosuchus minor* (Brochu 2006b). Maxillary tooth counts amongst crocodylians are known to vary by 1-3 alveoli in extant populations and do not increase in number throughout ontogeny (Bickelmann & Klein 2009; Brown et al. 2015; Iijima 2017). This suggests the difference in tooth

count here cannot be explained by ontogeny or intraspecific variation, and instead diagnoses two distinct *Argochampsa* species.

Maroccosuchus:

The distinct morphology of *Maroccosuchus brachygnathus,* MHNM.KHG 170, which is proportionately shorter and broader than *M*. *zennaroi*, is difficult to explain in terms of ontogenetic change and so is tentatively referred to a new species. This skull has a proportionally shorter and broader rostrum than *M. zennaroi* material of similar postorbital proportions.

The skull material referred to *Maroccosuchus zennaroi*, MHNM.KHG.171, MHNM.KHG.172 and MHNM.KHG.173, were compared to *Maroccosuchus zennaroi* (Jouve et al. 2014). They were also found to differ from previously published material (Jouve et al. 2014) in rostral proportions and some anatomical characters. In terms of rostral proportions, MHNM.KHG.171 and 173 are relatively slender with less pronounced lateral waves of the maxilla. The small size of the new material compared to the published material of *M. zennaroi* (typically >50cm skull length) and their relatively slender proportions, suggest that the new skulls may represent immature specimens of *M. zennaroi*. Furthermore, in MHNM.KHG.173 the alveoli become laterally compressed posteriorly and the prefrontal and lacrimal are the same length. In extant skulls of long-snouted species such as *Mecistops cataphractus* and generalist forms such as *Crocodylus porosus,* the posterior alveoli tend to show lateral compression in juvenile forms. Similarly, the position of the prefrontal with respect to the lacrimal, does show some intraspecific variation. As a result, the variation observed in MHNM.KHG.171, 172 and 173 does not fall outside of the range expected for a species, and therefore they were referred to *M. zennaroi.*

Feeding strategy and niche partitioning in the phosphates:

The high disparity seen amongst the skulls of the new taxa implies a range of different feeding strategies. By examining the skull morphology we can potentially make inferences about the dietary preference of these species in the marine environment (Busbey 1994; McHenry et al. 2006; Iijima 2017; McCurry et al. 2017; Walmsley et al. 2013).

The skull morphology of *Maroccosuchus zennaroi* can be classed as generalist (Brochu 2001). The dorsoventrally flattened and broad snout are adapted for high bite forces, and could tackle larger prey (Grigg & Kirshner 2015). Throughout ontogeny, as seen in our specimens MHNM.KGH.172 and MHNM.KHG.173, the skull and rostrum becomes wider and more robust to withstand the high bite forces imposed by this diet. The blunt, robust posterior maxillary and dentary teeth would have been effective in crushing hard-shelled prey items, potentially allowing the animal to expand its diet by incorporating hard shelled animals such as turtles, crustaceans, and/or molluscs.

Maroccosuchus brachygnathus (MHNM.KHG.170) has a shorter and broader snout than *M. zennaroi*. These proportions suggest adaptation towards crushing hard-shelled prey (Pierce et al. 2009; Erickson et al. 2004). The Cretaceous mosasaur fauna in the Moroccan phosphates included durophagous forms with blunt rounded teeth (Bardet, Suberbiola, Iarochène, Amalik, et al. 2005; Bardet et al. 2010). Though the teeth of MHNM.KHG.170 do not

show this extreme morphology, the tooth wear indicates that it may have moved to exploit this niche following the extinction of the mosasaurs at the K-Pg.

The three new gavialoid species described here all show variation within the longirostrine morphology. The long slender snouts, with homodont dentition and slender recurved teeth, imply a piscivorous diet (McHenry et al. 2006; Erickson et al. 2012). The slender teeth are not designed to withstand high pressures associated with biting, and are more suitable to spear/impale prey (Iijima 2017; Massare 1987). Lack of tooth wear on all the new material indicates that prey was likely to be docile and unarmoured. As the longirostrine snout experiences greater stresses during biting, the fusion of the nasals in Argochampsinae might have strengthened the rostrum by reducing the number of longitudinal sutures along its length- zones of weakness (Langston 1973). The separation of the nasal and premaxilla in *Phasmatosuchus* may have further strengthened the rostrum to these stresses. Additionally, increase in snout length has been correlated with an increase in the size of the supratemporal fenestrae, which implies rapid but weak jaw closure (Pierce et al. 2009; Pierce et al. 2008). The tubular design of the rostrum produces less drag in the water during lateral sweeps of the head, which favours the capture of agile prey (McHenry et al. 2006; Iijima 2017; McCurry et al. 2017; Pierce et al. 2008). The enlarged and pendulous basioccipital tubera, a diagnostic feature of the Argochampsinae, forms an enlarged area for muscle attachment (Schwarz-Wings 2014; Langston 1973; Iijima 2017). It is also observed in *Gavialis*, the function of which is thought to be advantageous for lateral sweeps of the head during the capture of prey (Iijima 2017). Low bite forces and homodont dentition suggest inertial feeding, where the prey is swallowed whole (Rieppel 2002; Iijima et al. 2016).

The disparity amongst the new taxa is expressed in three main ways. First in the proportional length of the rostrum, second in tooth count, and third, the orientation of the alveoli. Gavialoidea are typically are more variable in terms of tooth count compared to the rest of the crown group; this is particularly evident in the Argochampsinae (Table 2.1). The highest tooth counts amongst gavialoids were previously observed in the hyperelongate South American forms. These attained snout lengths 82-83% relative to total skull length and maxillary tooth counts of 28-30 (Sill 1970; Brochu & Rincon 2004; Kraus 1998; Riff et al. 2008; Langston & Gasparini 1997). *Phasmatosuchus decipulae* is similar in rostral length, 85%, but the tooth count far exceeds that of the South American forms. Higher tooth counts in gavialoids are thought to increase the area and chance of catching prey, whilst aiding transport of prey to the back of the pharynx during inertial feeding (Busbey 1994; Iijima 2017).

The proportionally shorter snout and reduced tooth count of *Argochampsa microrhynchus* would have created less surface area for prey capture in comparison to *Argochampsa krebsi*. The angular velocity achieved at the tip of the snout increases with length (Iijima 2017; McHenry et al. 2006), therefore *A. microrhynchus* may have favoured marginally slower/less agile prey compared to *A. krebsi*. The anterior maxillary alveoli are angled anteriorly in *A. microrhynchus* (Figure 2.3, 2.4); the procumbent teeth may have formed a mesh that could have acted as a fish trap (Rieppel 2002). However as there are no teeth preserved, this cannot be concluded with certainty.

Parvosuchus daouiensis has a higher tooth count and a proportionally longer rostrum that *Argochampsa microrhynchus,* which may have increased the likelihood of capturing very small and agile prey. The scalloping is much less pronounced on the maxilla, and the angle of the alveoli indicate that the teeth were only slightly procumbent. The main function was likely impaling the prey.

The rostrum of *Phasmatosuchus decipulae* is flattened dorsoventrally. However, the postorbital region of both skulls has retained a large degree of three-dimensionality, therefore the flattened profile of the rostrum is unlikely to be an entirely preservational artefact. Similarly, the orientation of the maxillary alveoli changes along the length of the rostrum (see Figure 2.15, 2.17, 2.18, 2.20). Posteriorly the alveoli are smaller and project ventrally. Anteriorly, the alveoli rotate to the lateral edge of the maxilla. This indicates that the lateral projection of the alveoli is likely a genuine feature and not preservational.

The length and flattened profile suggest that the jaw could achieve high speed and minimal drag in the water during lateral sweeps of the head, and the high number of teeth would increase the chance of catching small agile prey. However, the angle of the teeth and length of the rostrum suggest that biting would cause a very high degree of strain (Walmsley et al. 2013; Pierce et al. 2008). One hypothesis is that *Phasmatosuchus* used the elongate rostrum like extant sawfish, as has been suggested for *Euthecodon* (Brochu 2003)- the flattened profile would allow lateral swipes of the head, to stun prey (Wueringer et al. 2012). Sawfish and sawsharks have also been found to use the 'saw' to agitate the benthos and feed on benthic organisms (Wueringer et al. 2012; Nevatte et al. 2017).

Another hypothesis is that the arrangement of interlocking teeth could be used as a mesh to trap prey and strain them from the water. Unlike filter-feeders such as extant whales and pelicans which can actively expel water from the mouth, gavialoids have a long mandibular symphysis and narrow jaw which would prevent this style of feeding (Walmsley et al. 2013; McCurry et al. 2017). However, the closure of the jaw itself would create an outward flow of water and the interlocking teeth could form a trap against this. Examples of this type of feeding are seen in river dolphins (McCurry et al. 2017) and have been referred to as the "trap guild" for cryptoclidids and other plesiosaurs (Chatterjee & Small 1989; Noè et al. 2017).

In *Phasmatosuchus*, the alveolar spacing along the maxilla is 5mm, which suggests that macroscopic prey >3mm would have been trapped between the interlocking teeth. However, unlike the elongate slender teeth observed in plesiosaurs such as *Nothosaurus mirabilis* and *Cryptoclidus* (Rieppel 2002; Brown & Cruickshank 1994), the teeth preserved in *Phasmatosuchus* are relatively short in length. As a result, it is likely that the teeth would only interlock once the jaw was almost fully closed; if this is the case, then the strain/sieve feeding hypothesis is highly unlikely. The horizontal projection of the teeth would, however, increase the surface area available to trap or subdue small unarmoured prey in a sit-and-wait feeding strategy, either in the water column, or by stirring up or raking sediments on the seafloor (Noè et al. 2017).

Acknowledgements:

Thanks to M. Topham for assistance with preparation of specimens, to C. Underwood for identification of shark teeth for stratigraphic correlation, to M. Meharich and M&M Enterprises for invaluable assistance in Morocco, and to N.-E. Jalil and the MHNM (Museum of Natural History of Marrakech) for assistance with accessioning fossils. Thanks, and in memory of, M. Elgouni, without whom this project would not have been possible. Discussions with the University of Bath Palaeontology group, in particular, comments and suggestions for improvements provided by A. Roberts, C. Klein and E. Randle were greatly appreciated.

References:

Aguilera, O.A., Riff, D. & Bocquentin-Villanueva, J., 2006. A new giant *Purussaurus* (Crocodyliformes, Alligatoridae) from the Upper Miocene Urumaco Formation, Venezuela. *Journal of Systematic Palaeontology*, 4(3), pp.221–232.

Andrews, C.W., 1906. *A Descriptive Catalogue of the Tertiary Vertebrata of the Fayûm, Egypt.*, British Museum, London.

Arambourg, C., 1952. Les vertébrés fossiles des gisements de phosphates (Maroc-Algérie-Tunisie). *Service Géologique Maroc, Notes et Mémoires*, 92, pp.1–372.

Arambourg, C., 1935. *Note préliminaire sur les vertébrés fossiles des phosphates du Maroc*, Available at: https://books.google.co.uk/books?id=TtJ3nQEACAAJ.

Bardet, N., Suberbiola, X.P., Iarochène, M., Bouya, B., et al., 2005. A new species of *Halisaurus* from the Late Cretaceous phosphates of Morocco, and the phylogenetical relationships of the Halisaurinae (Squamata: Mosasauridae). *Zoological Journal of the Linnean Society*, 143, pp.447–472.

Bardet, N., Suberbiola, X.P., Iarochène, M., Amalik, M., et al., 2005. Durophagous Mosasauridae (Squamata) from the Upper Cretaceous phosphates of Morocco, with description of a new species of *Globidens*. *Geologie en Mijnbouw/Netherlands Journal of Geosciences*, 84, pp.167–175.

Bardet, N. et al., 2004. *Mosasaurus beaugei* Arambourg, 1952 (Squamata, Mosasauridae) from the Late Cretaceous Phosphates of Morocco. *Geobios*, 37, pp.315–324.

Bardet, N. et al., 2010. Reptilian assemblages from the latest Cretaceous – Palaeogene phosphates of Morocco: from Arambourg to present time. *Historical Biology*, 22(1–3), pp.186–199.

Bickelmann, C. & Klein, N., 2009. The late pleistocene horned crocodile *Voay robustus* (Grandidier & Vaillant, 1872) from Madagascar in the Museum fur Naturkunde Berlin. *Fossil Record*, 12(1), pp.13–21.

Brochu, C.A., 2004. A new Late Cretaceous gavialoid crocodylian from eastern North America and the phylogenetic relationships of thoracosaurs. *Journal of Vertebrate Paleontology*, 24(September), pp.610–633.

Brochu, C.A. et al., 2012. A new species of *Borealosuchus* (Crocodyliformes, Eusuchia) from the Late Cretaceous–early Paleogene of New Jersey. *Journal of Vertebrate Paleontology*, 32(1), pp.105–116.

Brochu, C.A., 2001. Crocodylian snouts in space and time: phylogenetic approaches toward adaptive radiation. *American Zoologist*, 41(3), pp.564–585.

Brochu, C.A., 2006a. *Eosuchus* (Crocodylia, Gavialoidea) from the lower Eocene of the Isle of Sheppey, England. *Journal of Vertebrate Paleontology*, 26(2), pp.466–470.

Brochu, C.A., 1997a. Morphology, fossils, divergence timing, and the phylogenetic relationships of *Gavialis*. *Systematic Biology*, 46(3), pp.479–522.

Brochu, C.A., 2006b. Osteology and phylogenetic significance of *Eosuchus minor* (Marsh, 1870) new combination, a longirostrine crocodylian from the Late Paleocene of North America. *Journal of Paleontology*, 80(1), pp.162–186.

Brochu, C.A., 2003. Phylogenetic approaches toward crocodylian history. *Annual Review of Earth and Planetary Sciences*, 31(1), pp.357–397.

Brochu, C.A., 2012. Phylogenetic relationships of Palaeogene ziphodont eusuchians and the status

of *Pristichampsus* Gervais, 1853. *Earth and Environmental Science Transactions of the Royal society of Edinburgh*, 103(3–4), pp.521–550.

Brochu, C.A., 1997b. *Phylogenetic systematics and taxonomy of Crocodylia*, University of Texas, Austin.

Brochu, C.A., 1999. Phylogenetics, taxonomy, and historical biogeography of Alligatoroidea. *Journal of Vertebrate Paleontology*, 19(January), pp.9–100.

Brochu, C.A., 2007. Systematics and taxonomy of Eocene tomistomine crocodylians from Britain and Northern Europe. *Palaeontology*, 50, pp.917–928.

Brochu, C.A. & Rincon, A.D., 2004. A gavialoid crocodylian from the Lower Miocene of Venezuela. *Special Papers in Palaeontology*, 71, pp.61–79.

Brown, C.M. et al., 2015. Tooth counts through growth in diapsid reptiles: implications for interpreting individual and size-related variation in the fossil record. *Journal of anatomy*, 226(4), pp.322–333.

Brown, D.S. & Cruickshank, A.R.I., 1994. The skull of the Callovian plesiosaur *Cryptoclidus eurymerus*, and the sauropterygian cheek. *Palaeontology*, 37(4), pp.941–953.

Busbey, A.B., 1994. The structural consequences of skull flattening in crocodilians. In J. J. Thomason, ed. *Functional Morphology in Vertebrate Paleontology*. Cambridge University Press, New York, pp. 173–192.

Carpenter, K., 1983. *Thoracosaurus neocesariensis* (de Kay, 1842) (Crocodylia : Crocodylidae) from the Late Cretaceous Ripley Formation of Mississippi. *Mississippi Geology*, 4, pp.1–10.

Chatterjee, S. & Small, B.J., 1989. New plesiosaurs from the Upper Cretaceous of Antarctica. *Geological Society, London, Special Publications*, 47(1), pp.197–215.

Delfino, M., Piras, P. & Smith, T., 2005. Anatomy and phylogeny of the gavialoid crocodylian *Eosuchus lerichei* from the Paleocene of Europe. *Acta Palaeontologica Polonica*, 50(3), pp.565–580.

Dollo, L., 1907. Nouvelle note sur les reptiles de l'Eocène inférieur de la Belgique et des régions voisines (*Eosuchus lerichei, Eopharsis gigas*). *Bulletin de la Société Belge de Géologie*, 21, pp.81–85.

Erickson, G.M. et al., 2004. Comparison of bite-force performance between long-term captive and wild American alligators (Alligator mississippiensis). *Journal of Zoology*, 262(1), pp.21–28.

Erickson, G.M. et al., 2012. Insights into the ecology and evolutionary success of crocodilians revealed through bite-force and tooth-pressure experimentation. *PLoS ONE*, 7(3).

Fitzinger, L.J.F.J., 1826. *Neue classification der reptilien nach ihren natürlichen verwandtschaften : nebst einer verwandtschafts-tafel und einem verzeichnisse der reptilien-sammlung des K. K. zoologischen museum's zu Wien / von L. J. Fitzinger.*, Wien : J. G. Heubner,.

Fortier, D.C., Perea, D. & Schultz, C.L., 2011. Redescription and phylogenetic relationships of *Meridiosaurus vallisparadisi* , a pholidosaurid from the Late Jurassic of Uruguay. *Zoological Journal of the Linnean Society*, 163, pp.S257–S272.

Gatesy, J. et al., 2003. Combined support for wholesale taxic atavism in gavialine crocodylians. *Systematic Biology*, 52(3), pp.403–422.

Gatesy, J., Baker, R.H. & Hayashi, C., 2004. Inconsistencies in arguments for the supertree approach: supermatrices versus supertrees of Crocodylia. *Systematic Biology*, 53(2), pp.342–355.

Ginsburg, L. & Buffetaut, E., 1978. *Euthecodon arambourgi* n. sp., et l'évolution du genre Euthecodon, Crocodilien du Néogène d'Afrique. *Géologie Méditerranéenne*, 5(2), pp.291–302.

Gold, M.E.L., Brochu, C.A. & Norell, M.A., 2014. An expanded combined evidence approach to the

Gavialis problem using geometric morphometric data from crocodylian braincases and eustachian systems. *PLoS ONE*, 9(9), pp.1–12.

Goloboff, P.A., Farris, J. & Nixon, K., 2003. T.N.T.: Tree Analysis Using New Technology.

Grigg, G.C. & Kirshner, D., 2015. *Biology and evolution of crocodylians*, Csiro Publishing.

Hall, P.M. & Portier, K.M., 1994. Cranial morphometry of New Guinea crocodiles (*Crocodylus novaeguineae*): ontogenetic variation in relative growth of the skull and an assessment of its utility as a predictor of the sex and size of individuals. *Herpetological Monographs*, 8, pp.203–225.

Harshman, J. et al., 2003. True and false gharials: a nuclear gene phylogeny of Crocodylia. *Systematic Biology*, 52(3), pp.386–402.

Hecht, M.K. & Malone, B., 1972. On the early history of the gavialid crocodilians. *Herpetologica*, 28(3), pp.281–284.

Hua, S. & Jouve, S., 2004. A primitive marine gavialoid from the Paleocene of Morocco. *Journal of Vertebrate Paleontology*, 24(2), pp.341–350.

Iijima, M., 2017. Assessment of trophic ecomorphology in non-alligatoroid crocodylians and its adaptive and taxonomic implications. *Journal of anatomy*, 231, pp.192–211.

Iijima, M., Takahashi, K. & Kobayashi, Y., 2016. The oldest record of *Alligator sinensis* from the Late Pliocene of Western Japan, and its biogeographic implication. *Journal of Asian Earth Sciences*, 124, pp.94–101.

Iordansky, N.N., 1973. The skull of the crocodilia. In C. Gans & T. Parsons, eds. *Biology of the Reptilia Vol. 4*. Academic Press, London, pp. 201–262.

Janke, A. et al., 2005. Mitogenomic analyses place the gharial (*Gavialis gangeticus*) on the crocodile tree and provide pre-K/T divergence times for most crocodilians. *Journal of Molecular Evolution*, 61(5), pp.620–626.

Jonet, S. & Wouters, G., 1977. *Maroccosuchus zennaroi,* crocodilien eusuchien nouveau des phosphates du Maroc. *Notes de la Service Geologique du Maroc*, 268, pp.177–203.

Jouve, S., Ne, M.I.È., et al., 2005. A new dyrosaurid crocodyliform from the Palaeocene of Morocco and a phylogenetic analysis of Dyrosauridae. *Acta Palaeontologica Polonica*, 50(3), pp.581–594.

Jouve, S. et al., 2006a. A new species of *Dyrosaurus* (Crocodylomorpha, Dyrosauridae) from the early Eocene of Morocco: phylogenetic implications. *Zoological Journal of the Linnean Society*, 148(4), pp.603–656.

Jouve, S. et al., 2014. *Maroccosuchus zennaroi* (Crocodylia: Tomistominae) from the Eocene of Morocco: phylogenetic and palaeobiogeographical implications of the basalmost tomistomine. *Journal of Systematic Palaeontology*, 13, pp.1–25.

Jouve, S. et al., 2006b. New material of *Argochampsa krebsi* (Crocodylia: Gavialoidea) from the Lower Paleocene of the Oulad Abdoun Basin (Morocco): phylogenetic implications. *Geobios*, 39(6), pp.817–832.

Jouve, S., Bardet, N. & Jalil, N.-E., 2008. The oldest African crocodylian: phylogeny, paleobiogeography, and differential survivorship of marine reptiles through the Cretaceous-Tertiary boundary. *Journal of Vertebrate Paleontology*, 28, pp.37–41.

Jouve, S., Bouya, B. & Amaghzaz, M., 2008. A long-snouted dyrosaurid (Crocodyliformes, Mesoeucrocodylia) from the Paleocene of Morocco: phylogenetic and palaeobiogeographic implications. *Palaeontology*, 51(2), pp.281–294.

Jouve, S., Bouya, B. & Amaghzaz, M., 2005. A short-snouted dyrosaurid (Crocodyliformes, Mesoeucrocodylia) from the Paleocene of Morocco. *Palaeontology*, 48(2), pp.359–369.

Kälin, J.A., 1933. Beiträge zur vergleichenden Osteologie des Crocodilidenschädels. *Zoologische Jahrbücher*, 57, pp.535–714.

Kobayashi, Y. et al., 2006. Anatomy of a Japanese tomistomine crocodylian, *Toyotamaphimeia machikanensis* (Kamei et Matsumoto, 1965), from the middle Pleistocene of Osaka Prefecture: the reassessment of its phylogenetic status within Crocodylia. *National Science Museum Monographs*.

Kocsis, L. et al., 2014. Comprehensive stable isotope investigation of marine biogenic apatite from the late Cretaceous-early Eocene phosphate series of Morocco. *Palaeogeography, Palaeoclimatology, Palaeoecology*, 394, pp.74–88.

Koken, E., 1888. *Thoracosaurus macrorhynchus* Bl. aus der Tuffkreide von Maastricht. *Zeitschrift der Deutschen Geologischen Gesellschaft*, 40(4), pp.754–773.

Kraus, R., 1998. The cranium of *Piscogavialis jugaliperforatus* n.gen., n.sp. (Gavialidae, Crocodylia) from the Miocene of Peru. *Paläontologische Zeitschrift*, 72, pp.389–406.

Langston Jr., W., 1966. *Mourasuchus* Price, *Nettosuchus* Langston, and the Family Nettosuchidae (Reptilia: Crocodilia). *Copeia*, 4, pp.882–885.

Langston Jr., W. & Gasparini, Z.B. de, 1997. Crocodilians, *Gryposuchus*, and the South American gavials. In R. F. Kay et al., eds. *Vertebrate Paleontology in the Neotropics. The Miocene Fauna of La Venta, Colombia*. Smithsonian Institution Press, Washington DC, pp. 113–154.

Langston, W., 1973. The crocodilian skull in historical perspective. In C. Gans & T. Parsons, eds. *Biology of the Reptilia Vol. 4*. Academic Press, London, pp. 263–284.

Langston, W. & Gasparini, Z., 1997. Crocodilians, Gryposuchus, and the South American gavials. In R. F. Kay et al., eds. *Vertebrate Paleontology in the Neotropics: the Miocene Fauna of La Venta, Colombia*. Smithsonian Institution Press, Washington DC, pp. 113–154.

de Lapparent de Broin, F., 2002. *Elosuchus* , a new genus of crocodile from the Lower Cretaceous of the North of Africa. *Comptes Rendus Palevol*, 1, pp.275–285.

Lucas, J. & Prevot-Lucas, L., 1996. Tethyan phosphates and bioproductites. In A. E. M. Nairn et al., eds. *The Ocean Basins and Margins*. Plenum Press, New York, pp. 367–391.

Martin, B.G.H. & Bellairs, A.D.A., 2009. The narial excrescence and pterygoid bulla of the gharial, *Gavialis gangeticus* (Crocodilia). *Journal of Zoology*, 182(4), pp.541–558.

Martin, J.E. et al., 2012. *Gavialis* from the Pleistocene of Thailand and its relevance for drainage connections from India to Java. *PloS ONE*, 7(9), pp.1–14.

Massare, J.A., 1987. Tooth morphology and prey preference of Mesozoic marine reptiles. *Journal of Vertebrate Paleontology*, 7(2), pp.121–137.

McAliley, L.R. et al., 2006. Are crocodiles really monophyletic? Evidence for subdivisions from sequence and morphological data. *Molecular Phylogenetics and Evolution*, 39(1), pp.16–32.

McCurry, M.R. et al., 2017. The remarkable convergence of skull shape in crocodilians and toothed whales. *Proceedings of the Royal Society B*, 284, pp.9–11.

McHenry, C.R. et al., 2006. Biomechanics of the rostrum in crocodilians: a comparative analysis using finite-element modeling. *The anatomical record. Part A, Discoveries in molecular, cellular, and evolutionary biology*, 288(May), pp.827–849.

Monteiro, L.R. & Soares, M., 1997. Allometric analysis of the ontogenetic variation and evolution of the skull in Caiman Spix, 1825 (Crocodylia: Alligatoridae). *Herpetologists League*, 53(1), pp.62–69.

Nevatte, R.J. et al., 2017. First insights into the function of the sawshark rostrum through examination of rostral tooth microwear. *Journal of Fish Biology*, 91(6), pp.1582–1602.

Noè, L.F., Taylor, M.A. & Gómez-pérez, M., 2017. An integrated approach to understanding the role

of the long neck in plesiosaurs. *Acta Palaeontologica Polonica*, 62(1), pp.137–162.

Oaks, J.R., 2011. A time-calibrated species tree of Crocodylia reveals a Recent radiation of the true crocodiles. *Evolution*, 65, pp.3285–3297.

Pierce, S.E., Angielczyk, K.D. & Rayfield, E.J., 2009. Morphospace occupation in thalattosuchian crocodylomorphs: Skull shape variation, species delineation and temporal patterns. *Palaeontology*, 52(5), pp.1057–1097.

Pierce, S.E., Angielczyk, K.D. & Rayfield, E.J., 2008. Patterns of morphospace occupation and mechanical performance in extant crocodilian skulls: A combined geometric morphometric and finite element modeling approach. *Journal of Morphology*, 269, pp.840–864.

Piras, P. et al., 2010. The *Gavialis-Tomistoma* debate: the contribution of skull ontogenetic allometry and growth trajectories to the study of crocodylian relationships. *Evolution & Development*, 12(6), pp.568–579.

Platt, S.G. et al., 2011. Size estimation, morphometrics, sex ratio, sexual size dimorphism, and biomass of *Crocodylus acutus* in the coastal zone of Belize. *Salamandra*, 47(4), pp.179–192.

Rieppel, O., 2002. Feeding mechanics in Triassic stem-group sauropterygians: the anatomy of a successful invasion of Mesozoic seas. *Zoological Journal of the Linnean Society*, 135(1), pp.33–63.

Riff, D., Conquista, V. & Aguilera, O.A., 2008. The world's largest gharials *Gryposuchus*: description of *G. croizati* n. sp (Crocodylia, Gavialidae) from the Upper Miocene Urumaco Formation, Venezuela. *Paläontologische Zeitschrift*, 82, pp.178–195.

Roos, J., Aggarwal, R.K. & Janke, A., 2007. Extended mitogenomic phylogenetic analyses yield new insight into crocodylian evolution and their survival of the Cretaceous-Tertiary boundary. *Molecular Phylogenetics and Evolution*, 45(2), pp.663–673.

Salas-Gismondi, R. et al., 2016. A new 13 million year old gavialoid crocodylian from proto-Amazonian mega-wetlands reveals parallel evolutionary trends in skull shape linked to longirostry. *PloS ONE*, 11(4), p.e0152453.

Salvan, H.M., 1954. Les invertébrés fossiles des phosphates Marocains. *N. Mém. Serv. Géol. Maroc (Rabat)*, 93, pp.1–258.

Schwarz-Wings, D., 2014. The feeding apparatus of dyrosaurids (Crocodyliformes). *Geological Magazine*, 151(01), pp.144–166.

Sereno, P.C. et al., 2001. The giant crocodyliform *Sarcosuchus* from the Cretaceous of Africa. *Science*, 294, pp.1516–1519.

Shan, H. et al., 2009. A new tomistomine (Crocodylia) from the Miocene of Taiwan. *Canadian Journal of Earth Sciences*, 46(7), pp.529–555.

Sill, W.D., 1970. Nota preliminar sobre un nuevo Gavial del Plioceno de Venezuela y una discusion de los Gaviales sudamericanos. *Ameghiniana*, 7(2), pp.151–159.

Storrs, G.W., 2003. Late Miocene-Early Pliocene crocodilian fauna of Lothagam, southwest Turkana Basin, Kenya. In M. G. Leakey & J. M. Harris, eds. *Lothagam: The Dawn of Humanity in Eastern Africa*. pp. 137–159.

Taplin, L.E., Grigg, G.C. & Beard, L., 1985. Salt gland function in fresh water Crocodiles: evidence for a marine phase in eusuchian evolution? In G. Grigg, R. Shine, & H. Ehmann, eds. *Biology of Australasian frogs and reptiles*. Royal Zoological Society of New South Wales, pp. 402–410.

Vélez-Juarbe, J., Brochu, C.A. & Santos, H., 2007. A gharial from the Oligocene of Puerto Rico: transoceanic dispersal in the history of a non-marine reptile. *Proceedings of the Royal Society B: Biological Sciences*, 274, pp.1245–1254.

Walmsley, C.W. et al., 2013. Why the long face? The mechanics of mandibular symphysis

proportions in crocodiles. *PloS ONE*, 8(1), p.e53873.

Watanabe, A. & Slice, D.E., 2014. The utility of cranial ontogeny for phylogenetic inference: A case study in crocodylians using geometric morphometrics. *Journal of Evolutionary Biology*, 27(6), pp.1078–1092.

Webb, G.J.W. & Messel, H., 1978. Morphometric analysis of *Crocodylus porosus* from the north coast of Arnhem Land, northern Australia. *Australian Journal of Zoology*, 26(1), pp.1–27.

Wueringer, B.E. et al., 2012. The function of the sawfish's saw. *Current Biology*, 22(5), pp.R150–R151.

Yans, J. et al., 2014. First carbon isotope chemostratigraphy of the Ouled Abdoun phosphate Basin, Morocco; implications for dating and evolution of earliest African placental mammals. *Gondwana Research*, 25, pp.257–269.

Young, M.T. et al., 2010. The evolution of Metriorhynchoidea (mesoeucrocodylia, thalattosuchia): an integrated approach using geometric morphometrics, analysis of disparity, and biomechanics. *Zoological Journal of the Linnean Society*, 158(4), pp.801–859.

2.3 Post-paper commentary:

2.3.1 Supplementary Information for paper:

Provenance and stratigraphy:

The specimens described here come from the Oulad Abdoun Basin and were recovered from the phosphate mines of Sidi Daoui and Sidi Chennane, near the town of Khouribga in northeast Morocco (Figure 2.1). Approximate data on locality (Sidi Daoui or Sidi Chennane), and in some cases, stratigraphic horizon ("Couche") were obtained by discussion with locals in the fossil trade. More precise stratigraphic constraint was made possible by examining the matrix surrounding the fossils and by using associated vertebrate fossils found in the matrix, primarily shark teeth, as index taxa to correlate the fossil.

The phosphates are largely devoid of invertebrate fossils or biostratigraphically useful microfossils such as foraminifera, dinoflagellates, or pollen (Kocsis *et al.*, 2014). However, the phosphates contain an exceptionally abundant and diverse selachian fauna, and the couches/beds have traditionally been correlated on this basis (Arambourg, 1952; Noubhani, 2010). More recently, carbon (Kocsis *et al.*, 2014; Yans *et al.*, 2014) and oxygen isotope stratigraphy have been used to refine the dating of the phosphates and their associated faunas (Kocsis *et al.*, 2014). The phosphates are broken up into a series of beds or "couches" (Noubhani and Cappetta, 1997; Kocsis *et al.*, 2014; Yans *et al.*, 2014). From top to bottom, these are Couche 0 and Couche I (Ypresian 52-56), Couche IIA and Couche IIB (Paleocene, 62-58Ma) and Couche III (Late Maastrichtian). Couche III is readily identifiable because the matrix contains a high density of sand-sized bone fragments, and frequently larger elements such as fish vertebrae and shark teeth, which often form dense and laterally extensive bonebed layers. The overlying Couche 0, I, and II beds tend to be composed primarily of phosphate pellets and small coprolites.

The fossil material described in this paper was prepared at the University of Bath. During preparation of the fossil material, we retained loose matrix and then dry sieved and graded the matrix. The sediment was picked for shark and ray teeth, which were then identified (C. Underwood, pers. comm. 2016) to correlate the fossils to Couche 0, I, IIA, or IIB. Associated matrix and shark teeth have all been retained and are catalogued with the specimens so that our biostratigraphic correlations can be verified by future workers.

The elasmobranch assemblage associated with the matrix of *Parvosuchus daouiensis* includes *Ixobatis mucronata, Palaeogaleus sp., Palaeogaleus ?brivisi, Triakis antunesi, Dasyatis sp.* (male morph), *?Danogaleus gueriri* and Lamniformes indet. (fragments preserved of the lamniforms might include *'Odontaspis' speyeri* and *Striatolamia whitei*). This assemblage is a mix of Danian and Maastrichtian taxa, however reworking of Maastrichtian material is common in the Grand Daoui region. Based on this information we assign a Danian age to this fossil (Arambourg, 1952; Noubhani and Cappetta, 1997; Cavin *et al.*, 2000; Tong and Meylan, 2013), which agrees with the Couche II age provided with the fossil.

Maroccosuchus zennaroi material was assigned to Couche I and 0. This is confirmed by the typical Ypresian assemblage of the associated elasmobranch material, which includes *Physogaleus secundus, Merabatis praealba, Abdounia beaugei, Archaeomanta melenhorsti, Chiloscyllium meraense,?Galeorhinus minutissimus* and a fragment of uncertain affinity,

possibly *Nebrius obliquus. Maroccosuchus brachygnathus* is preserved in one of the 'intercalaires'. This is an indurated layer and is very difficult to prepare, therefore no additional material has been gained from this matrix.

The matrix for *Argochampsa microrhynchus* was very sparse in associated elasmobranch material. Lamniformes indet. and a couple of triakids were recovered. *Triakis tanoutensis* might be present, but low preservation quality makes this uncertain. The matrix is distinctly different from the typical Couche III/Maastrichtian deposits, and as triakids are common in the Paleocene, a Paleocene age is assigned.

Examination of the associated material of *Phasmatosuchus decipulae* indicates Couche IIA/Late Paleocene age (Thanetian). The assemblage includes *Delpitoscyllium africanem, Hexanchus sp., Isurolamna inflate, Abdounia africana, Palaeogaleus ?prior* and *?Premontreia subulidens.*

Fossil preparation:

Fossils were received partially prepared, such that the dorsal face of all specimens was exposed and the fossil encased in a plaster jacket. Mechanical methods included the use of pin vice, brushes and construction of plaster jackets.

For the *Argochampsa microrhynchus* specimen, initial reconstructive work had been done, with plaster filling in damage on the fossil- the plaster has been highlighted in Figure 2.2. Examination of the surrounding fossil material suggests no forgery, as anatomical features or imperfections in the fossil are continuous across areas covered by plaster or matrix (Figure 2.6).

The *Parvosuchus daouiensis* specimen was partially prepared prior to acquisition. The posterior postorbital region of the skull was then fully prepared from the matrix. However, due to the state of preservation of the rostrum, which is heavily fractured, the rostral portion of the skull was left in the matrix. Photographs prior to preparation were taken as proof of the original position of the two parts of the skull with respect to each other.

The paratype of *Phasmatosuchus decipulae* was fully prepared prior to study, and reconstructive work had been carried out. Areas of reconstruction are highlighted in Figure 2.17-2.20 and discounted from anatomical interpretation.

Phylogenetic analysis:

Modifications were made to the character matrix from Jouve et al. (2014). Six new characters were added, and further modifications were made to three existing characters. After an examination of the character scorings for gavialoid taxa we modified scorings of the taxa listed below. An up to date character list and character matrix can be found in Appendix 1.

New characters:

239: Relationship between dentary tooth 1 and the premaxilla: no visible reception pit on ventral surface of premaxilla for receiving 1st dentary teeth (0), pit visible to receive the 1st dentary tooth on the ventral surface (1), deep pit on ventral surface to receive 1st dentary tooth and pierces the dorsal surface of the skull (2), occlusal notch for the first dentary tooth (3)

240: Diastema between the last premaxillary tooth and the first maxillary tooth: no diastema, alveolar spacing to accommodate caniniform tooth only (0), small diastema/no more than 2 teeth could fill the space (1), large diastema (2)

241: Size of the second maxillary alveolus: same size as the first (0), larger than the first (1), smaller than the first (2), same size as the first and the third larger (3)

242: Size of premaxilla at widest point: same size or smaller than the maxilla at widest point (0), wider than widest width of the maxilla (1)

243: Position of the 1st three premaxillary teeth: curved (0) or linear (1)

244: Width of interorbital bar: narrow (less than 30% of the midline width of the skull table) (0) or wide (>30%) (1)

Modified characters: (modifications shown in bold)

165: Edge of the maxillary tooth lower or at the same level than the space between toothrow (0), or edge of the maxillary tooth alveoli higher than the space between the toothrows (toothrow underlined) (1), **toothrow underlined and lateral margin becoming more deeply scalloped anteriorly (2)**

169: Less than 18 teeth (0), 18 to 22 teeth (1), 22-32 teeth (2) **or >32 teeth (3)** on maxilla

171: Frontal ends **posterior or at the same level (0)**, or extends well anterior (1) to the anterior extension of the prefrontal. [modified back to the coding in 2008 as examination of extant series show that there is too much variation to split character 0 into 2 characters]

Modifications were made in the character codings for the following taxa:

Eothoracosaurus mississippiensis
Thoracosaurus neocesariensis
Ikanogavialis gameroi
Euthecodon arambourgii
Euthecodon brumpti
Argochampsa krebsi
Maroccosuchus zennaroi

Additional analysis:

We ran an additional phylogenetic analysis which includes the more inclusive Crocodylomorpha (Turner, 2015). This was to check that the new taxa described here were in fact members of the crown group, and not one of the subsequent outgroups of the Crocodylomorpha. The results of the phylogenetic analysis indicate that these new fossils are crown crocodylians, and position with *Gavialis* and *Argochampsa* in the morphological matrix.

Character support:

Maroccosuchus:

The characters listed in Jouve et al (2014) for support for Tomistominae include 10 unambiguous synapomorphies: characters 43, 88, 93, 118, 119, 130, 153, 201, 204, and 235. In the morphology-only analysis, *Maroccosuchus* still forms the deepest branch of the Tomistominae. Character support is consistent with the result in the Jouve et al. (2014) analysis, but an additional character is found to support the grouping, spina quadratojugalis prominent at maturity (ch. 69). In the combined (morphology-with-molecular) analysis, *Maroccosuchus* is now defined as the basalmost member of the Gavialoidea (molecular definition), and is no longer included in the Tomistominae (which includes all taxa more closely related to *Tomistoma schlegelii* than *Gavialis gangeticus*). The results from the combined analyses find that the Gavialoidea is supported by a similar group of characters (43,88,93,118,119,201,204 and 235).

In the morphology-only analysis, *Maroccosuchus zennaroi* is supported by four synapomorphies; atlantal ribs possess large articular facets at anterior ends (ch. 15), pterygoid surface is pushed inward anterolateral to choanal aperture (ch. 73), supraoccipital exposure on dorsal skull table absent (ch. 82), and very large maxillary foramen for palatine ramus of cranial nerve five (ch. 111). There is one apomorphic character for *Maroccosuchus brachygnathus,* MHNM.KHG.170, wide interorbital bar relative to the width of the skull table (ch. 244). Three out of the four synapomorphies for *M. zennaroi* were not coded in MHNM.KHG.170 because of incomplete preservation, therefore cannot be directly compared. In the combined (morphology-with-molecular) analysis, support for the two *Maroccosuchus* species remains the same.

Argochampsinae:

In the morphology-only analysis, character support for the Argochampsinae includes very long posterior squamosal prongs (ch. 64), dorsal half of prefrontal pillar anteroposteriorly expanded (ch. 137), absence of a medial crest on the basioccipital tubera (ch. 180), pendulous basioccipital tubera (ch.187), presence of a smooth medial depression ventral to the basioccipital and posterior to medial eustachian foramen (ch. 188), no visible foramen aereum (ch. 199), and frontal forms a broad contact with the premaxilla (ch. 223).

The *Argochampsa* genus is united by an upturned orbital margin (ch. 103), strong scalloping of the maxillary edge anteriorly (ch. 165), premaxillary width is wider than the rostral width (ch. 242), and first three premaxillary teeth form a linear row (ch. 243). *Argochampsa krebsi* is supported by one character, 22-32 teeth (ch. 169), whereas *Argochampsa microrhynchus* is scored as <18 teeth. Additional character support for *A. microrhynchus* includes an expanded medial hemicondyle (ch. 112), short ventral premaxilla-maxilla suture (ch. 168), distance between the tip of the snout and anterior position of premaxilla-maxilla suture is longer than the distance between the anterior position of the suture and its posterior extremity (ch. 191), and wide interorbital bar relative to the width of the skull table (ch. 244).

Parvosuchus daouiensis is supported by the following characters; small and posteriorly projected pterygoid processes (ch. 98), ventral border of exoccipital does not hide the cranioquadrate passage from view (ch. 166), 18-22 maxillary teeth (ch. 169), anterior process of jugal well posterior to frontal (ch. 174), and choana positions far posterior to the suborbital fenestra and anterior to the posterior margin of the pterygoid wing (ch. 206). Synapomorphies

for *Phasmatosuchus decipulae* include the nasal and premaxilla not in contact (ch. 95), tooth count >32 (ch. 169), and anterior margin of suborbital fenestra strongly exceeds anterior margin of the orbits (ch. 200).

In the combined (morphology-with-molecular) analysis, character support for the Argochampsinae includes characters 137, 199, and 223 (as in the morphology) and an additional character, the short length of the posterior premaxillary processes (ch. 192). The characters also attributed to this clade in the morphology-only analysis (ch. 64,180,187,188), which describe the elongate squamosal prongs and the shape of the basioccipitals, unite the Argochampsinae with the Gryposuchinae in the combined topology (Vélez-Juarbe, Brochu and Santos, 2007).

Character support for the individual *Argochampsa* species, and the genus remain similar to the morphology-only analysis. The only differences being that *A. krebsi* is no longer supported by character 169 (number of maxillary teeth), and the genus is supported by an additional character, linear frontoparietal suture (ch. 86). In the combined analysis, character support for *Parvosuchus daouiensis* is reduced to characters 98, 166, and 174. Similarly, for *Phasmatosuchus decipulae*, support is reduced to just character 95. Improved resolution in the combined topology indicates a sister group relationship between *Parvosuchus* and *Phasmatosuchus*, supported by characters 151 and 189.

2.3.2 Ontogenetic justification:

The new fossil material prompted questions about ontogeny and intraspecific variation within a species, and more specifically, whether the new fossil material described here should be referred to an existing species or diagnosed as a new species. Extant crocodylian species are often distinguished based on soft tissue characters, however this data is rarely available for fossil material. Scale patterns, overall coloration, and eye colour are common diagnostic features (Grigg and Kirshner, 2015). In addition to this, molecular data can reveal cryptic species, such as *Crocodylus niloticus* (Hekkala *et al.*, 2011) and *Osteolaemus tetraspis* (Eaton *et al.*, 2009), in extant crocodylians, which could not be identified based on morphology.

Crocodylians grow allometrically and display huge levels of variation throughout ontogeny (Kälin, 1933; Iordansky, 1973; Foth, Bona and Desojo, 2013; Watanabe and Slice, 2014; Fernandez Blanco *et al.*, 2015; Grigg and Kirshner, 2015; Blanco and Brochu, 2016; Martin *et al.*, 2016). For example, in extant species, variation is typically observed in relative proportions of the orbits and supratemporal fenestra, and skulls generally become more robust and heavily ornamented with age. During ontogeny, it has been found that younger individuals have typically have slender rostra, less ornamentation, and less robust teeth. It is often observed at later stages of ontogeny that there is a shift towards widening of the rostrum. This is thought to correspond to dietary shifts to larger prey and the structural requirement of this kind of feeding (Hall and Portier, 1994; Monteiro, Cavalcanti and Sommer III, 1997; Platt *et al.*, 2011; Iijima, 2017). Additionally, crocodylians demonstrate continuous growth, however dwarfism within a species has been also been documented in populations of *Crocodylus niloticus* and *Crocodylus johnstoni* when there have been food shortages (Grigg and Kirshner, 2015). These are all confounding factors that should be considered when describing new material.

Characters described in the character matrix are often oriented towards adult specimens (Brochu, 1997c), as juvenile material can differ greatly in terms of character scorings (Kälin, 1933; Iordansky, 1973; Wu, Russell and Brinkman, 2001; Martin *et al.*, 2016). However, it is often the case that only one or few specimens are known for a species. It has been demonstrated that postcranial material such as the vertebrae can be informative about the ontogenetic age of a fossil, however this is more difficult with skull material. A smaller sized skull could represent a juvenile of an existing species, a dwarfed skull within a species, or a new species. Therefore, if the ontogenetic age is uncertain, characters with different scorings may erroneously split a specimen into a new species. In the literature, though there are abundant studies on ontogeny of extant species of crocodylian, it is difficult to translate this to fossil material, as the majority of studies focus on principal component analysis (PCA) or regression-based analyses rather than individual anatomical variations. The majority of studies are focussed on individual species as opposed to multiple species to find common ontogenetic trends within Crocodylia.

In order to examine this in detail, comparative data was collected from extant species amongst the Crocodylia. Nine different species were selected with a range of different skull morphologies within Crocodylia, ranging between 10-50 skulls per species from juveniles to adults. Photographs were taken in dorsal, ventral, occipital, and lateral views, to compile a comparative database on which to draw conclusions about this new fossil material. Due to similarities in overall morphology and phylogenetic position with respect to *Maroccosuchus*

zennaroi, ontogenetic series of *Crocodylus porosus, Mecistops cataphractus, Gavialis gangeticus* and *Tomistoma schlegelii* were compared (Figure 2.27-2.28). These four species were chosen as they are similar in terms of morphology and phylogenetic position.

The skull material referred to the species *Maroccosuchus zennaroi* in this chapter (MHNM.KHG.171, MHNM.KHG.172, MHNM.KHG.173) exhibits a range of characters inconsistent with the current scorings of *M. zennaroi*. The new specimens range in size between 42-55cm total skull length, whereas some of the larger published material is 70cm (Jouve *et al.*, 2014). It is therefore feasible that the variation observed in these individuals is due to ontogeny and intraspecific variation, rather than showing diagnostic characters for a new species. In addition to overall morphology, the differences in the shape of the supratemporal fenestrae, the shape of the jugals around the orbits, and the more slender teeth observed in these individuals can all be reconciled with ontogenetic changes in extant species.

A number of characters were scored differently in the new material compared to the published scorings for *Maroccosuchus zennaroi* (Jouve *et al.*, 2014). These include teeth laterally compressed posteriorly (ch. 194), ectopterygoid extends beyond anterior quarter of suborbital fenestra (ch. 173), and prefrontals elongate and extending well beyond anterior end of frontals (ch. 117, 171). However, when compared to the comparative sample of extant crocodylians, these characters are found to vary within the sample as well. This highlights problems with using the current phylogenetic matrix when fossil ontogenetic age is uncertain and suggests that a reassessment of the characters would assist future diagnosis of new fossil material.

As discussed in the paper, the skull proportions of *Maroccosuchus brachygnathus* sp. nov. do not reconcile well with ontogenetic variability for *M. zennaroi.* There are examples in the literature where fossil species have been identified using growth series when enough fossil material has been recovered (Wu, Russell and Brinkman, 2001; Blanco and Brochu, 2016; Martin *et al.*, 2016). Using a similar methodology, skull length vs. skull table width is plotted for available *M. zennaroi* specimens and compared with extant material (Figure 2.29). Skull table width is chosen over quadrate width, as the quadrates are incompletely preserved in some of the new material (data available in Appendix 1). The position of the *M. brachygnathus* specimen was found to be well outside of the range of variation seen in extant material, suggesting that the unusual skull proportions exhibited by this specimen is not due to intraspecific or ontogenetic variation.

Figure 2.27: Ontogenetic variation in extant crocodylian species, *Gavialis gangeticus* (left) and *Tomistoma schlegelii* (right). Skulls photographed in dorsal view, scale bar= 10cm. *Gavialis* skulls (smallest first): NHM 1896.7.7.4, NHM 1846.1.7.3, USNM 72562, NHM (no number), AMNH 173632, FL 118998, NHM 1935.6.4.1, AMNH 15176, AMNH 7138, NHM 1974.3009. *Tomistoma* skulls (smallest first): NHM 1899.1.31.1, FL 54210, NHM 1893.3.6.14, NHM 1848.10.31.19, RBINS 18141, NHM 1923.6.4.6, USNM 211323, AMNH 15177, RBINS 154c, NHM 1894.2.21.1.

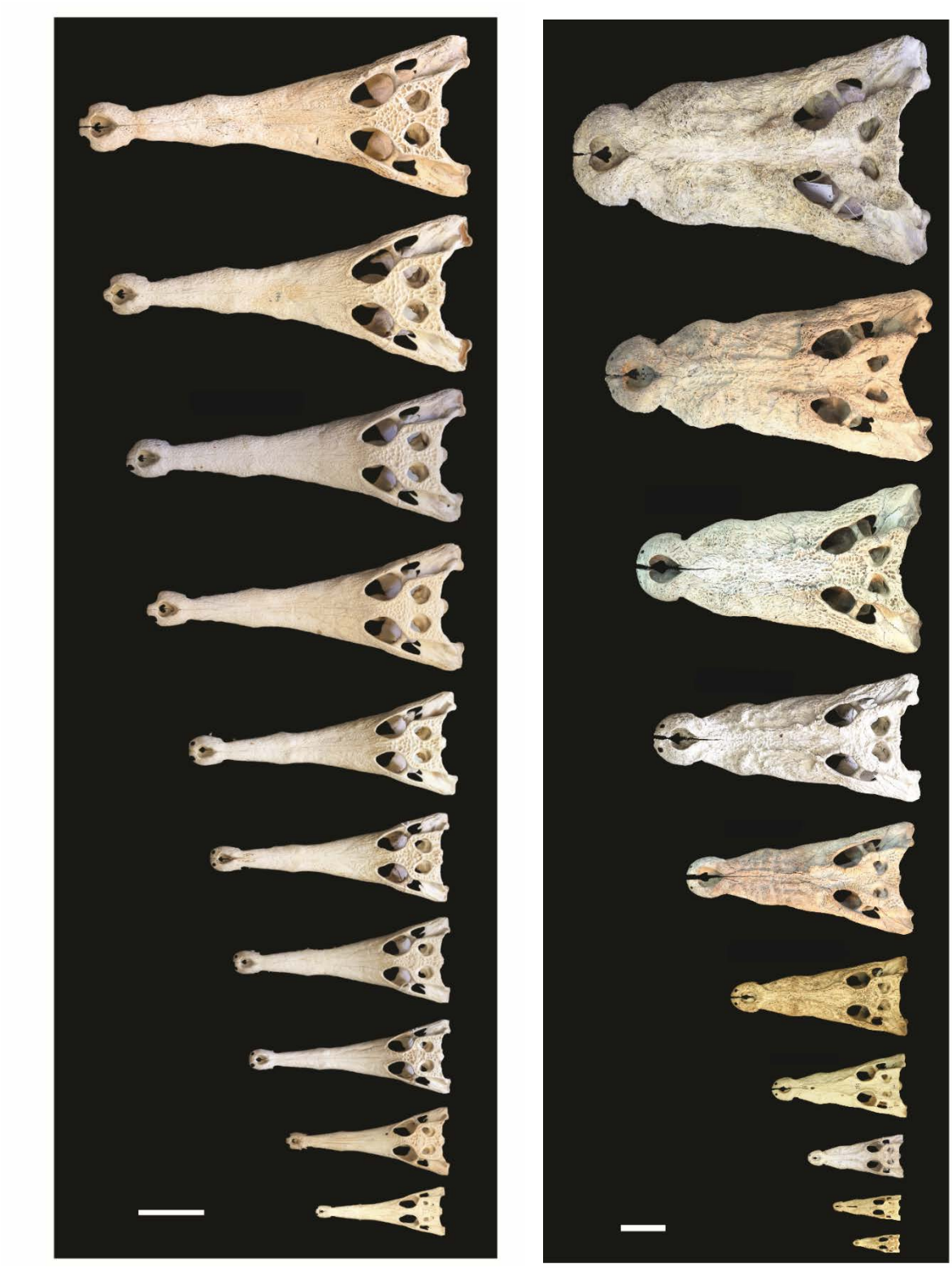

Figure 2.28: Ontogenetic variation in extant crocodylian species, *Mecistops cataphractus* (left) and *Crocodylus porosus* (right). Skulls photographed in dorsal view, scale bar= 10cm. *Mecistops* skulls (smallest first): AMNH 10074, RBINS 6031, RBINS 4976, RBINS 4983, RBINS 4977, RBINS 4981, RBINS 4989, RBINS 4998, RBINS 4990, RBINS 17967. *C. porosus* skulls (smallest first): AMNH 29298, AMNH 66383, RBINS 161, USNM 211309, AMNH 07131, NHM 1938.1.1.6, RBINS 13514, NHM 1865.8.22.1, NHM 1847.3.5.33, RBINS 161b.

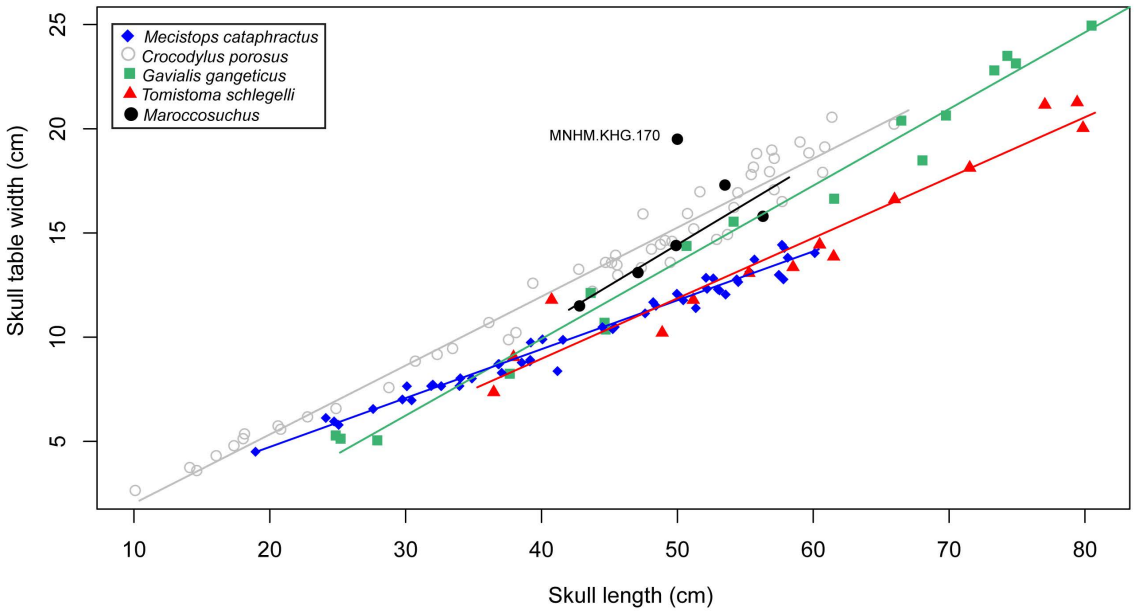

Figure 2.29: Cranial measurements of ontogenetic series of four extant crocodylians plotting skull length and skull table width. Linear regressions were calculated to compare variability in extant species to specimens of the genus *Maroccosuchus.* Measurements are provided in Appendix 1. Sample sizes: *Tomistoma schlegelii* = 14, *Gavialis gangeticus* = 17, *Mecistops cataphractus* = 50, *Crocodylus porosus*= 54, *Maroccosuchus*= 6.

2.3.3 Conclusion:

In this chapter, four new species of crown crocodylian have been described from the Paleocene-Eocene deposits of the Oulad Abdoun basin of Morocco. The new species are varied in skull morphology, suggesting a range of feeding habits. The results obtained from the two sets of phylogenetic analyses were broadly consistent with previous works in terms of the position of the Gavialoidea (Gold, Brochu and Norell, 2014; Jouve *et al.*, 2014).

The abundance of this crocodylian material in the Paleocene-Eocene deposits suggests the presence of interesting macroevolutionary patterns with respect to the recovery from the K-Pg mass extinction. In addition, as stratigraphically early members of the Gavialoidea and Tomistominae, they could help improve our understanding of the phylogenetic conflict. In the following chapter, the phylogenetic results from this chapter are examined in a time calibrated framework and stratigraphic congruence is assessed. The new species are also incorporated into a stratigraphic framework to examine disparity and body size evolution over the Cretaceous-Cenozoic, with an emphasis on the K-Pg.

Chapter 3: Diverse assemblage of marine Crocodylia following the K-Pg mass extinction

3.1 Pre-paper commentary:

The Moroccan phosphates are used as a case study in this thesis to investigate the effects of the K-Pg mass extinction on the Crocodylia. Both the extinction and the recovery can be studied as the stratigraphic record is continuous from the Late Cretaceous-Eocene (Kocsis *et al.*, 2014; Yans *et al.*, 2014). In the previous chapter, numerous new species of crocodylian were described from the recovery interval of the K-Pg mass extinction and placed into phylogenetic context. The aim of this chapter was to examine the macroevolutionary patterns of crocodylians and more specifically the gavialoids and tomistomines, incorporating the new taxa described in previous chapter. So far, there has been limited study on the crown crocodylians in terms of disparity and body size studies. The studies that do exist include the wider Crocodylomorpha (Langston, 1973; Sadleir and Makovicky, 2008; Wilberg, 2017), and therefore individual patterns within the crown group alone have not been examined in detail.

This chapter represents an in-depth study of a the macroevolutionary pattern amongst the Gavialoidea and Tomistominae, containing the most comprehensive set of fossils (not used in other macroevolutionary studies), a targeted phylogeny and a more detailed landmarking scheme to capture finer detail within the sample. Disparity and body size were investigated over the Cretaceous and Cenozoic with the new species incorporated into the known fossil record for these groups. In addition, the relationships between the gharial and false gharial remain controversial, as discussed in the previous chapter. In this chapter, a novel approach is taken to examine this conflict, by adding a stratigraphic time calibration to each phylogeny and comparing stratigraphic consistency indices. This time calibrated phylogenetic framework to assess how the differing hypotheses affect our understanding of crocodylian evolution, specifically over the K-Pg boundary.

This declaration concerns the article entitled:									
Diverse assemblage of marine Crocodylia following the K-Pg mass extinction									
Publication status (tick one)									
draft manuscript		**Submitted**		**In review**	X	**Accepted**		**Published**	
Publication details (reference)	Planned for resubmission of revisions to PloS Biology								
Candidate's contribution to the paper (detailed, and also given as a percentage).	Combination of ideas that formulate this paper were conceived by both N. Longrich and P Russell. Choice of methods for morphometrics, body size and stratigraphic congruence methods were chosen by Polly Russell with additional input from N. Longrich, M. Wills and E. Randle (in acknowledgements). All analyses and data collection were carried out by P. Russell. All figures were produced by P. Russell with suggestions for edits made by N. Longrich. The manuscript was predominantly written by Polly Russell and all supplemental material. N. Longrich contributed to the writing of the abstract, introduction and discussion. Additional input to the manuscript has been provided by numerous anonymous reviewers. Polly Russell 75%, Nick Longrich 25%								
Statement from Candidate	This paper reports on original research I conducted during the period of my Higher Degree by Research candidature.								
Signed						**Date**			

Diverse assemblage of marine Crocodylia following the K-Pg mass extinction

Polly Russell[a, b] and Nicholas R. Longrich[a, b,*]

[a] Department of Biology and Biochemistry and [b] Milner Centre for Evolution, University of Bath, Claverton Down, Bath, BA2 7AY, United Kingdom

Abstract:

The Cretaceous-Paleogene (K-Pg) mass extinction saw major upheaval in marine ecosystems, notably the extinction of large apex predators such as mosasaurs and plesiosaurs. However, other animals filling this ecological niche, such as marine crocodylomorphs, survived this catastrophic event without major drops in their diversity. The recent description of several new species of crown crocodylian from the Paleocene-Ypresian of Morocco belonging to the gavialoids and tomistomines have prompted an investigation into diversity and disparity of these groups over the K-Pg boundary. A combination of phylogenetic (morphological and molecular data) and morphometric analyses demonstrate that gavialoid crocodylians radiated, both taxonomically and morphologically during the early Cenozoic, with gavialoids from Morocco reaching a peak in diversity and disparity in the wake of the K-Pg extinction event. Gavialoids, along with dyrosaurid crocodylomorphs, palaeophiid and madtsoiid sea snakes, and chelonioid and bothremydid sea turtles formed a major component of the post-Cretaceous marine reptile radiation filling ecological niches left vacant by the mass extinctions victims.

Crocodylia| Gavialoidea | evolution | extinction | radiation | Paleogene

Introduction:

The Cretaceous-Paleogene (K-Pg) mass extinction, 66 Ma, was among the most severe extinctions in Earth's history, causing the demise of 40% of marine genera globally (Bambach 2006). Major extinctions were seen on land (Longrich et al. 2011; Longrich et al. 2012; Archibald & Bryant 1990), including the extinction of non-avian dinosaurs (Brusatte et al. 2015) and pterosaurs, as well as severe extinctions in marine environments, including ammonites and large apex predators such as mosasaurs (Polcyn et al. 2014) and plesiosaurs (Vincent et al. 2011). High levels of extinction and turnover were also seen within marine teleosts (Friedman 2009), sharks (Adolfssen & Ward 2014), bivalves (Jablonski 2008), nanoplankton and foraminifera (Schulte et al. 2010). Freshwater environments were not so strongly affected by the extinction (Robertson et al. 2013; Kaiho et al. 2016).

The K-Pg extinction marks a major shift in global faunal composition, from the reptile dominated fauna of the Mesozoic, to the mammal and bird dominated fauna of the Cenozoic (Jablonski & Chaloner 1994; Brusatte et al. 2015; Alroy 1999; Feduccia 1995; Prum et al. 2015; dos Reis et al. 2012). Throughout the Cenozoic, mammals radiated and became significant

components of terrestrial, marine and freshwater ecosystems. However, marine mammals did not become prevalent in marine ecosystems until the Eocene-Oligocene (Gingerich & Zouhri 2015; Domning 2001; Berta et al. 1989; Barnes & Goedert 2001; Bardet et al. 2010). Mounting evidence suggests that there was a recovery of marine reptiles in the aftermath of the K-Pg, represented by a diverse fauna of crocodylomorphs, snakes and turtles in low- to mid- latitude seas during the Early Paleogene (Bardet et al. 2010; Erickson 1998; Barbosa et al. 2008).

Crocodylia, the crown group, first appeared in the Late Cretaceous of North America (Brochu 2004; Wu et al. 2001) and represent one of three crocodylomorph lineages to survive the K-Pg mass extinction, alongside the marine Dyrosauridae and terrestrial Sebecidae (Kellner et al. 2014; Brochu 2003). The effect of the mass extinction on Crocodyliformes has previously been considered as relatively minor, with marine forms in particular showing increased taxon counts in the Paleocene (Puértolas-Pascual et al. 2016; Mannion et al. 2015; Bronzati et al. 2015; Kellner et al. 2014; Markwick 1998). This increased abundance following the extinction suggests that marine crocodyliformes may have benefited from the mass extinction, possibly stemming from lack of competition and predators in the early Cenozoic seas (Mannion et al. 2015). This pattern for marine Crocodyliformes is driven by the Dyrosauridae and the Gavialoidea, which share a specialised longirostrine (long and slender snout) morphology (Brochu 2001; McHenry et al. 2006; Mannion et al. 2015).

Aside from diversity trends, other patterns of Crocodylia evolution over the K-Pg boundary remain incompletely understood. Wilberg (2017) examined disparity amongst the Crocodylomorpha and found a significant decrease in disparity over the K-Pg boundary, however this is largely due to the loss of the diverse terrestrial crocodyliformes the Notosuchia. Patterns within the crown group alone have not been tested explicitly. Similarly, trends in body size evolution over the extinction event, though discussed in the literature, have not been tested in detail.

Recently, a number of new fossils have been described from Morocco (Figure 3.1), from the Paleocene-Ypresian (Russell and Longrich, in prep.). The new species have been diagnosed as members of the crown group with the Gavialoidea and Tomistominae. The relationships of the extant gharial (*Gavialis gangeticus*) and 'false' gharial (*Tomistoma schlegelii*) remain the source of much debate. Morphological data recover the Gavialoidea (all taxa more closely related to *Gavialis gangeticus* than *Crocodylus niloticus* and *Alligator mississippiensis* (Brochu 2003)) in a position basal to Crocodyloidea and Alligatoroidea, whilst Tomistominae remain nested within the Crocodyloidea. In contrast, mitochondrial DNA (Man et al. 2011; Janke et al. 2005; Aggarwal et al. 1994; McAliley et al. 2006; Meredith et al. 2011), nuclear DNA (Green et al. 2014; Harshman et al. 2003; Willis et al. 2007) and combined analyses (Gatesy et al. 2003; Gold et al. 2014) support a sister-group relationship between Gavialinae and Tomistominae (Russell and Longrich, in prep.). In the molecular context, Tomistominae becomes incorporated into Gavialoidea. This conflict limits our understanding of how these groups diversified with respect to each other, especially around the K-Pg boundary. The discovery of these new species in the Paleocene has therefore prompted an investigation into this conflict in a stratigraphic framework. Here, we frame this phylogenetic conflict in a new light by adding a stratigraphic time calibration to the conflicting topologies to assess stratigraphic congruence.

To date, up to seven species of gavialoid and tomistomine were known between the Paleocene-Ypresian (Jouve et al. 2006; Brochu 2006; Delfino et al. 2005; Jouve et al. 2014;

Brochu 2007; Troedsson 1924; Zarski et al. 1998). The addition of the four newly described Moroccan species therefore, adds significantly to the known diversity in this interval and suggests that there was much higher diversity than supposed hitherto after the K-Pg boundary (Figure 3.1). In this paper, we examine diversity, disparity and body size trends amongst the gavialoids and tomistomines with an emphasis on the K-Pg event. This was achieved using a combination of time calibrated phylogenetic and morphometric analyses to assess evolutionary relationships and shifts in morphospace occupation as expected with a radiation into newly vacant niches. Morphometric analyses suggest that marine crocodylians were able to diversify and occupy new niche space in the Early Paleogene, benefiting from the extinction of marine vertebrates in the K-Pg event.

Results

Phylogenetics

The phylogenetic analyses were carried out by Russell and Longrich (in prep.). The matrix used contains the largest number of Gavialoidea and Tomistominae, compared to previous analyses (Gold et al. 2014; Brochu 2012; Jouve et al. 2014), to provide a more targeted analysis of the phylogenetic conflict. The phylogenetic analyses carried out by Russell and Longrich (in prep.) included a morphological character matrix and a combined matrix of morphological and molecular data. Here, using the results from Russell and Longrich (in prep.), we time calibrated the strict consensus topologies to understand how this conflict affects the patterns of extinction and survival over the K-Pg event. In addition, we calculated stratigraphic congruence indices to assess fit with the fossil record. Time calibration was applied to each consensus topology based on stratigraphic first and last appearance dates.

The morphological phylogeny, which does not recover a relationship between gavialoids and tomistomines, is consistent with previous research using morphology (Jouve et al. 2014; Vélez-Juarbe et al. 2007; Brochu 2007). The strict consensus was produced from heuristic searches using morphological data only (Russell and Longrich, in prep.) and recovered 1,023 most parsimonious trees (MPT) with a tree length of 1,018 steps (CI: 0.32, RI: 0.725). Time calibration of the strict consensus from the morphology only dataset (Figure 3.2) is overall more consistent with the fossil record as inferred from ghost ranges. This was tested by using stratigraphic congruence indices (Figure 3.4). The indices were calculated from the most parsimonious trees from each analysis and not the strict consensus. For SCI, RCI and MSM all values closer to 1 suggest better fit to the stratigraphy. For the RCI, increasing positive values indicate improves stratigraphic congruence. Here the morphology-only phylogenetic analysis shows a consistently better fit to the fossil record than combined analysis (SCI: 0.563088, RCI: -262.846, GER: 0.833134, MSM*: 0.098571). Gavialoids first appear in the Cretaceous with multiple lineages crossing the K-Pg boundary and the Tomistominae originate and diversify in the Late Paleocene. The implication of the time calibrated phylogeny is that the majority of the gavialoids and tomistomines diversified after the K-Pg boundary, with the Argochampsinae diversifying in the Early Paleocene.

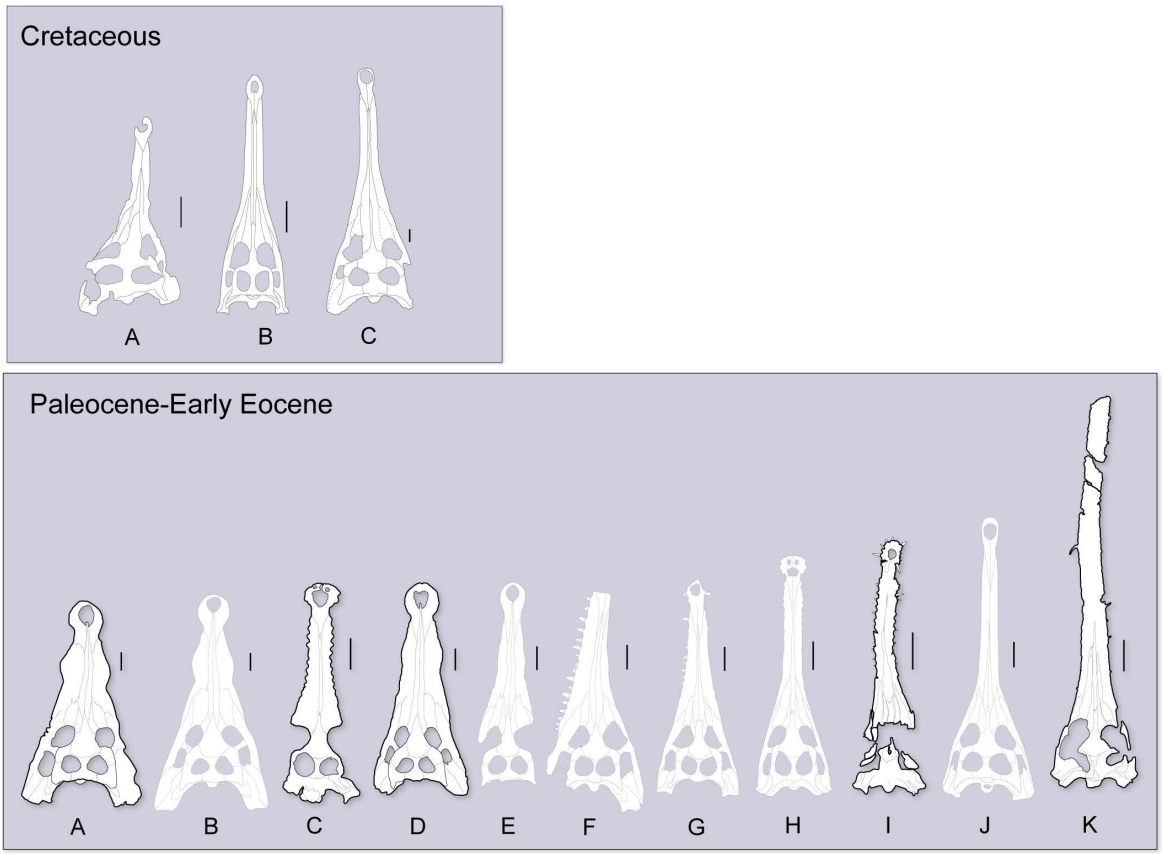

Figure 3.1. Variation in the skulls of the Gavialoidea (molecular context) in the Cretaceous, compared to the Paleocene-Ypresian, following of the K-Pg boundary. Skulls in dorsal view. Cretaceous: (A) *Thoracosaurus neocesariensis* (modified from (Laurent et al. 2000), (B) *Ocepesuchus eoafricanus* (modified from (Jouve, Bardet, et al. 2008)), (C) *Eothoracosaurus mississippiensis* (modified from (Brochu 2004)). Paleocene- Early Eocene: (A) *Maroccosuchus brachygnathus* sp. nov. (MHNM.KHG.170), (B) *M. zennaroi* (modified from (Jouve et al. 2014)), (C) *A. microrhynchus* sp. nov. , (D) *Maroccosuchus zennaroi* (MHNM.KHG.171), (E) *Kentisuchus spenceri* (modified from (Brochu 2007)), (F) *Eosuchus minor* (modified from (Brochu 2006)), (G) *Eosuchus lerichei* (modified from (Delfino et al. 2005)), (H) *Argochampsa krebsi* (modified from (Jouve et al. 2006)), (I) *Parvosuchus daouiensis* gen. et. sp. nov., (J) *Thoracosaurus scanicus* (syn. *T. macrorhynchus*) (modified from (Troedsson 1924)), (K) *Phasmatosuchus decipulae* gen. et. sp. nov. Drawings scaled to the same postorbital length, taxa in bold represent newly described species from Morocco. Scale = 5cm.

Phylogenetic analysis combining morphological and molecular data (Gold et al. 2014) found 32 MPTs each of 17,985 steps (CI: 0.562, RI: 0.628) (Russell and Longrich, in prep.). In summary, this topology was consistent with previous molecular and combined analyses (Harshman et al. 2003; Oaks 2011; Janke et al. 2005; Gatesy et al. 2003; Gold et al. 2014). Specifically, the Gavialoidea shifted from their basal position and form a sister relationship to the Crocodyloidea, while the Tomistominae were incorporated into the Gavialoidea (Russell and Longrich, in prep.). The term, Gavialidae is used to describe the last common ancestor of *Gavialis gangeticus* and *Tomistoma schlegelii* and all its descendants (Brochu 2003).

Time calibration of the combined consensus (morphology-with-molecular) (Figure 3.3), was less congruent with the fossil record of crocodylians as demonstrated by the increased number and length of ghost lineages (SCI: 0.401316, RCI: -433.649, GER: 0.745999, MSM*: 0.067033) (Figure 3.4). In the morphology-with-molecular phylogeny the Gavialoidea are in a highly nested position within the tree. This shift away from the root for the Gavialoidea increases the ghost lineages for taxa positioned more towards the root including the Tomistominae. This also creates a long ghost lineage for Crocodylidae and implies that the Crocodylia diversified rapidly in the Late Cretaceous (Figure 3.3). In comparison to the morphological hypothesis, this suggests a mass survival of the Gavialoidea across the K-Pg boundary. However, the Argochampsinae still diversifies in the earliest Paleocene, in the immediate aftermath of the K-Pg extinction.

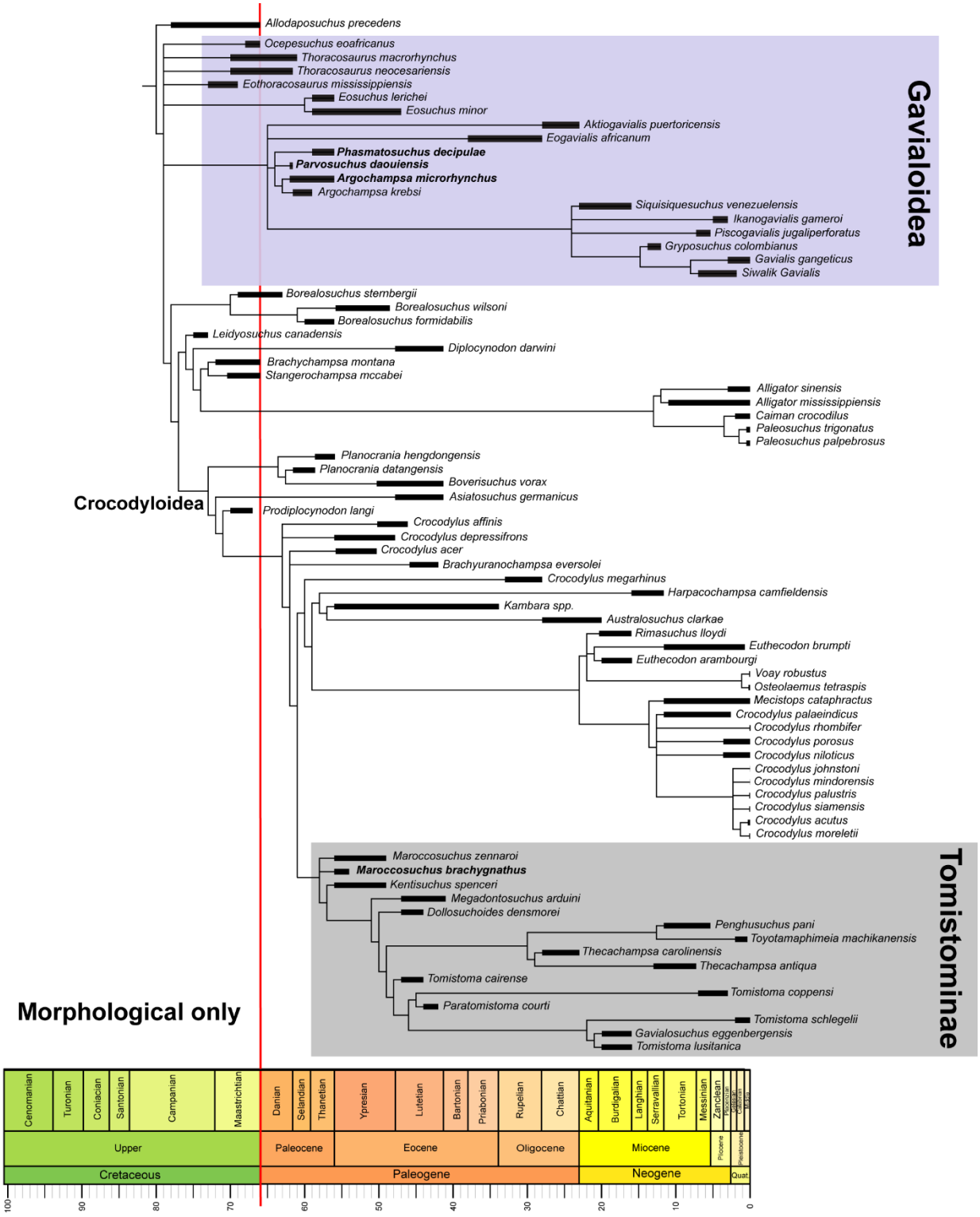

Figure 3.2. Strict consensus of 1023 most parsimonious cladograms from the morphological dataset (length= 1018 steps, CI= 0.32, RI= 0.725). Stratigraphic time calibration is based on first and last occurrence dates and *Bernissartia* and *Hylaeochampsa* were dropped from the figure after the analysis. Red bar = K-Pg mass extinction.

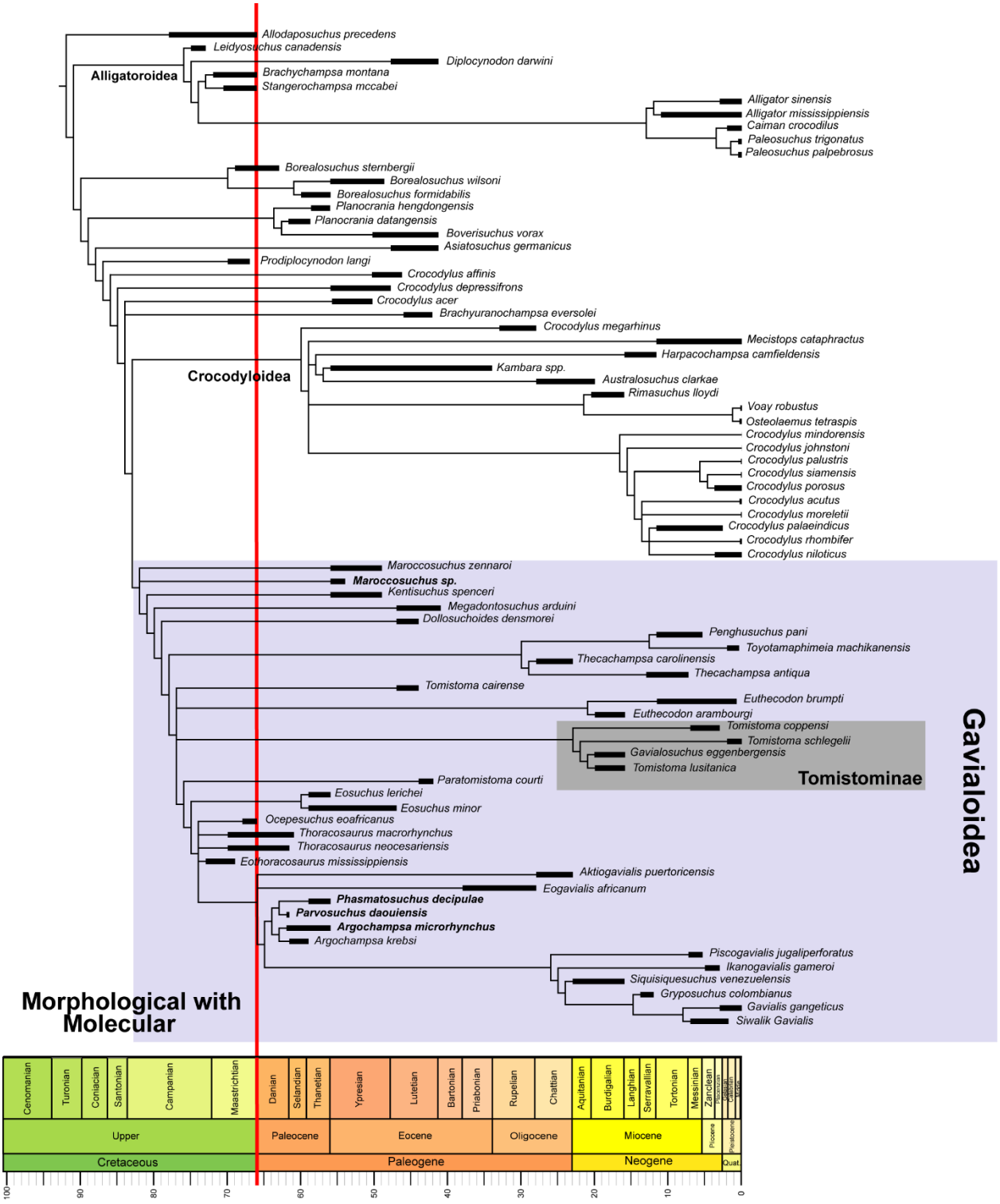

Figure 3.3. Strict consensus of 32 most parsimonious cladograms from the combined morphological and molecular datasets (length= 17,985 steps, CI= 0.562, RI= 0.628). Stratigraphic time calibration is based on first and last occurrence dates. *Bernissartia* and *Hylaeochampsa* were dropped from the figure after the analysis. Red bar = K-Pg mass extinction

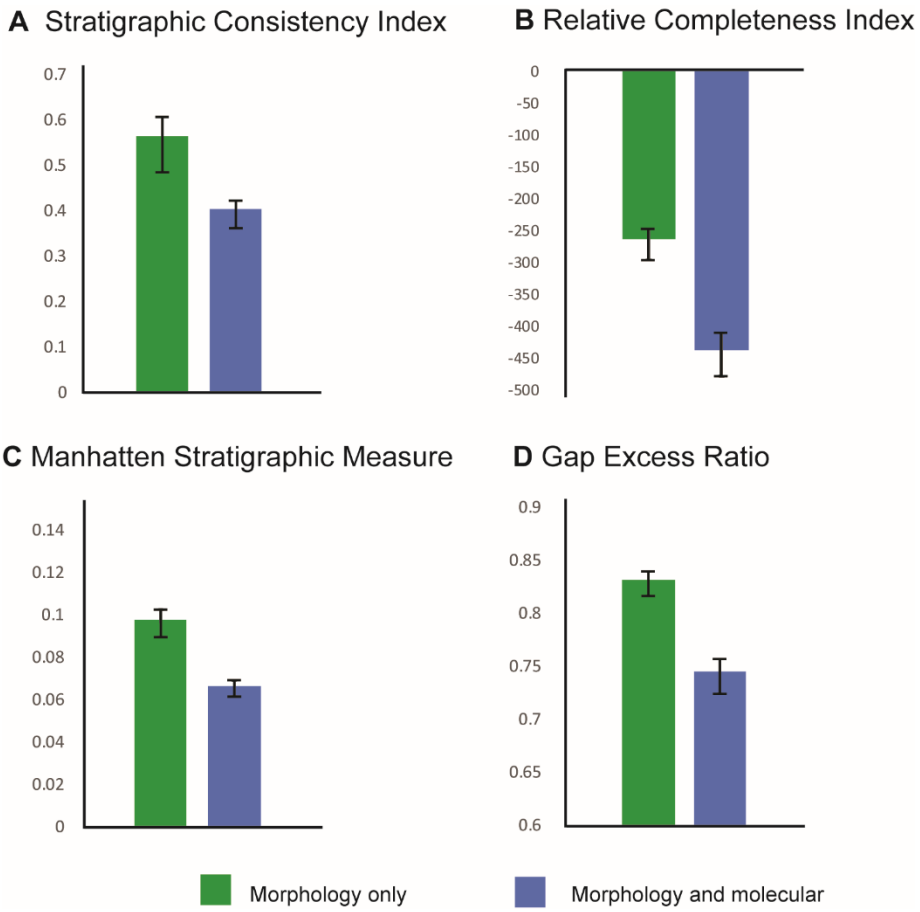

Figure 3.4: Stratigraphic congruence indices calculated for the morphology only and combined (morphology-with-molecular) analyses. Indices were calculated from the most parsimonious trees from each phylogenetic analysis, 1024 most parsimonious trees for the morphological analysis and 32 trees for the combined analysis.

Disparity

Snout morphology was quantified amongst the gavialoids and tomistomines using linear measurements (Figure 3.10A). Our results (Figure 3.5A, Table 3.1) indicate the largest amount of overall variation (sum and products of ranges and variances) (Table 3.1) is seen in the Paleocene-Early Eocene; the time bin following the K-Pg mass extinction event. In terms of relative snout length, the extreme regions of the Paleocene-Ypresian morphospace are occupied by two newly discovered species (Russell and Longrich, in prep.); *Maroccosuchus brachygnathus* and *Phasmatosuchus decipulae.* These species represent the shortest and most elongate rostra for the sampled fossil record of gavialoids and tomistomines respectively (Figure 3.1). The extremes of the relative orbital width (ROW) axis are similarly occupied by Moroccan species, *Maroccosuchus zennaroi* (Jouve et al. 2014) and *Argochampsa krebsi* (Hua & Jouve 2004).

Time Bin:	Sum of ranges	Root product of ranges	Sum of variance	Root product of variance
Results of the linear morphometrics				
Cretaceous	0.08878897	0.04090406	0.002268598	0.0008365711
Paleocene-Ypresian	0.4738932	0.2231729	0.01289415	0.004040516
Lutetian-Priabonian	0.2690427	0.1271959	0.0057141	0.002515217
Oligocene	0.1288048	0.06227898	0.001933204	0.0009108979
Miocene	0.2997212	0.1407292	0.005420314	0.002322964
Pliocene-Pleistocene	0.3257781	0.1524109	0.006224677	0.002429267
Results of the geometric morphometrics				
Cretaceous	0.1309204	0.01093131	0.001516766	0.0000597467
Paleocene-Ypresian	0.677479	0.0578129	0.01190509	0.0002966593
Lutetian-Priabonian	0.2650444	0.02567331	0.003215989	0.0001810538
Oligocene	0.2732934	0.05340198	0.003290122	0.0002016081
Miocene	0.4717324	0.05275353	0.004258561	0.0003482198
Pliocene-Pleistocene	0.5665943	0.0533793	0.007983991	0.0003037458

Table 3.1. Disparity results for each time bin using the stratigraphic binning scheme from Friedman (2010)

Results of the shape variation of crocodylian skull using geometric morphometric analysis are shown in Figure 3.5B and Figure 3.6, with PC1 and PC2 capturing 75.7% of the total variance. The first 8 PC axes account for 95% of the total variance (Table 3.3) and the first 5 PC axes suggest significant shape changes as they are to the left of the inflection point in the scree plot (Figure 3.11). PC1 accounts for 64.1% of total variance, describing overall snout shape variation, as shown by the vector plots (Figure 3.6). With increasingly negative loadings along PC1, the skull narrows and the rostrum becomes straighter and more elongate. The anterior extension of the nasal bone with respect to the premaxilla also contributes to shape variation along this axis. This character is phylogenetically informative amongst Gavialoidea and Tomistominae. The extreme negative values show the condition in *Phasmatosuchus* and *Gavialis* where the nasal and premaxilla are largely separated. Positive values show the plesiomorphic condition of the Crocodylia (as observed in *Maroccosuchus)*, with the nasal and premaxilla in contact and projecting into the external nares. PC2 explains 11.6% of total variance and captures shape changes entailing narrowing and elongation of the skull towards more negative loadings, as well as a reduction in the size of the skull table with an increase in size of the supratemporal fenestrae. The posterior portion of the rostrum is broader and less

tapered and the interorbital bar widens with positive loadings. PC3 through to PC5 inclusive describe 15.8% of the total variance and contribute very small amounts of shape variation. These are the length of the frontal, posterior extension of the premaxilla and shape of the skull table in PC3, and shape of the orbits, supratemporal fenestrae and length of the squamosals in PC4.

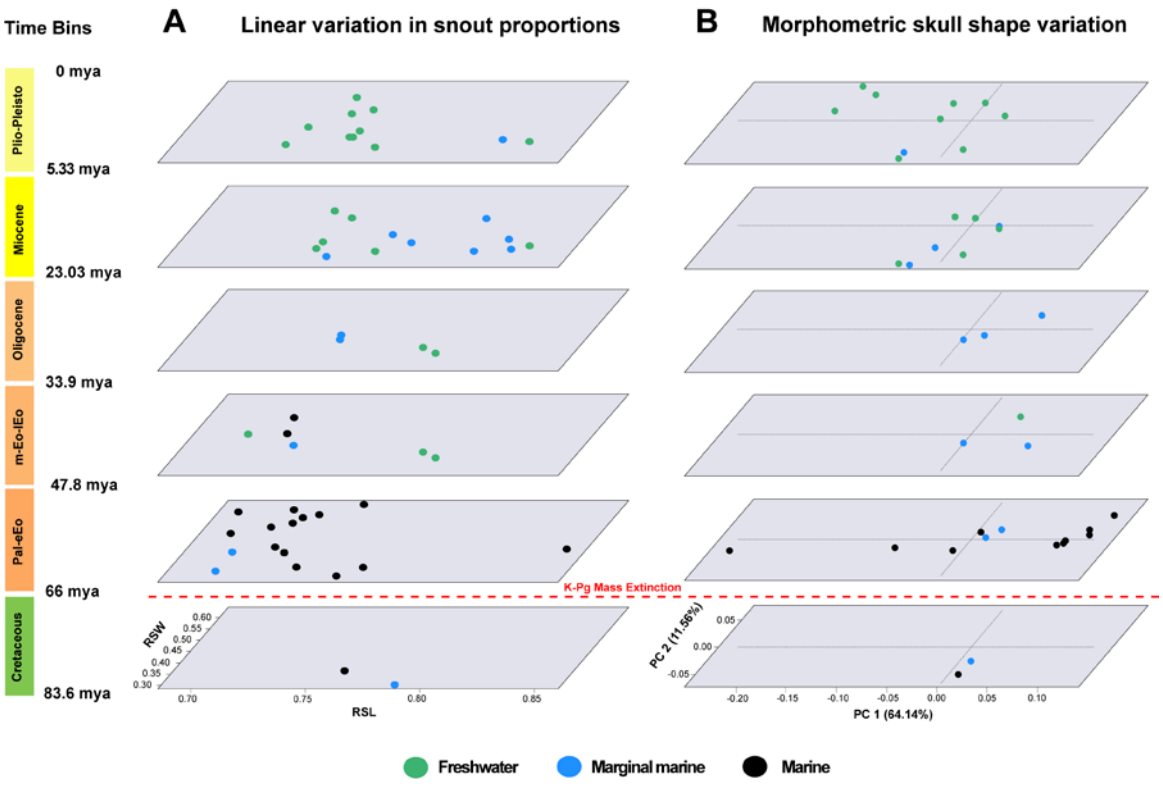

Figure 3.5. Results of the linear and geometric morphometrics analyses. (A) Stacked plot of relative snout length (RSL), rostral length/total skull length, vs. relative skull width (RSW), rostral width/postorbital width. (n=47). (B) Morphospace resulting from the principal components analysis of landmark data, showing principal components 1 and 2 which account for 75.7% of the total variation (n=35). The individual slices of the stacked plots represent taxa in each time slice.

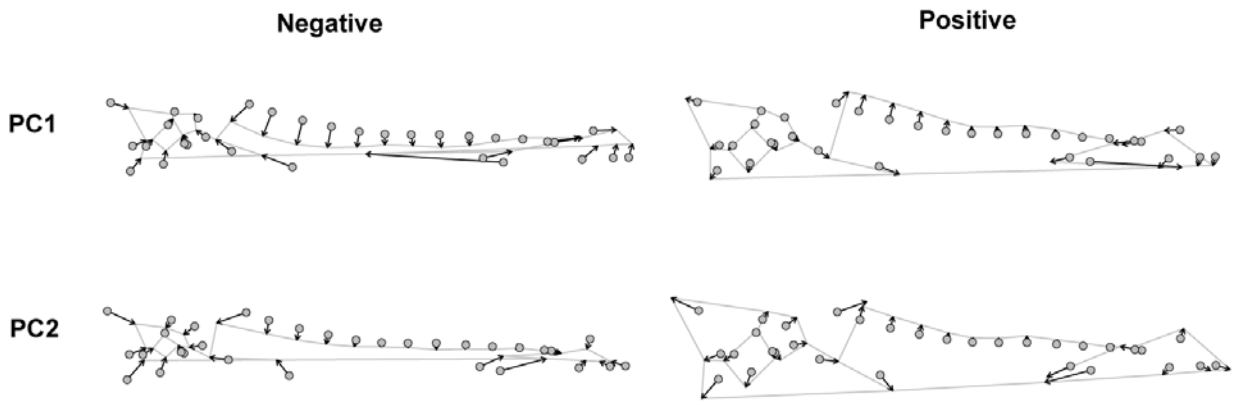

Figure 3.6. Vector plots for deformation along PC 1 and PC 2. Points show the configuration of landmarks for the mean shape. The arrows and lines indicate the configuration of landmarks at the extreme ends of the axes of PC1 and PC2.

The post-extinction time bin (Paleocene-Ypresian) occupies a large area of the morphospace showing the greatest spread across PC1 and is more restricted in PC2 (Figure 3.5B). Morphospace occupation is decreased in subsequent time bins showing greater spread across PC2 but increases in the Miocene and Plio-Pleistocene time bins. This increase in morphospace occupation in the Miocene-Pleistocene occurs in taxa that were found in coastal to freshwater settings, in comparison to the predominantly marine taxa in the Paleocene-Ypresian time bin. The sum and product of ranges and the sum of variances (Table 3.1) show that disparity is highest in the post extinction time bin. The product of variances, however indicates that the disparity is highest in the Miocene (0.00034) and Plio-Pleistocene (0.0003) bins (0.00029 in Paleo-Ypresian bin). Relative to the Cretaceous and mid-late Eocene time bins, the post-extinction time bin shows consistently higher disparity for all disparity metrics (Table 3.1).

The range metric gives an indication of overall variation in the sample but can be biased by sample size (Wills et al. 1994). Rarefaction (Figure 3.7B) was therefore carried out on the sum of ranges and the results were found to be broadly the same. We could not rarefy the Cretaceous time bin, as the bin contained only two taxa. Rarefied to a sample size of two, the sum of ranges indicates that the Cretaceous, Oligocene and mid-late Eocene time bins show the smallest amount of overall variation, and the Plio-Pleistocene and Paleocene-Ypresian time bins show the highest. The sum of variances was also rarefied (Figure 3.7A) and found to be robust to sample size; sum of variances is our chosen metric for disparity due to its relative insensitivity to sample size and outliers (Figure 3.7C, 3.8A) (Wills et al. 1994).

The 95% bootstrap confidence intervals do not overlap between the Cretaceous and post-extinction time bin, and therefore, disparity is significantly higher after the extinction (Figure 3.8A). The confidence intervals overlap with all subsequent time bins closer to the present. Though disparity is high in the post-extinction time bin, the results of the NPMANOVA

were not significant between subsequent time bins (Table 3.4), which indicates that they do not occupy a distinct area of morphospace and that there is overlap between morphospace of each time slice. The test for morphological outliers (Figure 3.7C) found that *Phasmatosuchus decipulae* is a significant outlier in morphology relative to other Gavialoidea and Tomistominae. As crocodylian skull morphology is highly indicative of diet (Brochu 2001; McHenry et al. 2006; Pierce et al. 2008), this occupation of a new area of morphospace suggests that this species had a unique feeding strategy amongst Gavialoidea.

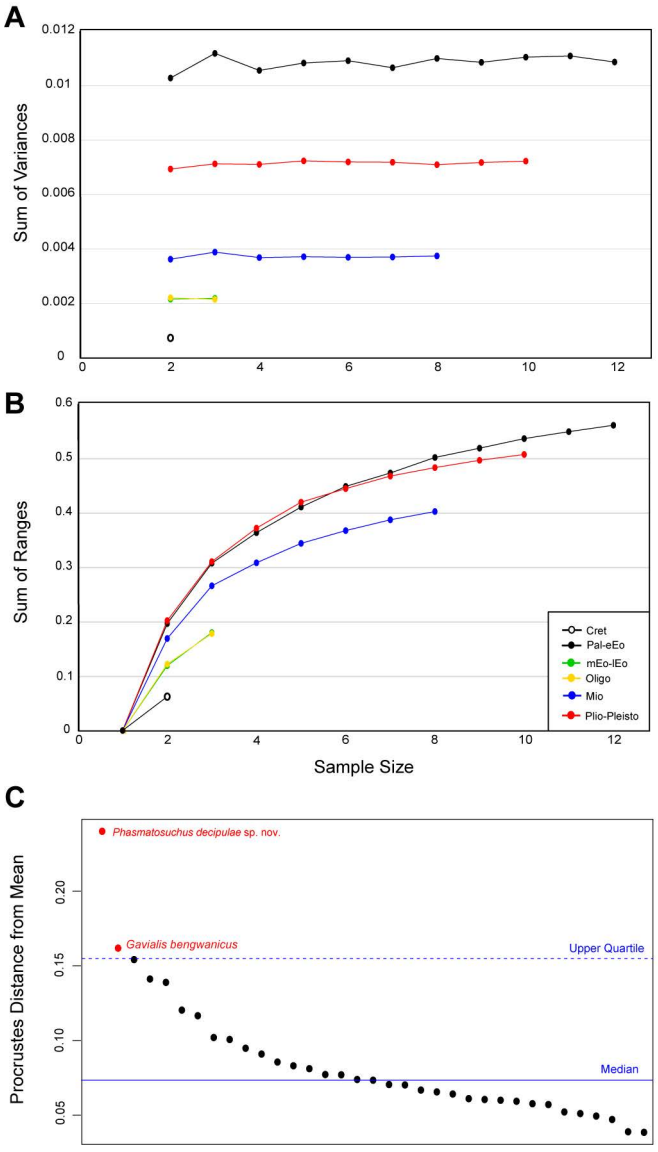

Figure 3.7. Results of the disparity analysis showing changes in disparity over time and morphological variation from the mean shape (test for outliers). (A) rarefaction analysis of sum of variances (B) rarefaction of the sum of ranges (C). GPA aligned landmark taxa plotted based on the Procrustes distance from the mean shape of all taxa. Taxa shown above the upper quartile are indicated in red.

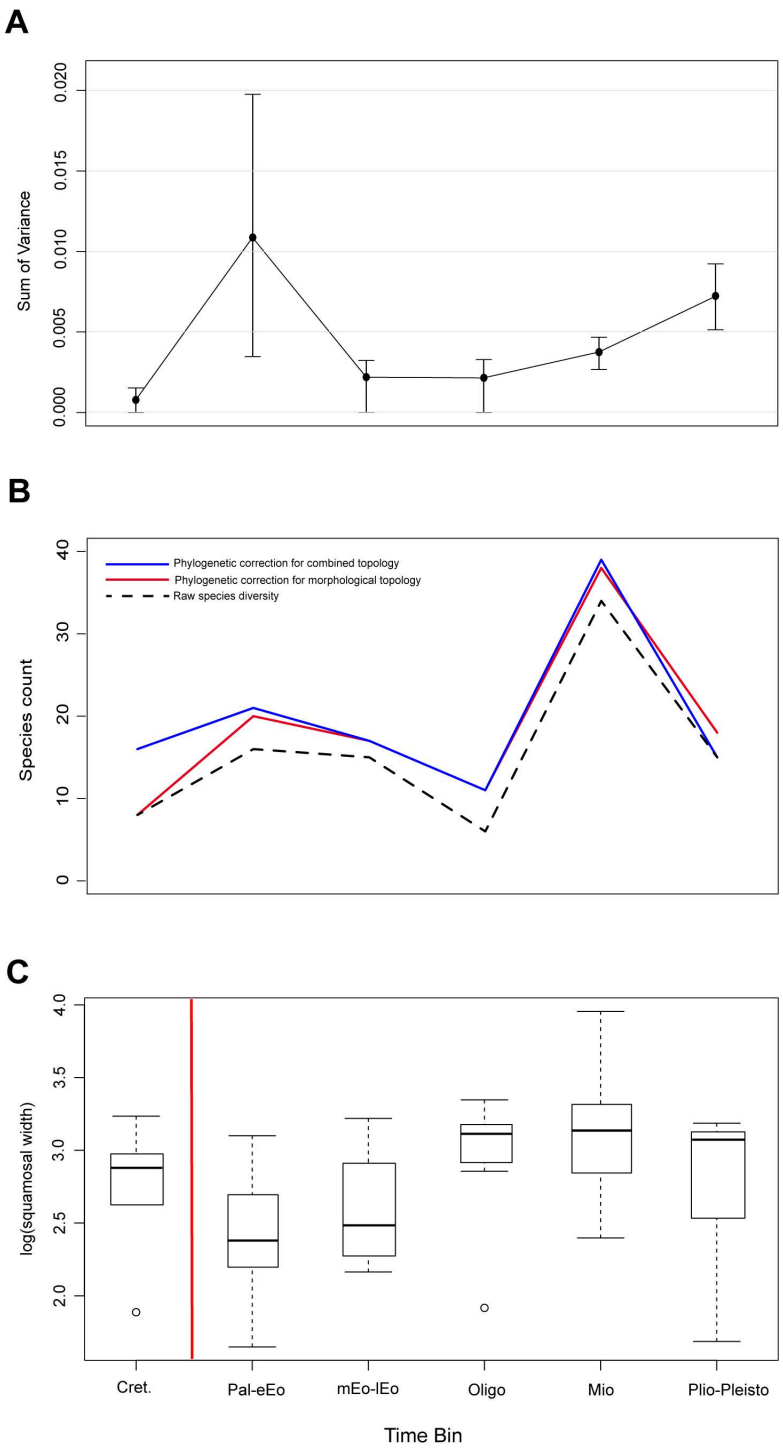

Figure 3.8 (A) Disparity in each time bin represented by the sum of variances, with 95% confidence intervals (based on bootstrap of 1000 replicates). (B) Diversity curves based on raw taxon counts and phylogenetically corrected counts (C) Boxplot of size through time for composite stage time bins. Mean values: Cretaceous= 2.7202, Paleocene-Ypresian= 2.4368, Lutetian-Priabonian= 2.5899, Oligocene= 2.9376, Miocene= 3.0852, Plio-Pleistocene= 2.7766. One-tailed t-test between the Cretaceous and Paleocene-Ypresian bin: t= 1.4575, p-value = 0.07897

The diversity curves show raw species diversity based on the fossil record and the phylogenetically corrected curves were calculated to account for bias in the fossil record (Figure 3.8B). The phylogenetic corrections are based on the two strict consensus topologies and factor in range expansions and ghost lineages, to account for the poor fossil record. The raw diversity curve largely matches the patterns of the phylogenetically corrected curves. All three curves indicate that species diversity increases over the K-Pg boundary, this is coupled with the increase in disparity. The main difference, as highlighted in the time-calibrated phylogeny (Figure 3.2,3.3) is the curve corrected for the combined phylogenetic analysis. This curve suggests that species diversity is much higher in the Cretaceous, implied by ghost ranges, therefore indicating higher rates of survival over the K-Pg extinction event. Following this initial rise in diversity after the K-Pg event, diversity decreases in the middle Eocene to Oligocene time bins, remaining coupled with disparity patterns. The Miocene diversity peak is not reflected as strongly in the disparity curve, which shows a small increase relative to diversity. As diversity drops in the most recent time bin, disparity continues to increase, becoming uncoupled from the diversity curve.

Investigation of skull size indicates that the post-extinction gavialoid and tomistomine fauna is characterised by small skull size, suggesting smaller body size (Figure 3.8C, 3.9). Mean skull size is lower than at any other point in the gavialoid fossil record, although the reduction in size is not statistically significant across the K-Pg boundary (one-tailed t-test: $t = 1.4575$, p-value = 0.07897 between the Cretaceous and Paleo-Ypresian time bin). In contrast, the dyrosaurids in the post-extinction time bin were much larger (Figure 3.9) and the difference in size between the gavialoids and dyrosaurs is statistically significant in the post-extinction time bin (one-tailed t-test: $t=3.7719$, $p= 0.0002916$). From the Late Eocene, we see an overall increase in size amongst the Gavialoidea and Tomistominae as well as a transition from predominantly marine fauna to estuarine/deltaic environmental preference.

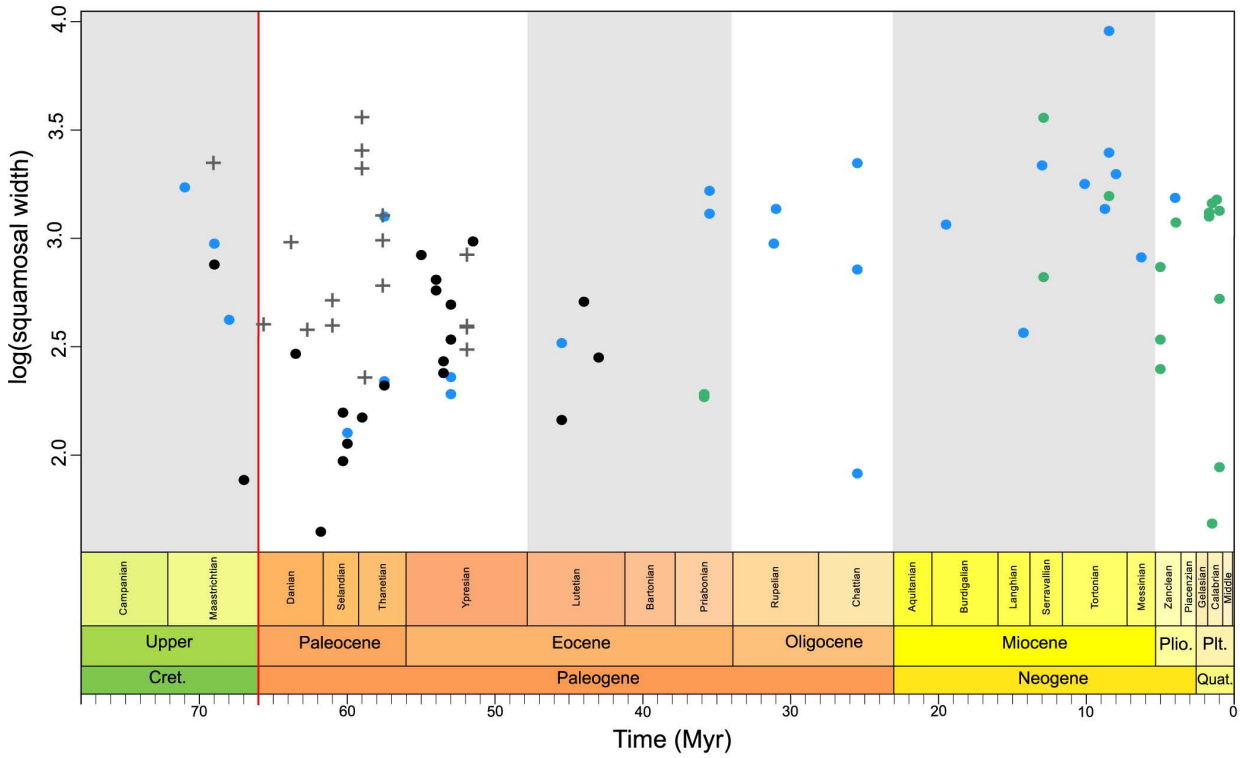

Figure 3.9. Skull sizes of Gavialoidea (molecular) from the Late Cretaceous to the Recent. Colours indicate environmental preference: black- marine, blue- marginal marine, green- freshwater. The crosses represent dyrosaurid taxa. The mid-point of the stratigraphic range of the taxa is plotted. Mean values by time bin: Cretaceous- **2.7202,** Paleocene-Ypresian- **2.4368,** Lutetian-Priabonian- **2.5899,** Oligocene- **2.9376,** Miocene- **3.0852,** Plio-Pleistocene- **2.7766.**

Discussion:

The number of lineages crossing the K-Pg boundary remains unclear as a result of the conflict between the morphological and combined (morphology-with-molecular) phylogenetic hypotheses (Figure 3.2, 3.3). The morphological dataset is more consistent with the fossil record, as inferred by a smaller number of ghost ranges. We calculated four stratigraphic congruence indices (Figure 3.4) to test this and found the morphological signal to consistently outperform the molecular-with-morphology signal. The diversification patterns from the morphology-only analysis (Figure 3.2) suggest that Paleogene diversity results from a few lineages surviving the extinction, then rapidly speciating and adapting to occupy new niches. Such a dynamic would be similar to neoavian birds, where Paleogene diversity results from rapid speciation of one or two survivors (Prum et al. 2015; Claramunt & Cracraft 2015).

Our combined consensus, alternatively, suggests that multiple crocodylian lineages crossed the boundary, including members of the Gavialidae and lineages of the Crocodyloidea. A similar dynamic is seen in placental mammals, where a diverse post-extinction community was the result of multiple lineages crossing the K-Pg boundary (Longrich et al. 2016;

Grossnickle & Newham 2016). The increased number of ghost lineages crossing the boundary in the morphology-with-molecular analysis suggests a cryptic missing early record for Crocodylia, perhaps suggesting unknown diversity and disparity prior to the K-Pg mass extinction. In both hypotheses, the Argochampsinae (Russell and Longrich, in prep.) originates after the K-Pg boundary, suggesting the disparity and diversity exhibited by these forms (*Phasmatosuchus* in particular) was not carried over the boundary and perhaps relates to a radiation into empty ecological niches. At present it is unclear if gavialoid diversity was driven primarily by rapid radiation of a few survivors (morphology only hypothesis) or mass survival (combined morphology-with-molecular hypothesis) and remains to be elucidated in future studies. In comparison to the low disparity of the Cretaceous, Paleogene gavialoids exhibit high diversity (Figure 3.1) and disparity (Figure 3.5, 3.8A) in the marine environment, suggesting occupation of a range of ecological niches (Russell and Longrich, in prep.) (McHenry et al. 2006; Pierce et al. 2008). The morphospace occupation shows brevirostrine forms (Figure 3.1, 3.5, 3.6) (Massare 1987; Rieppel & Labhardt 1979) with a broad, flattened rostrum more typical of extant crocodylids such as *Crocodylus niloticus*; these were likely to have been generalist feeders (Figure 3.1) (Brochu 2001). Longirostrine forms (long, tubular snouts) with needle-like teeth which presumably fed on fish and other small, unarmoured prey (see Russell and Longrich, in prep.). (McHenry et al. 2006; Walmsley et al. 2013; McCurry et al. 2017; Sadleir & Makovicky 2008). The most extreme morphology, and outlier in the morphospace (Figure 3.5, 3.7C), is the long-snouted *Phasmatosuchus* (Figure 3.1K). Possible feeding strategies for *Phasmatosuchus* have been hypothesised and range from the "trap guild" referred to cryptoclidid plesiosaurs (Chatterjee & Small 1989); or using the elongate rostrum to agitate the benthos and catch/stun small prey on the seafloor - similar to modern sawfish (see Russell and Longrich, in prep., for detailed discussion).

Regardless of the precise dietary habits of individual taxa in this bin, the disparity observed here suggests that gavialoids adapted rapidly, in the aftermath of the K-Pg. Lack of competition and predation as a result of the extinction of large apex predators such as the mosasaurs (Polcyn et al. 2014; Jouve, Bardet, et al. 2008) plesiosaurs (Vincent et al. 2013), selachians (Cappetta et al. 2014) and teleosts (Friedman 2009), may have helped drive this pattern.

Following this initial peak in disparity in the aftermath of the K-Pg, disparity is shown the decrease rapidly, remaining low from the middle Eocene to the Oligocene before increasing again towards the Recent (Figure 3.8). This appears, in part, to be coupled with diversity patterns, which show decrease in species diversity in the middle-Eocene to Oligocene time bins and the peak in the Miocene. However, the drop in disparity in the middle-late Eocene time bin in much more dramatic than the decrease in diversity. Examination of the morphospace through time (Figure 5) indicates that this decrease in disparity is the result of loss of the extreme morphologies in the morphospace- the hyperelongate and brevirostrine forms. One possibility is that following this initial burst in morphological variation as a result of reduced competition and predation. Increased competition over time rendered these morphologies unsuccessful and resulted in extinction. However, another possible explanation is that the disparity analysis has not been corrected for phylogeny, which may have introduced a bias by not accounting for ghost lineages. There is a similar pattern observed in the Miocene time bin, with diversity increasing much more rapidly than disparity. This suggests that though species diversity is high, they are morphologically uniform. Disparity and diversity become decoupled in the Pliocene-Pleistocene time bin with disparity increasing towards levels of the

Paleocene-Ypresian bin but diversity dropping, potentially indicating high levels of endemism amongst the remaining species.

When examining the occupation of morphospace in the post-extinction time bin, the extremes in morphospace (in both the linear and geometric morphometrics plots) are occupied by Moroccan taxa, which are all found in the same locality, the Oulad Abdoun Basin (Jouve et al. 2014; Jouve et al. 2006). In addition to 6 species of Gavialoid and tomistomine which are found in this locality in the aftermath of the K-Pg, several species of Dyrosauridae have also been described- a group of marine Crocodyliformes with a similar longirostrine skull morphology (Jouve 2007). Generally where numerous species of crocodyliformes are found to coexist (Salas-Gismondi et al. 2015; Scheyer et al. 2013), they occupy a range of disparate niches. For example, the endemic Miocene fauna of South America (Salas-Gismondi et al. 2015) includes blunt-snouted caimans, a longirostrine gharial and the "duck-faced" *Mourasuchus*. The range in skull morphology suggests they exhibited different feeding strategies and prey choice. However, in Morocco, this is not the case, the predominant skull morphology is longirostrine (with the exception of *Maroccosuchus*), this morphology is specialised towards impaling agile prey with needle-like teeth and assumed piscivory (McHenry et al. 2006; Walmsley et al. 2013; Brochu 2001). Within the constraints of this specialised morphology, the disparity amongst the Moroccan species is predominantly shown by changes in relative snout length and tooth count (Figure 3.1, 3.5) (Russell and Longrich, in prep.). Similar to the patterns observed with the Gavialoidea, the dyrosaurs in Morocco appear to exhibit similar patterns in terms of morphology from the short-snouted *Chenanisuchus lateroculi* (Jouve et al. 2005) to the hyperelongate snout of *Atlantosuchus caupatezi* (Jouve, Bouya, et al. 2008).

Here, it is possible that these smaller scale changes in rostral morphology have been driven by competitive interactions for similar resources. This has been observed in other reptile populations leading to niche partitioning, enhanced by ecological character displacement (Adams & Rohlf 2000; Pierce et al. 2009; Pierce et al. 2008). The variation is snout proportions observed in the Moroccan species likely allowed for a finer scale partitioning of resources within this specialised niche. The disparity amongst the dyrosaurs is not restricted to the marine phosphatic basins of Morocco, as similar short-snouted morphs have been discovered in Paleocene fluvial floodplain deposits of Colombia (*Cerrejonisuchus improcerus* (Hastings et al. 2010) and *Anthracosuchus balrogus* (Hastings et al. 2014)). Future fossil discoveries may reveal whether a global signal also applies to gavialoids and tomistomines.

The Dyrosauridae and Gavialoidea (molecular context) also vary in overall skull size. The dyrosaurs were all typically much larger in skull size relative to the gavialoids (Figure 3.9) (Jouve, Bouya, et al. 2008), which are unusually small in the Paleocene-Ypresian time bin compared to the rest of fossil record of the Gavialoidea and Tomistominae (Figure 3.8C, 3.9, Appendix 2). Gavialoids were typically larger in the Cretaceous (though the difference across the K-Pg is not significant) therefore, a selection for smaller body sizes may have occurred over the K-Pg mass boundary. Large gavialoids and tomistomines, approaching Cretaceous thoracosaurs in size (50-90cm skull length), did not appear until later in the Eocene, and the largest species did not appear until the Miocene (>1m skull length), alongside other giant crocodylians (Figure 3.8C, 3.9) (Aguilera et al. 2006; Kobayashi et al. 2006; Riff et al. 2008). This delayed evolution of large body size is strikingly similar to the pattern seen in mammals (Smith et al. 2010). For mammals, trends in body size evolution during the Cenozoic have been attributed to diversification to fill ecological niches as well as cooling temperatures throughout

the Cenozoic. It is possible that cooling temperatures over the course of the Cenozoic may have influenced this trend in gavialoid and tomistomine body as well (Seebacher et al. 1999).

Tethys supported a diverse marine reptile fauna, including not only gavialoids but dyrosaurids (Bardet et al. 2010; Barbosa et al. 2008), palaeophiid (Bardet et al. 2010) and madtsoiid (Rage et al. 2014) sea snakes, and chelonioid and bothremydid sea turtles (Bardet et al. 2010). Several factors could help explain why reptiles initially dominated the recovery fauna. Gavialoidea, Tomistominae, Dyrosauridae, Chelonioidea, and Bothremydidae were already adapted to marine ecosystems in the Cretaceous, while the ancestors of the Palaeophiidae, the Nigerophiidae, were already specialised for aquatic life (Rage & Prasad 1992). Thus, the amount of morphological and physiological changes required to occupy the marine realm was much smaller for animals whose ancestor already evolved aquatic adaptations. Additionally, freshwater habitats were thought to have been less affected by the K-Pg extinction than the marine environment (Sheehan & Fastovsky 1992). Though typically marine, dyrosaurs have been recovered from freshwater deposits (Hastings et al. 2011); gavialoids are also known from a range of marine and freshwater deposits later in the Cenozoic (Figure 3.9). It has been suggested that a freshwater lifestyle for juveniles, as seen in extant marine crocodiles, may explain the differential survivorship of the crocodylomorphs relative to the mosasaurs (Jouve, Bardet, et al. 2008). It would also account for the apparent lack of juvenile material in the phosphates. Warm Paleogene sea temperatures (Zachos et al. 2001) may also have contributed to the success of ectothermic marine reptiles.

Although gavialoids and other reptiles formed the first wave of marine recovery, they ultimately declined in the marine realm over the Cenozoic. Dyrosauridae, Palaeophiidae, and Bothremydidae are not known beyond the Eocene (Hastings et al. 2011; Snetkov 2011; Gaffney et al. 2006). Gavialoids and tomistomines are typically recovered in coastal to freshwater environments from the Miocene and ultimately disappeared from marine ecosystems in the Pliocene (Figure 3.5, 3.9). Chelonioid sea turtles represent the only members of this initial recovery fauna to maintain a significant presence in modern marine ecosystems.

The reasons for the decline of marine gavialoids, tomistomines and other marine reptiles are poorly understood. Competition with other groups such as whales may have played a role (Martin et al. 2014; Martin 2013), or it may be that climate was a significant driver (Markwick 1998). Sea-surface temperature has been linked to diversity of marine crocodylomorphs, favouring warmer temperatures (Martin et al. 2014) and therefore, as the planet cooled and transitioned from greenhouse conditions to an ice age regime (Zachos et al. 2001), possibly, ectothermic reptiles were no longer able to compete in marine environments. Alternatively, another study suggests that sea-surface temperature does not correlate with diversity, and decline in eustatic sea level over the Cenozoic is a more significant driver for this decline in diversity (Mannion et al. 2015)

In conclusion, the gavialoids provide a striking study in evolutionary innovation following a mass extinction. High disparity in the aftermath of the K-Pg can be attributed to competitive release, created by the extinction of other marine reptiles at the K-Pg, opening ecological niches and allowing the survivors to diversify and evolve morphologically. Whether diversity was the result of mass survival or rapid radiation from a few lineages is not clear and requires future research to resolve the phylogenetic conflict. Though successful in the short-term, these marine crocodyliformes ultimately declined in the marine realm becoming extinct in the case of the dyrosaurs, or ecomorphologically and biogeographically restricted in the case of the extant species, *Gavialis gangeticus* and *Tomistoma schlegelii.*

Material and Methods:

Data Availability:

All data used are available from the authors. Fossils were acquired from local sellers in Morocco and exported to the UK in accordance with export laws. Specimens are accessioned at the Museum of Natural History of Marrakech, Cadi Ayyad University, Marrakech, Morocco. The fossils were prepared and currently held on loan to and in trust by the University of Bath, Bath, UK.

Phylogenetic analyses:

Phylogenetic analyses were performed by Russell and Longrich (in prep.) which used both a morphological character matrix and a combined (morphology-with-molecular) matrix. The character matrix was modified from Jouve et al. (2014), we added 6 new characters and 13 taxa to the matrix, the new matrix consists of 244 characters and 77 ingroup taxa, with *Bernissartia fagesii* as an outgroup (see Russell and Longrich, in prep., Appendix 1). The molecular matrix was sourced from Gold et al. (2014). New taxa include 9 extant species and 4 fossil taxa, *Argochampsa microrhynchus, Parvosuchus daouiensis, Maroccosuchus brachygnathus* and *Phasmatosuchus decipulae*. Tree searches were carried out in TNT v 1.1 (Goloboff et al. 2003) using a traditional search of 1000 replicates of Wagner trees, holding 100 trees per replicate (TBR branch swapping).

The resulting strict consensus cladograms were time calibrated using stratigraphic first and last occurrence datums (FAD, LAD) in the Paleotree and Strap packages (Bapst 2012; Bell & Lloyd 2014) in R (R Core Team 2013). Stratigraphic ranges were sourced from the literature (Appendix 2) and dated using the minimum branch length (mbl) time-scaling method. This method scales all zero-length branches, so they are greater than or equal to a time variable, set to 1Myr. It should be noted that the time-scaling methods used will not provide realistic estimates of divergence dates, as noted in the package details, as it simply uses stratigraphic dates and no other information (such as sampling and extinction rate) is added. They are used here as a visual approximation of crocodylian divergence through time.

Stratigraphic congruence was calculated for each of the most parsimonious trees from each phylogenetic analysis to compare the fit of the trees to the fossil record. This was done following the methodology of the StratPhyloCongruence() function in Strap (Bell & Lloyd 2014) in R (R Core Team 2013). To account for uncertainties in the dating of the fossils, the function was set to randomly sample ages between the FAD and LAD for a sample size of 1000, stratigraphic congruence indices were calculated for all trees within this sample as well. The stratigraphic congruence measures calculated include: SCI-stratigraphic consistency index, which calculates the number of stratigraphically consistent nodes in the phylogeny (scale 0-1, where 1 is the most consistent); RCI- relative completeness index, this calculates the sum of the ghost ranges in the phylogeny (called the minimum implied gap, MIG) over the sum of observed ranges (more positive values, better stratigraphic congruence); MSM*- Manhattan stratigraphic measure, calculates the optimal fit to stratigraphy over the MIG (scale 0-1, where 1 is the most optimal tree fit); GER- gap excess ratio, compares the MIG to the most optimal and least optimal fit (values closer to 1 indicate an improved fit). A modified version of the GER is also calculated to assess whether the MIG of the observed parsimonious trees is better or worse than trees generated at random in strap (Bell & Lloyd 2014). If GER* is equal to 1, this indicates a better fit than all randomly generated trees. In addition, P-values were calculated

for the other three (SCI, RCI, MSM) indices to assess whether the values obtained for these trees were significantly different from randomly generated trees. For all trees in both the morphology-only and the combined (morphology-with-molecular) phylogenetic analyses, P-values and GER* were significant which show that the observed trees fit better to stratigraphy than by just chance alone.

Diversity curves:

In order to create the diversity curves, data was downloaded from the Paleobiology database, accessed through Fossilworks (http://fossilworks.org). The data included all species assigned to Gavialoidea and Tomistominae at the species level. Data was collected for both the generic and species level- the two were compared due to issues associated with wastebasket taxa etc… however the overall patterns recovered were largely similar, therefore just the species curve has been presented here. Raw counts were taken from the database and then to factor in ghost lineages on the phylogeny, we also used a phylogenetic correction on the raw taxon counts. Phylogenetic correction was applied to the raw counts using the results from both phylogenetic analyses, using the time-calibrated result on the strict consensus.

Morphometrics:

Linear and geometric morphometrics were used to quantify shape variation in gavialoid skulls, with data taken from photographed fossil material and published descriptions (Appendix 2). In both analyses, to maintain a larger sample size, we quantified shape on the dorsal aspect only, as the ventral side is not visible in several the fossil taxa used. If there was evident variation in morphology or size within a species (likely indicating ontogenetic variability) additional specimens were quantified for that species. For incomplete crocodylian skulls, specimens were either reconstructed by mirroring the complete side or using published reconstructions. Both *Phasmatosuchus* specimens have an incomplete rostrum and an absent premaxilla, we produced a reconstruction of its premaxilla and skull based upon closely related (phylogenetic sister) taxa.

The Paleobiology Database records 249 occurrences of gavialoids and tomistomines, excluding extant species and the newly described Moroccan taxa (Russell and Longrich, in prep.). Of these 249 occurrences, 82 entries describe non-skull material including lower jaw, teeth and postcrania and were therefore ignored. In addition, 47 of the entries belong to material that is not accessible- either listed in a paper but no accession number or not figured. The remaining 118 entries describe skull material that could have been utilised in the morphometric analyses. For the linear morphometrics, fragmentary/incomplete skull material in the database could not be used as the complete medial length of the skull was measured, as well as width of the rostrum. Removal of the entries describing incomplete skull material resulted in a dataset of 47 specimens. gavialoid and tomistomine skulls for the linear morphometric analysis (Appendix 2). This included two species of *Euthecodon*, as our combined (morphology-with-molecular) phylogeny placed them within Gavialoidea (Russell & Longrich, in prep.). The advantage of linear over a geometric morphometrics approach, is that a greater number of taxa can be included in the analysis as it relies on fewer data points – perfect for fossil data. We used linear measurements that include total skull length, rostrum length, width of the rostrum at the anterior border of the orbits and width of the rostrum

between the first and second wave of maxillary teeth (see Figure 3.10A). Measurements were collected using ImageJ (Schneider et al. 2012), and the results were plotted as relative snout length (rostral length/total skull length) vs. relative snout width (width of rostrum/width at orbits) to demonstrate the range of snout morphotypes (Salas-Gismondi et al. 2015).

Linear measurements only capture changes in general proportions and miss a lot of variation in shape. Hence, we also used geometric morphometrics to quantify changes in shape. Geometric morphometrics methods require that there are no missing data. As this dataset relies on fossil taxa, poor preservation (and therefore the loss of sutural information: ideal for landmarking) is a confounding factor. A total of 32 landmarks were chosen to retain a larger sample size and still capture the majority of morphological variation. Areas that demonstrate poor preservation and have been excluded from landmarking, include the sutural contacts of the preorbital bones (prefrontal, lacrimal and jugal), the postorbital bar and the quadrate region. The 32 landmarks are all taken from the left side of the skull comprising 20 fixed landmarks and 12 semilandmarks in 1 curve (Figure 3.10B, Table 3.2). The resultant dataset for the geometric morphometric analyses contains 35 skulls. As above, this was reduced from an original dataset containing 249 gavialoid and tomistomine specimens from the Paleobiology Database. The number is less than the number used in the linear analysis and the geometric morphometric method cannot deal with missing data and therefore complete and undeformed skull material was needed.

Due to varying complexity in the outline of the rostrum in our sample, there is a risk of over or under sampling the curve based on the number of semilandmarks used to adequately capture the shape- as per the methodology in extended eigenshape analysis (Macleod 1999). To determine the number of semilandmarks suitable for our sample of fossil material, we performed a sensitivity analysis using the methodology in Finlay and Cooper (2015). In order to avoid oversampling the curve, we degraded the number of semilandmarks in order to find the minimum number required to adequately capture the outline at 95% accuracy. The sensitive threshold at which 95% of the variation was captured was 12 semilandmarks; including more did not significantly change the results of the analysis and would contribute noise due to intraspecific variation, preservational bias and human error. Only half the skull was landmarked to reduce noise introduced by preservational distortion and natural asymmetry. Six landmarks were located along the midline. Where the right side showed better preservation, the image was flipped and taken from the left-hand side. The fixed landmarks were predominantly type 1 and type 2 (Zelditch et al. 2004). Landmark 32 was type 3 and used to define the end point of the semilandmark curve. The landmarks and scales of 35 skulls were digitised using tpsDig264 (Rohlf 2016a) and curves were appended in tpsUtil64 (Rohlf 2016b) (Appendix 2). A generalised Procrustes alignment (GPA) was performed with the gpagen() function in R to align the data by removing the effects of scale, position and orientation (Finlay & Cooper 2015; Zelditch et al. 2004), for semi-landmark sliding we used the Procrustes distance criterion. A principal components analysis (PCA) was performed on the Procrustes superimposed coordinates using Geomorph (Adams & Otarola-Castillo 2013) in R (R Core Team 2013). The time sliced plot was produced using the StackPlot() function from Claddis (Lloyd 2016) in R.

Disparity:

Disparity was assessed using the first 8 PC axes, which account for 95% of the total variance. To assess change in disparity through time we assigned taxon disparity values to time bins based on their FADs and LADs (Appendix 2). Due to the variability in epoch length in the

Cenozoic, we employed the stratigraphic binning used in Friedman (2010) (Friedman 2010), which combined geologic stages into composite bins of comparable duration.

The sum and product of ranges and variance was calculated per time bin to quantify disparity (Wills et al. 1994) (Table 3.1). The range metrics are useful to describe the overall variation within each time bin, whereas the variance gives an indication of average dissimilarity between bins. Range will be affected by the size of the sample; as larger samples will likely show higher amounts of variation. Variance is relatively robust to the effects of sample size and outliers in the data (Wills 1998), and therefore is used as our primary disparity metric. The range and variances were calculated in RARE (Wills 1998) and the 8^{th} root of the product of ranges and variance were taken to normalise the outcome. Due to the variable sample size per time bin we used rarefaction analysis and bootstrapping of 95% confidence intervals (1000 replicates) to examine disparity (Figure 3.7, 3.8A) using RARE (Wills et al. 1994). Significance was assessed using a NPMANOVA (non-parametric multivariate analysis of variance) and overlap or non-overlap of 95% bootstrap confidence intervals. The NPMANOVA (Table 3.4) was used to test if there was a significant difference in the distribution of taxa in morphospace. Euclidean distances were calculated using the first 8 PC axes (10000 permutations) from PAST (Hammer et al. 2001), p-values were calculated and adjusted using a Bonferroni correction (to reduce the likelihood of false positives i.e. type 1 errors). The relative position of taxa in morphospace (GPA coordinates) was plotted using Geomorph in R (R Core Team 2013) using their Procrustes distances (Figure 3.7C).

Skull size:

To investigate the variation in skull size amongst the gavialoids and tomistomines, we measured the width across the back of the skull table. To reduce measurement error relating to post-mortem damage and natural asymmetry of skull material, one half of the skull was measured between the midpoint of the parietal and the lateral edge of the skull and then doubled. Where poor preservation was apparent, the most complete side was used; a total of 63 specimens where measured in ImageJ (Schneider et al. 2012) and subsequently log transformed to normalise the data (Appendix 2). As above, the Paleobiology Database contain 118 occurrences of skull material of gavialoids and tomistomines. The proportion of this dataset that was not used in this analysis is represented by incomplete skull material that did not preserved the skull table, i.e. rostral fragments.

Skull width was chosen over total skull length as it is comparatively unaffected by variation in rostral proportions between species (Figure 3.1, 3.5A). It has been shown that measurements of the braincase region are more conservative when comparing across multiple crocodylian species, this has also been observed in ichthyosaurs (Hurlburt et al. 2003; Fischer et al. 2011). A number of studies have examined the use of skull table width as a proxy for body size using linear regressions, but these are restricted to individual species (Hall & Portier 1994; Webb & Messel 1978; Wu et al. 2006; Platt et al. 2011). These studies indicate that skull width would be a useful proxy for estimating snout-vent length, however it needs to be tested across a range of crocodylian species (gavialoids in particular).

Stratigraphic range of species and environmental preference were obtained from the literature (Appendix 2). If direct provenance data could not be obtained for the specimen, range for the species was used instead. Environmental preference was assigned based on discussions in the literature and information on the depositional environment; three main environmental categories were assigned: marine, marginal marine and freshwater (Appendix

2). Marginal marine was used when specimens were reported in coastal/deltaic and estuarine environments. This category was used in cases where the marine affinities of taxa were uncertain - i.e. found in coastal deposits but may also have washed-out from freshwater habitats inland. Time binning for this analysis was the same as the scheme used for the disparity analysis, using the composite stage level time bins (see disparity methods). To test whether skull size varied significantly before and after the K-Pg mass extinction, we used one-tailed t-tests with equal variance. Additional skull size data were collected for 17 dyrosaurid specimens. For the post-extinction time bin, we used a one-tailed t-test with equal variance to find if there was a significant difference in size between the Gavialoidea (molecular context) and the Dyrosauridae.

Acknowledgements:

Thanks to T. Astrop, T. Stubbs, M. Wills, C. Klein and University of Bath Palaeontology Group for discussion of methods, and to D. Ward for discussions of the phosphate fauna. Thanks to M. Topham for assistance with preparation, to C. Underwood for identification of shark teeth for stratigraphic correlation, to M. Meharich and M&M Enterprises for invaluable assistance in Morocco, and to N.-E. Jalil and the MHNM (Museum of Natural History of Marrakech) for assistance with accessioning fossils. Thanks, and in memory of, M. Elgouni, without whom this project would not have been possible.

References:

Adams, D.C. & Otarola-Castillo, E., 2013. geomorph: an R package for the collection and analysis of geometric morphometric shape data. *Methods in Ecology and Evolution*, 4, pp.393–399.

Adams, D.C. & Rohlf, F.J., 2000. Ecological character displacement in *Plethodon* : Biomechanical differences found from a geometric morphometric study. *Proceedings of the National Academy of Sciences*, 97(8), pp.4106–4111.

Adolfssen, J.S. & Ward, D.J., 2014. Crossing the boundary: an elasmobranch fauna from Stevns Klint, Denmark. *Palaeontology*, 57(3), pp.591–629.

Aggarwal, R.K. et al., 1994. Generic affinities among crocodilians as revealed by DNA fingerprinting with a Bkm-derived probe. *Proceedings of the National Academy of Sciences*, 91(22), pp.10601–10605.

Aguilera, O.A., Riff, D. & Bocquentin-Villanueva, J., 2006. A new giant *Purussaurus* (Crocodyliformes, Alligatoridae) from the Upper Miocene Urumaco Formation, Venezuela. *Journal of Systematic Palaeontology*, 4(3), pp.221–232.

Alroy, J., 1999. The fossil record of North American mammals : evidence for a Paleocene evolutionary radiation. *Systematic Biology*, 48(1), pp.107–118.

Archibald, J.D. & Bryant, L.J., 1990. Differential Cretaceous/Tertiary extinctions of nonmarine vertebrates; evidence from northeastern Montana. *Geological Society of America Special Papers*, 247, pp.549–562.

Bambach, R.K., 2006. Phanerozoic Biodiversity Mass Extinctions. *Annual Review of Earth and Planetary Sciences*, 34(1), pp.127–155.

Bapst, D.W., 2012. paleotree: an R package for paleontological and phylogenetic analyses of evolution. *Methods in Ecology and Evolution*, 3, pp.803–807.

Barbosa, J.A., Kellner, A.W.A. & Viana, M.S.S., 2008. New dyrosaurid crocodylomorph and evidences for faunal turnover at the K-P transition in Brazil. *Proceedings of the Royal Society B: Biological Sciences*, 275, pp.1385–1391.

Bardet, N. et al., 2010. Reptilian assemblages from the latest Cretaceous – Palaeogene phosphates of Morocco: from Arambourg to present time. *Historical Biology*, 22(1–3), pp.186–199.

Barnes, L.G. & Goedert, J.L., 2001. Stratigraphy and paleoecology of Oligocene and Miocene desmostylian occurrences in western Washington State, USA. *Bulletin of Ashoro Museum of Paleontology*, 2, pp.7–22.

Bell, M.A. & Lloyd, G.T., 2014. strap: stratigraphic tree analysis for palaeontology. , pp.1–17. Available at: https://cran.r-project.org/package=strap.

Berta, A., Ray, C.E. & Wyss, A.R., 1989. Skeleton of the oldest known pinniped, *Enaliarctos mealsi*. *Science*, 244(4900), pp.60–62.

Brochu, C.A., 2004. A new Late Cretaceous gavialoid crocodylian from eastern North America and the phylogenetic relationships of thoracosaurs. *Journal of Vertebrate Paleontology*, 24(September), pp.610–633.

Brochu, C.A., 2001. Crocodylian snouts in space and time: phylogenetic approaches toward adaptive radiation. *American Zoologist*, 41(3), pp.564–585.

Brochu, C.A., 2006. Osteology and phylogenetic significance of *Eosuchus minor* (Marsh, 1870) new combination, a longirostrine crocodylian from the Late Paleocene of North America. *Journal of Paleontology*, 80(1), pp.162–186.

Brochu, C.A., 2003. Phylogenetic approaches toward crocodylian history. *Annual Review of Earth and Planetary Sciences*, 31(1), pp.357–397.

Brochu, C.A., 2012. Phylogenetic relationships of Palaeogene ziphodont eusuchians and the status of *Pristichampsus* Gervais, 1853. *Earth and Environmental Science Transactions of the Royal society of Edinburgh*, 103(3–4), pp.521–550.

Brochu, C.A., 2007. Systematics and taxonomy of Eocene tomistomine crocodylians from Britain and Northern Europe. *Palaeontology*, 50, pp.917–928.

Bronzati, M., Montefeltro, F.C. & Langer, M.C., 2015. Diversification events and the effects of mass extinctions on Crocodyliformes evolutionary history. *Royal Society Open Science*, 2, pp.1–9.

Brusatte, S.L. et al., 2015. The extinction of the dinosaurs. *Biological Reviews*, 90(2), pp.628–642.

Cappetta, H. et al., 2014. Marine vertebrate faunas from the Maastrichtian phosphates of Benguerir (Ganntour Basin, Morocco): Biostratigraphy, palaeobiogeography and palaeoecology. *Palaeogeography, Palaeoclimatology, Palaeoecology*, 409, pp.217–238.

Chatterjee, S. & Small, B.J., 1989. New plesiosaurs from the Upper Cretaceous of Antarctica. *Geological Society, London, Special Publications*, 47(1), pp.197–215.

Claramunt, S. & Cracraft, J., 2015. A new time tree reveals Earth history's imprint on the evolution of modern birds. *Science Advances*, 1(11), pp.1–14.

Delfino, M., Piras, P. & Smith, T., 2005. Anatomy and phylogeny of the gavialoid crocodylian *Eosuchus lerichei* from the Paleocene of Europe. *Acta Palaeontologica Polonica*, 50(3), pp.565–580.

Domning, D.P., 2001. The earliest known fully quadrupedal sirenian. *Nature*, 413, pp.625–627.

Erickson, B.R., 1998. Crocodilians of the Black Mingo Group (Paleocene) of the South Carolina coastal plain. *Transactions of the American philosophical society*, 88(4), pp.196–214.

Feduccia, A., 1995. Explosive evolution in tertiary birds and mammals. *Science*, 267(5198), pp.637–638.

Finlay, S. & Cooper, N., 2015. Morphological diversity in tenrecs (Afrosoricida, Tenrecidae): comparing tenrec skull diversity to their closest relatives. *PeerJ*, 3, p.e927.

Fischer, V. et al., 2011. A new Barremian (Early Cretaceous) ichthyosaur from western Russia. *Journal of Vertebrate Paleontology*, 31(5), pp.1010–1025.

Friedman, M., 2009. Ecomorphological selectivity among marine teleost fishes during the end-Cretaceous extinction. *Proceedings of the National Academy of Sciences*, 106(13), pp.5218–5223.

Friedman, M., 2010. Explosive morphological diversification of spiny-finned teleost fishes in the aftermath of the end-Cretaceous extinction. *Proceedings of the Royal Society B: Biological Sciences*, 277, pp.1675–1683.

Gaffney, E.S., Tong, H. & Meylan, P.A., 2006. Evolution of the side-necked turtles: the families Bothremydidae, Euraxemydidae, and Araripemydidae. *Bulletin of the American Museum of Natural History*, 300, pp.1–698.

Gatesy, J. et al., 2003. Combined support for wholesale taxic atavism in gavialine crocodylians. *Systematic Biology*, 52(3), pp.403–422.

Gingerich, P.D. & Zouhri, S., 2015. New fauna of archaeocete whales (Mammalia, Cetacea) from the Bartonian middle Eocene of southern Morocco. *Journal of African Earth Sciences*, 111, pp.273–286.

Gold, M.E.L., Brochu, C.A. & Norell, M.A., 2014. An expanded combined evidence approach to the *Gavialis* problem using geometric morphometric data from crocodylian braincases and eustachian systems. *PLoS ONE*, 9(9), pp.1–12.

Goloboff, P.A., Farris, J. & Nixon, K., 2003. T.N.T.: Tree Analysis Using New Technology.

Green, R.E. et al., 2014. Three crocodilian genomes reveal ancestral patterns of evolution among archosaurs. *Science*, 346(6215), p.1335.

Grossnickle, D.M. & Newham, E., 2016. Therian mammals experience an ecomorphological radiation during the Late Cretaceous and selective extinction at the K–Pg boundary. *Proceedings of the Royal Society B: Biological Sciences*, 283(1832), p.20160256.

Hall, P.M. & Portier, K.M., 1994. Cranial morphometry of New Guinea crocodiles (*Crocodylus novaeguineae*): ontogenetic variation in relative growth of the skull and an assessment of its utility as a predictor of the sex and size of individuals. *Herpetological Monographs*, 8, pp.203–225.

Hammer, Ø., Harper, D.A.T. & Ryan, P.D., 2001. PAST: paleontological statistics software package for education and data analysis. *Palaeontologia Electronica*, 4(1), p.9pp.

Harshman, J. et al., 2003. True and false gharials: a nuclear gene phylogeny of Crocodylia. *Systematic Biology*, 52(3), pp.386–402.

Hastings, A.K. et al., 2010. A new small short-snouted dyrosaurid (Crocodylomorpha, Mesoeucrocodylia) from the Paleocene of northeastern Colombia. *Journal of Vertebrate Paleontology*, 30(January), pp.139–162.

Hastings, A.K., Bloch, J.I. & Jaramillo, C.A., 2014. A new blunt-snouted dyrosaurid, *Anthracosuchus balrogus* gen. et sp. nov. (Crocodylomorpha, Mesoeucrocodylia), from

the Palaeocene of Colombia. *Historical Biology*, pp.1–23.

Hastings, A.K., Bloch, J.I. & Jaramillo, C.A., 2011. A new longirostrine dyrosaurid (Crocodylomorpha, Mesoeucrocodylia) from the Paleocene of north-eastern Colombia: biogeographic and behavioural implications for New-World Dyrosauridae. *Palaeontology*, 54(5), pp.1095–1116.

Hua, S. & Jouve, S., 2004. A primitive marine gavialoid from the Paleocene of Morocco. *Journal of Vertebrate Paleontology*, 24(2), pp.341–350.

Hurlburt, G.R., Heckert, A.B. & Farlow, J.O., 2003. Body mass estimates of phytosaurs (Archosauria: Parasuchidae) from the Petrified Forest Formation (Chinle Group: Revueltian) based on skull and limb bone measurements. *New Mexico Museum of Natural History and Science Bulletin*, 24, pp.105–113.

Jablonski, D., 2008. Extinction and the spatial dynamics of biodiversity. *Proceedings of the National Academy of Sciences*, 105, pp.11528–11535.

Jablonski, D. & Chaloner, W.G., 1994. Extinctions in the fossil record [and discussion]. *Philosophical Transactions of the Royal Society B*, 344, pp.11–17.

Janke, A. et al., 2005. Mitogenomic analyses place the gharial (*Gavialis gangeticus*) on the crocodile tree and provide pre-K/T divergence times for most crocodilians. *Journal of Molecular Evolution*, 61(5), pp.620–626.

Jouve, S. et al., 2014. *Maroccosuchus zennaroi* (Crocodylia: Tomistominae) from the Eocene of Morocco: phylogenetic and palaeobiogeographical implications of the basalmost tomistomine. *Journal of Systematic Palaeontology*, 13, pp.1–25.

Jouve, S. et al., 2006. New material of *Argochampsa krebsi* (Crocodylia: Gavialoidea) from the Lower Paleocene of the Oulad Abdoun Basin (Morocco): phylogenetic implications. *Geobios*, 39(6), pp.817–832.

Jouve, S., 2007. Taxonomic revision of the dyrosaurid assemblage (Crocodyliformes: Mesoeucrocodylia) from the Paleocene of the Iullemmeden Basin, West Africa. *Journal of Paleontology*, 81(1), pp.163–175.

Jouve, S., Bardet, N. & Jalil, N.-E., 2008. The oldest African crocodylian: phylogeny, paleobiogeography, and differential survivorship of marine reptiles through the Cretaceous-Tertiary boundary. *Journal of Vertebrate Paleontology*, 28, pp.37–41.

Jouve, S., Bouya, B. & Amaghzaz, M., 2008. A long-snouted dyrosaurid (Crocodyliformes, Mesoeucrocodylia) from the Paleocene of Morocco: phylogenetic and palaeobiogeographic implications. *Palaeontology*, 51(2), pp.281–294.

Jouve, S., Bouya, B. & Amaghzaz, M., 2005. A short-snouted dyrosaurid (Crocodyliformes, Mesoeucrocodylia) from the Paleocene of Morocco. *Palaeontology*, 48(2), pp.359–369.

Kaiho, K. et al., 2016. Global climate change driven by soot at the K-Pg boundary as the cause of the mass extinction. *Scientific Reports*, 6(1), p.28427.

Kellner, A.W.A., Pinheiro, A.E.P. & Campos, D.A., 2014. A new sebecid from the paleogene of Brazil and the crocodyliform radiation after the K-Pg boundary. *PloS ONE*, 9(1), pp.1–11.

Kobayashi, Y. et al., 2006. Anatomy of a Japanese tomistomine crocodylian, *Toyotamaphimeia machikanensis* (Kamei et Matsumoto, 1965), from the middle Pleistocene of Osaka Prefecture: the reassessment of its phylogenetic status within Crocodylia. *National Science Museum Monographs*.

Laurent, Y., Buffetaut, E. & Le Loeuff, J., 2000. Un crâne de Thoracosaurine (Crocodylia, crocodylidae) dans le Maastrichtien spérieur du sud de la France. *Oryctos*, 3, pp.19–27.

Lloyd, G.T., 2016. Estimating morphological diversity and tempo with discrete character-taxon matrices: Implementation, challenges, progress, and future directions. *Biological Journal of the Linnean Society*, 118(1), pp.131–151.

Longrich, N.R., Bhullar, B.-A.S. & Gauthier, J.A., 2012. Mass extinction of lizards and snakes at the Cretaceous-Paleogene boundary. *Proceedings of the National Academy of Sciences*, 109(52), pp.21396–21401.

Longrich, N.R., Scriberas, J. & Wills, M.A., 2016. Severe extinction and rapid recovery of mammals across the Cretaceous-Palaeogene boundary, and the effects of rarity on patterns of extinction and recovery. *Journal of evolutionary biology*, 29(8), pp.1495–1512.

Longrich, N.R., Tokaryk, T. & Field, D.J., 2011. Mass extinction of birds at the Cretaceous-Paleogene (K-Pg) boundary. *Proceedings of the National Academy of Sciences*, 108(37), pp.15253–15257.

Macleod, N., 1999. Generalizing and extending the eigenshape method of shape space visualization and analysis. *Paleobiology*, 25(1), pp.107–138.

Man, Z. et al., 2011. Crocodilian phylogeny inferred from twelve mitochondrial protein-coding genes, with new complete mitochondrial genomic sequences for Crocodylus acutus and Crocodylus novaeguineae. *Molecular Phylogenetics and Evolution*, 60(1), pp.62–67.

Mannion, P.D. et al., 2015. Climate constrains the evolutionary history and biodiversity of crocodylians. *Nature communications*, 6, pp.1–9.

Markwick, P.J., 1998. Crocodilian diversity in space and time: the role of climate in paleoecology and its implication for understanding K/T extinctions. *Paleobiology*, 24(4), pp.470–497.

Martin, J.E. et al., 2014. Sea surface temperature contributes to marine crocodylomorph evolution. *Nature Communications*, 5, pp.1–7.

Martin, J.E., 2013. Surviving a potentially lethal injury? Bite mark and associated trauma in the vertebra of a dyrosaurid crocodilian. *Palaios*, 28(1), pp.6–8.

Massare, J.A., 1987. Tooth morphology and prey preference of Mesozoic marine reptiles. *Journal of Vertebrate Paleontology*, 7(2), pp.121–137.

McAliley, L.R. et al., 2006. Are crocodiles really monophyletic? Evidence for subdivisions from sequence and morphological data. *Molecular Phylogenetics and Evolution*, 39(1), pp.16–32.

McCurry, M.R. et al., 2017. The remarkable convergence of skull shape in crocodilians and toothed whales. *Proceedings of the Royal Society B*, 284, pp.9–11.

McHenry, C.R. et al., 2006. Biomechanics of the rostrum in crocodilians: a comparative analysis using finite-element modeling. *The anatomical record. Part A, Discoveries in molecular, cellular, and evolutionary biology*, 288(May), pp.827–849.

Meredith, R.W. et al., 2011. A phylogenetic hypothesis for *Crocodylus* (Crocodylia) based on mitochondrial DNA: evidence for a trans-Atlantic voyage from Africa to the New World. *Molecular Phylogenetics and Evolution*, 60(1), pp.183–191.

Oaks, J.R., 2011. A time-calibrated species tree of Crocodylia reveals a Recent radiation of the true crocodiles. *Evolution*, 65, pp.3285–3297.

Pierce, S.E., Angielczyk, K.D. & Rayfield, E.J., 2009. Morphospace occupation in thalattosuchian crocodylomorphs: Skull shape variation, species delineation and temporal patterns. *Palaeontology*, 52(5), pp.1057–1097.

Pierce, S.E., Angielczyk, K.D. & Rayfield, E.J., 2008. Patterns of morphospace occupation and mechanical performance in extant crocodilian skulls: A combined geometric morphometric and finite element modeling approach. *Journal of Morphology*, 269, pp.840–864.

Platt, S.G. et al., 2011. Size estimation, morphometrics, sex ratio, sexual size dimorphism, and biomass of *Crocodylus acutus* in the coastal zone of Belize. *Salamandra*, 47(4), pp.179–192.

Polcyn, M.J. et al., 2014. Physical drivers of mosasaur evolution. *Palaeogeography, Palaeoclimatology, Palaeoecology*, 400, pp.17–27.

Prum, R.O. et al., 2015. A comprehensive phylogeny of birds (Aves) using targeted next-generation DNA sequencing. *Nature*, 526(7574), pp.569–573.

Puértolas-Pascual, E. et al., 2016. Review of the Late Cretaceous-early Paleogene crocodylomorphs of Europe: Extinction patterns across the K-PG boundary. *Cretaceous Research*, 57, pp.565–590.

R Core Team, 2013. R: a language and environment for statistical computing. Available at: http://www.r-project.org/.

Rage, J.-C. et al., 2014. First report of the giant snake *Gigantophis* (Madtsoiidae) from the Paleocene of Pakistan: Paleobiogeographic implications. *Geobios*, 47(3), pp.147–153.

Rage, J.-C. & Prasad, G.V.R., 1992. New snakes from the late Cretaceous (Maastrichtian) of Naskal, India. *Neues Jahrbuch für Geologie und Paläontologie, Abhandlungen*, 187(1), pp.83–97.

dos Reis, M. et al., 2012. Phylogenomic datasets provide both precision and accuracy in estimating the timescale of placental mammal phylogeny. *Proceedings of the Royal Society B: Biological Sciences*, 279, pp.3491–3500.

Rieppel, O. & Labhardt, L., 1979. Mandibular mechanics in *Varanus niloticus* (Reptilia: Lacertilia). *Herpetologica*, 35(2), pp.158–163.

Riff, D., Conquista, V. & Aguilera, O.A., 2008. The world's largest gharials *Gryposuchus*: description of *G. croizati* n. sp (Crocodylia, Gavialidae) from the Upper Miocene Urumaco Formation, Venezuela. *Paläontologische Zeitschrift*, 82, pp.178–195.

Robertson, D.S. et al., 2013. K-Pg extinction patterns in marine and freshwater environments: The impact winter model. *Journal of Geophysical Research: Biogeosciences*, 118(3), pp.1006–1014.

Rohlf, F.J., 2016a. tpsDig, digitize landmarks and outlines, version 2.25. Department of Ecology and Evolution, State University of New York at Stony Brook.

Rohlf, F.J., 2016b. tpsUtil, file utility program, version 1.68. Department of Ecology and Evolution, State University of New York at Stony Brook.

Sadleir, R.W. & Makovicky, P.J., 2008. Cranial shape and correlated characters in crocodilian evolution. *Journal of Evolutionary Biology*, 21, pp.1578–1596.

Salas-Gismondi, R. et al., 2015. A Miocene hyperdiverse crocodylian community reveals peculiar trophic dynamics in proto-Amazonian mega-wetlands. *Proceedings of the Royal Society B: Biological Sciences*, 282, pp.4–8.

Scheyer, T.M. et al., 2013. Crocodylian diversity peak and extinction in the late Cenozoic of the northern Neotropics. *Nature communications*, 4(1907), pp.1–9.

Schneider, C.A., Rasband, W.S. & Eliceiri, K.W., 2012. NIH Image to ImageJ: 25 years of image

analysis. *Nature Methods*, 9(7), pp.671–675.

Schulte, P. et al., 2010. The Chicxulub asteroid impact and mass extinction at the Cretaceous-Paleogene boundary. *Science*, 327(1214), pp.1214–1218.

Seebacher, F., Grigg, G.C. & Beard, L.A., 1999. Crocodiles as dinosaurs: behavioural thermoregulation in very large ectotherms leads to high and stable body temperatures. *The Journal of experimental biology*, 202, pp.77–86.

Sheehan, P.M. & Fastovsky, D.E., 1992. Major extinctions of land-dwelling vertebrates at the Cretaceous-Tertiary boundary, eastern Montana. *Geology*, 20, pp.556–560.

Smith, F.A. et al., 2010. The evolution of maximum body size of terrestrial mammals. *Science*, 330(1216), pp.1216–1219.

Snetkov, P.B., 2011. Vertebrae of the sea snake *Palaeophis nessovi* Averianov (Acrochordoidea, Palaeophiidae) from the Eocene of western Kazakhstan and phylogenetic analysis of the superfamily Acrochordoidea. *Paleontological Journal*, 45(3), pp.305–313.

Troedsson, G.T., 1924. *On crocodilian remains from the Danian of Sweden*, Lund.

Vélez-Juarbe, J., Brochu, C.A. & Santos, H., 2007. A gharial from the Oligocene of Puerto Rico: transoceanic dispersal in the history of a non-marine reptile. *Proceedings of the Royal Society B: Biological Sciences*, 274, pp.1245–1254.

Vincent, P. et al., 2013. New plesiosaur specimens from the Maastrichtian Phosphates of Morocco and their implications for the ecology of the latest Cretaceous marine apex predators. *Gondwana Research*, 24(2), pp.796–805.

Vincent, P. et al., 2011. *Zarafasaura oceanis*, a new elasmosaurid (Reptilia: Sauropterygia) from the Maastrichtian Phosphates of Morocco and the palaeobiogeography of latest Cretaceous plesiosaurs. *Gondwana Research*, 19(4), pp.1062–1073.

Walmsley, C.W. et al., 2013. Why the long face? The mechanics of mandibular symphysis proportions in crocodiles. *PloS ONE*, 8(1), p.e53873.

Webb, G.J.W. & Messel, H., 1978. Morphometric analysis of *Crocodylus porosus* from the north coast of Arnhem Land, northern Australia. *Australian Journal of Zoology*, 26(1), pp.1–27.

Willis, R.E. et al., 2007. Evidence for placing the false gharial (*Tomistoma schlegelii*) into the family Gavialidae: Inferences from nuclear gene sequences. *Molecular Phylogenetics and Evolution*, 43(3), pp.787–794.

Wills, M.A., 1998. Crustacean disparity through the Phanerozoic: comparing morphological and stratigraphic data. *Biological Journal of the Linnean Society*, 65, pp.455–500.

Wills, M.A., Briggs, D.E.G. & Fortey, R.A., 1994. Disparity as an evolutionary index: a comparison of Cambrian and Recent arthropods. *Paleobiology*, 20(2), pp.93–130.

Wu, X.-C., Russell, A.P. & Brinkman, D.B., 2001. A review of *Leidyosuchus* Lambe, 1907 (Archosauria: Crocodylia) and an assessment of cranial variation based upon new material: Erratum. *Canadian Journal of Earth Sciences*, 38, pp.1665–1587.

Wu, X.B. et al., 2006. Regression analysis between body and head measurements of Chinese alligators (*Alligator sinensis*) in the captive population. *Animal Biodiversity and Conservation*, 29(1), pp.65–71.

Zachos, J.C. et al., 2001. Trends, rhythms, and aberrations in global climate 65 Ma to present. *Science*, 292(5517), pp.686–693.

Zarski, M., Jakubowski, G. & Gawor-Biedowa, E., 1998. The first Polish find of Lower Paleocene crocodile *Thoracosaurus* Leidy, 1852: geological and palaeontological description.

Geological Quarterly, 42(2), pp.141–160.

Zelditch, M.L. et al., 2004. *Geometric morphometrics for biologists*, Elsevier.

3.3 Post-paper commentary:

3.3.1 Supplementary material for the paper:

Geometric morphometrics:

For the landmark analysis, 32 landmarks were digitised onto 35 specimens. The landmarks comprise 20 fixed landmarks and 12 semilandmarks. The position of the landmarks is described in Table 3.2 and Figure 3.10B, coordinate data is presented in Appendix 2.

Landmark:	Description:
1	Anteriormost tip of the premaxillae
2	Posterior tip of the premaxilla contact at the narial opening
3	Posterior border of the narial opening along the medial axis
4	Anterior tip of the nasal bones
5	Frontal-nasal-nasal contact
6	Midline of the supraoccipital/or midline posterior point of the skull table
7	Point of maximal curvature along the lateral margin of the premaxilla
8	Point of inflection/minimal curvature between the premaxillae and maxillae
9	Premaxilla-maxilla midline contact
10	Frontal-prefrontal-orbit contact
11	Frontal-postorbital-orbit contact
12	Point of maximal curvature of the skull table at contact with postorbital bar
13	Frontal-parietal-postorbital contact
14	Anterior postorbital-supratemporal fenestra contact
15	Postorbital-squamosal contact with lateral margin of skull table
16	Postorbital-squamosal-supratemporal fenestra contact
17	Point of maximal curvature of the supratemporal fenestra along the parietal
18	Parietal-squamosal-supratemporal fenestra contact
19	Parietal-squamosal contact along posterior margin of skull table
20	Posterolateral tip of squamosal (prong)
21	Premaxilla-maxilla contact along lateral margin
32	Point along the lateral margin that is level with the anterior border of the orbits
Curve:	
1	10 semilandmarks between landmarks 21-32 along the left lateral margin

Table 3.2. Description of the position of the fixed landmarks and semilandmark curve

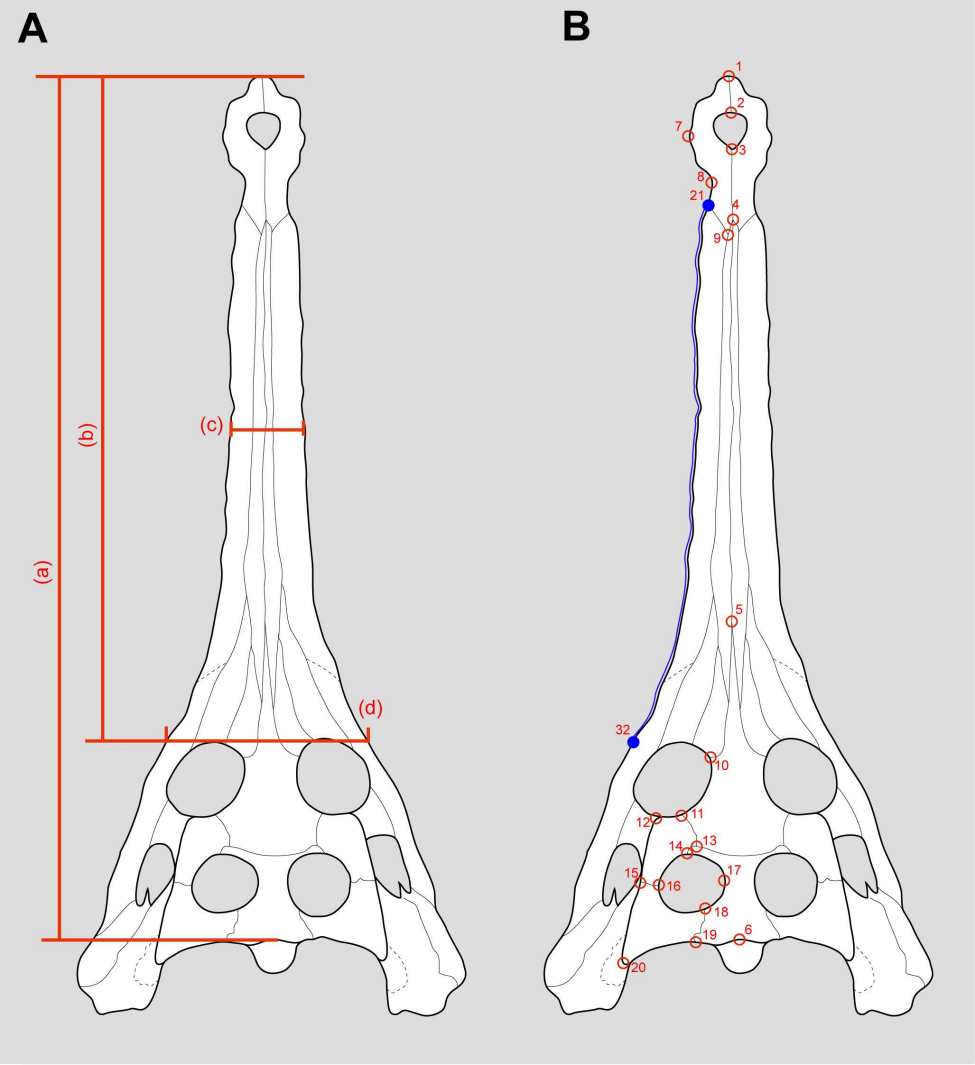

Figure 3.10 (A) Position of the linear measurements collected for ratios of relative snout length to relative snout width. (a) total skull length, (b) rostral length, (c) snout width, (d) width of the rostrum at the anterior border of the orbits. For the snout width (c), when the rostrum demonstrates lateral waves, as in *Maroccosuchus*, the constriction between the first and second maxillary wave was the position at which the measurement was taken. (B) Position of the landmarks used in the geometric morphometric analysis. Open circles show the fixed landmarks and blue curve indicates outline over which the semilandmarks are positioned. Landmark 21 and 32 are the first and last semilandmarks used to anchor the curve. Drawing of *Eogavialis andrewsi* (modified from (Storrs, 2003)).

Here we have provided additional results from the morphometric analysis not presented in the main paper. Table 3.3 shows the results of the principal component analysis (PCA) and the proportion of variance described by each principal component axis. There was a total of 30 principal components axes recovered from the PCA, the proportion of total variance is shown in Figure 3.11. The higher axes contribute minimally to the overall variance and likely describes noise in the dataset. The first 15 axes are detailed in Table 3.3 and describe 98.6% of the total variance. Only the first 8 principal components were used to calculate disparity in this paper as these describe 95% of the variance and as shown on the scree plot, show the most significant amount of variance in the data.

	Standard Deviation:	Proportion of Variance:	Cumulative Proportion:
PC1	0.07684	0.64145	0.64145
PC2	0.03262	0.11557	0.75702
PC3	0.02737	0.08139	0.83841
PC4	0.02167	0.05100	0.88941
PC5	0.01534	0.02556	0.91497
PC6	0.01186	0.01529	0.93026
PC7	0.01081	0.01268	0.94295
PC8	0.009649	0.01011	0.95306
PC9	0.008579	0.00800	0.96106
PC10	0.00763	0.00632	0.96738
PC11	0.007298	0.00579	0.97317
PC12	0.006113	0.00406	0.97723
PC13	0.005783	0.00363	0.98086
PC14	0.005155	0.00289	0.98375
PC15	0.005007	0.00272	0.98647

Table 3.3. Results of the principal components analysis- variance accounted for in the first 15 PC axes

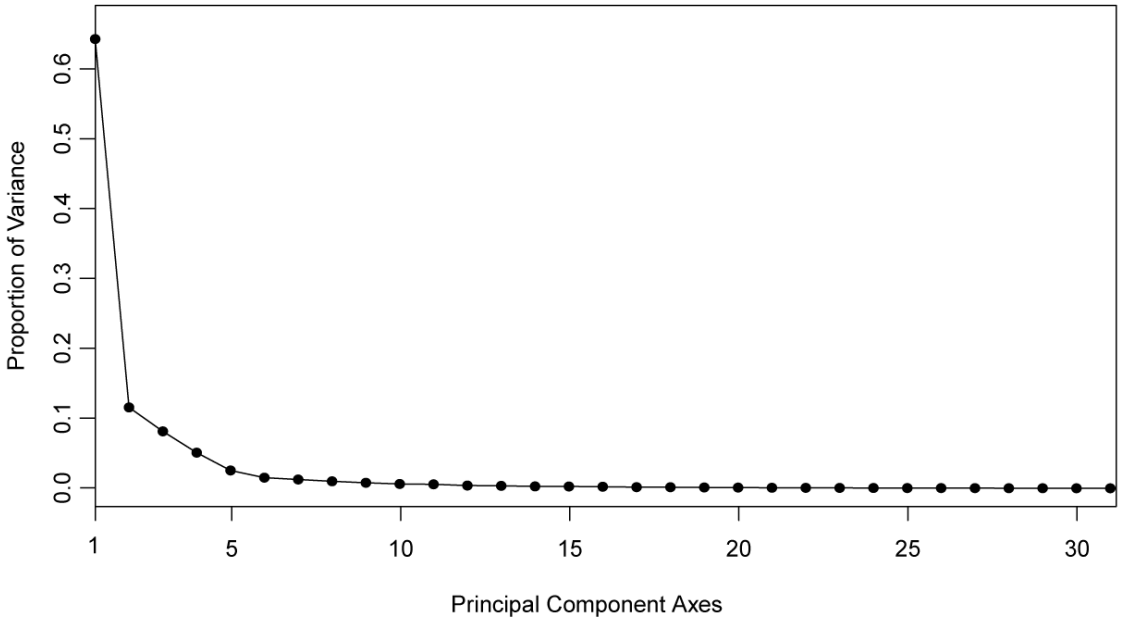

Figure 3.11: Scree plot of the proportion of total variance for all PC axes in the geometric morphometric analysis.

The results of the NPMANOVA (Table 3.4) were calculated from the first 8 principal component axes in PAST (Hammer, Harper and Ryan, 2001). The results were not significant between subsequent time bins, suggesting that gavialoids do not occupy significantly different areas of morphospace.

Time bin (Myrs)	Cretaceous	Pal-eEo	mEo-lEo	Oligocene	Miocene	Plio-Pleisto
Cretaceous		1	0.5759	1	1	1
Pal-eEo	0.1013		1	1	1	1
mEo-lEo	0.08779	0.2592		1	1	1
Oligocene	0.08589	0.2304	1		1	1
Miocene	0.0384	0.2432	0.4971	0.5524		1
Plio-Pleisto	0.09059	0.3293	0.09929	0.09729	0.4216	

Table 3.4: Results of the pairwise NPMANOVA showing Bonferroni-corrected P-values between each time bin (top right) and P-values for uncorrected significance (bottom left). This first 8 PC axes were used as they represent 95% of the total variance in the dataset.

3.3.2 Additional material not presented in the paper:

There is speculation that thoracosaurs may not be members of Gavialidae (Brochu, 2004a; Vélez-Juarbe, Brochu and Santos, 2007). Uncertainty about their gavialoid affinities have arisen as thoracosaurs typically exhibit primitive characters in their braincase morphology and tooth arrangements (Brochu, 2004a, 2006b; Gold, Brochu and Norell, 2014), suggesting that they are not in fact members of the Gavialoidea. Also, thoracosaurs evolve prior to the estimated divergence dates of Gavialinae and Tomistominae in the Cenozoic (based on molecular clocks) (Harshman *et al.*, 2003; Janke *et al.*, 2005). These divergence dates coincide with a gap in the fossil record of Gavialoidea (morphological context) in the middle Eocene. If these divergence times accurately reflect the evolutionary timescales for Crocodylia, then Cretaceous/Paleocene thoracosaurs cannot be crown members of Gavialidae (Brochu, 2004a).

To examine the consequences of this idea, the thoracosaurs were removed from the combined (morphology-with-molecular) matrix and an additional phylogenetic analysis was carried out, using the same tree searching methods as the previous analyses. Six species were removed from the matrix, *Eothoracosaurus mississippiensis, Thoracosaurus macrorhynchus, Thoracosaurus neocesariensis, Eosuchus minor, Eosuchus lerichei* and *Ocepesuchus eoafricanus.* The resultant phylogeny (64 most parsimonious cladograms, 17,939 steps, CI: 0.563, RI: 0.63) with time calibration (Figure 3.12) showed similar survival patterns across the K-Pg mass extinction as the original combined analysis (Figure 3.3), however, the ghost lineages were less extensive.

Stratigraphic congruence indices were calculated for this analysis, as well as the previous two phylogenetic analyses (Table 3.5 and Figure 3.4). Corrected GER indices and P-values indices were calculated to check whether the values obtained for these trees were significantly different from randomly generated trees; all p-values were significant. The RCI, GER and MSM* suggest that the combined analysis without the thoracosaur taxa are marginally more congruent with the stratigraphy when compared to the combined analysis with thoracosaurs. The morphology only trees, however, are consistently more stratigraphically congruent than the combined analyses.

We ran this analysis to test whether the outcome would be more consistent with the molecular clocks and stratigraphic record, as speculated in the literature; this was found not to be the case. The removal of the "thoracosaur" taxa did not affect the phylogenetic position of Argochampsinae which are also found prior to the "gharial gap". As a result, the *Gavialis-Tomistoma* divergence remains in the Cretaceous (see Figure 3.12) and inconsistent with Eocene-Miocene divergence dates from molecular clocks (Janke *et al.*, 2005; Roos, Aggarwal and Janke, 2007; Oaks, 2011). The Argochampsinae also exhibit characters typically associated with more derived members of the Gavialinae (Salas-Gismondi *et al.*, 2016), unlike the "thoracosaurs". It should be emphasised that the removal of the six species from the matrix, is not supported by the phylogenetic analysis, and that this was done to examine speculation in the literature.

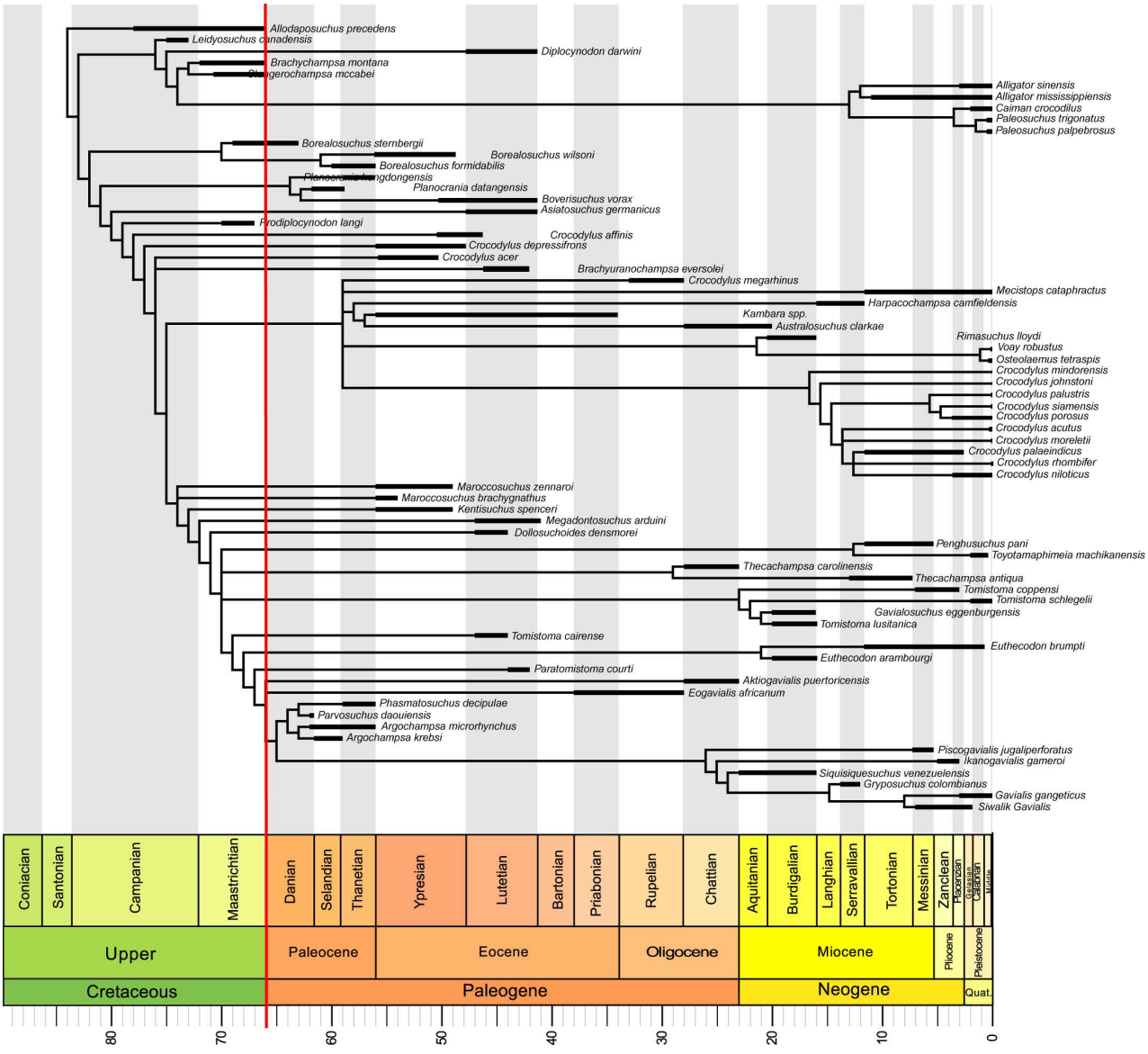

Figure 3.12: Strict consensus of 64 most parsimonious cladograms from the combined morphological and molecular datasets, with thoracosaur taxa removed (length= 17,939 steps, CI= 0.563, RI= 0.63). The matrix contains 72 taxa and 11,808 characters in interleaved format – 244 morphological characters and 11,564 molecular base pairs. Stratigraphic time calibration has been used and *Bernissartia*, *Hylaeochampsa* and *Iharkutosuchus* were dropped from the figure after the analysis. Red bar= K-Pg mass extinction.

Morphology only: calculated from 1024 most parsimonious trees			
	Mean	**Upper range**	**Lower range**
SCI	0.563088	0.605263	0.526316
RCI	-262.846	-248.404	-280.795
GER	0.833134	0.840502	0.823977
MSM*	0.098571	0.102622	0.093893
Combined (morphology-with-molecular): calculated from 32 most parsimonious trees			
	Mean	**Upper range**	**Lower range**
SCI	0.401316	0.421053	0.381579
RCI	-433.649	-412.712	-454.722
GER	0.745999	0.75668	0.735249
MSM*	0.067033	0.069735	0.064454
Combined analysis without thoracosaurs: calculated from 64 most parsimonious trees			
	Mean	**Upper range**	**Lower range**
SCI	0.396429	0.414286	0.385714
RCI	-426.047	-399.869	-454.299
GER	0.765568	0.778192	0.751943
MSM*	0.075987	0.079902	0.072056

Table 3.5: Stratigraphic congruence indices calculated from the most parsimonious trees from each phylogenetic analysis.

3.3.3 Conclusion:

In this chapter, the new species of crocodylian described in chapter 2 were incorporated into macroevolutionary study over the Cretaceous and Cenozoic, with a focus on how the K-Pg extinction has driven diversity and disparity patterns. Results showed patterns of high disparity in the marine environment following the K-Pg mass extinction. Disparity decreased in subsequent time bins but peaked again in the Miocene and Pliocene in the freshwater ecosystems, consistent with patterns that have been reported for the Crocodylomorpha (Mannion *et al.*, 2015; Wilberg, 2017).

Body size was investigated to look at size selectivity across the extinction boundary. It was found that though there was an apparent decrease in size amongst the Moroccan gavialoids, this was not significant and no Lilliput effect is observed. The dyrosaurs maintained large sizes before and after the K-Pg boundary. Increase in skull size amongst the gavialoids and tomistomines towards the Miocene is also observed. These patterns may be similar across other crocodylian groups, such as the Alligatoroidea, based on the primary literature (Langston Jr., 1966; Aguilera, Riff and Bocquentin-Villanueva, 2006). Future work is needed on the entire crown group to better understand these evolutionary patterns and drivers.

The phylogenetic conflict between the morphological and molecular signals was examined in a time calibrated framework and found that the different analyses had a strong impact on crocodylian evolution across the K-Pg boundary. In the morphological framework, a

few lineages survived and then rapidly diversified in the aftermath of the K-Pg, whereas in the combined analysis, there was mass survival of crocodylian over the K-Pg boundary. Stratigraphic congruence was measured using four different metrics and the morphological hypothesis was found to be consistently more congruent with the stratigraphy compared to the combined analyses. The removal of early gavialoids (thoracosaurs) from the matrix is not supported in the current phylogenetic framework and did not dramatically change the survival patterns across the K-Pg for the combined (morphological-with-molecular) analysis or stratigraphic congruence.

Previous morphospace studies have asserted that, though superficially similar, gavialoids and tomistomines cannot be closely related, as implied by the molecular hypothesis, as they occupy different areas of morphospace and therefore convergence best describes the groups' similarity (Pierce, Angielczyk and Rayfield, 2008). However, existing studies have only considered the extant fauna, which may not be useful for this problem as there are only two extant species and a wealth of fossil data is being disregarded (Pierce, Angielczyk and Rayfield, 2008; Sadleir and Makovicky, 2008; Piras *et al.*, 2010, 2014; Gold, Brochu and Norell, 2014; Watanabe and Slice, 2014). The inclusion of fossil material in this disparity analysis shows, that although the extant members do occupy distinct regions, the fossil taxa show distinct overlap across the morphospace. Only the most basal members of the clade- *Maroccosuchus, Kentisuchus, Megadontosuchus* and *Dollosuchoides*, occupy a distinct area on the far right of the PCA plot, and *Gavialis* and *Phasmatosuchus* on the far left (Figure 3.5). This overlap of fossil species suggests that the molecular hypothesis cannot be dismissed based on morphospace and highlights the importance of including fossil taxa to examine the *Gavialis-Tomistoma* debate in the future.

Chapter 4: An Alligatoroid from the Early Paleogene of North Africa and the Post-Extinction Dispersal of Alligators

4.1 Pre-paper commentary:

The previous chapters were focussed on the gavialoid/tomistomine fauna recovered from the Moroccan phosphates, and the wider implications of these new fossil finds. The aim of this chapter is the description of some additional crocodylian fossil material from the phosphate deposits of Morocco, spanning the Late Paleocene-Ypresian, within 10Myrs of the mass extinction. Unlike the preceding chapters, this species belongs to the Alligatoroidea; this is unusual for two reasons. First, this new taxon has been found in the marine horizons in the Oulad Abdoun basin, whereas alligatoroids are typically found in freshwater settings. Second, no alligatoroid material is conclusively known from Africa to date. Unlike the gavialoids which showed interesting patterns in terms of disparity following the K-Pg extinction, this fossil highlights interesting patterns of alligatoroid biogeography. This new species has proved important in shaping our understanding of the dispersal of the Alligatoroidea and how this relates to the K-Pg extinction.

This declaration concerns the article entitled:									
An Alligatoroid from the Early Paleogene of North Africa and the Post-Extinction Dispersal of Alligators									
Publication status (tick one)									
draft manuscript	**X**	**Submitted**		**In review**		**Accepted**		**Published**	
Publication details (reference)	Draft manuscript being prepared for Proceedings of the Royal Society B: Biological Sciences								
Candidate's contribution to the paper (detailed, and also given as a percentage).	N. Longrich recognised the fossil material as novel and obtained the material. Discussions of ideas for the manuscript were between N. Longrich and P. Russell. L. Steel provided access to additional fossil material at the NHM. Choice of methodology, data collection and analyses were carried out by P. Russell. Photographs of the NHM material was provided by L. Steel, all other photographs drawings and figures were made by P. Russell. The manuscript was written by P. Russell, N. Longrich advised at all stages and provided comments and edits on the drafts of the manuscript. Additional edits to the manuscript were provided by D. Field and C. Klein. P. Russell 80% N. Longrich 10%, L. Steel 10%								
Statement from Candidate	This paper reports on original research I conducted during the period of my Higher Degree by Research candidature.								
Signed						**Date**			

An Alligatoroid from the Early Paleogene of North Africa and the Post-Extinction Dispersal of the Alligatoroidea

Polly Russell[1], Nicholas R. Longrich[1] and Lorna Steel[2]

[1]Department of Biology and Biochemistry, and Milner Centre for Evolution, University of Bath, Claverton Down, Bath, BA2 7AY, United Kingdom

[2]Department of Earth Sciences, Natural History Museum, Cromwell Road, London SW7 5BD, UK

Alligatoroidea are a freshwater clade of Crocodylia that includes extant Alligatorinae and Caimaninae, and the extinct Diplocynodontidae. Intolerance to saltwater has restricted the biogeography of the group, with alligatorines occurring predominantly in North America, caimans in South America, and diplocynodontids in Europe. To date, there are no definitive alligatoroid fossils known from Africa. Here we describe a new diplocynodontid alligatoroid, *Diplocynodon africanum* sp. nov., from the Paleocene/Early Eocene of Morocco. Phylogenetic analysis places the new species in a derived position within Diplocynodontidae as sister to *Diplocynodon remensis* from the Paleocene of France. Time calibration combined with ancestral state and paleo-map reconstructions suggests that diplocynodontids dispersed into Africa from Europe in the Paleocene, prior to the Paleocene-Eocene Thermal Maximum. Similarly, dispersals from North America to South America, Europe, and perhaps Asia, are inferred to have taken place in the Paleocene in various alligatoroid clades. These patterns suggest that Alligatoroidea underwent a radiation and dispersal after the K-Pg mass extinction, with alligatoroids dispersing out of North America to occupy niches left vacant by the K-Pg mass extinction on other continents. Rather than a biogeographic distribution driven by vicariance, the patterns found here suggest that high rates of dispersal in the Paleogene may be driven by the extinction of competitors and predators across the K-Pg boundary, allowing survivors to successfully colonise new habitats amid reduced interspecific competition.

1. Introduction

Alligatoroidea, a freshwater crocodylian subclade including extant alligators and caimans, exhibit a fossil record extending back to the Late Cretaceous of North America (Brochu, 1999). Today, alligators (Alligatorinae) occur in North America and China, and caimans (Caimaninae) are distributed throughout South America (Grigg and Kirshner, 2015; IUCN, 2017). The extinct Diplocynodontidae are an early clade of alligatoroids known exclusively from Europe between the Late Paleocene and Miocene (Brochu, 1999; Piras and Buscalioni, 2006; Martin, 2010; Martin *et al.*, 2014; Díaz Aráez *et al.*, 2015).

Amongst crown crocodylians, alligators and caimans are unusual in being restricted to freshwater environments (Brochu, 1999). Whilst other crocodylians can disperse across marine barriers and are therefore biogeographically widespread, intolerance to saltwater has hindered the dispersal of alligatoroids and they are, as a result, biogeographically restricted.

Prior to the Cenozoic, alligatoroids are known exclusively from North America. During the Cenozoic, Alligatorinae are known from the Paleocene to the Recent in North America, Caimaninae are known from the Paleocene to Recent in South America, and Diplocynodontidae occur exclusively in the Paleocene to Miocene of Europe. In addition, there are rare examples of Alligatorinae in Europe (Kälin, 1939; Wassersug and Hecht, 1967) and Asia (Wu *et al.*, 2006; Martin and Lauprasert, 2010; Iijima, Takahashi and Kobayashi, 2016; Wang, Sullivan and Liu, 2016), and Caimaninae from North America (Brochu, 1999, 2010).

The Diplocynodontidae, containing nine currently recognised species, were until recently thought to have migrated from North America to Europe around the Paleocene-Eocene Thermal Maximum (PETM) (Martin *et al.*, 2014; Delfino *et al.*, 2017). However, reassessment of Late Paleocene material now suggest an earlier dispersal (Martin *et al.*, 2014; Delfino *et al.*, 2017). Whether diplocynodontids were tolerant to saltwater is uncertain, though their restriction to Europe suggests that they resembled their extant relatives in exhibiting limited salt tolerance (Delfino, Böhme and Rook, 2007). This implies that land bridges were the most likely mechanism for dispersal for alligatoroids (Brikiatis, 2014).

To date, there are no definitive alligatoroid remains from Africa. Fragmentary fossils have been reported from Libya (D'Erasmo, 1934) and Egypt (Rossmann, Muller and Forst, 2000) but these are too incomplete to be diagnostic and require further study (Delfino and Smith, 2012). Here, we describe two nearly complete skulls representing a new species of *Diplocynodon* from the Paleocene/Ypresian phosphate deposits of Morocco. The excellent preservation of the material provides the first conclusive evidence for Alligatoroidea in Africa, suggesting an Early Paleogene dispersal into Africa, with broader implications for the dispersal of vertebrates in the wake of the K-Pg mass extinction.

2. Geological Setting

The phosphates of the Oulad Abdoun basin (Figure 4.1) span the Late Cretaceous-Ypresian (Kocsis *et al.*, 2014; Yans *et al.*, 2014). The deposits have yielded a rich vertebrate fossil fauna including selachians, actinopterygian fish, reptiles and mammals (Arambourg, 1952; Cavin *et al.*, 2000; Gheerbrant *et al.*, 2003; Bardet *et al.*, 2010; Noubhani, 2010; Cappetta *et al.*, 2014). The depositional environment represents a warm, shallow epicontinental seaway; though the majority of species are marine, there are examples of rarer terrestrial material which has been transported in (Gheerbrant, 2009; Yans *et al.*, 2014; Longrich *et al.*, 2017). The Cretaceous marine reptile fauna was dominated by diverse mosasaurs, along with rarer occurrences of crocodylomorphs, plesiosaurs, marine turtles and birds (Longrich and Field, no date; Jouve, Bardet and Jalil, 2008; Bardet *et al.*, 2010, 2013; Vincent *et al.*, 2013; Cappetta *et al.*, 2014). High turnover over the K-Pg boundary resulted in a marine reptile fauna dominated by a diverse crocodylomorph assemblage along with abundant palaeophiid sea snakes and marine turtles in the aftermath (Bardet *et al.*, 2010). The known Palaeogene crocodylomorph assemblage was dominated by dyrosaurs, gavialoids and tomistomines (Russell and Longrich, in prep.).

The new fossil material presented here, including two complete skulls and part of a third, was found in the Sidi Daoui and Sidi Chennane localities in the Oulad Abdoun basin (Figure 4.1). The holotype, MHNM.KHG.178, is from Sidi Daoui and the other specimens (BMNH R36873, MHNH.KHG 167 and MHNH.KHG 168) come from Sidi Chennane and come from the Paleocene of Couche II and Early Eocene (Ypresian) of Couche I (see supplementary information).

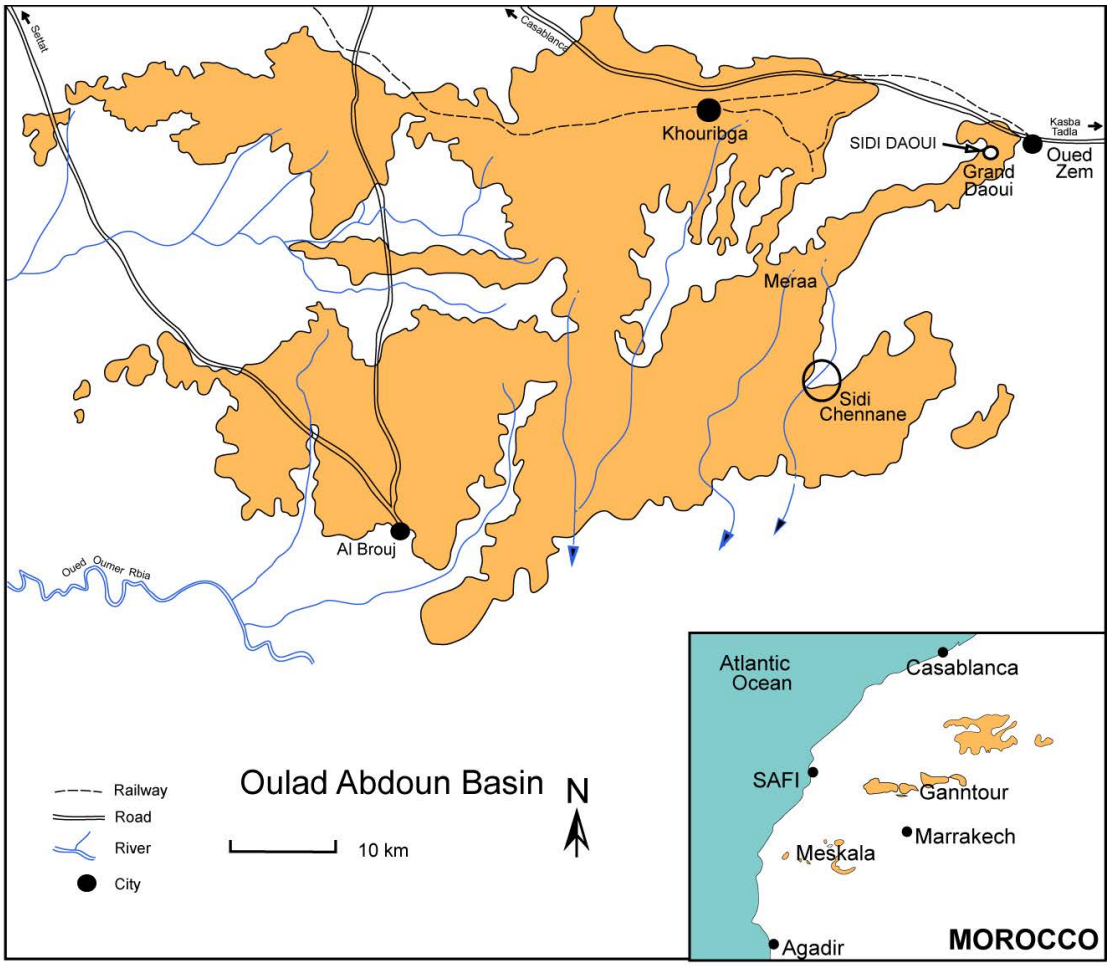

Figure 4.1: Geographic map of the Oulad Abdoun basin in Morocco, with the fossil localities, Sidi Daoui and Sidi Chennane shown (modified from (Yans *et al.*, 2014)).

Institutional abbreviations: **BMNH:** Natural History Museum, London; **CE**: Collection Eldonia, Gannat, France; **GMH**: Geiseltalsammlung, Zentralmagazin Naturwissenschaftlicher Sammlungen, Martin-Luther-Universität Halle-Wittenberg, Halle (Saale), Germany; **HLMD:** Hessisches Landesmuseum, Darmstadt, Germany; **IPS**: Institut de Paleontologia 'Miguel Crusafont', Sabadell, Barcelona, Spain; **MHNM:** Museum of Natural History, Cadi Ayyad University, Marrakech, Morocco;**MNHN:** Museum National d'Histoire Naturelle, Paris, France; **MUL:** Montanuniversität Leoben, Austria; **NMB:** Naturhistorisches Museum Basel, Switzerland; **Rhinopolis**: Association Rhinopolis, Gannat, Allier, France.

3. Systematic Palaeontology

Crocodylia Gmelin, 1789 (*sensu* Martin and Benton 2008)
Eusuchia Huxley, 1875
Alligatoroidea Gray, 1844
Diplocynodontidae Hua, 2004
Genus *Diplocynodon* Pomel, 1847

(a) Genus Diagnosis

Axial hypapophysis located toward the centrum; dorsal margin of the iliac blade rounded in shape, with a smooth border and a very deep posterior tip of the blade; splenial excluded from mandibular symphysis; a pair of enlarged maxillary (four and five) alveoli and confluent dentary (three and four) alveoli; parietal and squamosal approach each other on posterior wall of supratemporal fenestra without actually making contact; ectopterygoid adjacent to the posterior-most maxillary alveoli; dorsal margin of the infratemporal fenestra formed by the quadratojugal, preventing the quadrate from reaching the fenestra; lacrimal longer than prefrontal; nasals excluded, at least externally, from naris.

***Diplocynodon africanum* sp. nov.**

(b) Etymology

The species name refers to Africa, as this taxon represents the first definitive alligatoroid fossil material from the African continent.

(c) Diagnosis

Diplocynodontid distinguished from other species by the following combination of characters: enlarged posteriorly projecting lateral supraoccipital tuberosities, 14 maxillary teeth, surangular-dentary suture at posterodorsal angle of external mandibular fenestra, frontal ends at the same level to the anterior extension of the prefrontal.

(d) Material

Holotype: MHNM.KHG.178, skull, jaws and associated axis and cervical vertebrae (Figure 4.2);
Paratype: BMNH R36873 complete skull with associated dorsal vertebrae and ventral osteoderms (Figure 4.3)
Referred material: MHNH.KHG 167, MHNH.KHG 168 partial rostrum (Figure 4.6, 4.7)

(e) Locality and Horizon

Paleocene/Eocene of Sidi Daoui (type) and Sidi Chennane (MHNH.KHG.167, MHNH.KHG.168) in the Oulad Abdoun basin of Morocco.

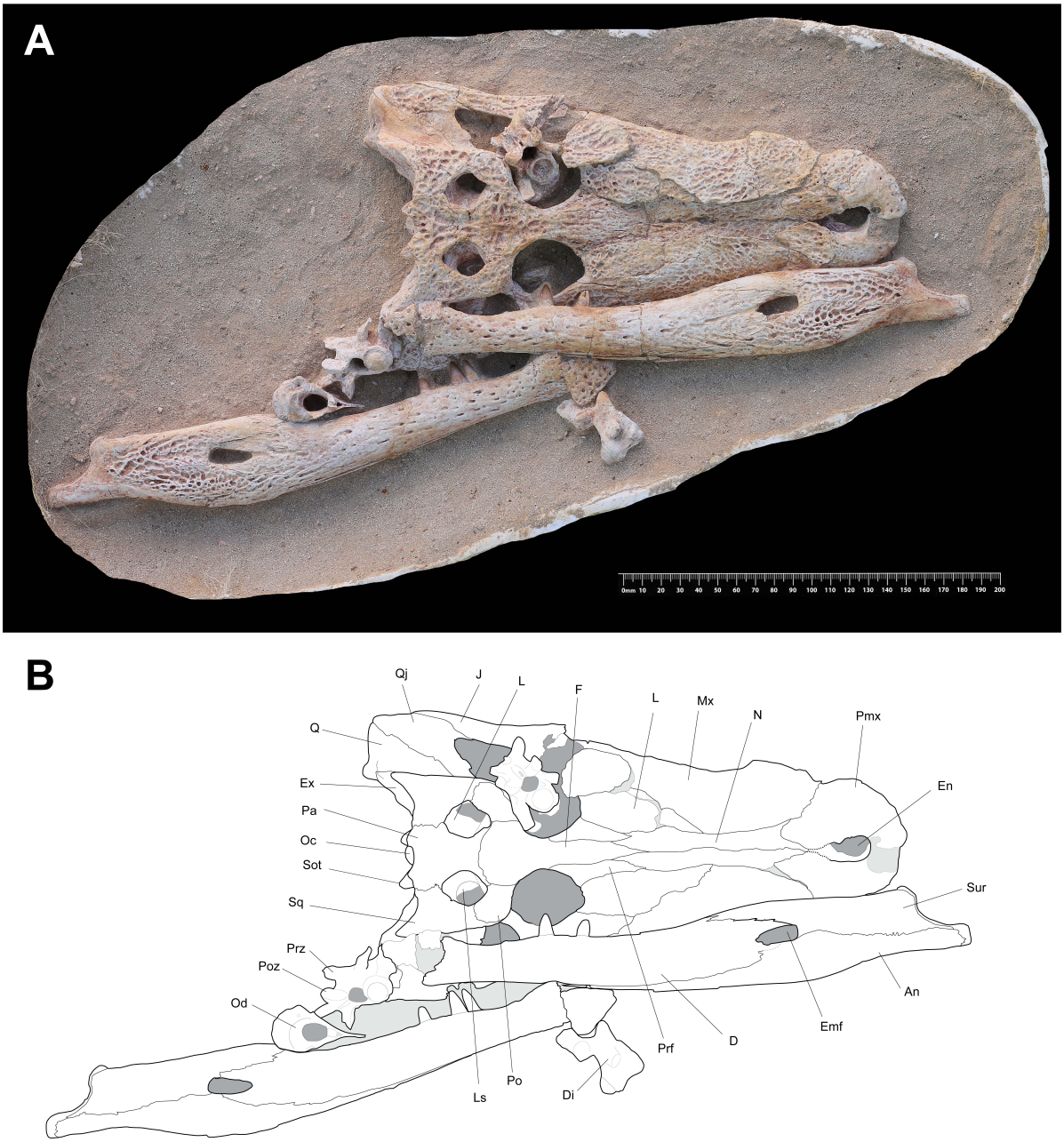

Figure 4.2: *Diplocynodon africanum* sp. nov., holotype MHNM.KHG.178 from Paleocene/Ypresian of Morocco. Skull in dorsal view. **Abbreviations: An,** angular, **D,** dentary, **Di,** diapophyses, **En,** external nares, **Emf,** external mandibular fenestra, **Ex,** exoccipital, **F,** frontal, **J,** jugal, **L,** lacrimal, **Ls,** laterosphenoid, **Mx,** maxilla, **N,** nasal, **Oc,** occipital condyle, **Od,** odontoid process, **Pa,** parietal, **Pmx,** premaxilla, **Po,** postorbital, **Poz,** postzygapophysis, **Prf,** prefrontal, **Prz,** prezygapophysis, **Q,** quadrate, **Qj,** quadratojugal, **Sot,** supraoccipital tuberosity, **Sq,** squamosal, **Sur,** surangular.

(f) Description and comparisons

Diplocynodon africanum sp. nov. is represented by three specimens. The holotype (MHNM.KHG.1780 and paratype (BMNH R36873) include complete skull material with associated vertebrae and osteoderms; the referred material (MHNM.KHG 167, MHNM.KHG.168) consists of fragments of maxilla, nasals, and palate. The skull of MHNM.KHG.178 measures 261 mm in length and the paratype measures 216 mm in length (Table 4.1). The lower jaw is partially preserved in the holotype and has become disarticulated and damaged at the anterior symphyseal region. Some dorsoventral compression is evident in the holotype and paratype; the ventral portion of the paratype is crushed ventrally, limiting interpretation of the palate, and there has been limited reconstruction performed on the left side of the paratype specimen prior to study (Figure 4.3).

The skull is broad-snouted and brevirostrine. There is a constriction at the maxilla-premaxillary contact, and in ventral view there is a shallow pit at this constriction where the fourth mandibular tooth would likely be received. This suggests that there was no notch present early in ontogeny (Character 91) favouring a referral to the Diplocynodontidae. Posteriorly, the maxillae flare at the level of the 4-5th maxillary alveoli. Overall skull morphology is similar to *Diplocynodon remensis, D. elavericus* and *D. hantoniensis,* though these species are larger overall. The snout shape contrasts with the more triangular shape of *D. tormis* and *D. ratelli*. In terms of relative snout length, *D. africanum* is most similar to *D. tormis D. ungeri,* which has the proportionally most elongate rostrum (65%) (Table 4.2).

The naris in *D. africanum* is subcircular and surrounded by the premaxilla. In contrast to Alligatorinae and Caimaninae, the nasals do not contact the nares. This feature is shared with all species of *Diplocynodon* except for *D. ratelli* (Character 82) (Díaz Aráez *et al.*, 2015). The orbits are sub-circular, similar to *D. tormis* (Buscalioni, Sanz and Casanovas, 1992), in contrast to the anteroposteriorly elongate shape exhibited by other species (Table 4.2). The step or spectacle anterior to the orbits is not observed in *D. africanum*, a feature shared with *D. hantoniensis* to the exclusion of other diplocynodontids. The supratemporal fenestrae are subcircular as in *D. remensis* (Martin *et al.*, 2014) and *D. ungeri* (Martin and Gross, 2011) in contrast to the oval, anteroposteriorly elongate shape seen in other *Diplocynodon*. Based on different sized specimens of *D. ratelli* and *D. hantoniensis* (BMNH 25167, BMNH 30393), larger skull sizes show more rounded supratemporal fenestrae suggesting ontogenetic variability in this feature (Díaz Aráez *et al.*, 2015). The incisive foramen (Character 88,89) is large, a feature shared with *D. elavericus* (Martin, 2010).

The premaxilla contains five teeth (Character 87). The first two are small relative to the third and fourth alveoli, with a large occlusal pit for the first dentary tooth between them. The dorsal posterior premaxillary processes are short, not extending posteriorly beyond the second maxillary alveolus, typical of all Alligatoroidea (Character 90). The ventral maxilla-premaxillary suture is linear, as is typical for diplocynodontids. The maxillary tooth count is 14, apomorphic to this species; diplocynodontids typically have 16-17 maxillary alveoli. The largest maxillary alveoli are the 4th and 5th (Character 93). Such enlarged double caniniform teeth are a synapomorphy of *Diplocynodon* (Piras and Buscalioni, 2006; Martin, 2010; Martin *et al.*, 2014). Occlusal pits are present between the 6th, 7th and 8th alveoli, with lingual pits present posteriorly (shared with *D. hantoniensis* and *D. elavericus*).

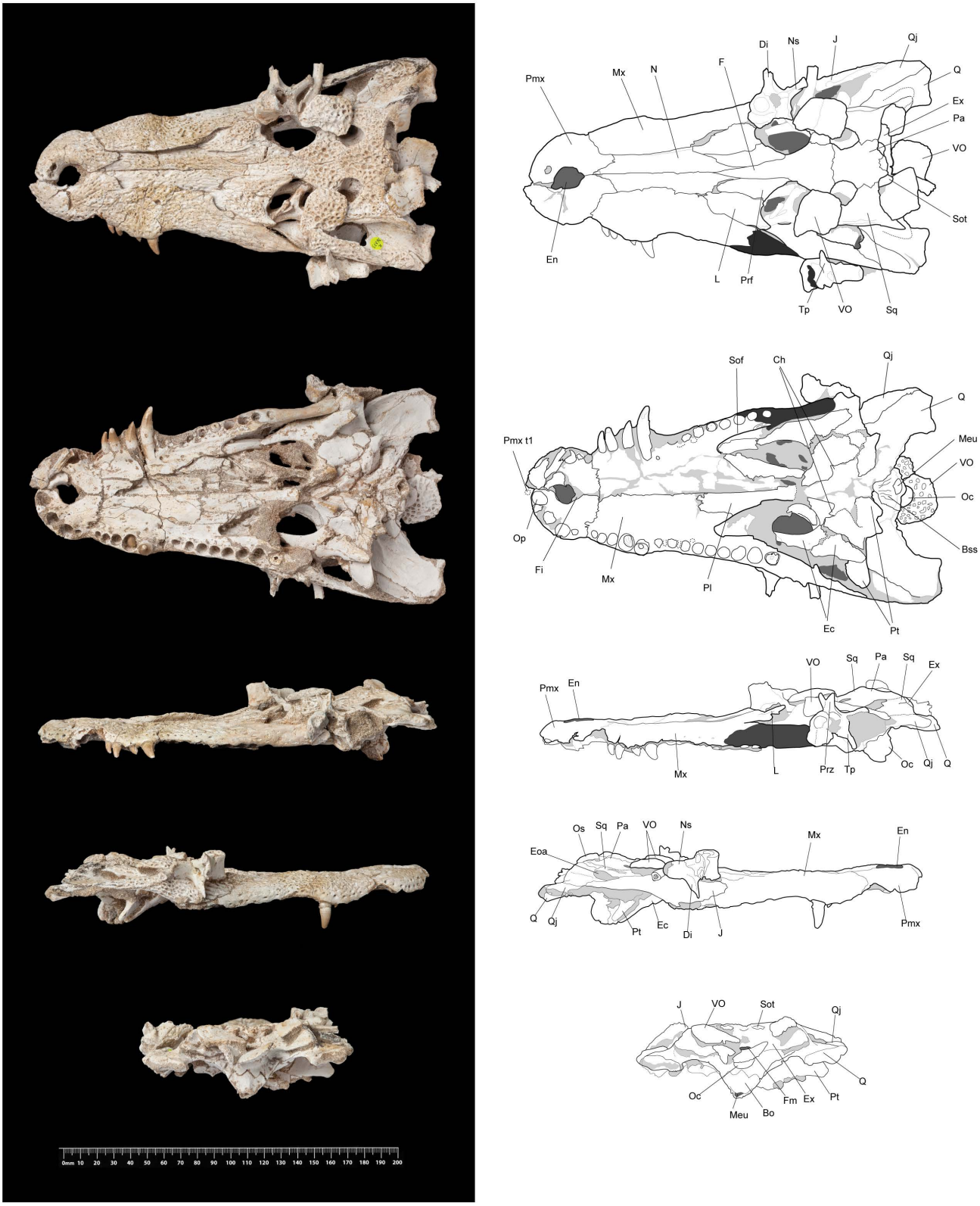

Figure 4.3: *Diplocynodon africanum* sp. nov., paratype BMNH R36873 from Ypresian of Morocco. Skull in dorsal, ventral, left lateral, right lateral and occipital view. Darkest shading highlights where the skull has been reconstructed with plaster. **Abbreviations: Bo,** basioccipital, **Bss,** basisphenoid suture surface, **Ch,** choana, **Di,** diapophyses, **Ec,** ectopterygoid, **En,** external nares, **Eoa,** external otic aperture, **Ex,** exoccipital, **F,** frontal, **Fi,** foramen incisivum, **Fm,** foramen magnum, **J,** jugal, **L,** lacrimal,

Meu, medial eustachian foramen, **Mx,** maxilla, **N,** nasal, **Ns,** neural spine, **Oc,** occipital condyle, **Op,** occlusion pit, **Os,** osteoderm, **Pa,** parietal, **Pl,** palatine, **Pmx,** premaxilla, **Pmx t1,** first premaxillary tooth, **Prf,** prefrontal, **Prz,** prezygapophysis, **Pt,** pterygoid, **Q,** quadrate, **Qj,** quadratojugal, **Sof,** suborbital fenestra, **Sot,** supraoccipital tuberosity, **Sq,** squamosal, **Tp,** transverse process, **VO,** ventral osteoderm.

	MHNM.KHG.178 (Holotype)	BMNH R36873 (Paratype)
Total length (posterior border of supraoccipital to tip of rostrum)	26.1	21.6
Rostral length (from anterior border of the orbits to tip of rostrum)	17.2	14
Length from supraoccipital to anterior border of the orbits	8.9	7.6
Rostrum width at anterior border of orbit	11.6*	9.1
Width at confluent alveoli	9.4*	7.5
Width of rostrum at maxilla-premaxilla contact	6.1*	4.9
Width between lateral quadrate condyles	14.2*	11.9
Width skull table (across the middle of the supratemporal fenestrae)	8	6.7
Width between squamosals	8.9	7.3
Orbit length	3.8	3.4
Orbital width (maximum)	3.1*	-
Supratemporal fenestra length	2.3	1.5
Supratemporal fenestra width	1.8	1.3
External naris length	-	1.7*
External nares width	-	1.8*
Premaxilla maximum width	7.4*	5.3*
Interorbital width	1.5	1.5
Interfenestral bar width	1.7	1.8
Incisive foramen length	-	1.6
Incisive foramen width	-	1.2*
Suborbital fenestra length	-	6.2
Suborbital fenestra width	-	2*
Interfenestral width of the palatines	-	1.4*

Table 4.1: Skull measurements of the holotype and paratype of *Diplocynodon africanum* sp. nov. (measurements in cm). Asterisks (*) show estimated values due to preservation.

The frontal is equal in length to the prefrontals (Character 181), an autapomorphy of the species. The lacrimals are longer than the prefrontals (Character 129). The fronto-parietal suture is linear as in all *Diplocynodon* species except for *D. ungeri* and *D. ratelli* where it is concavo-convex (Character 149). There is modest entry of the suture into the supratemporal fenestra (Character 148), shared with *D. remensis*. The squamosal shows parallel groves for external ear musculature, a crocodylian plesiomorphy, and has elongate prongs, as in *D. elavericus* and *D. hantoniensis*. The postorbital bar is damaged. The supraoccipital exposure on the dorsal skull table is small (Character 158), and *D. africanum* also shows significant posterior tuberosities of the supraoccipital on the occipital face. This character is also observed in *D. hantoniensis, D. elavericus* and other alligatoroids, *Leidyosuchus* (Farke *et al.*, 2014), *Brachychampsa* (Sullivan and Lucas, 2003) and *Tsoabichi* (Brochu, 2010).

The quadratojugal bears a long anterior process along the lower temporal bar (Character 142) and the quadratojugal spine is positioned between the posterior and superior angles of the infratemporal fenestra (Character 139), a plesiomorphic feature of Alligatoroidea. The quadratojugal extends to the superior angle and prevents the participation of the quadrate in the infratemporal fenestra (Character 143). As in other diplocynodontids, except *Diplocynodon elavericus*, the quadrates do not extend very far posteriorly beyond the skull table.

The palatine is broad and shows wing-shaped processes at the anterior border of the suborbital fenestrae, as in *Diplocynodon muelleri* (Piras and Buscalioni, 2006). The anterior extension is short, and does not extend beyond the ninth alveolus. The palatine extends further anteriorly in *D. elavericus, D. deponiae* and *D. tormis.* The ectopterygoid is broadly separated from the toothrow, as shown by the presence of a sutural surface on the maxilla, and is adjacent to the last two alveoli.

The extent of the mandibular symphysis and presence of confluent third and fourth dentary alveoli are unclear. The dentary-angular suture is positioned at the posteroventral margin of the external mandibular fenestra, and is more posteriorly positioned than in *Diplocynodon remensis*. The dentary-surangular suture meets at the posterodorsal corner of the external mandibular fenestra (Character 64), representing an apomorphy for this species. The surangular pinches off anterior to the tip of the retroarticular process (Character 72). The retroarticular process is posterodorsally directed, though the dorsal angle is shallow so that the process is nearly posteriorly directed (Character 71). This long, shallow process is very similar to the condition seen in *D. remensis* and *Leidyosuchus* (Martin *et al.*, 2014). The angular-surangular suture occurs at the posteroventral corner of the external mandibular fenestra (Character 60) and curves ventrally towards fenestra; in *D. remensis* this contact curves dorsally and is more dorsally positioned on the fenestra.

The dentary and maxillary teeth are typical of *Diplocynodon*, being short and bluntly conical with mediodistal carinae. The teeth curve lingually, and there is no obvious compression of the alveoli posteriorly.

Postcranial elements include the axis and three post-axial cervical vertebrae in the holotype and two posterior dorsal vertebrae and several osteoderms in the paratype. The axis is partially preserved and visible in anterior view. The odontoid process is fused with the centrum and weakly developed, and articular surfaces for the atlantal neural arch are positioned laterally to the odontoid process. The diaphophyses of the post-axial cervicals project ventrolaterally. The hypapophysis and parapophysis are only visible in one vertebra

(preserved in lateral view) and are not strongly developed; thus, this vertebra is likely to be an anterior cervical (Kobayashi *et al.*, 2006; Shan *et al.*, 2009). The dorsal vertebrae associated with the paratype are proceolous as in other Crocodylia. They lack a hypapophysis and parapophyses, and the diapophyses are laterally directed. Osteoderms are subrectangular in shape and show ornamentation in the form of deep circular pits. The osteoderms lack a median keel, suggesting that they are ventral osteoderms (Martin and Gross, 2011).

	Total length skull (cm)	Relative snout length	Relative snout width	Orbit shape
D. deponiae	8.8 *	49% *	-	87%
D. elavericus	34.5 *	55% *	75% *	65% *
D. muelleri	11.9	55%	89%	67%
D. hantoniensis	49	59%	90%	69%
D. remensis	29.8	59%	83% *	69%
D. darwini	15.5	59%	84%	74%
D. ratelli	40.9	61%	70%	76%
D. africanum	26.1	65%	81%	82%
D. ungeri	35.5 *	65% *	-	-
D. tormis	20.5	67%	83%	77%

Table 4.2: Comparative measurements amongst different species of *Diplocynodon.* Relative snout length (length rostrum/total skull length), relative snout width (width of rostrum level with 5th maxillary alveolus/width of rostrum at anterior border of orbits), orbit shape (width obit/length orbit). *D. deponiae:* HLMD Me7496 (Brochu, 1999), *D. elavericus:* Rhinopolis B3 (Martin, 2010), *D. muelleri:* NMB Spa 4 T2 (Piras and Buscalioni, 2006), *D. hantoniensis:* BMNH 30393 (Martin, 2010), *D. remensis:* CE0001 (Martin *et al.*, 2014), *D. darwini*: GMH 6074 (Hastings and Hellmund, 2015), *D. ratelli:* MNHN sg557 (Brochu, 1999), *D. africanum:* MHNM.KHG.178 (Holotype), *D. ungeri*: MUL Inv. No. 21 (Martin and Gross, 2011), *D. tormis*: IPS- 9001 (Buscalioni, Sanz and Casanovas, 1992).

4. Phylogenetics and Biogeography

Diplocynodon africanum was scored using the character-taxon matrix from Brochu (2012). We also scored four additional diplocynodontid species from the literature, including *D. deponiae* (Delfino and Smith, 2012) *D. ungeri, D. elavericus* and *D. remensis* (Martin *et al.*, 2014), so that all valid species of *Diplocynodon* were included in the analysis. Five additional alligatoroid taxa were added to the matrix including *Krabisuchus siamogallicus*- Brochu version (Martin and Lauprasert, 2010), *Globidentosuchus brachyrostris, Culebrasuchus mesoamericanus* (Hastings, Reisser and Scheyer, 2016), *Protoalligator huiningensis* and the Maoming specimen (Wang, Sullivan and Liu, 2016). Modifications were made to the scorings of *Leidyosuchus canadensis* (Farke *et al.*, 2014), *Diplocynodon ratelli* (Díaz Aráez *et al.*, 2015) and *D. remensis* (see supplementary). Four characters were added to the matrix from (Jouve *et al.*, 2014) (see supplementary). The new matrix consists of 183 characters and 107 taxa, with *Bernissartia* as an outgroup.

The matrix was analysed in TNT v. 1.1 (Goloboff, Farris and Nixon, 2003) using a heuristic search of 1000 random addition sequence replicates and TBR branch swapping, holding 100 trees per replicate. Preliminary searches found low resolution in the strict consensus tree (Figure 4.8), therefore "Pruned trees" in TNT and RogueNaRok (Aberer, Krompass and Stamatakis, no date) were used to identify unstable taxa. After the removal of these taxa (*Hassiacosuchus haupti, Protoalligator huiningensis* and Maoming specimen) we reran the search, resulting in 32 trees of 759 steps (CI: 0.31, RI: 0.788), and then calculated Bremer decay values (Figure 4.4, 4.9). The resulting consensus was time calibrated in R (R Core Team, 2013), using the Paleotree (Bapst, 2012) and Strap (Bell and Lloyd, 2014) packages, with stratigraphic ranges taken from the literature (Appendix 3). Analyses were performed for the entire matrix (Figure 4.10), but only the results for Alligatoroidea are presented here (Figure 4.4). Three dating methods were applied, using the "basic" and "equal" methods in DatePhylo() and the "mbl" method in timePaleoPhy(). The "basic" method makes the age of the internal node equal to the age of the oldest descendent, but a drawback of this method is that it can result in zero length branches, which is avoided with the "equal" and "mbl" methods.

Patterns of dispersal were inferred using ancestral state reconstruction in R (R Core Team, 2013). We used both maximum likelihood (ML) and Bayesian frameworks to test the robustness of the results with respect to the choice of model. We used the Phytools package in R (Revell, 2012) (make.simmap() for Bayesian and rerootingMethod() for ML), because they incorporate branch length information and accept polytomies in the phylogeny. After assessing model fit (Table 4.3), we used the equal rates model on the "mbl" time-scaled consensus tree for both analyses (ML and Bayesian), and a sample of 1000 stochastic maps for the Bayesian analysis. Results of the Bayesian analysis are presented in Figure 4.4. The results were consistent for the equal rates model between the make.simmap() and rerootingMethod() functions. The biogeographic distributions of the Alligatoroidea from the Cretaceous to the Eocene were plotted using paleoMap (Sara Varela and Sonja Rothkugel, 2016) in R. The biogeographic data used in this package were checked and modifications were made including removal of taxa with uncertain affinity and addition of *Diplocynodon africanum* (see supplementary information).

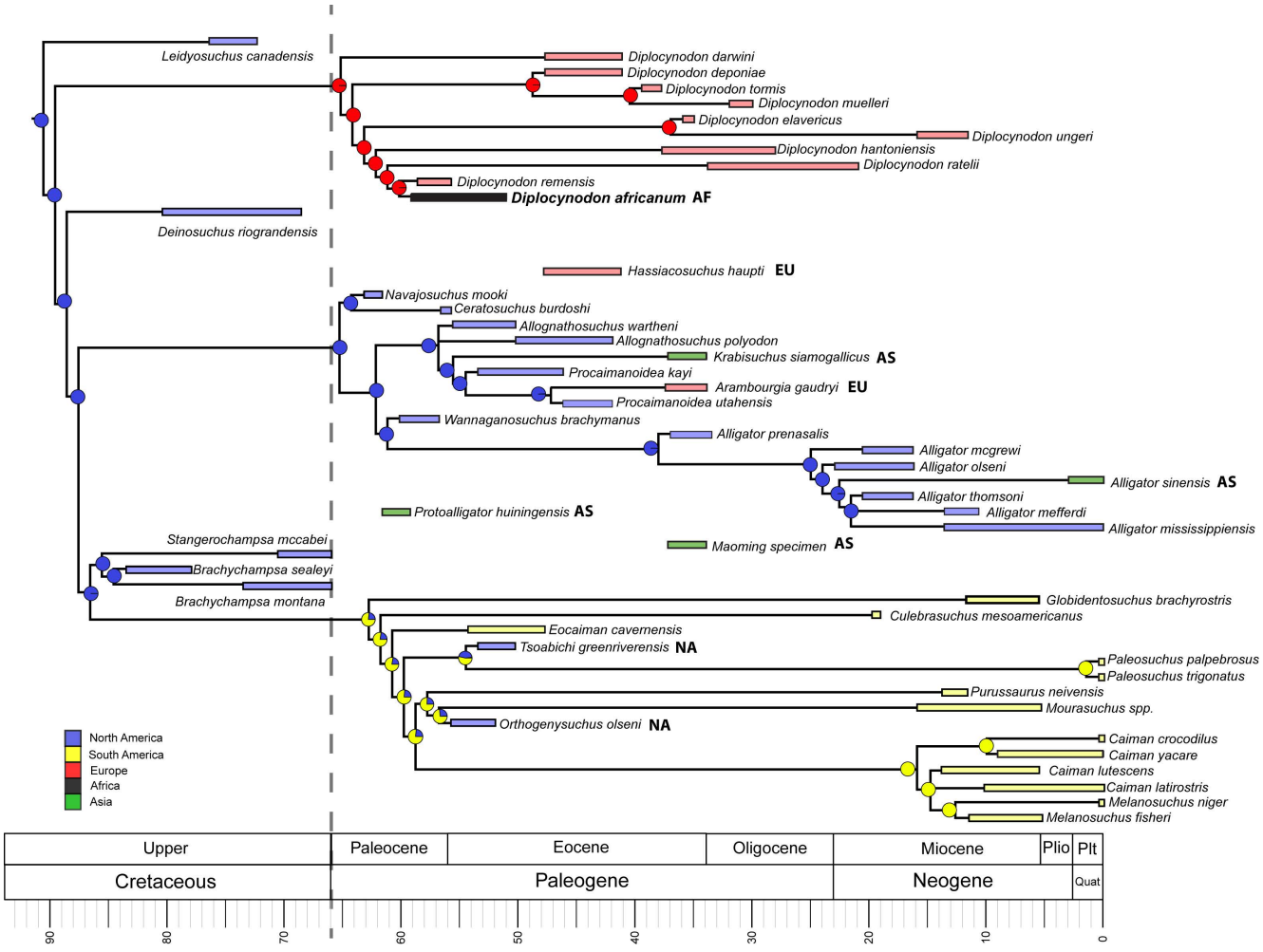

Figure 4.4: Time calibrated strict consensus of the Alligatoroidea. Result of 32 most parsimonious trees of 759 steps (CI: 0.31, RI: 0.788). Pie charts represent the ancestral state reconstruction. Floating taxa indicate rogue taxa that were removed from the analysis prior to the ancestral state reconstruction. Taxa that show isolated dispersal events are highlighted with their geographic location: **AF:** Africa, **AS:** Asia, **EU:** Europe, **NA:** North America.

5. Discussion

(a) Relationships of *Diplocynodon africanum* sp. nov.

Diplocynodon africanum can be referred to Alligatoroidea based on the separation of the ectopterygoid from the maxilla (Character 103), sub equal anterior surangular process (Character 61) and lingual occlusal pits on the maxilla (Character 92). Another typical feature of the Alligatoroidea, the lateral shift of the quadrate foramen aereum (Character 175), is not visible on either specimen. Characters shared with *Diplocynodon* include enlarged 4th and 5th maxillary alveoli, a lacrimal that is longer than prefrontal; an ectopterygoid positioned adjacent the last two maxillary alveoli; and a dorsal margin of the infratemporal fenestra formed by the quadratojugal, preventing the quadrate from reaching the fenestra. Diplocynodontidae is a stem alligatorid clade, outside of Globidonta (i.e. *Alligator mississippiensis* and all taxa closer to it than to *Diplocynodon ratelli*), but closer to the crown than *Leidyosuchus*, the earliest member of the Alligatoroidea.

In previous phylogenetic analyses *Diplocynodon darwini* and *D. deponiae* (Delfino and Smith, 2012) form the earliest diverging members of the group (Piras and Buscalioni, 2006; Martin, 2010; Delfino and Smith, 2012; Martin *et al.*, 2014). This is consistent with the results presented here, as *D. darwini* remains the earliest-diverging member of the clade, with strong bremer support for this position (Figure 4.9). The interrelationships between other members of the Diplocynodontidae vary considerable within the literature (Piras and Buscalioni, 2006; Martin, 2010; Delfino and Smith, 2012; Martin *et al.*, 2014), and the results presented here show a considerable rearrangement of species within Diplocynodontidae (Figure 4.4). Internal nodes within the Diplocynodontidae show weak support, based on the Bremer decay indices (Figure 4.9). The low bremer support values are a pervasive feature between prior studies and the phylogenetic results presented here, which helps to explain this taxonomic instability (Piras and Buscalioni, 2006; Martin and Gross, 2011; Martin *et al.*, 2014). In comparison to previous results, we find that *D. tormis* and *D. muelleri* remain sister taxa but shift from the most derived position in the tree to a deeper branching node with *D. deponiae*. *Diplocynodon remensis* has shifted to the most derived position in the present consensus and is sister taxon to the new species*, D. africanum*. These two species are closely related to *D. ratelli* and *D. hantoniensis*. The time calibrated tree reveals that this derived position for *D. remensis* and *D. africanum* is stratigraphically incongruent, as these two species are the stratigraphically earliest members of the group.

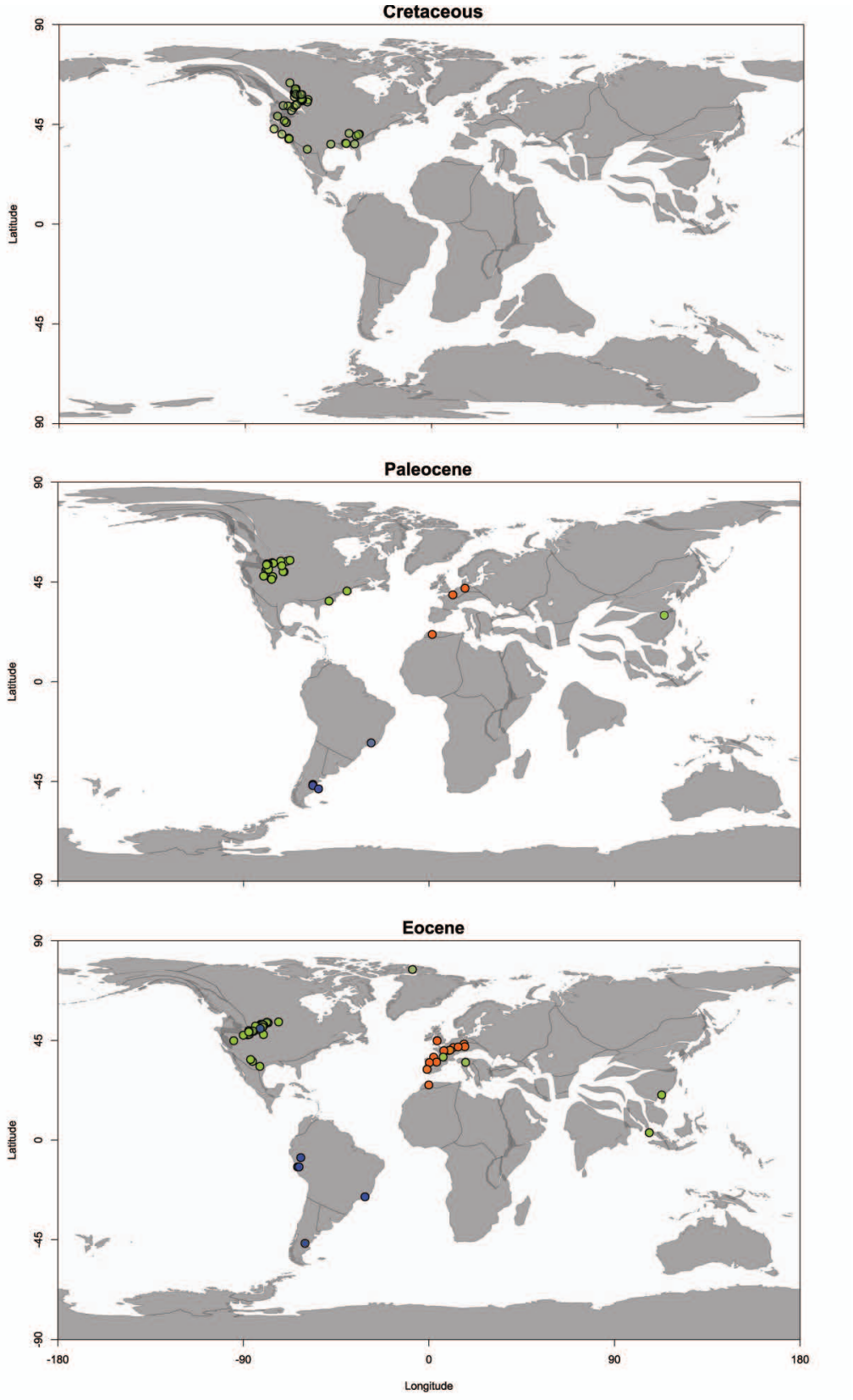

Figure 4.5: PaleoMap reconstructions of the Alligatoroidea in the Cretaceous, Paleocene and Eocene. Alligatoridae are shown in green, Caimaninae in blue, and Diplocynodontidae in orange.

(b) Biogeography

Africa:

There are several reports of alligatoroid fossils from Africa prior to this study, including a mandible fragment from the Upper Eocene Qasr-el-Sagha Formation in the Fayum (Rossmann, Muller and Forst, 2000), Egypt, and cranial and postcranial fragments from the Miocene, As Sahabi locality in Libya (D'Erasmo, 1934). The Libyan material was originally identified as *Diplocynodon sp.,* however subsequent examination suggests this material is too fragmentary to be diagnostic (Buffetaut, 1985; Brochu, 1999; Delfino, Böhme and Rook, 2007). The fragmentary nature of these fossils means that, until now, there has been no definitive evidence of African alligatoroids (Buffetaut, 1985). The description of *Diplocynodon africanum* provides confirmation that Alligatoroids dispersed into Africa. In light of this, further study of the Egyptian and Libyan fossils, and a closer examination of crocodylomorphs from Africa, is warranted.

Dispersal of *Diplocynodon* from Europe into Africa appears to have been an isolated event in the Early Paleocene (Figure 4.4). Palaeogeographic reconstructions suggest that there were no complete land bridges in the Paleocene between Europe and Africa (Gheerbrant and Rage, 2006). Although there are documented cases of mammals crossing between Europe and Africa during the Cretaceous and Eocene (Gheerbrant, 1990; Gheerbrant and Rage, 2006), African mammal faunas show limited European influence (Archibald and Bryant, 1990; Longrich, Scriberas and Wills, 2016), consistent with a scenario involving persistent marine barriers. Therefore, an oceanic dispersal is the most likely dispersal route. Dispersal may have been facilitated by the Mediterranean Tethyan Sill, a series of platforms emerging at low eustatic sea levels between Africa and western Eurasia. These platforms may have acted as stepping stones, breaking a long sea crossing into a series of short dispersals between islands.

Extant species of alligatoroid are restricted to freshwater habitats (Grigg and Kirshner, 2015). Lingual salt excreting glands and keratinised tongues are present in extant crocodylids and gavialoids, and aid long term exposure to saltwater. As a result, these lineages readily disperse across marine barriers. Crocodyloidea, for example, have dispersed from Africa to the New World (Meredith *et al.*, 2011; Oaks, 2011). The saltwater crocodile, *Crocodylus porosus,* is widely distributed along the coasts of Australia, Indonesia and Southeast Asia, and the American crocodile, *Crocodylus acutus*, is widespread in the Caribbean and along the coasts of North and South America (Grigg and Kirshner, 2015; IUCN, 2017). These adaptations to life in marine settings are not present in extant alligatorids and caimans (Taplin, Grigg and Beard, 1985).

Despite their general lack of specializations for saltwater-tolerance, there are rare instances of extant alligators and caimans inhabiting brackish or saline environments for short periods. For example, *Alligator mississippiensis* occurs in the Florida keys and *Caiman latirostris* has been observed in an estuary in Brazil with sources of freshwater close by (Grigg and Kirshner, 2015). There are also examples of oceanic dispersal across shorter distances, including between islands in archipelagos, such as *Caiman crocodilus* becoming established on Trinidad (Brochu, 1999).

Diplocynodontids lie outside crown group Alligatoridae (last common ancestor of *Alligator mississippiensis* and *Caiman crocodilus)* and therefore it is unknown if they were saltwater tolerant (Delfino, Böhme and Rook, 2007). The anatomical features associated with this tolerance involve soft tissue, and are therefore difficult to infer from fossil material

(Brochu, 1999). All previously described fossil *Diplocynodon* remains were found in lacustrine/freshwater deposits (Piras and Buscalioni, 2006; Martin, 2010; Martin and Gross, 2011; Díaz Aráez *et al.*, 2015), however, *D. africanum* is from a marine setting. Whether *D. africanum* inhabited a marine or freshwater environment is unclear. *D. africanum* is a rare component of the Moroccan fossil crocodylian fauna, especially when compared to the abundant dyrosaurids and gavialoids (Jouve *et al.*, 2006, 2014; Jouve, 2007; Jouve, Bouya and Amaghzaz, 2008). This may be consistent with the hypothesis that the remains were washed in from freshwater environments. Terrestrial mammal material is sometimes found in the marine horizons at these localities (Yans *et al.*, 2014), suggesting limited but important terrestrial input. Alternatively, *D. africanum* may have occupied brackish environments as sometimes seen in extant alligators, with access to freshwater (Grigg and Kirshner, 2015).

K-Pg:

The K-Pg mass extinction was a severe extinction event (Raup and Sepkoski, 1982) and saw high turnover in terrestrial ecosystems (Field *et al.*, no date; Feduccia, 1995; Alroy, 1999; Longrich, Tokaryk and Field, 2011; Grossnickle and Newham, 2016; Longrich, Scriberas and Wills, 2016; Feng *et al.*, 2017). However freshwater species, including crocodylians, appear to have been less affected (Archibald and Bryant, 1990; Sheehan and Fastovsky, 1992; Robertson *et al.*, 2013b). Whereas terrestrial and open-ocean food chains are highly dependent upon primary productivity, which was depressed following the Chicxulub asteroid impact (Alvarez *et al.*, 1980), freshwater food chains are dependent on dead plant and animal matter, which would have been abundant following the asteroid impact (Sheehan and Fastovsky, 1992). Furthermore, the impact would have resulted in dramatic temperature changes. The existence of a thermal pulse remains debated (Goldin and Melosh, 2009; Morgan, Artemieva and Goldin, 2013; Robertson *et al.*, 2013a; Brugger, Feulner and Petri, 2017) but evidence increasingly suggests that the aftermath of the impact was characterised by severe cooling (Vellekoop *et al.*, 2014; Kaiho *et al.*, 2016). In both cases, the high thermal inertia of water would have buffered freshwater ecosystems. Other factors may also have favoured the survival of crocodylians, including the ability to go for long periods with little or no food due to their low metabolic rates (Robertson *et al.*, 2004; Grigg and Kirshner, 2015), and a highly generalised feeding ecology that would have allowed them to exploit whatever resources were available (Busbey, 1994; Brochu, 2001; McHenry *et al.*, 2006).

As the largest-bodied carnivores surviving this extinction event, alligatoroids and marine crocodyliformes may have benefitted from the aftermath of the extinction by exploiting niches left vacant by the extinction of competitors and predators (Markwick, 1998; Mannion *et al.*, 2015; Puértolas-Pascual *et al.*, 2016). The time calibrated phylogeny (Figure 4.4) suggests a rapid diversification of alligatorines, caimanines, and diplocynodontids in the aftermath of the K-Pg extinction. This observation supports previous studies finding a shift in diversification rate for the Alligatoroidea after the K-Pg extinction (Bronzati, Montefeltro and Langer, 2015). The time tree suggests that this pattern results from a few survivors crossing the boundary, followed by a rapid diversification. Similar rapid post-K–Pg radiations have been reported in numerous vertebrate taxa, including birds (Jarvis *et al.*, 2014; Prum *et al.*, 2015; Berv and Field, 2017), frogs (Feng *et al.*, 2017), snakes (Klein et al. in prep.) and marine actinopterygians (Alfaro *et al.*, 2018).

The diversification following the K-Pg is coupled with a biogeographic dispersal. As exemplified by the ancestral state reconstruction (Figure 4.4) and paleogeographic maps (Figure 4.5), Cretaceous Alligatoroidea are restricted to North America. After the K-Pg event,

alligatoroids appear in the Paleocene of South America, Asia, Europe, Africa and North America. The most likely dispersal routes into Europe may have been the high latitude Thulian, De Geer, and Beringia routes, which connected North America with western and eastern Eurasia in the early Paleogene (Brikiatis, 2014). However, as these land bridges are at high latitudes, and alligatoroids are ectothermic, global temperatures likely restricted when these crossings were possible. Such a route could potentially involve a land bridge, with alligatoroids likely constrained to dispersing via rivers, lakes and swamps and short overland or sea crossings. The early Paleogene Arctic Ocean had relatively low salinity, with episodic surface water freshening (Brinkhuis *et al.*, 2006), which might have facilitated dispersal via sea crossings. By the Early Eocene, conditions were also warm enough for alligatoroids to inhabit the Arctic (Estes and Howard Hutchison, 1980). Due to the uncertain phylogenetic position of the Asian taxa, these were not included in the biogeographic analysis. However, the stratigraphic position of *Protolligator huiningensis* in the mid-Paleocene suggests that this species might also have dispersed close to the K-Pg boundary (Wang, Sullivan and Liu, 2016). Dispersal out of North America into Asia likely took place through Beringia or the Thulian route (Martin and Lauprasert, 2010).

We propose that early Paleogene dispersal may be driven by the same processes as diversification, namely the extinction of competitors and predators at the K-Pg boundary. The K-Pg extinction would not have affected the ability of alligatoroids to cross geographic barriers. However, successful dispersal would have been made more likely by the removal of these biotic barriers (Longrich *et al.*, 2015). Alligatoroidea may serve as a model for understanding how mass extinction has helped shape modern biogeographic patterns. Following the discovery of plate tectonics, discussions of biogeography have tended to emphasise the role of Mesozoic continental fragmentation and vicariance in driving biogeographic patterns (Cracraft, 1982). Yet groups originating and diversifying in the wake of the K-Pg extinction must have become widespread long after the breakup of the continents (Field and Hsiang, no date; Tarver *et al.*, 2016; Feng *et al.*, 2017; Kieren *et al.*, 2018)((Klein et.al., in prep). In these cases, modern biogeographic distributions may owe less to continental drift than to mass extinction.

Rather than being a phenomenon peculiar to the Alligatoroidea, these patterns may have characterised many groups of terrestrial vertebrates. Similar patterns are seen in amphisbaenians, which undertook several dispersal events in the early Paleocene (Longrich et al. 2015), and frogs which saw rapid diversification and dispersal of Natatanura and Microhylidae (Feng *et al.*, 2017). Other examples include the invasion of North America by Asian choristoderes (Gao and Fox, 1998) and cryptobranchid salamanders (Naylor, 1981), and the dispersal of Afrophidia into Asia (Klein et al., in prep.). Dispersal is also common in early Paleogene mammals. The early Paleocene of North America saw repeated invasions of mammals from Asia (Longrich, Scriberas and Wills, 2016) , while South America saw invasions of ungulates and marsupials (Muizon and Cifellii, 2000) from North America. Marsupials subsequently appeared in the early Eocene of Australia (Beck *et al.*, 2008), representing a dispersal from South America (Nilsson *et al.*, 2010). Dispersal between Laurasian continents was probably via high-latitude land bridges, but Africa, South America, and Australia were physically isolated by ocean barriers, suggesting trans-oceanic dispersal.

The results presented here, challenge ideas about alligatoroid biogeography. Diplocynodontidae were previously thought to be an exclusively European clade (Martin, 2010; Martin *et al.*, 2014). Reports of *Diplocynodon* in the Cretaceous and Paleocene of North America have since been referred to *Borealosuchus,* an early diverging clade within the

Crocodylia (Brochu, 1997; Brochu *et al.*, 2012; Delfino and Smith, 2012). Until recently, Diplocynodontidae were thought to diversify around the PETM, based on the stratigraphic occurrence of *D. darwini* and *D. deponiae*, from the mid-Eocene of Germany (Brochu, 1999; Delfino and Smith, 2012). Similar dispersals of non-marine groups including mammals, lizards and birds are observed at this time (Martin *et al.*, 2014). The new fossil material described here, indicate that Diplocynodontidae are not endemic to Europe and dispersed into Africa in the Early Paleocene. The highly nested position of *D. africanum*, in the Diplocynodontidae suggests a substantial missing fossil record for the Diplocynodontidae in the Paleocene (Figure 4.4). As a result, we find evidence for a major diversification for all alligatoroid groups in the wake of the K-Pg mass extinction.

Acknowledgements:

Thanks to M. Meharich for assistance in Oulad Bou Ali and to N.E. Jalil for assistance with accessioning specimens. Thanks also to Charlie Underwood, David Ward and Emmanuel Gheerbrandt for discussions. Comments and suggestions for improvements provided by Daniel J. Field and Catherine Klein were greatly appreciated.

References:

Aberer, A.J., Krompass, D. & Stamatakis, A., Pruning Rogue Taxa Improves Phylogenetic Accuracy: An Efficient Algorithm and Webservice. *Systematic Biology*.

Alfaro, M.E. et al., 2018. Explosive diversification of marine fishes at the Cretaceous–Palaeogene boundary. *Nature Ecology and Evolution*, 2, pp.688–696.

Alroy, J., 1999. The fossil record of North American mammals : evidence for a Paleocene evolutionary radiation. *Systematic Biology*, 48(1), pp.107–118.

Alvarez, L.W. et al., 1980. Extraterrestrial Cause for the Cretaceous-Tertiary Extinction. *Science*, 208, pp.1095–1108.

Arambourg, C., 1952. Les vertébrés fossiles des gisements de phosphates (Maroc-Algérie-Tunisie). *Service Géologique Maroc, Notes et Mémoires*, 92, pp.1–372.

Archibald, J.D. & Bryant, L.J., 1990. Differential Cretaceous/Tertiary extinctions of nonmarine vertebrates; evidence from northeastern Montana. *Geological Society of America Special Papers*, 247, pp.549–562.

Bapst, D.W., 2012. paleotree: an R package for paleontological and phylogenetic analyses of evolution. *Methods in Ecology and Evolution*, 3, pp.803–807.

Bardet, N. et al., 2013. A giant chelonioid turtle from the Late Cretaceous of Morocco with a suction feeding apparatus unique among tetrapods. *PLoS ONE*, 8(7), pp.1–10.

Bardet, N. et al., 2010. Reptilian assemblages from the latest Cretaceous – Palaeogene phosphates of Morocco: from Arambourg to present time. *Historical Biology*, 22(1–3), pp.186–199.

Beck, R.M.D. et al., 2008. Australia's oldest marsupial fossils and their biogeographical implications. *PLoS ONE*, 3(3).

Bell, M.A. & Lloyd, G.T., 2014. strap: stratigraphic tree analysis for palaeontology. , pp.1–17. Available at: https://cran.r-project.org/package=strap.

Berv, J.S. & Field, D.J., 2017. Genomic Signature of an Avian Lilliput Effect across the K-Pg Extinction. *Systematic Biology*, 67(1), pp.1–13.

Brikiatis, L., 2014. The de geer, thulean and beringia routes: Key concepts for understanding early cenozoic biogeography. *Journal of Biogeography*, 41(6), pp.1036–1054.

Brinkhuis, H. et al., 2006. Episodic fresh surface waters in the Eocene Arctic Ocean. *Nature*,

441(7093), pp.606–609.
Brochu, C.A., 2010. A new alligatorid from the lower Eocene Green River Formation of Wyoming and the origin of caimans. *Journal of Vertebrate Paleontology*, 30(4), pp.1109–1126.
Brochu, C.A. et al., 2012. A new species of *Borealosuchus* (Crocodyliformes, Eusuchia) from the Late Cretaceous–early Paleogene of New Jersey. *Journal of Vertebrate Paleontology*, 32(1), pp.105–116.
Brochu, C.A., 1997. A review of "*Leidyosuchus*" (Crocodyliformes, Eusuchia) from the Cretaceous through Eocene of North America. *Journal of Vertebrate Paleontology*, 17(4), pp.679–697.
Brochu, C.A., 2001. Crocodylian snouts in space and time: phylogenetic approaches toward adaptive radiation. *American Zoologist*, 41(3), pp.564–585.
Brochu, C.A., 1999. Phylogenetics, taxonomy, and historical biogeography of Alligatoroidea. *Journal of Vertebrate Paleontology*, 19(January), pp.9–100.
Bronzati, M., Montefeltro, F.C. & Langer, M.C., 2015. Diversification events and the effects of mass extinctions on Crocodyliformes evolutionary history. *Royal Society Open Science*, 2, pp.1–9.
Brugger, J., Feulner, G. & Petri, S., 2017. Baby, it's cold outside: Climate model simulations of the effects of the asteroid impact at the end of the Cretaceous. *Geophysical Research Letters*, 44(1), pp.419–427.
Buffetaut, E., 1985. Zoogeographical history of African crocodilians since the Triassic. In *Proceedings of the International Symposium on African Vertebrates: Systematics, Phylogeny and Evolutionary Ecology*. pp. 453–469.
Busbey, A.B., 1994. The structural consequences of skull flattening in crocodilians. In J. J. Thomason, ed. *Functional Morphology in Vertebrate Paleontology*. Cambridge University Press, New York, pp. 173–192.
Buscalioni, A.D., Sanz, J.L. & Casanovas, M.L., 1992. A new species of the eusuchian crocodile *Diplocynodon* from the Eocene of Spain. *Neues Jahrbuch für Geologie und Paläontologie Abhandlungen*, 187, pp.1–29.
Cappetta, H. et al., 2014. Marine vertebrate faunas from the Maastrichtian phosphates of Benguerir (Ganntour Basin, Morocco): Biostratigraphy, palaeobiogeography and palaeoecology. *Palaeogeography, Palaeoclimatology, Palaeoecology*, 409, pp.217–238.
Cavin, L. et al., 2000. A new Palaeocene albulid (Teleostei: Elopomorpha) from the Ouled Abdoun phosphatic basin, Morocco. *Geological Magazine*, 137(5), pp.583–591.
Cracraft, J., 1982. Geographic differentiation, cladistics , and vicariance biogeography : Reconstructing the tempo and mode of evolution. *American Zoologist*, 22(2), pp.411–424.
D'Erasmo, G., 1934. Su alcuni avanzi di vertebrati terziari della Sirtica. *Missione Scientifica della reale accademia Italiana a Cufra (1931-IX), 3 (studi paleontologici e litologici sulla Cirenaica e sulla Tripolitania orientale)*, pp.257–279.
Delfino, M. et al., 2017. Evidence for a pre-PETM dispersal of the earliest European crocodyloids. *Historical Biology*, 2963(December), pp.1–8.
Delfino, M., Böhme, M. & Rook, L., 2007. First European evidence for transcontinental dispersal of *Crocodylus* (late Neogene of southern Italy). *Zoological Journal of the Linnean Society*, 149(3), pp.293–307.
Delfino, M. & Smith, T., 2012. Reappraisal of the morphology and phylogenetic relationships of the middle Eocene alligatoroid *Diplocynodon deponiae* (Frey, Laemmert, and Riess, 1987) based on a three-dimensional specimen. *Journal of Vertebrate Paleontology*, 32(6), pp.1358–1369.
Díaz Aráez, J.L. et al., 2015. New remains of *Diplocynodon* (Crocodylia: Diplocynodontidae) from the Early Miocene of the Iberian Peninsula. *Comptes Rendus - Palevol*, 16(1), pp.12–26.

Estes, R. & Howard Hutchison, J., 1980. Eocene lower vertebrates from Ellesmere Island, Canadian Arctic Archipelago. *Palaeogeography, Palaeoclimatology, Palaeoecology*, 30, pp.325–347.
Farke, A.A. et al., 2014. *Leidyosuchus* (Crocodylia: Alligatoroidea) from the Upper Cretaceous Kaiparowits Formation (late Campanian) of Utah, USA. *PaleoBios*, 30(3), pp.72–88.
Feduccia, A., 1995. Explosive evolution in tertiary birds and mammals. *Science*, 267(5198), pp.637–638.
Feng, Y.-J. et al., 2017. Phylogenomics reveals rapid, simultaneous diversification of three major clades of Gondwanan frogs at the Cretaceous–Paleogene boundary. *Proceedings of the National Academy of Sciences*, 114(29), pp.E5864–E5870.
Field, D.J. et al., Early evolution of modern birds structured by global forest collapse at the end-Cretaceous mass extinction. *Current Biology*.
Field, D.J. & Hsiang, A.Y., A North American stem turaco, and the complex biogeographic history of modern birds. *BMC evolutionary biology*.
Gao, K. & Fox, R.C., 1998. New choristoderes (Reptilia: Diapsida) from the upper Cretaceous and Palaeocene, Alberta and Saskatchewan, Canada, and phylogenetic relationships of Choristodera. *Zoological Journal of the Linnean Society*, 124(4), pp.303–353.
Gheerbrant, E., 1990. On the early biogeographical history of the African placentals. *Historical Biology*, 4(2), pp.107–116.
Gheerbrant, E., 2009. Paleocene emergence of elephant relatives and the rapid radiation of African ungulates. *Proceedings of the National Academy of Sciences*, 106(26), pp.10717–10721.
Gheerbrant, E. et al., 2003. The mammal localities of Grand Daoui Quarries, Ouled Abdoun Basin, Morocco, Ypresian: a first survey. *Bulletin De La Societe Geologique De France*, 174(3), pp.279–293.
Gheerbrant, E. & Rage, J.-C., 2006. Paleobiogeography of Africa: How distinct from Gondwana and Laurasia? *Palaeogeography, Palaeoclimatology, Palaeoecology*, 241(2), pp.224–246.
Goldin, T.J. & Melosh, H.J., 2009. Self-shielding of thermal radiation by Chicxulub impact ejecta: Firestorm or fizzle? *Geology*, 37(12), pp.1135–1138.
Goloboff, P.A., Farris, J. & Nixon, K., 2003. T.N.T.: Tree Analysis Using New Technology.
Grigg, G.C. & Kirshner, D., 2015. *Biology and evolution of crocodylians*, Csiro Publishing.
Grossnickle, D.M. & Newham, E., 2016. Therian mammals experience an ecomorphological radiation during the Late Cretaceous and selective extinction at the K–Pg boundary. *Proceedings of the Royal Society B: Biological Sciences*, 283(1832), p.20160256.
Hastings, A.K. & Hellmund, M., 2015. Rare in situ preservation of adult crocodylian with eggs from the Middle Eocene of Geiseltal, Germany. *Palaios*, 30(6), pp.446–461.
Hastings, A.K., Reisser, M. & Scheyer, T.M., 2016. Character evolution and the origin of Caimaninae (Crocodylia) in the New World Tropics: New evidence from the Miocene of Panama and Venezuela. *Journal of Paleontology*, 90(2), pp.317–332.
Iijima, M., Takahashi, K. & Kobayashi, Y., 2016. The oldest record of *Alligator sinensis* from the Late Pliocene of Western Japan, and its biogeographic implication. *Journal of Asian Earth Sciences*, 124, pp.94–101.
IUCN, 2017. The IUCN Red List of Threatened Species. Version 2017-3. Available at: http://www.iucnredlist.org [Accessed December 5, 2017].
Jarvis, E.D. et al., 2014. Whole-genome analyses resolve early branches in the tree of life of modern birds. *Science*, 346(6215), pp.1320–1331.
Jouve, S. et al., 2014. *Maroccosuchus zennaroi* (Crocodylia: Tomistominae) from the Eocene of Morocco: phylogenetic and palaeobiogeographical implications of the basalmost tomistomine. *Journal of Systematic Palaeontology*, 13, pp.1–25.
Jouve, S. et al., 2006. New material of *Argochampsa krebsi* (Crocodylia: Gavialoidea) from the Lower Paleocene of the Oulad Abdoun Basin (Morocco): phylogenetic implications. *Geobios*, 39(6), pp.817–832.

Jouve, S., 2007. Taxonomic revision of the dyrosaurid assemblage (Crocodyliformes: Mesoeucrocodylia) from the Paleocene of the Iullemmeden Basin, West Africa. *Journal of Paleontology*, 81(1), pp.163–175.

Jouve, S., Bardet, N. & Jalil, N.-E., 2008. The oldest African crocodylian: phylogeny, paleobiogeography, and differential survivorship of marine reptiles through the Cretaceous-Tertiary boundary. *Journal of Vertebrate Paleontology*, 28, pp.37–41.

Jouve, S., Bouya, B. & Amaghzaz, M., 2008. A long-snouted dyrosaurid (Crocodyliformes, Mesoeucrocodylia) from the Paleocene of Morocco: phylogenetic and palaeobiogeographic implications. *Palaeontology*, 51(2), pp.281–294.

Kaiho, K. et al., 2016. Global climate change driven by soot at the K-Pg boundary as the cause of the mass extinction. *Scientific Reports*, 6(1), p.28427.

Kälin, J.A., 1939. Ein extrem kurzschnauziger Crocodilide aus den Phosphoriten des Quercy Arambourgia (nov. gen.) gaudryi de Stefano. *Abhandlungen der Schweizerischen Palaeontologischen Gesell- schaft*, 62, pp.1–18.

Kieren, S. et al., 2018. A biogeographic and ecological perspective to the evolution of reproductive behaviour in the family Salamandridae. *Molecular Phylogenetics and Evolution*, 121(January), pp.98–109.

Kobayashi, Y. et al., 2006. Anatomy of a Japanese tomistomine crocodylian, *Toyotamaphimeia machikanensis* (Kamei et Matsumoto, 1965), from the middle Pleistocene of Osaka Prefecture: the reassessment of its phylogenetic status within Crocodylia. *National Science Museum Monographs*.

Kocsis, L. et al., 2014. Comprehensive stable isotope investigation of marine biogenic apatite from the late Cretaceous-early Eocene phosphate series of Morocco. *Palaeogeography, Palaeoclimatology, Palaeoecology*, 394, pp.74–88.

Longrich, N.R. et al., 2017. An abelisaurid from the latest Cretaceous (late Maastrichtian) of Morocco, North Africa. *Cretaceous Research*, 76, pp.40–52.

Longrich, N.R. et al., 2015. Biogeography of worm lizards (Amphisbaenia) driven by end-Cretaceous mass extinction. *Proceedings of the Royal Society of London B: Biological Sciences*, 282(1806), p.20143034.

Longrich, N.R. & Field, D.J., An *Ichthyornis*-like bird from the late Maastrichtian of North Africa. Cretaceous Research. *Cretaceous Research*.

Longrich, N.R., Scriberas, J. & Wills, M.A., 2016. Severe extinction and rapid recovery of mammals across the Cretaceous-Palaeogene boundary, and the effects of rarity on patterns of extinction and recovery. *Journal of evolutionary biology*, 29(8), pp.1495–1512.

Longrich, N.R., Tokaryk, T. & Field, D.J., 2011. Mass extinction of birds at the Cretaceous-Paleogene (K-Pg) boundary. *Proceedings of the National Academy of Sciences*, 108(37), pp.15253–15257.

Mannion, P.D. et al., 2015. Climate constrains the evolutionary history and biodiversity of crocodylians. *Nature communications*, 6, pp.1–9.

Markwick, P.J., 1998. Crocodilian diversity in space and time: the role of climate in paleoecology and its implication for understanding K/T extinctions. *Paleobiology*, 24(4), pp.470–497.

Martin, J.E., 2010. A new species of *Diplocynodon* (Crocodylia, Alligatoroidea) from the Late Eocene of the Massif Central, France, and the evolution of the genus in the climatic context of the Late Palaeogene. *Geological Magazine*, 147(04), pp.596–610.

Martin, J.E. et al., 2014. Late Palaeocene eusuchian remains from Mont de Berru, France, and the origin of the alligatoroid *Diplocynodon*. *Zoological Journal of the Linnean Society*, 172(4), pp.867–891.

Martin, J.E. & Gross, M., 2011. Taxonomic clarification of *Diplocynodon* Pomel, 1847 (Crocodilia) from the Miocene of Styria, Austria. *Neues Jahrbuch für Geologie und Paläontologie - Abhandlungen*, 261(2), pp.177–193.

Martin, J.E. & Lauprasert, K., 2010. A new primitive alligatorine from the Eocene of Thailand:

Relevance of Asiatic members to the radiation of the group. *Zoological Journal of the Linnean Society*, 158(3), pp.608–628.
McHenry, C.R. et al., 2006. Biomechanics of the rostrum in crocodilians: a comparative analysis using finite-element modeling. *The anatomical record. Part A, Discoveries in molecular, cellular, and evolutionary biology*, 288(May), pp.827–849.
Meredith, R.W. et al., 2011. A phylogenetic hypothesis for *Crocodylus* (Crocodylia) based on mitochondrial DNA: evidence for a trans-Atlantic voyage from Africa to the New World. *Molecular Phylogenetics and Evolution*, 60(1), pp.183–191.
Morgan, J., Artemieva, N. & Goldin, T., 2013. Revisiting wildfires at the K-Pg boundary. *Journal of Geophysical Research: Biogeosciences*, 118(4), pp.1508–1520.
Muizon, C. De & Cifellii, R.L., 2000. The "condylarths" (archaic Ungulata, Mammalia) from the early Palaeocene of Tiupampa (Bolivia): implications on the origin of the South American ungulates. *Geodiversitas*, 22(1), pp.47–150.
Naylor, B.G., 1981. Cryptobranchid Salamanders from the Paleocene and Miocene of Saskatchewan. *Copeia*, 1981(1), pp.76–86.
Nilsson, M.A. et al., 2010. Tracking marsupial evolution using archaic genomic retroposon insertions. *PLoS Biology*, 8(7).
Noubhani, A., 2010. The selachians' faunas of the Moroccan phosphate deposits and the KT mass-extinctions. *Historical Biology*, 22(1–3), pp.71–77.
Oaks, J.R., 2011. A time-calibrated species tree of Crocodylia reveals a Recent radiation of the true crocodiles. *Evolution*, 65, pp.3285–3297.
Piras, P. & Buscalioni, A.D., 2006. *Diplocynodon muelleri* Comb. nov., an Oligocene diplocynodontine alligatoroid from Catalonia (Ebro Basin, Lleida Province, Spain). *Journal of Vertebrate Paleontology*, 26(3), pp.608–620.
Prum, R.O. et al., 2015. A comprehensive phylogeny of birds (Aves) using targeted next-generation DNA sequencing. *Nature*, 526(7574), pp.569–573.
Puértolas-Pascual, E. et al., 2016. Review of the Late Cretaceous-early Paleogene crocodylomorphs of Europe: Extinction patterns across the K-PG boundary. *Cretaceous Research*, 57, pp.565–590.
R Core Team, 2013. R: a language and environment for statistical computing. Available at: http://www.r-project.org/.
Raup, D.M. & Sepkoski, J.J., 1982. Mass extinctions in the marine fossil record. *Science*, 215(4539), pp.1501–1503.
Revell, L.J., 2012. phytools: An R package for phylogenetic comparative biology (and other things). *Methods in Ecology and Evolution*, 3, pp.217–223.
Robertson, D.S. et al., 2013a. K-Pg extinction: Reevaluation of the heat-fire hypothesis. *Journal of Geophysical Research: Biogeosciences*, 118(1), pp.329–336.
Robertson, D.S. et al., 2013b. K-Pg extinction patterns in marine and freshwater environments: The impact winter model. *Journal of Geophysical Research: Biogeosciences*, 118(3), pp.1006–1014.
Robertson, D.S. et al., 2004. Survival in the first hours of the Cenozoic. *Bulletin of the Geological Society of America*, 116(5–6), pp.760–768.
Rossmann, T., Muller, J. & Forst, M., 2000. Studies on Cenozoic crocodilians: 7. First evidence of an alligatorid from Africa and its implications for crocodilian palaeobiogeography. *Neues Jahrbuch fur Geologie und Palaontologie-Monatshefte*, (12), pp.705–714.
Sara Varela & Sonja Rothkugel, 2016. paleoMap: combine paleogeography and paleobiodiversity.
Shan, H. et al., 2009. A new tomistomine (Crocodylia) from the Miocene of Taiwan. *Canadian Journal of Earth Sciences*, 46(7), pp.529–555.
Sheehan, P.M. & Fastovsky, D.E., 1992. Major extinctions of land-dwelling vertebrates at the Cretaceous-Tertiary boundary, eastern Montana. *Geology*, 20, pp.556–560.
Sullivan, R.M. & Lucas, S.G., 2003. *Brachychampsa montana* Gilmore (Crocodylia Alligatoridae)

from the Kirtland Formation (Upper Campanian) San Juan Basin New Mexico. *Journal of Vertebrate Paleontology*, 23(December), pp.832–841.

Taplin, L.E., Grigg, G.C. & Beard, L., 1985. Salt gland function in fresh water Crocodiles: evidence for a marine phase in eusuchian evolution? In G. Grigg, R. Shine, & H. Ehmann, eds. *Biology of Australasian frogs and reptiles*. Royal Zoological Society of New South Wales, pp. 402–410.

Tarver, J.E. et al., 2016. The interrelationships of placental mammals and the limits of phylogenetic inference. *Genome Biology and Evolution*, 8(2), pp.330–344.

Vellekoop, J. et al., 2014. Rapid short-term cooling following the Chicxulub impact at the Cretaceous-Paleogene boundary. *Proceedings of the National Academy of Sciences*, 111(21), pp.7537–7541.

Vincent, P. et al., 2013. New plesiosaur specimens from the Maastrichtian Phosphates of Morocco and their implications for the ecology of the latest Cretaceous marine apex predators. *Gondwana Research*, 24(2), pp.796–805.

Wang, Y., Sullivan, C. & Liu, J., 2016. Taxonomic revision of *Eoalligator* (Crocodylia, Brevirostres) and the paleogeographic origins of the Chinese alligatoroids. *PeerJ*, 4, p.e2356.

Wassersug, R.J. & Hecht, M.K., 1967. The status of the crocodylid genera *Procaimanoidea* and *Hassiacosuchus* in the New World. *Herpetologica*, 23(1), pp.30–34.

Wu, X.B. et al., 2006. Regression analysis between body and head measurements of Chinese alligators (*Alligator sinensis*) in the captive population. *Animal Biodiversity and Conservation*, 29(1), pp.65–71.

Yans, J. et al., 2014. First carbon isotope chemostratigraphy of the Ouled Abdoun phosphate Basin, Morocco; implications for dating and evolution of earliest African placental mammals. *Gondwana Research*, 25, pp.257–269.

4.3 Post-paper commentary:

4.3.1 Supplementary material for the paper:

Provenance:

As with other fossils described from the Oulad Abdoun Basin, the fossils described here were collected by locals from the phosphate mines, and so precise provenance data are not available. However, discussions with local collectors, examination of the preservation of the fossil and associated matrix, and associated fossils make it possible to confidently constrain these fossils to the early Paleogene (Danian-Ypresian) phosphate beds of the Oulad Abdoun Basin.

Up to five beds or "Couches" are recognized in the phosphates; from top to bottom these are Couches 0-IV. Couche 0 and I are early Eocene (Ypresian) in age (Kocsis *et al.*, 2014; Yans *et al.*, 2014). Couche II is Paleocene in age, and is broken into two beds, Couche IIA and Couche IIB. Couche III is assigned to the Late Maastrichtian (Michard *et al.*, 2008; Yans *et al.*, 2014).

The matrix of Couche III is distinctive in containing numerous sand-sized grains of bone. Couche II and Couche I are both characterized by a matrix comprised primarily of small pelletal phosphate and abundant coprolitic pellets. The matrix of the fossils described here matches the matrix of either Couche II or I. The fossils differ in their preservation, indicating that they come from different localities and/or horizons.

Holotype. The holotype, MHNM.KHG.178, is reported as coming from Couche II, which is Paleocene in age, in Sidi Daoui. Preservation of the fossil and matrix are consistent with this assignment. Other fossils coming from the same horizon in the same quarry include a mammal, referable to *Ocepeia* sp. *Ocepeia* is known exclusively from the Paleocene (Couche II) of the Oulad Abdoun Basin, supporting a Paleocene age of the type.

Paratype. Ypresian (pending additional information)

Referred. The referred specimens, MHNM.KHG.167 and MHNM.KHG.168, are reported as coming from Sidi Chennane. The matrix surrounding these specimens was screened for shark/ray teeth to determine the age of the fossil based on selachian biozonation (Lucas and Prevot-Lucas, 1996; Noubhani, 2010). The following species were identified (Charlie Underwood, pers. comm.), *Striatolamia striata, Abdounia beaugei, Physogaleus secondus.* This suggests a likely Ypresian age, as these species are very common in the Ypresian, but they also known in the Upper Paleocene. With limited material a more precise determination was not possible.

Conclusions. All available information, including information obtained from local collectors, associated matrix, associated shark and mammal fossils, are consistent with the fossils coming from the Upper Paleocene-Ypresian of the phosphates.

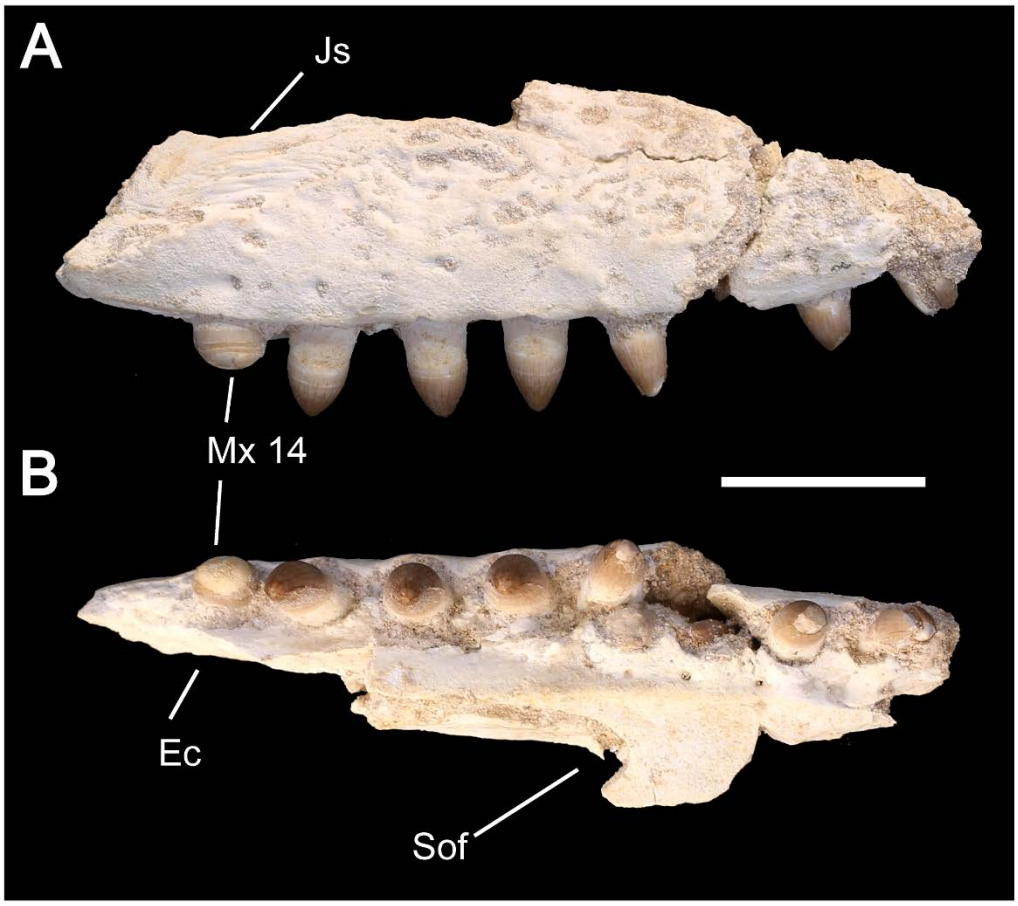

Figure 4.6: *Diplocynodon africanum* sp. nov., MHNM.KHG.167 from Paleocene/Ypresian of Morocco. Posterior fragment of the right maxilla. (A) maxilla in lateral view, (B) maxilla in ventral view. Scale = 2cm. **Abbreviations: Ec,** ectopterygoid suture surface on the maxilla, **Js,** suture surface for the jugal on the maxillary surface, **Mx 14,** maxillary tooth 14 (final maxillary tooth), **Sof,** anterior border of the suborbital fenestra.

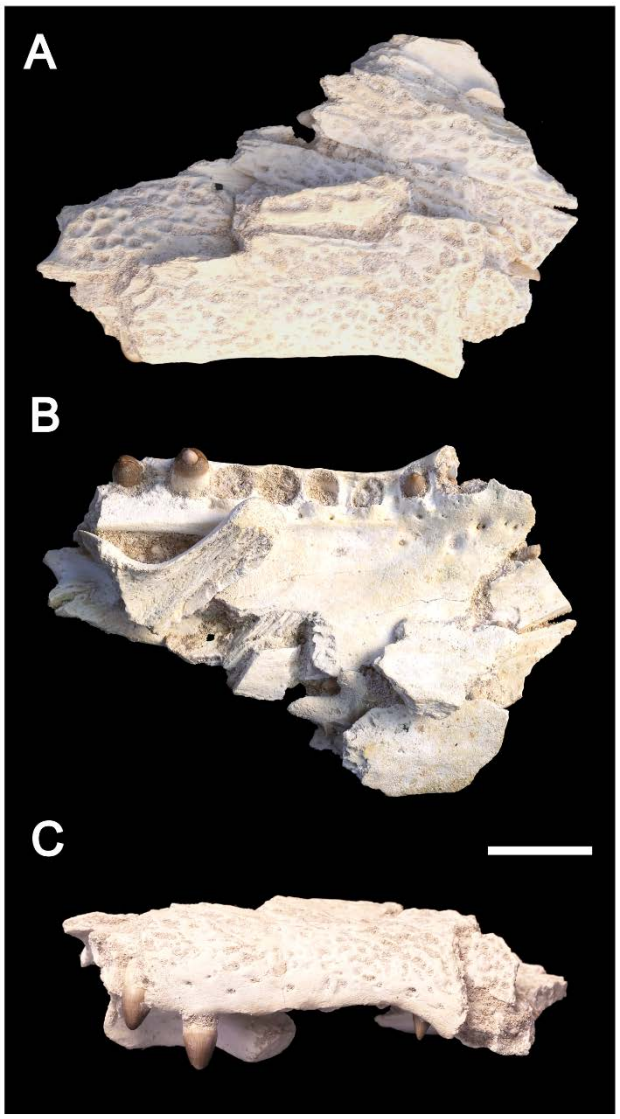

Figure 4.7: *Diplocynodon africanum* sp. nov., MHNM.KHG.168 from Paleocene/Ypresian of Morocco. Preserved portion of the rostrum between the fifth maxillary alveolus and the anterior border of the orbit. Scale= 2cm. (A) dorsal view, (B) ventral view, (C) right lateral view.

Phylogenetic analysis:

The character matrix used in this paper (Appendix 3) represents one of the most up-to-date matrices including the majority of known alligatoroid species. The matrix, sourced from Farke et al. (2014), is a modified version of the matrix used in Brochu et al. (2012). In our analysis we modified the codings for *Diplocynodon ungeri* and *D. elavericus* to those used in the more recent analysis by Martin et al. (2014). For *D. ungeri* modifications made in Martin et al. (2014) include character 114-1 and character 117-0, and *D. elavericus* character 112-0, 114-1, 116-0 and 118-1. *Diplocynodon remensis* was also added from Martin et al. (2014), and we modified character 72-1 and 148-1. We also updates character 82 for *D. ratelli* based on new fossil material (Díaz Aráez *et al.*, 2015).

Allognathosuchus is typically found in North America and is classed as a member of the Alligatorinae. There have been reports of European species, *A. woutersi* (Buffetaut, 1985a), *A. weigeti* and *A. brevirostris,* from the Eocene of Europe in Germany and Belgium (Brochu, 2004b). However, due to the fragmentary nature of the material it is uncertain if they represent distinct species or if they are synonymous with *Diplocynodon* or *Hassiacosuchus* (which are also European taxa) (Brochu, 2004b). Due to uncertainty in their taxonomic assignment, they have not been included in the phylogeny and biogeographic analysis. *Necrosuchus ionensis* (Brochu, 2011) was added to the matrix as it represents one of the earliest members of the Caimaninae. However, in preliminary analyses, the high percentage of missing data for this taxon greatly reduced resolution in the tree. It has been recognised as a wildcard taxon by previous researchers (Hastings *et al.*, 2013; Scheyer *et al.*, 2013; Hastings, Reisser and Scheyer, 2016). We therefore removed this taxon from the matrix.

Four additional characters were added from Jouve et al. (2014):

(180) Character 169: Less than 18 teeth (0), 18 to 22 teeth (1), or more than 22 teeth (2) on maxilla. [Jouve et al. 2008 (169), modified from Jouve 2004 (169)].

(181) Character 171: Frontal ends posterior (0) at the same level (1), or extends well anterior (2) to the anterior extension of the prefrontal. [Modified from Jouve et al. 2008 (171), and Jouve 2004 (172)].

(182) Character 201: Lateral posterior tuberosity of supraoccipital not visible (0), or visible in dorsal view (1). [Jouve 2004 (193)].

(183) Character 223: Anterior tip of frontal forms simple acute point (0) or forms broad, complex sutural contact with the nasals (1). [Brochu et al. 2011 (131)].

The initial heuristic search is presented in Figure 2.8, showing the strict consensus topology. The resolution is poor, with no distinction between Crocodyloidea and Alligatoroidea. Following the identification of rogue taxa, we reran the analysis. The strict consensus topology in presented in Figure 2.9, with Bremer decay values. This is the topology time calibrated for the ancestral state reconstruction (Figure 4.4, 4.10). Complete character matrix and character list are in Appendix 3.

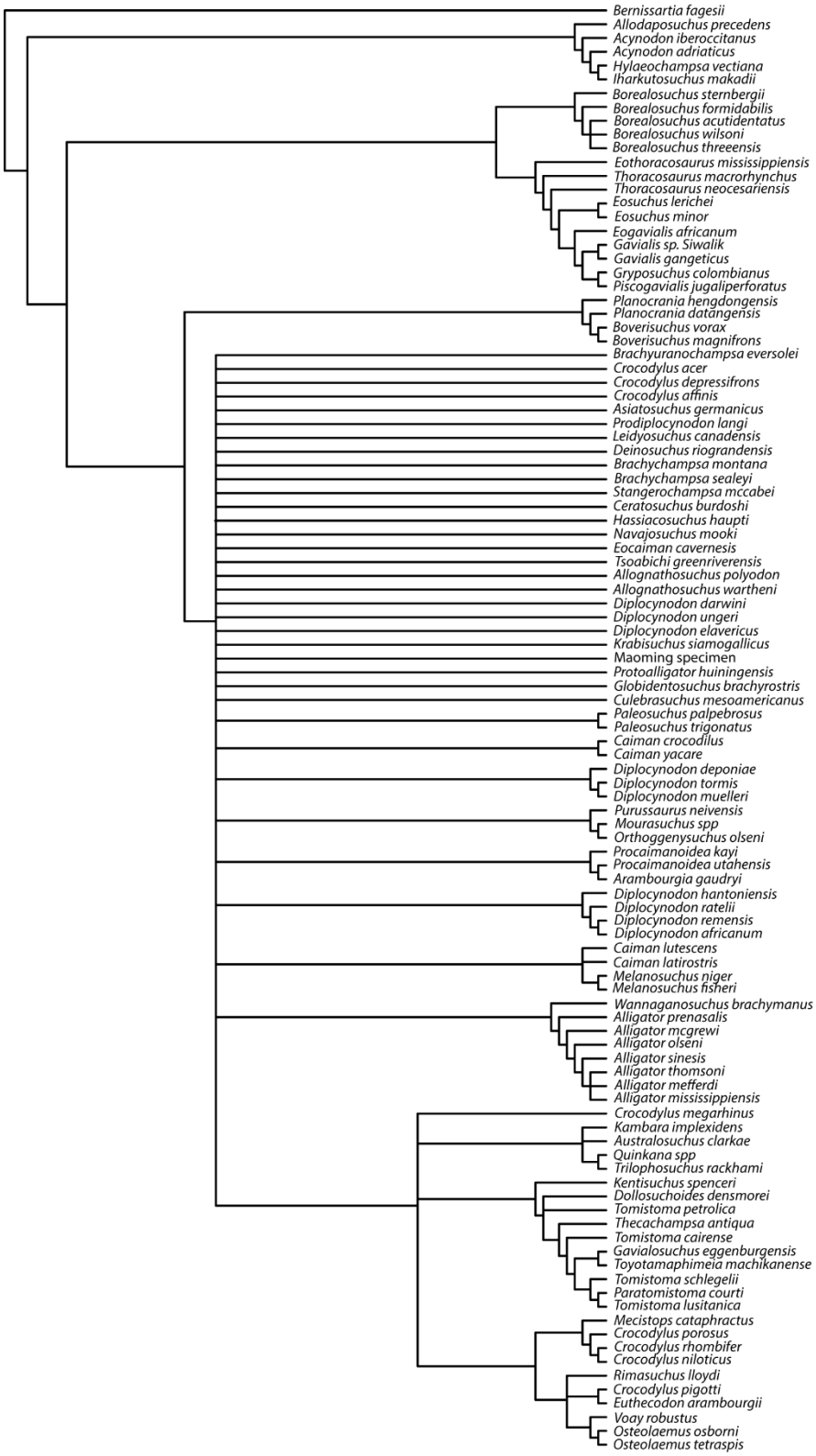

Figure 4.8: Strict consensus topology from preliminary analysis of the character matrix prior to the removal of rogue taxa (trees: 11,000 steps: 768, CI: 0.307, RI: 0.786).

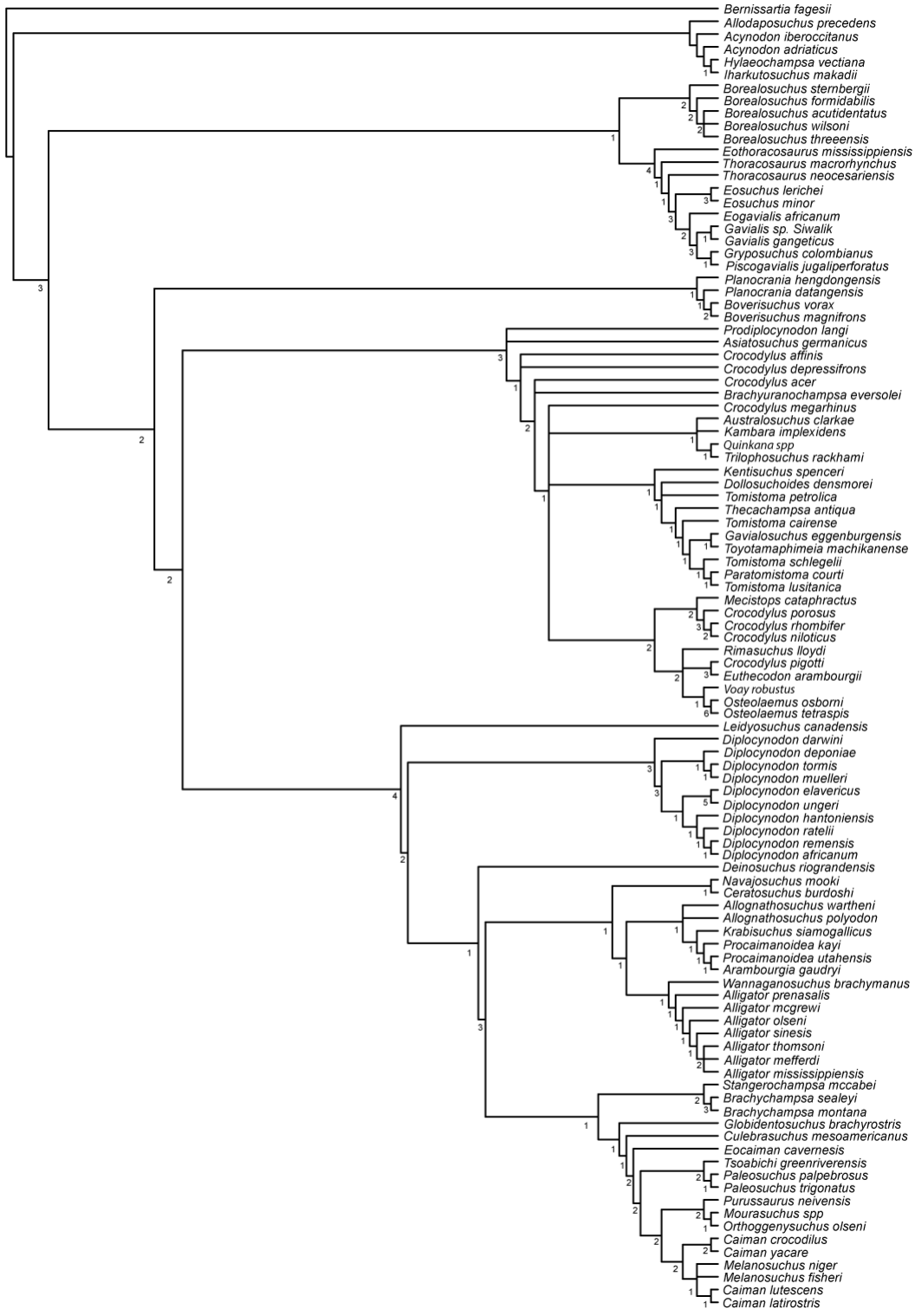

Figure 4.9: Strict consensus topology after removal of rogue taxa, result of 32 most parsimonious trees of 759 steps (CI: 0.31, RI: 0.788). Bremer decay values are indicated at each node.

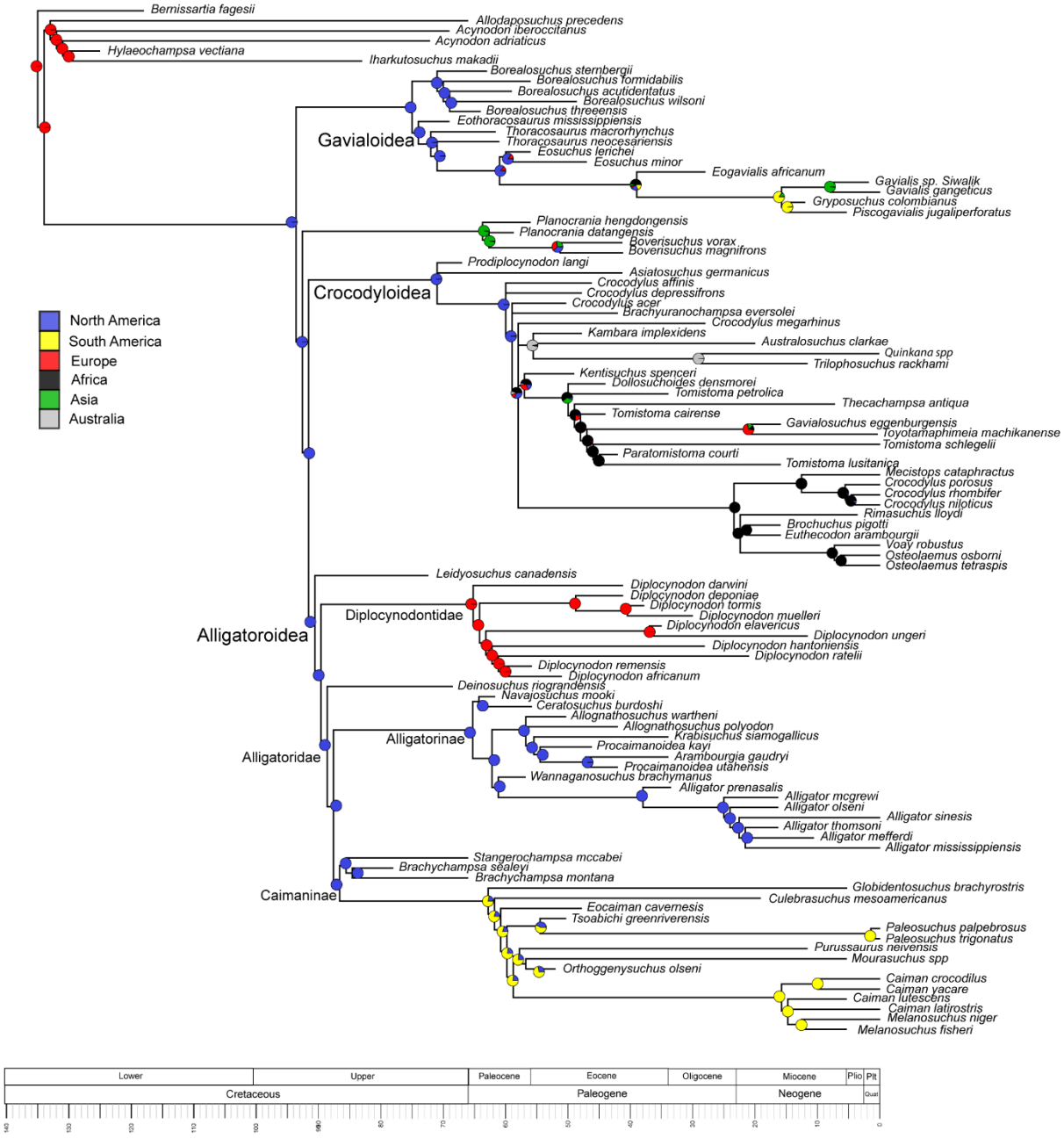

Figure 4.10: Ancestral state reconstruction of the time calibrated strict consensus of the Crocodylia. The phylogeny has been time-scaled based on FADs and LADs using the "mbl" method, and equal rates evolutionary model for the ancestral state reconstruction.

TREE DATING METHOD:		MODEL:		
		ER	**SYM**	**ARD**
BASIC	**Log likelihood**	-129.3632	-116.4568	-114.8272
	AIC	260.7264	262.9136	289.6544
	AICw	74.9%	25%	0.1%
EQUAL	**Log likelihood**	-130.0849	-114.4778	-110.4011
	AIC	262.1698	258.9556	280.8022
	AICw	16.6%	83.2%	0.1%
MBL	**Log likelihood**	-126.4012	-113.3326	-108.1987
	AIC	254.8024	256.6652	279.3973
	AICw	71.7%	28.2%	0.1%

Table 4.3: Results for the model support for Bayesian models on different time-scaled trees. The lower the AIC value, the better the support- the AIC is calculated from the log likelihood values and the number of parameters in the model. The red values show the best supported model uses the "mbl" time-tree with the equal rates model.

PaleoMaps reconstruction:

The paleoMaps package in R (Rothkugel and Varela, 2015) extracts data from the Paleobiology Database. Following examination of the data, the following modifications were made. All occurrences of *Diplocynodon* in the USA in the Cretaceous have been removed from the dataset. This is because this material has been referred to *Borealosuchus* by previous authors (Brochu, 1997a; Martin, Smith, *et al.*, 2014). *Borealosuchus*, though sharing a lot of similarities to diplocynodontids (Martin, Smith, *et al.*, 2014), does not class within the Alligatoroidea. Putative remains of *Allognathosuchus* in India and Argentina are based on isolated teeth only. As crocodylian teeth are known to be highly convergent based on diet, diagnosis of a species based purely on teeth should be treated with caution (Langston, 1973). Similarly, occurrences of *Brachychampsa* outside of America are based on remains that are not diagnostic, including teeth. All of these uncertain occurrences were removed from the dataset prior to plotting the maps. *Diplocynodon africanum* was added to the dataset, palaeolongitude: 1.53, paleolatitude: 21.34.

4.3.2 Conclusion:

In this chapter, additional new material was described and diagnosed from the abundant deposits of the Oulad Abdoun basin in Morocco. This new material represents the first definitive alligatoroid material from Africa and a new species of Diplocynodontidae. With the addition of this new species, the Moroccan phosphates are now recognised to contain an additional crocodyliform family, the Alligatoroidea. The range of crocodylian material preserved in these deposits emphasises the importance of this site for continued future research.

The fossil was diagnosed as a member of the Diplocynodontidae, an extinct group with a stratigraphic rage extending from the Late Paleocene to Miocene (Martin, 2010; Martin and Gross, 2011; Delfino and Smith, 2012; Martin, Smith, *et al.*, 2014). In this paper, we time calibrated the phylogeny and found that the three alligatoroid subfamilies (Alligatorinae, Caimaninae and Diplocynodontidae) diversify rapidly in the aftermath of the K-Pg mass extinction. This is associated with migration from North America into South America and Europe, and likely Asia. Ancestral state reconstruction suggest that this new species, *Diplocynodon africanum*, dispersed into Africa from Europe, which suggests that the Diplocynodontidae were already in Europe in the Paleocene, contrasting to prior hypotheses that they dispersed to Europe over the PETM (Brochu, 1999; Martin, Smith, *et al.*, 2014; Delfino *et al.*, 2017).

Rogue taxa identified in this chapter dramatically reduced resolution in the phylogenetic analysis. Two of these species, *Protoalligator huiningensis* (Wang, Sullivan and Liu, 2016) and Maoming specimen (Skutschas *et al.*, 2014) represent dispersals into Asia in the Paleogene, and therefore have interesting biogeographic implications with regards to the K-Pg. However, it is unclear at this stage which subfamily these Asian species belong to and therefore, how they dispersed into Asia. A reassessment of existing phylogenetic characters or addition of new characters to the matrix may help improve stability. Fragmentary material from Africa has previously been assigned to the Alligatoroidea, but the diagnosis has been questioned (D'Erasmo, 1934; Buffetaut, 1985c; Brochu, 1999; Rossmann, Muller and Forst, 2000; Delfino, Böhme and Rook, 2007). The new species identified in the chapter, indicating that Alligatoroidea were present in Africa, highlights the need for reassessment of this and other fragmentary material globally.

The Alligatoroidea form the focus of this biogeographic study. The results suggest that opportunities in the aftermath of the extinction, such as lack of predation and competition, played a significant role in shaping alligatoroid diversity and global distribution of this group. Expanding this study to the entire crown group, Crocodylia, would be an interesting future direction to identify if this pattern was pervasive to all crocodylians or restricted to this freshwater clade.

Chapter 5: Discussion and Future Work

The probability of any organism becoming fossilised, and the subsequent likelihood that this fossil ever becomes sampled in the fossil record, is extremely low. As a result, the quality of the fossil record is patchy and our understanding of evolution is limited. Therefore, the discovery of any new fossil material is vital, as it tests our current understanding and has the potential to radically change our perceptions about evolution for any particular group of organisms.

The purpose of this thesis was to describe numerous new fossil crown crocodylian specimens from the Paleocene-Eocene phosphate deposits of Morocco. The discovery of these fossils has provided new insights into disparity, biogeography, and competitive interactions in an interval relatively early in crown crocodylian history, which also spans the recovery phase from the K-Pg mass extinction. In the style of the alternative format thesis, each chapter is presented in the form of an academic paper. Each chapter contains a discussion relevant to that chapter. A brief summary for each chapter is provided here, followed by the implications of these results within the wider field and potential areas for future research.

5.1 Chapter 2:

The aim of this chapter was the description of numerous crocodylian skulls recovered from the Paleocene-Eocene phosphate deposits of Morocco. Numerous species of crocodylomorph have already been described from the phosphates including three species belonging to the crown group; *Ocepesuchus eoafricanus* (Maastrichtian) (Jouve, Bardet and Jalil, 2008), *Argochampsa krebsi* (Paleocene) (Hua and Jouve, 2004), and *Maroccosuchus zennaroi* (Ypresian) (Jouve *et al.*, 2014). Four new species, *Argochampsa microrhynchus* sp. nov., *Parvosuchus daouiensis* gen. et sp. nov., *Phasmatosuchus decipulae* gen. et. sp. nov. and *Maroccosuchus brachygnathus* sp. nov., and three additional specimens referred to *M. zennaroi* as juveniles/sub-adults are described in this chapter.

Phylogenetic analysis of morphological characters recovered gavialoid affinities for three of the new species (*Argochampsa microrhynchus, Parvosuchus* and *Phasmatosuchus*) forming a new clade with *A. krebsi*, the Argochampsinae. The new clade is endemic to Morocco and confined to the Paleocene. This clade exhibits a number of morphological characters in the braincase region which draws it closer to the more derived gavialoids, Gryposuchinae and *Gavialis,* and away from the deeper branching thoracosaurs. *Maroccosuchus brachygnathus* sp. nov. was recovered as the sister group of all other Tomistominae, with *M. zennaroi.* This position for *Maroccosuchus* is consistent with previous morphological analyses for the genus (Jouve *et al.*, 2014).

The phylogenetic position of the Gavialoidea and Tomistominae is a matter of conflict in the literature between morphological and molecular datasets (Brochu, 1997b). Morphology suggests that the Gavialoidea branch prior to the Alligatoroidea and Crocodyloidea, with Tomistominae nested within Crocodyloidea. Whereas the molecular data suggest that Gavialoidea forms a sister group to Crocodyloidea, with Alligatoroidea basal to this; Tomistominae becomes incorporated in the Gavialoidea. The new taxa described provided a fresh opportunity to examine the phylogenetic relationships in a combined (morphology-with-molecular) analysis. The results of this second phylogenetic analysis were congruent with the

molecular hypothesis (Oaks, 2011), with the Tomistominae becoming incorporated into the Gavialoidea. Other combined analyses have recovered similar results, consistent with the molecular hypothesis (Gatesy *et al.*, 2003; Gold, Brochu and Norell, 2014). However, here we incorporated a greater number of fossil species within the analysis and achieved greater resolution in the consensus topology. In contrast to prior studies, we also found that *Euthecodon,* a longirostrine crocodyloid, becomes incorporated into the Gavialoidea in the combined (morphology-with-molecular) analysis. In addition, the borealosuchids, which typically form one of the deepest branching clades in the Crocodylia are shifted crownwards, and the Alligatoroidea are positioned basal to the borealosuchids. This result is novel for the Alligatoroidea and challenges what might constitute the ancestral morphology for the Crocodylia.

The rostral proportions and tooth count in the newly described taxa vary dramatically, which suggested a range in dietary habits. However, the variability in skull proportions, especially amongst the *Maroccosuchus* material, also highlighted problems associated with ontogeny and intraspecific variation which is often difficult to diagnose in fossil material. Preliminary data was collected to establish the range of variability in skull material between extant species, to assist diagnosis of the new fossil material. The osteological data collected represents ontogenetic series from nine species of extant crocodylians to create a photographic comparative resource. In preliminary investigations into ontogeny, a number of characters in the morphological matrix were found to score differently between different individuals of the same species, either as a result of ontogeny or intraspecific variation. Similar problems were found amongst the referred *Maroccosuchus* material. The presence of these characters in the matrix is a potential issue as it may result in the erroneous diagnosis of new species. However, further work is needed to identify all of these problematic characters within the matrix and to assess their validity. These incongruences suggest that either the characters should be removed from the matrix entirely or revised in such a way that they remain taxonomically informative.

5.2 Chapter 3:

Chapter 3 investigates disparity and body size amongst the Gavialoidea and Tomistominae during the Late Cretaceous and Cenozoic, incorporating the new material described in chapter 2. In addition, the phylogenetic conflict of the Gavialoidea (morphology vs. morphology-with-molecular) is examined using stratigraphic congruence. The four new species have dramatically increased the known diversity of crocodylians in the aftermath of the K-Pg mass extinction. Results from the disparity analyses indicate higher levels of morphological variation in the aftermath of the K-Pg than in any other time bin during the Cretaceous-Cenozoic record for these crocodylians. Disparity drops following this initial peak, after the K-Pg, but increases towards the recent, showing another peak in disparity in the Plio-Pleistocene. The bizarre morphology of *Phasmatosuchus decipulae*, with a hyperelongate rostrum and numerous small laterally projecting teeth, contributes strongly to this increased disparity in the post-extinction time bin; it is identified as a morphological outlier within this dataset. It is proposed here that the high disparity amongst the gavialoids and tomistomines was driven by post-extinction opportunism. The extinction of the large mosasaurs and selachians that dominated the marine environment in the Cretaceous (Bardet *et al.*, 2010; Noubhani, 2010; Cappetta *et al.*, 2014) lead to reduced levels of predation and competition, allowing the Moroccan crocodylians to diversify rapidly in the aftermath.

Skull size data was collected to examine the evolution of body size through time for gavialoids and tomistomines. With the addition of the newly described species, body size in the aftermath of the K-Pg is found to be smaller than previously known. However, no significant difference is detected before and after the K-Pg to suggest a Lilliput effect amongst these marine crown crocodylians. Size data was also collected for the dyrosaurids, an extinct clade of marine crocodyliformes which were abundant in the Paleocene and Eocene. Though no trends in body size are detected before and after the K-Pg, there is a significant difference in size between the crown crocodylians and the dyrosaurids in the post extinction time bin. It is suggested that competition for similar resources between the surviving crocodylians, caused an additional element of competition, elevating disparity further.

Stratigraphic congruence of the two different phylogenetic analyses (i.e. morphological vs. combined morphology-with-molecular) was assed using stratigraphic occurrences of the fossil material and the phylogenetic trees (Chapter 2). The morphology-only analysis favours a scenario where a few crocodylian lineages cross the K-Pg boundary, followed by a diversification after the extinction, which is the most congruent with the fossil record as it is currently stands. The combined topology (morphology-with-molecular), suggests that the Crocodylia diversified rapidly in the Late Cretaceous with mass survival over the K-Pg extinction. This topology projects a large number of ghost lineages into the Cretaceous and suggests that there was much higher diversity, and likely, disparity in the Cretaceous which remains undetected in the fossil record. The combined topology suggests that *Gavialis*-*Tomistoma* divergence was in the Cretaceous, this result is highly inconsistent with existing molecular clock studies which suggest an Eocene-Miocene divergence (Janke *et al.*, 2005; Roos, Aggarwal and Janke, 2007; Oaks, 2011). Until this conflict is resolved, the work presented in this thesis highlights a potentially significant gap in our understanding of the early evolution of the Crocodylia and their survival over the K-Pg event.

5.3 Chapter 4:

The aim of chapter 4 is to describe new alligatoroid fossil material from Africa. To date, no definitive alligatoroid material has been recovered from Africa, as putative remains are highly fragmentary (Buffetaut, 1985c; Rossmann, Muller and Forst, 2000). Here, two complete skulls were described from the Late Paleocene-Ypresian horizons from the phosphates of the Oulad Abdoun basin, Morocco. Phylogenetic analysis indicates that this material represents a new species of alligatoroid, *Diplocynodon africanum* sp.nov., and the first definitive alligatoroid from Africa. The new species belongs to the Diplocynodontidae, an extinct clade within the Alligatoroidea that branches prior to the Globidonta- the clade containing the extant alligatoroid species. The Diplocynodontidae were previously thought to be endemic to Europe, migrating from North America around the Paleocene-Eocene Thermal Maximum - a rapid climatic warming event (Martin, Smith, *et al.*, 2014; Delfino *et al.*, 2017). Recent fossil material from the Late Paleocene (Martin, Smith, *et al.*, 2014) however, suggests an earlier migration, and the new material described here provides stronger support for this alternative hypothesis. To examine the implications of these stratigraphically earlier fossils, time calibration of the consensus topology and ancestral state reconstruction were carried out in this chapter. The results suggest that Diplocynodontidae diversified and became established in Europe rapidly after the K-Pg event. This pattern of rapid diversification and geographic dispersal is also detected in the other alligatoroid groups e.g. alligators and caimans (Brochu, 1999; Bronzati, Montefeltro and Langer, 2015; Mannion *et al.*, 2015). It is suggested in this

chapter that lack of predation and competition following the K-Pg mass extinction drove the rapid diversification and geographic dispersal of the Alligatoroidea.

5.4 Future work:

Crocodylians show huge variability throughout ontogeny, which can be a confounding factor in the description and diagnosis of new fossil material. Preliminary work found that numerous characters in the morphological matrix are only applicable to adult specimens however, when describing fossil material, it is often difficult to ascertain the age. Though ontogeny of extant skulls is heavily discussed and studied, most studies are confined to individual species (Kälin, 1933; Iordansky, 1973; Webb and Messel, 1978; Hall and Portier, 1994; Monteiro, Cavalcanti and Sommer III, 1997; Foth, Bona and Desojo, 2013; Fernandez Blanco *et al.*, 2015). A detailed study across numerous species with different morphologies (longirostrine, blunt, and generalist) would help to identify characters which vary throughout ontogeny. It would be interesting to establish if there are common trends within a particular morphology (such as longirostry) or uniting all extant crocodylians. This would aid the future diagnosis of new fossil material as an up to date comparative resource is currently lacking.

The methods used in this thesis to understand disparity patterns of gavialoids and tomistomines through time could be built on in a number of ways. Sample sizes were small in the geometric morphometrics analyses (Chapter 3) because some fossil taxa could not be included due to missing data. One approach to counter this would be to use models to estimate the location of missing landmarks (Adams and Otarola-Castillo, 2013). Methods to do this usually implement multivariate regressions or use thin-plate splines from the existing sample of taxa. Alternatively, phylogenetic corrections, factoring in ghost lineages, can model disparity through time, in order to compensate for a poor fossil record (Friedman, 2010; Wilberg, 2017). This would be a particularly interesting application with the Gavialoidea. However, whilst the conflict over phylogenetic relationships and divergence times of the Gavialoidea remains, using phylogenetic corrections for disparity will be equally uncertain.

To increase our understanding of Crocodylia evolution and turnover over the K-Pg boundary, and gavialoids in particular, the phylogenetic conflict between molecular and morphological datasets needs to be addressed. To date, combined analyses on the Crocodylia have only been carried out using parsimony methods, which treats the data included within each partition equally. Molecular characters greatly outnumber the morphological characters in many phylogenetic analyses, which in parsimony analyses biases the result towards the signal in the molecular dataset (Poe, 1996; Brochu, 1997b; Gatesy *et al.*, 2003; Gold, Brochu and Norell, 2014). It has been suggested that parsimony-based combined analyses may not be useful for recovering evolutionary relationships amongst Crocodylia as the strongest data partition will overpower the signal (Brochu, 1997b). With the advancement of Bayesian and Maximum Likelihood methods, and improved evolutionary models, a total evidence analysis employing tip-dating may provide a novel insight into the conflict. Tip-dating would allow stratigraphic data to be incorporated into divergence time estimation, which might help deal with the stratigraphic incongruence of molecular data and molecular clock analyses.

In addition to improving tree searching methods for the combined analyses, an additional approach would be to re-examine the source data. Numerous molecular datasets using a range of nuclear and mitochondrial data have been analysed and all consistently recover a sister relationship between *Gavialis gangeticus* and *Tomistoma schlegelii* (Harshman *et al.*, 2003; Janke *et al.*, 2005; Roos, Aggarwal and Janke, 2007; Man *et al.*, 2011; Oaks, 2011).

The morphological data consistently recovers gavialoids in a position basal to Tomistominae, but in contrast to the molecular analyses, the morphological analyses are almost entirely restricted the Brochu (1999) matrix. This matrix has formed the basis of most phylogenetic analyses for the last 20 years, though it has been substantially modified and expanded with the addition of new fossil species and characters (Salisbury, 2002; Hua and Jouve, 2004; Brochu, 2006b, 2010; Martin and Gross, 2011; Brochu and Storrs, 2012; Delfino and Smith, 2012; Conrad *et al.*, 2013; Jouve *et al.*, 2014). This is potentially problematic as errors may have propagated within the matrix and there is limited comparative data. In this thesis, the morphological phylogeny contains a large number of homoplastic characters, as exemplified by the consistency index (Figure 3.2-3.3). This points to the high levels of convergence amongst the crocodylians (Brochu, 2001; Sadleir and Makovicky, 2008), which has led to confusion in taxonomic placement, particularly with taxa such as the thoracosaurs, *Gavialosuchus* (Koken, 1888; Erickson and Sawyer, 1996; Brochu, 2004a, 2006b; Delfino, Piras and Smith, 2005) and *Euthecodon* (Ginsburg and Buffetaut, 1978; Storrs, 2003). At this stage, a novel matrix of morphological characters may shed new light on phylogenetic relationships amongst the crown group.

5.5 Conclusions:

In this thesis, the diagnosis and description of five new species of crown crocodylian have helped improve our understanding of extinction recovery within the crown group and how this major environmental change has driven patterns in biogeography, diversity and disparity throughout the Cenozoic. The new Moroccan material shows that there was much greater Palaeogene diversity than previously known and that the recovery from the K-Pg extinction was rapid. New fossil species from a range of fossil groups continue to be described from the Moroccan phosphatic basins (Arambourg, 1952; Gheerbrant *et al.*, 2003; Bardet *et al.*, 2010; Longrich *et al.*, 2017), greatly adding to our understanding of many fossil groups. The phosphates represent an important area for future research in the K-Pg mass extinction.

There are few studies that investigate macroevolutionary patterns within Crocodylia over the K-Pg extinction, and even fewer during the recovery (Brochu, 2001; Bronzati, Montefeltro and Langer, 2015; Mannion *et al.*, 2015; Wilberg, 2017). To address this gap in knowledge, the work presented in chapter 3 investigates body size and disparity amongst the gavialoids and tomistomines, based on the newly described species. This builds on previous analyses by including a much greater sample size within this subset of crocodylians and using a more detailed landmarking scheme. Increased disparity in the aftermath extinction suggests that these crocodylians were able to benefit from extinction.

The G*avialis-Tomistoma* conflict remains unresolved (Gatesy *et al.*, 2003; Oaks, 2011; Brochu and Storrs, 2012; Gold, Brochu and Norell, 2014). However, in a novel approach to the problem, time calibration was applied to the conflicting topologies (chapter 3). The results have major implications for understanding crocodylian survival over the K-Pg, if the combined (morphology-with-molecular) topology is more accurate it implies that the crocodylians diversified in the Cretaceous and there was mass survival of this group over the boundary. This is in complete contrast to the known fossil record to date and poses interesting questions about the selectivity of the K-Pg mass extinction.

Time-calibration of the phylogeny of the Alligatoroidea found that all three alligatoroid groups diversify and disperse rapidly in the wake of the K-Pg, suggesting the extinction was a strong driver for the biogeographic distribution of this group (chapter 4). This contrasts with

previous hypotheses of alligatoroid dispersal (Martin, Smith, *et al.*, 2014; Delfino *et al.*, 2017) and highlights the importance of new fossil finds to challenge out understanding of macroevolutionary trends in the fossil record.

Macroevolutionary trends deduced from the fossil record, especially during times of environmental stress, can help us to make future predictions about a groups evolutionary success, but translating these trends for use in conservation is not without complications (Barnosky *et al.*, 2011). The macroevolutionary trends identified in this thesis focus on time scales of millions of years, making it difficult to use for short-term conservation solutions. In addition, unlike examples of past mass extinctions and environmental change, the changes affecting extant crocodylian populations are heavily linked to human activity- e.g. habitat encroachment, global climate change or the direct killing of species. The human impact is too rapid to be compared to geologic timescales and cannot be compared to any previous event in Earth history. However, the results from this thesis do show that crocodylians were resilient in the face of major environmental stress and were able to recover rapidly after K-Pg event. The fact that the recovery was accompanied by experimentation in skull morphology and rapid biogeographic dispersal shows that Crocodylia are highly adaptable.

The Crocodylomorpha have survived multiple mass extinction events and perturbations in global climate. Though there has been a recent drive to explore these macroevolutionary trends particularly in the crown group (Sadleir and Makovicky, 2008; Jouve *et al.*, 2014; Martin, Amiot, *et al.*, 2014; Bronzati, Montefeltro and Langer, 2015; Mannion *et al.*, 2015; Salas-Gismondi *et al.*, 2015; Wilberg, 2017), the Cretaceous-Cenozoic fossil record of this group remains incompletely understood. From the work presented in this thesis, we now have a better understanding of the effect of a mass extinction on crocodylians. In the face of a sixth mass extinction in Earth history (Barnosky *et al.*, 2011; Ceballos *et al.*, 2015; Ceballos, Ehrlich and Dirzo, 2017), a thorough knowledge of the groups past survival and recovery of these events is necessary to help us understand macroevolutionary processes and the effects of future climate change on this group.

References:

Adams, D.C. & Otarola-Castillo, E., 2013. geomorph: an R package for the collection and analysis of geometric morphometric shape data. *Methods in Ecology and Evolution*, 4, pp.393–399.

Adolfssen, J.S. & Ward, D.J., 2014. Crossing the boundary: an elasmobranch fauna from Stevns Klint, Denmark. *Palaeontology*, 57(3), pp.591–629.

Aggarwal, R.K. et al., 1994. Generic affinities among crocodilians as revealed by DNA fingerprinting with a Bkm-derived probe. *Proceedings of the National Academy of Sciences*, 91(22), pp.10601–10605.

Aguilera, O.A., Riff, D. & Bocquentin-Villanueva, J., 2006. A new giant *Purussaurus* (Crocodyliformes, Alligatoridae) from the Upper Miocene Urumaco Formation, Venezuela. *Journal of Systematic Palaeontology*, 4(3), pp.221–232.

Albertão, G.A. & Martins, P.P., 1996. A possible tsunami deposit at the Cretaceous-Tertiary boundary in Pernambuco, northeastern Brazil. *Sedimentary Geology*, 104(1–4), pp.189–201.

Alroy, J., 1999. The fossil record of North American mammals : evidence for a Paleocene evolutionary radiation. *Systematic Biology*, 48(1), pp.107–118.

Alvarez, L.W. et al., 1980. Extraterrestrial Cause for the Cretaceous-Tertiary Extinction. *Science*, 208, pp.1095–1108.

Alvarez, W., 1997. T. rex *and the crater of doom*, Princeton, N.J. : Princeton University Press.

Alvarez, W., Asaro, F. & Montanari, A., 1990. Iridium Profile for 10 Million Years Across the Cretaceous-Tertiary Boundary at Gubbio (Italy). *Science*, 250(4988), pp.1700–1702.

Andrews, C.W., 1906. *A Descriptive Catalogue of the Tertiary Vertebrata of the Fayûm, Egypt.*, British Museum, London.

Arambourg, C., 1952. Les vertébrés fossiles des gisements de phosphates (Maroc-Algérie-Tunisie). *Service Géologique Maroc, Notes et Mémoires*, 92, pp.1–372.

Archibald, J.D. & Bryant, L.J., 1990. Differential Cretaceous/Tertiary extinctions of nonmarine vertebrates; evidence from northeastern Montana. *Geological Society of America Special Papers*, 247, pp.549–562.

Aureliano, T. et al., 2015. Morphometry, bite-force, and paleobiology of the Late Miocene caiman *Purussaurus brasiliensis*. *PLoS ONE*, 10(2), pp.1–14.

Bambach, R.K., 2006. Phanerozoic Biodiversity Mass Extinctions. *Annual Review of Earth and Planetary Sciences*, 34(1), pp.127–155.

Bardet, N., Suberbiola, X.P., Iarochène, M., Bouya, B., et al., 2005. A new species of *Halisaurus* from the Late Cretaceous phosphates of Morocco, and the phylogenetical relationships of the Halisaurinae (Squamata: Mosasauridae). *Zoological Journal of the Linnean Society*, 143, pp.447–472.

Bardet, N., Suberbiola, X.P., Iarochène, M., Amalik, M., et al., 2005. Durophagous Mosasauridae (Squamata) from the Upper Cretaceous phosphates of Morocco, with description of a new species of *Globidens*. *Geologie en Mijnbouw/Netherlands Journal of Geosciences*, 84, pp.167–175.

Bardet, N. et al., 2004. *Mosasaurus beaugei* Arambourg, 1952 (Squamata, Mosasauridae) from the Late Cretaceous Phosphates of Morocco. *Geobios*, 37, pp.315–324.

Bardet, N. et al., 2010. Reptilian assemblages from the latest Cretaceous – Palaeogene phosphates

of Morocco: from Arambourg to present time. *Historical Biology*, 22(1–3), pp.186–199.

Barnosky, A.D. et al., 2011. Has the Earth's sixth mass extinction already arrived? *Nature*, 471(7336), pp.51–57.

Belben, R.A. et al., 2017. Ecological impact of the end-Cretaceous extinction on lamniform sharks. *PLoS ONE*, 12(6).

Belcher, C.M., 2009. Reigniting the Cretaceous-Palaeogene firestorm debate. *Geology*, 37, pp.1147–1148.

Benson, R.B.J. & Butler, R.J., 2011. Uncovering the diversification history of marine tetrapods: ecology influences the effect of geological sampling biases. *Geological Society, London, Special Publications*, 358(1), pp.191–208.

Benton, M.J., 1999. Early origins of modern birds and mammals: molecules vs. morphology. *BioEssays*, 21(12), pp.1043–1051.

Bernard, A. et al., 2010. Regulation of body temperature by some Mesozoic marine reptiles. *Science*, 328(5984), pp.1379–1382.

Berv, J.S. & Field, D.J., 2017. Genomic Signature of an Avian Lilliput Effect across the K-Pg Extinction. *Systematic Biology*, 67(1), pp.1–13.

Blanco, A. & Brochu, C.A., 2016. Intra- and interspecific variability in allodaposuchid crocodylomorphs and the status of western European taxa. *Historical Biology*, 2963(July), pp.1–14.

Böhme, M., 2003. The Miocene Climatic Optimum: evidence from ectothermic vertebrates of Central Europe. *Palaeogeography, Palaeoclimatology, Palaeoecology*, 195(3–4), pp.389–401.

Bohor, B.F., Modreski, P.J. & Foord, E.E., 1987. Shocked quartz in the Cretaceous-Tertiary boundary clays : evidence for a global distribution. *Science*, 236(4802), pp.705–709.

Bourdon, E., Amaghzaz, M. & Bouya, B., 2010. Pseudotoothed Birds (Aves, Odontopterygiformes) from the Early Tertiary of Morocco. *American Museum Novitates*, (3704), pp.1–72.

Bourgeois, J., 2009. Geologic effects and records of tsunamis. In *The Sea, Volume 15: Tsunamis*. Harvard University Press, pp. 53–91.

Brochu, C.A., 2010. A new alligatorid from the lower Eocene Green River Formation of Wyoming and the origin of caimans. *Journal of Vertebrate Paleontology*, 30(4), pp.1109–1126.

Brochu, C.A., 2004a. A new Late Cretaceous gavialoid crocodylian from eastern North America and the phylogenetic relationships of thoracosaurs. *Journal of Vertebrate Paleontology*, 24(September), pp.610–633.

Brochu, C.A. et al., 2012. A new species of *Borealosuchus* (Crocodyliformes, Eusuchia) from the Late Cretaceous–early Paleogene of New Jersey. *Journal of Vertebrate Paleontology*, 32(1), pp.105–116.

Brochu, C.A., 1997a. A review of "*Leidyosuchus*" (Crocodyliformes, Eusuchia) from the Cretaceous through Eocene of North America. *Journal of Vertebrate Paleontology*, 17(4), pp.679–697.

Brochu, C.A., 2004b. Alligatorine phylogeny and the status of *Allognathosuchus* Mook, 1921. *Journal of Vertebrate Paleontology*, 24(4), pp.857–873.

Brochu, C.A., 2001. Crocodylian snouts in space and time: phylogenetic approaches toward adaptive radiation. *American Zoologist*, 41(3), pp.564–585.

Brochu, C.A., 2006a. *Eosuchus* (Crocodylia, Gavialoidea) from the lower Eocene of the Isle of Sheppey, England. *Journal of Vertebrate Paleontology*, 26(2), pp.466–470.

Brochu, C.A., 1997b. Morphology, fossils, divergence timing, and the phylogenetic relationships of *Gavialis*. *Systematic Biology*, 46(3), pp.479–522.

Brochu, C.A., 2006b. Osteology and phylogenetic significance of *Eosuchus minor* (Marsh, 1870) new combination, a longirostrine crocodylian from the Late Paleocene of North America. *Journal of Paleontology*, 80(1), pp.162–186.

Brochu, C.A., 2003. Phylogenetic approaches toward crocodylian history. *Annual Review of Earth and Planetary Sciences*, 31(1), pp.357–397.

Brochu, C.A., 2011. Phylogenetic relationships of *Necrosuchus ionensis* Simpson, 1937 and the early history of caimanines. *Zoological Journal of the Linnean Society*, 163, pp.S228–S256.

Brochu, C.A., 2012. Phylogenetic relationships of Palaeogene ziphodont eusuchians and the status of *Pristichampsus* Gervais, 1853. *Earth and Environmental Science Transactions of the Royal society of Edinburgh*, 103(3–4), pp.521–550.

Brochu, C.A., 1997c. *Phylogenetic systematics and taxonomy of Crocodylia*, University of Texas, Austin.

Brochu, C.A., 1999. Phylogenetics, taxonomy, and historical biogeography of Alligatoroidea. *Journal of Vertebrate Paleontology*, 19(January), pp.9–100.

Brochu, C.A., 2007. Systematics and taxonomy of Eocene tomistomine crocodylians from Britain and Northern Europe. *Palaeontology*, 50, pp.917–928.

Brochu, C.A. & Gingerich, P.D., 2000. New tomistomine crocodylian from the Middle Eocene (Bartonian) of Wadi Hitan, Fayum Province, Egypt. *Contributions of the Museum of Paleontology*, 30(10), pp.251–268.

Brochu, C.A. & Storrs, G.W., 2012. A giant crocodile from the Plio-Pleistocene of Kenya, the phylogenetic relationships of Neogene African crocodylines, and the antiquity of *Crocodylus* in Africa. *Journal of Vertebrate Paleontology*, 32(3), pp.587–602.

Bronzati, M., Montefeltro, F.C. & Langer, M.C., 2012. A species-level supertree of Crocodyliformes. *Historical Biology*, 24(April), pp.598–606.

Bronzati, M., Montefeltro, F.C. & Langer, M.C., 2015. Diversification events and the effects of mass extinctions on Crocodyliformes evolutionary history. *Royal Society Open Science*, 2, pp.1–9.

Brugger, J., Feulner, G. & Petri, S., 2017. Baby, it's cold outside: Climate model simulations of the effects of the asteroid impact at the end of the Cretaceous. *Geophysical Research Letters*, 44(1), pp.419–427.

Brusatte, S.L. et al., 2015. The extinction of the dinosaurs. *Biological Reviews*, 90(2), pp.628–642.

Bryant, H.N., 1989. Non-dinosaurian lower vertebrates across the Cretaceous-Tertiary Boundary in northeastern Montana. *University of California Publications in Geological Sciences*, 134, pp.1–107.

Buckley, G. et al., 2000. A pug-nosed crocodyliform from the Late Cretaceous of Madagascar. *Nature*, 405(6789), pp.941–944.

Buffetaut, E., 1981. Die biogeographische Geschichte der Krokodilier, mit Beschreibung einer neuen Art, *Araripesuchus wegeneri*. *Geologische Rundschau*, 70, pp.611–624.

Buffetaut, E., 1985a. Les crocodiliens de l'Eocène inférieur de Dormaal (Brabant, Belgique). *Bulletin de la Société Belge de Géologie*, 94(1), pp.51–59.

Buffetaut, E., 1985b. The place of *Gavialis* and *Tomistoma* in Eusuchian evolution: a reconciliation of palaeontological and biochemical data. *Neues jahrbuch für geologie und paläontologie, Monatshefte*, 12, pp.707–716.

Buffetaut, E., 1990. Vertebrate extinctions and survival across the Cretaceous-Tertiary boundary. *Tectonophysics*, 171(1–4), pp.337–345.

Buffetaut, E., 1985c. Zoogeographical history of African crocodilians since the Triassic. In

Proceedings of the International Symposium on African Vertebrates: Systematics, Phylogeny and Evolutionary Ecology. pp. 453–469.

Busbey, A.B., 1994. The structural consequences of skull flattening in crocodilians. In J. J. Thomason, ed. *Functional Morphology in Vertebrate Paleontology*. Cambridge University Press, New York, pp. 173–192.

Callahan, W. et al., 2015. A nearly complete specimen of *Hyposaurus rogersii* (Crocodylomorpha , Dyrosauridae) from the Late Cretaceous-Early Paleogene of New Jersey. In p. 1.

Cappetta, H. et al., 2014. Marine vertebrate faunas from the Maastrichtian phosphates of Benguerir (Ganntour Basin, Morocco): Biostratigraphy, palaeobiogeography and palaeoecology. *Palaeogeography, Palaeoclimatology, Palaeoecology*, 409, pp.217–238.

Carpenter, K., 1983. *Thoracosaurus neocesariensis* (de Kay, 1842) (Crocodylia : Crocodylidae) from the Late Cretaceous Ripley Formation of Mississippi. *Mississippi Geology*, 4, pp.1–10.

Cavin, L. et al., 2000. A new Palaeocene albulid (Teleostei: Elopomorpha) from the Ouled Abdoun phosphatic basin, Morocco. *Geological Magazine*, 137(5), pp.583–591.

Cavin, L., 2002. Effects of the Cretaceous-Tertiary boundary event on bony fishes. *Geological and biological effects of impact events*, pp.141–158.

Ceballos, G. et al., 2015. Accelerated modern human – induced species losses: entering the sixth mass extinction. *Sciences Advances*, 1(e1400253), pp.1–5.

Ceballos, G., Ehrlich, P.R. & Dirzo, R., 2017. Biological annihilation via the ongoing sixth mass extinction signaled by vertebrate population losses and declines. *Proceedings of the National Academy of Sciences*, p.201704949.

Ciampaglio, C.N., Kemp, M. & Mcshea, D.W., 2016. Detecting changes in morphospace occupation patterns in the fossil record : Characterization and analysis of measures of disparity. *Paleobiology*, 27(4), pp.695–715.

Claeys, P., Kiessling, W. & Alvarez, W., 2002. Distribution of Chicxulub ejecta at the Cretaceous-Tertiary boundary. *Special Paper 356: Catastrophic events and mass extinctions: impacts and beyond*, pp.55–68.

Clark, J.M. et al., 2004. A Middle Jurassic 'sphenosuchian' from China and the origin of the crocodylian skull. *Nature*, 430, pp.8–10.

Clark, J.M., 1994. Patterns of evolution in Mesozoic Crocodyliformes. In N. C. Fraser & H.-D. Sues, eds. *In the shadow of the dinosaurs: Early Mesozoic tetrapods*. Cambridge University Press New York, pp. 84–97.

Clark, J.M., Jacobs, L.L. & Downs, W.R., 1989. Mammal-like dentition in a Mesozoic crocodylian. *Science*, 244(4908), pp.1064–1066.

Conrad, J.L. et al., 2013. New specimens of '*Crocodylus' pigotti (Crocodylidae) from Rusinga Island, Kenya, and generic reallocation of the species*.' *Journal of Vertebrate Paleontology*, 33(3), pp.629–646.

Coxall, H.K., D'Hondt, S. & Zachos, J.C., 2006. Pelagic evolution and environmental recovery after the Cretaceous-Paleogene mass extinction. *Geology*, 34(4), pp.297–300.

D'Erasmo, G., 1934. Su alcuni avanzi di vertebrati terziari della Sirtica. *Missione Scientifica della reale accademia Italiana a Cufra (1931-IX), 3 (studi paleontologici e litologici sulla Cirenaica e sulla Tripolitania orientale)*, pp.257–279.

D'Hondt, S. et al., 1996. Planktic foraminifera, asteroids, and marine production: Death and recovery at the Cretaceous-Tertiary boundary. *The Cretaceous-Tertiary event and other catastrophes in earth history. Geological Society of America Special Paper*, 307, pp.303–317.

Dameron, S.N. et al., 2017. Extinction, dissolution, and possible ocean acidification prior to the

Cretaceous/Paleogene (K/Pg) boundary in the tropical Pacific. *Palaeogeography, Palaeoclimatology, Palaeoecology*, 485, pp.433–454.

Darwin, C., 1859. *The origin of species: by means of natural selection, or the preservation of favoured races in the struggle for life*, London: Murray.

Debiasse, M.B. & Hellberg, M.E., 2015. Discordance between morphological and molecular species boundaries among Caribbean species of the reef sponge Callyspongia. *Ecology and Evolution*, 5(3), pp.663–675.

Delfino, M. et al., 2017. Evidence for a pre-PETM dispersal of the earliest European crocodyloids. *Historical Biology*, 2963(December), pp.1–8.

Delfino, M., Böhme, M. & Rook, L., 2007. First European evidence for transcontinental dispersal of *Crocodylus* (late Neogene of southern Italy). *Zoological Journal of the Linnean Society*, 149(3), pp.293–307.

Delfino, M., Piras, P. & Smith, T., 2005. Anatomy and phylogeny of the gavialoid crocodylian *Eosuchus lerichei* from the Paleocene of Europe. *Acta Palaeontologica Polonica*, 50(3), pp.565–580.

Delfino, M. & Smith, T., 2012. Reappraisal of the morphology and phylogenetic relationships of the middle Eocene alligatoroid *Diplocynodon deponiae* (Frey, Laemmert, and Riess, 1987) based on a three-dimensional specimen. *Journal of Vertebrate Paleontology*, 32(6), pp.1358–1369.

Densmore, L.D. & Dessauer, H.C., 1984. Low levels of protein divergence detected between *Gavialis* and *Tomistoma*: evidence for crocodilian monophyly? *Comparative Biochemistry and Physiology Part B: Comparative Biochemistry*, 77(4), pp.715–720.

Díaz Aráez, J.L. et al., 2015. New remains of *Diplocynodon* (Crocodylia: Diplocynodontidae) from the Early Miocene of the Iberian Peninsula. *Comptes Rendus - Palevol*, 16(1), pp.12–26.

Donoghue, M.J. & Sanderson, M.J., 1992. The suitability of molecular and morphological evidence in reconstructing plant phylogeny. In *Molecular systematics of plants*. Springer, pp. 340–368.

Eaton, M.J. et al., 2009. Species-level diversification of African dwarf crocodiles (Genus Osteolaemus): a geographic and phylogenetic perspective. *Molecular Phylogenetics and Evolution*, 50(3), pp.496–506.

Efimov, M.B., 1982. A two-fanged crocodile from the Upper Cretaceous in Tadzhikistan. *Paleontological Journal*, 1982, pp.103–105.

Elewa, A.M.T. & Dakrory, A.M., 2008. Causes of mass extinction at the K/Pg boundary: A case study from the North African Plate. In *Mass Extinction*. Springer, pp. 133–148.

Erickson, B.R., 1982. *Wannaganosuchus*, a new alligator from the Paleocene of North America. *Journal of Paleontology*, 56(2), pp.492–506.

Erickson, B.R. & Sawyer, G.T., 1996. *The estuarine crocodile* Gavialosuchus carolinensis *n. sp. (Crocodylia: Eusuchia) from the late Oligocene of South Carolina, North America*, Science Museum of Minnesota.

Erickson, G.M. et al., 2012. Insights into the ecology and evolutionary success of crocodilians revealed through bite-force and tooth-pressure experimentation. *PLoS ONE*, 7(3).

Erickson, G.M. & Brochu, C.A., 1999. How the 'terror crocodile' grew so big. *Nature*, 398(318651), pp.205–206.

Estes, R. & Howard Hutchison, J., 1980. Eocene lower vertebrates from Ellesmere Island, Canadian Arctic Archipelago. *Palaeogeography, Palaeoclimatology, Palaeoecology*, 30, pp.325–347.

Farke, A.A. et al., 2014. *Leidyosuchus* (Crocodylia: Alligatoroidea) from the Upper Cretaceous Kaiparowits Formation (late Campanian) of Utah, USA. *PaleoBios*, 30(3), pp.72–88.

Feduccia, A., 1995. Explosive evolution in tertiary birds and mammals. *Science*, 267(5198), pp.637–638.

Feng, G. et al., 2010. Two complete mitochondrial genomes of *Crocodylus* and implications for phylogeny. *Amphibia-Reptilia*, 31, pp.299–309.

Feng, Y.-J. et al., 2017. Phylogenomics reveals rapid, simultaneous diversification of three major clades of Gondwanan frogs at the Cretaceous–Paleogene boundary. *Proceedings of the National Academy of Sciences*, 114(29), pp.E5864–E5870.

Fernandez Blanco, M. V. et al., 2015. Ontogenetic variation in the skulls of *Caiman* : the case of *Caiman latirostris* and *Caiman yacare* (Alligatoridae, Caimaninae). *The Herpetological Journal*, 25(2), pp.65–73.

Ferrow, E. et al., 2011. Multiproxy analysis of a new terrestrial and a marine Cretaceous-Paleogene (K-Pg) boundary site from New Zealand. *Geochimica et Cosmochimica Acta*, 75(2), pp.657–672.

Font, E. et al., 2016. Mercury anomaly, deccan volcanism, and the end-cretaceous mass extinction. *Geology*, 44(2), pp.171–174.

Foth, C., Bona, P. & Desojo, J.B., 2013. Intraspecific variation in the skull morphology of the black caiman *Melanosuchus niger* (Alligatoridae, Caimaninae). *Acta Zoologica*, 96, pp.1–13.

Friedman, M., 2009. Ecomorphological selectivity among marine teleost fishes during the end-Cretaceous extinction. *Proceedings of the National Academy of Sciences*, 106(13), pp.5218–5223.

Friedman, M., 2010. Explosive morphological diversification of spiny-finned teleost fishes in the aftermath of the end-Cretaceous extinction. *Proceedings of the Royal Society B: Biological Sciences*, 277, pp.1675–1683.

Gardin, S. & Monechi, S., 1998. Palaeoecological change in middle to low latitude calcareous nannoplankton at the Cretaceous/Tertiary boundary. *Bulletin de la Société géologique de France*, 169(5), pp.709–723.

de Gasparini, Z.B., 1971. Los Notosuchia del Cretácico de América del Sur como un nuevo infraorden de los Mesosuchia (Crocodilia). *Ameghiniana*, 8(2), pp.83–103.

Gatesy, J. et al., 2003. Combined support for wholesale taxic atavism in gavialine crocodylians. *Systematic Biology*, 52(3), pp.403–422.

Gatesy, J., Baker, R.H. & Hayashi, C., 2004. Inconsistencies in arguments for the supertree approach: supermatrices versus supertrees of Crocodylia. *Systematic Biology*, 53(2), pp.342–355.

Gheerbrant, E., 2009. Paleocene emergence of elephant relatives and the rapid radiation of African ungulates. *Proceedings of the National Academy of Sciences*, 106(26), pp.10717–10721.

Gheerbrant, E. et al., 2003. The mammal localities of Grand Daoui Quarries, Ouled Abdoun Basin, Morocco, Ypresian: a first survey. *Bulletin De La Societe Geologique De France*, 174(3), pp.279–293.

Gheerbrant, E. & Rage, J.-C., 2006. Paleobiogeography of Africa: How distinct from Gondwana and Laurasia? *Palaeogeography, Palaeoclimatology, Palaeoecology*, 241(2), pp.224–246.

Ginsburg, L. & Buffetaut, E., 1978. *Euthecodon arambourgi* n. sp., et l'évolution du genre Euthecodon, Crocodilien du Néogène d'Afrique. *Géologie Méditerranéenne*, 5(2), pp.291–302.

Gold, M.E.L., Brochu, C.A. & Norell, M.A., 2014. An expanded combined evidence approach to the *Gavialis* problem using geometric morphometric data from crocodylian braincases and

eustachian systems. *PLoS ONE*, 9(9), pp.1–12.

Goldin, T.J. & Melosh, H.J., 2009. Self-shielding of thermal radiation by Chicxulub impact ejecta: Firestorm or fizzle? *Geology*, 37(12), pp.1135–1138.

Green, R.E. et al., 2014. Three crocodilian genomes reveal ancestral patterns of evolution among archosaurs. *Science*, 346(6215), p.1335.

Grigg, G.C. & Kirshner, D., 2015. *Biology and evolution of crocodylians*, Csiro Publishing.

Grossnickle, D.M. & Newham, E., 2016. Therian mammals experience an ecomorphological radiation during the Late Cretaceous and selective extinction at the K–Pg boundary. *Proceedings of the Royal Society B: Biological Sciences*, 283(1832), p.20160256.

Guggisberg, C.A., 1972. *Crocodiles: their natural history, folklore and conservation*,

Haddi, H. El, Benbouziane, A. & Mouflih, M., 2014. Geochemical Siliceous and Silicified Facies of Phosphate Series of Ouled Abdoun Basin (Morocco). *Open Journal of Geology*, 4, pp.295–302.

Hall, P.M. & Portier, K.M., 1994. Cranial morphometry of New Guinea crocodiles (*Crocodylus novaeguineae*): ontogenetic variation in relative growth of the skull and an assessment of its utility as a predictor of the sex and size of individuals. *Herpetological Monographs*, 8, pp.203–225.

Hammer, Ø., Harper, D.A.T. & Ryan, P.D., 2001. PAST: paleontological statistics software package for education and data analysis. *Palaeontologia Electronica*, 4(1), p.9pp.

Harshman, J. et al., 2003. True and false gharials: a nuclear gene phylogeny of Crocodylia. *Systematic Biology*, 52(3), pp.386–402.

Hastings, A.K. et al., 2013. Systematics and biogeography of crocodylians from the Miocene of Panama. *Journal of Vertebrate Paleontology*, 33(2), pp.239–263.

Hastings, A.K., Bloch, J.I. & Jaramillo, C.A., 2014. A new blunt-snouted dyrosaurid, *Anthracosuchus balrogus* gen. et sp. nov. (Crocodylomorpha, Mesoeucrocodylia), from the Palaeocene of Colombia. *Historical Biology*, pp.1–23.

Hastings, A.K., Reisser, M. & Scheyer, T.M., 2016. Character evolution and the origin of Caimaninae (Crocodylia) in the New World Tropics: New evidence from the Miocene of Panama and Venezuela. *Journal of Paleontology*, 90(2), pp.317–332.

Hekkala, E. et al., 2011. An ancient icon reveals new mysteries: Mummy DNA resurrects a cryptic species within the Nile crocodile. *Molecular Ecology*, 20(20), pp.4199–4215.

Hill, R. V. et al., 2008. Dyrosaurid (Crocodyliformes: Mesoeucrocodylia) fossils from the Upper Cretaceous and Paleogene of Mali: implications for phylogeny and survivorship across the K/T boundary. *American Museum Novitates*, 3631, pp.1–19.

Hua, S. & Jouve, S., 2004. A primitive marine gavialoid from the Paleocene of Morocco. *Journal of Vertebrate Paleontology*, 24(2), pp.341–350.

Hughes, M., Gerber, S. & Wills, M.A., 2013. Clades reach highest morphological disparity early in their evolution. *Proceedings of the National Academy of Sciences*, 110(34), pp.13875–13879.

Hutchison, J.H., 1982. Turtle, crocodilian, and champsosaur diversity changes in the Cenozoic of the north-central region of western United States. *Palaeogeography, Palaeoclimatology, Palaeoecology*, 37(2–4), pp.149–164.

Iijima, M., 2017. Assessment of trophic ecomorphology in non-alligatoroid crocodylians and its adaptive and taxonomic implications. *Journal of anatomy*, 231, pp.192–211.

Iijima, M., Takahashi, K. & Kobayashi, Y., 2016. The oldest record of *Alligator sinensis* from the Late Pliocene of Western Japan, and its biogeographic implication. *Journal of Asian Earth Sciences*,

124, pp.94–101.

Iordansky, N.N., 1973. The skull of the crocodilia. In C. Gans & T. Parsons, eds. *Biology of the Reptilia Vol. 4*. Academic Press, London, pp. 201–262.

IUCN, 2015. The IUCN red list of threatened species. *Version 2015-3.* Available at: %3Cwww.iucnredlist.org%3E [Accessed September 26, 2015].

Jablonski, D., 2005. Mass extinctions and macroevolution. *Paleobiology*, 31(2), pp.192–210.

Jalil, N.-E. et al., 2009. *Euclastes acutirostris*, a new species of littoral turtle (Cryptodira, Cheloniidae) from the Palaeocene phosphates of Morocco (Oulad Abdoun Basin, Danian-Thanetian). *Comptes Rendus Palevol*, 8(5), pp.447–459.

Janke, A. et al., 2005. Mitogenomic analyses place the gharial (*Gavialis gangeticus*) on the crocodile tree and provide pre-K/T divergence times for most crocodilians. *Journal of Molecular Evolution*, 61(5), pp.620–626.

Jenner, R.A., 2004. When molecules and morphology clash: reconciling conflicting phylogenies of the Metazoa by considering secondary character loss. *Evolution & development*, 6(5), pp.372–378.

Jonet, S. & Wouters, G., 1977. *Maroccosuchus zennaroi,* crocodilien eusuchien nouveau des phosphates du Maroc. *Notes de la Service Geologique du Maroc*, 268, pp.177–203.

Jouve, S., 2005. A new description of the skull of *Dyrosaurus phosphaticus* (Thomas, 1893) (Mesoeucrocodylia: Dyrosauridae) from the Lower Eocene of North Africa. *Canadian Journal of Earth Sciences*, 42(3), pp.323–337.

Jouve, S., Ne, M.I.È., et al., 2005. A new dyrosaurid crocodyliform from the Palaeocene of Morocco and a phylogenetic analysis of Dyrosauridae. *Acta Palaeontologica Polonica*, 50(3), pp.581–594.

Jouve, S. et al., 2014. *Maroccosuchus zennaroi* (Crocodylia: Tomistominae) from the Eocene of Morocco: phylogenetic and palaeobiogeographical implications of the basalmost tomistomine. *Journal of Systematic Palaeontology*, 13, pp.1–25.

Jouve, S. et al., 2006. New material of *Argochampsa krebsi* (Crocodylia: Gavialoidea) from the Lower Paleocene of the Oulad Abdoun Basin (Morocco): phylogenetic implications. *Geobios*, 39(6), pp.817–832.

Jouve, S., 2007. Taxonomic revision of the dyrosaurid assemblage (Crocodyliformes: Mesoeucrocodylia) from the Paleocene of the Iullemmeden Basin, West Africa. *Journal of Paleontology*, 81(1), pp.163–175.

Jouve, S., Bardet, N. & Jalil, N.-E., 2008. The oldest African crocodylian: phylogeny, paleobiogeography, and differential survivorship of marine reptiles through the Cretaceous-Tertiary boundary. *Journal of Vertebrate Paleontology*, 28, pp.37–41.

Jouve, S., Bouya, B. & Amaghzaz, M., 2008. A long-snouted dyrosaurid (Crocodyliformes, Mesoeucrocodylia) from the Paleocene of Morocco: phylogenetic and palaeobiogeographic implications. *Palaeontology*, 51(2), pp.281–294.

Jouve, S., Bouya, B. & Amaghzaz, M., 2005. A short-snouted dyrosaurid (Crocodyliformes, Mesoeucrocodylia) from the Paleocene of Morocco. *Palaeontology*, 48(2), pp.359–369.

Kaiho, K. et al., 2016. Global climate change driven by soot at the K-Pg boundary as the cause of the mass extinction. *Scientific Reports*, 6(1), p.28427.

Kälin, J.A., 1933. Beiträge zur vergleichenden Osteologie des Crocodilidenschädels. *Zoologische Jahrbücher*, 57, pp.535–714.

Kälin, J.A., 1939. Ein extrem kurzschnauziger Crocodilide aus den Phosphoriten des Quercy Arambourgia (nov. gen.) gaudryi de Stefano. *Abhandlungen der Schweizerischen*

Palaeontologischen Gesell- schaft, 62, pp.1–18.

Kälin, J.A., 1955. Zur stammesgeschichte der Crocodilia. *Revue Suisse de Zoologie*, 62, pp.347–356.

Katsura, Y., 2004. Paleopathology of *Toyotamaphimeia machikanensis* (Diapsida, Crocodylia) from the Middle Pleistocene of Central Japan. *Historical Biology*, 16(2–4), pp.93–97.

Keller, G. et al., 2004. Chicxulub impact predates the K-T boundary mass extinction. *Proceedings of the National Academy of Sciences*, 101(11), pp.3753–3758.

Keller, G. et al., 2010. Cretaceous Extinctions: Evidence Overlooked J. Sills, ed. *Science*, 328(5981), p.974 LP-975. Available at: http://science.sciencemag.org/content/328/5981/974.1.abstract.

Keller, G., 2014. Deccan volcanism, the Chicxulub impact, and the end-Cretaceous mass extinction : Coincidence? Cause and effect? *Geological society of America Special Papers*, 505(03), pp.57–89.

Keller, G. et al., 2003. Multiple impacts across the Cretaceous–Tertiary boundary. *Earth-Science Reviews*, 62(3–4), pp.327–363.

Kellner, A.W.A., Pinheiro, A.E.P. & Campos, D.A., 2014. A new sebecid from the paleogene of Brazil and the crocodyliform radiation after the K-Pg boundary. *PloS ONE*, 9(1), pp.1–11.

Kobayashi, Y. et al., 2006. Anatomy of a Japanese tomistomine crocodylian, *Toyotamaphimeia machikanensis* (Kamei et Matsumoto, 1965), from the middle Pleistocene of Osaka Prefecture: the reassessment of its phylogenetic status within Crocodylia. *National Science Museum Monographs*.

Kocsis, L. et al., 2014. Comprehensive stable isotope investigation of marine biogenic apatite from the late Cretaceous-early Eocene phosphate series of Morocco. *Palaeogeography, Palaeoclimatology, Palaeoecology*, 394, pp.74–88.

Koken, E., 1888. *Thoracosaurus macrorhynchus* Bl. aus der Tuffkreide von Maastricht. *Zeitschrift der Deutschen Geologischen Gesellschaft*, 40(4), pp.754–773.

Kraus, R., 1998. The cranium of *Piscogavialis jugaliperforatus* n.gen., n.sp. (Gavialidae, Crocodylia) from the Miocene of Peru. *Paläontologische Zeitschrift*, 72, pp.389–406.

Kring, D.A., 1997. Air blast produced by the meteor crater impact event and a reconstruction of the affected environment. *Meteoritics and Planetary Science*, 32(4), pp.517–530.

Kring, D.A., 2007. The Chicxulub impact event and its environmental consequences at the Cretaceous-Tertiary boundary. *Palaeogeography, Palaeoclimatology, Palaeoecology*, 255(1–2), pp.4–21.

Kruge, M.A. et al., 1994. Fossil charcoal in Cretaceous-Tertiary boundary strata: Evidence for catastrophic firestorm and megawave. *Geochimica et Cosmochimica Acta*, 58(4), pp.1393–1397.

Labandeira, C.C., Johnson, K.R. & Lang, P., 2002. Preliminary assessment of insect herbivory across the Cretaceous-Tertiary boundary: major extinction and minimum rebound. *Geological society of America Special Papers*, 361, pp.297–327.

Landman, N.H. et al., 2014. Ammonite extinction and nautilid survival at the end of the Cretaceous. *Geology*, 42(8), pp.707–710.

Lang, J.W. & Andrews, H. V., 1994. Temperature-dependent sex determination in crocodilians. *Journal of Experimental Zoology*, 270(1), pp.28–44.

Langston Jr., W., 1966. *Mourasuchus* Price, *Nettosuchus* Langston, and the Family Nettosuchidae (Reptilia: Crocodilia). *Copeia*, 4, pp.882–885.

Langston, W., 1973. The crocodilian skull in historical perspective. In C. Gans & T. Parsons, eds. *Biology of the Reptilia Vol. 4*. Academic Press, London, pp. 263–284.

Łaska, W., Rodríguez-Tovar, F.J. & Uchman, A., 2017. Evaluating macrobenthic response to the Cretaceous–Palaeogene event: A high-resolution ichnological approach at the Agost section (SE Spain). *Cretaceous Research*, 70, pp.96–110.

Lloyd, G.T., 2016. Estimating morphological diversity and tempo with discrete character-taxon matrices: Implementation, challenges, progress, and future directions. *Biological Journal of the Linnean Society*, 118(1), pp.131–151.

Lockwood, R., 2005. Body size , extinction events , and the early Cenozoic record of veneroid bivalves : a new role for recoveries? *Paleobiology*, 31(4), pp.578–590.

Longrich, N.R. et al., 2017. An abelisaurid from the latest Cretaceous (late Maastrichtian) of Morocco, North Africa. *Cretaceous Research*, 76, pp.40–52.

Longrich, N.R. et al., 2015. Biogeography of worm lizards (Amphisbaenia) driven by end-Cretaceous mass extinction. *Proceedings of the Royal Society of London B: Biological Sciences*, 282(1806), p.20143034.

Longrich, N.R., Bhullar, B.-A.S. & Gauthier, J.A., 2012. Mass extinction of lizards and snakes at the Cretaceous-Paleogene boundary. *Proceedings of the National Academy of Sciences*, 109(52), pp.21396–21401.

Longrich, N.R., Sciberras, J. & Wills, M.A., Mammals across the Cretaceous-Paleogene boundary: spatial dynamics obscure extinction and recovery. *Journal of Evolutionary Biology*.

Longrich, N.R., Scriberas, J. & Wills, M.A., 2016. Severe extinction and rapid recovery of mammals across the Cretaceous-Palaeogene boundary, and the effects of rarity on patterns of extinction and recovery. *Journal of evolutionary biology*, 29(8), pp.1495–1512.

Longrich, N.R., Tokaryk, T. & Field, D.J., 2011. Mass extinction of birds at the Cretaceous-Paleogene (K-Pg) boundary. *Proceedings of the National Academy of Sciences*, 108(37), pp.15253–15257.

Lucas, J. & Prevot-Lucas, L., 1996. Tethyan phosphates and bioproductites. In A. E. M. Nairn et al., eds. *The Ocean Basins and Margins*. Plenum Press, New York, pp. 367–391.

Macleod, N., 1999. Generalizing and extending the eigenshape method of shape space visualization and analysis. *Paleobiology*, 25(1), pp.107–138.

Man, Z. et al., 2011. Crocodilian phylogeny inferred from twelve mitochondrial protein-coding genes, with new complete mitochondrial genomic sequences for Crocodylus acutus and Crocodylus novaeguineae. *Molecular Phylogenetics and Evolution*, 60(1), pp.62–67.

Mannion, P.D. et al., 2015. Climate constrains the evolutionary history and biodiversity of crocodylians. *Nature communications*, 6, pp.1–9.

Marinho, T.S. & Carvalho, I.S., 2009. An armadillo-like sphagesaurid crocodyliform from the Late Cretaceous of Brazil. *Journal of South American Earth Sciences*, 27(1), pp.36–41.

Markwick, P.J., 1998a. Crocodilian diversity in space and time: the role of climate in paleoecology and its implication for understanding K/T extinctions. *Paleobiology*, 24(4), pp.470–497.

Markwick, P.J., 1994. “Equability”, continentality, and Tertiary “climate”: the crocodilian perspective. *Geology*, 22, pp.613–616.

Markwick, P.J., 1998b. Fossil crocodilians as indicators of Late Cretaceous and Cenozoic climates: implications for using palaeontological data in reconstructing palaeoclimate. *Palaeogeography, Palaeoclimatology, Palaeoecology*, 137(3–4), pp.205–271.

Martin, J.E., 2010. A new species of *Diplocynodon* (Crocodylia, Alligatoroidea) from the Late Eocene of the Massif Central, France, and the evolution of the genus in the climatic context of the Late Palaeogene. *Geological Magazine*, 147(04), pp.596–610.

Martin, J.E., Smith, T., et al., 2014. Late Palaeocene eusuchian remains from Mont de Berru,

France, and the origin of the alligatoroid *Diplocynodon*. *Zoological Journal of the Linnean Society*, 172(4), pp.867–891.

Martin, J.E. et al., 2016. New specimens of *Allodaposuchus precedens* from France: Intraspecific variability and the diversity of European Late Cretaceous eusuchians. *Zoological Journal of the Linnean Society*, 176(3), pp.607–631.

Martin, J.E., Amiot, R., et al., 2014. Sea surface temperature contributes to marine crocodylomorph evolution. *Nature Communications*, 5, pp.1–7.

Martin, J.E. & Gross, M., 2011. Taxonomic clarification of *Diplocynodon* Pomel, 1847 (Crocodilia) from the Miocene of Styria, Austria. *Neues Jahrbuch für Geologie und Paläontologie - Abhandlungen*, 261(2), pp.177–193.

Martin, J.E. & Lauprasert, K., 2010. A new primitive alligatorine from the Eocene of Thailand: Relevance of Asiatic members to the radiation of the group. *Zoological Journal of the Linnean Society*, 158(3), pp.608–628.

Martínez-Díaz, J.L. et al., 2016. Lilliput effect in a retroplumid crab (Crustacea: Decapoda) across the K/Pg boundary. *Journal of South American Earth Sciences*, 69, pp.11–24.

Maruoka, T. & Koeberl, C., 2003. Acid-neutralizing scenario after the Cretaceous-Tertiary impact event. *Geology*, 31(6), pp.489–492.

McAliley, L.R. et al., 2006. Are crocodiles really monophyletic? Evidence for subdivisions from sequence and morphological data. *Molecular Phylogenetics and Evolution*, 39(1), pp.16–32.

McGregor, J., 2005. Crocodile crimes: people versus wildlife and the politics of postcolonial conservation on Lake Kariba, Zimbabwe. *Geoforum*, 36(3), pp.353–369.

McHenry, C.R. et al., 2006. Biomechanics of the rostrum in crocodilians: a comparative analysis using finite-element modeling. *The anatomical record. Part A, Discoveries in molecular, cellular, and evolutionary biology*, 288(May), pp.827–849.

Meganathan, P.R. et al., 2011. Complete mitochondrial genome sequences of three *Crocodylus* species and their comparison within the Order Crocodylia. *Gene*, 478(1–2), pp.35–41.

Meyer, E.R., 1984. Crocodilians as living fossils. In *Living Fossils*. Springer, pp. 105–131.

Michard, A. et al., 2008. *Continental evolution: The geology of Morocco: Structure, stratigraphy, and tectonics of the Africa-Atlantic-Mediterranean triple junction*, Springer.

Monteiro, L.R., Cavalcanti, M.J. & Sommer III, H.J.S., 1997. Comparative ontogenic shape changes in the skull of *Caiman* species (Crocodylia, Alligatoridae). *Journal of Morphology*, 231(1), pp.53–62.

Mook, C.C., 1941. A new crocodilian from the Lance Formation. *American Museum Novitates*, 1128, pp.1–6.

Mook, C.C., 1942. A new fossil crocodilian from the Paleocene of New Mexico. *American Museum Novitates*, No. 1189(1189), pp.1–4.

Moraes-Santos, H., Villanueva, J.B. & Toledo, P.M., 2011. New remains of a gavialoid crocodilian from the late Oligocene−early Miocene of the Pirabas Formation, Brazil. *Zoological Journal of the Linnean Society*, 163, pp.S132–S139.

Morgan, J., Artemieva, N. & Goldin, T., 2013. Revisiting wildfires at the K-Pg boundary. *Journal of Geophysical Research: Biogeosciences*, 118(4), pp.1508–1520.

Mukhopadhyay, S., Farley, K.A. & Montanari, A., 2001. A 35 Myr record of helium in pelagic limestones from Italy: Implications for interplanetary dust accretion from the early Maastrichtian to the middle Eocene. *Geochimica et Cosmochimica Acta*, 65(4), pp.653–669.

Müller, L., 1927. Ergebnisse der Forschungsreisen Prof. E. Stromers in den Wüsten Ägyptens. V.

Tertiäre Wirbeltiere. *Beiträge zur Kenntnis der Krokodilier des ägyptischen Tertiärs. Abhandlungen der Bayerischen Akademie der Wissenschaften*, 31(2), pp.1–97.

Nesbitt, S.J., 2011. The early evolution of archosaurs: Relationships and the origin of major clades. *Bulletin of the American Museum of Natural History*, 352(352), pp.1–292.

Nichols, D.J. et al., 1992. A new Cretaceous-Tertiary boundary locality in the western Powder River basin, Wyoming: biological and geological implications. *Cretaceous Research*, 13(1), pp.3–30.

Nichols, D.J. & Johnson, K.R., 2008. *Plants and the KT boundary*, Cambridge University Press.

Norell, M.A., 1989. The higher level relationships of the extant Crocodylia. *Journal of Herpetology*, 23(4), pp.325–335.

Norris, R.D. et al., 2000. Mass failure of the North Atlantic margin triggered by the Cretaceous-Paleogene bolide impact. *Geology*, 28(12), pp.1119–1122.

Noubhani, A., 2010. The selachians' faunas of the Moroccan phosphate deposits and the KT mass-extinctions. *Historical Biology*, 22(1–3), pp.71–77.

Noubhani, A. & Cappetta, H., 1997. *Les Orectolobiformes, Carcharhiniformes et Myliobatiformes (Elasmobranchii, Neoselachii) des Bassins à phosphate du Maroc (Maastrichtien-Lutétien basal): systématique, biostratigraphie, évolution et dynamique des faunes*, Verlag Friedrich Pfeil.

O'Connor, P.M. et al., 2010. The evolution of mammal-like crocodyliforms in the Cretaceous Period of Gondwana. *Nature*, 466(7307), pp.748–751.

Oaks, J.R., 2011. A time-calibrated species tree of Crocodylia reveals a Recent radiation of the true crocodiles. *Evolution*, 65, pp.3285–3297.

Ohno, S. et al., 2014. Production of sulphate-rich vapour during the Chicxulub impact and implications for ocean acidification. *Nature Geoscience*, 7(4), pp.279–282.

Ollivier-Pierre, M.F., 1982. La microflore du Paléocène et de l'Eocène des séries phosphatées des Ganntour (Maroc). *Bulletin des Sciences Géologiques*, 35, pp.117–127.

Petersen, S. V., Dutton, A. & Lohmann, K.C., 2016. End-Cretaceous extinction in Antarctica linked to both Deccan volcanism and meteorite impact via climate change. *Nature Communications*, 7(May), pp.1–9.

Pierazzo, E., Kring, D.A. & Melosh, H.J., 1998. Hydrocode simulation of the Chicxulub impact event and the production of climatically active gases. *Journal of Geophysical Research*, 103, p.28607.

Pierce, S.E., Angielczyk, K.D. & Rayfield, E.J., 2009. Morphospace occupation in thalattosuchian crocodylomorphs: Skull shape variation, species delineation and temporal patterns. *Palaeontology*, 52(5), pp.1057–1097.

Pierce, S.E., Angielczyk, K.D. & Rayfield, E.J., 2008. Patterns of morphospace occupation and mechanical performance in extant crocodilian skulls: A combined geometric morphometric and finite element modeling approach. *Journal of Morphology*, 269, pp.840–864.

Piras, P. et al., 2014. Morphological integration and functional modularity in the crocodilian skull. *Integrative zoology*, 9(4), pp.498–516.

Piras, P. et al., 2007. Phylogenetic position of the crocodylian *Megadontosuchus arduini* and tomistomine palaeobiogeography. *Acta Palaeontologica Polonica*, 52(2), pp.315–328.

Piras, P. et al., 2010. The *Gavialis-Tomistoma* debate: the contribution of skull ontogenetic allometry and growth trajectories to the study of crocodylian relationships. *Evolution & Development*, 12(6), pp.568–579.

Piras, P. et al., 2009. The shadow of forgotten ancestors differently constrains the fate of

Alligatoroidea and Crocodyloidea. *Global Ecology and Biogeography*, 18(1), pp.30–40.

Piras, P. & Buscalioni, A.D., 2006. *Diplocynodon muelleri* Comb. nov., an Oligocene diplocynodontine alligatoroid from Catalonia (Ebro Basin, Lleida Province, Spain). *Journal of Vertebrate Paleontology*, 26(3), pp.608–620.

Platt, S.G. et al., 2011. Size estimation, morphometrics, sex ratio, sexual size dimorphism, and biomass of *Crocodylus acutus* in the coastal zone of Belize. *Salamandra*, 47(4), pp.179–192.

Poe, S., 1996. Data set incongruence and the phylogeny of crocodilians. *Systematic Biology*, 45(4), pp.393–414.

Pol, D. & Leardi, J.M., 2015. Diversity patterns of Notosuchia (Crocodyliformes, Mesoeucrocodylia) during the Cretaceous of Gondwana. *Publicación Electrónica de la Asociación Paleontológica Argentina*, 15(1), pp.172–186.

Pol, D. & Powell, J.E., 2011. A new sebecid mesoeucrocodylian from the Rio Loro Formation (Palaeocene) of north-western Argentina. *Zoological Journal of the Linnean Society*, 163, pp.S7-36.

Polcyn, M.J. et al., 2014. Physical drivers of mosasaur evolution. *Palaeogeography, Palaeoclimatology, Palaeoecology*, 400, pp.17–27.

Pope, K.O. et al., 1997. Energy, volatile production, and climatic effects of the Chicxulub Cretaceous/ Tertiary impact. *Journal of Geophysical Research*, 102(E9), pp.21645–21664.

Puértolas-Pascual, E. et al., 2016. Review of the Late Cretaceous-early Paleogene crocodylomorphs of Europe: Extinction patterns across the K-PG boundary. *Cretaceous Research*, 57, pp.565–590.

Puértolas, E., Canudo, J.I. & Cruzado-Caballero, P., 2011. A new crocodylian from the late Maastrichtian of Spain: implications for the initial radiation of crocodyloids. *PloS ONE*, 6(6), pp.1–12.

Punekar, J. et al., 2016. A multi-proxy approach to decode the end-Cretaceous mass extinction. *Palaeogeography, Palaeoclimatology, Palaeoecology*, 441, pp.116–136.

Renne, P.R. et al., 2013. Time scales of critical events around the Cretaceous-Paleogene boundary. *Science*, 339(6120), pp.684–687.

Richard, L., 1888. *Catalogue of the fossil Reptilia and Amphibia in the British Museum (Natural history). Part 1.*, London,Printed by order of the Trustees,. Available at: http://www.biodiversitylibrary.org/item/125711.

Rieppel, O. & Reisz, R.R., 1999. The origin and early evolution of turtles. *Annual Review of Ecology and Systematics*, 30(1), pp.1–22.

Riff, D., Conquista, V. & Aguilera, O.A., 2008. The world's largest gharials *Gryposuchus*: description of *G. croizati* n. sp (Crocodylia, Gavialidae) from the Upper Miocene Urumaco Formation, Venezuela. *Paläontologische Zeitschrift*, 82, pp.178–195.

Rivera-Sylva, H.E. et al., 2011. A *Deinosuchus riograndensis* (Eusuchia: Alligatoroidea) from Coahuila, North Mexico. *Revista Mexicana de Ciencias Geologicas*, 28(2), pp.267–274.

Robertson, D.S. et al., 2013a. K-Pg extinction: Reevaluation of the heat-fire hypothesis. *Journal of Geophysical Research: Biogeosciences*, 118(1), pp.329–336.

Robertson, D.S. et al., 2013b. K-Pg extinction patterns in marine and freshwater environments: The impact winter model. *Journal of Geophysical Research: Biogeosciences*, 118(3), pp.1006–1014.

Robertson, D.S. et al., 2004. Survival in the first hours of the Cenozoic. *Bulletin of the Geological Society of America*, 116(5–6), pp.760–768.

Roos, J., Aggarwal, R.K. & Janke, A., 2007. Extended mitogenomic phylogenetic analyses yield new insight into crocodylian evolution and their survival of the Cretaceous-Tertiary boundary. *Molecular Phylogenetics and Evolution*, 45(2), pp.663–673.

Rossmann, T., Muller, J. & Forst, M., 2000. Studies on Cenozoic crocodilians: 7. First evidence of an alligatorid from Africa and its implications for crocodilian palaeobiogeography. *Neues Jahrbuch fur Geologie und Palaontologie-Monatshefte*, (12), pp.705–714.

Rothkugel, S. & Varela, S., 2015. paleoMap: spatial paleobiodiversity combined with paleogeography. Available at: https://github.com/NonaR/paleoMap.

Russell, A.P. & Wu, X., 1997. The Crocodylomorpha at and between geological boundaries: the Baden-Powell approach to change? *Zoology*, 100(3), pp.164–182.

Sadleir, R.W. & Makovicky, P.J., 2008. Cranial shape and correlated characters in crocodilian evolution. *Journal of Evolutionary Biology*, 21, pp.1578–1596.

Salas-Gismondi, R. et al., 2015. A Miocene hyperdiverse crocodylian community reveals peculiar trophic dynamics in proto-Amazonian mega-wetlands. *Proceedings of the Royal Society B: Biological Sciences*, 282, pp.4–8.

Salas-Gismondi, R. et al., 2016. A new 13 million year old gavialoid crocodylian from proto-Amazonian mega-wetlands reveals parallel evolutionary trends in skull shape linked to longirostry. *PloS ONE*, 11(4), p.e0152453.

Salas-Gismondi, R. et al., 2007. Middle Miocene crocodiles from the Fitzcarrald Arch. *European meeting of the palaeontology and stratigraphy of LatinAmerica*, 8, pp.355–360.

Salisbury, S.W., 2002. Crocodilians from the Lower Cretaceous (Berriasian) Purbeck Limestone Group of Dorset. *Special Papers in Palaeontology*, 68, pp.121–144.

Salisbury, S.W. & Willis, P.M.A., 1996. A new crocodylian from the Early Eocene of south-eastern Queensland and a preliminary investigation of the phylogenetic relationships of crocodyloids. *Alcheringa: An Australasian Journal of Palaeontology*, 20(3), pp.179–226.

Salvan, H.M., 1954. Les invertébrés fossiles des phosphates Marocains. *N. Mém. Serv. Géol. Maroc (Rabat)*, 93, pp.1–258.

Scheyer, T.M. et al., 2013. Crocodylian diversity peak and extinction in the late Cenozoic of the northern Neotropics. *Nature communications*, 4(1907), pp.1–9.

Schoene, B. et al., 2015. U-Pb geochronology of the Deccan Traps and relation to the end-Cretaceous mass extinction. *Science*, 347(6218), pp.182–184.

Schulte, P. et al., 2010. The Chicxulub asteroid impact and mass extinction at the Cretaceous-Paleogene boundary. *Science*, 327(1214), pp.1214–1218.

Schwarz, D., 2002. A new species of *Goniopholis* from the Upper Jurassic of Portugal. *Palaeontology*, 45(1), pp.185–208.

Schwarz, D. & Salisbury, S.W., 2005. A new species of *Theriosuchus* (atoposauridae, crocodylomorpha) from the Late Jurassic (Kimmeridgian) of Guimarota, Portugal. *Geobios*, 38(6), pp.779–802.

Sepkoski, J.J., 1996. Patterns of Phanerozoic Extinction: a Perspective from Global Data Bases. In O. H. Walliser, ed. *Global Events and Event Stratigraphy in the Phanerozoic: Results of the International Interdisciplinary Cooperation in the IGCP-Project 216 ``Global Biological Events in Earth History''*. Berlin, Heidelberg: Springer Berlin Heidelberg, pp. 35–51.

Sereno, P.C. et al., 2001. The giant crocodyliform *Sarcosuchus* from the Cretaceous of Africa. *Science*, 294, pp.1516–1519.

Sereno, P.C. & Larsson, H.C.E., 2009. Cretaceous crocodyliforms from the Sahara. *ZooKeys*, 28, pp.1–143.

Sheehan, P.M. & Fastovsky, D.E., 1992. Major extinctions of land-dwelling vertebrates at the Cretaceous-Tertiary boundary, eastern Montana. *Geology*, 20, pp.556–560.

Silber, S., Geisler, J.H. & Bolortsetseg, M., 2011. Unexpected resilience of species with temperature-dependent sex determination at the Cretaceous-Palaeogene boundary. *Biology letters*, 7, pp.295–298.

Sill, W.D., 1970. Nota preliminar sobre un nuevo Gavial del Plioceno de Venezuela y una discusion de los Gaviales sudamericanos. *Ameghiniana*, 7(2), pp.151–159.

Sill, W.D., 1968. The zoogeography of the Crocodilia. *Copeia*, 1968(1), pp.76–88.

Skutschas, P.P. et al., 2014. The first discovery of an alligatorid (Crocodylia, Alligatoroidea, Alligatoridae) in the Eocene of China. *Journal of Vertebrate Paleontology*, 34(2), pp.471–476.

Smit, J. & Hertogen, J., 1980. An extraterrestrial event at the Creataceous-Tertiary boundary. *Nature*, 285, pp.198–200.

Solé, F. et al., 2009. Further evidence of the African antiquity of hyaenodontid ("Creodonta", Mammalia) evolution. *Zoological Journal of the Linnean Society*, 156(4), pp.827–846.

Storrs, G.W., 2003. Late Miocene-Early Pliocene crocodilian fauna of Lothagam, southwest Turkana Basin, Kenya. In M. G. Leakey & J. M. Harris, eds. *Lothagam: The Dawn of Humanity in Eastern Africa*. pp. 137–159.

Storrs, G.W. & Efimov, M.B., 2000. Mesozoic crocodyliforms of north-central Eurasia. In M. J. Benton et al., eds. *The age of dinosaurs in Russia and Mongolia*. Cambridge University Press Cambridge, pp. 402–419.

Stubbs, T.L. et al., 2013. Morphological and biomechanical disparity of crocodile-line archosaurs following the end-Triassic extinction. *Proceedings of the Royal Society B: Biological Sciences*, 280, pp.1–9.

Stubbs, T.L. & Benton, M.J., 2016. Ecomorphological diversifications of Mesozoic marine reptiles: The roles of ecological opportunity and extinction. *Paleobiology*, 42(4), pp.547–573.

Suberbiola, X.P. et al., 2004. The first record of a sauropod dinosaur from the Late Cretaceous phosphates of Morocco. *Journal of African Earth Sciences*, 40(1–2), pp.81–88.

Sullivan, R.M. & Lucas, S.G., 2003. *Brachychampsa montana* Gilmore (Crocodylia Alligatoridae) from the Kirtland Formation (Upper Campanian) San Juan Basin New Mexico. *Journal of Vertebrate Paleontology*, 23(December), pp.832–841.

Taplin, L.E., Grigg, G.C. & Beard, L., 1985. Salt gland function in fresh water Crocodiles: evidence for a marine phase in eusuchian evolution? In G. Grigg, R. Shine, & H. Ehmann, eds. *Biology of Australasian frogs and reptiles*. Royal Zoological Society of New South Wales, pp. 402–410.

Tarsitano, S.F., Frey, E. & Riess, J., 1989. The evolution of the Crocodilia: a conflict between morphological and biochemical data. *Integrative and Comparative Biology*, 29(3), pp.843–856.

Tennant, J.P., Mannion, P.D. & Upchurch, P., 2016. Environmental drivers of crocodyliform extinction across the Jurassic/Cretaceous transition. *Proceedings of the Royal Society B: Biological Sciences*, 283(1826), p.20152840.

Toljagić, O. & Butler, R.J., 2013. Triassic–Jurassic mass extinction as trigger for the Mesozoic radiation of crocodylomorphs. *Biology Letters*, 9(3), pp.1–4.

Tong, H. & Meylan, P.A., 2013. Morphology and relationships of *Brachyopsemys tingitana* gen. et sp. nov. from the Early Paleocene of Morocco and recognition of the new eucryptodiran turtle family: Sandownidae. In *Morphology and evolution of turtles*. pp. 187–212. Available at: http://sysbio.oxfordjournals.org/cgi/doi/10.1093/sysbio/syt031.

Toula, F. & Kail, J.A., 1885. *Über einen Krokodil-Schädel aus den Tertiärablagerungen von*

Eggenburg in Niederösterreich: eine paläontologische Studie, Kaiserl. Königl. Staatsdr.

Troedsson, G.T., 1924. *On crocodilian remains from the Danian of Sweden*, Lund.

Troxell, E.L., 1925. *Hyposaurus*, a marine crocodilian. *American Journal of Science*, 54, pp.489–514.

Trueman, J.W., 1998. Reverse successive weighting. *Systematic biology*, 47(4), pp.733–737.

Turner, A.H., 2015. A review of *Shamosuchus* and *Paralligator* (Crocodyliformes, Neosuchia) from the Cretaceous of Asia. *PloS ONE*, 10(2), p.e0118116.

Vajda, V. & Bercovici, A., 2014. The global vegetation pattern across the Cretaceous-Paleogene mass extinction interval: A template for other extinction events. *Global and Planetary Change*, 122, pp.29–49.

Vélez-Juarbe, J., Brochu, C.A. & Santos, H., 2007. A gharial from the Oligocene of Puerto Rico: transoceanic dispersal in the history of a non-marine reptile. *Proceedings of the Royal Society B: Biological Sciences*, 274, pp.1245–1254.

Vellekoop, J. et al., 2014. Rapid short-term cooling following the Chicxulub impact at the Cretaceous-Paleogene boundary. *Proceedings of the National Academy of Sciences*, 111(21), pp.7537–7541.

Vincent, P. et al., 2013. New plesiosaur specimens from the Maastrichtian Phosphates of Morocco and their implications for the ecology of the latest Cretaceous marine apex predators. *Gondwana Research*, 24(2), pp.796–805.

Wagner, P.J., 2010. Paleontological perspectives on morphological evolution. In L. J. Bell MA, Futuyma DJ, Eanes WF, ed. *Evolution since Darwin: the first 150 years*. Sunderland, MA: Sinauer., pp. 451–578.

Walmsley, C.W. et al., 2013. Why the long face? The mechanics of mandibular symphysis proportions in crocodiles. *PloS ONE*, 8(1), p.e53873.

Wang, Y., Sullivan, C. & Liu, J., 2016. Taxonomic revision of *Eoalligator* (Crocodylia, Brevirostres) and the paleogeographic origins of the Chinese alligatoroids. *PeerJ*, 4, p.e2356.

Wassersug, R.J. & Hecht, M.K., 1967. The status of the crocodylid genera *Procaimanoidea* and *Hassiacosuchus* in the New World. *Herpetologica*, 23(1), pp.30–34.

Watanabe, A. & Slice, D.E., 2014. The utility of cranial ontogeny for phylogenetic inference: A case study in crocodylians using geometric morphometrics. *Journal of Evolutionary Biology*, 27(6), pp.1078–1092.

Webb, G.J.W. & Messel, H., 1978. Morphometric analysis of *Crocodylus porosus* from the north coast of Arnhem Land, northern Australia. *Australian Journal of Zoology*, 26(1), pp.1–27.

Wiest, L.A. et al., 2018. Terrestrial evidence for the Lilliput effect across the Cretaceous-Paleogene (K-Pg) boundary. *Palaeogeography, Palaeoclimatology, Palaeoecology*, 491, pp.161–169.

Wiest, L.A. et al., 2015. Trace fossil evidence suggests widespread dwarfism in response to the end-Cretaceous mass extinction: Braggs, Alabama and Brazos River, Texas. *Palaeogeography, Palaeoclimatology, Palaeoecology*, 417, pp.105–111.

Wilberg, E.W., 2017. Investigating patterns of crocodyliform cranial disparity through the Mesozoic and Cenozoic. *Zoological Journal of the Linnean Society*, XX(February), pp.1–20.

Wilf, P. et al., 2006. Decloupled plant and insect diversity after the end-Cretaceous extinction. *Science*, 313(5790), pp.1112–1115.

Wilkinson, M., Thorley, J.L. & Upchurch, P., 2000. A chain is no stronger than its weakest link: double decay analysis of phylogenetic hypotheses. *Systematic Biology*, 49(4), pp.754–776.

Williamson, T.E., 1996. ?*Brachychampsa sealeyi,* sp. nov., (Crocodylia, Alligatoroidea) from the Upper Cretaceous (Lower Campanian) Menefee Formation, Northwestern New Mexico.

Journal of Vertebrate Paleontology, 16(3), pp.421–431.

Willis, P. & Stilwell, J.D., 2000. A probable piscivorous crocodile from Eocene deposits of McMurdo Sound, East Antarctica. *Paleobiology and Paleoenvironments of Eocene Rocks: McMurdo Sound, East Antarctica*, pp.355–358.

Willis, P.M.A., Murray, P.F. & Megirian, D., 1990. *Baru darrowi* gen. et sp. nov., a large broad-snouted crocodyline (Eusuchia: Crocodylidae) from mid-Tertiary freshwater limestones in northern Australia. *Memoirs of the Queensland Museum*, 29(2), pp.521–540.

Willis, R.E. et al., 2007. Evidence for placing the false gharial (*Tomistoma schlegelii*) into the family Gavialidae: Inferences from nuclear gene sequences. *Molecular Phylogenetics and Evolution*, 43(3), pp.787–794.

Wills, M.A., Briggs, D.E.G. & Fortey, R.A., 1994. Disparity as an evolutionary index: a comparison of Cambrian and Recent arthropods. *Paleobiology*, 20(2), pp.93–130.

Wilson, G.P., 2013. Mammals across the K/Pg boundary in northeastern Montana, U.S.A.: dental morphology and body-size patterns reveal extinction selectivity and immigrant-fueled ecospace filling. *Paleobiology*, 39(03), pp.429–469.

Wu, X.-C., Russell, A.P. & Brinkman, D.B., 2001. A review of *Leidyosuchus* Lambe, 1907 (Archosauria: Crocodylia) and an assessment of cranial variation based upon new material: Erratum. *Canadian Journal of Earth Sciences*, 38, pp.1665–1587.

Wu, X., Russell, A.P. & Cumbaa, S.L., 2001. *Terminonaris* (Archosauria, Crocodyliformes): new material from Saskatchewan, Canada, and comments on its phylogenetic relationships. *Journal of Vertebrate Paleontology*, 21(3), pp.492–514.

Wu, X., Sues, H.-D. & Sun, A., 1995. A plant-eating crocodyliform reptile from the Cretaceous of China. *Nature*, 376(6542), pp.678–680.

Yans, J. et al., 2014. First carbon isotope chemostratigraphy of the Ouled Abdoun phosphate Basin, Morocco; implications for dating and evolution of earliest African placental mammals. *Gondwana Research*, 25, pp.257–269.

Young, M.T. et al., 2010. The evolution of Metriorhynchoidea (mesoeucrocodylia, thalattosuchia): an integrated approach using geometric morphometrics, analysis of disparity, and biomechanics. *Zoological Journal of the Linnean Society*, 158(4), pp.801–859.

Zachos, J.C. et al., 2001. Trends, rhythms, and aberrations in global climate 65 Ma to present. *Science*, 292(5517), pp.686–693.

Zarski, M., Jakubowski, G. & Gawor-Biedowa, E., 1998. The first Polish find of Lower Paleocene crocodile *Thoracosaurus* Leidy, 1852: geological and palaeontological description. *Geological Quarterly*, 42(2), pp.141–160.

Zelditch, M.L. et al., 2004. *Geometric morphometrics for biologists*, Elsevier.

Zittel, K.A. von et al., 1890. *Handbuch der palaeontologie, Vol. 3. Vertebrata (Pisces, Amphibia, Reptilia, Aves)*, München,R. Oldenbourg,.

Appendix 1: Supplementary Data for Chapter 2

Character list used in Chapter 2 and 3:

Modifications to the matrix from Jouve et al. (2014) are highlighted in **bold.**

1. Ventral tubercle of proatlas at least one half (0) or less than one half (1) the width of the dorsal crest.
2. Proatlas boomerang shaped (0), strap shaped (1), or massive and block shaped (2).
3. Posterior half of axis neural spine wide (0) or narrow (1).
4. Axis neural arch lacks (0) or possesses (1) a lateral process ("diapophysis'").
5. Atlas intercentrum wedge shaped in lateral view with insignificant parapophyseal processes (0) or plate shaped in lateral view with prominent parapophyseal processes at maturity (1).
6. Axial hypapophysis located toward the centre of centrum (0) or toward the anterior end of centrum (1).
7. Hypapophyseal keels extend to 11th vertebra behind atlas (0), 12th vertebra behind atlas (1), or 10th vertebra behind atlas (2).
8. First postaxial cervical vertebra with prominent hypapophysis (0) or lacks prominent hypapophysis (1).
9. Neural spine on first postaxial cervical vertebra wide with dorsal tip at least half the length of the centrum without the cotyle (0) or narrow with dorsal tip acute and less than half the length of the centrum without the cotyle (1).
10. Proatlas with prominent anterior process (0) or lacks anterior process (1).
11. Anterior half of axis neural spine oriented horizontally (0) or slopes anteriorly (1).
12. Axis neural spine crested (0) or not crested (1).
13. Anterior sacral capitulum projects far anteriorly of tuberculum and is broadly visible in dorsal view (0) or anterior margins of tuberculum and capitulum nearly in same plane and capitulum largely obscured dorsally (1).
14. Dorsal margin of atlantal rib generally smooth with modest dorsal process (0) or with prominent process (1).
15. Atlantal ribs lack (0) or possess (1) large articular facets for each other at anterior ends.
16. Atlantal ribs without (0) or with (1) very thin medial laminae at anterior end.
17. Proatlas has tall dorsal keel (0) or lacks tall dorsal keel and has a smooth dorsal side (1).
18. Presacral centra amphicoelous (0) or procoelous (1).

19. Axial hypapophysis with (0) or without (1) deep fork.

20. Axial rib tuberculum wide with broad dorsal tip (0) or narrow with acute dorsal tip (1).

21. Axial rib tuberculum contacts diapophysis late in ontogeny if at all (0) or early in ontogeny (1).

22. Scapular blade flares dorsally at maturity (0) or sides of scapular blade subparallel with minimal dorsal flare at maturity (1).

23. Deltoid crest of scapula very thin at maturity with sharp margin (0) or very wide at maturity with broad margin (1).

24. Scapulocoracoid synchondrosis closes very late in ontogeny (0) or relatively early in ontogeny (1).

25. Scapulocoracoid facet anterior to glenoid fossa uniformly narrow (0) or broad immediately anterior to glenoid fossa and tapering anteriorly (1).

26. Proximal edge of deltopectoral crest emerges smoothly from proximal end of humerus and is not obviously concave (0) or emerges abruptly from proximal end of humerus and is obviously concave (1).

27. Olecranon process of ulna narrow and subangular (0) or wide and rounded (1).

28. Dorsal margin of iliac blade rounded with smooth border (0), rounded with modest dorsal indentation (1), rounded with strong dorsal indentation (wasp-waisted) (2), narrow with dorsal indentation (3), or rounded with smooth border and posterior tip of blade very deep (4).

29. *M. teres major* and *M. dorsalis scapulae* insert separately on humerus and scars can be distinguished dorsal to deltopectoral crest (0) or insert with common tendon and single insertion scar (1).

30. Interclavicle flat along length without dorsoventral flexure (0), with moderate dorsoventral flexure (1), or with severe dorsoventral flexure (2).

31. Anterior end of interclavicle flat (0) or rodlike (1).

32. Supraacetabular crest narrow (0) or broad (1).

33. Limb bones relatively robust and hind limb much longer than forelimb at maturity (0) or limb bones very long and slender and forelimb and hind limb more equal in length at maturity (1).

34. Iliac anterior process prominent (0) or virtually absent (1).

35. Dorsal osteoderms not keeled (0) or keeled (1).

36. Dorsal midline osteoderms rectangular (0) or nearly square (1).

37. Accessory osteoderms absent (0) or maximum of one longitudinal row of transversely contiguous accessory osteoderms (1) or maximum of two longitudinal rows of transversely contiguous accessory osteoderms (2) or maximum of three sagittal longitudinal rows of transversely contiguous accessory osteoderms (3).

38. Nuchal shield grades continuously into dorsal shield (0), differentiated from dorsal shield with four nuchal osteoderms (1), differentiated from dorsal shield with six nuchal osteoderms, four central and two lateral (2), or differentiated from dorsal shield with eight nuchal osteoderms in two parallel rows (3).

39. Ventral osteoderms present, polygonal (0) or present, square (1) or present, paired ossifications that suture together (2) or absent (3).

40. Anterior margin of dorsal midline osteoderms with anterior process (0) or smooth and without process (1).

41. Splenial with anterior perforation for mandibular ramus of cranial nerve V (0) or lacks anterior perforation for mandibular ramus of cranial nerve V (1).

42. Mandibular ramus of cranial nerve V exits splenial anteriorly only (0), splenial has singular perforation for mandibular ramus of cranial nerve V posteriorly (1), or splenial has double perforation for mandibular ramus of cranial nerve V posteriorly (2).

43. Splenial participates in mandibular symphysis and splenial symphysis adjacent to no more than one dentary alveoli (0), splenial excluded from mandibular symphysis and anterior tip of splenial passes ventral to Meckelian groove (1), splenial excluded from mandibular symphysis and anterior tip of splenial passes dorsal to Meckelian groove (2), participates in the mandibular symphysis over the length of two to five teeth (3); deep splenial symphysis, participates in the mandibular symphysis over the length of five to seven teeth, and forms wide "V" within symphysis (4), or deep splenial symphysis participates in the mandibular symphysis over the length of five to seven teeth, and splenial constricted within symphysis and forms narrow "V" (5), or deep splenial symphysis, longer than seven dentary alveoli (6).

44. Articular–surangular suture simple (0) or articular bears anterior lamina dorsal to lingual foramen (1) or articular bears anterior lamina ventral to lingual foramen (2) or bears laminae above and below foramen (3).

45. Lingual foramen for articular artery and alveolar nerve perforates surangular entirely (0), or perforates surangular-angular suture (1).

46. Coronoid bounds posterior half of foramen intermandibularis medius (0), completely surrounds foramen intermandibularis medius at maturity (1), or obliterates foramen intermandibularis medius at maturity (2).

47. Angular-surangular suture contacts external mandibular fenestra at posterior angle at maturity (0) or passes broadly along ventral margin of external mandibular fenestra late in ontogeny (1).

48. Anterior processes of surangular unequal (0) or subequal to equal (1).

49. Foramen aerum at extreme lingual margin of retroarticular process (0) or set in from margin of retroarticular process (1).

50. Retroarticular process projects posteriorly (0) or projects posterodorsally (1).

51. Surangular extends to posterior end of retroarticular process (0) or pinched off anterior to tip of retroarticular process (1).

52. Alveoli for dentary teeth 3 and 4 nearly same size and confluent (0), fourth alveolus larger than third and alveoli are separated (1), or same size and separated (2).

53. Anterior dentary teeth strongly procumbent (0) or project anterodorsally (1).

54. Superior edge of coronoid slopes strongly anteriorly (0) or almost horizontal (1).

55. Inferior process of coronoid laps strongly over inner surface of Meckelian fossa (0) or remains largely on medial surface of mandible (1).

56. Coronoid imperforate (0) or with perforation posterior to foramen intermandibularis medius (1).

57. Dorsal projection of hyoid cornu flat (0) or rod-like (1).

58. Dorsal projection of hyoid cornu narrow with parallel sides (0) or flared (1).

59. Process of splenial separates angular and coronoid (0) or there is no splenial process between angular and coronoid (1).

60. Sulcus between articular and surangular (0) or articular flush against surangular (1).

61. Surangular with spur bordering the dentary throw lingually for at least one alveolus length (0) or lacking such spur (1).

62. External mandibular fenestra absent (0) or present as narrow slit, no discrete fenestral concavity on angular dorsal margin (1) or present with discrete concavity on angular dorsal margin (2) present and very large; most of foramen intermandibularis caudalis visible in lateral view (2).

63. Dorsal anterior projection of coronoid longer than ventral (0) or ventral projection longer than dorsal (1).

64. Mature skull table with significant squamosal prongs (0), with no squamosal prongs (1), or with very long posterior squamosal prongs (2).

65. Surangular-dentary suture intersects external mandibular fenestra anterior to posterodorsal corner (0) or at posterodorsal corner (1).

66. Angular extends dorsally toward or beyond anterior end of foramen intermandibularis caudalis and anterior tip acute (0) or does not extend dorsally beyond anterior end of foramen intermandibularis caudalis and anterior tip very blunt (1).

67. Surangular-angular suture lingually meets articular at ventral tip (0) or dorsal to ventral tip (1).

68. Dentary gently curved (0), deeply curved (1), or linear (2) between 4th and 10th alveoli.

69. Spina quadratojugalis prominent at maturity (0) or greatly reduced or absent at maturity (1).

70. Postorbital bar massive and anteroposteriorly extended (0) or slender and rounded in cross section (1).

71. Palatine forms anterior half of the choanal opening (0), forms anterior margin of choanal opening (1), or choanal opening entirely surrounded by the pterygoid (2).

72. Choana projects posteroventrally (0) or anteroventrally (1) at maturity.

73. Pterygoid surface lateral and anterior to internal choana flush, with choanal margin (0) or pushed inward anterolateral to choanal aperture (1) or pushed inward around choana to form neck surrounding aperture (2) or everted from flat surface to form neck surrounding aperture (3).

74. Extensive exposure of prootic on external braincase wall (0) or prootic largely obscured by quadrate and laterosphenoid externally (1).

75. Quadratojugal forms posterior angle of infratemporal fenestra (0), jugal forms posterior angle of infratemporal fenestra (1), or quadratojugal-jugal suture lies at posterior angle of infratemporal fenestra (2).

76. Postorbital contacts neither quadrate nor quadratojugal medially (0), contacts quadratojugal but not quadrate medially (1), contacts quadrate and quadratojugal at dorsal angle of infratemporal fenestra (2), or contacts quadratojugal with significant descending process (3).

77. Dentary tooth 4 occludes in notch between premaxilla and maxilla early in ontogeny (0) or occludes in pit between premaxilla and maxilla and there is no notch early in ontogeny (1).

78. All dentary teeth occlude lingual to maxillary teeth (0), occlusion pit between 7th and 8th maxillary teeth and all other dentary teeth occlude lingually (1), or dentary teeth occlude in line with maxillary toothrow (2).

79. Naris projects anterodorsally (0) or dorsally (1).

80. Quadratojugal extends to superior angle of infratemporal fenestra (0) or does not extend to superior angle of infratemporal fenestra and quadrate participates in fenestra (1).

81. Frontoparietal suture deeply within supratemporal fenestra and frontal prevents broad contact between postorbital and parietal (0), suture makes modest entry into supratemporal fenestra at maturity and postorbital and parietal are in broad contact (1), or suture on skull table entirely (2).

82. Supraoccipital exposure on dorsal skull table small (0), points posteriorly to the caudal margin of the parietal (1), absent (2), large (3), or large such that parietal is excluded from posterior edge of table (4).

83. Quadratojugal sends long anterior process along lower temporal bar (0) or sends modest process or none at all along lower temporal bar (1).

84. Dorsal and ventral rims of squamosal groove for external ear valve musculature parallel (0) or squamosal groove flares anteriorly (1).

85. Palatine-pterygoid suture nearly at (0) or far from (1) posterior angle of suborbital fenestra.

86. Frontoparietal suture concavo-convex (0) or linear (1).

87. Supratemporal fenestra with fossa and dermal bones of skull roof do not overhang rim at maturity (0), dermal bones of skull roof overhang rim of supratemporal fenestra near maturity (1), or supratemporal fenestra closes during ontogeny (2).

88. Pterygoid ramus of ectopterygoid straight, posterolateral margin of suborbital fenestra linear (0) or ramus bowed, posterolateral margin of fenestra concave (1).

89. Largest maxillary alveolus in the "first wave" is no. 3 (0), no. 5 (1), no. 4 (2), no. 4 and no. 5 are same size (3), no. 6 (4), or maxillary teeth homodont (5), or maxillary alveoli increase in diameter posteriorly toward penultimate or ultimate alveolus (6), or no. 7 (7).

90. Lateral edges of palatines parallel posteriorly (0) or flare posteriorly, producing a shelf (1).

91. Ectopterygoid abuts the last two maxillary teeth (0), does not about the maxillary teeth, and the ectopterygoid-maxillary suture parallels the toothrow (1), or maxilla broadly separates ectopterygoid from maxillary toothrow (2).

92. Shallow fossa at anteromedial corner of supratemporal fenestra (0) or no such fossa and anteromedial corner of supratemporal fenestra smooth (1).

93. Lacrimal makes broad contact with nasal and there is no posterior process of maxilla (0), maxilla sends posterior process within lachrymal (1), maxilla sends posterior process between lacrimal and prefrontal (2), or between lacrimal and nasal (3).

94. Lateral edges of palatines smooth anteriorly (0) or with lateral process projecting from palatines into suborbital fenestrae (1).

95. External naris bisected by nasals (0), nasals contact external naris but do not bisect it (1), nasals excluded, at least externally, from naris and nasals and premaxillae still in large contact (2), nasals excluded from naris and nasals and premaxillae in weak contact (3), or nasals and premaxillae not in contact (4).

96. Palpebral forms from single ossification (0) or from multiple ossifications (1).

97. Premaxilla has five teeth (0) or four teeth (1) early in posthatchling ontogeny.

98. Posterior pterygoid processes tall and prominent (0), small and project posteroventrally (1), or small and project posteriorly (2).

99. Prefrontal pillar solid (0) or with large pneumatic sinus (prefrontal recess of Witmer 1997) (1).

100. Prefrontals separated by frontals and nasals (0) or prefrontals meet medially (1).

101. Dorsal surface of rostrum curves smoothly (0) or bears medial dorsal boss (1).

102. Caudal margin of otic aperture not defined and gradually merging into the exoccipital (0) or smooth and continuous with the paroccipital process (1) or caudal margin of otic aperture inset (2).

103. Margin of orbit flush with skull surface (0), dorsal edge of orbit upturned (1), or orbital margin telescoped (2).

104. Medial parietal wall of supratemporal fenestra imperforate (0) or bearing foramina (1).

105. Maxilla has linear medial margin adjacent to suborbital fenestra (0) or bears broad shelf extending into fenestra, making lateral margin concave (1).

106. Surangular continues to dorsal tip of lateral wall of glenoid fossa (0) or truncated and not continuing dorsally (1).

107. Posterior rim of internal choana not deeply notched (0) or deeply notched (1).

108. Anterior face of palatine process rounded or pointed anteriorly (0) or invaginate (1).

109. Anterior ectopterygoid process tapers to a point (0) or is forked (1).

110. Palatine process extends (0) or does not extend (1) significantly beyond anterior end of suborbital fenestra.

111. Maxillary foramen for palatine ramus of CN-V small or not present (0) or very large (1).

112. Quadrate with small ventrally reflected medial hemicondyle (0), with small medial hemicondyle and dorsal notch for foramen aerum (1), with prominent dorsal projection between hemicondyles (2), or with expanded medial hemicondyle (3).

113. Basisphenoid thin (0) or anteroposteriorly long (1) anterior to the basioccipital.

114. Spina quadratojugalis low and near posterior angle of infratemporal fenestra (0) or high and between posterior and superior angles of infratemporal fenestra (1).

115. Laterosphenoid bridge comprised entirely of laterosphenoid (0) or with ascending process or palatine (1).

116. Ectopterygoid-pterygoid flexure disappears during ontogeny (0) or remains throughout ontogeny (1).

117. Lacrimal longer than prefrontal (0), prefrontal longer than lacrimal (1), or lacrimal and prefrontal both elongate and nearly the same length (2).

118. Palatine process generally broad anteriorly (0) or in form of thin wedge (1).

119. Basisphenoid not broadly exposed ventral to basioccipital at maturity and pterygoid short ventral to median eustachian opening (0) or basisphenoid exposed as broad sheet ventral to basioccipital at maturity and pterygoid tall ventral to median eustachian opening (1).

120. Medial jugal foramen small (0) or very large (1).

121. Quadrate foramen aerum on mediodorsal angle (0) or on dorsal surface (1) of quadrate.

122. Sulcus on anterior braincase wall lateral to basisphenoid rostrum (0) or braincase wall lateral to basisphenoid rostrum smooth with no sulcus (1).

123. Skull table surface slopes ventrally from sagittal axis (0) or is planar (1) at maturity.

124. Incisive foramen small and less than half the greatest width of premaxillae (0), extremely reduced and thin (1), large and more than half the greatest width of premaxillae (2), or large and intersects premaxillary-maxillary suture (3).

125. Vomer entirely obscured by premaxilla and maxilla (0) or exposed on palate at premaxillary-maxillary suture (1).

126. Vomer entirely obscured by maxillae and palatines (0) or exposed on palate between palatines (1).

127. Significant ventral quadrate process on lateral braincase wall (0) or quadrate-pterygoid suture linear from basisphenoid exposure to foramen ovale (1).

128. Lateral carotid foramen opens lateral (0) or dorsal (1) to basisphenoid lateral exposure at maturity.

129. Basisphenoid not exposed extensively (0) or exposed extensively (1) on braincase wall anterior to foramen ovale.

130. Capitate process of laterosphenoid oriented laterally (0) or anteroposteriorly (1) toward midline.

131. Parietal and squamosal widely separated by quadrate on posterior wall of supratemporal fenestra (0), parietal and squamosal approach each other on posterior wall of supratemporal fenestra without actually making contact (1), or parietal and squamosal meet along posterior wall of supratemporal fenestra (2).

132. Quadrate and squamosal not in contact on the external surface of the skull, posteriorly to the external auditory meatus (0) or quadratosquamosal suture extends dorsally along caudal margin of the external auditory meatus (1) or extends only to the caudoventral corner of the external auditory meatus (2).

133. Ectopterygoid extends along medial face of postorbital bar (0) or stops abruptly ventral to postorbital bar (1).

134. Two prominent projections (0) or single projection that is generally not prominent (1) on postorbital bar.

135. Maxillary toothrow laterally convex or linear (0) or laterally convex and flaring posterior to first six maxillary alveoli (1), or flaring laterally from 2nd or 3rd maxillary alveoli (2).

136. Medial process of prefrontal pillar expanded dorsoventrally (0) or anteroposteriorly (1).

137. Dorsal half of prefrontal pillar narrow (0) or expanded anteroposteriorly in dorsal half (1).

138. Medial process of prefrontal pillar wide (0) or constricted (1) at base.

139. Lateral edge of the jugal raises laterally to the postorbital bar and a gutter separates this edge from the postorbital bar (0), or lateral edge of the jugal raises laterally to the postorbital bar, and projects a shelf laterally to the postorbital bar, and the dorsal margin of the jugal is not gently convex dorsally, but shows a gentle step in lateral view (1), or lateral edge of the jugal raises laterally to the postorbital bar, but there is no or shallow gutter between the latter and postorbital bar, and the dorsal margin of the jugal is not gently convex dorsally but exhibits a step in lateral view (2) or no jugal lateral edge laterally to the postorbital bar, jugal not widens laterally and presence of a prominent notch on the ventral margin of the orbit (3).

140. Mature skull table with broad lateral curvature (0), with nearly straight lateral sides (1), or strong lateral curvature of the squamosal and only squamosal (2).

141. Exoccipital with very prominent boss on paroccipital process and process lateral to cranioquadrate opening short (0) or exoccipital with small or no boss on paroccipital process and process lateral to cranioquadrate opening long (1).

142. Premaxillary surface lateral to naris smooth (0) or with deep notch lateral to naris (1).

143. Canthi rostrales absent or very modest (0) or very prominent (1) at maturity.

144. Preorbital ridges absent or very modest (0) or very prominent (1) at maturity.

145. Dorsal premaxillary processes short and not extending beyond third maxillary alveolus (0) or long and extending beyond third maxillary alveolus (1).

146. Anterolateral border of the suborbital fenestra narrow (0) or very broad and at least twice wider than the diameter of the adjacent tooth (1).

147. Lateral eustachian canals open dorsal (0) or lateral (1) to medial eustachian canal.

148. Surface of maxilla within narial canal imperforate (0) or with multiple cecal recesses (1).

149. Ectopterygoid extends (0) or does not extend (1) to posterior tip of lateral pterygoid flange at maturity.

150. Squamosal does not extend (0) or extends (1) ventrolaterally to lateral extent of exoccipital and quadrate.

151. Otoccipitals terminate dorsal to basioccipital tubera (0), send robust process ventrally and participate in basioccipital tubera (1), or send slender process ventrally to basioccipital tubera (2).

152. Internal choana not septate (0), with septum that remains recessed within choana (1), or with septum that projects out of choana (2).

153. Posterior margin of the foramen incisivum far posterior to the last premaxillary tooth (0), posterior to the posterior margin of the penultimate premaxillary tooth (1), posterior to the posterior margin of the tooth anterior to the penultimate premaxillary tooth (2), or at the level or anterior to the tooth anterior to the penultimate premaxillary tooth (3).

154. Parietal with sinus communicating with pneumatic system (0) or solid and without sinus (1).

155. Ventral scales have (0) or lack (1) follicle gland pores.

156. Ventral collar scales not enlarged relative to other ventral scales (0), in a single enlarged row (1), or in two parallel enlarged rows (2).

157. Median pelvic keel scales form two parallel rows along most of tail length (0), form single row along tail (1), or merge with lateral keel scales to form Y-shaped keel (2).

158. Lingual osmoregulatory pores small (0) or large (1).

159. Tongue with (0) or without (1) keratinized surface.

160. M. caudofemoralis with single head (0) or with double head (longus and brevis) (1).

161. Naris circular or keyhole shaped (0) or wider than long (1) or anteroposteriorly long and prominently teardrop-shaped (2).

162. Surangular-articular suture oriented anteroposteriorly (0) or bowed strongly laterally (1) within glenoid fossa.

163. Postorbital-squamosal suture oriented ventrally (0) or passes medially (1) ventral to skull table.

164. Anterior foramen for palatine ramus of cranial nerve VII ventrolateral (0) or ventral (1) to basisphenoid rostrum.

165. Edge of the maxillary tooth lower or at the same level than the space between toothrow (0), or edge of the maxillary tooth alveoli higher than the space between the toothrows (toothrow underlined) (1), **toothrow underlined and lateral margin becoming more deeply scalloped anteriorly (2)**

166. Ventral border of the exoccipital: convex and ventrally projected, hiding the posterior opening of the cranioquadrate passage from the occipital view (0); straight, sharpen or smoothly convex and does not hide the posterior opening of the cranioquadrate passage from occipital view (1).

167. Occipital surface sloped, visible in dorsal view (0) or vertical and not visible in dorsal view (1) at maturity.

168. Ventral premaxilla-maxilla suture short and ends posteriorly before the 3rd maxillary teeth (0), or elongated and extends or exceeds the 3rd maxillary alveoli (1).

169. Less than 18 teeth (0), 18 to 22 teeth (1), or more than 22 teeth (2) **or >32 teeth (3)** on maxilla.

170. Lateral edge of the skull table at the level of the postorbital-squamosal suture situated laterally at the same level as (0), or medially to (1) the quadrate condyle in dorsal view at maturity.

171. Frontal ends **posterior or at the same level (0)**, or extends well anterior **(1)** to the anterior extension of the prefrontal.

172. Maxillary posterior process without tooth, short or absent (0) or long, longer than the distance between the three last teeth (1) in ventral view.

173. The ectopterygoid does not extend (0), extends anteriorly beyond the anterior quarter of the suborbital fenestra (1), or is such extended that it nearly excludes the maxillary from the margin of the suborbital fenestra (2).

174. Anterior process of jugal extends anterior or at the same level as (0), well posterior to the anterior process of frontal (1), or does not exceeds the anterior margin of the orbit (2).

175. Anterior process of frontal extending far anterior (0) or at the same level or posterior (1) to the anterior margin of the orbit.

176. Symphysis less extended posteriorly than the level of the thirteenth dentary tooth (0), extended between the level of the fourteenth and twentieth tooth (1) or extended beyond the twenty first tooth (2).

177. Interorbital space narrower (0), or broader (1) than the minimal width of the rostrum.

178. Ventral margin of jugal strongly convex dorsally (0) or straight (1).

179. Posterior edge of the supratemporal fenestra very thick, thicker than the lateral margin (0), as thick as the lateral margin (1), thinner than the lateral margin (2), or forms a thin crest (1).

180. Presence (0) or absence (1) of a medial crest on the basioccipital.

181. Posterior process of jugal ends posterior to (0), anterior or at the level as (1) the posterior margin of the basioccipital tubera.

182. Absence (0) or presence (1) of a posterior dentary process between splenial and angular on the ventral side.

183. Infratemporal fenestra not or slightly (0), or largely (1) visible in ventral view, laterally to the pterygoid flange.

184. Postorbital bar strongly inclined laterally (0), or vertical and not visible in dorsal view (1).

185. Dorsal margin of the articular on retroarticular process largely visible in lateral view (0), or slightly or not visible in lateral view (1).

186. Posterior margin of the orbit anterior to the posterior margin of the suborbital fenestra (0), or posterior or at the same level as the posterior margin of the suborbital fenestra (1).

187. Posterior surface of basioccipital ventral to the occipital condyle long, flat and nearly vertical (0), or short and gently curved (1).

188. Absence (0) or presence (1) of a smooth medial depression ventral to the basioccipital and posterior to the medial eustachian foramen.

189. Ventral processes of the exoccipital oriented ventrally or medioventrally (0), or oriented lateroventrally (1) in occipital view.

190. Antorbital fenestra present (0) or absent (1).

191. Distance between the tip of the snout and the anteriormost position of the premaxilla-maxilla suture in dorsal view is longer (0), or shorter (1) than the distance between the anteriormost position of the premaxilla-maxilla suture in dorsal view and the posterodorsal extremity of the premaxilla.

192. Length of the posterior process of the premaxilla: distance between the posterior margin of the external nares to the posterodorsal extremity of the premaxilla is less than twice longer (0), or at least twice longer (1) than the length between the tip of the snout and the posterior margin of the external nares.

193. Anterolateral margin of the suborbital fenestra longer (0) or as long as, or shorter (1) than the posterolateral margin.

194. Teeth and alveoli of maxilla and/or dentary circular in cross-section (0), or posterior teeth laterally compressed (1), or all teeth compressed (2).

195. Dentary symphysis extends to fourth or fifth alveolus (0) or sixth through eighth alveolus (1) or behind eighth alveolus (2).

196. Largest dentary alveolus immediately caudal to fourth is 13 or 14 (0), 13 or 14 and a series behind it (1), 11 or 12 (2), no differentiation (3), or behind 14 (4).

197. Anterolateral limit of the maxilla-premaxilla suture in dorsal view: at the level as or posterior (0), or far anterior (1) to the posterior margin of the external nares.

198. Supratemporal fenestra small and rounded (0), large, quadrangular, much wider than long, and posterior margin straight and laterally oriented (1), or wider than long, and posterior margin straight and posterolaterally oriented (2) at maturity.

199. Foramen aereum small (0), comparatively large (1), or absent (2).

200. Anterior margin of suborbital fenestra: exceeds strongly (0) or does not exceed (1) the level of the anterior margin of orbit.

201. Lateral posterior tuberosity of supraoccipital not visible (0), or visible in dorsal view (1).

202. Relative position of the three last premaxillary teeth: curves laterally or aligned in an anteroposterior line (0), or aligned in a posteromedial line (1).

203. Size of the first to tenth maxillary teeth: variation, homodontie (0), or only one tooth larger, other ones being of nearly same size (1).

204. Position of the last premaxillary tooth relative to the tooth immediately anterior: posterior (0), posterolateral (1), or posteromedial (2).

205. Premaxillae do not contact each other or in weak contact (0) or contact largely each other (1) posterior to the external nares.

206. Anterior margin of the choana anterior (0), or at the level as the posterior margin of the suborbital fenestra (1), or far posterior to the posterior margin of the suborbital fenestra and posterior margin of the choana anterior or at the level as the posterior margin of the pterygoidian wing (2), or posterior margin of the choana posterior to the posterior margin of the pterygoidian wing (3)

207. Posterolateral margin of squamosal horizontal or nearly so (0) or upturned to form a discrete horn (1).

208. Lateral margin of the orbit lateral (0) or medial or at the level as the lateral margin of the maxillary waves at the level of the 3-6 teeth (1).

209. Ventral surface of quadrate smooth or with simple muscle scars (0) or with developed ridges that form a folded surface rising ventrally to the quadrate surface and placed at its posteromedial margin (1) or with a protuberant bulky insertion near the contact with quadrate that may extend toward the centre of the quadrate (2).

210. Vertical ridge on occipital surface of paroccipital process just lateral to distal end, absent (0) or present (1).

211. Posterior margin of the choanae thick (0), or as a thin lamina (1).

212. Height of peduncle of neural arch on caudal cervical vertebrae approximately equivalent to that of peduncle on neural arch of each of the thoracic, sacral and cranial most caudal vertebrae (0) or considerably greater (1).

213. Cervical vertebrae all amphicoelous (0) or some amphicoelous and some procoelous (1) or all procoelous (2).

214. Caudal vertebrae all amphicoelous (0) or first caudal vertebra opisthoceolous or procoelous, remainder of caudal vertebrae amphicoelous (1) or first caudal vertebra opisthoceolous or procoelous, remainder of caudal vertebrae procoelous, with the degree of procoely decreasing terminally (2) or first caudal vertebra biconvex, remainder of caudal vertebrae procoelous, with the degree of procoely decreasing terminally (3).

215. Distal extremity of the ulna expanded transversely with respect to the long axis of the bone; maximum width equivalent to that of the proximal extremity (0) or proximal extremity of the ulna considerably wider than the distal extremity (1)

216. Maxillary and dentary teeth with smooth carinae (0) or serrated (1).

217. Cervical and anterior dorsal centra lack (0) or bear (1) deep pits on the ventral surface of the centrum.

218. External naris of reproductively mature males remains similar to that of females (0) or develops bony excrescence (ghara) (1).

219. External naris opens flush with dorsal surface of premaxillae (0) or circumscribed by thin crest (1).

220. Maxilla terminates in palatal view anterior to lower temporal bar (0) or comprises part of the lower temporal bar (1).

221. Penultimate maxillary alveolus less than (0) or more than (1) twice the diameter of the last maxillary alveolus.

222. Prefrontal dorsal surface smooth adjacent to orbital rim (0) or bearing discrete knob-like processes (1).

223. Anterior tip of frontal forms simple acute point (0) or forms broad, complex sutural contact with the nasals (1).

224. Premaxillary interalveolar space homogeneous (0), or second tooth separated from the first and close to the third (1).

225. Premaxillary teeth: all of nearly same size or increase in size up to the last (0), penultimate is the largest (1), or penultimate and antepenultimate nearly equal in size (2).

226. Prefrontal does not send (0) or sends (1) a process within the nasal.

227. Largest maxillary tooth in the second “wave”, posterior to the 9^{th} tooth: 9^{th} to 11^{th} (0), 12 or posterior (1), or homodont (2).

228. Anterior margin of the coronoid far anterior (0), or levelled or posterior (1) to the anterior margin of the foramen intermandibularis caudalis when exists, or the anterodorsal process of the angular on the medial surface of the mandible.

229. Iris greenish/yellowish (0) or brown (1).

230. Two or more (0) or one (1) row of postoccipital osteoderms.

231. Palatine-maxillary suture intersects suborbital fenestra at its anteromedial margin or maxilla sends a medial process that exceeds posteriorly the anterior margin of the suborbital fenestra (0) or intersects the suborbital fenestra nearly at its anteriormost limit, and no posteromedial maxillary process (1).

232. Frontal lacks (0) or bears (1) prominent midsagittal crest between orbits.

233. All cervical neural spines anteroposteriorly broad (0) or posterior neural spines thin and rod-like (1).

234. Postorbital bar continuous with anterolateral edge of skull table (0) or inset (1).

235. Maxillary teeth not widely spaced, and 7^{th} and 8^{th} teeth not more spaced than other teeth (0), maxillary teeth widely spaced and 7^{th} and 8^{th} teeth not more spaced than other teeth (1), maxillary teeth not widely spaced, and distance between 7^{th} and 8^{th} maxillary teeth wider than other intervals (2), or maxillary teeth widely spaced, and distance between 7^{th} and 8^{th} maxillary teeth wider than other intervals (3).

236. Primary choanae rounded or oval (0), or triangular in shape, and anterior margin sharp anteriorly (1).

237. Pterygoid at least 50% wider than its minimal length (0) or nearly as wide as its minimal length (1).

238. Interfenestral bar wide (0) or narrow (1).

239. Relationship between dentary tooth 1 and the premaxilla: no visible pit on ventral surface of premaxilla for receiving 1st dentary teeth (0), pit visible to receive the 1st dentary tooth on the ventral surface (1), deep pit on ventral surface to receive 1^{st} dentary tooth and pierces the dorsal surface of the skull (2), occlusal notch for the first dentary tooth (3)

240. Diastema between the last premaxillary tooth and the first maxillary tooth: no diastema, alveolar spacing to accommodate caniniform tooth only (0), small diastema/no more than 2 teeth could fill the space (1), large diastema (2)

241. Size of the second maxillary alveolus: same size as the first (0), larger than the first (1), smaller than the first (2), same size as the first and the third larger (3)

242. Size of premaxilla at widest point: same size or smaller than the maxilla at widest point (0), wider than widest width of the maxilla (1)

243. Position of the 1st three premaxillary teeth: curved (0) or linear (1)

244. Width of interorbital bar: narrow (less than 30% of the midline width of the skull table) (0) or wide (>30%) (1)

Morphological Character Matrix:

#NEXUS

BEGIN TAXA;
TITLE Taxa;
DIMENSIONS NTAX=78;
TAXLABELS
Bernissartia_fagesii Iharkutosuchus_makadii Hylaeochampsa_vectiana Allodaposuchus_precedens Borealosuchus_formidabilis Borealosuchus_wilsoni Borealosuchus_sternbergii Leidyosuchus_canadensis Boverisuchus_vorax Planocrania_datangensis Planocrania_hengdongensis Diplocynodon_darwini Stangerochampsa_mccabei Brachychampsa_montana Alligator_mississippiensis Caiman_crocodilus Mecistops_cataphractus Crocodylus_niloticus Crocodylus_porosus Crocodylus_rhombifer Crocodylus_palaeindicus Osteolaemus_tetraspis Voay_robustus Rimasuchus_lloydi Crocodylus_megarhinus Euthecodon_arambourgi Euthecodon_brumpti Brachyuranochampsa_eversolei Crocodylus_depressifrons Crocodylus_acer Crocodylus_affinis Asiatosuchus_germanicus Prodiplocynodon_langi Australosuchus_clarkae Kambara Harpacochampsa_camfieldensis Tomistoma_schlegelii Tomistoma_lusitanica Thecachampsa_antiqua Tomistoma_cairense Gavialosuchus_eggenburgensis Paratomistoma_courti Dollosuchoides_densmorei Toyotamaphimeia_machikanensis Megadontosuchus_arduini Penghusuchus_pani Thecachampsa_carolinensis Tomistoma_coppensi Eothoracosaurus_mississippiensis Thoracosaurus_neocesariensis Thoracosaurus_macrorhynchus Eosuchus_minor Eosuchus_lerichei Eogavialis_africanum Piscogavialis_jugaliperforatus Ikanogavialis_gameroi Siquisiquesuchus_venezuelensis Aktiogavialis_puertoricensis Gryposuchus_colombianus Siwalik_Gavialis Gavialis_gangeticus Kentisuchus_spenceri Maroccosuchus_sp. Maroccosuchus_zennaroi Ocepesuchus_eoafricanus Argochampsa_krebsi Argochampsa_microrhynchus Parvosuchus_daouiensis Phasmatosuchus_decipulae Alligator_sinensis Paleosuchus_palpebrosus Paleosuchus_trigonatus Crocodylus_moreletii Crocodylus_acutus Crocodylus_siamensis Crocodylus_palustris Crocodylus_mindorensis Crocodylus_johnstoni
;

END;
BEGIN CHARACTERS;
TITLE Character_Matrix;
DIMENSIONS NCHAR=244;
FORMAT DATATYPE = STANDARD GAP = - MISSING = ? SYMBOLS = " 0 1 2 3 4 5 6 7";
MATRIX
Bernissartia_fagesii
??11?1210?010????00??0?0?0000??00010101000?0?????0100??????110?0?00000100?2?00000001011003020301?00?00110100100?000?000?0???0??????0??00??0100000010?00001?????????00??000?0?0001000?0?0?0?00??0100001?0000000?0101000003?00?00000??01???00?1?00000?000

Iharkutosuchus_makadii
??0???1???20??????110?1???210200?0?1000?

3001120600?201?00?00?0?000000?00??0100???1000???1??0?0????00000100?1000???????0???00110000220001?01?1??0?0?11010141?0100010200210????0??011010001???10?1001?000010

Hylaeochampsa_vectiana
??1?????0200??1?0?000?01100600120???0?000100?0000?00??0101???0??000?1000000?0100?00?100?000????????0?001??000?21?0?00??1??00001???0???0011?????0?210????????1101??0????10?1?0?00??0?0

Allodaposuchus_precedens
??0?????120???1120000?0110?2?00??1?0??000100?00000?0???00011?000010?1?0010???110000001??0001???????0?0?000000??0?0?0?000?????010100?0??000000010?0110?????0??0000?0200????0?100?0003000

Borealosuchus_formidabilis
00000101001100??01?000000000100010000?200030000?020010?00100120000000120 0?020000001100301100200000010000000000000?021100?100000??010?1010111000000?10002???????000?0100110?000000100000110001010012000000011200000123000?00000120????00?10000002000

Borealosuchus_wilsoni
???????10???0????1???00000001???10000?20??10?0000?0010?0???011?000000120000102000100?11003011002?00000100000?00?00000211??01????0??01001?1?111????0??1000?????????000?0??01??0????0?10??????????10000020000?00?120?00??????0?0000012?????00?10??000?0?1

Borealosuchus_sternbergii
??0001?10?110000?11000000000010001000???000300?0001001???00?00200000001200001010000000100130110 12?000001000000000000?000110010000001010 11?1?111000000010001 0??????000?010011000?000010000011000100000000000000120000 0????00?000001200????00?10000003000

Leidyosuchus_canadensis
????????????????1???????1?01???0111??110?300?011110?????????2?0000001200001000000001001302101 1?000002001000000101000010101000000?101?10?1?111000010?10001?????????000?0?00110000000000?000100010010110000100102010 00???3?00?0000112010??00?10010001000

Boverisuchus_vorax
??000101??01???0?10??00000111??00010???100001?0??1?11????????2?00000?1200?0100002000100030010 01?0000011000000020?0000100?1000?1?102010???111001000?10001?????????00?0?11001000010001 00?00110001001 1?0000001020000 0?23?10?00001010????00?1?0?0102001

Planocrania_datangensis
??11??????????0?????12?????000?00?0?00?30?1?01?0??00210?????00??????0????1?00????0???0?????10001?0?????????????0???0?1?0????0100010???1??0??11002??0000000?0?00???????1??0?001???????00?12??000?001

Planocrania_hengdongensis
??0????01?11????????(1
2)?0???0?12?????010??0?0100030?1?01????002000?????01????????1????????10???0????1
1????00??0??????????00??0???00??????0010???11?00?1??0211000000010?0000?????1??0
0001?1??????0?1???0?0?000

Diplocynodon_darwini
100000?0000101000101?000?1141??00110112100101001111101??000?1?2?00000112?0?011
0000000110131?1002?00000200000000?101?000101?1000?0??12?10???111000010?10001?
??????000?011001?????0000000?0110??1000011000000010?0?000123100?00001?20????00
?100?0?0?000

Stangerochampsa_mccabei
??00?1?00?010????11??000?11010000101??110100?001??111???????12?011001121010210
1010000012121201?00?002000000?00101?0001?1?1300???????10???111000110?1?010???
????000?0110010020100010??0110001101011100100010200000 12?100?0000101010??00?
10010103010

Brachychampsa_montana
10001??00111?10001?10?00011010000?10311110100?0111111???00?112?00?00112101021
0101300000111212 01?000002000001000101000010101300000112110?1?111000110?10010
???????000?01100100201?001000?0110001101011100110010201000123100000000010000
0000010010103010

Alligator_mississippiensis
1000110001010100110111101111100001112131112010011111110000111300000011210102
1010220001012121200000100210010000010110101010100000012211011011110001001002
1011001100110110010000000000000001100010010001001000102010001231000000000100
0000010010103010

Caiman_crocodilus
1000110001100101110111011111100001111221112201111101101001110200011011210102
1111240000112121101000000211101000010101001010100000012211011021100001001021
(1 2)011101100110110010000100000000011000100(0 1)002000(0
1)000102000001231000000000100000000010010103000

Mecistops_cataphractus
100001000?001100?10101001112120001111131101110100101110010011210000001200110
0211201010011001002001000210010010030000010101100011110101011101100000011000
2101010101010110010010000010000011000100001200000002120000112310000000111001
0000013010203000

Crocodylus_niloticus
1010010011101000110101001112120001111231101110100101110010011210000001200110
0211201010011001001001000210010010030000000101100011110101011101100000111000
1101010101010110010010000010000011000100002000000000201001123100000000110010
0100012010103000

Crocodylus_porosus
1110011011001000110101000112120001111231101110100101110010011200000001200110
0211201010011001001001000210010010030000000101100011110101011101100100111000

1101010101010110010010000010000011000100000200000000020100112310000000001100101000012010103000

Crocodylus_rhombifer

0010010011101000110101001111120001111231101110100101110010011200000001202110021120101001100100100100121001001003000000010110001111010101110110000011100011010101010101100100000000100?0011000100000200000001021100012310000000011100?0100012010101000

Crocodylus_palaeindicus

????????????1????1?????????????????1??????1011?0100??111?0??0112000000012001100211221010011 0?1001?0100021001?0100300?000010010001111010101110110000011?10001????????010?0?1001??0???001???00?1000100000?000?00000?0100?????0??0000011?0???00?12?1010100?

Osteolaemus_tetraspis

??1001100100100?1101010011111201011111111011100001011100100112010000112021100210201011111001010111000210100001030000001101100011110101011111110010000110011010101011101100100000000000000011000100010200000001020000012310 0?0000101001110011001200100?1201010000?

Voay_robustus

????????????1????10???????111??101?????1101110001101110 0??0112000001120211002112210101110010 11?0100021001000103000000010?1000111101010111011001000011001????????011101100100000000000000110001000012000000010211000?23100?0000001001??00?1201010000?

Rimasuchus_lloydi

??1?????????????????????0????0120?11002112010?00?1?011?1?0100021000?0000300??00?1011000?11101?1011101100100 0??10?1???????0?0??1?001?0????001????0??00?100?012000000010201 00?????00?0000?11?0???00?12??0101000

Crocodylus_megarhinus

????????0????????1??????????????????????101???000?011??????112?000000120002?02112?101?013001?01?0100021000000 0?300000001011000?11?01010???011000000?1000?????????010?011001?0????00100??01?000100?0??000?00000?0100?????00?0000011?0???00?12010103000

Euthecodon_arambourgi

??4?????????????????????1?????1????1002112010?10?50?1?03?0?00021000?0000301??00?10?1100?1?1010101110110011 00??1003???????0???2?110?0??00?000?0??0?????101?023000000001?0000?????0??000001201???00?110?0?02000

Euthecodon_brumpti

????????????????????????????????????10???1?0411?000?021??????002110?02?12021100211 1010110150?1003?01?00210010010030??00001011100?11101010???011001100011003?????????011?2111110?0?0200000?00?0000111002300000000120000?????0??000001202???00?11010203000

Brachyuranochampsa_eversolei
??2?0?????1200?0?021020
0011011001001??00002000?0?0?030??00?0?0?1?00?1?????10???011000100?1000????????
0?0?0110010?0?0?00100?00?1000100101200000000020?000????0??00000?101???00?120?
0?01000

Crocodylus_depressifrons
???000100???1????10??00001111??00110???11010??0001011??????112?00?000120100201
10230010011001?01?01?0020000?0011301?000010?1000?1?10?010?1?01100000000100?2??
????00???011001000000000??01?000100?012000000010?0100?123101?00001110?????0
?120?0101000

Crocodylus_acer
??0????01200?0?021120
0010011001001?00?00?000?000103000000?01100011??01010?1?011000100?1000???????
?0?0?01100100000?00100?00?100010000???000000?0200000????0??00001??0????00?1?00
010?000

Crocodylus_affinis
000001000110110011010000011110000110???11010000001011100000112000000001200?01
011?2000100110010 01?0000020000000 1130?000000011000?1??01010???011000000?10001
1??????010?011001000000001000001100010000120000000002000001231 01?00001?100???
00?12010100010

Asiatosuchus_germanicus
001001?01100????1101?000?11?1???01?????1000???0001011???00??12?00000?1201?0100
001000?10?10?10?1?000002000000001130??000??0?100??1??01?10???0110000?0?10001???
????000?0110?10???10001?00?011???100?010000?0001020?000?2??00?0?001?10?????0?1
?01000300?

Prodiplocynodon_langi
??0?????1200?0?001?10
001?013?01?01?00??02000?0001130?00?01?01100001?1???10?10011000?00?10001???????
0?0?011001?00???00100?00?1000100?0??000?00000201000????0??0000?12?0???00?12010
103000

Australosuchus_clarkae
?????1?0??????????1???????1??1???0?10???110111?000?011??????112?0000001????200211
2210?00?1?11001?0?00021000?0000100?00101011000?11102010?1?0110001000100?11???
???010????001000000001?00?0?????100?002000000010?0?0??????0??0000?1100???00?12
??0102000

Kambara
??????????????????1???????1?11??00110???110111?0001011??????112?0000001201120021
120101000101100 1?0100121000000100000000101100011111 00020?010101?0110010100 11??
???010?000110010000000010??001100010000??000000010?00???????00?000001100????0?
120?0102000

Harpacochampsa_camfieldensis
??0????01?0?12?021121
1???0?1?1???1?01???2?????????000?0??0?0?100?1????201????0010??0?0??00?2???????0?

0??1?0?1?0?????0100?10?0000?00?0??000?00000?0?00?????0??000??11????????1?0?010200?

Tomistoma_schlegelii
021001001100100011010000111111000110133110500010010110000000020000020120000102102210110010111020110002100000010300000101011101111101010111011000100010003101010101010110010000010000000011000111002000001112130000012310000000?2101110011101020100 0

Tomistoma_lusitanica ??????????????????1??????????????????10???1??(35)?0?000101?????????2?000020120000102112 2?1110010?1002?0100021000000003000001010110011?1110101011?011000100?10003???????0?0?011001(0 1)??(01)00002?00001?00?10100(1 2)202?0?1121310000????00?00000120????00?110?1203000

Thecachampsa_antiqua
021001?000001000010??01011?11???01?0???1??531?????0111000????2000002?0200001021?22111000100?102?0100021000000030?000101?11000?1?001010???111000100?100031?????010?01?00110000000201?00?000010100120020100013000001????00?000000200???00?13100?0?000

Tomistoma_cairense
??501?????01???????0?2?00002?0200?01?2??20?1100050?100?????00?100000?0?30?00010?011??0?1??01?10???011?00?0???000????????10???1??10??0100000??00110001??00??0000??0?131000?????????0000??02???00?11?00202000

Gavialosuchus_eggenburgensis
??????????????????1??0?????120??0?021?2??11?0020?1302???000?100??0?0?0???001????10?0???1????0?0111100010???0??3???????0???0110010?000?00200??0??0001?100??02?0?1121?1000?????0??00?001200???00?11??1?1?0?0

Paratomistoma_courti
??00?0?010????????0?2?00?0??1???0?1?2??20?1?00????10?????000?10?0??????0?0?0?????0???10100?????1??11??0?00??00??????????10?1?1???1??00???00????1?0001???0???0??1?????0????????0?????00??0?????0?????0????0

Dollosuchoides_densmorei
0010?1?00111?????1??????011????0010???????3???00?1111???????02?00??2?0200?0?021?20?1100010011 02?11?00?000001?0?3???0011?0?1000???????10???011000100?100?2?????010?0110010000000300??0110001010012000011020200000 12?100?00001?200???00?13001201000

Toyotamaphimeia_machikanensis
001100001111?1?0010??010111111000000???100500?10?10?????00??02?00?02?020??0?001?2?1?1?007011?02?01?00210000000300??000???100??0?0??010???011000101?10?03?????00??0?10010000010030000011000111 00?20000?00213000011231 00?0000?11?1???00?10?00102000

Megadontosuchus_arduini ??????????????????1??????????????????1???????(35)???1?0??11??????0?2?00??0?0????0?021?20?0?10?1??1??1????00?1?????????????1????

10???????1??0??20110001O????1?????????0???0?1?011???010?1????0?????1?1?0???0?0100?0?0???0?2??0?????00110?????0?1???0?0?000

Penghusuchus_pani
00100?101000?01101?10?10111111?00000???110501?0001?1????00???2?00?02?0201????2??2???1??0701?10???1100?1?000000030??0210?1?1??0?0?0??010111011?00?00?1000?????????01?011?0100000100?0??00110001??0010?000??0??30000112310O??0001??11???0011010??1?000

Thecachampsa_carolinensis
???001?01???1000?10??0?01??????00100???1?0531?00??011??????002?00?02?0200?0?021?22?110001001?02?01?00?10010?00030??0010???10??????????0????11000100?100?3?????01??0110011?0?000??01?00?0000101001?0020?000130000112?100???0000200???00?1?100?03000

Tomistoma_coppensi
??3??????1?11????????2?0????2?12?????021?201010001??1(0 1
3)?2?0??0021?00???0?3???00???0?0??0???????10???01100010???00?3???????0???0110010000?0000000?00?10?010?001?0000?1121?0000????????00000120?????0?11??0200000

Eothoracosaurus_mississippiensis
??????????????????1????000??????00?00???0??40???001101??????0?0?00??2?1200?01021?00?1100050?1?03?00?00100000000000???01000?0?0??????1?00???111000100?1?001?????00??1001101?010110000??010000100?0230000?0021?0000?????00?0000002?2???00?11??0010001

Thoracosaurus_neocesariensis
???1?1?1????0????11??????01?0???0000???0??40????01?11????????1?00?0201200001021?0101100050?1003?000001100000000000?010?00000000000?000?0?111000100?10011?????000?100???0?000?1?10???1?000?1??002300001?0?1?00001?23?00?0?000???2???00?110?0?00001

Thoracosaurus_macrorhynchus
??11?1?1??0??????11??????0??0????000???0??400??00?11???????0?100000201200?0102100101110050?1003??000011000000000000?1010?000000?0?0?1000?0?111000100?10012?????000?1001100??00110100?10?000011100230000000213000O1??3?00?000001202???00?11000000000

Eosuchus_minor
???1?1????0??????11??00?0?100??000000??0?040000001111O?0??00?2?00?02?1200?0102102001100050110O2?00000?00000000030???0100000000?0?1010020?0111000100?1?1?3?????????000?10100?00000?0?100???10000101002300101?0?1?00000?2??00?00000??02???00?110?0010000

Eosuchus_lerichei
???0?1???????????1????????1???????0???????4????????11??????????0???201200?0?021?2?0110005011002?00?00?000?00000300?001000?0000????010?2?0?11100010??10113??????0?0?110100?0000010?100????000010100230010?0021200000?2?100?000010202???00?11000010000

Eogavialis_africanum
?????1??????0?????11?????????????0?????0?060??10?1111??????1?2?00002002000010210
1101100050010 02?020001200000000000000100000100?0?00100000010100010 0?101030??
????000?100100000001012 01?110000111100230000110213000 01????00?000001202????0?
110?0210000

Piscogavialis_jugaliperforatus
????????????????????????????????????0?????6????0???11???????0(1
2)?2????2?1200?000211210110005011?03?12?00?100?0000?00??001?00001000??001000???
12100010??10103???????0?0?1001201111?2013?1?11?01?1111002300001002130000 1??3?
0??000000002???10?11000200000

Ikanogavialis_gameroi
??60???00??11??????0?2?20?02?120????020?2
10??10?501?0?3?02?00?20???0?0?00???010?0?01???0??0??00???321000100??01?3???????
00??2?0?20?101020?3??????0?1111100230100100 21?00??1????0???0000?202???10?110?0
?0?0?0

Siquisiquesuchus_venezuelensis
??????????????????1?????????????0?????????60?0??0??110?0???????2????2??2???0?021??
1?1??0?50?1?0??02??01200??000?0?????10?0?0????0?????00???321000100???1?????????0
0??1?0?20??1??20?3?????0000?111?02301?11?0?1?00?0?????0????00????2????0?11??02?
0000

Aktiogavialis_puertoricensis
??0???????0?1??????11
???10????1?????2???120??0?????1?????0??00?????0001?????????????????1???????????
???0???????????10??????0011???????0??1?????0???1?????????????????????1???0??????

Gryposuchus_colombianus
??1?0?????00?????1????000?????????????0?0600000011111 00???00202000200200101021
0110101005011103?02000120000000?0100001000001000000001000???321000100?10103???
????000?100?10(0
1)0100111311?1100111101002301011102130000 1????00100000??021??10?110?0200101

Siwalik_Gavialis
????????????0????????????????????????????60???0?????????????2?0000200200?01?2?0?
101??00?01??04??20?012000?000?010????000001?000??01000???311????00?10102???????
000?1001?011110?11311?1100111100102301011102130000 1????00?000001202???10?1100
0202101

Gavialis_gangeticus
021101011000000001100000001001000 0?0003000600000011110000100020000020020000 1
021011011100501110400200012000000000100001000001000000010000003110001000101 0
200000000000100120111102113111110011110010230101110213000010231001000001202 0
0010011000202101

Kentisuchus_spenceri
??????????????????1?????????????????????????311?0?0???1??????1?2?0000??1200???02102
0?010001001101?0?000?100??100?30??0011???100011?????10???011000100?10002??????
00?0?0?1001000100001 00?001100010100??00?010020200?00??3?0??00000110????00?130
00113000

Maroccosuchus_brachygnathus
??3????0?1?11????????2?00??0?0????0???1?20?0?00?1??11?1????00?10????????????0?????1??????????10???0110001????00?????????010?0?1?010??0000?1????0?????100??1200??????0?00?0?????0??0??00??0?????0?1???0?0?001

Maroccosuchus_zennaroi
??????????????1????????????1???00110???1??30??00?1011??????112?00?0000201?00021122101000100110 1?01?0021000010013?0?0011?0?1000???001010?1?01100010??10002??????0010?011?0100000000 1000?011000100001200001002020000 0??3?0??0000011001??00?13010103000

Ocepesuchus_eoafricanus
??0?????1????0??????1???10?5??00??????00??0????????????2???1?0???????????0???11??00?????00?????????????1?0???0???0?0?1???????0001???????00???????0????????0?????00??0?????0?????0?????0

Argochampsa_krebsi ??11??????0??00???10?????0????????0??????(46)????????11??????????2????2?1200?000210110??10?5??1003?0??001100?00?000????01???00000???0?1010?1?10100010???01?0???????0?0?2001200?000?0?111?10?01111100023002010021300 00???2??0??0?0010002???00?110?0110110

Argochampsa_microrhynchus
??2????????????1?????10?5??1??3?0??00110???0???3?????1????000??????1??0????010000????0??1???????0?0?2000000???0?0?11??????111100?0??002??0021?0000????????0?0010002????0??1??0110111

Parvosuchus_daouiensis
??2??????200?????1????1???5???0?3?00?001?0??0????00???0?00??????????01??0?????10??0?0?1000????????0??110?1?0??10????1??????110110?0??0?2??002120?00?????0??0???10002???????10??02000?

Phasmatosuchus_decipulae
??2??????200?0??2??1?0?100?50?1004??20001200?00?0?00???010???0??0???0?1??001???1?00??0?1000?????????????100?300??00?01111?1??01101???0???0211?0???00001????0???0001??02????0??1000??????

Alligator_sinensis
1000111001110100110111101111100001112121012010011111 1?00??111300000011210102101022000001212110000000021010000001011010101010000001221101102111000100100210111011001101 1?0100001000000?00110001001010100100010201000123100000001010001100112010101000

Paleosuchus_palpebrosus
1000111010010111110110011113121001111321122002111101111101???200011011210102101123000111212101111000021?00110001010100101010000001221101102110000000010212011201100110110010000000 0??0?0011???10000120000000102000001231000000011100011100110010101000

Paleosuchus_trigonatus
1000111000010111110110011113121001111321122002111101111101111200011011210102
1011230001112121011110000021?0011000101010010101000000122110110211000000010212
0112011001101100100000000?0000011000100001200000001020100012310000000011100
0100011001010100

Crocodylus_moreletii
0010010011101000010 1?1001112120001111231101110100101110010011200000001200110
0211201010011001101001001210010 0(0
1)0030000000101100011110101011101100000111001101010100110011001001000001000 0
0110001000002000000010201001123100000000110010100112010101001

Crocodylus_acutus
0010010011101000011 1?1001112120001110231101110100101110010011200000001200110
0211201010011001101001001210010 0(0
1)0030000000101100011110101011101100000111001201010100110011001001000001000 0
0110001000002000000010200001123100000000110010100112010103001

Crocodylus_siamensis
1110010001111000010 1?1001012120001111231101110100101110010011200000001200110
0211201010011001001001000210010 0(0
1)0030000000101100011110101011101100100111001201010100110011001000100001000 0
0110001000002000000010201001123100000000110010101112010101001

Crocodylus_palustris
1010010111001000010 1?1001112121101111231101110100101110010011210000001200110
0211201010011001001001000210010 0(0
1)0030000000101100011110101011101100100111001201010100110011001000001000100 0
0110001000002000000010201001123100000000110010100112010103001

Crocodylus_mindorensis
1110011011001000010 1?1000112120001111231101110100101110010011200000001200110
0211201010011001001001000210010 0(0
1)0030000000101100011110101011101100100111001201010100110011001000100000100 0
0110001000002000000010201001123100000000110010100112010103001

Crocodylus_johnstoni
1110011011001000010 1?1000112120001111231101110100101110010011200000001200110
0211201010011001001001000210010 0(0
1)0030000010101100011110101011101100100111001201010100110011001001100001000 0
0100001000?2000000011200001123100000000110210100111010103000

;

END;

Table A1.1: Data for Ontogenetic regressions:

Genus	Species	Catalogue no.	Skull length (cm)	Skull table width (cm)
Crocodylus	porosus	AMNH R 7131	38.12	10.22
Crocodylus	porosus	AMNH R 7859	20.803	5.58
Crocodylus	porosus	AMNH R 15179	65.948	20.221
Crocodylus	porosus	AMNH R 24957	48.754	14.45
Crocodylus	porosus	AMNH R 24958	57.708	16.507
Crocodylus	porosus	AMNH R 29298	10.096	2.646
Crocodylus	porosus	AMNH R 58015	49.605	14.599
Crocodylus	porosus	AMNH R 58016	55.599	18.158
Crocodylus	porosus	AMNH R 66383	14.626	3.601
Crocodylus	porosus	AMNH R 66644	16.051	4.313
Crocodylus	porosus	AMNH R 69125	18.14	5.361
Crocodylus	porosus	UF 71779	49.089	14.641
Crocodylus	porosus	UF 134586	47.466	15.914
Crocodylus	porosus	USNM 38081	36.127	10.702
Crocodylus	porosus	USNM 61206	42.739	13.26
Crocodylus	porosus	USNM 67735	49.471	13.588
Crocodylus	porosus	USNM 67736	45.609	12.976
Crocodylus	porosus	USNM 122063	33.456	9.459
Crocodylus	porosus	USNM 164811	56.95	18.977
Crocodylus	porosus	USNM 210131	51.658	16.977
Crocodylus	porosus	USNM 211309	28.767	7.582
Crocodylus	porosus	USNM 211315	45.156	13.574
Crocodylus	porosus	USNM 211316	47.344	13.337
Crocodylus	porosus	USNM 211318	52.888	14.693
Crocodylus	porosus	USNM 228411	30.71	8.85
Crocodylus	porosus	USNM 228415	44.712	13.588
Crocodylus	porosus	USNM 228416	57.131	18.58
Crocodylus	porosus	USNM 509454	55.836	18.812
Crocodylus	porosus	RBINS 160	43.749	12.203
Crocodylus	porosus	RBINS 160c	18.038	5.131
Crocodylus	porosus	RBINS 161	20.608	5.742
Crocodylus	porosus	RBINS 161c	56.783	17.941
Crocodylus	porosus	RBINS 3303	17.361	4.794
Crocodylus	porosus	RBINS 13514	55.437	17.802
Crocodylus	porosus	RBINS 18140	39.36	12.589
Crocodylus	porosus	NHM 1843.8.18.4	60.694	17.906
Crocodylus	porosus	NHM 1847.3.5.33	61.374	20.553
Crocodylus	porosus	NHM 1852.12.9.2	54.449	16.933
Crocodylus	porosus	NHM 1860.9.29.2	54.161	16.223
Crocodylus	porosus	NHM 1864.9.11.1	57.121	17.074
Crocodylus	porosus	NHM 1865.8.22.1	59.025	19.366
Crocodylus	porosus	NHM 1867.4.2.188	45.551	13.468
Crocodylus	porosus	NHM 1883.6.29.3	32.32	9.17

Crocodylus	porosus	NHM 1886.5.20.3	37.569	9.879
Crocodylus	porosus	NHM 1889.5.13.12	51.204	15.2
Crocodylus	porosus	NHM 1889.5.13.13	50.742	15.93
Crocodylus	porosus	NHM 1897.12.31.2	45.451	13.932
Crocodylus	porosus	NHM 1929.2.22.5	24.872	6.578
Crocodylus	porosus	NHM 1932.8.19.1	22.779	6.176
Crocodylus	porosus	NHM 1938.1.1.6	48.09	14.224
Crocodylus	porosus	NHM LV5.9.2015	59.678	18.841
Crocodylus	porosus	NHM no data	53.692	14.927
Crocodylus	porosus	NHM no number	60.846	19.126
Crocodylus	porosus	NHM no number3	14.11	3.746
Gavialis	gangeticus	AMNH R 7138	68.036	18.481
Gavialis	gangeticus	AMNH R 15176	66.483	20.393
Gavialis	gangeticus	AMNH R 131377	43.617	12.123
Gavialis	gangeticus	AMNH R 173632	50.676	14.378
Gavialis	gangeticus	UF 118998	54.139	15.544
Gavialis	gangeticus	UF 70592	24.854	5.286
Gavialis	gangeticus	USNM 72562	37.665	8.246
Gavialis	gangeticus	NHM 1846.1.7.3	27.908	5.05
Gavialis	gangeticus	NHM 1847.12.20.4	74.921	23.134
Gavialis	gangeticus	NHM 1869.8.28.159	69.77	20.635
Gavialis	gangeticus	NHM 1896.7.7.4	44.637	10.692
Gavialis	gangeticus	NHM 1935.6.4.1	61.537	16.642
Gavialis	gangeticus	NHM 1974.3009	74.287	23.498
Gavialis	gangeticus	NHM 2005.1601	73.331	22.798
Gavialis	gangeticus	NHM found with 1896.7.7.4	25.214	5.128
Gavialis	gangeticus	NHM no number	44.717	10.367
Gavialis	gangeticus	NHM no data	80.484	24.947
Maroccosuchus	brachygnathus	MNHM.KHG.170	50	19.5
Maroccosuchus	zennaroi	MHNM.KHG.171	49.9	14.4
Maroccosuchus	zennaroi	MHNM.KHG.172	47.1	13.1
Maroccosuchus	zennaroi	MHNM.KHG.173	42.8	11.5
Maroccosuchus	zennaroi	OCP DEK-GE 385	56.3	15.8
Maroccosuchus	zennaroi	MHNT.PAL.2006.80.11	53.5	17.3
Mecistops	cataphractus	AMNH R 10074	18.946	4.502
Mecistops	cataphractus	AMNH R 10075	41.173	8.371
Mecistops	cataphractus	AMNH R 29299	39.209	9.745
Mecistops	cataphractus	AMNH R 29300	45.239	10.387
Mecistops	cataphractus	AMNH R 75424	25.07	5.79
Mecistops	cataphractus	AMNH R 107634	30.093	7.645
Mecistops	cataphractus	AMNH R 160902	36.876	8.711
Mecistops	cataphractus	UF 166780	48.217	11.677
Mecistops	cataphractus	UF 166781	37.07	8.29
Mecistops	cataphractus	RBINS 3302	57.808	12.775
Mecistops	cataphractus	RBINS 4975	34.023	8.03
Mecistops	cataphractus	RBINS 4976	29.758	7.009
Mecistops	cataphractus	RBINS 4977	34.879	8.018

Mecistops	cataphractus	RBINS 4978	39.167	8.909
Mecistops	cataphractus	RBINS 4979	36.819	8.704
Mecistops	cataphractus	RBINS 4980	32.62	7.65
Mecistops	cataphractus	RBINS 4981	38.543	8.781
Mecistops	cataphractus	RBINS 4982	33.96	7.66
Mecistops	cataphractus	RBINS 4983	32.004	7.724
Mecistops	cataphractus	RBINS 4984	24.731	5.957
Mecistops	cataphractus	RBINS 4985	27.604	6.554
Mecistops	cataphractus	RBINS 4987	53.093	12.247
Mecistops	cataphractus	RBINS 4988	54.371	12.771
Mecistops	cataphractus	RBINS 4989	45.39	10.486
Mecistops	cataphractus	RBINS 4990	52.107	12.85
Mecistops	cataphractus	RBINS 4993	53.55	12.044
Mecistops	cataphractus	RBINS 4994	54.482	12.645
Mecistops	cataphractus	RBINS 4995	52.64	12.819
Mecistops	cataphractus	RBINS 4996	50.429	11.772
Mecistops	cataphractus	RBINS 4997	57.696	14.431
Mecistops	cataphractus	RBINS 4998	48.419	11.505
Mecistops	cataphractus	RBINS 4999	51.357	11.394
Mecistops	cataphractus	RBINS 5000	57.872	14.28
Mecistops	cataphractus	RBINS 5001	57.471	12.989
Mecistops	cataphractus	RBINS 5225	52.184	12.319
Mecistops	cataphractus	RBINS 5233	40.073	9.896
Mecistops	cataphractus	RBINS 6031	24.127	6.125
Mecistops	cataphractus	RBINS 17962	47.625	11.141
Mecistops	cataphractus	RBINS 17963	55.668	13.725
Mecistops	cataphractus	RBINS 17964	58.121	13.814
Mecistops	cataphractus	RBINS 17967	55.3	13.133
Mecistops	cataphractus	RBINS 18374	31.878	7.656
Mecistops	cataphractus	NHM 1862.6.30.8	52.982	12.295
Mecistops	cataphractus	NHM 1865.4.6.1	49.965	12.083
Mecistops	cataphractus	NHM 1886.12.30.2	41.58	9.873
Mecistops	cataphractus	NHM 1900.2.27.1	50.061	12.019
Mecistops	cataphractus	NHM 1904.9.9.2	44.483	10.48
Mecistops	cataphractus	NHM 1924.5.10.1	60.114	14.033
Mecistops	cataphractus	NHM 1934.10.24.2	30.445	6.97
Mecistops	cataphractus	NHM 1934.10.24.3	39.143	8.839
Tomistoma	schlegelii	AMNH R 15177	71.517	18.129
Tomistoma	schlegelii	UF 54210	37.94	9.046
Tomistoma	schlegelii	UF 84888	40.743	11.792
Tomistoma	schlegelii	USNM 52972	51.168	11.79
Tomistoma	schlegelii	USNM 211322	79.857	20.035
Tomistoma	schlegelii	USNM 211323	65.98	16.614
Tomistoma	schlegelii	RBINS 154c	77.049	21.154
Tomistoma	schlegelii	RBINS 18141	60.473	14.442
Tomistoma	schlegelii	NHM 1848.10.31.19	55.265	13.078
Tomistoma	schlegelii	NHM 1860.11.6.8	58.512	13.359
Tomistoma	schlegelii	NHM 1893.3.6.14	48.883	10.213

Tomistoma	schlegelii	NHM 1894.2.21.1	79.428	21.267
Tomistoma	schlegelii	NHM 1899.1.31.1	36.482	7.36
Tomistoma	schlegelii	NHM 1923.6.4.6	61.502	13.864

Appendix 2: Supplementary data for Chapter 3:

Table A2.1:

Data and sources used for the time calibration of the phylogenetic trees. All references were cross checked with the PaleobiologyDatabase

Species	FAD	LAD	Reference
Bernissartia_fagesii	129	118	[1]
Iharkutosuchus_makadii	86	83	[2]
Hylaeochampsa_vectiana	129	125	[3]
Allodaposuchus_precedens	78	66	[4–6]
Borealosuchus_sternbergii	69	63	[7]
Borealosuchus_formidabilis	60	56	[7]
Borealosuchus_wilsoni	56	48.6	[7,8]
Boverisuchus_vorax	50.3	41.3	[9]
Planocrania_datangensis	61.7	58.7	[9]
Planocrania_hengdongensis	58.7	56	[9]
Asiatosuchus_germanicus	47.8	41.3	[10]
Prodiplocynodon_langi	70	67	[11,12]
Brachyuranochampsa_eversolei	46	42	[13]
Crocodylus_acer	55.8	50.3	[14]
Crocodylus_megarhinus	33	28	[15]
Mecistops_cataphractus	11.608	0	[16]
Euthecodon_arambourgi	20	15.9	[17]
Euthecodon_brumpti	11.6	0.7	[16,17]
Crocodylus_niloticus	3.6	0	[18]
Crocodylus_porosus	3.6	0	[19]
Crocodylus_rhombifer	0.01	0	[18]
Crocodylus_palaeindicus	11.608	2.588	[20]
Rimasuchus_lloydi	20.4	15.9	[21]
Osteolaemus_tetraspis	0.2	0	[18]
Voay_robustus	0.01	0	[22,23]
Harpacochampsa_camfieldensis	15.97	11.608	[24]
Australosuchus_clarkae	28	20	[25]
Kambara	56	33.9	[25,26]
Kentisuchus_spenceri	56	49	[27]
Megadontosuchus_arduini	47	41	[28]
Dollosuchoides_densmorei	47	44	[27]
Tomistoma_cairense	47	44	[29]
Tomistoma_coppensi	7	3	[30]
Tomistoma_schlegelii	2	0	[18]
Tomistoma_lusitanica	20	15.9	[28,31]
Gavialosuchus_eggenburgensis	20	15.9	[32]
Thecachampsa_antiqua	13	7.246	[33]

Thecachampsa_carolinensis	28	23	[34]
Toyotamaphimeia_machikanensis	2	0.37	[35]
Penghusuchus_pani	11.608	5.332	[36]
Paratomistoma_courti	44	42	[37]
Ocepesuchus_eoafricanus	68	66	[38]
Eothoracosaurus_mississippiensis	73	69	[39]
Thoracosaurus_macrorhynchus	70	61	[40–42]
Thoracosaurus_neocesariensis	70	61.6	[43,44]
Eogavialis_africanum	38	28	[29,45]
Aktiogavialis_puertoricensis	28	23	[46]
Piscogavialis_jugaliperforatus	7.25	5.33	[47]
Ikanogavialis_gameroi	5	3	[48]
Siquisiquesuchus_venezuelensis	23.03	15.97	[49]
Gryposuchus_colombianus	13.8	12	[50]
Siwalik_Gavialis	7	1.8	[51,52]
Gavialis_gangeticus	3	0	[53]
Argochampsa_krebsi	61.6	59	[54,55]
Argochampsa_microrhynchus	62	56	
Parvosuchus_daouiensis	62	61.6	
Phasmatosuchus_decipulae	59	56	
Eosuchus_minor	59	47	[56,57]
Eosuchus_lerichei	59	56	[58]
Maroccosuchus_zennaroi	56	49	[31,59]
Maroccosuchus_sp.	56	54	
Crocodylus_depressifrons	56	47.8	[60]
Crocodylus_affinis	50.3	46.2	[61]
Leidyosuchus_canadensis	75	73	[7,62,63]
Diplocynodon_darwini	47.8	41.3	[64]
Stangerochampsa_mccabei	70.6	66	[65]
Brachychampsa_montana	72	66	[64,66]
Alligator_mississippiensis	11	0	[64]
Caiman_crocodilus	2	0	[64]
Alligator_sinensis	3	0	[67]
Paleosuchus_palpebrosus	0.5	0	[64]
Paleosuchus_trigonatus	0.5	0	[64]
Crocodylus_moreletii	0.1	0	[18]
Crocodylus_acutus	0.3	0	[18]
Crocodylus_siamensis	0.1	0	[18]
Crocodylus_palustris	0.1	0	[18]
Crocodylus_mindorensis	0.012	0	[18]
Crocodylus_johnstoni	0.012	0	[18]

Table A2.2:

Data and sources used for the linear morphometrics of skull proportions

Species	Catalogue no.	Skull length	Rostral length	Snout width	Width in front orbits
Argochampsa krebsi	OCP DEK-GE 1201	40.4	29.9	2.9	8.2
Argochampsa krebsi	OCP DEK-GE 333	34.3	26.1	2.2	7
Argochampsa microrhynchus	MHNM.KHG.169	30.3	22.1	3.3	7.9
Dollosuchoides densmorei	IRSNB 1748	45.3	33.2	4.6	10.9
Eogavialis africanum	SMNS 11785	82.3	65.2	7.6	19.4
Eogavialis africanum	SMF R 452	99.9	79.9	8.2	22.4
Eogavialis andrewsi	KNM-LT 22943	72.2	55.9	6.1	17.1
Eogavialis gavialoides	BMNH PV R 3329	57.5	43.3	5.5	12.9
Eosuchus lerichei	IRSNB R 48	43.6	30.8	4.5	10.7
Eosuchus minor	USNM 299730	39.5	27.9	3.9	11.6
Eothoracosaurus mississippiensis	MSU 3293	90.2	71	7.3	23.9
Euthecodon arambourgi	MNHN ZEL 001	60.2	48.8	6.3	12.6
Euthecodon brumpti	KNM-ER 70 FS 53	81.7	68.6	5.5	14.5
Gavialis bengewanicus	DMR-KS-201202-1	70.2	53.3	5.5	13.7
Gavialis gangeticus	University of Bath	76.5	58.2	6.9	17.2
Gavialis gangeticus	BMNH 1846.1.7.3	28.5	21.7	1.5	3.5
Gavialosuchus eggenbergensis	KME	73.6	57.9	7.7	19.4
Gryposuchus colombianus	IGM 184696	97.8	72.5	11.6	21.6
Gryposuchus croizati	MCN-URU-2002-77	109.4	89.4	10.6	29.5
Gryposuchus croizati	AMU-CURS-58	150.9	113.9	14.4	42.9
Ikanogavialis gameroi	VF- 1165	98.9	81.8	8.4	21.5
Kentisuchus spenceri	BMNH 38975	42.8	30.9	6.2	11.3
Kentisuchus spenceri	BMNH 1753	57.1	39.9	9.5	18.9
Maomingosuhus petrolica	DM-F0001	34.2	24.25	4	8.5
Maroccosuchus brachygnathus	MNHM.KHG.170	50	34.7	11.3	18.9
Maroccosuchus zennaroi	MHNM.KHG.171	49.9	35.8	9.3	15.3
Maroccosuchus zennaroi	MHNM.KHG.172	47.1	34.4	9.2	15.7
Maroccosuchus zennaroi	MHNM.KHG.173	42.8	31	7.1	12.4
Maroccosuchus zennaroi	OCP DEK-GE 385	56.3	42	13.5	21.4
Maroccosuchus zennaroi	MHNT.PAL.2006.80.11	53.5	38.2	10.3	19.4
Megadontosuchus arduini	MGPD 1Z	56.3	40.7	9.2	16.9
Ocepesuchus eoafricanus	OCP DEK-GE 45	35	26.6	2.9	7.9
Penghusuchus pani	NMNS-005645	80.6	58.3	11.8	26.8
Parvogavialis daouiensis	MHNM.KHG.168	33.3	24.9	2.7	6.8
Phasmatosuchus decipulae	MHNM.KHG.166	59.8	50.91	3.6	8.3
Piscogavialis jugaliperforatus	SMNK 1282 PAL	114.2	95.1	7.1	19.4

Siquisiquesuchus venezuelensis	MBLUZ-P-5050	103.5	85.7	7.7	18.7
Thecachampsa antiqua	USNM 25243	93.4	69.8	9.2	24.8
Thecachampsa carolinensis	ChM PV 4279	83.4	62.7	14.3	32
Thoracosaurus scanicus	LO 3076	52.9	40.7	3.7	10.5
Tomistoma cairense	SMNS 10575	37.9	27.5	3.9	8.2
Tomistoma coppensi	NK 527'88	50.3	37.8	6	11.9
Tomistoma dowsoni	BMNH PV R 4769	98	76	12.5	28.9
Tomistoma schlegelii	BMNH 1894.2.21.1	79.6	59.5	13.1	22.7
Tomistoma schlegelii	BMNH 1899.1.31.1	36.5	26.8	2.1	5.7
Tomistoma schlegelii	BMNH 1860.11.6.8	58.3	43	5.7	12.8
Toyotamaphimaeia machikanensis	MOUF00001	102.7	78	17.8	34.1

Table A2.3:

List of taxa used in the morphometric analyses and associated information. Time bins were assigned based on FADs and LADs.

Species	Source	Reconstruction?	FAD	LAD	Environment	Reference	Figure Reference
Argochampsa krebsi	OCP DEK-GE 1201	no	61.6	59	marine	[54]	Fig. 2
Argochampsa microrhynchus	MHNM.KHG.169	yes	62	56	marine	-	Photograph
Dollosuchoides densmorei	IRSNB 1748	no	47	44	marginal marine	[27]	Text-Fig. 3
Eogavialis africanum	SMF R 452	yes	38	28	marginal marine	[29]	Tafel 1/Table p.48
Eogavialis andrewsi	KNM-LT 22943	yes	7	3	freshwater	[16]	Fig. 4.26
Eogavialis gavialoides	BMNH PV R 3329	yes	33.9	28.4	marginal marine	[45]	Plate XXIII, Fig. 3A
Eosuchus lerichei	IRSNB R 48	no	59	56	marginal marine	[58]	Fig. 2
Eosuchus minor	USNM 299730	yes	59	47	marginal marine	[56]	Fig. 9
Eothoracosaurus mississippiensis	MSU 3293	no	73	69	marginal marine	[39]	Fig. 1
Euthecodon arambourgi	MNHN ZEL 001	yes	23.03	15.97	marginal marine	[17]	Fig. 1
Euthecodon brumpti	KNM-ER 70 FS 53	no	11.608	0.781	freshwater	[16]	Photograph
Gavialis bengwanicus	DMR-KS-201202-1	no	2.6	0.8	freshwater	[68]	Fig. 2
Gavialis gangeticus (1)	BMNH 1846.1.7.3	no	3	0	freshwater	-	Photograph
Gavialis gangeticus (2)	University of Bath	no	3	0	freshwater	-	Photograph
Gavialosuchus eggenbergensis	KME	no	15	11	marginal marine	[32]	Tafel 1
Gryposuchus colombianus	IGM 184696	yes	13.8	12	freshwater	[50]	Fig. 8.5
Ikanogavialis gameroi	VF- 1165	yes	5	3	marginal marine	[48]	Fig. 1
Kentisuchus spenceri	BMNH 38975	yes	56	49	marine	[27]	Text-Fig. 2
Maomingosuchus petrolica	DM-F0001	no	37.8	33.9	freshwater	[69]	Fig. 2
Maroccosuchus brachygnathus	MNHM.KHG.170	no	56	54	marine	-	Photograph
Maroccosuchus zennaroi (1)	MHNM.KHG.171	no	56	49	marine	-	Photograph
Maroccosuchus zennaroi (2)	MHNM.KHG.172	no	56	49	marine	-	Photograph

Maroccosuchus zennaroi (3)	MHNM.KHG.173	no	56	49	marine	-	Photograph
***Maroccosuchus zennaroi* (4)**	MHNT.PAL.2006.80.11	no	56	49	marine	[31]	Fig. 8
Ocepesuchus eoafricanus	OCP DEK-GE 45	yes	68	66	marine	[38]	Fig. 4
Penghusuchus pani	NMNS-005645	yes	11.608	5.332	freshwater	[36]	Fig. 2-3
Phasmatosuchus decipulae	MHNM.KHG.166	yes	59	56	marine	-	Photograph
Piscogavialis jugaliperforatus	SMNK 1282 PAL	no	7.25	5.33	marginal marine	[47]	Fig. 2
Thecachampsa antiqua	USNM 25243	no	13	7.246	freshwater	[33]	Fig. 5b
Thecachampsa carolinensis	ChM PV 4279	no	28	23	marginal marine	[34]	Fig. 1
Thoracosaurus scanicus	LO 3076	yes	66	61	marine	[41]	Text-Fig. 3
Tomistoma schlegelii (1)	BMNH 1860.11.6.8	no	2	0	freshwater	-	Photograph
Tomistoma schlegelii (2)	BMNH 1899.1.31.1	no	2	0	freshwater	-	Photograph
Tomistoma schlegelii (3)	BMNH 1894.2.21.1	no	2	0	freshwater	-	Photograph
Toyotamaphimeia machikanensis	MOUF00001	no	2	0.37	freshwater	[35]	Fig. 7
Additional taxa included in the linear morphometrics							
Argochampsa krebsi	OCP DEK-GE 333		61.6	59	marine	[55]	Fig. 1b
Eogavialis africanum	SMNS 11785		38	28	marginal marine	[29]	Tafel 2 Fig. 4a/Table p.48
Gryposuchus croizati	MCN- URU-2002-77		11.608	5.332	marginal marine	[70]	Fig. 1
Gryposuchus croizati	AMU-CURS-58		11.608	5.332	marginal marine	[70]	Fig. 2
Kentisuchus spenceri	BMNH 1753		56	49	marine	-	Photograph
Maroccosuchus zennaroi	OCP DEK-GE 385		56	49	marine	[31]	Fig. 3b
Megadontosuchus arduini	MGPD 1Z		47	41	marine	[28]	Fig. 1
Parvosuchus daouiensis	MHNM.KHG.168		62	61.6	marine	-	Photograph
Siquisiquesuchus venezuelensis	MBLUZ-P-5050		23.03	15.97	marginal marine	[49]	Text-Fig. 1
Tomistoma cairense	SMNS 10575		47	44	marine	[29]	Tafel II Fig. 1a
Tomistoma coppensi	NK 527'88		7	3	marine	[30]	Plate III Fig. 1
Tomistoma dowsoni	BMNH PV R 4769		15.9	11.608	marginal marine	-	Photograph

Landmark file: Landmark coordinates for all specimens in the geometric morphometric analysis, quantified in TPSDig [71]. ID: arkr- *Argochampsa krebsi*, armi- *Argochampsa microrhynchus,* dolde- *Dollosuchoides densmorei*, eoaf- *Eogavialis africanum*, eoand- *Eogavialis andrewsi*, eogav- *Eogavialis gavialoides*, eole- *Eosuchus lerichei*, eomin- *Eosuchus minor*, eomis- *Eothoracosaurus mississippiensis*, euaram- *Euthecodon arambourgii*, eubr- *Euthecodon brumpti*, gavben- *Gavialis bengewanicus*, gavga1- *Gavialis gangeticus (1)*, gavga2- *Gavialis gangeticus (2)*, gegg- *Gavialosuchus eggenbergensis*, grcol- *Gryposuchus colombianis*, ikgam- *Ikanogavialis gameroi*, kensp- *Kentisuchus spenceri*, maopet- *Maomingosuchus petrolica*, marbr- *Maroccosuchus brachygnathus*, marze171- *Maroccosuchus zennaroi (1)*, marze172- *M. zennaroi (2)*, marze173- *M. zennaroi (3)*, marze- *M.zennaroi (4)*, oce- *Ocepesuchus eoafricanus*, pepan- *Penghusuchus pani*, phas- *Phasmatosuchus decipulae*, pisc- *Piscogavialis jugaliperforatus*, than- *Thecachampsa antiqua*, thcar- *Thecachampsa carolinensis*, thsc- *Thoracosaurus scanicus*, tomsch1- *Tomistoma schlegelii (1)*, tomsch2- *Tomistoma schlegelii (2),* tomsch3- *Tomistoma schlegelii* (3), toy- *Toyotamaphimeia machikanensis*

LM=32
633.00000 1049.00000
633.00000 1004.00000
635.00000 966.00000
637.00000 844.00000
641.00000 423.00000
649.00000 124.00000
579.00000 1001.00000
607.00000 960.00000
632.00000 822.00000
612.00000 334.00000
594.00000 269.00000
565.00000 254.00000
594.00000 233.00000
594.00000 233.00000
559.00000 196.00000
575.00000 191.00000
640.00000 185.00000
619.00000 148.00000
620.00000 130.00000
538.00000 76.00000
605.00000 947.00000
599.00000 893.00000
602.00000 838.00000
600.00000 783.00000
601.00000 729.00000
599.00000 674.00000
597.00000 619.00000
601.00000 565.00000
587.00000 514.00000
577.00000 460.00000
562.00000 407.00000
543.00000 356.00000

ID=arkr
SCALE=0.043288
LM=32
1441.00000 8150.00000
1462.00000 7914.00000
1472.00000 7340.00000
1495.00000 6414.00000
1519.00000 3610.00000
1612.00000 1338.00000
839.00000 7558.00000
1181.00000 7177.00000
1451.00000 6207.00000
1238.00000 2851.00000
855.00000 2174.00000
748.00000 2132.00000
1093.00000 2052.00000
1093.00000 2052.00000
753.00000 1935.00000
878.00000 1893.00000
1511.00000 1701.00000
1246.00000 1434.00000
1231.00000 1302.00000
554.00000 952.00000
1167.00000 7068.00000
1104.00000 6713.00000
1094.00000 6351.00000
1128.00000 5990.00000
1154.00000 5629.00000
1132.00000 5268.00000
1093.00000 4909.00000
1039.00000 4551.00000
935.00000 4206.00000
869.00000 3854.00000

778.00000 3504.00000
674.00000 3157.00000
ID=armi
SCALE=0.004413
LM=32
105.00000 417.00000
104.00000 403.00000
102.00000 376.00000
102.00000 368.00000
99.00000 166.00000
95.00000 46.00000
82.00000 396.00000
88.00000 346.00000
91.00000 295.00000
87.00000 126.00000
73.00000 105.00000
54.00000 97.00000
83.00000 87.00000
83.00000 84.00000
45.00000 79.00000
56.00000 73.00000
94.00000 65.00000
74.00000 52.00000
74.00000 49.00000
44.00000 37.00000
87.00000 338.00000
82.00000 322.00000
83.00000 303.00000
81.00000 284.00000
79.00000 265.00000
76.00000 247.00000
77.00000 228.00000
75.00000 209.00000
69.00000 191.00000
63.00000 173.00000
57.00000 155.00000
50.00000 137.00000
ID=dolde
SCALE=0.116248
LM=32
2046.00000 4002.00000
2045.00000 3901.00000
2046.00000 3782.00000
2052.00000 3410.00000
2096.00000 2301.00000
2092.00000 1582.00000
1924.00000 3879.00000
1984.00000 3588.00000
2032.00000 3127.00000
2015.00000 1970.00000
1933.00000 1919.00000
1892.00000 1923.00000
1999.00000 1819.00000
1992.00000 1815.00000
1808.00000 1803.00000
1854.00000 1782.00000
2076.00000 1723.00000
1974.00000 1666.00000
1967.00000 1604.00000
1755.00000 1422.00000
1985.00000 3572.00000
1960.00000 3434.00000
1962.00000 3293.00000
1962.00000 3152.00000
1955.00000 3011.00000
1949.00000 2870.00000
1957.00000 2729.00000
1951.00000 2588.00000
1931.00000 2448.00000
1900.00000 2310.00000
1848.00000 2179.00000
1793.00000 2049.00000
ID=eoaf
SCALE=0.038095
LM=32
178.00000 901.00000
181.00000 864.00000
182.00000 830.00000
184.00000 762.00000
181.00000 376.00000
188.00000 83.00000
142.00000 840.00000
163.00000 795.00000
177.00000 749.00000
162.00000 254.00000
136.00000 200.00000
109.00000 192.00000
148.00000 171.00000
139.00000 163.00000
96.00000 136.00000
113.00000 134.00000
176.00000 136.00000
156.00000 111.00000
148.00000 81.00000
80.00000 60.00000
159.00000 778.00000
151.00000 731.00000
149.00000 684.00000

150.00000 637.00000
152.00000 590.00000
148.00000 543.00000
145.00000 495.00000
142.00000 449.00000
138.00000 401.00000
129.00000 355.00000
112.00000 311.00000
89.00000 269.00000
ID=eoand
SCALE=0.105240
LM=32
262.00000 913.00000
262.00000 896.00000
263.00000 844.00000
264.00000 754.00000
269.00000 376.00000
267.00000 123.00000
216.00000 880.00000
233.00000 796.00000
260.00000 636.00000
249.00000 279.00000
214.00000 249.00000
186.00000 247.00000
214.00000 223.00000
214.00000 223.00000
163.00000 212.00000
184.00000 197.00000
256.00000 186.00000
225.00000 148.00000
225.00000 128.00000
137.00000 79.00000
229.00000 782.00000
227.00000 738.00000
228.00000 694.00000
227.00000 650.00000
226.00000 607.00000
224.00000 563.00000
224.00000 519.00000
222.00000 475.00000
215.00000 432.00000
209.00000 388.00000
197.00000 346.00000
182.00000 305.00000
ID=eogav
SCALE=0.070360
LM=32
327.00000 1592.00000
330.00000 1550.00000
337.00000 1474.00000
347.00000 1285.00000
355.00000 662.00000
352.00000 238.00000
270.00000 1488.00000
299.00000 1402.00000
343.00000 1167.00000
321.00000 519.00000
289.00000 474.00000
220.00000 447.00000
283.00000 435.00000
280.00000 408.00000
199.00000 382.00000
241.00000 358.00000
345.00000 335.00000
303.00000 284.00000
282.00000 256.00000
176.00000 217.00000
299.00000 1385.00000
285.00000 1317.00000
284.00000 1247.00000
279.00000 1175.00000
282.00000 1103.00000
272.00000 1032.00000
262.00000 961.00000
252.00000 890.00000
235.00000 820.00000
217.00000 751.00000
200.00000 681.00000
183.00000 611.00000
ID=eole
SCALE=0.031055
LM=32
641.00000 1329.00000
641.00000 1324.00000
650.00000 1259.00000
653.00000 1154.00000
644.00000 782.00000
638.00000 517.00000
607.00000 1288.00000
619.00000 1221.00000
642.00000 1098.00000
622.00000 698.00000
596.00000 673.00000
554.00000 657.00000
606.00000 647.00000
604.00000 640.00000
543.00000 622.00000
561.00000 612.00000

631.00000 593.00000
604.00000 555.00000
597.00000 538.00000
514.00000 516.00000
619.00000 1207.00000
615.00000 1165.00000
611.00000 1124.00000
609.00000 1082.00000
604.00000 1041.00000
597.00000 999.00000
588.00000 958.00000
574.00000 918.00000
559.00000 879.00000
545.00000 840.00000
532.00000 800.00000
516.00000 761.00000
ID=eomin
SCALE=0.047610
LM=32
880.00000 912.00000
882.00000 899.00000
886.00000 849.00000
893.00000 765.00000
898.00000 440.00000
912.00000 89.00000
852.00000 867.00000
864.00000 823.00000
889.00000 747.00000
875.00000 243.00000
851.00000 218.00000
816.00000 204.00000
855.00000 191.00000
855.00000 189.00000
803.00000 169.00000
823.00000 159.00000
894.00000 150.00000
872.00000 129.00000
877.00000 96.00000
787.00000 57.00000
865.00000 814.00000
860.00000 767.00000
862.00000 719.00000
863.00000 671.00000
862.00000 623.00000
861.00000 575.00000
858.00000 527.00000
849.00000 480.00000
840.00000 432.00000
829.00000 386.00000
819.00000 339.00000
807.00000 292.00000
ID=eomis
SCALE=0.104076
LM=32
1066.00000 2984.00000
1063.00000 2919.00000
1064.00000 2822.00000
1068.00000 2410.00000
1059.00000 1575.00000
1051.00000 911.00000
976.00000 2774.00000
1009.00000 2648.00000
1055.00000 2380.00000
1007.00000 1248.00000
982.00000 1154.00000
916.00000 1116.00000
981.00000 1092.00000
981.00000 1092.00000
907.00000 1048.00000
959.00000 1047.00000
1036.00000 1038.00000
1019.00000 995.00000
1007.00000 922.00000
855.00000 860.00000
1004.00000 2627.00000
992.00000 2505.00000
987.00000 2382.00000
974.00000 2260.00000
968.00000 2137.00000
967.00000 2014.00000
966.00000 1892.00000
959.00000 1769.00000
936.00000 1649.00000
900.00000 1531.00000
866.00000 1415.00000
840.00000 1295.00000
ID=euaram
SCALE=0.029239
LM=32
210.00000 919.00000
208.00000 887.00000
210.00000 861.00000
215.00000 707.00000
221.00000 308.00000
224.00000 145.00000
188.00000 875.00000
199.00000 808.00000
209.00000 696.00000

205.00000 259.00000
200.00000 226.00000
185.00000 216.00000
208.00000 200.00000
208.00000 200.00000
178.00000 183.00000
198.00000 183.00000
218.00000 183.00000
206.00000 167.00000
197.00000 144.00000
171.00000 135.00000
199.00000 798.00000
195.00000 750.00000
196.00000 702.00000
195.00000 653.00000
195.00000 604.00000
192.00000 556.00000
192.00000 507.00000
190.00000 459.00000
184.00000 411.00000
171.00000 364.00000
162.00000 317.00000
153.00000 269.00000
ID=eubr
SCALE=0.105257
LM=32
599.00000 962.00000
600.00000 932.00000
604.00000 860.00000
601.00000 542.00000
593.00000 429.00000
576.00000 178.00000
547.00000 910.00000
577.00000 857.00000
604.00000 731.00000
523.00000 347.00000
502.00000 306.00000
469.00000 302.00000
543.00000 270.00000
544.00000 262.00000
463.00000 265.00000
486.00000 258.00000
557.00000 230.00000
528.00000 204.00000
530.00000 187.00000
451.00000 160.00000
576.00000 845.00000
575.00000 798.00000
575.00000 752.00000
576.00000 705.00000
575.00000 659.00000
571.00000 612.00000
567.00000 566.00000
564.00000 520.00000
556.00000 474.00000
542.00000 429.00000
524.00000 387.00000
496.00000 381.00000
ID=gavben
SCALE=0.089229
LM=32
1933.00000 4887.00000
1934.00000 4692.00000
1933.00000 4508.00000
1861.00000 2573.00000
1845.00000 1795.00000
1817.00000 342.00000
1759.00000 4720.00000
1831.00000 4400.00000
1920.00000 3904.00000
1691.00000 1295.00000
1591.00000 1030.00000
1415.00000 1009.00000
1662.00000 836.00000
1670.00000 803.00000
1394.00000 766.00000
1477.00000 725.00000
1765.00000 609.00000
1673.00000 502.00000
1672.00000 422.00000
1403.00000 318.00000
1822.00000 4347.00000
1806.00000 4077.00000
1796.00000 3805.00000
1791.00000 3532.00000
1778.00000 3259.00000
1760.00000 2987.00000
1746.00000 2715.00000
1728.00000 2442.00000
1704.00000 2170.00000
1675.00000 1899.00000
1617.00000 1633.00000
1475.00000 1414.00000
ID=gavga1
SCALE=0.006206
LM=32
1399.00000 5147.00000
1386.00000 4968.00000

1389.00000 4727.00000
1391.00000 3201.00000
1386.00000 2582.00000
1399.00000 1195.00000
1144.00000 4944.00000
1252.00000 4596.00000
1392.00000 4193.00000
1143.00000 2001.00000
1032.00000 1850.00000
848.00000 1827.00000
1062.00000 1702.00000
1062.00000 1702.00000
841.00000 1567.00000
908.00000 1542.00000
1326.00000 1491.00000
1184.00000 1312.00000
1195.00000 1279.00000
820.00000 1065.00000
1250.00000 4558.00000
1241.00000 4333.00000
1232.00000 4108.00000
1233.00000 3882.00000
1223.00000 3657.00000
1213.00000 3432.00000
1206.00000 3207.00000
1193.00000 2982.00000
1167.00000 2758.00000
1118.00000 2538.00000
979.00000 2232.00000
884.00000 2171.00000
ID=gavga2
SCALE=0.019607
LM=32
398.00000 1332.00000
399.00000 1313.00000
401.00000 1231.00000
409.00000 1081.00000
432.00000 507.00000
441.00000 192.00000
341.00000 1267.00000
363.00000 1135.00000
400.00000 860.00000
402.00000 371.00000
349.00000 324.00000
312.00000 304.00000
387.00000 298.00000
395.00000 284.00000
303.00000 284.00000
336.00000 241.00000
433.00000 246.00000
362.00000 200.00000
376.00000 176.00000
236.00000 71.00000
362.00000 1110.00000
355.00000 1048.00000
354.00000 985.00000
353.00000 923.00000
352.00000 860.00000
351.00000 797.00000
349.00000 735.00000
347.00000 672.00000
332.00000 611.00000
317.00000 550.00000
298.00000 490.00000
280.00000 430.00000
ID=gegg
SCALE=0.064101
LM=32
1275.00000 3197.00000
1273.00000 3109.00000
1275.00000 3023.00000
1292.00000 2629.00000
1305.00000 1882.00000
1307.00000 1262.00000
1136.00000 3074.00000
1196.00000 2882.00000
1287.00000 2626.00000
1201.00000 1698.00000
1133.00000 1611.00000
1029.00000 1619.00000
1149.00000 1531.00000
1149.00000 1531.00000
1005.00000 1487.00000
1050.00000 1461.00000
1278.00000 1432.00000
1157.00000 1364.00000
1161.00000 1332.00000
963.00000 1168.00000
1195.00000 2871.00000
1196.00000 2767.00000
1192.00000 2664.00000
1196.00000 2560.00000
1192.00000 2457.00000
1188.00000 2353.00000
1186.00000 2250.00000
1188.00000 2146.00000
1177.00000 2043.00000
1160.00000 1941.00000

1130.00000 1842.00000
1072.00000 1756.00000
ID=grcol
SCALE=0.051535
LM=32
214.00000 1501.00000
214.00000 1495.00000
214.00000 1425.00000
215.00000 1163.00000
225.00000 579.00000
234.00000 240.00000
162.00000 1446.00000
181.00000 1369.00000
211.00000 1160.00000
193.00000 425.00000
176.00000 365.00000
115.00000 361.00000
183.00000 330.00000
181.00000 324.00000
93.00000 293.00000
114.00000 286.00000
214.00000 289.00000
179.00000 259.00000
187.00000 247.00000
90.00000 236.00000
180.00000 1361.00000
164.00000 1277.00000
165.00000 1191.00000
162.00000 1106.00000
160.00000 1020.00000
160.00000 934.00000
157.00000 849.00000
151.00000 763.00000
142.00000 678.00000
140.00000 593.00000
117.00000 516.00000
88.00000 436.00000
ID=ikgam
SCALE=0.080622
LM=32
468.00000 859.00000
469.00000 843.00000
468.00000 777.00000
468.00000 777.00000
453.00000 375.00000
455.00000 66.00000
416.00000 793.00000
434.00000 724.00000
447.00000 611.00000
422.00000 241.00000
401.00000 200.00000
361.00000 178.00000
420.00000 167.00000
415.00000 163.00000
347.00000 142.00000
372.00000 124.00000
444.00000 127.00000
413.00000 94.00000
406.00000 68.00000
344.00000 43.00000
432.00000 703.00000
425.00000 664.00000
419.00000 624.00000
412.00000 586.00000
406.00000 546.00000
407.00000 506.00000
399.00000 467.00000
390.00000 429.00000
375.00000 392.00000
362.00000 354.00000
350.00000 316.00000
336.00000 279.00000
ID=kensp
SCALE=0.052629
LM=32
390.00000 1963.00000
391.00000 1932.00000
388.00000 1786.00000
385.00000 1616.00000
376.00000 1011.00000
383.00000 397.00000
294.00000 1868.00000
328.00000 1706.00000
371.00000 1479.00000
321.00000 794.00000
271.00000 706.00000
202.00000 666.00000
300.00000 630.00000
297.00000 623.00000
187.00000 562.00000
225.00000 555.00000
365.00000 534.00000
285.00000 483.00000
279.00000 393.00000
139.00000 314.00000
323.00000 1674.00000
314.00000 1598.00000
308.00000 1522.00000

303.00000 1446.00000
290.00000 1372.00000
286.00000 1296.00000
285.00000 1220.00000
276.00000 1144.00000
257.00000 1070.00000
234.00000 998.00000
207.00000 926.00000
180.00000 855.00000
ID=maopet
SCALE=0.021833
LM=32
1029.00000 3559.00000
1031.00000 3508.00000
1050.00000 3242.00000
1045.00000 3287.00000
1011.00000 2120.00000
987.00000 1147.00000
802.00000 3276.00000
897.00000 3155.00000
1016.00000 2879.00000
884.00000 1794.00000
763.00000 1612.00000
649.00000 1584.00000
805.00000 1513.00000
784.00000 1477.00000
596.00000 1418.00000
687.00000 1391.00000
946.00000 1330.00000
822.00000 1253.00000
822.00000 1131.00000
553.00000 988.00000
858.00000 3023.00000
801.00000 2927.00000
746.00000 2830.00000
696.00000 2731.00000
701.00000 2621.00000
727.00000 2514.00000
704.00000 2408.00000
659.00000 2306.00000
626.00000 2199.00000
591.00000 2094.00000
562.00000 1986.00000
530.00000 1879.00000
ID=marbr
SCALE=0.021186
LM=32
3021.00000 9256.00000
2976.00000 8849.00000
3034.00000 8285.00000
3019.00000 8513.00000
3033.00000 4528.00000
3068.00000 2011.00000
2415.00000 8551.00000
2674.00000 7986.00000
2905.00000 7102.00000
2744.00000 3660.00000
2530.00000 3260.00000
2323.00000 3130.00000
2722.00000 2900.00000
2668.00000 2831.00000
2134.00000 2849.00000
2409.00000 2594.00000
2937.00000 2568.00000
2708.00000 2304.00000
2711.00000 2064.00000
2157.00000 1707.00000
2674.00000 7916.00000
2552.00000 7587.00000
2455.00000 7228.00000
2332.00000 6877.00000
2338.00000 6510.00000
2356.00000 6139.00000
2304.00000 5774.00000
2226.00000 5411.00000
2145.00000 5048.00000
2088.00000 4681.00000
2046.00000 4312.00000
1957.00000 3951.00000
ID=marze171
SCALE=0.006935
LM=32
8324.00000 8885.00000
8322.00000 8660.00000
8307.00000 8021.00000
8313.00000 8246.00000
8356.00000 4737.00000
8275.00000 2077.00000
7732.00000 8152.00000
7958.00000 7648.00000
8198.00000 6870.00000
8110.00000 3724.00000
7848.00000 3370.00000
7576.00000 3260.00000
7977.00000 3020.00000
7932.00000 2965.00000
7366.00000 2860.00000
7687.00000 2686.00000

8255.00000 2607.00000
7893.00000 2369.00000
7842.00000 2165.00000
7252.00000 2011.00000
7955.00000 7582.00000
7824.00000 7261.00000
7718.00000 6931.00000
7608.00000 6602.00000
7592.00000 6256.00000
7713.00000 5801.00000
7636.00000 5617.00000
7492.00000 5302.00000
7368.00000 4978.00000
7267.00000 4646.00000
7162.00000 4316.00000
7059.00000 3985.00000
ID=marze172
SCALE=0.006916
LM=32
672.00000 919.00000
672.00000 888.00000
674.00000 831.00000
674.00000 839.00000
673.00000 422.00000
688.00000 135.00000
611.00000 844.00000
635.00000 780.00000
659.00000 689.00000
642.00000 321.00000
630.00000 263.00000
599.00000 243.00000
652.00000 228.00000
637.00000 215.00000
581.00000 212.00000
619.00000 184.00000
670.00000 191.00000
646.00000 155.00000
641.00000 127.00000
580.00000 91.00000
635.00000 778.00000
624.00000 741.00000
616.00000 702.00000
605.00000 664.00000
597.00000 624.00000
598.00000 584.00000
603.00000 544.00000
597.00000 505.00000
586.00000 466.00000
576.00000 427.00000
568.00000 387.00000
563.00000 347.00000
ID=marze173
SCALE=0.053760
LM=32
1166.00000 911.00000
1167.00000 900.00000
1165.00000 847.00000
1165.00000 850.00000
1164.00000 515.00000
1164.00000 270.00000
1113.00000 842.00000
1133.00000 799.00000
1151.00000 731.00000
1131.00000 437.00000
1112.00000 399.00000
1085.00000 376.00000
1127.00000 358.00000
1127.00000 357.00000
1069.00000 350.00000
1096.00000 328.00000
1153.00000 325.00000
1129.00000 301.00000
1128.00000 280.00000
1053.00000 242.00000
1132.00000 788.00000
1122.00000 759.00000
1113.00000 728.00000
1098.00000 700.00000
1092.00000 669.00000
1096.00000 638.00000
1104.00000 608.00000
1088.00000 581.00000
1076.00000 551.00000
1066.00000 521.00000
1060.00000 490.00000
1051.00000 460.00000
ID=marze
SCALE=0.084022
LM=32
165.00000 800.00000
165.00000 784.00000
165.00000 757.00000
164.00000 704.00000
162.00000 407.00000
160.00000 208.00000
140.00000 756.00000
147.00000 740.00000
158.00000 663.00000

150.00000 326.00000
126.00000 284.00000
111.00000 276.00000
131.00000 273.00000
131.00000 273.00000
108.00000 255.00000
117.00000 254.00000
154.00000 245.00000
137.00000 217.00000
138.00000 210.00000
101.00000 204.00000
146.00000 740.00000
143.00000 704.00000
141.00000 669.00000
141.00000 632.00000
139.00000 596.00000
138.00000 560.00000
136.00000 525.00000
132.00000 489.00000
127.00000 453.00000
116.00000 419.00000
105.00000 385.00000
95.00000 350.00000
ID=oce
SCALE=0.058136
LM=32
289.00000 876.00000
289.00000 857.00000
289.00000 827.00000
289.00000 672.00000
286.00000 328.00000
285.00000 82.00000
259.00000 841.00000
261.00000 788.00000
284.00000 645.00000
258.00000 260.00000
234.00000 225.00000
199.00000 208.00000
246.00000 187.00000
247.00000 179.00000
185.00000 186.00000
212.00000 163.00000
268.00000 154.00000
246.00000 128.00000
238.00000 90.00000
154.00000 61.00000
258.00000 781.00000
251.00000 737.00000
241.00000 693.00000
239.00000 648.00000
229.00000 604.00000
235.00000 559.00000
234.00000 514.00000
225.00000 469.00000
209.00000 427.00000
192.00000 385.00000
176.00000 342.00000
162.00000 299.00000
ID=pepan
SCALE=0.102036
LM=32
533.00000 1599.00000
533.00000 1584.00000
532.00000 1527.00000
540.00000 680.00000
531.00000 404.00000
527.00000 192.00000
494.00000 1555.00000
508.00000 1490.00000
535.00000 1357.00000
509.00000 326.00000
480.00000 295.00000
439.00000 290.00000
475.00000 277.00000
475.00000 277.00000
436.00000 254.00000
443.00000 248.00000
515.00000 240.00000
486.00000 209.00000
479.00000 199.00000
414.00000 166.00000
506.00000 1474.00000
507.00000 1372.00000
507.00000 1270.00000
507.00000 1168.00000
509.00000 1066.00000
507.00000 964.00000
503.00000 863.00000
505.00000 761.00000
504.00000 659.00000
497.00000 557.00000
477.00000 457.00000
445.00000 361.00000
ID=phas
SCALE=0.050666
LM=32
216.00000 1452.00000
217.00000 1418.00000

217.00000 1374.00000
220.00000 1164.00000
214.00000 573.00000
199.00000 145.00000
169.00000 1376.00000
188.00000 1323.00000
217.00000 1161.00000
179.00000 344.00000
139.00000 285.00000
91.00000 275.00000
145.00000 255.00000
146.00000 250.00000
90.00000 219.00000
106.00000 213.00000
188.00000 212.00000
141.00000 176.00000
169.00000 160.00000
68.00000 70.00000
188.00000 1321.00000
185.00000 1238.00000
188.00000 1154.00000
183.00000 1066.00000
179.00000 978.00000
177.00000 889.00000
171.00000 800.00000
170.00000 712.00000
164.00000 623.00000
147.00000 535.00000
124.00000 449.00000
98.00000 364.00000
ID=pisc
SCALE=0.079355
LM=32
697.00000 964.00000
698.00000 947.00000
697.00000 881.00000
697.00000 787.00000
695.00000 416.00000
697.00000 131.00000
651.00000 898.00000
664.00000 823.00000
686.00000 716.00000
674.00000 307.00000
637.00000 263.00000
602.00000 248.00000
646.00000 224.00000
646.00000 221.00000
590.00000 197.00000
611.00000 182.00000
687.00000 184.00000
646.00000 148.00000
640.00000 128.00000
572.00000 97.00000
661.00000 804.00000
655.00000 761.00000
655.00000 717.00000
656.00000 674.00000
652.00000 630.00000
646.00000 588.00000
642.00000 544.00000
635.00000 501.00000
620.00000 460.00000
609.00000 418.00000
597.00000 376.00000
590.00000 333.00000
ID=than
SCALE=0.111962
LM=32
821.00000 935.00000
821.00000 901.00000
821.00000 869.00000
821.00000 785.00000
818.00000 488.00000
798.00000 262.00000
771.00000 847.00000
779.00000 800.00000
809.00000 709.00000
785.00000 395.00000
764.00000 370.00000
722.00000 359.00000
767.00000 338.00000
761.00000 335.00000
708.00000 334.00000
728.00000 320.00000
799.00000 308.00000
754.00000 293.00000
751.00000 264.00000
661.00000 240.00000
778.00000 798.00000
767.00000 765.00000
764.00000 730.00000
764.00000 695.00000
756.00000 661.00000
750.00000 626.00000
751.00000 591.00000
742.00000 558.00000
727.00000 525.00000
708.00000 497.00000

686.00000 469.00000
671.00000 437.00000
ID=thcar
SCALE=0.119014
LM=32
416.00000 1146.00000
418.00000 1115.00000
419.00000 1059.00000
416.00000 797.00000
409.00000 429.00000
406.00000 140.00000
383.00000 1089.00000
396.00000 1023.00000
416.00000 864.00000
379.00000 315.00000
352.00000 275.00000
307.00000 257.00000
347.00000 248.00000
347.00000 248.00000
296.00000 218.00000
316.00000 214.00000
389.00000 204.00000
348.00000 172.00000
355.00000 150.00000
286.00000 107.00000
395.00000 1009.00000
387.00000 949.00000
385.00000 888.00000
382.00000 828.00000
383.00000 767.00000
382.00000 707.00000
379.00000 646.00000
376.00000 586.00000
370.00000 525.00000
354.00000 467.00000
331.00000 411.00000
307.00000 355.00000
ID=thsc
SCALE=0.051010
LM=32
1835.00000 5539.00000
1843.00000 5399.00000
1853.00000 5180.00000
1903.00000 4167.00000
2006.00000 2431.00000
2101.00000 1129.00000
1680.00000 5315.00000
1756.00000 4846.00000
1891.00000 4031.00000
1940.00000 2083.00000
1840.00000 1812.00000
1717.00000 1740.00000
1906.00000 1614.00000
1886.00000 1587.00000
1679.00000 1496.00000
1788.00000 1493.00000
2020.00000 1395.00000
1917.00000 1282.00000
1923.00000 1123.00000
1629.00000 1007.00000
1753.00000 4780.00000
1751.00000 4553.00000
1761.00000 4324.00000
1771.00000 4095.00000
1766.00000 3867.00000
1781.00000 3639.00000
1791.00000 3410.00000
1791.00000 3181.00000
1773.00000 2953.00000
1742.00000 2727.00000
1701.00000 2501.00000
1661.00000 2276.00000
ID=tomsch1
SCALE=0.008239
LM=32
2214.00000 4830.00000
2190.00000 4670.00000
2168.00000 4457.00000
2082.00000 3417.00000
1970.00000 1970.00000
1884.00000 781.00000
2010.00000 4608.00000
2026.00000 4165.00000
2049.00000 3354.00000
1813.00000 1676.00000
1730.00000 1435.00000
1580.00000 1367.00000
1771.00000 1247.00000
1728.00000 1212.00000
1538.00000 1172.00000
1614.00000 1115.00000
1853.00000 1060.00000
1716.00000 954.00000
1696.00000 792.00000
1320.00000 647.00000
2014.00000 4115.00000
1988.00000 4064.00000
1952.00000 3712.00000

1913.00000 3465.00000
1875.00000 3406.00000
1883.00000 3303.00000
1832.00000 2891.00000
1792.00000 2687.00000
1734.00000 2488.00000
1663.00000 2293.00000
1590.00000 2098.00000
1522.00000 1902.00000
ID=tomsch2
SCALE=0.014486
LM=32
1590.00000 5425.00000
1563.00000 5198.00000
1535.00000 4925.00000
1487.00000 3956.00000
1389.00000 2227.00000
1311.00000 875.00000
1269.00000 5054.00000
1313.00000 4613.00000
1434.00000 3825.00000
1226.00000 1812.00000
1058.00000 1517.00000
943.00000 1488.00000
1166.00000 1357.00000
1131.00000 1311.00000
838.00000 1251.00000
978.00000 1189.00000
1271.00000 1139.00000
1106.00000 1003.00000
1127.00000 838.00000
649.00000 675.00000
1297.00000 4528.00000
1251.00000 4301.00000
1210.00000 4072.00000
1152.00000 3848.00000
1112.00000 3620.00000
1073.00000 3392.00000
1024.00000 3165.00000
984.00000 2937.00000
932.00000 2711.00000
876.00000 2485.00000
810.00000 2263.00000
736.00000 2043.00000
ID=tomsch3
SCALE=0.017482
LM=32
189.00000 684.00000
189.00000 674.00000
193.00000 637.00000
196.00000 542.00000
191.00000 255.00000
186.00000 74.00000
159.00000 645.00000
169.00000 580.00000
189.00000 460.00000
171.00000 200.00000
155.00000 166.00000
124.00000 149.00000
157.00000 149.00000
158.00000 149.00000
121.00000 137.00000
134.00000 127.00000
181.00000 105.00000
155.00000 84.00000
156.00000 79.00000
94.00000 64.00000
171.00000 578.00000
166.00000 545.00000
162.00000 511.00000
157.00000 477.00000
148.00000 444.00000
146.00000 410.00000
144.00000 376.00000
131.00000 345.00000
117.00000 314.00000
105.00000 282.00000
94.00000 250.00000
87.00000 217.00000
ID=toy
SCALE=0.166656

Sliders file to designate semilandmarks in R:

#Landmark 21 and 32 represent the anchor points for the curve

before	slide	after
21	22	23
22	23	24
23	24	25
24	25	26
25	26	27
26	27	28
27	28	29
28	29	30
29	30	31
30	31	32

Table A2.4: List of taxa and specimens used in the skull size analysis with associated groupings and data

Species	Source	FAD	LAD	log(squamosal)	Continent	Environment	Main Reference	Figure Reference
Aktiogavialis puertoricensis	UPRMP 3094	28	23	1.916922612	South America	marginal marine	[46]	Fig. 2
Argochampsa krebsi	OCP DEK-GE 1201	61.6	59	2.197224577	Africa	marine	[54]	Fig. 2
Argochampsa krebsi	OCP DEK-GE 333	61.6	59	1.974081026	Africa	marine	[55]	Fig. 1a
Argochampsa microrhynchus	MHNM.KHG.169	62	56	2.174751721	Africa	marine	-	Photograph
Dollosuchoides densmorei	IRSNB 1748	47	44	2.517696473	Europe	marginal marine	[27]	Text-Fig. 3
Eogavialis africanum	SMF R 452	38	28	3.218875825	Africa	marginal marine	[29]	Tafel 1
Eogavialis africanum	SMNS 11785	38	28	3.113515309	Africa	marginal marine	[29]	Tafel 2, Fig. 4a
Eogavialis andrewsi	KNM-LT 22943	7	3	2.867898902	Africa	freshwater	[16]	Fig. 4.25/26
Eogavialis andrewsi	KNM LT 23295	7	3	2.397895273	Africa	freshwater	[16]	Fig. 4.28b
Eogavialis gavialoides	BMNH PV R 3329	33.9	28.4	2.975529566	Africa	marginal marine	[45]	Plate XXIII, Fig. 3A
Eogavialis gavialoides	AMNH 5068	33.9	28.4	3.135494216	Africa	marginal marine	-	Photograph
Eosuchus lerichei	IRSNB R 48	59	56	2.341805806	Europe	marginal marine	[58]	Fig. 2
Eosuchus minor	NJSM 15437	59	47	2.104134154	North America	marginal marine	[56]	Fig. 2
Eosuchus minor	USNM 181577	59	47	2.360854001	North America	marginal marine	[56]	Fig. 11
Eosuchus minor	USNM 299730	59	47	2.282382386	North America	marginal marine	[56]	Fig. 9
Eothoracosaurus mississippiensis	MSU 3293	73	69	3.234749174	North America	marginal marine	[39]	Fig. 1
Eothoracosaurus mississippiensis	PPM p2001.1.260	73	69	2.975529566	North America	marginal marine	[39]	Fig. 3
Gavialis bengewanicus	DMR-KS-201202-1	2.6	0.8	3.117949906	Asia	freshwater	[68]	Fig. 2
Gavialis bengewanicus	DMR-KS-03-25-23	2.6	0.8	3.100092289	Asia	freshwater	[68]	Fig. 7/8
Gavialis gangeticus	University of Bath	3	0	3.161246712	Asia	freshwater	-	Photograph

Gavialis gangeticus	BMNH 1846.1.7.3	3	0	1.686398954	Asia	freshwater	-	Photograph
Gavialis lewisi	YPM3226	5.332	2.555	3.072693315	Asia	freshwater	[51]	Fig. 1/photograph
Gavialosuchus eggenbergensis	KME	15	11	3.335769576	Europe	marginal marine	[32]	Tafel 1
Gryposuchus neogaeus	MLP 26-413	9	6.8	3.295836866	South America	marginal marine	[50]	Table 8.3
Gryposuchus colombianus	UCMP3358	13.8	12	2.821378886	South America	freshwater	[50]	Table 8.3
Gryposuchus colombianus	IGM 184696	13.8	12	3.555348061	South America	freshwater	[50]	Table 8.3
Gryposuchus croizati	MCN- URU-2002-77	11.608	5.332	3.394508394	South America	marginal marine	[70]	Fig. 2
Gryposuchus croizati	AMU-CURS-58	11.608	5.332	3.955082495	South America	marginal marine	[70]	Fig. 3
Ikanogavialis gameroi	VF- 1165	5	3	3.186352633	South America	marginal marine	[48]	Fig. 1
Kentisuchus spenceri	BMNH 38975	56	49	2.379546134	Europe	marine	[27]	Text-Fig. 2
Kentisuchus spenceri	BMNH 1753	56	49	2.985681938	Europe	marine	-	Photograph
Maomingosuchus petrolica	DM-F0001	37.8	33.9	2.280543962	Asia	freshwater	[69]	Fig. 2A
Maomingosuchus petrolica	NMNS002060-F027511	37.8	33.9	2.26633596	Asia	freshwater	[69]	Fig. 2D
Maroccosuchus zennaroi	MHNM.KHG.171	56	49	2.76000994	Africa	marine	-	Photograph
Maroccosuchus brachygnathus	MNHM.KHG.170	56	54	2.923161581	Africa	marine	-	Photograph
Maroccosuchus zennaroi	MHNM.KHG.173	56	49	2.468099531	Africa	marine	-	Photograph
Maroccosuchus zennaroi	MHNM.KHG.172	56	49	2.517696473	Africa	marine	-	Photograph
Maroccosuchus zennaroi	OCP DEK-GE 385	56	49	2.76000994	Africa	marine	[31]	Fig. 3b
Maroccosuchus zennaroi	MHNT.PAL.2006.80.11	56	49	2.809402695	Africa	marine	[31]	Fig. 8
Megadontosuchus arduini	MGPD 1Z	47	41	2.708050201	Europe	marine	[28]	Fig. 1
Ocepesuchus eoafricanus	OCP DEK-GE 45	68	66	1.887069649	Africa	marine	[38]	Fig. 4
Paratomistoma courti	CGM 421 88	44	42	2.451005098	Africa	marine	[37]	Fig. 2-3
Parvosuchus daouiensis	MHNM.KHG.168	62	61.6	1.648658626	Africa	marine	-	Photograph
Penghusuchus pani	NMNS-005645	11.608	5.332	3.194583132	Asia	freshwater	[36]	Fig. 2-3
Phasmatosuchus decipulae	MHNM.KHG.166	59	56	2.32238772	Africa	marine	-	Photograph

Phasmatosuchus decipulae	MHNM.KHG.167	59	56	2.054123734	Africa	marine	-	Photograph
Piscogavialis jugaliperforatus	SMNK 1282 PAL	7.25	5.33	2.912350665	South America	marginal marine	[47]	Fig. 2
Siquisiquesuchus venezuelensis	MBLUZ-P-5050	23.03	15.97	3.063390922	South America	marginal marine	[49]	Text. Fig 1
Thecachampsa antiqua	USNM 25243	13	7.246	3.250374492	North America	marginal marine	[33]	Fig. 5b
Thecachampsa antiqua	AMNH 5663	13	7.246	3.135494216	North America	marginal marine	-	Photograph
Thecachampsa carolinensis	SCSM 90.93.1	28	23	2.856470206	North America	marginal marine	[34]	Fig. 4.28 b
Thecachampsa carolinensis	ChM PV 4279	28	23	3.346389145	North America	marginal marine	[34]	Fig. 1
?Thecachampsoides minor	ANSP 10079	59.2	56	3.100092289	North America	marginal marine	[39]	Photograph
Thoracosaurus borissiaki	TsNIGRI c. 3373no. 709	70.6	66	2.879198457	Europe	marine	[72]	Fig.20.11
Thoracosaurus neocesariensis	AMNH 2842	70	61.6	2.624668592	North America	marginal marine	-	Photograph
Thoracosaurus scanicus	LO 3076	66	61	2.468099531	Europe	marine	[41]	Text-Fig. 3
Tomistoma cairense	SMNS 10575	47	44	2.163323026	Africa	marine	[29]	Tafel II Fig. 1a
Tomistoma coppensi	NK 527'88	7	3	2.533696814	Africa	freshwater	[30]	Plate III Fig. 1
Tomistoma dowsoni	BMNH PV R 4769	15.9	11.608	2.564949357	Africa	marginal marine	-	Photograph
Tomistoma schlegelii	BMNH 1894.2.21.2	2	0	3.126760536	Asia	freshwater	-	Photograph
Tomistoma schlegelii	BMNH 1860.11.6.8	2	0	2.721295428	Asia	freshwater	-	Photograph
Tomistoma schlegelii	BMNH 1899.1.31.1	2	0	1.945910149	Asia	freshwater	-	Photograph
Toyotamaphimaeia machikanensis	MOUF00001	2	0.37	3.17805383	Asia	freshwater	[35]	Fig. 7
Dyrosauridae								
Atlantosuchus coupatezi	OCP-DEK-GE 51	66	61.6	2.985479897	Africa	marine	[73]	Text Fig. 4
Chenanisuchus lateroculi	OCP DEK-GE 262	59.2	56	2.785011242	Africa	marine	[74]	Text Fig. 2

Chenanisuchus lateroculi	OCP DEK-GE 61	59.2	56	3.109060959	Africa	marine	[74]	Text Fig. 4
Hyposaurus rogersii	NJSM 23368	72.1	59.2	2.606091301	North America	marine	[75]	Fig. 1 (poster)
Congosaurus bequaerti	recon	66	56	2.600613457	Africa	marine	[76]	Fig. 2
Sokotosuchus ianwilsoni	recon	72.1	66	3.351656936	Africa	marine	[77]	Fig. 4
Phophatosaurus gavialoides	recon	56	47.8	2.92777458	Africa	marine	[77]	Fig. 4
Arambourgisuchus khouribgaensis	recon	59.2	56	2.994030827	Africa	marine	[78]	Fig. 4
Dryosaurus maghribensis	recon	56	47.8	2.591666186	Africa	marine	[79]	Fig. 5
Dyrosaurus phosphaticus	MNHN ALG 1	56	47.8	2.489562461	Africa	marine	[80]	Fig. 1
Dyrosaurus phosphaticus	MNHN ALG 2	56	47.8	2.599127794	Africa	marine	[80]	Fig. 1
Rhabdognathus keiniensis	MNHN TGE 4031	66	56	2.716943868	Africa	marine	[81]	Fig. 7
Cerrejonisuchus improcerus	UF/IGM 29	61.6	56	2.360854001	South America	marine	[82]	Fig. 3
Guarinisuchus munzini	DG-CTG-UFPE 5723	63.8	61.6	2.581125508	South America	marine	[83]	Fig. 2
Anthracosuchus balrogus	UF/IGM 67	60	58	3.562125046	South America	marine	[84]	Fig. 2
Anthracosuchus balrogus	UF/IGM 68	60	58	3.408437773	South America	marine	[84]	Fig. 3
Anthracosuchus balrogus	UF/IGM 69	60	58	3.325970835	South America	marine	[84]	Fig. 4

References:

1. Buscalioni AD, Sanz JL. The small crocodile *Bernissartia fagesii* from the Lower Cretaceous of Galve (Teruel, Spain). Bulletin de l'Institut Royal des Sciences naturelles de Belgique. Sciences de la Terre. 1990. pp. 129–150.
2. Ősi A. Cranial osteology of *Iharkutosuchus makadii*, a Late Cretaceous basal eusuchian crocodyliform from Hungary. Neues Jahrbuch für Geologie und Paläontologie - Abhandlungen. 2008. pp. 279–299. doi:10.1127/0077-7749/2008/0248-0279
3. Clark JM, Norell MA. The early Cretaceous crocodylomorph *Hylaeochampsa vectiana* from the Wealden of the Isle of Wight. Am Museum Novit. 1992;3032: 1–19.
4. Martin JE, Delfino M, Garcia G, Godefroit P, Berton S, Valentin X. New specimens of *Allodaposuchus precedens* from France: Intraspecific variability and the diversity of European Late Cretaceous eusuchians. Zool J Linn Soc. 2016;176: 607–631. doi:10.1111/zoj.12331
5. Delfino M, Codrea V, Folie A, Dica P, Godefroit P, Smith T. A complete skull of *Allodaposuchus precedens* Nopsca, 1928 (Eusuchia) and a reassessment of the morphology of the taxon based on the Romanian remains. J Vertebr Paleontol. 2008;28: 111–122.
6. Buscalioni AD, Ortega F, Weishampel DB, Jianu CM. A revision of the Crocodyliform *Allodaposuchus precedens* from the Upper Cretaceous of the Hateg Basin, Romania. Its relevance in the phylogeny of Eusuchia. J Vertebr Paleontol. 2001;21: 74–86. doi:10.1671/0272-4634(2001)021[0074:AROTCA]2.0.CO;2
7. Brochu CA. A review of "*Leidyosuchus*" (Crocodyliformes, Eusuchia) from the Cretaceous through Eocene of North America. J Vertebr Paleontol. 1997;17: 679–697. doi:10.1080/02724634.1997.10011017
8. Brochu CA, Parris DC, Grandstaff BS, Denton RK, Gallagher WB. A new species of *Borealosuchus* (Crocodyliformes, Eusuchia) from the Late Cretaceous–early Paleogene of New Jersey. J Vertebr Paleontol. 2012;32: 105–116. doi:10.1080/02724634.2012.633585
9. Brochu CA. Phylogenetic relationships of Palaeogene ziphodont eusuchians and the status of *Pristichampsus* Gervais, 1853. Earth Environ Sci Trans R Soc Edinburgh. 2012;103: 521–550. doi:10.1017/S1755691013000200
10. Vasse D. Un crâne d'*Asiatosuchus germanicus* du Lutétien d'Issel (Aude). Bilan sur le genre *Asiatosuchus* en Europe. Geobios. 1992. pp. 293–304. doi:10.1016/S0016-6995(06)80407-9
11. Mook CC. A new crocodilian from the Lance Formation. Am Museum Novit. 1941;1128: 1–6.
12. Puértolas E, Canudo JI, Cruzado-Caballero P. A new crocodylian from the late Maastrichtian of Spain: implications for the initial radiation of crocodyloids. PLoS One. 2011;6: 1–12. doi:10.1371/journal.pone.0020011
13. Zangerl R. *Brachyuranochampsa eversolei,* gen. et. sp. nov., a new crocodilian from the Washakie Eocene of Wyoming. Ann Carnegie Museum. 1944;30: 77–84.
14. Mook CC. The skull of *Crocodilus acer* Cope. Bull Am Museum Nat Hist. 1882;9: 117–121.
15. Mook CC. The Skull Characters of *Crocodilus megarhinus* Andrews. Am Museum Novit. 1927;289: 1–8.
16. Storrs GW. Late Miocene-Early Pliocene crocodilian fauna of Lothagam, southwest Turkana Basin, Kenya. In: Leakey MG, Harris JM, editors. Lothagam: The Dawn of Humanity in Eastern Africa. 2003. pp. 137–159.
17. Ginsburg L, Buffetaut E. *Euthecodon arambourgi* n. sp., et l'évolution du genre Euthecodon, Crocodilien du Néogène d'Afrique. Géologie Méditerranéenne. 1978;5: 291–302.
18. Brochu CA. Crocodylian snouts in space and time: phylogenetic approaches toward adaptive radiation. Am Zool. 2001;41: 564–585. doi:10.1668/0003-1569(2001)041[0564:CSISAT]2.0.CO;2

19. Molnar RE. *Pallimnarchus* and other Cenozoic crocodiles of Queensland. Mem Queensl Museum. 1982;20: 657–673.

20. Badam CL. On a partial skull of *Crocodylus palaeindicus* Falconer from the Pinjor Formation of the Upper Siwalik Group, north India. Bull Indian Geol Assoc. 1977;10: 29–35.

21. Brochu CA, Storrs GW. A giant crocodile from the Plio-Pleistocene of Kenya, the phylogenetic relationships of Neogene African crocodylines, and the antiquity of *Crocodylus* in Africa. J Vertebr Paleontol. 2012;32: 587–602. doi:10.1080/02724634.2012.652324

22. Bickelmann C, Klein N. The late pleistocene horned crocodile *Voay robustus* (Grandidier & Vaillant, 1872) from Madagascar in the Museum fur Naturkunde Berlin. Foss Rec. 2009;12: 13–21. doi:10.1002/mmng.200800007

23. Brochu CA, Njau J, Blumenschine RJ, Densmore LD. A new horned crocodile from the Plio-Pleistocene hominid sites at Olduvai Gorge, Tanzania. PLoS One. 2010;5: 1–13. doi:10.1371/journal.pone.0009333

24. Megirian D, Murray PF, Willis PMA. A new crocodile of the gavial ecomorph morphology from the Miocene of Northern Australia. Beagle Rec Museums Art Gall North Territ. 1991;8: 135–158.

25. Salisbury SW, Willis PMA. A new crocodylian from the Early Eocene of south-eastern Queensland and a preliminary investigation of the phylogenetic relationships of crocodyloids. Alcheringa An Australas J Palaeontol. 1996;20: 179–226. doi:10.1080/03115519608619189

26. Willis PMA, Molnar RE, Scanlon JD. An Early Eocene crocodilian from Murgon, Southeastern Queensland. Kaupia Darmstädter Beiträge zur Naturgeschichte. 1993;3: 27–33.

27. Brochu CA. Systematics and taxonomy of Eocene tomistomine crocodylians from Britain and Northern Europe. Palaeontology. 2007;50: 917–928.

28. Piras P, Delfino M, Favero L Del, Kotsakis T. Phylogenetic position of the crocodylian *Megadontosuchus arduini* and tomistomine palaeobiogeography. Acta Palaeontol Pol. 2007;52: 315–328.

29. Müller L. Ergebnisse der Forschungsreisen Prof. E. Stromers in den Wüsten Ägyptens. V. Tertiäre Wirbeltiere. Beiträge zur Kenntnis der Krokodilier des ägyptischen Tertiärs Abhandlungen der Bayer Akad der Wissenschaften. 1927;31: 1–97.

30. Pickford M. Late Cenozoic crocodiles (Reptilia: Crocodylidae) from the Western Rift Uganda. Geology and Palaeobiology of the Albertine Rift Valley, Uganda-Zaire, Vol II - Palaeobiology. 1994. pp. 137–155.

31. Jouve S, Bouya B, Amaghzaz M, Meslouh S. *Maroccosuchus zennaroi* (Crocodylia: Tomistominae) from the Eocene of Morocco: phylogenetic and palaeobiogeographical implications of the basalmost tomistomine. J Syst Palaeontol. 2014;13: 1–25. doi:10.1080/14772019.2014.913078

32. Toula F, Kail JA. Über einen Krokodil-Schädel aus den Tertiärablagerungen von Eggenburg in Niederösterreich: eine paläontologische Studie. Kaiserl. Königl. Staatsdr.; 1885.

33. Myrick AC. *Thecachampsa antiqua* (Leidy, 1852) (Crocodylidae: Thoracosaurinae) from fossil marine deposits at Lee Creek Mine, Aurora, North Carolina, USA. Smithonian Contrib to Paleobiol. 2001;90: 219–225.

34. Erickson BR, Sawyer GT. The estuarine crocodile *Gavialosuchus carolinensis* n. sp. (Crocodylia: Eusuchia) from the late Oligocene of South Carolina, North America. Science Museum of Minnesota; 1996.

35. Kobayashi Y, Tomida Y, Kamei T, Eguchi T. Anatomy of a Japanese tomistomine crocodylian, *Toyotamaphimeia machikanensis* (Kamei et Matsumoto, 1965), from the middle Pleistocene of Osaka Prefecture: the reassessment of its phylogenetic status within Crocodylia. Natl Sci Museum Monogr. 2006;

36. Shan H, Wu X, Cheng Y, Sato T. A new tomistomine (Crocodylia) from the Miocene of Taiwan. Can J Earth Sci. NRC Research Press; 2009;46: 529–555. doi:10.1139/E09-036

37. Brochu CA, Gingerich PD. New tomistomine crocodylian from the Middle Eocene (Bartonian) of Wadi Hitan, Fayum Province, Egypt. Contrib Museum Paleontol. 2000;30: 251–268.

38. Jouve S, Bardet N, Jalil N-E. The oldest African crocodylian: phylogeny, paleobiogeography, and differential survivorship of marine reptiles through the Cretaceous-Tertiary boundary. J Vertebr Paleontol. 2008;28: 37–41. doi:10.1671/0272-4634(2008)28

39. Brochu CA. A new Late Cretaceous gavialoid crocodylian from eastern North America and the phylogenetic relationships of thoracosaurs. J Vertebr Paleontol. 2004;24: 610–633. doi:10.1671/0272-4634(2004)024

40. Koken E. *Thoracosaurus macrorhynchus* Bl. aus der Tuffkreide von Maastricht. Zeitschrift der Dtsch Geol Gesellschaft. Stuttgart, Germany: Schweizerbart Science Publishers; 1888;40: 754–773.

41. Troedsson GT. On crocodilian remains from the Danian of Sweden. Lund; 1924.

42. Puértolas-Pascual E, Blanco A, Brochu CA, Canudo JI. Review of the Late Cretaceous-early Paleogene crocodylomorphs of Europe: Extinction patterns across the K-PG boundary. Cretac Res. 2016;57: 565–590. doi:http://dx.doi.org/10.1016/j.cretres.2015.08.002

43. Laurent Y, Buffetaut E, Le Loeuff J. Un crâne de Thoracosaurine (Crocodylia, crocodylidae) dans le Maastrichtien spérieur du sud de la France. Oryctos. 2000;3: 19–27.

44. Cook JJ, Ramsdell RC. Macrofossils from the Vincentown Formation (Paleocene) of New Jersey. Bull New Jersey Acad Sci. 1991;36: 11–15.

45. Andrews CW. A Descriptive Catalogue of the Tertiary Vertebrata of the Fayûm, Egypt. British Museum, London; 1906.

46. Vélez-Juarbe J, Brochu CA, Santos H. A gharial from the Oligocene of Puerto Rico: transoceanic dispersal in the history of a non-marine reptile. Proc R Soc B Biol Sci. 2007;274: 1245–1254. doi:10.1098/rspb.2006.0455

47. Kraus R. The cranium of *Piscogavialis jugaliperforatus* n.gen., n.sp. (Gavialidae, Crocodylia) from the Miocene of Peru. Paläontologische Zeitschrift. 1998;72: 389–406.

48. Sill WD. Nota preliminar sobre un nuevo Gavial del Plioceno de Venezuela y una discusion de los Gaviales sudamericanos. Ameghiniana. 1970;7: 151–159.

49. Brochu CA, Rincon AD. A gavialoid crocodylian from the Lower Miocene of Venezuela. Spec Pap Palaeontol. 2004;71: 61–79.

50. Langston Jr. W, Gasparini ZB de. Crocodilians, *Gryposuchus*, and the South American gavials. In: Kay RF, Madden RH, Cifelli RL, Flynn JJ, editors. Vertebrate Paleontology in the Neotropics The Miocene Fauna of La Venta, Colombia. Smithsonian Institution Press, Washington DC; 1997. pp. 113–154.

51. Lull RS. Fossil gavials from north India. American Journal of Science. 1944. pp. 417–430. doi:10.2475/ajs.242.8.417

52. Mook CC. A new species of fossil gavial from the Siwalik beds. Am Museum Novit. 1932;514: 1–5.

53. Sen PK, Banerjee M. On the occurrence of reptilian remains in the peat bed of Barrackpore, 24-Parganas, West Bengal. J Palaeontol Soc India. 1983;29: 47–51.

54. Hua S, Jouve S. A primitive marine gavialoid from the Paleocene of Morocco. J Vertebr Paleontol. 2004;24: 341–350.

55. Jouve S, Iarochène M, Bouya B, Amaghzaz M. New material of *Argochampsa krebsi* (Crocodylia: Gavialoidea) from the Lower Paleocene of the Oulad Abdoun Basin (Morocco): phylogenetic implications. Geobios. 2006;39: 817–832. doi:10.1016/j.geobios.2005.07.003

56. Brochu CA. Osteology and phylogenetic significance of *Eosuchus minor* (Marsh, 1870) new combination, a longirostrine crocodylian from the Late Paleocene of North America. Journal of

Paleontology. 2006. pp. 162–186. doi:10.1666/0022-3360(2006)080[0162:OAPSOE]2.0.CO;2

57. Brochu CA. *Eosuchus* (Crocodylia, Gavialoidea) from the lower Eocene of the Isle of Sheppey, England. Journal of Vertebrate Paleontology. 2006. pp. 466–470. doi:10.1671/0272-4634(2006)26[466:ECGFTL]2.0.CO;2

58. Delfino M, Piras P, Smith T. Anatomy and phylogeny of the gavialoid crocodylian *Eosuchus lerichei* from the Paleocene of Europe. Acta Palaeontol Pol. 2005;50: 565–580.

59. Jonet S, Wouters G. *Maroccosuchus zennaroi,* crocodilien eusuchien nouveau des phosphates du Maroc. Notes la Serv Geol du Maroc. 1977;268: 177–203.

60. Delfino M, Smith T. A reassessment of the morphology and taxonomic status of *"Crocodylus" depressifrons* Blainville, 1855 (Crocodylia, Crocodyloidea) based on the Early Eocene remains from Belgium. Zool J Linn Soc. 2009;156: 140–167. doi:10.1111/j.1096-3642.2008.00478.x

61. Mook CC. Description of a skull of a Bridger crocodilian. Bull Am Museum Nat Hist. 1904;8: 111–116.

62. Mook CC. A new species of fossil crocodile of the genus *Leidyosuchus* from the Green River beds. Am Museum Novit. 1959;1933: 1–6.

63. Wu X-C, Russell AP, Brinkman DB. A review of *Leidyosuchus* Lambe, 1907 (Archosauria: Crocodylia) and an assessment of cranial variation based upon new material: Erratum. Can J Earth Sci. 2001;38: 1665–1587. doi:10.1139/e02-900

64. Brochu CA. Phylogenetics, taxonomy, and historical biogeography of Alligatoroidea. J Vertebr Paleontol. Taylor & Francis; 1999;19: 9–100. doi:10.1080/02724634.1999.10011201

65. Wu X, Brinkman DB, Russell AP. A new alligator from the upper cretaceous of canada and the relationships of early eusuchians. Palaeontology. 1996. pp. 351–375.

66. Norell MA, Clark JM, Hutchison JH. The Late Cretaceous alligatoroid *Brachychampsa montana* (Crocodylia): new material and putative relationships. Am Museum Novit. 1994;3116: 1–26.

67. Shan H, Cheng Y, Wu X. The first fossil skull of *Alligator sinensis* from the Pleistocene, Taiwan, with a paleogeographic implication of the species. J Asian Earth Sci. Elsevier Ltd; 2013;69: 17–25. doi:10.1016/j.jseaes.2012.05.026

68. Martin JE, Buffetaut E, Naksri W, Lauprasert K, Claude J. *Gavialis* from the Pleistocene of Thailand and its relevance for drainage connections from India to Java. PLoS One. 2012;7: 1–14. doi:10.1371/journal.pone.0044541

69. Shan H, Wu X, Cheng Y, Sato T. *Maomingosuchus petrolica*, a restudy of 'Tomistoma' petrolica Yeh, 1958. Palaeoworld. "Elsevier B.V. and NANJING INSTITUTE OF GEOLOGY AND PALAEONTOLOGY, CAS"; 2017; doi:10.1016/j.palwor.2017.03.006

70. Riff D, Conquista V, Aguilera OA. The world's largest gharials *Gryposuchus*: description of *G. croizati* n. sp (Crocodylia, Gavialidae) from the Upper Miocene Urumaco Formation, Venezuela. Paläontologische Zeitschrift. 2008;82: 178–195. doi:10.1007/BF02988408

71. Rohlf FJ. tpsDig, digitize landmarks and outlines, version 2.25. Department of Ecology and Evolution, State University of New York at Stony Brook. 2016.

72. Storrs GW, Efimov MB. Mesozoic crocodyliforms of north-central Eurasia. In: Benton MJ, Shishkin MA, Unwin DM, Kurochkin EN, editors. The age of dinosaurs in Russia and Mongolia. Cambridge University Press Cambridge; 2000. pp. 402–419. doi:10.1086/343364

73. Jouve S, Bouya B, Amaghzaz M. A long-snouted dyrosaurid (Crocodyliformes, Mesoeucrocodylia) from the Paleocene of Morocco: phylogenetic and palaeobiogeographic implications. Palaeontology. 2008;51: 281–294. doi:10.1111/j.1475-4983.2007.00747.x

74. Jouve S, Bouya B, Amaghzaz M. A short-snouted dyrosaurid (Crocodyliformes, Mesoeucrocodylia) from the Paleocene of Morocco. Palaeontology. 2005;48: 359–369.

75. Callahan W, Pellegrini R, Schein JP, Parris DC, McCauley JD. A nearly complete specimen of

Hyposaurus rogersii (Crocodylomorpha , Dyrosauridae) from the Late Cretaceous-Early Paleogene of New Jersey. 2015. p. 1. doi:10.13140/RG.2.1.2253.2724

76. Jouve S, Schwarz D. *Congosaurus bequaerti,* a Paleocene Dyrosaurid (Crocodyliformes; Mesoeucrocodylia) from Landana (Angola). Bull l'Institut R des Sci Nat Belqique, Sci la Terre. 2004;74: 129–146.

77. Buffetaut E. *Sokotosuchus ianwilsoni* and the evolution of the dyrosaurid crocodilians. 1979.

78. Jouve S, Ne MIÈ, Bouya B, Amaghzaz M. A new dyrosaurid crocodyliform from the Palaeocene of Morocco and a phylogenetic analysis of Dyrosauridae. Acta Palaeontol Pol. 2005;50: 581–594.

79. Jouve S, Iarochène M, Bouya B, Amaghzaz M. A new species of *Dyrosaurus* (Crocodylomorpha, Dyrosauridae) from the early Eocene of Morocco: phylogenetic implications. Zool J Linn Soc. 2006;148: 603–656. doi:10.1111/j.1096-3642.2006.00241.x

80. Jouve S. A new description of the skull of *Dyrosaurus phosphaticus* (Thomas, 1893) (Mesoeucrocodylia: Dyrosauridae) from the Lower Eocene of North Africa. Can J Earth Sci. 2005;42: 323–337. doi:10.1139/e05-008

81. Jouve S. Taxonomic revision of the dyrosaurid assemblage (Crocodyliformes: Mesoeucrocodylia) from the Paleocene of the Iullemmeden Basin, West Africa. Journal of Paleontology. 2007. pp. 163–175. doi:10.1666/0022-3360(2007)81[163:TROTDA]2.0.CO;2

82. Hastings AK, Bloch JI, Cadena EA, Jaramillo CA. A new small short-snouted dyrosaurid (Crocodylomorpha, Mesoeucrocodylia) from the Paleocene of northeastern Colombia. J Vertebr Paleontol. 2010;30: 139–162. doi:10.1080/02724630903409204

83. Barbosa JA, Kellner AWA, Viana MSS. New dyrosaurid crocodylomorph and evidences for faunal turnover at the K-P transition in Brazil. Proc R Soc B Biol Sci. 2008;275: 1385–1391. doi:10.1098/rspb.2008.0110

84. Hastings AK, Bloch JI, Jaramillo CA. A new blunt-snouted dyrosaurid, *Anthracosuchus balrogus* gen. et sp. nov. (Crocodylomorpha, Mesoeucrocodylia), from the Palaeocene of Colombia. Hist Biol. Taylor & Francis; 2014; 1–23. doi:10.1080/08912963.2014.918968

Appendix 3: Supplementary Data for Chapter 4:

Character list used for phylogenetic analysis in Chapter 4:

The character list here is the character list from Brochu (2012) [1]. Any modifications to the characters from this source are highlighted in **bold.**

1. Ventral tubercle of proatlas more than one-half (0); or no more than one half (1) the width of the dorsal crest.
2. Fused proatlas boomerang-shaped (0); strap-shaped(1); or massive and block-shaped (2).
3. Proatlas with prominent anterior process (0); or lacks anterior process (1).
4. Proatlas has tall dorsal keel (0); or lacks tall dorsal keel; dorsal side smooth (1).
5. Atlas intercentrum wedge-shaped in lateral view, with insignificant parapophyseal processes (0); or plate-shaped in lateral view, with prominent parapophyseal processes at maturity (1).
6. Dorsal margin of atlantal rib generally smooth with modest dorsal process (0); or with prominent process (1).
7. Atlantal ribs without (0); or with (1) very thin medial laminae at anterior end.
8. Atlantal ribs lack (0); or possess (1) large articular facets at anterior ends for each other.
9. Axial rib tuberculum wide, with broad dorsal tip (0); or narrow, with acute dorsal tip (1).
10. Axial rib tuberculum contacts diapophysis late in ontogeny, if at all (0); or early in ontogeny (1).
11. Anterior half of axis neural spine oriented horizontally (0); or slopes anteriorly (1).
12. Axis neural spine crested (0); or not crested (1).
13. Posterior half of axis neural spine wide (0); or narrow (1).
14. Axis neural arch lacks (0); or possesses (1) a lateral process (diapophysis).
15. Axial hypapophysis located toward the center of centrum (0); or toward the anterior end of centrum (1).
16. Axial hypapophysis without (0); or with (1) deep fork.
17. Hypapophyseal keels present on eleventh vertebra behind atlas (0); twelfth vertebra behind atlas (1); or tenth vertebra behind atlas (2).
18. Third cervical vertebra (first postaxial) with prominent hypapophysis (0); or lacks prominent hypapophysis (1).
19. Neural spine on third cervical long, dorsal tip at least half the length of the centrum without the cotyle (0); or short, dorsal tip acute and less than half the length of the centrum without the cotyle (1).
20. Cervical and anterior dorsal centra lack (0); or bear (1) deep pits on the ventral surface of the centrum.
21. Presacral centra amphicoelous (0); or procoelous (1).

22. Anterior sacral rib capitulum projects far anteriorly of tuberculum and is broadly visible in dorsal view (0); or anterior margins of tuberculum and capitulum nearly in same plane, and capitulum largely obscured dorsally (1).
23. Scapular blade flares dorsally at maturity (0); or sides of scapular blade sub-parallel; minimal dorsal flare at maturity (1).
24. Deltoid crest of scapula very thin at maturity, with sharp margin (0); or very wide at maturity, with broad margin (1).
25. Scapulocoracoid synchondrosis closes very late in ontogeny (0); or relatively early in ontogeny (1).
26. Scapulocoracoid facet anterior to glenoid fossa uniformly narrow (0); or broad immediately anterior to glenoid fossa, and tapering anteriorly (1).
27. Proximal edge of deltopectoral crest emerges smoothly from proximal end of humerus and is not obviously concave (0); or emerges abruptly from proximal end of humerus and is obviously concave (1).
28. M. teres major and M. dorsalis scapulae insert separately on humerus; scars can be distinguished dorsal to deltopectoral crest (0); or insert with common tendon; single insertion scar (1).
29. Olecranon process of ulna narrow and sub-angular (0); or wide and rounded (1).
30. Distal extremity of ulna expanded transversely with respect to long axis of bone; maximum width equivalent to that of proximal extremity (0); or proximal extremity considerably wider than distal extremity (1).
31. Interclavicle flat along length, without dorsoventral flexure (0); or with moderate dorsoventral flexure (1); or with severe dorsoventral flexure (2).
32. Anterior end of interclavicle flat (0); or rod-like (1).
33. Iliac anterior process prominent (0); or virtually absent (1).
34. Dorsal margin of iliac blade rounded with smooth border (0); or rounded, with modest dorsal indentation (1); or rounded, with strong dorsal indentation (wasp-waisted) (2); or narrow, with dorsal indentation(3); or rounded with smooth border; posterior tip of blade very deep (4).
35. Supraacetabular crest narrow (0); or broad (1).
36. Limb bones relatively robust, and hind limb much longer than forelimb at maturity (0); or limb bones very long and slender (1).
37. M. caudofemoralis with single head (0); or with double head (1).
38. Dorsal osteoderms not keeled (0); or keeled (1).
39. Dorsal midline osteoderms rectangular (0); or nearly square (1).
40. Four (0); six (1); eight (2); or ten (3) contiguous dorsal osteoderms per row at maturity.
41. Nuchal shield grades continuously into dorsal shield (0); or differentiated from dorsal shield, with four nuchal osteoderms (1); or differentiated from dorsal shield and six nuchal osteoderms with four central and two lateral (2); or differentiated from dorsal shield, with eight nuchal osteoderms in two parallel rows (3).
42. Ventral armor absent (0); or present and comprising single ventral osteoderms (1); or present and comprising paired ventral ossifications that suture together (2).

43. Anterior margin of dorsal midline osteoderms with anterior process (0); or smooth, without process (1).
44. Ventral scales have (0); or lack (1) follicle gland pores.
45. Ventral collar scales not enlarged relative to other ventral scales (0); or in a single enlarged row (1); or in two parallel enlarged rows (2).
46. Median pelvic keel scales form two parallel rows along most of tail length (0); or form single row along tail (1); or merge with lateral keel scales (2).
47. Alveoli for dentary teeth 3 and 4 nearly same size and confluent (0); or fourth alveolus larger than third, and alveoli are separated (1).
48. Anterior dentary teeth strongly procumbent (0); or project anterodorsally (1).
49. Dentary symphysis extends to fourth or fifth alveolus (0); or sixth through eighth alveolus (1); or behind eighth alveolus (2).
50. Dentary gently curved (0); deeply curved (1); or linear (2) between fourth and tenth alveoli.
51. Largest dentary alveolus immediately caudal to fourth is (0) 13 or 14; (1) 13 or 14 and a series behind it; (2) 11 or 12; or (3) no differentiation; or (4) behind 14.
52. Splenial with anterior perforation for mandibular ramus of cranial nerve V (0); or lacks anterior perforation for mandibular ramus of cranial nerve V (1).
53. Mandibular ramus of cranial nerve V exits splenial anteriorly only (0); or splenial has singular perforation for mandibular ramus of cranial nerve V posteriorly (1); or splenial has double perforation for mandibular ramus of cranial nerve V posteriorly (2).
54. Splenial participates in mandibular symphysis; splenial symphysis adjacent to no more than five dentary alveoli (0); or splenial excluded from mandibular symphysis; anterior tip of splenial passes ventral to Meckelian groove (1); or splenial excluded from mandibular symphysis; anterior tip of splenial passes dorsal to Meckelian groove (2); or deep splenial symphysis, longer than five dentary alveoli; splenial forms wide 'V' within symphysis (3); or deep splenial symphysis, longer than five dentary alveoli; splenial constricted within symphysis and forms narrow V (4).
55. Coronoid bounds posterior half of foramen intermandibularis medius (0); or completely surrounds foramen intermandibularis medius at maturity (1); or obliterates foramen intermandibularis medius at maturity (2).
56. Superior edge of coronoid slopes strongly anteriorly (0); or almost horizontal (1).
57. Inferior process of coronoid laps strongly over inner surface of Meckelian fossa (0); or remains largely on medial surface of mandible (1).
58. Coronoid imperforate (0); or with perforation posterior to foramen intermandibularis medius (1).
59. Process of splenial separates angular and coronoid (0); or no splenial process between angular and coronoid (1).
60. Angular-surangular suture contacts external mandibular fenestra at posterior angle at maturity (0); or passes broadly along ventral margin of external mandibular fenestra late in ontogeny (1).
61. Anterior processes of surangular unequal (0); or sub-equal to equal (1).
62. Surangular with spur bordering the dentary tooth row lingually for at least one alveolus length (0); or lacking such spur (1).

63. External mandibular fenestra absent (0); or present (1); or present and very large; most of foramen intermandibularis caudalis visible in lateral view (2).
64. Surangular-dentary suture intersects external mandibular fenestra anterior to posterodorsal corner (0); or at posterodorsal corner (1).
65. Angular extends dorsally toward or beyond anterior end of foramen intermandibularis caudalis; anterior tip acute (0); or does not extend dorsally beyond anterior end of foramen intermandibularis caudalis; anterior tip very blunt (1).
66. Surangular-angular suture lingually meets articular at ventral tip (0); or dorsal to tip (1).
67. Surangular continues to dorsal tip of lateral wall of glenoid fossa (0); or truncated and not continuing dorsally (1).
68. Articular-surangular suture simple (0); or articular bears anterior lamina dorsal to lingual foramen (1); or articular bears anterior lamina ventral to lingual foramen (2); or bears laminae above and below foramen (3).
69. Lingual foramen for articular artery and alveolar nerve perforates surangular entirely (0); or perforates surangular/angular suture (1).
70. Foramen aerum at extreme lingual margin of retroarticular process (0); or set in from margin of retroarticular process (1).
71. Retroarticular process projects posteriorly (0); or projects posterodorsally (1).
72. Surangular extends to posterior end of retroarticular process (0); or pinched off anterior to tip of retroarticular process (1).
73. Surangular-articular suture oriented anteroposteriorly (0); or bowed strongly laterally (1) within glenoid fossa.
74. Sulcus between articular and surangular (0); or articular flush against surangular (1).
75. Dorsal projection of hyoid cornu flat (0); or rodlike (1).
76. Dorsal projection of hyoid cornu narrow, with parallel sides (0); or flared (1).
77. Lingual osmoregulatory pores small (0); or large (1).
78. Tongue with (0); or without (1) keratinized surface.
79. Teeth and alveoli of maxilla and/or dentary circular in cross-section (0); or posterior teeth laterally compressed (1); or all teeth compressed (2) .
80. Maxillary and dentary teeth with smooth carinae (0); or serrated (1).
81. Naris projects anterodorsally (0); or dorsally (1).
82. External naris bisected by nasals (0); or nasals contact external naris, but do not bisect it (1); or nasals excluded, at least externally, from naris; nasals and premaxillae still in contact (2); or nasals and premaxillae not in contact (3).
83. Naris circular or keyhole-shaped (0); or wider than long (1); or anteroposteriorly long and prominently teardrop-shaped (2).
84. External naris of reproductively mature males remains similar to that of females (0); or develops bony excrescence (ghara) (1).
85. External naris opens flush with dorsal surface of premaxillae (0); or circumscribed by thin crest (1).
86. Premaxillary surface lateral to naris smooth (0); or with deep notch lateral to naris (1).

87. Premaxilla has five teeth (0); or four teeth (1) early in post-hatching ontogeny.

88. Incisive foramen small, less than half the greatest width of premaxillae (0); or large, more than half the greatest width of premaxillae (1); or large, and intersects premaxillary-maxillary suture (2).

89. Incisive foramen completely situated far from premaxillary tooth row, at the level of the second or third alveolus (0); or abuts premaxillary tooth row (1); or projects between first premaxillary teeth (2).

90. Dorsal premaxillary processes short, not extending beyond third maxillary alveolus (0); or long, extending beyond third maxillary alveolus (1).

91. Dentary tooth 4 occludes in notch between premaxilla and maxilla early in ontogeny (0); or occludes in a pit between premaxilla and maxilla; no notch early in ontogeny (1).

92. All dentary teeth occlude lingual to maxillary teeth (0); or occlusion pit between seventh and eight maxillary teeth; all other dentary teeth occlude lingally (1); or dentary teeth occlude in line with maxillary tooth row (2).

93. Largest maxillary alveolus is 3 (0); 5 (1); 4 (2); 4 and 5 are same size (3); 6 (4); or maxillary teeth homodont (5); or maxillary alveoli gradually increase in diameter posteriorly toward penultimate alveolus (6).

94. Maxillary tooth row curved medially or linear (0); or curves laterally broadly (1) posterior to first six maxillary alveoli.

95. Dorsal surface of rostrum curves smoothly (0); or bears medial dorsal boss (1).

96. Canthi rostralii absent or very modest (0); or very prominent (1) at maturity.

97. Preorbital ridges absent or very modest (0); or very prominent (1) at maturity.

98. Vomer entirely obscured by premaxilla and maxilla (0); or exposed on palate at premaxillary-maxillary suture (1).

99. Vomer entirely obscured by maxillae and palatines (0); or exposed on palate between palatines (1).

100. Surface of maxilla within narial canal imperforate (0); or with a linear array of pits (1).

101. Medial jugal foramen small (0); or very large (1).

102. Maxillary foramen for palatine ramus of cranial nerve V small or not present (0); or very large (1).

103. Ectopterygoid abuts maxillary tooth row (0); or maxilla broadly separates ectopterygoid from maxillary tooth row (1).

104. Maxilla terminates in palatal view anterior to lower temporal bar (0); or comprises part of the lower temporal bar (1).

105. Penultimate maxillary alveolus less than (0); or more than (1) twice the diameter of the last maxillary alveolus.

106. Prefrontal dorsal surface smooth adjacent to orbital rim (0); or bearing discrete knoblike processes (1).

107. Dorsal half of prefrontal pillar narrow (0); or expanded anteroposteriorly (1).

108. Medial process of prefrontal pillar expanded dorsoventrally (0); or anteroposteriorly (1).

109. Prefrontal pillar solid (0); or with large pneumatic recess (1).

110. Medial process of prefrontal pillar wide (0); or constricted (1) at base.

111. Maxilla has linear medial margin adjacent to suborbital fenestra (0); or bears broad shelf extending into fenestra, making lateral margin concave (1).

112. Anterior face of palatine process rounded or pointed anteriorly (0); or notched anteriorly (1).

113. Anterior ectopterygoid process tapers to a point (0); or forked (1).

114. Palatine process extends (0); or does not extend (1) significantly beyond anterior end of suborbital fenestra.

115. Palatine process generally broad anteriorly (0); or in form of thin wedge (1).

116. Lateral edges of palatines smooth anteriorly (0); or with lateral process projecting from palatines into suborbital fenestrae (1).

117. Palatine-pterygoid suture nearly at (0); or far from (1) posterior angle of suborbital fenestra.

118. Pterygoid ramus of ectopterygoid straight, posterolateral margin of suborbital fenestra linear (0); or ramus bowed, posterolateral margin of fenestra concave (1).

119. Lateral edges of palatines parallel posteriorly (0); or flare posteriorly, producing shelf (1).

120. Anterior border of the choana is comprised of the palatines (0); or choana entirely surrounded by pterygoids (1).

121. Choana projects posteroventrally (0); or anteroventrally (1) at maturity.

122. Pterygoid surface lateral and anterior to internal choana flush with choanal margin (0); or pushed inward anterolateral to choanal aperture (1); or pushed inward around choana to form neck surrounding aperture (2); or everted from flat surface to form neck surrounding aperture (3).

123. Posterior rim of internal choana not deeply notched (0); or deeply notched (1).

124. Internal choana not septate (0); or with septum that remains recessed within choana (1); or with septum that projects out of choana (2).

125. Ectopterygoid-pterygoid flexure disappears during ontogeny (0); or remains throughout ontogeny (1).

126. Ectopterygoid extends (0); or does not extend (1) to posterior tip of lateral pterygoid flange at maturity.

127. Lacrimal makes broad contact with nasal; no posterior process of maxilla (0); or maxilla with posterior process within lacrimal (1); or maxilla with posterior process between lacrimal and prefrontal (2).

128. Prefrontals separated by frontals and nasals (0); or prefrontals meet medially (1).

129. Lacrimal longer than prefrontal (0); or prefrontal longer than lacrimal (1); or lacrimal and prefrontal both elongate and nearly the same length (2).

130. Ectopterygoid extends along medial face of postorbital bar (0); or stops abruptly ventral to postorbital bar (1).

131. Postorbital bar massive (0); or slender (1).

132. Postorbital bar bears process that is prominent, dorsoventrally broad, and divisible into two spines (0); or bears process that is short and generally not prominent (1).

133. Ventral margin of postorbital bar flush with lateral jugal surface (0); or inset from lateral jugal surface (1).

134. Postorbital bar continuous with anterolateral edge of skull table (0); or inset (1).

135. Margin of orbit flush with skull surface (0); or dorsal edges of orbits upturned (1); or orbital margin telescoped (2).

136. Ventral margin of orbit circular (0); or with prominent notch (1).

137. Palpebral forms from single ossification (0); or from multiple ossifications (1).

138. Quadratojugal spine prominent at maturity (0); or greatly reduced or absent at maturity (1).

139. Quadratojugal spine low, near posterior angle of infratemporal fenestra (0); or high, between posterior and superior angles of infratemporal fenestra (1).

140. Quadratojugal forms posterior angle of infratemporal fenestra (0); or jugal forms posterior angle of infratemporal fenestra (1); or quadratojugal-jugal suture lies at posterior angle of infratemporal fenestra (2).

141. Postorbital neither contacts quadrate nor quadratojugal medially (0); or contacts quadratojugal, but not quadrate, medially (1); or contacts quadrate and quadratojugal at dorsal angle of infratemporal fenestra (2); or contacts quadratojugal with significant descending process (3).

142. Quadratojugal bears long anterior process along lower temporal bar (0); or bears modest process, or none at all, along lower temporal bar (1).

143. Quadratojugal extends to superior angle of infratemporal fenestra (0); or does not extend to superior angle of infratemporal fenestra; quadrate participates in fenestra (1).

144. Postorbital-squamosal suture oriented ventrally (0); or passes medially (1) ventral to skull table.

145. Dorsal and ventral rims of squamosal groove for external ear valve musculature parallel (0); or squamosal groove flares anteriorly (1).

146. Squamosal-quadrate suture extends dorsally along posterior margin of external auditory meatus (0); or extends only to posteroventral corner of external auditory meatus (1).

147. Posterior margin of otic aperture smooth (0); or bowed (1).

148. Frontoparietal suture deeply within supratemporal fenestra; frontal prevents broad contact between postorbital and parietal (0); or suture makes modest entry into supratemporal fenestra at maturity; postorbital and parietal in broad contact (1); or suture on skull table entirely (2).

149. Frontoparietal suture concavoconvex (0); or linear (1) between supratemporal fenestrae.

150. Supratemporal fenestra with fossa; dermal bones of skull roof do not overhang rim at maturity (0); or dermal bones of skull roof overhang rim of supratemporal fenestra near maturity (1); or supratemporal fenestra closes during ontogeny (2).

151. Shallow fossa at anteromedial corner of supratemporal fenestra or no such fossa (0); anteromedial corner of supratemporal fenestra smooth (1).

152. Medial parietal wall of supratemporal fenestra imperforate (0); or bearing foramina (1).

153. Parietal and squamosal widely separated by quadrate on posterior wall of supratemporal fenestra (0); or parietal and squamosal approach each other on posterior wall of

supratemporal fenestra without actually making contact (1); or parietal and squamosal meet along posterior wall of supratemporal fenestra (2).

154. Skull table surface slopes ventrally from sagittal axis (0); or planar (1) at maturity.

155. Posterolateral margin of squamosal horizontal or nearly so (0); or upturned to form a discrete horn (1).

156. Mature skull table with broad curvature; short posterolateral squamosal rami along paroccipital process or with nearly horizontal sides (0); or significant posterolateral squamosal rami along paroccipital process (1), **or with very long squamosal rami (2). [character originally added in** [1]**]**

157. Squamosal does not extend (0); or extends (1) ventrolaterally to lateral extent of paroccipital process.

158. Supraoccipital exposure on dorsal skull table small (0); absent (1); large (2); or large such that parietal is excluded from posterior edge of table (3).

159. Anterior foramen for palatine ramus of cranial nerve VII ventrolateral (0); or ventral (1) to basisphenoid rostrum.

160. Sulcus on anterior braincase wall lateral to basisphenoid rostrum (0); or braincase wall lateral to basisphenoid rostrum smooth; no sulcus (1).

161. Basisphenoid not exposed extensively (0); or exposed extensively (1) on braincase wall anterior to trigeminal foramen.

162. Extensive exposure of prootic on external braincase wall (0); or prootic largely obscured by quadrate and laterosphenoid externally (1).

163. Laterosphenoid bridge comprised entirely of laterosphenoid (0); or with ascending process or palatine (1).

164. Capitate process of laterosphenoid oriented laterally (0); or anteroposteriorly (1) toward midline.

165. Parietal with recess communicating with pneumatic system (0); or solid, without recess (1).

166. Significant ventral quadrate process on lateral braincase wall (0); or quadrate-pterygoid suture linear from basisphenoid exposure to trigeminal foramen (1).

167. Lateral carotid foramen opens lateral (0); or dorsal (1) to basisphenoid at maturity.

168. External surface of basioccipital ventral to occipital condyle oriented posteroventrally (0); or posteriorly (1) at maturity.

169. Posterior pterygoid processes tall and prominent (0); or small and project posteroventrally (1); or small and project posteriorly (2).

170. Basisphenoid thin (0); or anteroposteriorly wide (1) ventral to basioccipital.

171. Basisphenoid not broadly exposed ventral to basioccipital at maturity; pterygoid short ventral to median eustachian opening (0); or basisphenoid exposed as broad sheet ventral to basioccipital at maturity; pterygoid tall ventral to median eustachian opening (1).

172. Exoccipital with very prominent boss on paroccipital process; process lateral to cranioquadrate opening short (0); or exoccipital with small or no boss on paroccipital process; process lateral to cranioquadrate opening long (1).

173. Lateral eustachian canals open dorsal (0); or lateral (1) to medial eustachian canal.

174. Exoccipitals terminate dorsal to basioccipital tubera (0); or send robust process ventrally and participate in basioccipital tubera (1); or send slender process ventrally to basioccipital tubera (2).

175. Quadrate foramen aerum on mediodorsal angle (0); or on dorsal surface (1) of quadrate.

176. Quadrate foramen aereum is small (0); comparatively large (1); or absent (2) at maturity.

177. Quadrate lacks (0); or bears (1) prominent, mediolaterally thin crest on dorsal surface of ramus.

178. Attachment scar for posterior mandibular adductor muscle on ventral surface of quadrate ramus forms modest crests (0); or prominent knob (1).

179. Quadrate with small, ventrally-reflected medial hemicondyle (0); or with small medial hemicondyle; dorsal notch for foramen aerum (1); or with prominent dorsal projection between hemicondyles (2); or with expanded medial hemicondyle (3).

180. Less than 18 teeth (0), 18 to 22 teeth (1), or more than 22 teeth (2) on maxilla. [[2] **(ch. 169)].**

181. Frontal ends posterior (0) at the same level (1), or extends well anterior (2) to the anterior extension of the prefrontal. [(Jouve et al. 2014) [2] (ch. 171)].

182. Lateral posterior tuberosity of supraoccipital not visible (0), or visible in dorsal view (1). [(Jouve et al. 2014) [2] (ch. 201)].

183. Anterior tip of frontal forms simple acute point (0) or forms broad, complex sutural contact with the nasals (1). [(Jouve et al. 2014)[2] (ch.223)].

Character matrix for TNT:

xread
183 105
Bernissartia_fagesii
??????0???0111102100?00?0?000???0000?100010???0010?000???????10?0?00?001
?1????000?0?0000?00030?00?????1000????1?0000?000??0100?0??000100?0?0??0?0?0010?
0??00??0????????000?0000?0000000
Allodaposuchus_precedens
??
??00010?0000001230000000?100000????000000010103000110001011000???01000000001100
10000?????1??01?010001?0000?00
Acynodon_iberoccitanus
??10104101????????0????????0?0??
???00010?0000001060000000??00100????0000000101?00???20000?0100?110?0000??01010
0000?1?????????1???0????01002?1
Acynodon_adriaticus
?????1?????????????01?100?1??????????010?10?????????01????????0???0??100??
00??00010?000?0?1060000?0????110????00?00011010000?1?11?0?0100???0????0??010?0
?0010?????????????1???01?00101
Iharkutosuchus_makadii
??10124?????????110???00??10?1?
???0001??0000011061000?0???0110????000000100110000120100 1?100?1?0?00?0???12???
100?2?????1???1000000??1100001
Hylaeochampsa_vectiana
??0???
??0??????????0?0?1000?00??0110?0?0000000100100 0?0?2110000120????1?0?0000101000
00000????1?001001000?0110?011
Eothoracosaurus
??????0????????????01??000????????00?00???0????122???3??????0?????00?011?0
????00120?000??102500000??000000????000010100100 0????00?000100???01???10000010
?001?00????????1000100000012?0
Thoracosaurus_neocesariensis
??????0??????111?1?010????0011??0??0?00???0???1122???3????????10?000?01?0
?????00120?0000?1025000000??000000?0?000010100100 00?00000110?00010??1?0000
10000100000000?00100?10000000?010
Thoracosaurus_macrorhynchus
??????0???0?1111?1?01?????00????0????00???0???1?22???3??????0?10000000110
0????00120?00?0?1025000000??000000?0?000010100100 0011000000110?000100?100010
10?0010000???0??01000100000001000
Eosuchus_minor
??????0???0??111???01?00?0?01???0000?000??0???1122??0300?0000?10?0000011
00????00120?0000?1025?00000?000000?0000000101001 00000000110???0100?10?10
0100001?0100??1???1010101010030010
Eosuchus_lerichei
??????0??????01????01????????1????????0????????1122???3?????????????????0??

???00120?0000?1025000000?0000000???0000010100100000100000?0110?000?0??10?20010
00010?1????????10?01?10100300?1
Eogavialis_africanum
????????1?????11???010??????????0?????????0???1122??03?????10?100000??110
1????00120?000?01025?00000?000000000000001010010000010000000121?000100?100100
1000010100?000??01010101000000010
Piscogavialis_jugaliperforatus
????????????????????????????????1?????????????11?2???3?????0001???????10???
???00120?0010010250000000?000000????0000010100100000?000000111?1?0001010020010
000200?0?1?0?0?12??1?10?0002210
Gryposuchus_colombianus
????0?0???001??????01??000?????????????????0???11223?030100?0001000000011
00????0012010000?1025?00000?0?0000??0?0000101001000001100000012 1?000100?10011
0100002000001 00?001210101000001[1 2]10
Gavialis_gangeticus
??????????????????010?????????????????????????22???3??????0?100000??1?0?
????00?30?0??????2??0???0?0?0000??0?0000?0?00100?0?1???0000121?000100?100??0?00
0010000?????001210101000002210
Gavialis_sp_Siwalik
020000000?00111101101000000011100000 0?000000011223003000000001000000
011000100001301000001025?000000000000000000001010010000011000000121000010001
00110100001000000000001210101000 00?210
Borealosuchus_threeensis
????0?????????????01???????0??????1?00??20???01002??1?????10?11?00000100
0??
??????????????????????????????
Borealosuchus_formidabilis
000?000?0?1100100100100000010100000 1?000?20???0110200000?000?110000000
100001??00020?0000?0023100000?000000100000001010010001010020 1?11000000?00?00
0010100101000??????001001100000001000
Borealosuchus_wilsoni
??????0??????????1001000000101??00?1?000?20???01002??100?0?0011000002010
00????00020?0?0???0231000?????00001?0?0?00101001000101002010 1100?000100??0011
01001010000?00???010011?0?00001??0
Borealosuchus_acutidentatus
????????????????????????????0?????????????????????002???????????000??????0??
???00020?0?00??0231000?????0000????0?0??0????????1??002?1?1100?0?0?0??0?011010?1
01000???????010??1?0?00001000
Borealosuchus_sternbergii
000000000?110010?100100000010100000 1?00???0???01102000000?00010000000
100000??00020?0000000131000000100000 1?0?000001110100010100001111 00?000100?00
0000100101000000?1?001001100000001000
Boverisuchus_magnifrons
????0?0???01001001?01?00000111??0100?10???1???1110?000?????0??1000001?1?
0?????21010?0000?0003000100?000000??0?0000001001000101000011111 0???0100?01000
0100101000???01??11001100000020100

Boverisuchus_vorax

????????????0?0???01?000?0??1??0100?1???1????11102000??????0?1????0??1?1?????21?20?0000000030001???000000????0000001001010??10000111110?0?0?00?0?010010?10100?????????1???100000020100

Planocrania_hengdongensis

????????????????????1?????????????????????????1110???1????????1????0?01?0??????20010?0?????01300??????0?000????0????01001???????0??1?1100????????0?0?00100?0100?????1???1???10?100010?00

Planocrania_datangensis

??11?????0??????????????????????20010?000??1003000000??0?000???????000??01???????0??1?1110????????0?000010010??0?????????????10??0?0?0?00

Mecistops_cataphractus

10?001001?000010000011100111112012000111101101111041010100010010001110101?100100120000001002100000001000001101000010110100010100001111100001011100120010010100011101011110010000030100

Crocodylus_niloticus

101000001?101010001011100111112012000111201101110021010100010110001110101110010011000000100210000000110000011010010001101000101100011111100001011100120010010100011101011110011000030000

Crocodylus_porosus

111000001?001010101011100011112012000111201101110021010100010110001110101110010011000000100210001001100000110100100011010001010000111110000101110012001001010001110101111001100000030000

Crocodylus_rhombifer

001000001?101010001011100111112011000111201101110021010100010110001110101110010011000000100210100001100000011010010001101000101100011111100001011100120010011100011101011110011000030000

Euthecodon_arambourgii

??0?????????????????1?????00020?0000?1025000100?1000001101000000??0????0???000111110??11011?001210100101100????1??11?0?1000?0030100

Osteolaemus_tetraspis

??1?00001?001010100011100111112011100111111110111002101010001011000011010111001101000001010021000100010000011011001011101010101000011111010010101001211100101100111010111101100000030001

Osteolaemus_osborni

??1?00001?001010100011100111112011100111111110111002101010000011000011010111001101100001010021000100010000011011001001001010101000011111010010101001211100101100111010111101100000030000

Voay_robustus

??????0????????0???011?????111??1110??????1???111021010100000110001111101101???00110?0000?00210001000100000110100010111010101010000111110?00101110012011001111107?1101?111100100000030000

Rimasuchus_lloydi

??1?????????????????1???

??00110?0000?0021000100?1000001101000000????10??1??100?111110?001011?001200100
101100111?1??1110?1000?0030?00
Brochuchus_pigotti
??????????00?010?00?11??01111????????10???0???11102??1????????1???111???1
?????00010?0100?00210001000100000????00101011010100001?0?0111110???1?1??001210
100101100??1?1??1100?100000030100
Crocodylus_megarhinus
??????0???????????001?????????????????????????????11102101?????00110000??01011
????00110?0000?002300000001?0000??0?000000110100010120001111110?002?11?0012?01
001010?01100???1110010000030?00
Australosuchus_clarkae
??????0????????1??0??1?????11???????0?10???1???1110?101?????00110000110101
1????00110?000011021000000010000001?0?000000???????10100001111110?002011?011200
100101000011??1??11?001000?001000?
Kambara_implexidens
??????0????????????01?????11????1100?10???1???11102101?????00110000110101
1????00110?000011021000000010000001?0100000010010001010000111110?002011?00120
010010100011101?111100100000010100
Trilophosuchus_rackhami
??
??0?????0???????2?0??0?0?1000????0?1?000001010???01?0?0111110??1201110112101000
0102011101?111?0?1000?001??1?
Quinkana_spp
??11?0???1?????????????????1??
???21010?0000?10[0 2][1 5]00[0
1]0000100000????0?0??????????1??1000111?10?00201110012101001010 2?11101?11??01?
000???1????
Tomistoma_schlegelii
021000001?00101000101100011111101100010130110111 22?104000001001000000
010100001001200000011021000001010000011010001001001000101100011111000001101 0
012101001010001100101111001000000030010
Tomistoma_lusitanica
??????0????????????01??????????????????10???1???1??2???4?????00?10000??0101?
????00120?0000?1021?00001?100000110?000010100100010100001111 10?0001?1?1012101
0010100011001??11100100000030[1 2]?0
Toyotamaphimeia_machikanense
00100100??11111100101100011111101100?00???1?????22??04?????10010?0000?1
01000??00120?00001100400000???00000????0000?010010000?10000011110??00?1??1??2
1010?1010??????????110010?0000300??
Gavialosuchus_eggenburgensis
??????????????????????1??
??00120?0000?1024000000??00000????00?0101001000?01200?0?1110?0??????1?121010?1
0100????????11???10000000301?0
Paratomistoma_courti
??0??10?000001010?
???00????????????2??0?0??????0001?0????????????????????000?1??11?????1???1??20010000
1000?1000?101?0?100??00??210

Tomistoma_cairense
??1??2???4????????1000001?1010?
???00?20?0?????025?0???0????000??0?000010100100010?00??011110???01???10?200100
1010001??0???11?001?000003?0?0
Thecachampsa_antiqua
02000000??001010?00011010111?1??11?0?00???1???1122???4?100????1000031?1
01?0???00120?0000110210000000?100000??0?0000101?0100010110000111110???011??1012
00100101010??00???11100100?20030210
Tomistoma_petrolica
??????????????????????????1?????????????????????????04??????0010?0?01?1?10?
???00???????????2?00?0?0???00001???0?00101001??????1?0?0?1110?0?2?0??0??200?000
0100?????????1???1????003??0?
Dollosuchoides_densmorei
001???0???111010?0001?0?001111??1?00??????????1120???0?????000100?0??010
1?????00120?00?0?1021000000??00000????01?0101001000101100?011110????????1??200
10?1010001???????10?01000?0030011
Kentisuchus_spenceri
??????0??1?????0?????0??1000?1101?11?
???00110?0000?1021000000???0000??0?010010100100?101100?111110??????0?0??20010?
10100???????111?0?100?0?030010
Brachyuranochampsa_eversolei
??
??0011??00???1021000000??00000??0?0?0??01101000101000?111100???2?00?0?121010?1
01000???????11000100000030000
Crocodylus_acer
??
??00110?0000?1021000000??000001???000100?10100010100000111100?002?01?00?200100
1010001??0??111000100000030001
Crocodylus_depressifrons
???00?00??1100001001110000111??1100?10???1???11102101?????001100000001
011????00110?0000?1011000000?1100001?0?0001001?01000101?000111100?010200?0012
0010010100011001?111000100000030001
Crocodylus_affinis
001001001?1000100001110000111100110 0?10???1???111021010100000110000000
101100??00110?0000100110000000?010000??0?000100110100010100000111100?0?010??001
2001001010001??0???11000100000030000
Asiatosuchus_germanicus
001?0?0?1?001010?0101?000?1111??1??0??????1???11102000?????00110000??010
1?00??00010?0000?000100000???10000??0?00010???01000101000?111100???0100?00111
0100101000???????1100?10000003?000
Prodiplocynodon_langi
??
??00110?0000??003000000??100001??000010011?1000101????111100???0?0??0?11?010?1
010001??01?011001100000030?00
Leidyosuchus_canadensis
????0?0????????1????010000011?1??10?0?11??11???0110000000?0?0101000000111

01????00010?000000003000000000100010001000011101000101000011110?01010010010
0010010100000001?001001100100011011
Deinosuchus_riograndensis
??????0????????????01????????????????00???1???0110???001?0?11?10??0??11?0?
????00??1?0??????0?0000???0??00011?00?0????????????000111120?012210?111000100
1?1000??000?0?????1??100?1????
Brachychampsa_montana
101011001?1100???0001??000111100?000?103111???11101101?????01110?000011
10100??00110?0002?1101000000?0010001?0?0100000111100101200111110?110200?0111
0010110102000101?001001100100010011
Brachychampsa_sealeyi
??????????????????????????????????????10???1???11101??0???????11??000011?1
????001?0?0002?110100000???010??????????00????????10?2001101?00???????????100????
???2?????????????1??10??10?0?
Stangerochampsa_mccabei
????110???010010?000100000111100100?01??11???111010100????0111110000?1
10?????00110?0002?1102000000?001000????000000011110010120011111100?110200?0?11
00102101000??1?1??01001100100010001
Ceratosuchus_burdoshi
??????????????????????????????????0?1????????11111??0?????01?10??00?11?01
????00010?0?01?0102000000???1000??0????00???01???1?1??0?111100????????0????010?
111???????????10??100100010?0?
Hassiacosuchus_haupti
001?1?0?1??????0???01?000?1111?????0??11?11???111110?0?????01?10??0??111
01????00010?00???010?0000??????0001?0??????0?????????1100?111100?1?0200?0112001
0210101????????01???10010001?001
Navajosuchus_mooki
??????0?1??????0???0?00???1111??1??0?111111???11111010?????01?10??00??110
?????00010?0001?01020000???0?1000??0???00?00?111001011001111100???020??0112?01
02101000????1??010??100100010001
Procaimanoidea_kayi
????110?1??????0???010?00?1111??10?0?112121?????010?1??100?01?1100000111
0?????10?????0???010?0000???0?1000??0?000000001110?0?110111111000??0200?011200
102101010???????0100110010001?001
Procaimanoidea_utahensis
??110100?00??01011110??0011101
????10110?0100?01020?0000??01000????0000000?11100101101?111100?1?0200?0112001
0?101000???????0100110010001?001
Arambourgia_gaudryi
??11010??0?????01?100?0??1110?
????1001??010??01020000?0???10001000??000????11?0??1101?111100?1102?0?0?1210?0
210100?????????10011?010?01?001
Wannaganosuchus_brachymanus
????1?0???1?00?0???010000?1111001000?11???1???111110?0?????0??100?00?11?
0?????00110?0000??10200??00???1000??0?100000???1??01?1101?111100????????0?12001
??101000????????10011?0100010001

Alligator_sinensis
101011101?1100101000101101111100110001121111101100001 20?0010112000001
11101??1100100001000010200000000010001100100000011110010110111111100110200 10
1120010210101000111100100110010001 0001
Alligator_mississippiensis
101011001?0100100000101101111100110001121011001100011201001011200010 1
1110100110010000100001020000000001000111000000001111001011011111110011020010
1121010210101000111100100110010001 0001
Alligator_mefferdi
??????????????????????????????1?????????11???????1100001201000011200010111 10
100??00100?0100?0102000000?0?10001?1?0000000?1110010110111111110?110200?011210
102101010??1???00100110010001 0?01
Alligator_thomsoni
??????????????????01????????1?????0?1????????110000?2?????01120001001110
1????00100?010000102000?0??0010001?1?000000????1?????1011111110?1?0200101?2101
0210101?001?11?01001100100010 0001
Alligator_olseni
??????0?1?????10???01?10011111???100?11???????11010010?????0112000000111
01????00100?01000?10200??00???1000??0?0?000101111101011011111110?110200?01120
0102101010??????00100?1?0100010 0001
Alligator_mcgrewi
100010001?010010?00010000111?1101??0?11???1???11110010?100?011100000111
101????00000?0100?0102000000?0010001?0010000001111001011011111100011020 0?0112
00102101010?01???001001100100010 0001
Alligator_prenasalis
10001?0?1?????10?0?01000011111??1000?112111???11111010?????011100000111
10100??00000?0100?0102000000?0010001100100000011110010110111111100?110200?011
200102101000001?1?001001100100010 0001
Eocaiman_cavernensis
??1110???2?????11?1?????????????
???00????0??????0???????????100???0?1??0000???????0?????1??1?0?????0???????0?????1
?3??????????0??1?2?????????
Tsoabichi_greenriverensis
??????????????????01??????????????????10??20???1100???2????????1??????11???
01??00010?10????10??000????????0?????????????????????000?1111?0?1?0????0??211???1
01?2?????????????????100???011
Purussaurus_neivensis
101?100?1?000010?0??1????011???????0?11???1???1?00??1?1010?1112011000110
01????00110?0001?0102000000?0010001?0?0?000001111012111111111110?110201?01120
11?210102000101??010??10210001000?
Orthogenysuchus_olseni
??00??????????????????????0???
??00121?0?01??10?0?0???????000????01?000?????????????????11110????????0????11??101
??0?????????????????10001????
Mourasuchus_spp
10??100?1?00?010?00?1?10?011????1300?11???1???1102?112?????01110?1000110

00????00121?0000?1105000100?0010001?0?0100000111101 2?1011?111110?110?00????21
11??111?30????1???100110?10001300?
Caiman_yacare
101111001?1000100000101011111100110001112211101100211210101110101102011001011100110000000011200000000010001100100000011110121111011111100110201101120111210103000101100100110210001000 1
Caiman_crocodilus
101111001?1000100000101011111100110001112211101100211210101110101102011001011100110000000011200000000010001100100000011110121110011111100110201101120111210103000101100100110210001000 1
Caiman_latirostris
101110001?100010000010 10?111100110001112212101100211210101 11?10110201100???1100110000000010200100000010001100100000011110121110011111100110201101121111210103000101100100110210001000 1
Caiman_lutescens
??0????????????????????????????00110?0000?0102001000?001000????10000001111012112 00?1?1?10?????0???????1????0??????????????????100?1??0?
Melanosuchus_fisheri
??????0????????0????????????????????????????????02????????1?11011????10?1???001?0?0000??102001010???1000??0???0????11????2?11???111110????????0????11??1010?????????010??1?2?0001000?
Melanosuchus_niger
101111001?1?0010000010101111110011000111221210110021121010111110110201100 1??1100110000000010200101000010001100100000011110121110011111100110201101121111121010300010110010011021000100 01
Paleosuchus_trigonatus
100111111?0100101000100011111121130001113211201100212221111111110110001100101111011000010001020000000001000110001000101111011110001111110111020110112111?2101020001011001001102100010001
Paleosuchus_palpebrosus
100111111?0100101010100011111121130001113211201100212221 11?11?10110001100?0111101100001000102000000000100011000100010111101111000111111011102011011211 1?2101020001011001001102100010001
Allognathosuchus_polyodon
??11111010?????01?11??00?111?1????00010?000??01020000?0?????00??0?00?00?0?111001?1?01?111100????????0??20010?101???????????1???1??1???1?0?1
Allognathosuchus_wartheni
????1?0????????????0?0000?1111??1000?11???1???11111010?100?0111100000111101????00010?0000?0102000000000010001?0?000000?0111001?11011111100?110200?01120010210100 00?1?1?0010011001?001?001
Diplocynodon_ratelii
??????0??????000???010?00?1111001400?10??21???01002101?????0111000001?1101????00110?0000001230000000101000??0?0000001111000101000011110 0??10100100000010110100000001?101001100100010211

Diplocynodon_hantoniensis
100???1?1?0100001000100001111??1400?101?21???011021010????011100000111
101????00120?0?000?11300?000?1010001?0?000000101100010100001111100?110100?0010
10101101000??0?1??010011?0100010?11
Diplocynodon_muelleri
??????????????????????1?01??1?????14?0?10??21???01002??2?????01110??1001110
0????00120?10000012300000000101000????000001111100000100 0?1?1100?110??0?01?010
10110100????????01001100100010001
Diplocynodon_tormis
??????????????????????1?????1??????????10??21???01?021?1?????01?1?00????11??
????0?120??00000123000000?1010001???000000111100?0?10000111100?11010000010101
0110100?0???1?001?0110010000100?1
Diplocynodon_darwini
100001001?010000?00010000?1111??1400?101121???011020010??0?01?10000011
110100??00020?0000?0103000000?0??000??0?0000001111?00101000?111100?110100?011
010101101000???????0100110010001 0?01
Diplocynodon_deponiae 10000?????????0?????1?00??1?????14?0?10?[1
2]21???0110210[1
2]?????01?10??0??111??????0?120??00??0113000000?101???????000000111100001 1000?1
11?00?11010100??01110[0 1]1?1?0??????????0??1??1???10?01
Diplocynodon_ungeri
??1????????0110210100?0100010101???110?
????0?120??000000?3000000???0???????0001110011???1010000111?000100010??112000?
?1?112???0????0?0????01???1?200
Diplocynodon_elavericus
??10???0???0?102??1????????1????0?1???1?
???1?1??????10?1131??000??00???????100110010110?101?0?01?1?0??????10?1110?00021
?110???0???11?0??0?11???00?1?
Diplocynodon_africanum
??????????????????01?????????????????????????????0?????????01?11??0???11???
???00120?0000001130000000??01?00????00000011?1?0???1000?111100??10?00?0??11010?
10100??????????00?100??00?0110
Diplocynodon_remensis
??10??20???01002000?????01110?00011110
1????00?20?0000000131000000100???1???0000001101000101000001?1100???01000000110
10110100???1?1??01001100100010200
Krabisuchus_siamogallicus
??????????????????????1??0????????020??11???1???11010??1?????00?110100?0100
1????00010?0?00?01020?0000???10?0????10000010111000010000110100?1?00?0?0??2001
??10112??????????????????10??1020?
Maoming_specimen
??
????11??00????1???000????????0?????????????????????????000?1???00???????????200???101?
?????????????????????????101
Protoalligator_huiningensis
??110021????????111????????????

???00100?000??1101000?????????????????????????????????00?1?1??0?????????????????????
??????????????????????????0??0
Globidentosuchus_brachyrostris
????????????????????01?????????????????????????????11101??0?11?10?1101103111011
????0012??000??01?20000???1?10?0??????0???0?11?????111??1?1100??????0?0??2011??
101?3?????????1???1?????0??0?0
Culebrasuchus_mesoamericanus
??11?2???2?????0??20???????????
???001???0?????1000000???????001?0?????????????????????1?1?0???????????121010210
?03??01????01?0?1?0?????0?0?
;
proc /;
comments 0
;

Table A3.1:

Data file for time calibration and ancestral state reconstruction

Species	FAD	LAD	Continent	Reference
Bernissartia_fagesii	129	118	Europe	[3]
Allodaposuchus_precedens	78	66	Europe	[4–6]
Acynodon_iberoccitanus	73	69	Europe	[7]
Acynodon_adriaticus	84	72.1	Europe	[8]
Iharkutosuchus_makadii	86	83	Europe	[9]
Hylaeochampsa_vectiana	129	125	Europe	[10]
Eothoracosaurus	73	69	North America	[11]
Thoracosaurus_neocesariensis	70	61	North America	[12,13]
Thoracosaurus_macrorhynchus	70	61.6	Europe	[14–16]
Eosuchus_minor	59	47	North America	[17,18]
Eosuchus_lerichei	59	56	Europe	[19]
Eogavialis_africanum	38	28	Africa	[20,21]
Piscogavialis_jugaliperforatus	7.25	5.33	South America	[22]
Gryposuchus_colombianus	13.8	12	South America	[23]
Gavialis_gangeticus	3	0	Asia	[24]
Gavialis_sp_Siwalik	7	1.8	Asia	[25,26]
Borealosuchus_threeensis	68	64	North America	[27]
Borealosuchus_formidabilis	60	56	North America	[28]
Borealosuchus_wilsoni	56	48.6	North America	[28,27]
Borealosuchus_acutidentatus	60	59	North America	[27]
Borealosuchus_sternbergii	69	63	North America	[28]
Boverisuchus_magnifrons	47.8	41.2	Europe	[29]
Boverisuchus_vorax	50.3	41.3	North America	[29]
Planocrania_hengdongensis	58.7	56	Asia	[29]
Planocrania_datangensis	61.7	58.7	Asia	[29]
Mecistops_cataphractus	11.608	0	Africa	[30]
Crocodylus_niloticus	3.6	0	Africa	[31]
Crocodylus_porosus	3.6	0	Australia	[32]
Crocodylus_rhombifer	0.5	0	North America	[31]
Euthecodon_arambourgii	20	15.9	Africa	[33]
Osteolaemus_tetraspis	0.2	0	Africa	[31]
Osteolaemus_osborni	0.5	0	Africa	[34]
Voay_robustus	0.01	0	Africa	[35,36]
Rimasuchus_lloydi	20	15.9	Africa	[37]
Brochuchus_pigotti	20.43	15.97	Africa	[38]
Crocodylus_megarhinus	33	28	Africa	[39]
Australosuchus_clarkae	28	20	Australia	[40]
Kambara_implexidens	54.6	47.8	Australia	[40,41]
Trilophosuchus_rackhami	15.97	11.63	Australia	[42]
Quinkana_spp	28.1	0.126	Australia	[43–45]
Tomistoma_schlegelii	2	0	Asia	[31]
Tomistoma_lusitanica	20	15.9	Africa	[46,2]
Toyotamaphimeia_machikanense	2	0.37	Asia	[47]

Gavialosuchus_eggenburgensis	20	15.9	Europe	[48]
Paratomistoma_courti	44	42	Africa	[49]
Tomistoma_cairense	47	44	Africa	[21]
Thecachampsa_antiqua	13	7.246	North America	[50]
Tomistoma_petrolica	37.2	33.9	Asia	[51]
Dollosuchoides_densmorei	47	44	Europe	[52]
Kentisuchus_spenceri	56	49	Europe	[52]
Brachyuranochampsa_eversolei	46	42	North America	[53]
Crocodylus_acer	55.8	50.3	North America	[54]
Crocodylus_depressifrons	56	47.8	Europe	[55]
Crocodylus_affinis	50.3	46.2	North America	[56]
Asiatosuchus_germanicus	47.8	41.3	Europe	[57]
Prodiplocynodon_langi	70	67	North America	[58,59]
Leidyosuchus_canadensis	76.5	72.4	North America	[28,60,61]
Deinosuchus_riograndensis	80.5	70.6	North America	[62]
Brachychampsa_montana	73.4	66	North America	[63–65]
Brachychampsa_sealeyi	83.6	78	North America	[66]
Stangerochampsa_mccabei	70.6	66	North America	[67]
Ceratosuchus_burdoshi	56.8	55.8	North America	[68]
Navajosuchus_mooki	63.3	61.7	North America	[69]
Procaimanoidea_kayi	53.5	46.2	North America	[64]
Procaimanoidea_utahensis	46.2	42	North America	[70]
Arambourgia_gaudryi	37.2	33.9	Europe	[71]
Wannaganosuchus_brachymanus	60.2	56.8	North America	[72]
Alligator_sinensis	3	0	Asia	[73]
Alligator_mississippiensis	13.6	0	North America	[64]
Alligator_mefferdi	13.6	10.6	North America	[74]
Alligator_thomsoni	20.6	16.3	North America	[64,75]
Alligator_olseni	23.03	16.3	North America	[64,76]
Alligator_mcgrewi	20.6	16.3	North America	[64,77]
Alligator_prenasalis	37	33.5	North America	[64]
Eocaiman_cavernensis	54	47.8	South America	[78]
Tsoabichi_greenriverensis	53.5	50.3	North America	[79]
Purussaurus_neivensis	13.82	11.63	South America	[64,80]
Orthogenysuchus_olseni	55.8	52	North America	[64]
Mourasuchus_spp	15.97	5.332	South America	[81–83]
Caiman_yacare	9	0	South America	[84,85]
Caiman_crocodilus	0.5	0	South America	[64]
Caiman_latirostris	10.29	0	South America	[64,80,84]
Caiman_lutescens	13.8	6.8	South America	[64,84]
Melanosuchus_fisheri	11.608	5.332	South America	[86,87]
Melanosuchus_niger	0.5	0	South America	[80]
Paleosuchus_trigonatus	0.5	0	South America	[64]
Paleosuchus_palpebrosus	0.5	0	South America	[64]
Allognathosuchus_polyodon	50.3	42	North America	[88]
Allognathosuchus_wartheni	55.8	50.3	North America	[88]
Diplocynodon_ratelii	33.9	21	Europe	[89,90]
Diplocynodon_hantoniensis	37.8	28.1	Europe	[91–93]

Diplocynodon_muelleri	32	30	Europe	[94]
Diplocynodon_tormis	39.5	37.8	Europe	[95]
Diplocynodon_darwini	47.8	41.2	Europe	[64]
Diplocynodon_deponiae	47.8	41.2	Europe	[64,96]
Diplocynodon_ungeri	15.97	11.6	Europe	[97]
Diplocynodon_elavericus	36	35	Europe	[98]
Diplocynodon_africanum	59.2	51	Africa	-
Diplocynodon_remensis	58.7	55.8	Europe	[99]
Krabisuchus_siamogallicus	37.2	33.9	Asia	[100]
Globidentosuchus_brachyrostris	11.6	5.3	South America	[81]
Culebrasuchus_mesoamericanus	19.83	19.12	South America	[101]

Strict consensus tree:

(Bernissartia_fagesii ,((Allodaposuchus_precedens ,(Acynodon_iberoccitanus ,(Acynodon_adriaticus ,(Iharkutosuchus_makadii ,Hylaeochampsa_vectiana)))),(((Eothoracosaurus ,(Thoracosaurus_macrorhynchus ,(Thoracosaurus_neocesariensis ,((Eosuchus_minor ,Eosuchus_lerichei),(Eogavialis_africanum ,((Piscogavialis_jugaliperforatus ,Gryposuchus_colombianus),(Gavialis_gangeticus ,Gavialis_sp_Siwalik)))))),(Borealosuchus_sternbergii ,(Borealosuchus_formidabilis ,(Borealosuchus_threeensis ,Borealosuchus_wilsoni ,Borealosuchus_acutidentatus)))),((Planocrania_hengdongensis ,(Planocrania_datangensis ,(Boverisuchus_magnifrons ,Boverisuchus_vorax))),((Asiatosuchus_germanicus ,Prodiplocynodon_langi ,(Crocodylus_depressifrons ,Crocodylus_affinis ,(Brachyuranochampsa_eversolei ,Crocodylus_acer ,(Crocodylus_megarhinus ,((Mecistops_cataphractus ,(Crocodylus_porosus ,(Crocodylus_niloticus ,Crocodylus_rhombifer))),(Rimasuchus_lloydi ,(Euthecodon_arambourgii ,Brochuchus_pigotti),(Voay_robustus ,(Osteolaemus_tetraspis ,Osteolaemus_osborni)))),(Australosuchus_clarkae ,Kambara_implexidens ,(Trilophosuchus_rackhami ,Quinkana_spp)),(Kentisuchus_spenceri ,(Tomistoma_petrolica ,Dollosuchoides_densmorei ,(Thecachampsa_antiqua ,(Tomistoma_cairense ,((Tomistoma_schlegelii ,(Tomistoma_lusitanica ,Paratomistoma_courti)),(Toyotamaphimeia_machikanense ,Gavialosuchus_eggenburgensis))))))))),(Leidyosuchus_canadensis ,((Deinosuchus_riograndensis ,(((Stangerochampsa_mccabei ,(Brachychampsa_montana ,Brachychampsa_sealeyi)),(Globidentosuchus_brachyrostris ,(Culebrasuchus_mesoamericanus ,(Eocaiman_cavernensis ,((Tsoabichi_greenriverensis ,(Paleosuchus_trigonatus ,Paleosuchus_palpebrosus)),((Purussaurus_neivensis ,(Orthogenysuchus_olseni ,Mourasuchus_spp)),((Caiman_yacare ,Caiman_crocodilus),(Caiman_latirostris ,Caiman_lutescens ,(Melanosuchus_fisheri ,Melanosuchus_niger)))))))),((Ceratosuchus_burdoshi ,Navajosuchus_mooki),((Allognathosuchus_polyodon ,Allognathosuchus_wartheni ,(Krabisuchus_siamogallicus ,(Procaimanoidea_kayi ,(Procaimanoidea_utahensis ,Arambourgia_gaudryi)))),(Wannaganosuchus_brachymanus ,(Alligator_prenasalis ,(Alligator_mcgrewi ,(Alligator_olseni ,(Alligator_sinensis ,(Alligator_mississippiensis ,Alligator_mefferdi ,Alligator_thomsoni))))))))),(Diplocynodon_darwini ,(((Diplocynodon_hantoniensis ,(Diplocynodon_ratelii ,(Diplocynodon_africanum ,Diplocynodon_remensis))),(Diplocynodon_ungeri ,Diplocynodon_elavericus)),(Diplocynodon_deponiae ,(Diplocynodon_muelleri ,Diplocynodon_tormis))))))))));

R scripting for time calibration of the strict consensus:

```
#Required packages for the time calibration and ancestral state reconstruction

library("paleotree", lib.loc="~/R/win-library/3.2")
library("ape", lib.loc="~/R/win-library/3.2")
library("strap", lib.loc="~/R/win-library/3.2")
library("phytools", lib.loc="~/R/win-library/3.2")



tree<-read.tree("filename.txt")
ages<- read.csv("filename.csv", header=TRUE)
FAD<- ages[,2]
LAD<- ages[,3]
names<-ages[,1]
treeages<-cbind(FAD,LAD)
rownames(treeages)<-names
AGES<-treeages[match(tree$tip.label,rownames(treeages)),]
equalstrict<-DatePhylo(tree, AGES, method= "equal", add.terminal = T, rlen=1)
basicstrict<-DatePhylo(tree, AGES, method= "basic", add.terminal = T)
mblstrict<-timePaleoPhy(tree, AGES, type="mbl", add.term=T, plot=T, vartime=1)
continent<-ages[,4]
continent<-as.character(continent)
names(continent)<- ages[,1]
states_equal<-continent[match(equalstrict$tip.label,names)]
states_basic<-continent[match(basicstrict$tip.label,names)]
states_mbl<-continent[match(mblstrict$tip.label,names)]
geoscalePhylo(equalstrict,AGES, cex.ts=1, cex.tip=0.7,width=1.6)
geoscalePhylo(basicstrict,AGES, cex.ts=1, cex.tip=0.7,width=1.6)
geoscalePhylo(mblstrict,AGES, cex.ts=1, cex.tip=0.7,width=1.6)
```

References:

1. Brochu CA, Rincon AD. A gavialoid crocodylian from the Lower Miocene of Venezuela. Spec Pap Palaeontol. 2004;71: 61–79.
2. Jouve S, Bouya B, Amaghzaz M, Meslouh S. *Maroccosuchus zennaroi* (Crocodylia: Tomistominae) from the Eocene of Morocco: phylogenetic and palaeobiogeographical implications of the basalmost tomistomine. J Syst Palaeontol. 2014;13: 1–25. doi:10.1080/14772019.2014.913078
3. Buscalioni AD, Sanz JL. The small crocodile *Bernissartia fagesii* from the Lower Cretaceous of Galve (Teruel, Spain). Bulletin de l'Institut Royal des Sciences naturelles de Belgique. Sciences de la Terre. 1990. pp. 129–150.
4. Martin JE, Delfino M, Garcia G, Godefroit P, Berton S, Valentin X. New specimens of *Allodaposuchus precedens* from France: Intraspecific variability and the diversity of European Late Cretaceous eusuchians. Zool J Linn Soc. 2016;176: 607–631. doi:10.1111/zoj.12331
5. Delfino M, Codrea V, Folie A, Dica P, Godefroit P, Smith T. A complete skull of *Allodaposuchus precedens* Nopsca, 1928 (Eusuchia) and a reassessment of the morphology of the taxon based on the Romanian remains. J Vertebr Paleontol. 2008;28: 111–122.
6. Buscalioni AD, Ortega F, Weishampel DB, Jianu CM. A revision of the Crocodyliform *Allodaposuchus precedens* from the Upper Cretaceous of the Hateg Basin, Romania. Its relevance in the phylogeny of Eusuchia. J Vertebr Paleontol. 2001;21: 74–86. doi:10.1671/0272-4634(2001)021[0074:AROTCA]2.0.CO;2
7. Martin JE. New material of the Late Cretaceous globidontan *Acynodon iberoccitanus* (Crocodylia) from Southern France. J Vertebr Paleontol. 2007;27: 362–372. doi:10.1671/0272-4634(2007)27[362:NMOTLC]2.0.CO;2
8. Delfino M, Martin JE, Buffetaut E. A new species of *Acynodon* (Crocodylia) from the upper cretaceous (Santonian-Campanian) of Villaggio del Pescatore, Italy. Palaeontology. 2008;51: 1091–1106. doi:10.1111/j.1475-4983.2008.00800.x
9. Ősi A. Cranial osteology of *Iharkutosuchus makadii*, a Late Cretaceous basal eusuchian crocodyliform from Hungary. Neues Jahrbuch für Geologie und Paläontologie - Abhandlungen. 2008. pp. 279–299. doi:10.1127/0077-7749/2008/0248-0279
10. Clark JM, Norell MA. The early Cretaceous crocodylomorph *Hylaeochampsa vectiana* from the Wealden of the Isle of Wight. Am Museum Novit. 1992;3032: 1–19.
11. Brochu CA. A new Late Cretaceous gavialoid crocodylian from eastern North America and the phylogenetic relationships of thoracosaurs. J Vertebr Paleontol. 2004;24: 610–633. doi:10.1671/0272-4634(2004)024
12. Laurent Y, Buffetaut E, Le Loeuff J. Un crâne de Thoracosaurine (Crocodylia, crocodylidae) dans le Maastrichtien spérieur du sud de la France. Oryctos. 2000;3: 19–27.
13. Cook JJ, Ramsdell RC. Macrofossils from the Vincentown Formation (Paleocene) of New Jersey. Bull New Jersey Acad Sci. 1991;36: 11–15.
14. Koken E. *Thoracosaurus macrorhynchus* Bl. aus der Tuffkreide von Maastricht. Zeitschrift der Dtsch Geol Gesellschaft. Stuttgart, Germany: Schweizerbart Science Publishers; 1888;40: 754–773.
15. Troedsson GT. On crocodilian remains from the Danian of Sweden. Lund; 1924.
16. Puértolas-Pascual E, Blanco A, Brochu CA, Canudo JI. Review of the Late Cretaceous-early Paleogene crocodylomorphs of Europe: Extinction patterns across the K-PG boundary. Cretac Res. 2016;57: 565–590. doi:http://dx.doi.org/10.1016/j.cretres.2015.08.002
17. Brochu CA. Osteology and phylogenetic significance of *Eosuchus minor* (Marsh, 1870) new combination, a longirostrine crocodylian from the Late Paleocene of North America. Journal of Paleontology. 2006. pp. 162–186. doi:10.1666/0022-3360(2006)080[0162:OAPSOE]2.0.CO;2

18. Brochu CA. *Eosuchus* (Crocodylia, Gavialoidea) from the lower Eocene of the Isle of Sheppey, England. Journal of Vertebrate Paleontology. 2006. pp. 466–470. doi:10.1671/0272-4634(2006)26[466:ECGFTL]2.0.CO;2

19. Delfino M, Piras P, Smith T. Anatomy and phylogeny of the gavialoid crocodylian *Eosuchus lerichei* from the Paleocene of Europe. Acta Palaeontol Pol. 2005;50: 565–580.

20. Andrews CW. A Descriptive Catalogue of the Tertiary Vertebrata of the Fayûm, Egypt. British Museum, London; 1906.

21. Müller L. Ergebnisse der Forschungsreisen Prof. E. Stromers in den Wüsten Ägyptens. V. Tertiäre Wirbeltiere. Beiträge zur Kenntnis der Krokodilier des ägyptischen Tertiärs Abhandlungen der Bayer Akad der Wissenschaften. 1927;31: 1–97.

22. Kraus R. The cranium of *Piscogavialis jugaliperforatus* n.gen., n.sp. (Gavialidae, Crocodylia) from the Miocene of Peru. Paläontologische Zeitschrift. 1998;72: 389–406.

23. Langston Jr. W, Gasparini ZB de. Crocodilians, *Gryposuchus*, and the South American gavials. In: Kay RF, Madden RH, Cifelli RL, Flynn JJ, editors. Vertebrate Paleontology in the Neotropics The Miocene Fauna of La Venta, Colombia. Smithsonian Institution Press, Washington DC; 1997. pp. 113–154.

24. Sen PK, Banerjee M. On the occurrence of reptilian remains in the peat bed of Barrackpore, 24-Parganas, West Bengal. J Palaeontol Soc India. 1983;29: 47–51.

25. Lull RS. Fossil gavials from north India. American Journal of Science. 1944. pp. 417–430. doi:10.2475/ajs.242.8.417

26. Mook CC. A new species of fossil gavial from the Siwalik beds. Am Museum Novit. 1932;514: 1–5.

27. Brochu CA, Parris DC, Grandstaff BS, Denton RK, Gallagher WB. A new species of *Borealosuchus* (Crocodyliformes, Eusuchia) from the Late Cretaceous–early Paleogene of New Jersey. J Vertebr Paleontol. 2012;32: 105–116. doi:10.1080/02724634.2012.633585

28. Brochu CA. A review of "*Leidyosuchus*" (Crocodyliformes, Eusuchia) from the Cretaceous through Eocene of North America. J Vertebr Paleontol. 1997;17: 679–697. doi:10.1080/02724634.1997.10011017

29. Brochu CA. Phylogenetic relationships of Palaeogene ziphodont eusuchians and the status of *Pristichampsus* Gervais, 1853. Earth Environ Sci Trans R Soc Edinburgh. 2012;103: 521–550. doi:10.1017/S1755691013000200

30. Storrs GW. Late Miocene-Early Pliocene crocodilian fauna of Lothagam, southwest Turkana Basin, Kenya. In: Leakey MG, Harris JM, editors. Lothagam: The Dawn of Humanity in Eastern Africa. 2003. pp. 137–159.

31. Brochu CA. Crocodylian snouts in space and time: phylogenetic approaches toward adaptive radiation. Am Zool. 2001;41: 564–585. doi:10.1668/0003-1569(2001)041[0564:CSISAT]2.0.CO;2

32. Molnar RE. *Pallimnarchus* and other Cenozoic crocodiles of Queensland. Mem Queensl Museum. 1982;20: 657–673.

33. Ginsburg L, Buffetaut E. *Euthecodon arambourgi* n. sp., et l'évolution du genre Euthecodon, Crocodilien du Néogène d'Afrique. Géologie Méditerranéenne. 1978;5: 291–302.

34. Eaton MJ, Martin A, Thorbjarnarson JB, Amato G. Species-level diversification of African dwarf crocodiles (Genus Osteolaemus): a geographic and phylogenetic perspective. Mol Phylogenet Evol. Elsevier Inc.; 2009;50: 496–506. doi:10.1016/j.ympev.2008.11.009

35. Bickelmann C, Klein N. The late pleistocene horned crocodile *Voay robustus* (Grandidier & Vaillant, 1872) from Madagascar in the Museum fur Naturkunde Berlin. Foss Rec. 2009;12: 13–21. doi:10.1002/mmng.200800007

36. Brochu CA, Njau J, Blumenschine RJ, Densmore LD. A new horned crocodile from the Plio-Pleistocene hominid sites at Olduvai Gorge, Tanzania. PLoS One. 2010;5: 1–13. doi:10.1371/journal.pone.0009333

37. Brochu CA, Storrs GW. A giant crocodile from the Plio-Pleistocene of Kenya, the phylogenetic

relationships of Neogene African crocodylines, and the antiquity of *Crocodylus* in Africa. J Vertebr Paleontol. 2012;32: 587–602. doi:10.1080/02724634.2012.652324

38. Conrad JL, Jenkins K, Lehmann T, Manthi FK, Peppe DJ, Nightingale S, et al. New specimens of *"Crocodylus" pigotti* (Crocodylidae) from Rusinga Island, Kenya, and generic reallocation of the species. J Vertebr Paleontol. 2013;33: 629–646. doi:10.1080/02724634.2013.743404

39. Mook CC. The Skull Characters of *Crocodilus megarhinus* Andrews. Am Museum Novit. 1927;289: 1–8.

40. Salisbury SW, Willis PMA. A new crocodylian from the Early Eocene of south-eastern Queensland and a preliminary investigation of the phylogenetic relationships of crocodyloids. Alcheringa An Australas J Palaeontol. 1996;20: 179–226. doi:10.1080/03115519608619189

41. Willis PMA, Molnar RE, Scanlon JD. An Early Eocene crocodilian from Murgon, Southeastern Queensland. Kaupia Darmstädter Beiträge zur Naturgeschichte. 1993;3: 27–33.

42. Willis PMA. *Trilophosuchus rackhami* gen. et sp. nov., a new crocodilian from the early miocene limestones of riversleigh, northwestern queensland. J Vertebr Paleontol. 1993;13: 90–98. doi:10.1080/02724634.1993.10011489

43. Molnar RE. Pleistocene ziphodont crocodilians of Queensland. Rec Aust Museum. 1981;33: 803–834. doi:10.3853/j.0067-1975.33.1981.198

44. Willis PMA, Mackness BS. *Quinkana babarra*, a new species of ziphodont mekosuchine Crocodile from the early Pliocene Bluff Downs local fauna, northern Australia with a revision of the genus. Proceedings of the Linnean Society of New South Wales. LINNEAN SOCIETY OF NEW SOUTH WALES; 1996. pp. 143–152.

45. Willis PMA. New crocodilians from the Late Oligocene White Hunter Site, Riversleigh, northwestern Queensland. Mem Queensl Museum. QUEENSLAND MUSEUM; 1997;41: 423–438.

46. Piras P, Delfino M, Favero L Del, Kotsakis T. Phylogenetic position of the crocodylian *Megadontosuchus arduini* and tomistomine palaeobiogeography. Acta Palaeontol Pol. 2007;52: 315–328.

47. Kobayashi Y, Tomida Y, Kamei T, Eguchi T. Anatomy of a Japanese tomistomine crocodylian, *Toyotamaphimeia machikanensis* (Kamei et Matsumoto, 1965), from the middle Pleistocene of Osaka Prefecture: the reassessment of its phylogenetic status within Crocodylia. Natl Sci Museum Monogr. 2006;

48. Toula F, Kail JA. Über einen Krokodil-Schädel aus den Tertiärablagerungen von Eggenburg in Niederösterreich: eine paläontologische Studie. Kaiserl. Königl. Staatsdr.; 1885.

49. Brochu CA, Gingerich PD. New tomistomine crocodylian from the Middle Eocene (Bartonian) of Wadi Hitan, Fayum Province, Egypt. Contrib Museum Paleontol. 2000;30: 251–268.

50. Myrick AC. *Thecachampsa antiqua* (Leidy, 1852) (Crocodylidae: Thoracosaurinae) from fossil marine deposits at Lee Creek Mine, Aurora, North Carolina, USA. Smithonian Contrib to Paleobiol. 2001;90: 219–225.

51. Shan H, Wu X, Cheng Y, Sato T. *Maomingosuchus petrolica*, a restudy of '*Tomistoma' petrolica</i> Yeh, 1958*. Palaeoworld. "Elsevier B.V. and NANJING INSTITUTE OF GEOLOGY AND PALAEONTOLOGY, CAS"; 2017; doi:10.1016/j.palwor.2017.03.006

52. Brochu CA. Systematics and taxonomy of Eocene tomistomine crocodylians from Britain and Northern Europe. Palaeontology. 2007;50: 917–928.

53. Zangerl R. *Brachyuranochampsa eversolei,* gen. et. sp. nov., a new crocodilian from the Washakie Eocene of Wyoming. Ann Carnegie Museum. 1944;30: 77–84.

54. Mook CC. The skull of *Crocodilus acer* Cope. Bull Am Museum Nat Hist. 1882;9: 117–121.

55. Delfino M, Smith T. A reassessment of the morphology and taxonomic status of *'Crocodylus' depressifrons* Blainville, 1855 (Crocodylia, Crocodyloidea) based on the Early Eocene remains from Belgium. Zool J Linn Soc. 2009;156: 140–167. doi:10.1111/j.1096-3642.2008.00478.x

56. Mook CC. Description of a skull of a Bridger crocodilian. Bull Am Museum Nat Hist. 1904;8: 111–116.

57. Vasse D. Un crâne d'*Asiatosuchus germanicus* du Lutétien d'Issel (Aude). Bilan sur le genre *Asiatosuchus* en Europe. Geobios. 1992. pp. 293–304. doi:10.1016/S0016-6995(06)80407-9

58. Mook CC. A new crocodilian from the Lance Formation. Am Museum Novit. 1941;1128: 1–6.

59. Puértolas E, Canudo JI, Cruzado-Caballero P. A new crocodylian from the late Maastrichtian of Spain: implications for the initial radiation of crocodyloids. PLoS One. 2011;6: 1–12. doi:10.1371/journal.pone.0020011

60. Mook CC. A new species of fossil crocodile of the genus *Leidyosuchus* from the Green River beds. Am Museum Novit. 1959;1933: 1–6.

61. Wu X-C, Russell AP, Brinkman DB. A review of *Leidyosuchus* Lambe, 1907 (Archosauria: Crocodylia) and an assessment of cranial variation based upon new material: Erratum. Can J Earth Sci. 2001;38: 1665–1587. doi:10.1139/e02-900

62. Rivera-Sylva HE, Frey E, Guzmán-Gutierrez JR, Palomino-Sánchez F, Stinnesbeck W. A *Deinosuchus riograndensis* (Eusuchia: Alligatoroidea) from Coahuila, North Mexico. Rev Mex Ciencias Geol. 2011;28: 267–274.

63. Norell MA, Clark JM, Hutchison JH. The Late Cretaceous alligatoroid *Brachychampsa montana* (Crocodylia): new material and putative relationships. Am Museum Novit. 1994;3116: 1–26.

64. Brochu CA. Phylogenetics, taxonomy, and historical biogeography of Alligatoroidea. J Vertebr Paleontol. Taylor & Francis; 1999;19: 9–100. doi:10.1080/02724634.1999.10011201

65. Sullivan RM, Lucas SG. *Brachychampsa montana* Gilmore (Crocodylia Alligatoridae) from the Kirtland Formation (Upper Campanian) San Juan Basin New Mexico. J Vertebr Paleontol. 2003;23: 832–841. doi:10.1671/A1082-8

66. Williamson TE. ?*Brachychampsa sealeyi,* sp. nov., (Crocodylia, Alligatoroidea) from the Upper Cretaceous (Lower Campanian) Menefee Formation, Northwestern New Mexico. J Vertebr Paleontol. 1996;16: 421–431.

67. Wu X, Brinkman DB, Russell AP. A new alligator from the upper cretaceous of canada and the relationships of early eusuchians. Palaeontology. 1996. pp. 351–375.

68. Bartels WS. Osteology and systematic affinities of the horned alligator *Ceratosuchus* (Reptilia, Crocodilia). J Paleontol. 1984;58: 1347–1353.

69. Mook CC. A new fossil crocodilian from the Paleocene of New Mexico. Am Museum Novit. 1942;No. 1189: 1–4.

70. Gilmore CW. A New Crocodilian from the Eocene of Utah. J Paleontol. 1946;20: 62–67.

71. Kälin JA. Ein extrem kurzschnauziger Crocodilide aus den Phosphoriten des Quercy Arambourgia (nov. gen.) gaudryi de Stefano. Abhandlungen der Schweizerischen Palaeontol Gesell- schaft. Birkhauser; 1939;62: 1–18.

72. Erickson BR. *Wannaganosuchus*, a new alligator from the Paleocene of North America. J Paleontol. SEPM Society for Sedimentary Geology; 1982;56: 492–506. doi:10.2307/1304478

73. Shan H, Cheng Y, Wu X. The first fossil skull of *Alligator sinensis* from the Pleistocene, Taiwan, with a paleogeographic implication of the species. J Asian Earth Sci. Elsevier Ltd; 2013;69: 17–25. doi:10.1016/j.jseaes.2012.05.026

74. Mook CC, Mefferd R. A new Pliocene alligator from Nebraska. American Museum of Natural History; 1946.

75. Mook CC, Thomson A. A new species of Alligator from the Snake Creek beds. By order of the Trustees of The American Museum of Natural History; 1923.

76. White TE. A new alligator from the Miocene of Florida. Copeia. JSTOR; 1942;1942: 3–7.

77. Schmidt KP. A new fossil alligator from Nebraska. Geol Ser F Museum Nat Hist. na; 1941;8: 27–32.

78. Pinheiro AEP, Fortier DC, Pol D, Campos DA, Bergqvist LP. A new *Eocaiman* (Alligatoridae, Crocodylia)

from the Itaboraí Basin, Paleogene of Rio de Janeiro, Brazil. Hist Biol. 2013;25: 327–337. doi:10.1080/08912963.2012.705838

79. Brochu CA. A new alligatorid from the lower Eocene Green River Formation of Wyoming and the origin of caimans. J Vertebr Paleontol. 2010;30: 1109–1126. doi:10.1080/02724634.2010.483569

80. Salas-gismondi R, Flynn JJ, Baby P, Wesselingh FP, Antoine P-O. A Miocene hyperdiverse crocodylian community reveals peculiar trophic dynamics in proto-Amazonian mega-wetlands. Proc R Soc B Biol Sci. 2015;282: 4–8.

81. Scheyer TM, Delfino M. The late Miocene caimanine fauna (Crocodylia: Alligatoroidea) of the Urumaco Formation , Venezuela. Palaeontol Electron. 2016;19.3.48A: 1–57.

82. Langston Jr. W. *Mourasuchus* Price, *Nettosuchus* Langston, and the Family Nettosuchidae (Reptilia: Crocodilia). Copeia. 1966;4: 882–885. doi:10.2307/1441424

83. Bocquentin J, Pereira J, Filho DES. O crogodiliana sul-americano *Carandaisuchus* como sinonímia de *Mourasuchus* (Nettosuchidae). Rev Bras Geociências. 1990;20: 230–233.

84. Bona P, Barrios F. The Alligatoroidea of Argentina: an update of its fossil record. Publicación Electrónica la Asoc Paleontológica Argentina. 2015;15: 143–158. doi:10.5710/PEAPA.15.06.2015.103

85. Grigg GC, Kirshner D. Biology and evolution of crocodylians. Csiro Publishing; 2015.

86. Medina CJ. Crocodilians from the Late Tertiary of northwestern Venezuela: *Melanosuchus* fisheri sp. nov. Museum of Comparative Zoology; 1976.

87. Bona P, Blanco MVF, Schever TM, Both C. Shedding light on the taxonomic diversity of the South American miocene caimans: The status of *Melanosuchus fisheri* (Crocodylia, Alligatoroidea). Ameghiniana. 2017;54: 681–687. doi:10.5710/AMGH.08.06.2017.3103

88. Brochu CA. Alligatorine phylogeny and the status of *Allognathosuchus* Mook, 1921. J Vertebr Paleontol. 2004;24: 857–873. doi:10.1043/0272-4634(2004)024<0857:apatso>2.0.co;2

89. Brinkmann W, Rauhe M. *Diplocynodon ratelii* POMEL, 1847 (Crocodylia, Leidyosuchidae) from the Lower Oligocene of Cereste (Southern France). Neues Jahrb fur Geol und Palaontologie-Abhandlungen. Stuttgart: E. Schweizerbart'sche Verlagsbuchhandlung, 1950-; 1998;209: 295–322.

90. Díaz Aráez JL, Delfino M, Luján ÀH, Fortuny J, Bernardini F, Alba DM. New remains of *Diplocynodon* (Crocodylia: Diplocynodontidae) from the Early Miocene of the Iberian Peninsula. Comptes Rendus - Palevol. Academie des sciences; 2015;16: 12–26. doi:10.1016/j.crpv.2015.11.003

91. Vignaud P, Brunet M, Guevel B, Jehenne Y. Un crâne de *Diplocynodon* (Crocodylomorpha, Alligatoridae) de l'Oligocène inférieur de Dordogne (France). Comptes rendus l'Académie des Sci Série 2 Sci la terre des planètes. Elsevier; 322: 595–601.

92. Owen R. A history of British fossil reptiles. Cassell & company limited; 1849.

93. Lydekker R. IV.—Note on the Hordwell and other Crocodilians. Geol Mag. Cambridge University Press; 1887;4: 307–312.

94. Piras P, Buscalioni AD. *Diplocynodon muelleri* Comb. nov., an Oligocene diplocynodontine alligatoroid from Catalonia (Ebro Basin, Lleida Province, Spain). Journal of Vertebrate Paleontology. 2006. pp. 608–620. doi:10.1671/0272-4634(2006)26[608:DMCNAO]2.0.CO;2

95. Buscalioni AD, Sanz JL, Casanovas ML. A new species of the eusuchian crocodile *Diplocynodon* from the Eocene of Spain. Neues Jahrb für Geol und Paläontologie Abhandlungen. 1992;187: 1–29.

96. Delfino M, Smith T. Reappraisal of the morphology and phylogenetic relationships of the middle Eocene alligatoroid *Diplocynodon deponiae* (Frey, Laemmert, and Riess, 1987) based on a three-dimensional specimen. J Vertebr Paleontol. 2012;32: 1358–1369. doi:10.1080/02724634.2012.699484

97. Martin JE, Gross M. Taxonomic clarification of *Diplocynodon* Pomel, 1847 (Crocodilia) from the Miocene of Styria, Austria. Neues Jahrb für Geol und Paläontologie - Abhandlungen. 2011;261: 177–193. doi:10.1127/0077-7749/2011/0159

98. Martin JE. A new species of *Diplocynodon* (Crocodylia, Alligatoroidea) from the Late Eocene of the

Massif Central, France, and the evolution of the genus in the climatic context of the Late Palaeogene. Geol Mag. 2010;147: 596–610. doi:10.1017/S0016756809990161

99. Martin JE, Smith T, de Lapparent de Broin F, Escuillie F, Delfino M. Late Palaeocene eusuchian remains from Mont de Berru, France, and the origin of the alligatoroid *Diplocynodon*. Zool J Linn Soc. 2014;172: 867–891. doi:10.1111/zoj.12195

100. Martin JE, Lauprasert K. A new primitive alligatorine from the Eocene of Thailand: Relevance of Asiatic members to the radiation of the group. Zool J Linn Soc. 2010;158: 608–628. doi:10.1111/j.1096-3642.2009.00582.x

101. Hastings AK, Bloch JI, Jaramillo CA, Rincon AF, Macfadden BJ. Systematics and biogeography of crocodylians from the Miocene of Panama. J Vertebr Paleontol. 2013;33: 239–263. doi:10.1080/02724634.2012.713814